ASTRONOMY AND ASTROPHYSICS LIBRARY

Series Editors: I. Appenzeller · G. Börner · M. Harwit · R. Kippenhahn
P. A. Strittmatter · V. Trimble

Springer
New York
Berlin
Heidelberg
Barcelona
Budapest
Hong Kong
London
Milan
Paris
Santa Clara
Singapore
Tokyo

ASTRONOMY AND ASTROPHYSICS LIBRARY

Series Editors: I. Appenzeller · G. Börner · M. Harwit · R. Kippenhahn
P. A. Strittmatter · V. Trimble

Theory of Orbits (2 volumes)
Volume 1: Integrable Systems and Non-perturbative Methods
Volume 2: Perturbative and Geometrical Methods
By D. Boccaletti and G. Pucacco

Galaxies and Cosmology
By F. Combes, P. Boissé, A. Mazure, and A. Blanchard

The Solar System 2nd Edition By T. Encrenaz and J.-P. Bibring

Compact Stars
Nuclear Physics, Particle Physics, and General Relativity
By N. K. Glendenning

The Physics and Dynamics of Planetary Nebulae
By G. A. Gurzadyan

Astrophysical Concepts 2nd Edition By M. Harwit

Stellar Structure and Evolution By R. Kippenhahn and A. Weigert

Modern Astrometry By J. Kovalevsky

Supernovae Editor: A. Petschek

General Relativity, Astrophysics, and Cosmology
By A. K. Raychaudhuri, S. Banerji, and A. Banerjee

Tools of Radio Astronomy 2nd Edition
By K. Rohlfs and T. L. Wilson

Atoms in Strong Magnetic Fields
Quantum Mechanical Treatment and Applications
in Astrophysics and Quantum Chaos
By H. Ruder, G. Wunner, H. Herold, and F. Geyer

The Stars By E. L. Schatzman and F. Praderie

Gravitational Lenses By P. Schneider, J. Ehlers, and E. E. Falco

Relativity in Astrometry, Celestial Mechanics, and Geodesy
By M. H. Soffel

The Sun An Introduction By M. Stix

Galactic and Extragalactic Radio Astronomy 2nd Edition
Editors: G. L. Verschuur and K. I. Kellermann

Reflecting Telescope Optics (2 volumes)
Volume I: Basic Design Theory and its Historical Development
Volume II: Manufacture, Testing, Alignment, Modern Techniques
By R. N. Wilson

Norman K. Glendenning

Compact Stars

Nuclear Physics, Particle Physics, and General Relativity

With 87 figures

Springer

Norman K. Glendenning
Lawrence Berkeley National Laboratory
University of California
Berkeley, CA 94720
USA

Series Editors

Immo Appenzeller
Landassternwarte, Königstuhl
D-69117 Heidelberg, Germany

Gerhand Börner
MPI für Physik und Astrophysik
Institut für Astrophysik
Karl-Schwarzschild-Strasse 1
D-85748 Garching, Germany

Martin Harwit
511 H Street SW
Washington, DC 20024, USA

Rudolf Kippenhahn
Rautenbreite 2
D-37077 Göttingen, Germany

Peter A. Strittmatter
Steward Observatory
The University of Arizona
Tucson, AZ 85721, USA

Virginia Trimble
Astronomy Program
University of Maryland
College Part, MD 20742, USA
and Department of Physics
University of California
Irvine, CA 92717, USA

Cover picture: Shock wave produced by the nearest millisecond pulsar, PSR J0437−4715, seen in the Hydrogen-alpha emission line with the CTIO telescope. The faint star directly behind shock is the white-dwarf companion of the pulsar. The distance between the shock wave and the star is about 1400 AU. Color image by Andrew S. Fruchter (Space Telescope Science Institute), courtesy of Cerro Tololo Inter-American Observatory).

Library of Congress Cataloging-in-Publication Data
Glendenning, Norman K.
Compact stars : nuclear physics, particle physics, and general relativity / Norman K. Glendenning.
p. cm.—(Astronomy and astrophysics library)
Includes bibliographical references and index.
ISBN-13: 978-1-4684-0493-7 e-ISBN-13: 978-1-4684-0491-3
DOI: 10.1007/978-1-4684-0491-3
1. Neutron stars. 2. White dwarfs. 3. General relativity (Physics) I. Title. II. Series.
QB843.N4G54 1996
523.8′874—dc20 96-31724

Printed on acid-free paper.

© 1997 Springer-Verlag New York, Inc.
Softcover reprint of the hardcover 1st edition 1997
All rights reserved. This work may not be translated or copied in whole or in part without the written permission of the publisher (Springer-Verlag New York, Inc., 175 Fifth Avenue, New York, NY 10010, USA), except for brief excerpts in connection with reviews or scholarly analysis. Use in connection with any form of information storage and retrieval, electronic adaptation, computer software, or by similar or dissimilar methodology now known or hereafter developed is forbidden.
The use of general descriptive names, trade names, trademarks, etc., in this publication, even if the former are not especially identified, is not to be taken as a sign that such names, as understood by the Trade Marks and Merchandise Marks Act, may accordingly be used freely by anyone.

Production managed by Steven Pisano; manufacturing supervised by Johanna Tschebull.
Photocomposed copy prepared from the author's LaTeX files.

9 8 7 6 5 4 3 2 1

ISBN-13: 978-1-4684-0493-7

To my children,
Alan, Elke, Nathan

Preface

The heavens are a wonder to us all. When keenly observed they present, not a vast and unchanging panoply, but a cycle of life that embraces our own. Stars are born in primordial clouds of diffuse gases. They lead an active and ever changing life for millions of years as they synthesize their store of hydrogen into ever heavier elements. Then they collapse and die. Their last gasp is an enormous explosion—a supernova—which lights the day-time sky for months as it disperses to the heavens the very elements of which the planets, and we ourselves, are made. From the primordial clouds, enriched by the elements of such stellar deaths, new stars are born.

Contemplating these marvels, we arrive at the thought that in the vast reaches of the universe the laws of nature are explored and realized in innumerable imagined—and as yet unimagined forms. In this spirit compact stars, especially neutron stars, are studied in this book. Neutron stars were a great surprise when first discovered as pulsars, highly magnetized rotating neutron stars that illuminate sensitive radio telescopes at each rotation. They continue to amaze us with their multitude of associated phenomena. These include a high velocity pulsar with a white dwarf companion creating a luminous nebula in the interstellar gas as the pair streaks through space (see cover picture), and a miniature planetary system consisting of a neutron star and three planets—the first planets discovered outside our own solar system.

Neutron stars—the smallest densest stars known—are as massive as the sun but much smaller than the earth, yet some of them spin hundreds of times in a second. The very high mass concentration and very rapid rotation of some pulsars warps the fabric of spacetime. Neutron stars are fully relativistic objects.

There are admirable and comprehensive treatises on General Relativity, those of Misner,Thorne and Wheeler, and of Weinberg. When I began my study of compact stars a little more than ten years ago, I would have found it useful to have the theory from its origins through to the equations of relativistic stellar structure set down rigorously and directly—along a geodesic path so to speak. With that limited goal, it is done here in a chapter.

This book differs from the excellent one of Shapiro and Teukolsky in

several respects. The range of topics dealt with in this book is narrower, but in general they are treated in greater depth. Also emphasis is placed on emerging topics—the many forms in which "neutron" stars may be realized in nature—hyperon stars, hybrids stars with intricate crystalline interiors of quark and nuclear matter, and strange quark stars and dwarfs sheathed in nuclear material. These marvelous objects challenge our understanding of dense matter physics both nuclear and particle, not to mention our imagination.

There is an immense body of data and lore on the subject of compact stars which can only be ferreted slowly from the literature, learning this here, that there, and then with enough—making the connections. The reader may profit in the time it takes to read these several hundred pages, from what I learned in this respect.

The physics of compact objects attracts the interest of many researchers and students, not only in astrophysics, but in other fields of the physical sciences such as nuclear and particle physics. The book is self-contained. The author writes in the hope that his book will inform, fire the imagination, and provide a basis for further investigations by newcomers as well as experienced researchers who want to familiarize themselves with a modern view of the topic.

I appreciate the forbearance of T. von Foerster, Editor in Chief of Physics at Springer-Verlag New York through the six years this book has been in preparation. To my great fortune he very wisely assigned an outstanding editor, D. A. Oliver whom I thank; with his help and prodding the presentation was vastly improved over many revisions. Over the last half dozen years F. Weber and I have collaborated on many projects, especially concerning stellar rotation. This book is, in part, a beneficiary of our collaboration. Most of all I thank Laura for who she is.

Norman K. Glendenning
Berkeley, California
October 17, 1996

Contents

Preface **vii**

1 Introduction **1**
1.1 Compact Stars 2
1.2 Compact Stars and Relativistic Physics 4
1.3 Compact Stars and Dense-Matter Physics 5

2 General Relativity **7**
2.1 Lorentz Invariance 8
2.1.1 Lorentz transformations 8
2.1.2 Covariant vectors 10
2.1.3 Energy-momentum tensor of a perfect fluid 12
2.1.4 Light cone 12
2.2 Scalars, Vectors, and Tensors in Curvilinear Coordinates . . 13
2.3 Principle of Equivalence of Inertia and Gravitation 18
2.3.1 Photon in a gravitational field 20
2.3.2 Tidal gravity 21
2.3.3 Curvature of spacetime 21
2.3.4 Energy conservation and curvature 22
2.4 Gravity 23
2.4.1 Mathematical definition of local Lorentz frames . . . 26
2.4.2 Geodesics 26
2.4.3 Comparison with Newton's gravity 29
2.5 Covariance 30
2.5.1 Principle of General Covariance 30
2.5.2 Covariant Differentiation 30
2.5.3 Geodesic equation from covariance principle 31
2.5.4 Covariant divergence and conserved quantities . . . 33
2.6 Riemann Curvature Tensor 36
2.6.1 Second covariant derivative of scalars and vectors . . 36
2.6.2 Symmetries of the Riemann tensor 36
2.6.3 Test for flatness 37
2.6.4 Second covariant derivative of tensors 37

2.6.5 Bianchi identities 38
2.6.6 Einstein tensor 39
2.7 Einstein's Field Equations 40
2.8 Relativistic Stars 42
2.8.1 Metric in static isotropic spacetime 42
2.8.2 The Schwarzschild solution 44
2.8.3 Riemann tensor outside a Schwarzschild star 45
2.8.4 Energy-Momentum tensor of matter 46
2.8.5 The Oppenheimer–Volkoff equations 47
2.8.6 Gravitational collapse and limiting mass 51
2.9 Action Principle in Gravity 52

3 Compact Stars: From Dwarfs to Black Holes 55
3.1 Birth and Death of Stars 55
3.2 Objective 61
3.3 Gravitational Units and Neutron Star Size 62
3.4 Partial Decoupling of Matter from Gravity 66
3.5 Equations of Relativistic Stellar Structure 67
3.6 Electrical Neutrality of Stars 71
3.7 "Constancy" of the Chemical Potential 72
3.8 Gravitational Redshift 73
3.8.1 Integrity of an atom in strong fields 73
3.8.2 Redshift in a general static field 75
3.8.3 Comparison of emitted and received light 78
3.8.4 Measurements of M/R from redshift 79
3.9 White Dwarfs and Neutron Stars 79
3.9.1 Overview 79
3.9.2 Fermi-Gas equation of state for nucleons and electrons 81
3.9.3 High- and low-density limits 86
3.9.4 Polytropes and Newtonian white dwarfs 87
3.9.5 Stability 91
3.9.6 Nonrelativistic electron region 93
3.9.7 Relativistic electron region: asymptotic white dwarf mass 94
3.9.8 Nature of limiting mass of dwarfs and neutron stars 96
3.9.9 Degenerate ideal gas neutron star 98
3.10 Improvements in White Dwarf Models 99
3.10.1 Nature of matter at dwarf densities 99
3.10.2 Carbon and oxygen white dwarfs 102
3.11 Stellar Sequences from White Dwarfs to Neutron Stars . . . 105
3.12 Star of Uniform Density 107
3.13 Baryon Number of a Star 110
3.14 Bound on Maximum Mass of Neutron Stars 112
3.15 Beyond Maximum-Mass Neutron Stars 116

3.16 Black Holes 117
3.16.1 Interior and Exterior Regions 117
3.16.2 No statics within 120
3.16.3 Black hole densities 122

4 Relativistic Nuclear Field Theory 124
4.1 Motivation 124
4.2 Lagrange Formalism 129
4.3 Symmetries and Conservation Laws 130
4.3.1 Internal global symmetries 131
4.3.2 Spacetime symmetries 132
4.4 Boson and Fermion Fields 135
4.4.1 Uncharged and charged scalar fields 135
4.4.2 Uncharged and charged vector fields 136
4.4.3 Dirac fields 138
4.4.4 Neutron and proton 140
4.4.5 Electromagnetic field 142
4.5 Properties of Nuclear Matter 143
4.6 The $\sigma - \omega$ Model 147
4.7 Stationarity of Energy Density 156
4.8 Model with Scalar Self-Interactions 156
4.8.1 Algebraic determination of the coupling constants . 158
4.8.2 Symmetric nuclear matter equation of state 161
4.8.3 Negative self-interaction 162
4.9 Introduction of Isospin Force 164
4.10 Inclusion of the Octet of Baryons 169
4.11 High-Density Limit 173
4.12 Effective vs. Renormalized Theory 173
4.13 Bound vs. Unbound Neutron Matter 175
4.13.1 Bound neutron matter 176
4.13.2 First-Order phase transition 176
4.14 Note on Dimensions 178
4.15 Summary 178

5 Neutron Stars 180
5.1 Introduction 180
5.2 Pulsars: The Observational Basis of Neutron Stars 183
5.2.1 Important pulsar discoveries 183
5.2.2 Pulsar periods 186
5.2.3 Individual pulses and pulse profiles 187
5.2.4 Detection biases 189
5.2.5 Two populations of pulsars 190
5.2.6 Supernova associations with pulsars 191
5.2.7 Why pulsars are neutron stars 193
5.2.8 Pulsar masses 197

5.2.9 Pulsar ages 200
5.2.10 Evolution of the braking index[5] 202
5.3 Theory of Neutron Stars 206
5.3.1 Nuclear and neutron star matter: Similarities and differences 206
5.3.2 Chemical equilibrium in a star 208
5.3.3 Hadronic composition of neutron stars 212
5.3.4 Neutron star matter 214
5.3.5 Hints for computation 219
5.3.6 Isospin- and charge-favored baryon species 221
5.3.7 Surface of neutron stars 221
5.3.8 Reprise of white dwarfs to neutron stars 222
5.3.9 Development of neutron star sequences 223
5.3.10 Mass as a function of central density 224
5.3.11 Radius–Mass characteristic relationship 225
5.4 Constitution of Neutron Stars 227
5.4.1 Limiting mass and the equation of state 227
5.4.2 Beta equilibrium and symmetry energy 228
5.4.3 Hyperon stars 229
5.4.4 Limiting mass and hyperon populations 233
5.4.5 Compression modulus and effective nucleon mass . . 234
5.4.6 Pion and kaon condensation 236
5.4.7 Charge neutrality achieved among baryons 240
5.5 Tables of Equations of State 242
5.5.1 Low density 242
5.5.2 High density 244

6 Rotating Neutron Stars 247
6.1 Motivation 247
6.2 Dragging of Local Inertial Frames 249
6.3 Interior Solution for the Dragging Frequency 253
6.4 Kepler Angular Velocity in General Relativity 255
6.5 Effect of Frame Dragging on Kepler Frequency 258
6.6 Hartle–Thorne Perturbative Solution 260
6.6.1 Comparison of Perturbative and Numerical Solutions 261
6.7 Imprint of Angular Momentum 262
6.8 Rotating Stars with Realistic Equations of State 263
6.9 Effect of Rotation on Stellar Structure 264
6.10 Gravitational-Wave Instabilities 265

7 Limiting Rotational Period of Neutron Stars 275
7.1 Motivation 275
7.2 The Minimal Constraints 277
7.3 Variational Ansatz 278
7.4 Limiting Value of Rotational Period as a Function of Mass . 279

7.5 Test of Sensitivity of Results 281
7.6 General Relativistic Limit on Rotation 285
7.7 Discussion and Alternatives 286
7.8 Summary 288

8 Quark Stars 289
8.1 Introduction 289
8.2 Quark Matter Equation of State 289
8.2.1 Zero Temperature 290
8.2.2 Massless quark approximation 291
8.2.3 First order in α_s 292
8.3 Quark Star Matter 293
8.4 Strange and Charm Stars 295
8.5 Beyond White Dwarfs and Neutron Stars 301

9 Hybrid Stars 303
9.1 Introduction 303
9.2 Constant-Pressure Phase Transition 305
9.3 The Confined-Deconfined Phase Transition in Neutron Stars 308
9.3.1 Conservation laws are global—not local 308
9.4 Degrees of Freedom in a Multicomponent System 309
9.4.1 Coulomb lattice structure of the mixed phase 313
9.4.2 Phase diagram 313
9.4.3 Two energy scales 314
9.5 Gross Structure of a Hybrid Star 315
9.5.1 Energy budget in the reapportionment of charge . . 317
9.6 Crystalline Structure 319
9.6.1 Crystalline structure as a function of stellar mass . . 323
9.6.2 Possible implications for glitches 325
9.7 Mechanism for Formation of Low-Mass Black Holes 326
9.7.1 Hyperonization-Induced collapse 328
9.7.2 Deconfinement-Induced collapse 329
9.7.3 Density profiles 330
9.7.4 Discussion 331
9.8 Tables of Equation of State for Hybrid Stars 333

10 Strange Stars 337
10.1 The Strange Matter Hypothesis 337
10.2 Compatibility of the Hypothesis with Present Knowledge . 338
10.2.1 Energetic considerations 338
10.2.2 The universe and its evolution 339
10.2.3 Stability of nuclei against decay to strange matter . 340
10.2.4 Stability of nuclei to conversion by strange nuggets . 341
10.2.5 Terrestrial searches 341
10.2.6 Summary, prospects and challenges 343

10.3 Submillisecond Pulsars 343
10.3.1 The fine-tuning problem 343
10.3.2 Limits to neutron star rotation 344
10.3.3 Implausibly high central densities 345
10.3.4 Strange stars as fast rotors 346
10.3.5 Out of the impasse 347
10.3.6 Motivation for searches and prospects for discovery . 348
10.4 Structure of Strange Stars 348
10.5 Strange Stars to Strange Dwarfs 350
10.5.1 Strange stars with nuclear crusts 350
10.5.2 Strange dwarfs with nuclear crusts 355
10.5.3 Stability 357
10.5.4 Possible new class of dense white dwarfs 360
10.6 Conclusion 361

Appendix A: Useful Astronomical Data **362**

Books for Further Study **363**

References **365**

Index **383**

1

Introduction

"In the deathless boredom of the sidereal calm we cry with regret for a lost sun ..."
Jean de la Ville de Mirmont, L'Horizon Chimérique.

Compact stars—broadly grouped as neutron stars and white dwarfs—are the ashes of luminous stars. One or the other is the fate that awaits the cores of most stars after a lifetime of tens to thousands of millions of years. Whichever of these objects is formed at the end of the life of a particular luminous star, the compact object will live in all essential respects unchanged from the state in which it was formed. Neutron stars themselves can take several forms—hyperon, hybrid, or strange quark star. Likewise white dwarfs take different forms though only in the dominant nuclear species. A black hole is probably the fate of the most massive stars, an inaccessible region of spacetime into which the entire star, ashes and all, falls at the end of the luminous phase.

Neutron stars are the smallest, densest stars known. Like all stars, neutron stars rotate—some as many as a few hundred times a second. A star rotating at such a rate will experience an enormous centrifugal force that must be balanced by gravity else it will be ripped apart. The balance of the two forces informs us of the lower limit on the stellar density. Neutron stars are 10^{14} times denser than Earth. Some neutron stars are in binary orbit with a companion. Application of orbital mechanics allows an assessment of masses in some cases. The mass of a neutron star is typically 1.5 solar masses. We can therefore infer their radii: about ten kilometers. Into such a small object, the entire mass of our sun and more, is compressed.

We infer the existence of neutron stars from the occurrence of supernova explosions (the release of the gravitational binding of the neutron star) and observe them in the periodic emission of pulsars. Just as neutron stars acquire high angular velocities through conservation of angular momentum, they acquire strong magnetic fields through conservation of magnetic flux during the collapse of normal stars. The two attributes, rotation and strong magnetic dipole field, are the means by which neutron stars can be detected—the beamed periodic signal of pulsars.

The extreme characteristics of neutron stars set them apart in the phys-

ical principles they require for their understanding. All other stars can be described in Newtonian gravity with atomic and low-energy nuclear physics (under conditions essentially known in the laboratory[1]). Neutron stars in their several forms push matter to such extremes of density that nuclear and particle physics—pushed to their extremes—are essential for their description. Further, the intense concentration of matter in neutron stars can be described only in General Relativity, Einstein's theory of gravity which alone describes the way the weakest force in nature arranges the distribution of the mass and constituents of the densest objects in the universe.

1.1 Compact Stars

Of what are compact stars made? The name "neutron star" is suggestive and at the same time misleading. No doubt neutron stars are made of baryons like nucleons and hyperons but also likely contain cores of quark matter in some cases. These physically compelling possibilities will be examined in the various chapters of this book, neutron stars, quark stars, hybrid stars, and strange stars.

We use "neutron star" in a generic sense to refer to stars as compact as described above. How does a star become so compact as neutron stars and why is there little doubt that they are made of baryons or quarks? The notion of a neutron star made from the ashes of a luminous star at the end point of its evolution goes back to 1934 and the study of supernova explosions by Baade and Zwicky [1].

During the luminous life of a star, part of the original hydrogen is converted in fusion reactions to heavier elements by the heat produced by gravitational compression. When sufficient iron—the end point of exothermic fusion—is made, the core containing this heaviest ingredient collapses and an enormous energy is released in the explosion of the star. Baade and Zwicky guessed that the source of such a magnitude as makes these stellar explosions visible in daylight and for weeks thereafter must be gravitational binding energy. This energy is released by the solar mass core as the star collapses to densities high enough to tear all nuclei apart into their constituents.

By a simple calculation one learns that the gravitational energy acquired by the collapsing core is more than enough to power such explosions as Baade and Zwicky were detecting. Their view as concerns the compactness of the residual star has since been supported by many detailed calcula-

[1]Luminous stars evolve through thermonuclear reactions. These are nuclear reactions induced by high temperatures but involving collision energies that are small on the nuclear scale. In some cases the reaction cross-sections can be measured on nuclear accelerators, and in others measured cross-sections must be extrapolated to lower energy.

tions, and most spectacularly by the supernova explosion of 1987 in the Large Magellanic Cloud, a nearby minor galaxy visible in the southern hemisphere. The pulse of neutrinos observed in several large detectors carried the evidence for an integrated energy release over 4π steradians of the expected magnitude.

The gravitational binding energy of a neutron star is about 10 percent of its mass. Compare this with the nuclear binding energy of 9 MeV per nucleon in iron which is one percent of the nucleon mass. We conclude that the release of gravitational binding energy at the death of a massive star is of the order ten times greater than the energy released by nuclear fusion reactions during the entire luminous life of the star. The evidence that the source of energy for a supernova is the binding energy of a compact star—a neutron star—is compelling. How else could a tenth of a solar mass of energy be generated and released in such a short time?

Neutron stars are more dense than was thought possible by physicists at the turn of the century. At that time astronomers were grappling with the thought of white dwarfs whose densities were inferred to be about a million times denser than the earth. It was only following the discovery of the quantum theory and Fermi-Dirac statistics that very dense, degenerate Fermi systems were conceived. Prior to that the high density inferred for the white dwarf Sirius seemed to present a dilemma. For while the high density was understood as arising from the ionization of the atoms in the hot star making possible their compaction by gravity, what would become of this dense object when ultimately it had consumed its nuclear fuel? Cold matter was known only in the form it is on earth with densities of a few grams per cubic centimeter. The great scientist Sir Arthur Eddington surmised for a time that the star had "got itself into an awkward fix"—that it must some how reexpand to matter of familiar densities as it cooled, but it had no remaining source of energy to do so. The perplexing problem of how a hot dense body without a source of energy could cool persisted until R. H. Fowler "came to the rescue"[2] by showing that Fermi-Dirac degeneracy allowed the star to cool by remaining comfortably in a previously unknown state of cold matter. It was this dense, degenerate state which Baade and Zwicky a little later conceived of as the resting place of nucleons in the stellar core after the final supernova explosion.

The constituents of neutron stars—leptons, baryons and quarks—are degenerate. They lie helplessly in the lowest energy states available to them. They must. Fusion reactions in the original star have reached the end point for energy release—the core has collapsed, and the immense gravitational energy converted to neutrinos has been carried away. The star has no remaining source of energy to excite the fermions. Only the Fermi pressure and the short-range repulsion of the nuclear force sustain the neutron star against further gravitational collapse—sometimes. At other times the mass

[2]Eddington in an address in 1936 at Harvard University.

is so concentrated that it falls into a black hole, a dynamical object whose existence and external properties can be understood in the Classical Theory of General Relativity.

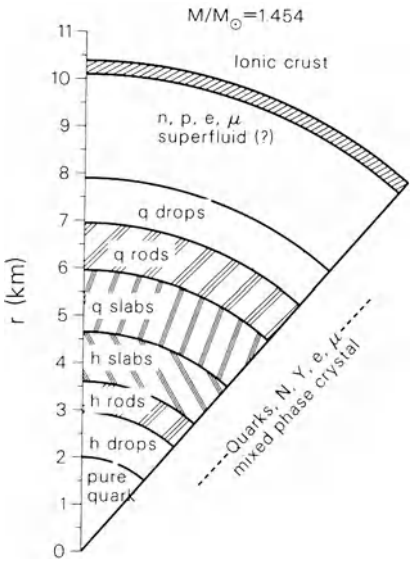

FIGURE 1.1. A section through a neutron star model that contains an inner sphere of pure quark matter surrounded by a crystalline region of mixed hadronic and quark matter. The mixed phase region consists of various geometrical objects of the rare phase immersed in the dominant one labeled by h(adronic) drops immersed in quark matter ... through to q(uark) drops immersed in hadronic matter. The particle composition of these regions is quarks, nucleons, hyperons, and leptons. A liquid of neutron star matter containing nucleons and leptons surrounds the mixed phase. A thin crust of heavy ions forms the stellar surface.

1.2 Compact Stars and Relativistic Physics

Classical General Relativity is completely adequate for the description of neutron stars, white dwarfs, and for the most part, the exterior region of black holes as well as some aspects of the interior.[3] The first chapter is devoted to General Relativity. The goal is to rigorously arrive at the equations that describe the structure of relativistic stars—the Oppenheimer–Volkoff equations—the form that Einstein's equations take for spherical static stars. Two important facts emerge immediately. No form of matter whatsoever can support a relativistic star above a certain mass called the limiting mass. Its value depends on the nature of matter but the existence of the limit does not. The implied fate of stars more massive than the limit is that either mass is lost in great quantity during the evolution of the star or it collapses to form a black hole.

Black holes—the most mysterious objects of the universe—are treated

[3]The density at which quantum gravity would be relevant is 10^{78} higher than found in neutron stars.

at the classical level in this book and only briefly. The peculiar difference between time as measured at a distant point and on an object falling into the hole is discussed. And it is shown that in black holes there is no statics. Everything at all times must approach the central singularity. Unlike neutron stars and white dwarfs, the question of their internal constitution does not arise at the classical level. They are enclosed within a horizon from which no information can be received. The ultimate fate of black holes is unknown.

Luminous stars are known to rotate because of the Doppler broadening of spectral lines. Therefore their collapsed cores, spun up by conservation of angular momentum, may rotate very rapidly. Consequently, no account of compact stars would be complete without a discussion of rotation, its effects on the structure of the star and spacetime in the vicinity, the limits on rotation imposed by mass loss at the equator and by gravitational radiation, and the nature of compact stars that would be implied by very rapid rotation.

Rotating relativistic stars set local inertial frames into rotation with respect to the distant stars. An object falling from rest at great distance toward a rotating star would fall—not toward its center but would acquire an ever larger angular velocity as it approached. The effect of rotating stars on the fabric of spacetime acts back upon the structure of the stars and so is essential to our understanding.

1.3 Compact Stars and Dense-Matter Physics

The physics of dense matter is not as simple as the final resting place of stars imagined by Baade and Zwicky. The constitution of matter at the high densities attained in a neutron star—the particle types, abundances and their interactions—pose challenging problems in nuclear and particle physics. How should matter at surpernuclear densities be described? In addition to nucleons, what exotic baryon species constitute it? Does a transition in phase from quarks confined in nucleons to the deconfined phase of quark matter occur in the density range of such stars? And how is the transition to be calculated? What new structure is introduced into the star? Do other phases like pion or kaon condensates play a role in their constitution?

In Fig. 1.1 we show a computation of the possible constitution and interior crystalline structure of a neutron star near the limiting mass of such stars (Chapter 9). Only now are we beginning to appreciate the complex and marvelous structure of these objects. Surely the study of neutron stars and their astronomical realization in pulsars will serve as a guide in the search for a solution to some of the fundamental problems of dense many-body physics both at the level of nuclear physics—the physics of baryons and mesons—and ultimately at the level of their constituents—quarks and

gluons. And neutron stars may be the only objects in which a Coulomb lattice structure (Fig. 1.1) formed from two phases of one and the same substance (hadronic matter) exists.

White dwarfs are the cores of stars whose demise is less spectacular than a supernova—a more quiescent thermal expansion of the envelope of a low mass star into a planetary nebula. White dwarf constituents are nuclei immersed in an electron gas and therefore arranged in a Coulomb lattice. White dwarfs are supported against collapse by Fermi pressure—as are neutron stars—except that the pressure is provided by degenerate electrons. White dwarfs pose less severe and less fundamental problems than neutron stars. The nuclei will comprise varying proportions of helium, carbon, and oxygen, and in some cases heavier elements like magnesium, depending on how far in the chain of exothermic nuclear fusion reactions the precursor star burned before it was disrupted by instabilities leaving behind the dwarf. White dwarfs are barely relativistic.

Of a vastly different nature than neutron stars are *strange stars*. Like neutron stars they are, if they exist, very dense, of the same order as neutron stars. However their very existence hinges on a hypothesis that at first sight seems absurd. According to the hypothesis, sometimes referred to as the *strange-matter hypothesis*, quark matter—consisting of an approximately equal number of up, down and strange quarks—has an equilibrium energy per nucleon that is lower than the mass of the nucleon or the energy per nucleon of the most bound nucleus, iron. In other words, under the hypothesis, strange quark matter is the *absolute* ground state of the strong interaction.

We customarily find that systems, if not in their ground state, readily decay to it. Of course this is not always so. Even in well known objects like nuclei, there are certain excited states whose structure is such that the transition to the ground state is hindered. The first excited state of ^{180}Ta has a half-life of 10^{15} years, five orders of magnitude longer than the age of the universe! We will discuss why the strange-matter hypothesis is consistent with the present universe—a long-lived excited state—if strange matter is the ground state. The structure of strange stars is fascinating as are some of their properties. Special attention is placed on what sort of observation on pulsars would count as a virtually irrefutable proof of the strange-matter hypothesis.

2

General Relativity

"Scarcely anyone who fully comprehends this theory can escape its magic."
A. Einstein

"Beauty is truth, truth beauty–that is all
Ye know on earth, and all ye need to know."
J. Keats

General Relativity, Einstein's theory of gravitation and spacetime, is the most beautiful and elegant of physical theories. Not only is it a beautiful theory; it is the foundation for our understanding of compact stars. Neutron stars and black holes owe their very existence to gravity as formulated by Einstein [2, 3]. Dense objects like neutron stars could also exist in Newton's theory, but they would be very different objects. Chandrasekhar found (in connection with white dwarfs) that all degenerate stars have a maximum possible mass. In Newton's theory such a maximum mass is attained asymptotically when all fermions whose pressure supports the star are ultrarelativistic. Under such conditions stars populated by heavy quarks would exist. Such unphysical stars do not occur in Einstein's theory.[1]

Perhaps the beauty of Einstein's theory can be attributed to the essentially simple answer it provides to a fundamental question: what meaning is attached to the absolute equality of inertial and gravitational masses? If all bodies move in gravitational fields in precisely the same way, no matter what their constitution or binding forces, then does this not mean that their motion has nothing to do with their nature but rather with the nature of spacetime? And if spacetime determines the motion of bodies, then according to the notion of action and reaction, does this not imply that spacetime in turn is shaped by bodies whose motion and form it determines?

Beautiful or not, the predictions of theory have to be tested. The first three tests of General Relativity were proposed by Einstein, the gravitational redshift, the deflection of light by massive bodies and the perihelion shift of Mercury. The latter had already been measured. Einstein computed

[1] See Section 8.5.

the anomalous part of the precession to be 43 arcseconds per century compared to the measurement of 42.98 ± 0.04. A fourth test was suggested by Shapiro in 1964—the time delay in the radar echo of a signal sent to a planet whose orbit is carrying it toward superior conjunction[2] with the sun. Eventually agreement to 0.1 percent with the prediction of Einstein's theory was achieved in these difficult and remarkable experiments. It should be remarked that all of the above tests involved weak gravitational fields.

The crowning experimental achievement was the 20 year study by Taylor and his colleagues of the Hulse–Taylor pulsar binary discovered in 1974. Their work yielded a measurement of 4.22663 degrees per year for the periastron shift of the orbit of the neutron star binary and a measurement of the decay of the orbital period by $7.60 \pm 0.03 \times 10^{-7}$ seconds per year. This rate of decay agrees to less than 1 percent with careful calculations of the effect of loss of energy through gravitational radiation predicted by Einstein's theory [4]. A fuller discussion of these experiments and other intricacies involved in the tests of relativity can be found in [5].

2.1 Lorentz Invariance

The Special Theory of Relativity, which holds in the absence of gravity, plays a central role in physics; for even in the strongest gravitational fields the laws of physics must conform to it in a sufficiently small locality of any spacetime event. The Special Theory plays a central role even in the development of the General Theory of Relativity and its applications.

2.1.1 Lorentz transformations

The Lorentz transformation leaves invariant the *proper time* or *invariant interval* in Minkowski spacetime

$$d\tau^2 = dt^2 - dx^2 - dy^2 - dz^2, \qquad (\text{units } c = 1) \tag{2.1}$$

as measured by observers in frames moving with constant relative velocity. Historically, this invariant was associated with the observed invariance of the speed of light in vacuo [6]. This invariant is a local property of the spacetime continuum in which we live. Together with the constant c, it can in principle be verified without resort to propagation of light signals or any other dynamical means but with only measuring rods and clocks [7]. The constant c may be thought of as the conversion factor which gives time and distance the same dimension.

A *pure* Lorentz transformation is one without spatial rotation, while a general Lorentz transformation is the product of a rotation in space and a

[2]Superior conjunction refers to the situation when the earth and the planet are on opposite sides of the sun.

pure Lorentz transformation. We recall the pure transformation, sometimes also referred to as a *boost*. For convenience, define

$$x^0 = t, \quad x^1 = x, \quad x^2 = y, \quad x^3 = z\,. \tag{2.2}$$

(In spacetime a point such as above is sometimes referred to as an *event*.) The linear homogeneous transformation connecting two reference frames can be written

$$x'^\mu = \Lambda^\mu{}_\nu x^\nu\,. \tag{2.3}$$

(We shall use the convenient notation introduced by Einstein whereby repeated indices are summed—Greek over time and space, Roman over space.)

Any set of four quantities A^μ, $(\mu = 0, 1, 2, 3)$ that transforms under a change of reference frame in the same way as the coordinates is a *contravariant* Lorentz four-vector,

$$A'^\mu = \Lambda^\mu{}_\nu A^\nu\,. \tag{2.4}$$

The invariant interval (also variously called the proper time, the line element, or the separation formula) can be written

$$d\tau^2 = \eta_{\mu\nu}\, dx^\mu\, dx^\nu\,, \tag{2.5}$$

where $\eta_{\mu\nu}$ is the Minkowski metric (sometimes also referred to as Galilean) which in rectilinear coordinates is

$$\eta_{\mu\nu} \equiv \begin{pmatrix} 1 & 0 & 0 & 0 \\ 0 & -1 & 0 & 0 \\ 0 & 0 & -1 & 0 \\ 0 & 0 & 0 & -1 \end{pmatrix}. \tag{2.6}$$

The condition of the invariance of $d\tau^2$ is

$$\eta_{\alpha\beta}\, dx^\alpha\, dx^\beta = \eta_{\mu\nu}\, dx'^\mu\, dx'^\nu = \eta_{\mu\nu}\Lambda^\mu{}_\alpha \Lambda^\nu{}_\beta\, dx^\alpha\, dx^\beta\,. \tag{2.7}$$

Since this holds for any dx^α, dx^β we conclude that the $\Lambda^\mu{}_\nu$ must satisfy the fundamental relationship assuring invariance of the proper time:

$$\eta_{\alpha\beta} = \eta_{\mu\nu}\Lambda^\mu{}_\alpha \Lambda^\nu{}_\beta\,. \tag{2.8}$$

For the special case of a boost along the x-axis arranged so that the origins of the two frames in uniform motion coincide at $t = 0$ and the primed x-axis x'^1 is moving along x^1 with velocity v we obtain,

$$\begin{aligned} \Lambda^0{}_0 &= \Lambda^1{}_1 = \gamma\,, \\ \Lambda^1{}_0 &= \Lambda^0{}_1 = -v\gamma\,, \\ \Lambda^2{}_2 &= \Lambda^3{}_3 = 1\,, \end{aligned} \tag{2.9}$$

where

$$\gamma \equiv (1 - v^2)^{-1/2} . \tag{2.10}$$

A boost in an arbitrary direction with the primed axis having velocity $\boldsymbol{v} = (v^1, v^2, v^3)$ relative to the unprimed is

$$\begin{aligned} \Lambda^0{}_0 &= \gamma , \\ \Lambda^0{}_j &= \Lambda^j{}_0 = -v^j \gamma , \\ \Lambda^j{}_k &= \Lambda^k{}_j = \delta^j_k + (\gamma - 1) v^j v^k / \boldsymbol{v}^2 . \end{aligned} \tag{2.11}$$

2.1.2 Covariant vectors

Two contravariant Lorentz vectors such as

$$A^\mu \equiv (A^0, A^1, A^2, A^3) \tag{2.12}$$

and B^μ may be used to create a *scalar* product (Lorentz scalar)

$$A' \cdot B' \equiv \eta_{\mu\nu} A'^\mu B'^\nu = \eta_{\mu\nu} \Lambda^\mu{}_\alpha \Lambda^\nu{}_\beta A^\alpha B^\beta = \eta_{\alpha\beta} A^\alpha B^\beta \equiv A \cdot B . \tag{2.13}$$

Because of the minus signs in the Minkowski metric we have

$$A \cdot B = A^0 B^0 - \boldsymbol{A} \cdot \boldsymbol{B} , \tag{2.14}$$

and the *covariant* Lorentz vector is defined by

$$A_\mu \equiv (A^0, -A^1, -A^2, -A^3) . \tag{2.15}$$

A *covariant* Lorentz vector is obtained from its contravariant dual by the process of lowering indices with the metric tensor,

$$A_\mu = \eta_{\mu\nu} A^\nu . \tag{2.16}$$

Conversely, raising of indices is achieved by

$$A^\mu = \eta^{\mu\nu} A_\nu . \tag{2.17}$$

It is straightforward to show that

$$\eta^{\mu\alpha} \eta_{\alpha\nu} \equiv \eta^\mu_\nu = \delta^\mu_\nu , \tag{2.18}$$

where δ^μ_ν is the Kroneker delta. It follows that

$$\eta_{\mu\nu} = \eta^{\mu\nu} . \tag{2.19}$$

The Lorentz transformation for a covariant vector is written in analogy with that of a contravariant vector:

$$A'_\mu = \Lambda_\mu{}^\nu A_\nu . \tag{2.20}$$

To obtain the elements of $\Lambda_\mu{}^\nu$ we write the above in two different ways,

$$\eta_{\mu\beta}\Lambda^\beta{}_\alpha A^\alpha = \eta_{\mu\beta}A'^\beta = A'_\mu = \Lambda_\mu{}^\nu A_\nu = \Lambda_\mu{}^\nu \eta_{\nu\alpha}A^\alpha \,. \tag{2.21}$$

This holds for arbitrary A^μ so

$$\Lambda_\mu{}^\nu = \eta_{\mu\alpha}\Lambda^\alpha{}_\beta \eta^{\beta\nu} \,. \tag{2.22}$$

Using (2.18) in the above we get the inverse relationship

$$\Lambda^\mu{}_\nu = \eta^{\mu\alpha}\Lambda_\alpha{}^\beta \eta_{\beta\nu} \,. \tag{2.23}$$

Multiplying (2.22) by $A^\mu{}_\sigma$, summing on μ, and employing the fundamental condition of invariance of the proper time (2.8) we find

$$\Lambda^\mu{}_\sigma \Lambda_\mu{}^\tau = \delta^\tau_\sigma \,. \tag{2.24}$$

We can now invert (2.3) and find that $\Lambda_\mu{}^\nu$ is the inverse Lorentz transformation,

$$x^\mu = \Lambda_\nu{}^\mu x'^\nu \,. \tag{2.25}$$

The elements of the inverse transformation are given in terms of (2.9) or (2.11) by (2.22). We have

$$\begin{aligned} \Lambda_0{}^0 &= \Lambda_1{}^1 = \gamma \,, \\ \Lambda_1{}^0 &= \Lambda_0{}^1 = v\gamma \,, \\ \Lambda_2{}^2 &= \Lambda_3{}^3 = 1 \,. \end{aligned} \tag{2.26}$$

A boost in an arbitrary direction with the primed axis having velocity $\boldsymbol{v} = (v^1, v^2, v^3)$ relative to the unprimed is

$$\begin{aligned} \Lambda_0{}^0 &= \gamma \,, \\ \Lambda_0{}^j &= \Lambda_j{}^0 = v^j\gamma \,, \\ \Lambda_j{}^k &= \Lambda_k{}^j = \delta^j_k + (\gamma - 1)v^j v^k/\boldsymbol{v}^2 \,. \end{aligned} \tag{2.27}$$

The *four-velocity* is a vector of particular interest and defined as

$$u^\mu = \frac{dx^\mu}{d\tau} \,. \tag{2.28}$$

Since $d\tau$ is an invariant scalar and dx^μ is a vector, u^μ is obviously a contravariant vector. From the expression for the invariant interval we have

$$d\tau = \sqrt{1 - \boldsymbol{v}^2}\, dt, \qquad \boldsymbol{v} \equiv \frac{d\boldsymbol{r}}{dt} \,, \tag{2.29}$$

with $\boldsymbol{r} = (x^1, x^2, x^3)$; it therefore follows that

$$u^0 \equiv \frac{dt}{d\tau} = \gamma, \qquad u^i \equiv \frac{dx^i}{d\tau} = \frac{dx^i}{dt}\frac{dt}{d\tau} = v^i\gamma \,, \tag{2.30}$$

or

$$u^\mu = \gamma(1, v^1, v^2, v^3), \qquad u_\mu = \gamma(1, -v^1, -v^2, -v^3), \qquad u^\mu u_\mu = 1\,. \quad (2.31)$$

The transformation of a tensor under a Lorentz transformation follows from (2.4) and (2.20) according to the position of the indices; for example,

$$T'^{\mu\nu} = \Lambda^\mu{}_\alpha \Lambda^\nu{}_\beta T^{\alpha\beta}\,. \quad (2.32)$$

We note that according to (2.8), the Minkowski metric $\eta^{\mu\nu}$ is a tensor; moreover it has the same constant form in every Lorentz frame.

2.1.3 Energy-momentum tensor of a perfect fluid

A perfect fluid is a medium in which the pressure is isotropic in the rest frame of each fluid element, and shear stresses and heat transport are absent. If at a certain point the velocity of the fluid is $\boldsymbol{v}$, an observer with this velocity will observe the fluid in the neighborhood as isotropic with an energy density ϵ and pressure p. In this local frame the energy-momentum tensor is

$$T'^{\mu\nu} \equiv \begin{pmatrix} \epsilon & 0 & 0 & 0 \\ 0 & p & 0 & 0 \\ 0 & 0 & p & 0 \\ 0 & 0 & 0 & p \end{pmatrix}. \quad (2.33)$$

As viewed from an arbitrary frame, say the laboratory system, let this fluid element be observed to have velocity $\boldsymbol{v}$. According to (2.25) we obtain the transformation

$$T^{\mu\nu} = \Lambda_\alpha{}^\mu \Lambda_\beta{}^\nu T'^{\alpha\beta}\,. \quad (2.34)$$

The elements of the transformation are given by (2.26) in the case that the fluid element is moving with velocity v along the laboratory x-axis, or by (2.27) if it has the general velocity $\boldsymbol{v}$. It is easy to check that in the arbitrary frame

$$T^{\mu\nu} = -p\eta^{\mu\nu} + (p+\epsilon)u^\mu u^\nu \quad (2.35)$$

and reduces to the diagonal form above when $\boldsymbol{v} = 0$. We have used the four-velocity defined above by (2.30). Relative to the laboratory frame it is the four-velocity of the fluid element.

2.1.4 Light cone

For vanishing proper time intervals, $d\tau = 0$ given by (2.1) is the equation of a double cone in the four-dimensional space x^μ with the time axis as

the axis of the cone. Events separated from the vertex event for which the proper time, (or invariant interval) vanishes ($d\tau = 0$), are said to have null separation. They can be connected to the event at the vertex by a light signal. Events separated from the vertex by a real interval $d\tau^2 > 0$ can be connected by a subluminal signal—a material particle can travel from one event to the other. An event for which $d\tau^2 < 0$ refers to an event outside the two cones; a light signal cannot join the vertex event to such an event. Therefore, events in the cone with t greater than that of the vertex of the cone lie in the future of the event at the vertex, while events in the other cone lie in its past. Events lying outside the cone are not causally connected to the vertex event.

2.2 Scalars, Vectors, and Tensors in Curvilinear Coordinates

In the last section we dealt with inertial frames of reference in flat spacetime. We now wish to allow for curvilinear coordinates. Our scalars, vectors, and tensors now refer to a point in spacetime. Their components refer to the reference frame at that point.

A scalar field $S(x)$ is a function of position, but its value does not depend on the coordinate system. An example is the temperature as registered on thermometers located in various rooms in a house. Each registered temperature may be different, and therefore a function of position, but independent of the coordinates used to specify the locations:

$$S'(x') = S(x). \tag{2.36}$$

A vector is a quantity whose components change under a coordinate transformation. One important vector is the displacement vector between adjacent points. Near the point x^μ we consider another, $x^\mu + dx^\mu$. The four displacements dx^μ are the components of a vector. Choose units so that time and distance are measured in the same units ($c = 1$). In Cartesian coordinates we can write the *invariant interval* $d\tau$ of the Special Theory of Relativity sometimes called the *proper time* as

$$d\tau^2 = (dx^0)^2 - (dx^1)^2 - (dx^2)^2 - (dx^3)^2. \tag{2.37}$$

Under a coordinate transformation from these rectilinear coordinates to arbitrary coordinates, $x^\mu \to x'^\mu$, we have (from the rules of partial differentiation)

$$dx'^\mu = \frac{\partial x'^\mu}{\partial x^\nu} dx^\nu. \tag{2.38}$$

As before, repeated indices are summed. We can as well write the inverse of the above equation and substitute for the spacetime differentials in the

invariant interval to obtain an equation of the form

$$d\tau^2 = g_{\mu\nu} dx^\mu dx^\nu \,, \tag{2.39}$$

where the $g_{\mu\nu}$ are defined in terms of products of the partial derivatives of the coordinate transformation.

Depending on the nature of the coordinate system, say rectilinear, oblique, or curvilinear, or on the presence of a gravitational field, the invariant interval may involve bilinear products of different dx^μ, and the $g_{\mu\nu}$ will be functions of position and time. They are field quantities—the components of a tensor called the *metric tensor*. Since $g_{\mu\nu}$ appear in a quadratic form (2.39), we may take them to be symmetric:

$$g_{\mu\nu} = g_{\nu\mu} \,. \tag{2.40}$$

In the rectilinear system of the Special Theory of Relativity in which the invariant interval was expressed in (2.37), the metric tensor $g_{\mu\nu}$ is equal to the Minkowski tensor (2.6) which is a constant and diagonal. It is appropriate for the flat spacetime of the special theory and holds locally anywhere at any time. We shall refer to reference frames in which the metric is given by the Minkowski tensor as *Lorentz frames*.

The invariant interval $d\tau$ is real for a timelike interval and imaginary for a spacelike[3]. The connotation *proper time* is seen to be appropriate because, when two events occur at the same *space* point, what remains of the invariant interval is dt.

Any four quantities A^μ that transform as dx^μ is a *contravariant vector*

$$A'^\mu = \frac{\partial x'^\mu}{\partial x^\nu} A^\nu \,, \tag{2.41}$$

and

$$g_{\mu\nu} A^\mu A^\nu \equiv A^2 \tag{2.42}$$

is its invariant squared length. It is obviously invariant under the same transformations that leave (2.37) invariant because the four quantities A^μ form a four-vector like dx^μ.

A covariant vector can be obtained through the process of *lowering* indices with the metric tensor:

$$A_\mu = g_{\mu\nu} A^\nu \,. \tag{2.43}$$

In terms of this vector, the magnitude equation (2.42) can be written

$$A_\mu A^\mu = A^2 \,. \tag{2.44}$$

[3]The opposite convention $ds^2 = -d\tau^2$ could also be employed. It is often referred to as the line element.

Let A^μ and B^μ be distinct contravariant vectors. Then so is $A^\mu + \lambda B^\mu$ for all finite λ. The quantity

$$g_{\mu\nu}\big(A^\mu + \lambda B^\mu\big)\big(A^\nu + \lambda B^\nu\big)$$

is the invariant squared length. Since this is true for all λ, the coefficient of each power of λ is also an invariant, in particular the coefficient of λ,

$$g_{\mu\nu}\big(A^\mu B^\nu + B^\mu A^\nu\big) = 2g_{\mu\nu}A^\mu B^\nu\,, \tag{2.45}$$

where we have used the symmetry of $g_{\mu\nu}$. Thus, we obtain the invariant scalar product of two vectors:

$$g_{\mu\nu}A^\mu B^\nu = A_\nu B^\nu = A\cdot B\ . \tag{2.46}$$

To derive the transformation law for a covariant vector use the fact, just proven, that $A_\mu B^\mu$ is a scalar. Then using the law of transformation of a contravariant vector (2.41), we have

$$A'_\mu B'^\mu = A_\alpha B^\alpha = A_\alpha \frac{\partial x^\alpha}{\partial x'^\mu} B'^\mu\ , \tag{2.47}$$

where A'_μ is the same vector as A_μ but referred to the primed reference frame. From the above equation it follows that

$$\big(A'_\mu - \frac{\partial x^\alpha}{\partial x'^\mu} A_\alpha\big) B'^\mu = 0\,. \tag{2.48}$$

Since B^μ is any vector, the quantity in brackets must vanish, so we have the law of transformation of a covariant vector,

$$A'_\mu = \frac{\partial x^\nu}{\partial x'^\mu} A_\nu\,. \tag{2.49}$$

Compare this transformation law with that of (2.41).

Let the determinant of $g_{\mu\nu}$ be g,

$$g = \det|g_{\mu\nu}|\,. \tag{2.50}$$

As long as g does not vanish, the equations (2.43) can be inverted. Let the coefficients of the inverse be called $g^{\mu\nu}$. Then find

$$A^\nu = g^{\nu\mu}A_\mu\,. \tag{2.51}$$

Multiply (2.43) by $g^{\alpha\mu}$ and sum on μ with the result

$$A^\alpha = g^{\alpha\mu}A_\mu = g^{\alpha\mu}g_{\mu\nu}A^\nu\,, \tag{2.52}$$

or

$$(g^{\alpha\mu}g_{\mu\nu} - \delta^\alpha_\nu)A^\nu = 0\ , \tag{2.53}$$

where δ^α_ν is the Kroneker delta. Since this equation holds for any vector, we have

$$g^\alpha_\beta \equiv g^{\alpha\mu} g_{\mu\beta} = \delta^\alpha_\beta \,. \tag{2.54}$$

The two g's, one with subscripts, the other with superscripts, are inverses. In the same way as $g_{\mu\nu}$ can be used to lower an index, $g^{\mu\nu}$ can be used to raise one. Both are symmetric;

$$g_{\mu\nu} = g_{\nu\mu}, \qquad g^{\mu\nu} = g^{\nu\mu} \,. \tag{2.55}$$

The derivative of a scalar field $S(x) = S'(x')$ is a vector field,

$$\frac{\partial S}{\partial x'^\mu} = \frac{\partial x^\nu}{\partial x'^\mu} \frac{\partial S}{\partial x^\nu} \,, \tag{2.56}$$

since it obeys the rules for transformation of a covariant vector, that is, differentiation of a scalar field with respect to the components of a contravariant position vector yields a covariant vector field and vice versa. Accordingly, we shall sometimes use the abbreviations

$$\partial_\mu \equiv \frac{\partial}{\partial x^\mu}, \qquad \partial^\mu \equiv \frac{\partial}{\partial x_\mu} \tag{2.57}$$

especially in writing Lagrangians of fields. In relativity it is also useful to have an even more compact notation for the coordinate derivative—the 'comma subscript':

$$S_{,\mu} \equiv \frac{\partial S}{\partial x^\mu} \,. \tag{2.58}$$

Tensors are similar to vectors but with more than one index. A simple tensor is one formed from the product of the components of two vectors, $A^\mu B^\nu$. But this is special because of the relationships between its components. A general tensor of the second rank can be formed by a sum of such products:

$$T^{\mu\nu} = A^\mu B^\nu + C^\mu D^\nu + \cdots \,. \tag{2.59}$$

The superscripts can be lowered as with a vector, either one index, or both,

$$T_\mu{}^\nu = g_{\mu\alpha} T^{\alpha\nu} \,, \qquad T^\nu_{\ \mu} = T^{\nu\alpha} g_{\alpha\mu} \,, \qquad T_{\mu\nu} = g_{\mu\alpha} g_{\nu\beta} T^{\alpha\beta} \,. \tag{2.60}$$

Similarly we may have tensors of higher rank, either contravariant with respect to all indices, or covariant, or mixed. The position of the indices on the mixed tensor (the lower to the left or right of the upper) refers to the position of the index that was lowered. If $T^{\mu\nu}$ is symmetric, then $T^\mu_{\ \nu} = T_\nu{}^\mu$ and it is unimportant to keep track of the position of the index

that has been lowered (or raised). But if $T^{\mu\nu}$ is antisymmetric, then the two orderings differ by a sign.

If two of the indices on a tensor, one a superscript the other a subscript, are set equal and summed, the rank is reduced by two. This process is called *contraction*. If it is done on a second rank mixed tensor, the result is a scalar,

$$S = T^{\mu}_{\ \mu} = T_{\mu}^{\ \mu}. \tag{2.61}$$

When $T^{\mu\nu}$ is antisymmetric, the contractions $T_{\mu}^{\ \mu}$ and $T^{\mu}_{\ \mu}$ are identically zero.

The test of tensor character is whether the object in question transforms under a coordinate transformation in the obvious generalization of a vector. For example,

$$T'^{\mu}_{\ \nu} = \frac{\partial x'^{\mu}}{\partial x^{\alpha}} \frac{\partial x^{\beta}}{\partial x'^{\nu}} T^{\alpha}_{\ \beta} \tag{2.62}$$

is a tensor.

In general we deal with curved spacetime in General Relativity. We must therefore deal with curvilinear coordinates. Vectors and tensors at a point in such a spacetime have components referring to the axis at that point. The components will change according to the above laws, depending on the way the axes change at that point. Therefore, the metric tensors $g_{\mu\nu}, g^{\mu\nu}$ cannot be constants. They are field quantities which vary from point to point. As we shall see, they can be referred to collectively as the gravitational field. Since the formalism of this section is expressed by local equations, it holds in curved spacetime; for curved spacetime is flat in a sufficiently small locality.

Because the derivative of a scalar field is a vector (2.56), one might have thought that the derivative of a vector field is a tensor. However by checking the transformation properties one finds that this supposition is not true.

We have referred invariably to the $g_{\mu\nu}$ as tensors. Now we show that this is so. Let A^{μ}, B^{ν} be arbitrary vector fields, and consider two coordinate systems such that the same point P has the coordinates x^{μ} and x'^{μ} when referred to the two systems respectively. Then we have

$$g'_{\alpha\beta} A'^{\alpha} A'^{\beta} = g_{\mu\nu} A^{\mu} A^{\nu} = g_{\mu\nu} \frac{\partial x^{\mu}}{\partial x'^{\alpha}} \frac{\partial x^{\nu}}{\partial x'^{\beta}} A'^{\alpha} A'^{\beta}. \tag{2.63}$$

Because this holds for arbitrary vectors, we have

$$g'_{\alpha\beta} = g_{\mu\nu} \frac{\partial x^{\mu}}{\partial x'^{\alpha}} \frac{\partial x^{\nu}}{\partial x'^{\beta}} \ , \tag{2.64}$$

which, by comparison with (2.49), shows that $g_{\mu\nu}$ is a covariant tensor. Similarly $g^{\mu\nu}$ is a contravariant tensor:

$$g'^{\alpha\beta} = g^{\mu\nu} \frac{\partial x'^{\alpha}}{\partial x^{\mu}} \frac{\partial x'^{\beta}}{\partial x^{\nu}} \ . \tag{2.65}$$

These are called the *fundamental tensors*. Of course the above tensor character of the metric is precisely what is required to make the square of the interval $d\tau^2$ of (2.39) an invariant, as is trivially verified.

Mixed tensors of arbitrary rank transform, for each index, according to the transformation laws (2.41, 2.49) depending on whether the index is a superscript or a subscript, as can be derived in obvious analogy to the above manipulations.

Tensors and tensor algebra are very powerful techniques for carrying the consequences discovered in one frame to another. That the linear combination of tensors of the same rank and arrangement of upper and lower indices is also a tensor, that the direct product of two tensors of the same or different rank and arrangement of indices, $A^{\mu\cdots}_{\alpha\cdots}B^{\nu\cdots}_{\cdots} = T^{\mu\cdots\nu\cdots}_{\alpha\cdots}$ is also a tensor, that contraction (defined above) of a pair of indices, one upper, one lower produces a tensor of rank reduced by two, are all easy theorems that we do not need to prove, but only note in passing. Of particular note, if the difference of two tensors of the same transformation rule vanishes in one frame, then it vanishes in all, i.e., the two tensors are equal in all frames.

2.3 Principle of Equivalence of Inertia and Gravitation

> "The possibility of explaining the numerical equality of inertia and gravitation by the unity of their nature gives to the general theory of relativity, according to my conviction, such a superiority over the conceptions of classical mechanics, that all the difficulties encountered in development must be considered as small in comparison." *A. Einstein* [3]

Eötvös established that all bodies have the same ratio of inertial to gravitational mass with high precision [8]. With an appropriate choice of units, the two masses are equal for all bodies to the accuracy established for the ratio. One might have expected such conceptually different properties, one having to do with inertia to motion (m_I), the other with 'charge' (m_G), in an expression of mutual attraction between bodies, to be entirely different. The relation between the force exerted by the gravitational attraction of a body of mass M at a distance R upon the object, and the acceleration imparted to it are expressed by Newton's equation, valid for weak fields and small material velocities:

$$m_I a = G\frac{m_G M}{R^2}\,. \tag{2.66}$$

Einstein reasoned that the near equality of two such different properties must be more than mere coincidence and that inertial and gravitational masses must be exactly equal: $m_I = m_G = m$. The mass drops out! In that

case all bodies experience precisely the same acceleration in a gravitational field, as was presaged by Galileo's experiments centuries earlier. For all other forces that we know, the acceleration is inverse to the mass.

The equivalence of inertial and gravitational mass is established to high accuracy for atomic and nuclear binding energies[4]. As well, as a result of very careful lunar laser-ranging experiments, the earth and moon are found to fall with equal acceleration toward the sun to a precision of almost 1 part in 10^{13}, better than the most accurate Eötvös type experiments on laboratory bodies. This exceedingly important test involving bodies of relatively different gravitational binding was conceived by Nordtvedt [9]. The essentially null result establishes the so-called *strong* statement of equivalence of inertial and gravitational mass: Free bodies—no matter their nature or constituents, nor how much or little those constituents are bound, nor by what force—all move in the spacetime of an arbitrary gravitational field as if they were identical test particles! *Since their motion has nothing to do with their nature, it evidently has to do with the nature of spacetime.*

Einstein felt certain a deep meaning was attached to the equivalence, and his conviction led him to the formulation of the *equivalence principle.* The equivalence principle provides the link between the physical laws as we discern them in our laboratories and their form under any circumstance in the universe, more precisely, in arbitrarily strong and varying gravitational fields. It also provides a tool for the development of the theory of gravitation itself as we shall see throughout the sequel.

The universe is populated by massive objects moving relative to one another. The gravitational field may be arbitrarily changing in time and space. However, the presence of gravity cannot be detected in a sufficiently small reference frame falling freely with a particle under no influence other than gravity. The particle will remain at rest in such a frame. It is a *local inertial frame.* A local inertial frame and a *local Lorentz frame* are synonymous. The laws of Special Relativity hold in inertial frames and therefore in the neighborhood of a *freely falling frame.*

Associated with a given spacetime event there are an infinity of locally inertial frames related by Lorentz transformations. All are equivalent for the description of physical phenomena in a sufficiently small region of spacetime. So we arrive at a statement of the equivalence principle: *At every spacetime point in an arbitrary gravitational field (meaning anytime and anywhere in the universe), a local inertial (Lorentz) frame can be chosen so that the laws of physics take on the form they have in Special Relativity.* This is the meaning of the equality of inertial and gravitational masses that Einstein sought. The restricted validity of inertial frames to small localities of any event suggested the very fruitful analogy with local flatness on a

[4]Eötvös' experiments on such diverse media as wood, platinum, copper, glass, and others involve different molecular, atomic, and nuclear binding energies and different ratios of neutrons and protons.

curved surface.

The equivalence principle has great power. It is the instrument by which all the special relativistic laws of physics—valid in a gravity-free universe—can be generalized to a gravity-filled universe. We shall see how Einstein was able to give dynamic meaning to the spacetime continuum as an integral part of the physical world quite distinct from the conception of an absolute spacetime in which the rest of physical processes take place.

2.3.1 Photon in a gravitational field

Employing the conservation of energy and Newtonian physics, Einstein reasoned that the gravitational field acts on photons. Let a photon be emitted from z_1 vertically to z_2, and only for simplicity, let the field be uniform. A device located at z_2 converts its energy on arrival to a particle of mass m with perfect efficiency. The particle drops to z_1 where its energy is now $m + mgh$, where g is the acceleration due to the uniform field. A device at z_1 converts it into a photon of the same energy as possessed by the particle. The photon again is directed to z_2. If the original (and each succeeding photon) does not lose energy $(h\nu)gh$ in climbing the gravitational field equal to the energy gained in dropping in the field, we would have a device that creates energy. By the law of conservation of energy Einstein discovered the gravitational redshift, commonly designated by the factor z and equal in this case to gh. The shift in energy of a photon by falling (in this case blue shifted) in the earth's gravitational field has been directly confirmed in an experiment performed by Pound and Rebka [10].

In the above discussion the equivalence principle entered when the photon's inertial mass $(h\nu)$ was used also as its gravitational mass in computing the gravitational work. One can also see the role of the equivalence principle by considering a pulse of light emitted over a distance h along the axis of a spaceship in uniform acceleration g in outer space. The time taken for the light to reach the detector is $t = h$ (we use units $G = c = 1$). The difference in velocity of the detector acquired during the light travel time is $v = gt = gh$, the Doppler shift z in the detected light. This experiment, carried out in the gravity-free environment of a spaceship whose rockets produce an acceleration g, must yield the same result for the energy shift of the photon in a uniform gravitational field g according to the equivalence principle. The Pound–Rebka experiment can therefore be regarded as an experimental proof of the equivalence principle.

We may regard a radiating atom as a clock, with each wave crest regarded as a tick of the clock. Imagine two identical atoms situated one at some height above the other in the gravitational field of the earth. Since, by dropping in the gravitational field, the light is blue shifted when compared to the radiation of an identical atom (clock) at the bottom, the clock at the top is seen to be running faster than the one at the bottom. Therefore identical clocks, stationary with respect to the earth, run at different rates

according to their different heights above the earth. Time flows at different rates in different gravitational fields.

The trajectory of photons is also bent by the gravitational field. Imagine a freely falling elevator in a constant gravitational field. Its walls constitute an inertial frame as guaranteed by the equivalence principle. Therefore, a photon (as for a free particle) directed from one wall to the opposite along a path parallel to the floor will arrive at the other wall at the same height from which it started. But relative to the earth, the elevator has fallen during the traversal time. Therefore the photon has been deflected toward the earth and follows a curved path as observed from a frame fixed on the earth.

2.3.2 Tidal gravity

Einstein predicted that a clock near a massive body would run more slowly than an identical distant clock. In doing so he arrived at a hint of the deep connection of the structure of spacetime and gravity. Two parallel straight lines never meet in the gravity-free, flat spacetime of Minkowski. A single inertial frame would suffice to describe all of spacetime. In formulating the equivalence principle (knowing that gravitational fields are not uniform and constant but depend on the motion of gravitating bodies and the position where gravitational effects are experienced), Einstein understood that only in a suitably small locality of spacetime do the laws of Special Relativity hold. Gravitational effects will be observed on a larger scale. *Tidal gravity* refers to the deviation from uniformity of the gravitational field at nearby points.

These considerations led Einstein to the notion of spacetime curvature. Whatever the motion of a free body in an arbitrary gravitational field, it will follow a straight line trajectory over any small locality as guaranteed by the equivalence principle. And in a gravity-endowed universe, free particles whose trajectories are parallel in a local inertial frame, will not remain parallel over a large region of spacetime. This has a striking analogy with the surface of a sphere on which two straight lines that are parallel over a small region do meet and cross. What if in fact the particles are freely falling in curved spacetime? In this way of thinking, the law that free particles move in straight lines remains true in an arbitrary gravitational field, thus obeying the principle of relativity in a larger sense. Any sufficiently small region of curved spacetime is locally flat. The paths in curved spacetime that have the property of being locally straight are called geodesics.

2.3.3 Curvature of spacetime

Let us now consider a thought experiment. Two nearby bodies released from rest above the earth follow parallel trajectories over a small region of their trajectories, as we know from the equivalence principle. (Any small

spacetime region is inertial.) But if holes were drilled in the earth through which the bodies could fall, the bodies would meet and cross at the earth's center. So there is clearly no single Minkowski spacetime that covers a large region or the whole region containing a massive body.

Einstein's view was that spacetime curvature caused the bodies to cross, bodies that in this curved spacetime were following straight line paths in every small locality, just as they would have done in the whole of Minkowski (flat) spacetime in the absence of gravitational bodies. The presence of gravitating bodies denies the existence of a global inertial frame. Spacetime can be flat everywhere only if there exists such a global frame. Hence, spacetime is curved by massive bodies. In their presence a test particle follows a geodesic path, one that is always locally straight. The concept of a "gravitational force" has been replaced by the curvature of spacetime, and the natural free motions of particles in it are defined by geodesics.

2.3.4 Energy conservation and curvature

Interestingly, the conservation of energy can also be used to inform us that spacetime is curved. Consider a static gravitational field. Let us conjecture that spacetime is flat so that the Minkowski metric holds; we will arrive at a contradiction.

Imagine the following experiment performed by observers and their apparatus at rest with respect to the gravitational field and their chosen Lorentz frame in the supposed flat spacetime of Minkowski. At a height z_1 in the field, let a monochromatic light signal be emitted upward a height h to $z_2 = z_1 + h$. Let the pulse be emitted for a specific time dt_1 during which N wavelengths (or photons) are emitted. Let the time during which they are received at z_2 be measured as dt_2. (Since the spacetime is assumed to be described by the Minkowski metric and the source and receiver are at rest in the chosen frame, the proper times and coordinate times are equal.)

Since the field in the above experiment is static, the path in the $z-t$ plane will have the same shape for both the beginning and ending of the pulse (as for each photon) as they trace their path in the Minkowski space we postulate to hold. The trajectories will not be straight lines at 45 degrees because of the field, but the curved paths will be congruent; a translation in time will make the paths lie one upon the other. Therefore $d\tau_2 = dt_2 = dt_1 = d\tau_1$ will be measured at the stationary detector if spacetime is Minkowskian. In this case, the frequency (and hence the energy received at z_2) is the same as that sent from z_1. But this cannot be. The photons comprising the signal must loose energy in climbing the gravitational field (Section 2.3.1).

The conjecture that spacetime in the presence of a gravitational field is Minkowskian must therefore be false. We conclude that the presence of the gravitational field has caused spacetime to be curved. Such a line of reasoning was first conceived by Schild [11, 12, 13].

2.4 Gravity

Massive bodies generate curvature, and since the galaxies, stars and other bodies are in motion, the curvature of spacetime is everywhere changing. For this reason there is no "prior geometry". There are no immutable reference frames to which events in spacetime can be referred. Indeed, the changing geometry of spacetime and of the motion and arrangement of mass-energy in spacetime are inseparable parts of the description of physical processes. This is a very different idea of space and time from that of Newton and even of the Special Theory of Relativity. We now take up the unified discussion of gravitating matter and motion.

The power of the equivalence principle in informing us so simply as above that spacetime must be curved by the presence of massive bodies in the universe suggests a fruitful way of beginning. Following Weinberg [14], we seek the connection between an arbitrary reference frame and a reference frame that is freely falling with a particle that is moving only under the influence of an arbitrary gravitational field. In this freely falling and therefore locally inertial frame, the particle moves in a straight line. Denote the coordinates by ξ^α. The equations of motion are

$$\frac{d^2\xi^\alpha}{d\tau^2} = 0 \,, \tag{2.67}$$

and the invariant interval (or proper time) between two neighboring spacetime events expressed in this frame, from (2.5), is

$$d\tau^2 = \eta_{\alpha\beta} d\xi^\alpha d\xi^\beta \,. \tag{2.68}$$

The freely falling coordinates may be regarded as functions of the coordinates x^μ of any arbitrary reference frame—curvilinear, accelerated, or rotating. We seek the connection between the equations of motion in the freely falling frame and the arbitrary one which might, for example, be the laboratory frame. From the chain rule for differentiation we can rewrite (2.67) as

$$\begin{aligned} 0 &= \frac{d}{d\tau}\left(\frac{\partial\xi^\alpha}{\partial x^\mu}\frac{dx^\mu}{d\tau}\right) \\ &= \frac{\partial\xi^\alpha}{\partial x^\mu}\frac{d^2x^\mu}{d\tau^2} + \frac{\partial^2\xi^\alpha}{\partial x^\mu \partial x^\nu}\frac{dx^\mu}{d\tau}\frac{dx^\nu}{d\tau} \,. \end{aligned}$$

Multiply by $\partial x^\lambda/\partial\xi^\alpha$, and use the chain rule again to obtain

$$\frac{dx^\lambda}{dx^\mu} = \frac{\partial x^\lambda}{\partial\xi^\alpha}\frac{\partial\xi^\alpha}{\partial x^\mu} = \delta^\lambda_\mu \,. \tag{2.69}$$

The equation of motion of the particle in an arbitrary frame when the particle is moving in an arbitrary gravitational field therefore is

$$\frac{d^2x^\lambda}{d\tau^2} + \Gamma^\lambda_{\mu\nu}\frac{dx^\mu}{d\tau}\frac{dx^\nu}{d\tau} = 0 \,. \tag{2.70}$$

Here $\Gamma^{\lambda}_{\mu\nu}$ defined by

$$\Gamma^{\lambda}_{\mu\nu} \equiv \frac{\partial x^{\lambda}}{\partial \xi^{\alpha}} \frac{\partial^2 \xi^{\alpha}}{\partial x^{\mu} \partial x^{\nu}} \tag{2.71}$$

is called the *affine connection*. The affine connection is symmetric in its lower indices.

The path defined by equation (2.70) is called a *geodesic*, the extremal path in the spacetime of an arbitrary gravitational field. We do not see here that it is an extremal, but this is hinted at inasmuch as it defines the same path of (2.67), the straight line path of a free particle as observed from its freely falling frame. In the next section we will see that locally a geodesic path is a straight line.

The invariant interval (2.68) can also be expressed in the arbitrary frame by writing $d\xi^{\alpha} = (\partial \xi^{\alpha}/\partial x^{\mu}) dx^{\mu}$ so that

$$d\tau^2 = g_{\mu\nu} dx^{\mu} dx^{\nu} \tag{2.72}$$

with

$$g_{\mu\nu} = \frac{\partial \xi^{\alpha}}{\partial x^{\mu}} \frac{\partial \xi^{\beta}}{\partial x^{\nu}} \eta_{\alpha\beta} \,. \tag{2.73}$$

In the new and arbitrary reference frame, the second term of (2.70) causes a deviation from a straight line motion of the particle in this frame. The second term therefore represents the effect of the gravitational field. (To be sure, the connection coefficients also represent any other noninertial effects that may have been introduced by the choice of reference frame, such as rotation.)

The affine connection (2.71) appearing in the geodesic equation clearly plays an important role in gravity, and we study it further. We first show that the affine connection is a nontensor, and then show how it can be expressed in terms of the metric tensor and its derivatives. In this sense the metric behaves as the gravitational potential and the affine connection as the force. Write $\Gamma^{\lambda}_{\mu\nu}$ expressed in (2.71) in another coordinate system x'^{μ} and use the chain rule several times to rewrite it:

$$\begin{aligned}
\Gamma'^{\lambda}_{\mu\nu} &= \frac{\partial x'^{\lambda}}{\partial x^{\rho}} \frac{\partial x^{\rho}}{\partial \xi^{\alpha}} \frac{\partial}{\partial x'^{\mu}} \left(\frac{\partial x^{\sigma}}{\partial x'^{\nu}} \frac{\partial \xi^{\alpha}}{\partial x^{\sigma}} \right) \\
&= \frac{\partial x'^{\lambda}}{\partial x^{\rho}} \frac{\partial x^{\rho}}{\partial \xi^{\alpha}} \left[\frac{\partial x^{\sigma}}{\partial x'^{\nu}} \frac{\partial x^{\tau}}{\partial x'^{\mu}} \frac{\partial^2 \xi^{\alpha}}{\partial x^{\tau} \partial x^{\sigma}} + \frac{\partial^2 x^{\sigma}}{\partial x'^{\mu} \partial x'^{\nu}} \frac{\partial \xi^{\alpha}}{\partial x^{\sigma}} \right] \\
&= \frac{\partial x'^{\lambda}}{\partial x^{\rho}} \frac{\partial x^{\tau}}{\partial x'^{\mu}} \frac{\partial x^{\sigma}}{\partial x'^{\nu}} \Gamma^{\rho}_{\tau\sigma} + \frac{\partial x'^{\lambda}}{\partial x^{\rho}} \frac{\partial^2 x^{\rho}}{\partial x'^{\mu} \partial x'^{\nu}} \,.
\end{aligned} \tag{2.74}$$

According to the transformation laws of tensors developed in section 2.2, the second term on the right spoils the transformation law of the affine connection. It is therefore a nontensor.

Let us now obtain the expression of the affine connection in terms of the derivatives of the metric tensor. Form the derivative of (2.64):

$$\frac{\partial}{\partial x'^{\kappa}} g'_{\mu\nu} = \frac{\partial}{\partial x'^{\kappa}} \left(g_{\rho\sigma} \frac{\partial x^{\rho}}{\partial x'^{\mu}} \frac{\partial x^{\sigma}}{\partial x'^{\nu}} \right) .$$

Take the derivatives and form the following combination and find that it is equal to the above derivative:

$$\frac{\partial g'_{\kappa\nu}}{\partial x'^{\mu}} + \frac{\partial g'_{\kappa\mu}}{\partial x'^{\nu}} - \frac{\partial g'_{\mu\nu}}{\partial x'^{\kappa}} = \frac{\partial x^{\tau}}{\partial x'^{\kappa}} \frac{\partial x^{\rho}}{\partial x'^{\mu}} \frac{\partial x^{\sigma}}{\partial x'^{\nu}} \left(\frac{\partial g_{\sigma\tau}}{\partial x^{\rho}} + \frac{\partial g_{\rho\tau}}{\partial x^{\sigma}} - \frac{\partial g_{\rho\sigma}}{\partial x^{\tau}} \right) + 2 g_{\rho\sigma} \frac{\partial x^{\sigma}}{\partial x'^{\kappa}} \frac{\partial^2 x^{\rho}}{\partial x'^{\mu} \partial x'^{\nu}} .$$

Multiply this equation by $\frac{1}{2}$ and the left and right sides by the left and right sides respectively of the law of transformation (2.65), namely,

$$g'^{\lambda\kappa} = g^{\alpha\beta} \frac{\partial x'^{\lambda}}{\partial x^{\alpha}} \frac{\partial x'^{\kappa}}{\partial x^{\beta}} .$$

Use the chain rule and rename several dummy indices to obtain

$$\left\{ {\lambda \atop \mu\nu} \right\}' = \frac{\partial x'^{\lambda}}{\partial x^{\rho}} \frac{\partial x^{\tau}}{\partial x'^{\mu}} \frac{\partial x^{\sigma}}{\partial x'^{\nu}} \left\{ {\rho \atop \tau\sigma} \right\} + \frac{\partial x'^{\lambda}}{\partial x^{\rho}} \frac{\partial^2 x^{\rho}}{\partial x'^{\mu} \partial x'^{\nu}} , \tag{2.75}$$

where the prime on $\{\}$ means that it is evaluated in the x'^{μ} frame and the symbol stands for

$$\left\{ {\lambda \atop \mu\nu} \right\} = \tfrac{1}{2} g^{\lambda\kappa} \left[\frac{\partial g_{\kappa\nu}}{\partial x^{\mu}} + \frac{\partial g_{\kappa\mu}}{\partial x^{\nu}} - \frac{\partial g_{\mu\nu}}{\partial x^{\kappa}} \right] . \tag{2.76}$$

This is called a *Christoffel symbol of the second kind.* It is seen to transform in exactly the same way as the affine connection (2.74). Subtract the two to obtain

$$\left[\Gamma^{\lambda}_{\mu\nu} - \left\{ {\lambda \atop \mu\nu} \right\} \right]' = \frac{\partial x'^{\lambda}}{\partial x^{\rho}} \frac{\partial x^{\tau}}{\partial x'^{\mu}} \frac{\partial x^{\sigma}}{\partial x'^{\nu}} \left[\Gamma^{\rho}_{\tau\sigma} - \left\{ {\rho \atop \tau\sigma} \right\} \right] . \tag{2.77}$$

This shows that the difference is a tensor. According to the equivalence principle, at anyplace and anytime there is a local inertial frame ξ^{α} in which the effects of gravitation are absent, the metric is given by (2.6), and $\Gamma^{\lambda}_{\mu\nu}$ vanishes (compare (2.67) and (2.70)). Since the first derivatives of the metric tensor vanish in such a local inertial system, the Christoffel symbol also vanishes. Because the difference of the affine connection and the Christoffel symbol is a tensor which vanishes in this frame, the difference vanishes in all reference frames. So everywhere we find

$$\Gamma^{\lambda}_{\mu\nu} = \left\{ {\lambda \atop \mu\nu} \right\} = \tfrac{1}{2} g^{\lambda\kappa} \left(g_{\kappa\nu,\mu} + g_{\kappa\mu,\nu} - g_{\mu\nu,\kappa} \right) . \tag{2.78}$$

We use the 'comma subscript' notation introduced earlier to denote differentiation (2.58).

Sometimes it is useful to have the superscript lowered on the affine connection

$$\Gamma_{\kappa\mu\nu} = g_{\kappa\lambda}\Gamma^{\lambda}_{\mu\nu} \ . \tag{2.79}$$

It is equal to the Christoffel symbol of the first kind

$$\Gamma_{\kappa\mu\nu} = \begin{bmatrix} \kappa \\ \mu\nu \end{bmatrix} = \tfrac{1}{2}\big(g_{\kappa\nu,\mu} + g_{\kappa\mu,\nu} - g_{\mu\nu,\kappa}\big) \ . \tag{2.80}$$

The above formulas provide a means of computing the affine connection from the derivatives of the metric tensor and will prove very useful. It is trivial from the above to prove that

$$\Gamma_{\kappa\mu\nu} + \Gamma_{\mu\kappa\nu} = g_{\mu\kappa,\nu} \ . \tag{2.81}$$

2.4.1 Mathematical definition of local Lorentz frames

Spacetime is globally curved by the massive bodies in the universe. Therefore, we need to define mathematically the meaning of "local Lorentz frame". In a rectilinear Lorentz frame the metric tensor is $\eta_{\mu\nu}$ (2.6). Therefore locally at an event P (point in the four-dimensional spacetime continuum), the metric tensor, its coordinate derivatives, and the affine connection have the following values:

$$g_{\mu\nu}(P) = \eta_{\mu\nu}, \qquad g_{\mu\nu,\alpha}(P) = 0, \qquad \Gamma^{\lambda}_{\mu\nu}(P) = 0. \tag{2.82}$$

The third of these equations follows from the second and from (2.78). All local effects of gravitation disappear in such a frame. The geodesic equation (2.70) defining the path followed by a free particle in an arbitrary gravitational field becomes locally the equation of a uniform straight line in accord with the equivalence principle.

Of course physical measurements are always subject to the precision of the measuring devices. The extent of the local region around P, in which the above equations will hold and in which spacetime is said to be flat, will depend on the accuracy of the devices and therefore their ability to detect deviations from the above conditions as one measures further from P.

2.4.2 Geodesics

In the Special Theory of Relativity a free particle remains at rest or moves with constant velocity in a straight line. A straight line is the shortest distance between two points in Euclidean three-dimensional space. In Minkowski spacetime a straight line is the longest interval between two events as we

shall shortly see. Both situations are covered by saying that a straight line is an extremal path between two points. We shall show that in an arbitrary gravitational field, a particle moving under the influence of only gravity, follows a path that is, in the sense that we shall define, the straightest line possible in curved spacetime.

We first show that a straight-line path between two events in Minkowski spacetime maximizes the proper time. This is easily proved. Orient the axis so that the two events marking the ends of the path, A and B, lie on the t-axis with coordinates $(0,0,0,0)$ and $(T,0,0,0)$, and consider an alternate path in the $t-x$ plane that consists of two straight-line segments that pass from A to B through $(T/2, R/2, 0, 0)$. The proper time as measured on the second path is

$$\tau = 2\sqrt{(T/2)^2 - (R/2)^2} = \sqrt{T^2 - R^2}\,. \tag{2.83}$$

For any finite R, τ is smaller than the proper time along the straight-line path from A to B, namely, T. Therefore the straight-line path is a maximum in proper time.

We have referred to the equation of motion of a particle moving freely in an arbitrary gravitational field (2.70) as a geodesic equation. In general a geodesic that is not null (a null geodesic, as is the case for a light particle, has $d\tau = 0$), is the extremal path of

$$\int_A^B d\tau \tag{2.84}$$

where A to B refer to spacetime events on the geodesic. To prove this result, let $x^\mu(\tau)$ denote the coordinates along the geodesic path, parameterized by the proper time, and let $x^\mu(\tau) + \delta x^\mu(\tau)$ denote a neighboring path with the same end points, A to B. From

$$d\tau^2 = g_{\mu\nu} dx^\mu dx^\nu\,, \tag{2.85}$$

we have to first order in the variation,

$$\begin{aligned} 2d\tau\,\delta(d\tau) &= \delta g_{\mu\nu} dx^\mu dx^\nu + 2g_{\mu\nu} dx^\mu \delta(dx^\nu) \\ &= dx^\mu dx^\nu g_{\mu\nu,\lambda}\delta x^\lambda + 2g_{\mu\nu} dx^\mu d(\delta x^\nu)\,. \end{aligned} \tag{2.86}$$

Recalling the four-velocity, $u^\mu = dx^\mu/d\tau$, we have

$$\delta(d\tau) = \Big(\tfrac{1}{2}u^\mu u^\nu g_{\mu\nu,\lambda}\delta x^\lambda + g_{\mu\lambda}u^\mu \frac{d}{d\tau}\delta x^\lambda\Big)d\tau\,. \tag{2.87}$$

Thus

$$\delta\int_A^B d\tau = \int_A^B \Big[\tfrac{1}{2}u^\mu u^\nu g_{\mu\nu,\lambda} - \frac{d}{d\tau}\Big(g_{\mu\lambda}u^\mu\Big)\Big]\delta x^\lambda\, d\tau \tag{2.88}$$

where an integration by parts in the second term was performed. Since the variation of the path δx^λ is arbitrary save for its end points being zero, we obtain as the extremal condition,

$$\frac{d}{d\tau}\Big(g_{\mu\lambda}u^\mu\Big) - \tfrac{1}{2}u^\mu u^\nu g_{\mu\nu,\lambda} = 0\,. \tag{2.89}$$

The first and second terms can be rewritten:

$$\begin{aligned}\frac{d}{d\tau}\Big(g_{\mu\lambda}u^\mu\Big) &= g_{\mu\lambda}\frac{du^\mu}{d\tau} + g_{\mu\lambda,\nu}u^\mu u^\nu\,,\\ g_{\mu\lambda,\nu}u^\mu u^\nu &= \tfrac{1}{2}(g_{\mu\lambda,\nu} + g_{\lambda\nu,\mu})u^\mu u^\nu\,.\end{aligned} \tag{2.90}$$

Now using the relationship (2.80), we find

$$g_{\mu\lambda}\frac{du^\mu}{d\tau} + \Gamma_{\lambda\mu\nu}u^\mu u^\nu = 0\,. \tag{2.91}$$

Multiplying by $g^{\sigma\lambda}$ and summing on λ, we obtain the geodesic equation (2.70):

$$\frac{du^\sigma}{d\tau} + \Gamma^\sigma_{\mu\nu}u^\mu u^\nu = 0\,. \tag{2.92}$$

This completes the proof that the path defined by the geodesic equation, the equation of motion of a particle in a purely gravitational field, extremizes the proper time between any two events on the path.

The straight-line path between two events in Minkowski spacetime maximizes the interval between the events. We proved that a geodesic path, in the general case that a gravitational field is present, will be an extremum, but if the spacetime separation of the ends of the path is large, there may be two geodesic paths, one of minimum and one of maximum length. The geodesic path of a particle in spacetime is frequently referred to as its *world line*.

In a region of spacetime sufficiently small that the Minkowski metric holds, (the existence of which locality is guaranteed by the equivalence principle), we see that the geodesic equation reduces to that for uniform straight-line motion,

$$\frac{du^\mu}{d\tau} = 0\,. \tag{2.93}$$

Therefore the path of a particle moving under the influence of a general gravitational field will be locally straight. But since we know that no global Lorentz frame exists in the presence of gravitating bodies, geodesic paths will in general be curved. However, in the above sense they will be as straight as possible in curved spacetime.

2.4.3 Comparison with Newton's gravity

We confirm the assertion made earlier that the metric tensor $g_{\mu\nu}$ takes the place in General Relativity that the Newtonian potential occupies in Newton's theory. Of course this must be done in a weak field situation for it is only there that Newton's theory applies. For this reason, of the ten independent $g_{\mu\nu}$, only one can be involved in the correspondence.

We consider a particle moving slowly in a weak static gravitational field. From the Special Theory of Relativity we have

$$d\tau = \left(dt^2 - d\boldsymbol{r}^2\right)^{1/2} = \left(1 - \boldsymbol{v}^2\right)^{1/2} dt, \qquad \boldsymbol{v} = \frac{d\boldsymbol{r}}{dt}\,, \tag{2.94}$$

where boldface symbols denote three-vectors. The slowly moving assumption is

$$\frac{d\boldsymbol{r}}{dt} << \frac{dt}{d\tau} \approx 1\,. \tag{2.95}$$

So the geodesic equation (2.70) can be written with the neglect of the velocity terms as

$$\frac{d^2x^\mu}{d\tau^2} + \Gamma^\mu_{00}\left(\frac{dt}{d\tau}\right)^2 = 0\,. \tag{2.96}$$

Since the field is static, the time derivatives of $g_{\mu\nu}$ vanish. Consequently,

$$\Gamma^\mu_{00} = \tfrac{1}{2}g^{\mu\nu}\left(2g_{\nu 0,0} - g_{00,\nu}\right) = -\tfrac{1}{2}g^{\mu\nu}g_{00,\nu}(1-\delta^\nu_0)\,. \tag{2.97}$$

Because the field is weak we may take

$$g_{00} = (1+\delta)\eta_{00}\ , \tag{2.98}$$

where $\delta << 1$ and similarly for the other $g_{\mu\nu}$. To first order in the small quantities, we have

$$\Gamma^\mu_{00} = -\tfrac{1}{2}\eta^{\mu\nu}\eta_{00}\frac{d\delta}{dx^\nu}(1-\delta^\nu_0)\,. \tag{2.99}$$

Thus the geodesic equations become

$$\frac{d^2\boldsymbol{r}}{d\tau^2} = -\tfrac{1}{2}\left(\frac{dt}{d\tau}\right)^2\nabla\delta, \qquad \frac{d^2t}{d\tau^2} = 0\,. \tag{2.100}$$

The second of these tells us that $\tau = at + b$. So we may write the first as

$$\frac{d^2\boldsymbol{r}}{dt^2} = -\tfrac{1}{2}\nabla\delta\,. \tag{2.101}$$

Newton's equation is

$$\frac{d^2\boldsymbol{r}}{dt^2} = -\nabla V\ , \tag{2.102}$$

where V is the gravitational potential. Comparing, we have

$$g_{00} = 1 + 2V \,. \tag{2.103}$$

In particular, if the gravitational field is produced by a body of mass M,

$$V = -\frac{GM}{r} \quad \Longrightarrow \quad g_{00} = 1 - \frac{2GM}{r} \,, \tag{2.104}$$

where G is Newton's constant. Thus we see for weak fields how the metric is related to the Newtonian potential.

2.5 Covariance

2.5.1 Principle of General Covariance

Physical laws in their form ought to be independent of the frame in which they are expressed and of the location in the universe, that is, on the gravitational field. The principle of general covariance states that a law of physics holds in a general gravitational field if it holds in the absence of gravity and its form is invariant to any coordinate transformation. Physical laws frequently involve space-time derivatives of scalars, vectors, or tensors. We have seen that the derivative of a scalar is a vector but that the ordinary derivative of a vector or a tensor is not a tensor (page 17). Therefore we need a type of derivative—a covariant derivative—that reduces to ordinary differentiation in the absence of gravity and which retains its form under any coordinate transformation, that is, in any gravitational field.

2.5.2 Covariant Differentiation

Take the derivative of the expression of the covariant vector transformation law (2.49),

$$\frac{dA'_\mu}{dx'^\rho} = \frac{\partial x^\nu}{\partial x'^\mu}\frac{\partial x^\sigma}{\partial x'^\rho}\frac{\partial A_\nu}{\partial x^\sigma} + \frac{\partial^2 x^\nu}{\partial x'^\rho \partial x'^\mu} A_\nu \,.$$

If only the first term were present we would have the correct transformation law for a covariant tensor. Now multiply the left and right sides of (2.74) by the left and right sides of (2.49), respectively, and rearrange to find

$$\Gamma'^\lambda_{\mu\nu} A'_\lambda = \frac{\partial x^\alpha}{\partial x'^\mu}\frac{\partial x^\beta}{\partial x'^\nu}\Gamma^\kappa_{\alpha\beta} A_\kappa + \frac{\partial^2 x^\kappa}{\partial x'^\mu \partial x'^\nu} A_\kappa \,.$$

Subtracting the above two equations after renaming some dummy indices of summation, we get

$$\left(\frac{dA'_\mu}{dx'^\nu} - \Gamma'^\lambda_{\mu\nu} A'_\lambda\right) = \frac{\partial x^\alpha}{\partial x'^\mu}\frac{\partial x^\beta}{\partial x'^\nu}\left(\frac{dA_\alpha}{dx^\beta} - \Gamma^\lambda_{\alpha\beta} A_\lambda\right) \,, \tag{2.105}$$

which proves the tensor character of the quantity in brackets. This we call the *covariant derivative* of a covariant vector. We denote it by

$$A_{\mu;\nu} \equiv \frac{dA_\mu}{dx^\nu} - \Gamma^\lambda_{\mu\nu} A_\lambda \ , \tag{2.106}$$

and the 'semicolon subscript' shall denote the covariant derivative, and imply the operations shown on the right. The covariant derivative is a second-rank covariant tensor which reduces to ordinary differentiation in inertial frames—and therefore locally in any gravitational field.

Through similar manipulations we find the covariant derivative of a contravariant vector,

$$A^\mu{}_{;\nu} \equiv \frac{dA^\mu}{dx^\nu} + \Gamma^\mu_{\sigma\nu} A^\sigma \ . \tag{2.107}$$

This is a second-rank mixed tensor because its transformation law is

$$\left(\frac{dA'^\mu}{dx'^\nu} + \Gamma'^\mu_{\lambda\nu} A'^\lambda\right) = \frac{\partial x'^\mu}{\partial x^\alpha}\frac{\partial x^\beta}{\partial x'^\nu}\left(\frac{dA^\alpha}{dx^\beta} + \Gamma^\alpha_{\kappa\beta} A^\kappa\right) . \tag{2.108}$$

The covariant derivative of a mixed tensor of arbitrary order can be obtained by successive application of the above two rules to each index; there is one ordinary derivative of the tensor and an affine connection for each index with sign as indicated by the above.

In particular, the covariant derivative of the metric tensor is

$$g_{\mu\nu;\lambda} = \frac{\partial g_{\mu\nu}}{\partial x^\lambda} - \Gamma^\rho_{\mu\lambda} g_{\rho\nu} - \Gamma^\rho_{\nu\lambda} g_{\rho\mu} \ . \tag{2.109}$$

In a local inertial frame, where the affine connection and the derivative of the metric tensor vanish, we see that the covariant derivative of the metric tensor vanishes in that frame. But since this itself is a tensor, it must vanish in all frames. Similarly, for the covariant derivative of $g^{\mu\nu}$,

$$g_{\mu\nu;\lambda} = 0 = g^{\mu\nu}{}_{;\lambda} \, . \tag{2.110}$$

2.5.3 Geodesic equation from covariance principle

As an important example of the application of the covariant derivative, consider the four-velocity of a free particle in a Lorentz frame in the absence of gravity. We denote the four-velocity by $u^\mu = dx^\mu/d\tau$ and its equation of motion is $du^\mu/d\tau = 0$, or equivalently in differential form,

$$du^\mu = 0 \, . \tag{2.111}$$

The covariant derivative (2.108) was introduced to preserve the vector or tensor character so that a law expressed in such form is preserved in form for all coordinate transformations in accord with the principle of relativity. The

equation expressing the law is said to be covariant if its form is preserved. Therefore the law of free motion (2.111) in a Lorentz frame in the absence of gravity is generalized to frames in arbitrary gravitational fields by requiring that the covariant differential of the four-velocity vanish:

$$\begin{aligned} 0 = u^{\mu}{}_{;\nu} dx^{\nu} &= \frac{du^{\mu}}{dx^{\nu}} dx^{\nu} + \Gamma^{\mu}_{\sigma\nu} u^{\sigma} dx^{\nu} \\ &= du^{\mu} + \Gamma^{\mu}_{\sigma\nu} u^{\sigma} dx^{\nu} . \end{aligned} \tag{2.112}$$

Dividing the above equation by $d\tau$ yields the expected result—the geodesic equation (2.70)—the equation of motion derived previously for a free particle in an arbitrary gravitational field:

$$\frac{d^2 x^{\lambda}}{d\tau^2} + \Gamma^{\lambda}_{\mu\nu} \frac{dx^{\mu}}{d\tau} \frac{dx^{\nu}}{d\tau} = 0 . \tag{2.113}$$

This is an example of the application of the principle of general covariance and it is seen to rest on the equivalence principle, which assures us that a Lorentz frame can be erected locally. To restate the procedure briefly, *any law that holds in the special theory of relativity and in the absence of gravity can be generalized by replacing the metric* $\eta_{\mu\nu}$ by $g_{\mu\nu}$ *and replacing derivatives by covariant derivatives.*

We obtain an additional result that we need later, namely, the equations of motion for the covariant components of the four-velocity. The law of motion of a free particle in the special theory, $du^{\mu} = 0$, implies at once that $du_{\mu} = g_{\mu\nu} du^{\nu} = 0$. The covariant statement of this fact is

$$0 = u_{\mu;\nu} dx^{\nu} = \frac{du_{\mu}}{dx^{\nu}} dx^{\nu} - \Gamma^{\lambda}_{\mu\nu} u_{\lambda} dx^{\nu} \tag{2.114}$$

or

$$\frac{d^2 x_{\mu}}{d\tau^2} - \Gamma^{\lambda}_{\mu\nu} \frac{dx_{\lambda}}{d\tau} \frac{dx^{\nu}}{d\tau} = 0 . \tag{2.115}$$

This is the equation corresponding to (2.113) for the covariant acceleration. We carry the analysis a step further. Examine the second term on the left.

$$\begin{aligned} \Gamma^{\lambda}_{\mu\nu} u_{\lambda} u^{\nu} &= \tfrac{1}{2} g^{\lambda\kappa} \big(g_{\kappa\nu,\mu} + g_{\kappa\mu,\nu} - g_{\mu\nu,\kappa} \big) u_{\lambda} u^{\nu} \\ &= \tfrac{1}{2} \big(g_{\kappa\nu,\mu} + g_{\kappa\mu,\nu} - g_{\mu\nu,\kappa} \big) u^{\kappa} u^{\nu} . \end{aligned} \tag{2.116}$$

Because of the symmetry of the product $u^{\kappa} u^{\nu}$, the last two terms in the bracket cancel. We are left

$$\frac{du_{\mu}}{d\tau} = \tfrac{1}{2} g_{\kappa\nu,\mu} u^{\kappa} u^{\nu} . \tag{2.117}$$

This proves that if all the $g_{\alpha\beta}$ are independent of some coordinate component, say x^{μ}, then the covariant velocity u_{μ} is a constant along the particle's

trajectory. We will use this result in a much later chapter during a discussion of the phenomenon of dragging of local inertial frames by a rotating star (according to which a body dropped freely from a great distance falls, not toward the star's center, but is dragged ever more strongly in the sense of the star's rotation).

2.5.4 Covariant divergence and conserved quantities

The element of four-volume transforms under coordinate change is

$$dx'^0 dx'^1 dx'^2 dx'^3 = J\, dx^0 dx^1 dx^2 dx^3\,, \tag{2.118}$$

where J is the Jacobian of the transformation,

$$J = \det \left| \frac{\partial x'^\rho}{\partial x^\mu} \right| . \tag{2.119}$$

For brevity the four volume element is often written d^4x.

The transformation law for the metric tensor is

$$g_{\mu\nu} = \frac{\partial x'^\alpha}{\partial x^\mu} g'_{\alpha\beta} \frac{\partial x'^\beta}{\partial x^\nu} . \tag{2.120}$$

We may regard this as an element in the product of three matrices. The corresponding determinant equation is

$$g = Jg'J = J^2 g' \tag{2.121}$$

where $g = \det|g_{\mu\nu}|$ and is a negative quantity according to the convention used in this book, as can be verified by looking at the Minkowski metric. Thus, we may write

$$\sqrt{-g} = J\sqrt{-g'}\,. \tag{2.122}$$

If $S = S'$ is a scalar field, then

$$\int_{V_4} S\sqrt{-g}\, d^4x = \int_{V_4} S\sqrt{-g'}\, J\, d^4x = \int_{V_4} S'\sqrt{-g'}\, d^4x' \tag{2.123}$$

is an invariant where V_4 is a prescribed 4-volume. The quantity

$$\mathcal{S} \equiv S\sqrt{-g} \tag{2.124}$$

is called a *scalar density*, and its integral over a region of spacetime is invariant to a coordinate transformation. Also, and very important to us, $\sqrt{-g}\, d^4x$ is the invariant volume element.

The covariant derivative of a vector A^μ is given by (2.107). If we contract indices, according to (2.61) we have a scalar. This is the *covariant divergence* of A^μ:

$$A^\mu{}_{;\mu} \equiv A^\mu{}_{,\mu} + \Gamma^\mu_{\nu\mu} A^\nu \,. \tag{2.125}$$

From (2.78) we find

$$\Gamma^\nu_{\mu\nu} = \tfrac{1}{2} g^{\nu\kappa}\big(g_{\kappa\nu,\mu} + g_{\kappa\mu,\nu} - g_{\mu\nu,\kappa}\big) \,. \tag{2.126}$$

Interchange the names of the dummy summation indices in the second term on the right to see that it cancels the third. Thus

$$\Gamma^\nu_{\mu\nu} = \tfrac{1}{2} g^{\nu\kappa} g_{\kappa\nu,\mu} \,. \tag{2.127}$$

We need still another result. Denote the cofactor of the element $g_{\alpha\beta}$ by $C^{\alpha\beta}$. The determinant $g = \det|g_{\alpha\beta}|$ can be expanded in any of the set of minors (i.e., any $\alpha = 0, 1, 2,$ or 3) in the equation

$$g = g_{(\alpha)\beta} C^{(\alpha)\beta}, \qquad \text{(no sum on } \alpha). \tag{2.128}$$

Since the cofactor contains no elements $g_{(\alpha)\beta}$, we find

$$\frac{\partial g}{\partial g_{\alpha\nu}} = \frac{\partial(g_{(\alpha)\beta} C^{(\alpha)\beta})}{\partial g_{\alpha\nu}} = \frac{\partial g_{\alpha\mu}}{\partial g_{\alpha\nu}} C^{\alpha\mu} = \delta^\nu_\mu C^{\alpha\mu} = C^{\alpha\nu} \,. \tag{2.129}$$

Therefore,

$$g_{,\alpha} = \frac{\partial g}{\partial g_{\mu\nu}} g_{\mu\nu,\alpha} = C^{\mu\nu} g_{\mu\nu,\alpha} \,. \tag{2.130}$$

We need the expression,

$$C^{\mu\nu} = g g^{\mu\nu} \,, \tag{2.131}$$

which can be proved by multiplying by $g_{\mu\nu}$ and summing only over ν,

$$g_{(\mu)\nu} C^{(\mu)\nu} = g_{(\mu)\nu} g^{(\mu)\nu} g = g \,. \tag{2.132}$$

This is the determinant expansion in minors (2.128). Thus we have derived the result,

$$g_{,\alpha} = g g^{\mu\nu} g_{\mu\nu,\alpha} \,. \tag{2.133}$$

Hence,

$$\Gamma^\nu_{\mu\nu} = \tfrac{1}{2} g^{-1} g_{,\mu} = \tfrac{1}{2}\big(\ln(-g)\big)_{,\mu} = \frac{1}{\sqrt{-g}}\big(\sqrt{-g}\big)_{,\mu} \,. \tag{2.134}$$

With this in (2.125), we obtain the important result for the covariant divergence,

$$\sqrt{-g}A^{\mu}{}_{;\mu} = \left(\sqrt{-g}A^{\mu}\right)_{,\mu}. \tag{2.135}$$

The left side is a scalar density. From the invariance of the integral of a scalar density over a prescribed four-volume, we have the invariant

$$\int_{V_4} \sqrt{-g}A^{\mu}{}_{;\mu}\, d^4x = \int_{V_4} \left(\sqrt{-g}A^{\mu}\right)_{,\mu} d^4x. \tag{2.136}$$

The right side can be converted to a surface integral over a three-volume at a definite time x^0 by Gauss' theorem.

If the covariant divergence vanishes, we get a conservation law as follows:

$$A^{\mu}{}_{;\mu} = 0 \quad \Longrightarrow \quad \left(\sqrt{-g}A^{\mu}\right)_{,\mu} = 0. \tag{2.137}$$

As a result, we obtain

$$\left(\sqrt{-g}A^0\right)_{,0} = -\left(\sqrt{-g}A^m\right)_{,m} \quad \text{(summed over } m = 1,2,3). \tag{2.138}$$

Integrate the above expression over a three-volume at definite time x^0 to find

$$\frac{\partial}{\partial x^0}\int_V \sqrt{-g}A^0\, d^3x = -\int_V \left(\sqrt{-g}A^m\right)_{,m} d^3x = -\int_S \sqrt{-g}\boldsymbol{A}\cdot d\boldsymbol{S}. \tag{2.139}$$

If there is no three-current $\sqrt{-g}\boldsymbol{A}$ crossing the surface, then the quantity of density $\sqrt{-g}A^0$ contained within V is constant,

$$\int_V \sqrt{-g}A^0\, d^3x = \text{ constant} \tag{2.140}$$

This quantity is frequently referred to as the total charge of whatever A^{μ} represents. We will apply these results in Chapter 3, Section 3.13 and in Chapter 5 to calculate the distribution of various baryon species in neutron stars.

We can apply precisely the same reasoning to the covariant divergence of an antisymmetric tensor $A^{\mu\nu}$ and find

$$\sqrt{-g}A^{\mu\nu}{}_{;\nu} = \left(\sqrt{-g}A^{\mu\nu}\right)_{,\nu}, \tag{2.141}$$

where the quantity on the left is a *vector density* according to the previous section. Similarly we can derive conservation laws for the three-volume integral of the four densities $\sqrt{-g}A^{\mu 0}$ if the covariant divergence vanishes and there is no three-flux through the surface of the volume. However, if the tensor is not antisymmetric, the above theorem does not generally apply in curved spacetime to a tensor of more than one index.

2.6 Riemann Curvature Tensor

The order of ordinary differentiation in flat spacetime does not matter. The order of covariant differentiation does matter in curved spacetime. From an investigation of this fact we arrive at a measure of curvature.

2.6.1 Second covariant derivative of scalars and vectors

If we take the covariant derivative of a scalar twice and then invert the order, the answer is easily verified to be the same:

$$S_{;\mu;\nu} = S_{;\mu,\nu} - \Gamma^{\alpha}_{\mu\nu} S_{;\alpha} = S_{,\mu,\nu} - \Gamma^{\alpha}_{\mu\nu} S_{;\alpha}\,, \tag{2.142}$$

where we use the fact in the second equality that the covariant derivative of a scalar is the ordinary derivative $S_{;\mu} = S_{,\mu}$. The above result is symmetrical in μ, ν.

However for vectors and tensors, a changed order of differentiation in general produces a different result. The operations involved, all defined above, are many but straightforward. The result for the vector A_σ is

$$A_{\sigma;\mu;\nu} - A_{\sigma;\nu;\mu} = A_\rho R^{\rho}_{\sigma\mu\nu}\,, \tag{2.143}$$

where

$$R^{\rho}_{\sigma\mu\nu} \equiv \Gamma^{\rho}_{\sigma\nu,\mu} - \Gamma^{\rho}_{\sigma\mu,\nu} + \Gamma^{\alpha}_{\sigma\nu}\Gamma^{\rho}_{\alpha\mu} - \Gamma^{\alpha}_{\sigma\mu}\Gamma^{\rho}_{\alpha\nu} \tag{2.144}$$

is the *Riemann–Christoffel curvature tensor*. We know that it is a tensor because the left side of (2.143) is a tensor and A_ν is any tensor. Riemann is the only tensor that can be constructed from the metric tensor and its first and second derivatives (cf. Ref. [14], p. 133).

2.6.2 Symmetries of the Riemann tensor

Riemann has a number of symmetry properties that can be easily derived from the above expression:

$$R^{\mu}_{\nu\rho\sigma} = -R^{\mu}_{\nu\sigma\rho}\,, \tag{2.145}$$

$$R^{\alpha}_{\nu\rho\sigma} + R^{\alpha}_{\sigma\nu\rho} + R^{\alpha}_{\rho\sigma\nu} = 0\,. \tag{2.146}$$

Lowering the index on the Riemann tensor, we get

$$R_{\rho\sigma\mu\nu} = g_{\rho\alpha} R^{\alpha}_{\sigma\mu\nu}\,. \tag{2.147}$$

The additional symmetries follow:

$$R_{\mu\nu\rho\sigma} = -R_{\nu\mu\rho\sigma} = -R_{\mu\nu\sigma\rho}\,, \tag{2.148}$$

$$R_{\mu\nu\rho\sigma} = R_{\rho\sigma\mu\nu} = R_{\sigma\rho\nu\mu}\,. \tag{2.149}$$

As a consequence of the symmetries only 20 of the $4^4 = 256$ components of Riemann are independent. In two dimensions there are 15 such symmetry relationships. Consequently, there are $2^4 - 15 = 1$ independent components of the Riemann tensor, namely, the Gaussian curvature. See Ref. [15] (p. 60 and appendix B) for a discussion of curvature in two dimensions.

We shall encounter two additional objects that are obtained from the Riemann tensor, the *Ricci tensor*,

$$R_{\mu\nu} = R^{\rho}_{\mu\nu\rho}\,, \tag{2.150}$$

and the *scalar curvature*,

$$R = g^{\mu\nu} R_{\mu\nu}\,. \tag{2.151}$$

Multiply the left and right side of (2.149) by $g^{\mu\sigma}$ and then rename indices to find

$$R_{\mu\nu} = R_{\nu\mu}\,. \tag{2.152}$$

Because of this symmetry, when we raise an index on the Ricci tensor, it is unnecessary to preserve the location,

$$R^{\mu}{}_{\nu} = R_{\nu}{}^{\mu} = R^{\mu}_{\nu}\,. \tag{2.153}$$

From the definition of the Ricci tensor in terms of the Riemann tensor, we have the following explicit expression:

$$R_{\mu\nu} = \Gamma^{\alpha}_{\mu\alpha,\nu} - \Gamma^{\alpha}_{\mu\nu,\alpha} - \Gamma^{\alpha}_{\mu\nu}\Gamma^{\beta}_{\alpha\beta} + \Gamma^{\alpha}_{\mu\beta}\Gamma^{\beta}_{\nu\alpha}\,. \tag{2.154}$$

The first term might appear to contradict the assertion that $R_{\mu\nu}$ is symmetric in μ, ν. However the result (2.134) proves that the Ricci tensor is symmetric.

2.6.3 Test for flatness

If spacetime is flat, then we may choose a rectilinear coordinate system in which case the metric tensor is a constant throughout spacetime. Then according to (2.78) the nontensor $\Gamma^{\lambda}_{\mu\nu}$ vanishes in this frame in all spacetime. So also do the derivatives of $\Gamma^{\lambda}_{\mu\nu}$. Therefore the Riemann tensor (2.144) vanishes everywhere at all times in flat spacetime. Since this is a statement about a tensor, it is true in any coordinate system, rectilinear or not. The converse is true but more difficult to prove: If Riemann vanishes, spacetime is flat. We prove this later in Section 2.8.3

2.6.4 Second covariant derivative of tensors

An arbitrary second rank tensor can be expressed as the sum of products $A_\mu B_\nu$. It is simpler to start by examining the second covariant derivative

of such a product:

$$\begin{aligned}(A_\mu B_\nu)_{;\rho;\sigma} &= (A_{\mu;\rho}B_\nu + A_\mu B_{\nu;\rho})_{;\sigma} \\ &= A_{\mu;\rho;\sigma}B_\nu + A_\mu B_{\nu;\rho;\sigma} + A_{\mu;\rho}B_{\nu;\sigma} + A_{\mu;\sigma}B_{\nu;\rho}\,.\end{aligned}$$

Interchange ρ, σ, and subtract to find

$$\begin{aligned}(A_\mu B_\nu)_{;\rho;\sigma} &= (A_\mu B_\nu)_{;\sigma;\rho} \\ &= A_\mu(B_{\nu;\rho;\sigma} - B_{\nu;\sigma;\rho}) + (A_{\mu;\rho;\sigma} - A_{\mu;\sigma;\rho})B_\nu \\ &= A_\mu B_\alpha R^\alpha_{\nu\rho\sigma} + A_\alpha R^\alpha_{\mu\rho\sigma}B_\nu\,.\end{aligned}$$

We can form an arbitrary linear combination of such products of first-rank tensors to obtain the result for a general tensor,

$$T_{\mu\nu;\rho;\sigma} - T_{\mu\nu;\sigma;\rho} = T_{\mu\alpha}R^\alpha_{\nu\rho\sigma} + T_{\alpha\nu}R^\alpha_{\mu\rho\sigma}\,. \tag{2.155}$$

2.6.5 Bianchi identities

The Bianchi identities are extremely important for the further development of the theory of gravity, allowing us to prove that the Einstein tensor, which we come to next, has vanishing divergence.

Apply the above result to the particular case that the second-rank tensor is the covariant derivative of a vector $T_{\mu\nu} = A_{\mu;\nu}$,

$$A_{\mu;\nu;\rho;\sigma} - A_{\mu;\nu;\sigma;\rho} = A_{\mu;\alpha}R^\alpha_{\nu\rho\sigma} + A_{\alpha;\nu}R^\alpha_{\mu\rho\sigma}\,. \tag{2.156}$$

Now write down the additional two equations obtained from this by cyclic permutation of the indices $(\nu\rho\sigma)$, and add the three equations. First study the left side of the sum. Use (2.143) to get

$$\begin{aligned}\text{LHS} &= (A_{\mu;\nu;\rho} - A_{\mu;\rho;\nu})_{;\sigma} + (A_{\mu;\sigma;\nu} - A_{\mu;\nu;\sigma})_{;\rho} + (A_{\mu;\rho;\sigma} - A_{\mu;\sigma;\rho})_{;\nu} \\ &= (A_\alpha R^\alpha_{\mu\nu\rho})_{;\sigma} + (A_\alpha R^\alpha_{\mu\sigma\nu})_{;\rho} + (A_\alpha R^\alpha_{\mu\rho\sigma})_{;\nu}\,.\end{aligned}$$

Using (2.146) in the sum of the right-hand sides of the cyclic permutation, we are left with

$$\text{RHS} = A_{\alpha;\nu}R^\alpha_{\mu\rho\sigma} + A_{\alpha;\sigma}R^\alpha_{\mu\nu\rho} + A_{\alpha;\rho}R^\alpha_{\mu\sigma\nu}\,.$$

Equating left and right sides and cancelling common terms, we get

$$A_\alpha(R^\alpha_{\mu\nu\rho;\sigma} + R^\alpha_{\mu\sigma\nu;\rho} + R^\alpha_{\mu\rho\sigma;\nu}) = 0\,. \tag{2.157}$$

Since A_α is any vector,

$$R^\alpha_{\mu\nu\rho;\sigma} + R^\alpha_{\mu\sigma\nu;\rho} + R^\alpha_{\mu\rho\sigma;\nu} = 0\,. \tag{2.158}$$

In addition to the symmetry relationships, the Riemann tensor satisfies the differential equations above known as *Bianchi identities* as well as certain symmetry relationships written above.

2.6.6 Einstein tensor

Let us multiply the differential equations for the Bianchi identities (2.158) by $g^{\mu\nu}$, contract σ with α, and use the fact, already established, that the covariant derivatives of the metric tensor vanish:

$$\begin{aligned} 0 &= g^{\mu\nu}(R^{\alpha}_{\mu\nu\rho;\sigma} + R^{\alpha}_{\mu\sigma\nu;\rho} + R^{\alpha}_{\mu\rho\sigma;\nu}) \\ &= (g^{\mu\nu}R^{\alpha}_{\mu\nu\rho})_{;\alpha} + (g^{\mu\nu}R^{\alpha}_{\mu\alpha\nu})_{;\rho} + (g^{\mu\nu}R^{\alpha}_{\mu\rho\alpha})_{;\nu}\,. \end{aligned} \tag{2.159}$$

Examine each term in brackets using the Riemann tensor symmetries. The first term is

$$g^{\mu\nu}R^{\alpha}_{\mu\nu\rho} = g^{\mu\nu}g^{\alpha\beta}R_{\beta\mu\nu\rho} = g^{\mu\nu}g^{\alpha\beta}R_{\mu\beta\rho\nu} = g^{\alpha\beta}R^{\nu}_{\beta\rho\nu} = g^{\alpha\beta}R_{\beta\rho} = R^{\alpha}_{\rho}\,.$$

The second term is

$$g^{\mu\nu}R^{\alpha}_{\mu\alpha\nu} = -g^{\mu\nu}R^{\alpha}_{\mu\nu\alpha} = -g^{\mu\nu}R_{\mu\nu} = -R\,.$$

The third term is

$$g^{\mu\nu}R^{\alpha}_{\mu\rho\alpha} = g^{\mu\nu}R_{\mu\rho} = R^{\nu}_{\rho}\,.$$

Now put these results back into their brackets with the covariant derivatives as indicated in (2.159) to obtain

$$0 = R^{\alpha}_{\rho;\alpha} - R_{;\rho} + R^{\nu}_{\rho;\nu} = 2R^{\alpha}_{\rho;\alpha} - R_{;\rho}\,.$$

Multiply by $g^{\mu\rho}$, and note that

$$\begin{aligned} g^{\mu\rho}R^{\alpha}_{\rho;\alpha} = (g^{\mu\rho}R^{\alpha}_{\rho})_{;\alpha} &= R^{\mu\alpha}{}_{;\alpha} = R^{\mu\nu}{}_{;\nu} \\ g^{\mu\rho}R_{;\rho} &= g^{\mu\nu}R_{;\nu} \end{aligned}$$

to arrive immediately at

$$(R^{\mu\nu} - \tfrac{1}{2}g^{\mu\nu}R)_{;\nu} = 0\,. \tag{2.160}$$

The object in the brackets is called the *Einstein curvature tensor*,

$$G^{\mu\nu} \equiv R^{\mu\nu} - \tfrac{1}{2}g^{\mu\nu}R\,. \tag{2.161}$$

The Einstein tensor is constructed from the Riemann curvature tensor and has an identically vanishing covariant divergence. It is symmetric and of second rank. Einstein was motivated to seek a tensor that contained no differentials of the $g^{\mu\nu}$ higher than the second—a tensor which was a linear homogeneous combination of terms linear in the second derivative or quadratic in the first (in analogy with Poisson's equation for the gravitational potential in Newton's theory:

$$\nabla^2 V = 4\pi\rho\,, \tag{2.162}$$

where ρ is the mass density generating the field). For the expression of energy and momentum conservation, it is important that the divergence vanish. The energy-momentum tensor of matter accomplishes this and is of second rank.

2.7 Einstein's Field Equations

We know that other bodies will experience gravity in the vicinity of massive bodies. So mass is a source of gravity, and from the Special Theory of Relativity we must say in general that mass and energy are sources. We have just seen that a construction from the Riemann curvature tensor, namely Einstein's tensor, has vanishing divergence. We have three possibilities,

$$G^{\mu\nu} = 0\,, \tag{2.163}$$

or

$$G^{\mu\nu} = kT^{\mu\nu}\,, \tag{2.164}$$

where $T^{\mu\nu}$ is a symmetric divergenceless tensor constructed from the mass-energy properties of the material medium, or

$$G^{\mu\nu} = kT^{\mu\nu} + \Lambda g^{\mu\nu}\,. \tag{2.165}$$

The constant Λ is the so-called *cosmological constant*. It was not present in the original theory and was added to obtain a static cosmology before it was known that the universe is expanding. Einstein regarded its numerical value as a matter to be settled by experiment—"The curvature constant [Λ] is, however, essentially determinable, and an increase in the precision of data derived from observations will enable us in the future to fix its sign and determine its value" [16].

It is apparent that the cosmological constant corresponds to a constant energy density $\Lambda/(8\pi)$ and a constant negative pressure of the same numerical value. The cosmological constant is sometimes referred to as the vacuum energy density. In any case it is small if not zero ($\Lambda < 10^{-29}$ g/cm^3), as estimated, for example, as the limiting value that would leave Newtonian celestial mechanics unchanged as concerns its predictions for small clusters of galaxies [17]. Its effect is indeed cosmological; stellar structure is unaffected by it. We need not consider the cosmological term further.

The first set of differential equations (2.163) are those that must be satisfied by the metric in empty space outside material bodies and energy concentrations. An example is the gravitational fields outside a star.

The second set of differential equations (2.164) determine the gravitational fields $g^{\mu\nu}$ inside a spacetime region of mass-energy and in addition determine how the mass-energy is arranged by gravity. With appropriate $T^{\mu\nu}$ it would provide the equations of stellar structure. We have yet to fix the constant k. This can be done by looking to the weak field limit where the General Theory of Relativity should agree with Newton's well-tested, weak-field theory.

There are several remarkable notes we can make at this point. Einstein's field equations tell spacetime how to curve and mass-energy how to configure itself and how to move. Spacetime acts upon matter and in turn

is acted upon by matter. This was Einstein's intuition and motivation in seeking a theory that placed spacetime and matter as codeterminers in nature. He was displeased with the Special Theory of Relativity as anything but a local theory, for it gave spacetime an absolute status.

Second, the Einstein field equations are nonlinear in the fields $g^{\mu\nu}$. (This can be verified by tracing back through the objects from which the Einstein tensor is constructed.) Nonlinearity means that the gravitational field interacts with itself. This is because the field carries energy, and mass-energy in any form is a source of gravity. The nonlinearity of the Einstein equations accounts for some of the extraordinary phenomena encountered in strong gravity, including black holes [18] and the reversal of the centrifugal force in their vicinity [19].

We have seen in (2.160) that the Einstein tensor has identically vanishing covariant divergence. Hence (2.164) requires of the matter tensor that

$$T^{\mu\nu}{}_{;\nu} = 0\,. \tag{2.166}$$

The corresponding equation in flat space is

$$T^{\mu\nu}{}_{,\nu} = 0\,. \tag{2.167}$$

The vanishing of the ordinary divergence of the energy-momentum tensor in the Special Theory of Relativity corresponds to the conservation of energy and momentum. However, (2.166) does not assure us of the constancy of any quantity in time. In fact (2.164) ensures that matter and the gravitational fields exchange energy, or in other words do work on each other, for it is the divergence of $G^{\mu\nu} - kT^{\mu\nu}$ that vanishes. So neither matter nor the gravitational field can by itself conserve energy in any sense. There is no contradiction with laboratory experiments performed on earth. Over the dimensions of a typical laboratory, spacetime is essentially flat, and nothing that could be done in a laboratory could possibly disturb this flatness.

This brings us back to the comparison of the weak-field limit between Newton's theory and Einstein's. The inverse-square law of the force between massive objects is not required by the inner structure of Newton's theory. He could have postulated an inverse α law, that force $F \sim Mm/r^{\alpha}$, and then attempted to fit α to the astronomical data of the solar system. Depending on what weight was given to the precession of planets, one would have found a value of α close to two.

Einstein's theory does not possess the flexibility of Newton's in this regard. We saw in (2.104) that Einstein predicts precisely the inverse square law. In this sense, he could claim as his own all the successes of the Newtonian theory in explaining the motion of planets in the solar system. They were computed with the inverse-square law, there being no flexibility in the choice of the power in his theory.

Concerning the precession of planets, an isolated planet in orbit about the sun under an inverse square law is an ellipse whose orientation is fixed

in space. However the total precession of the orbit of Mercury is observed to be about 5600 seconds/century. Most of this is caused by the fact that an earthbound observer is not in an inertial frame far from the sun. For example, suppose that Mercury did not orbit about the sun, but instead held a fixed position. Nevertheless, from the earth it would be appear to move, sometimes to the left of the sun, sometimes to the right, and alternately passing in front of and in back of the sun. Taking account of this correction to the apparent motion of Mercury due to the earth's own motion, the precession of Mercury is about 574 seconds/century. This value is about 43 seconds/century larger than the precession computed by Newtonian physics as due to the perturbation of the orbit by other planets, a small but disturbing discrepancy. An early triumph of Einstein was that he calculated, within the observational errors, the precise value of the excess precession. In Newton's theory only mass contributes to gravity, whereas in Einstein's theory, the kinetic energy of the motion of the planets contributes as well.

2.8 Relativistic Stars

Einstein's field equations are completely general and simple in appearance. They are however exceedingly complicated because of their nonlinear character and because spacetime and matter act upon each other. As already remarked, there is no prior geometry of spacetime. There are a few cases in which solutions can be found in closed form. One of the most important closed-form solutions is the Schwarzschild metric outside a static spherical star. Another is the Kerr metric outside a rotating black hole. Einstein's equations can also be numerically solved as the coupled differential equations for the interior structure of a spherical static star—the Oppenheimer–Volkoff equations.

In this section we take up the important problem of deriving the equations that govern spacetime and the arrangement of matter in the case of relativistic spherical static stars. They are the basic equations that underlie the development of neutron star models in the rest of the book. They also demonstrate the mathematical existence of Schwarzschild black holes. They can also be used to develop white dwarf models, though Newtonian gravity is a good approximation for these stars.

2.8.1 Metric in static isotropic spacetime

We seek solutions to Einstein's field equations in static isotropic regions of spacetime such as would be encountered in the interior and exterior regions of static stars. Under these conditions the $g_{\mu\nu}$ are independent of time ($x^0 \equiv t$) and $g^{0m} = 0$. We choose spatial coordinates $x^1 = r,\ x^2 = \theta,$

and $x^3 = \phi$. The most general form of the line element is then

$$d\tau^2 = U(r)\,dt^2 - V(r)\,dr^2 - W(r)r^2(\,d\theta^2 + \sin^2\theta\,d\phi^2)\,. \tag{2.168}$$

We may replace r by any function of r without disturbing the spherical symmetry. We do so in such a way that $W(r) \equiv 1$. Then we may write

$$d\tau^2 = e^{2\nu(r)}\,dt^2 - e^{2\lambda(r)}\,dr^2 - r^2\,d\theta^2 - r^2\sin^2\theta\,d\phi^2\ , \tag{2.169}$$

where λ, ν are functions only of r. Comparing with $d\tau^2 = g_{\mu\nu}\,dx^\mu\,dx^\nu$, we read off [5]

$$g_{00} = e^{2\nu(r)}, \quad g_{11} = -e^{2\lambda(r)}, \quad g_{22} = -r^2, \quad g_{33} = -r^2\sin^2\theta,$$
$$g_{\mu\nu} = g^{\mu\nu} = 0, \quad (\mu \neq \nu)\,. \tag{2.170}$$

Hence, from $g_{\mu\nu}g^{\nu\rho} = \delta^\rho_\mu$, we have in this special case

$$g_{\mu\mu} = 1/g^{\mu\mu} \qquad \text{(not summed)}\,. \tag{2.171}$$

According to its definition as a contraction of the Riemann tensor, the Ricci tensor can be written

$$R_{\mu\nu} = \Gamma^\alpha_{\mu\alpha,\nu} - \Gamma^\alpha_{\mu\nu,\alpha} - \Gamma^\alpha_{\mu\nu}\Gamma^\beta_{\alpha\beta} + \Gamma^\alpha_{\mu\beta}\Gamma^\beta_{\nu\alpha}\,. \tag{2.172}$$

We can derive the nonvanishing affine connections (2.78), which are symmetric in their lower indices, from the metric tensor whose general form for static isotropic regions was derived above:

$$\begin{array}{ll} \Gamma^1_{00} = \nu'\,e^{2(\nu-\lambda)}\ , & \Gamma^0_{10} = \nu'\ , \\ \Gamma^1_{11} = \lambda'\ , & \Gamma^2_{12} = \Gamma^3_{13} = 1/r\ , \\ \Gamma^1_{22} = -re^{-2\lambda}\ , & \Gamma^3_{23} = \cot\theta\ , \\ \Gamma^1_{33} = -r\sin^2\theta\,e^{-2\lambda}\ , & \Gamma^2_{33} = -\sin\theta\cos\theta\,. \end{array} \tag{2.173}$$

The primes denote differentiation with respect to the r-coordinate. Hence, for static isotropic spacetime

$$\begin{aligned} R_{00} &= \left(-\nu'' + \lambda'\nu' - \nu'^2 - \frac{2\nu'}{r}\right)e^{2(\nu-\lambda)}\ , \\ R_{11} &= \nu'' - \lambda'\nu' + \nu'^2 - \frac{2\lambda'}{r}\ , \\ R_{22} &= (1 + r\nu' - r\lambda')e^{-2\lambda} - 1\ , \\ R_{33} &= R_{22}\sin^2\theta\,. \end{aligned} \tag{2.174}$$

[5]Note that in (2.169) some authors use the opposite signs for time and space components, and some use the functions ν, λ but without the factor 2, or use different notation altogether for the metric. Great care has to be exercised in using results from different sources.

2.8.2 The Schwarzschild solution

In the empty space outside a static star Einstein's equation is $G_{\mu\nu} = 0$, or equivalently

$$R_{\mu\nu} = \tfrac{1}{2} g_{\mu\nu} R\,. \tag{2.175}$$

Multiply by $g^{\alpha\mu}$, and sum on the dummy index to find

$$R^{\alpha}_{\nu} = \tfrac{1}{2} \delta^{\alpha}_{\nu} R\,. \tag{2.176}$$

Contract by setting $\alpha = \nu$, and sum to get

$$R = 2R \quad \Longrightarrow \quad R = 0\,. \tag{2.177}$$

Hence, the vanishing of Einstein's tensor implies

$$G_{\mu\nu} = 0 \quad \Longrightarrow \quad R = 0, \quad R_{\mu\nu} = 0\,. \tag{2.178}$$

In empty space Einstein's equation is equivalent to the vanishing of the Ricci tensor or, equivalently, the scalar curvature. Its form for static isotropic spacetime was worked out in the previous section.

From the vanishing of R_{00}, R_{11} we find that

$$\lambda' + \nu' = 0\,. \tag{2.179}$$

(Do not confuse ν and λ when used to denote indices and when used to denote the metric functions as in the above equation.) For large r, space must be unaffected by the star and therefore flat so that λ and ν tend to zero; therefore

$$\lambda + \nu = 0\,. \tag{2.180}$$

Using these results in $R_{22} = 0$, we find that

$$(1 + 2r\nu')e^{2\nu} = 1\,. \tag{2.181}$$

This condition integrates to

$$g_{00} \equiv e^{2\nu} = 1 - \frac{2GM}{r}\,, \qquad (r > R)\,, \tag{2.182}$$

where M is the constant of integration, and we introduced Newton's constant. Having studied the Newtonian approximation, one identifies M with the mass of the star. From the foregoing results,

$$g_{11} = -e^{2\lambda} = -e^{-2\nu} = -\left(1 - \frac{2GM}{r}\right)^{-1}, \qquad (r > R). \tag{2.183}$$

This completes the derivation of the *Schwarzschild solution* (1916) of Einstein's equations outside a spherical static star. It was the first exact solution found for Einstein's equations. The proper time is

$$d\tau^2 = \left(1 - \frac{2GM}{r}\right)dt^2 - \left(1 - \frac{2GM}{r}\right)^{-1} dr^2 - r^2 d\theta^2 - r^2 \sin^2\theta d\phi^2, \quad (r > R), \tag{2.184}$$

where R, in this context, denotes the radius of the star.

Let us summarize the Schwarzschild solution found above:

$$g_{00}(r) = e^{2\nu(r)} = \left(1 - \frac{2GM}{r}\right), \qquad r > R\,,$$
$$g_{11}(r) = -e^{2\lambda(r)} = -\left(1 - \frac{2GM}{r}\right)^{-1}, \qquad r > R\,,$$

and

$$g_{22}(r) = -r^2, \qquad g_{33}(r,\theta) = -r^2 \sin^2\theta\,. \tag{2.185}$$

Notice that the Schwarzschild metric is singular at the radius $r = r_S \equiv 2M$. This does not mean that spacetime itself is singular at that radius, but only that this particular metric is. Other nonsingular metrics have been found, in particular, the Kruskal-Szerkeres metric [20, 21]. However, further analysis shows that if r_S lies outside the star where the Schwarzschild solution holds, then it is a black hole—no particle or even light can leave the region $r < r_S$. This radius r_S is called the *Schwarzschild radius* or *Schwarzschild horizon.* But since the above metric holds only outside the star, r_S has no special significance if it is smaller than the radius of the star. For then a different metric holds inside the star which does not possess a singularity. We come to this solution shortly.

2.8.3 Riemann tensor outside a Schwarzschild star

If spacetime is flat, then the Riemann curvature tensor vanishes (section 2.6.3). We are now prepared to address the converse (albeit not rigorously): if spacetime is curved some components of the Riemann tensor are finite (which components, of course, will depend upon how convoluted spacetime is).

The metric tensor and, indeed, the affine connection for the empty space outside a massive body were computed in the preceding section. We have seen in Section 2.3.3 that massive bodies curve spacetime. So we know that the Schwarzschild metric tensor refers to curved spacetime. Referring to the definition of the Riemann tensor (2.144) and the specific form that the affine connection takes for a static spherical star (2.173), we can compute

$$R^1_{010} = \left(\nu'' + 2\nu'^2 - \nu'\lambda'\right)e^{2(\nu-\lambda)}\,. \tag{2.186}$$

Thus we exhibit at least one nonvanishing component of the Riemann tensor in the curved spacetime outside a Schwarzschild star. This suggests that Riemann is not identically zero in curved spacetime. An actual proof that if Riemann is finite then spacetime is curved requires the formulation of parallel transport, which we do not take up here. We declare, without rigorous proof, that the Riemann tensor vanishes if and only if spacetime is flat. Notice that, far from an isolated star where spacetime approaches flatness, Riemann approaches zero as it should.

2.8.4 Energy-Momentum tensor of matter

From the success of Newtonian physics in describing celestial mechanics and other weak gravitational field phenomena, we know that mass is a source of gravity. From the experimental verifications of the Special Theory of Relativity, we know that all forms of energy are equivalent and must contribute equally as sources of gravity. Normally of course, it is mass that dominates, and that is why Newtonian physics is so accurate under the typical conditions mentioned above.

An essential aspect of Einstein's curvature tensor is that it automatically has vanishing covariant divergence (2.160). It is also a symmetric second-rank tensor. Accordingly, mass-energy—the source of the gravitational field—must be incorporated into a divergenceless, symmetric, second-rank tensor in flat space. As a tensor, it can be transcribed immediately to its form in an arbitrary spacetime frame by the general covariance principle. Such a tensor is the energy-momentum tensor.

In other parts of this book we shall be interested in specific theories of dense matter from which we will be able to explicitly construct the energy-momentum tensor of the theory. Here we are interested in the general form such a tensor takes. Frequently, matter may be regarded as a perfect fluid. The fluid velocity is assumed to vary continuously from point to point. The perfect fluid energy-momentum tensor in the Special Theory of Relativity can be expressed in terms of the local values of the pressure p and energy density ϵ as in (2.35). The General Relativistic energy-momentum tensor can be written immediately using the Principle of General Covariance spelled out on page 32[6]:

$$T^{\mu\nu} = -pg^{\mu\nu} + (p+\epsilon)u^\mu u^\nu \,, \tag{2.187}$$

$$g_{\mu\nu}u^\mu u^\nu = 1 \,. \tag{2.188}$$

[6]Carrying over to General Relativity the assumption about the perfect fluid character of the medium presupposes that the local region of flat spacetime (guaranteed by the equivalence principle) is actually sufficiently large that the assumption is valid. This will have to be verified in any particular application.

In the above equations, u^μ is the local fluid four-velocity

$$u^\mu = \frac{dx^\mu}{d\tau} \tag{2.189}$$

and satisfies (2.188) because of (2.39).

The pressure and total energy density (including mass) are related by the equation of state of matter, frequently written in the form

$$p = p(\epsilon) \tag{2.190}$$

or its inverse, where p and ϵ are the pressure and energy density (including mass) in the local rest-frame of the fluid. In the next section we shall see how the equations for stellar structure involve these quantities and this relationship.

2.8.5 The Oppenheimer–Volkoff equations

We are now prepared to derive the differential equations for the structure of a static, spherically symmetric, relativistic star. For the region outside a star, we found that the vanishing of the Einstein tensor was equivalent to the vanishing of the Ricci tensor or the scalar curvature. This is not the case for the interior of the star. We need both the Ricci tensor and scalar curvature to construct the Einstein tensor. The general form of the metric for a static isotropic spacetime was obtained in (2.170). From Section 2.8.1 we find the scalar curvature,

$$\begin{aligned} R &= g^{\mu\nu}R_{\mu\nu} = e^{-2\nu}R_{00} - e^{-2\lambda}R_{11} - \frac{2}{r^2}R_{22} \\ &= e^{-2\lambda}\left\{-2\nu'' + 2\lambda'\nu' - 2\nu'^2 - \frac{2}{r^2} + 4\frac{\lambda'}{r} - 4\frac{\nu'}{r}\right\} + \frac{2}{r^2}\,. \end{aligned} \tag{2.191}$$

It is more convenient to work with mixed tensors. For example,

$$G_0^{\ 0} = R_0^{\ 0} - \tfrac{1}{2}R \tag{2.192}$$

is obtained with the results of Section 2.8.1 for a static isotropic field, namely,

$$g_0^0 = g_{0\nu}g^{0\nu} = g_{00}g^{00} = 1\,. \tag{2.193}$$

So using results obtained earlier in this section we can find that the components of the Einstein tensor are

$$\begin{aligned} r^2G_0^{\ 0} &\equiv e^{-2\lambda}(1 - 2r\lambda') - 1 = -\frac{d}{dr}[r(1 - e^{-2\lambda})]\,, \\ r^2G_1^{\ 1} &\equiv e^{-2\lambda}(1 + 2r\nu') - 1\,, \\ G_2^{\ 2} &\equiv e^{-2\lambda}(\nu'' + \nu'^2 - \lambda'\nu' + \frac{\nu' - \lambda'}{r})\,, \\ G_3^{\ 3} &= G_2^{\ 2}. \end{aligned} \tag{2.194}$$

Because of the assumption that the star is static, the three-velocity of every fluid element is zero, so

$$u^\mu = 0 \quad (\mu \neq 0), \qquad u^0 = 1/\sqrt{g_{00}}\,, \tag{2.195}$$

according to (2.188). For the energy-momentum tensor expressed as a mixed tensor, we have the nonzero components in the present metric,

$$T_0{}^0 = \epsilon, \quad T_\mu{}^\mu = -p, \quad (\mu \neq 0). \tag{2.196}$$

So the (00) component of the Einstein equations gives

$$r^2 G_0{}^0 = -\frac{d}{dr}\{r(1 - e^{-2\lambda(r)})\} = kr^2 T_0{}^0 = kr^2 \epsilon(r)\,. \tag{2.197}$$

This can be integrated immediately to yield

$$e^{-2\lambda(r)} = 1 + \frac{k}{r}\int_0^r \epsilon(r) r^2 dr\,. \tag{2.198}$$

Let us define

$$M(r) \equiv 4\pi \int_0^r \epsilon(r) r^2 dr\ , \tag{2.199}$$

and let R denote the radius of the star, the radial coordinate exterior to which the pressure vanishes. Zero pressure defines the edge of the star because zero pressure can support no material against the gravitational attraction from within. Denote the corresponding value of $M(R)$ by

$$M \equiv M(R)\,. \tag{2.200}$$

Now comparing (2.104, 2.182, 2.183) we see that, to obtain agreement with the Newtonian limit, we must choose

$$k = -8\pi G \tag{2.201}$$

and interpret M as the *gravitational mass* of the star and, therefore, $M(r)$ as the mass within the coordinate r. So Einstein's field equations can now be written

$$G^{\mu\nu} = -8\pi G T^{\mu\nu}. \tag{2.202}$$

From the above, we have found so far that

$$g_{11}(r) = -e^{2\lambda(r)} = -\Big(1 - \frac{2GM(r)}{r}\Big)^{-1}\ , \tag{2.203}$$

which agrees with (2.183), but now we see that $g_{11}(r)$ has the same form inside and outside the star although it is the included mass $M(r)$, not the total mass, that appears in the interior solution.

Having learned the constant of proportionality in Einstein's equations (2.202), let us now write out the field equations for a spherically symetric static star, including the one we have already solved. In passing we note that our solution gives a relationship between the included mass $M(r)$ at any radial coordinate and the metric function $g_{11}(r)$ or $\lambda(r)$, but we have yet to learn how to compute one or the other. The differential equations from (2.194) are

$$G_0^{\ 0} \equiv e^{-2\lambda}\big(1-\frac{2\lambda'}{r}\big)-\frac{1}{r^2}=-8\pi G\epsilon(r)\,, \tag{2.204}$$

$$G_1^{\ 1} \equiv e^{-2\lambda}\big(\frac{1}{r^2}+\frac{2\nu'}{r}\big)-\frac{1}{r^2}=8\pi Gp(r)\,, \tag{2.205}$$

$$G_2^{\ 2} \equiv e^{-2\lambda}\big(\nu''+\nu'^2-\lambda'\nu'+\frac{\nu'-\lambda'}{r}\big)=8\pi Gp(r)\,, \tag{2.206}$$

$$G_3^{\ 3} = G_2^{\ 2}=8\pi Gp(r)\,. \tag{2.207}$$

The last equation contains no information additional to that provided by those preceding it.

To simplify notation, choose units so that $G=c=1$. Solve (2.204) to find

$$2r\lambda'=(1-8\pi r^2\epsilon)e^{2\lambda}-1 \tag{2.208}$$

and (2.205) to find

$$2r\nu'=(1+8\pi r^2p)e^{2\lambda}-1\,. \tag{2.209}$$

Take the derivative of (2.209):

$$2r\nu'+2r^2\nu''=\Big[2r\lambda'(1+8\pi r^2p)+(16\pi r^2p+8\pi r^3p')\Big]e^{2\lambda}\,.$$

Solve for ν'' using (2.209, 2.208):

$$2r^2\nu''=1+(16\pi r^2p+8\pi r^3p')e^{2\lambda}-(1+8\pi r^2p)(1-8\pi r^2\epsilon)e^{4\lambda}\,. \tag{2.210}$$

Square (2.209) to obtain the result

$$2r^2\nu'^2=\tfrac{1}{2}(1+8\pi r^2p)^2e^{4\lambda}-(1+8\pi r^2p)e^{2\lambda}-\tfrac{1}{2}\,. \tag{2.211}$$

We now have expressions for λ', ν', ν'', and ν'^2 in terms of p, p', ϵ, and $e^{2\lambda}$ the latter of which, according to (2.203), can be expressed in terms of the included mass. Therefore the metric can be eliminated altogether by substituting in the remaining field equation (2.206). After a number of cancellations, we emerge with the result

$$\frac{dp}{dr}=-\frac{\big[p(r)+\epsilon(r)\big]\big[M(r)+4\pi r^3p(r)\big]}{r\big(r-2M(r)\big)}\,. \tag{2.212}$$

This and equation (2.199) represent the reduction of Einstein's equations for the interior of a spherical, static, relativistic star. These equations are frequently referred to as the Oppenheimer–Volkoff equations. The stars they describe—static and spherically symmetric—are sometimes referred to as Schwarzschild stars.

It will be noted that since the radial distribution of pressure is prescribed by the above equation, so is the distribution of energy density through the equation of state $\epsilon(r) = \epsilon\big(p(r)\big)$.

It may seem curious that the expression (2.199) for mass has precisely the same form as one would write in nonrelativistic physics for the mass whose distribution is given by $\epsilon(r)$. How can this be, inasmuch as we know that spacetime is curved by mass and mass in turn is moved and arranged by spacetime in accord with Einstein's equations? The answer is that (2.199) is not a prescription for computing the total mass of an arbitrary distribution $\epsilon(r)$. There are no arbitrary distributions in gravity; rather $\epsilon(r)$ is precisely prescribed by another of Einstein's equations (2.212). As such, M comprises the mass of the star and its gravitational field. Because of the mutual interaction of mass-energy and spacetime, there is no meaning to the question "What is the mass of the star?" in isolation from the field energy. That is why we refer to M as the gravitational mass or the mass-energy of the star. It is the only type of mass that enters Einstein's theory and is the only stellar mass to which we will refer in this book. Therefore, we shall generally refer to a star's mass as simply the mass without the adjective 'gravitational'. Sometimes a so-called proper mass is defined. It appears nowhere in Einstein's equations and is an artifact.

It does make sense to inquire about the mass of the totality of nucleons in a star if they were dispersed to infinity. This mass is referred to as the baryon mass. The difference between gravitational mass and baryon mass, if negative, is the gravitational binding of the star. As we shall find, the gravitational binding is of the order of 100 MeV per nucleon in stars near the mass limit as compared to 10 MeV binding by the strong force in nuclei.

Notice that, according to (2.212), the pressure is a monotonic decreasing function from the inside of the star to its edge because all the factors in (2.212) are positive, leaving the explicit negative sign. This makes sense. Any region is weighted down by all that lies above. We have assumed that the denominator in (2.212) is positive. Overall this is true of the earth, the sun, and a neutron star. In fact, as we shall see in Section 3.12, $2M/R < 8/9$ for any static stable star. It can also be shown that $2M(r)/r < 1$ for all regions of a stable star [22]; so indeed we are justified in taking the last factor in (2.212) as positive.

In (2.184) we saw a singularity in the Schwarzschild solution if a star lies within $r = 2M$. Such stars are highly relativistic objects called black holes. No light or particle can escape from within their Schwarzschild radius. A luminous star is highly nonrelativistic. A neutron star is relativistic. Newtonian gravity would not produce the same results as General Relativity.

This fact is clear, given that $2M$ can be as large as $\frac{8}{9}R$ for a neutron star, which makes the denominator of (2.212) a large correction (as much as 9 instead of 1).

We already have an expression for the radial metric function both inside and outside a star. It is sometimes useful to have the time metric function g_{00}. No general expression for the solution can be obtained, as for g_{11}, (2.203). However using the latter in (2.209) we obtain a differential equation,

$$\frac{d\nu}{dr} = \frac{M(r) + 4\pi r^3 p(r)}{r(r - 2M(r))}\,. \tag{2.213}$$

The solution must match the exterior solution (2.183). This is easily accomplished. If $\nu(r)$ is a solution, we can add any constant to it and still have a solution. We obtain the correct condition at R if we make the change

$$\nu(r) \longrightarrow \nu(r) - \nu(R) + \tfrac{1}{2}\ln\Big(1 - \frac{2M}{R}\Big), \qquad r \le R. \tag{2.214}$$

We can start the integration at $r = 0$ with any convenient value of $\nu(0)$, say zero.

Alternately, once the Oppenheimer–Volkoff equations have been solved so that $p(r)$ and hence $\epsilon(r)$ are known, one can find $\nu(r)$ by integration of

$$\frac{d\nu}{dr} = -\frac{1}{p+\epsilon}\frac{dp}{dr}\,, \tag{2.215}$$

namely,

$$\nu(r) = -\int_0^r \frac{1}{p+\epsilon}\frac{dp}{dr} + \text{constant}, \qquad \nu(\infty) = 0\,. \tag{2.216}$$

The Oppenheimer–Volkoff equations can be integrated from the origin with the initial conditions $M(0) = 0$ and an arbitrary value for the central energy density $\epsilon(0)$, until the pressure $p(r)$ becomes zero at, say R. Since zero pressure can support no overlying matter against the gravitational attraction, R defines the gravitational radius of the star and $M(R)$ its gravitational mass. For the given equation of state, there is a unique relationship between the mass and central density $\epsilon(0)$. So for each possible equation of state , there is a unique family of stars, parameterized by, say, the central density or the central pressure. Such a family is often referred to as the *single parameter sequence* of stars corresponding to the given equation of state.

2.8.6 Gravitational collapse and limiting mass

In Newtonian physics mass alone generates gravity. In the Special Theory of Relativity mass is equivalent to energy so in the general theory all forms

of energy contribute to gravity. It is surprising that pressure also plays a most consequential role in the structure of relativistic stars beyond the role it plays in Newtonian gravity. Pressure supports stars against gravity, but surprisingly, it ultimately assures the gravitational collapse of relativistic stars whose mass lies above a certain limit.

Pressure appears together with energy density in determining the monotonic decrease of pressure (2.212) in a relativistic star. Gravity acts to compress the material of the star. As it does so, the pressure of the material is increased toward the center. But inasmuch as pressure appears on the right side of the equation, this increase serves to further enhance the grasp of gravity on the material. Therefore for stars of increasing mass, for which the supporting pressure must correspondingly increase, the pressure gradient (which is negative) is increased in magnitude, making the radius of the star smaller since its edge necessarily occurs at $p = 0$. As a consequence, if the mass of a relativistic star exceeds a critical value, there is no escape from gravitational collapse to a black hole [23]. Whatever the equation of state, the one-parameter sequence of stable configurations belonging to that equation of state is terminated by a maximum-mass compact star. The mass of this star is referred to as the *mass limit* or *limiting mass* of the sequence.

2.9 Action Principle in Gravity

We arrived at Einstein's equations by noting the vanishing divergence of the Einstein curvature tensor and equating it to the divergenceless, energy-momentum tensor of matter as the source of the gravitational field. We did not comment on how the energy-momentum tensor might be obtained. In general, this tensor is not given but must be calculated from a theory of matter. In what frame should the theory be solved? Evidently in the general frame of the gravitational field. But this is an entirely different problem than is normally solved in many-body theory.

We are accustomed to solving problems in nuclear and particle theory in flat spacetime (or even flat space) in which the constant Minkowski metric $\eta_{\mu\nu}$ appears, not a general and as yet unspecified field $g_{\mu\nu}(x)$. In passing from the energy-momentum tensor in a Lorentz frame (2.35) to its form (2.187) in a general frame by means of the principle of general covariance, as was done in deriving the Oppenheimer–Volkoff equations of stellar structure, a tacit assumption is made. The local region over which every Lorentz frame extends is assumed to be sufficiently large that the equations of motion of the matter fields can be solved in a Lorentz frame, that is, in the absence of gravity, and the corresponding energy-momentum tensor constructed from the solution for such a region.

As we shall see in the next chapter, the local inertial frames in the gravitational field of neutron stars (and therefore for the less dense white dwarfs

and all other stars) are sufficiently extensive that the matter from which they are constituted can be described by theories in flat spacetime. We shall refer to such a situation as a partial decoupling of matter from gravity. In other words, in the equations of motion for the matter and radiation fields, the Minkowski metric can be used, but the general metric functions $g_{\mu\nu}(x)$ reappear on the right side of Einstein's field equations in the energy-momentum tensor referred to a general frame in accord with the principle of general covariance. Therefore the metric functions $g_{\mu\nu}(x)$ still appear on both sides of Einstein's field equations, and matter shapes spacetime just as spacetime shapes matter.

There are conceivable situations where the partial decoupling just described may not hold. In that case the equations of motion themselves contain, not the Minkowski metric tensor (a diagonal tensor with constant elements), but the general, spacetime-dependent, metric tensor. This is the fully coupled problem and obviously would be enormously difficult to solve. While we do not encounter this situation in this book (see as an example where strong coupling is used, ref. [24]), nonetheless it is worth seeing in symbolic form what the fully coupled problem looks like. The expectation that the stress-energy tensor should be obtained in general from a theory of matter by solving the field equations of the theory in a general gravitational field will be verified.

We employ the gravitational action principle. As in all cases, the Lagrangian of gravity ought to be a scalar. We have encountered the Ricci scalar curvature $R = g^{\mu\nu}R_{\mu\nu}$, and from it, as Hilbert did, the Lagrangian density can be formed (with a prefactor that can be known only in hindsight):

$$\mathcal{L}_g = -\frac{1}{16\pi G} R\sqrt{-g}\,. \tag{2.217}$$

Here G is Newton's constant and g is the determinant of the metric $g_{\mu\nu}$, which is negative. We also define the Lagrangian density

$$\mathcal{L}_m = L_m\sqrt{-g} \tag{2.218}$$

from the Lagrangian L_m of the matter fields which we denote collectively as ϕ. The total action is

$$I = \int (\mathcal{L}_g + \mathcal{L}_m)\, d^4x\,. \tag{2.219}$$

The coupled field equations for the matter and metric functions emerge as the conditions that yield vanishing variation of the action with respect to all the fields—gravitational described by $g_{\mu\nu}$ and matter fields described by ϕ. The manipulations are quite tedious and not germane to our purpose. The field equations obtained are

$$\frac{\delta\mathcal{L}_m}{\delta\phi} - \partial_\mu \frac{\delta\mathcal{L}_m}{\delta(\partial_\mu\phi)} = 0\,, \tag{2.220}$$

$$G^{\mu\nu} = -8\pi G T^{\mu\nu} , \tag{2.221}$$

where $G^{\mu\nu} \equiv R^{\mu\nu} - \frac{1}{2} g^{\mu\nu} R$ is the Einstein tensor. The first of the field equations reduces to the familiar Euler–Lagrange equations in the limit of weak gravitational fields. We shall encounter them in studying theories of dense nuclear matter. The second are Einstein's field equations (2.202).

The matter-radiation energy-momentum tensor that emerges from the variational principle is given by

$$T^{\mu\nu} \equiv -g^{\mu\nu} L_m + 2 \frac{\partial L_m}{\partial g_{\mu\nu}} . \tag{2.222}$$

The second term is

$$2 \frac{\partial L_m}{\partial g_{\mu\nu}} = 2 \frac{\partial L_m}{\partial(\partial_\alpha \phi)} \frac{1}{2} \frac{\partial(g_{\alpha\beta} \partial^\beta \phi)}{\partial g_{\mu\nu}} = \frac{\partial L_m}{\partial(\partial_\mu \phi)} \partial^\nu \phi .$$

Combining these results yields the canonical form of the energy-momentum tensor in field theory (for example, see (2.8.4)) except that the Minkowski tensor is replaced by the general metric of gravity. Thus we have

$$T^{\mu\nu} = -g^{\mu\nu} L_m + \sum_\phi \frac{\partial L_m}{\partial(\partial_\mu \phi)} g^{\nu\alpha} \partial_\alpha \phi , \tag{2.223}$$

where the sum is over the various fields ϕ in L_m. In this way we see how the equations couple all matter and gravitational fields, $\phi(x), \cdots, g^{\mu\nu}(x)$ in the general case.

3

Compact Stars: From Dwarfs to Black Holes

3.1 Birth and Death of Stars

> "A star is drawing on some vast reservoir of energy.... This reservoir can scarcely be other than the subatomic energy.... There is sufficient in the Sun to maintain its output of heat for 15 billion years."
> *A. Eddington*, 1920 [25]

Clouds of interstellar gas consisting mostly of molecular hydrogen and a little dust are the incubators of stars. The horsehead nebula in Orion is an especially beautiful example. The clouds are diffuse and highly nonuniform, with clumps and filaments interspersed throughout. The gas spans a wide range of temperature. Most of it is cold at 10 K, but some regions are as hot as 2000 K. Interstellar clouds range in size from less than a light year to several hundred light years and in mass from 10 to $10^7 M_\odot$. A compression of the order 10^{20} is involved in forming a star from this diffuse gas. Stars more massive than a few $M_\odot$ are observed to form in small groups in the densest regions of the clouds. The motion of a given star often suggests the gravitational influence of several nearby stars. About half of all stars are in binaries.

Important factors in stellar formation are gravity, dust, gas pressure, rotation, magnetic fields, winds and radiation from nearby young stars, and radiative shock waves. Our understanding of how these factors conspire to induce collapse of a relatively small region of an otherwise long-lived dynamic, but stable, *molecular cloud* is at a rudimentary level.

The dust in molecular clouds originates on the cool stellar surfaces of *supergiants*, massive stars in a late stage of stellar evolution. Dust shields cloud interiors from ultraviolet starlight, enabling their centers to cool. With lower thermal pressure, gravitational collapse of the denser regions of clouds becomes inevitable.

At some stage a perturbation (such as the passage of a shock wave or of a shell of expanding gas from a supernova remnant) induces an instability in a critical mass of cloud. Sir James Jeans derived the critical mass (now

TABLE 3.1. Evolutionary times of stars

$M/M_\odot$	years
30	5×10^6
15	1×10^7
10	2×10^7
5	7×10^7
1	1×10^{10}
0.1	3×10^{12}

known as the Jeans mass)[1] in the early twentieth century. A clump of gas then begins a fall toward its mass center under the attraction of gravity. Gravitational energy is converted to heat by the compression. The opacity of the gas increases as its density and establishes a temperature and thermal pressure gradient which approximately balances gravity in a state of quasi-hydrostatic equilibrium. Energy loss by radiation at the *protostar's* surface causes further slow contraction and heating until the core temperature rises to the ignition point for fusing hydrogen into helium. Thereafter fusion becomes the dominant energy source and the thermal and radiation pressure will now nearly balance gravity for millions to billions of years, a time scale depending approximately on the inverse square of the stellar mass (Table 3.1).

The protostar has now joined the *main sequence* of stars, the evolutionary pathway of stars first proposed by H. N. Russell. The star will spend most of its luminous life in this state of suspended collapse as it burns its large store of hydrogen, slowly radiating energy from its surface.

Thermonuclear fusion[2] provides the energy for the "great furnace", in the phrase of Eddington, which evolves stars through the various stages of combustion— helium, carbon, neon, oxygen, magnesium, and silicon. Fusion will end when iron, the most bound nuclear species, is reached. Beyond iron, fusion is no longer exothermic.

After hydrogen is spent in the core, the next phase of burning—helium—will commence. Hydrogen in a surrounding shell will continue to burn. The star is hottest in its center and heat is transported by radiation, conduction and convection to the surface where it is radiated. Ever higher temperatures are required to drive quantum mechanical nuclear tunnelling—first explained by George Gamow—through the increasing Coulomb barriers along the reaction chain. Hydrogen and then helium burning in the core

[1]The Jeans mass depends sensitively on the temperature of the gas cloud.

[2]Thermonuclear fusion refers to nuclear fusion induced by tunneling through the Coulomb barrier between nuclei. Thermal motion provides the energy for tunnelling. Fusion is exothermic up to iron.

sustain the star on the main sequence for most of its life. As helium burns, a carbon core is formed. Concentric burning shells are established as one element after another is synthesized [26]. Carbon burning in the core lasts for only a few thousand years. Copious gamma rays in the core produce electron-positron pairs which annihilate producing neutrino pairs. Neutrino losses increase as a high power of the temperature. At this stage the loss is so great that succeeding burning stages progress ever more rapidly—oxygen in a year, silicon in a week. At the exhaustion of each elemental fuel, the core contracts further until the ignition temperature for the next step in the chain is reached. In some cases the heat output from combustion in a succeeding step will be so great as to cause a reexpansion of the outer parts of the star.

The cessation of nuclear fusion signals the end of the luminous stage of the star. The duration of the fusion stage (in which a star spends most of its life) as well as its final evolution depends on the stellar mass. Combustion to the iron end point is attained in massive stars[3] which end through a complex terminal stage either as neutron stars or black holes. Combustion is slower and incomplete in light stars. They end as white dwarfs. Whatever the final end point—dwarf, neutron star, or black hole—it is the gravity of the star's mass that drives stellar evolution and its rate from beginning to end.

For light stars up to a few solar masses, contraction begins again when hydrogen is exhausted in the core. As the temperature increases, hydrogen begins to burn in the outer layers. The envelope expands slowly to become a *red giant* while the core continues to contract and heat. At 10^8 K three helium nuclei fuse to form carbon followed by an additional helium to form oxygen. These reactions sometimes begin explosively. Eventually, pulsations in the envelope become unstable, and most of the star is shaken off to form a *planetary nebula*.

The remaining core of the star is composed mostly of helium, carbon, or oxygen (sometimes a mixture) depending on how far the reactions proceeded before the instability removed the compressing weight of the bulk of the star. With insufficient mass to maintain combustion temperature, the core contracts under its own gravity to form a white dwarf, a star whose high surface temperature (8000 K) makes it appear white. A white dwarf has a radius of a few thousand kilometers and an average density of the order of 10^6 that of the earth. (See Table 3.2). After formation, a white dwarf radiates the residue of its earlier hot existence as photons for 10^{10} years. It cools, crystallizes, and disappears as a *black dwarf*. It is possible that the universe is not yet old enough for the final state of dwarfs to have formed.

Because of the low mass of the progenitor, gravity propels light stars through their evolution at a much slower rate than massive stars. Stars

[3]We shall usually use massive stars to refer to those with mass $M \geq 8M_\odot$.

that terminate their life as dwarfs typically attain great age before the dwarf stage. The sun, presently of age 4.5×10^9 years, is expected to live to 12 billion years before collapsing to the dwarf stage, according to modern theory. Eddington's 1920 estimate is in remarkable agreement.

Stars above eight solar masses evolve more rapidly than the progenitors of dwarfs. Most importantly, the thermonuclear reactions proceed further, the star becoming ever hotter until it expands into a super red giant.[4] In the central region of the star, the reactions burn to the iron end point. The core of the star is now supported against collapse only by the pressure of degenerate nonrelativistic electrons. Nuclear burning continues in surrounding shells of Si, O, ... overlying the now inert, central region of iron. The core has a radius of only several thousand kilometers lying within the red supergiant of radius $> 10^8$ km.

Burning in the outer shells adds to the iron core mass. Gravity crushes the core to such a density that electrons become relativistic. The pressure they provide now increases less rapidly with increasing density than was the case at the earlier stage when the electrons were nonrelativistic. Moreover, the kinetic energies of the relativistic electrons have reached the point that capture on protons—*inverse beta decay*—produces an energetically more favorable state. The supporting electron pressure is thus diminished below the point at which it can support further growth in the mass of the iron core against gravity. The core has attained its maximum possible mass named after S. Chandrasekhar who first discovered the limit for an object supported by the pressure of ultrarelativistic, degenerate electrons.

The core then commences a rapid implosion taking less than a second. It becomes extremely hot, attaining temperatures toward the end of collapse of the order of tens of MeV ($\sim 10^{11}$ K). The core is bloated with energetic neutrinos produced by inverse beta decay in the continued *neutronization* of the core material during collapse. The cross-section for the interaction of energetic neutrinos and nuclei is sufficiently large to trap the neutrinos by collision in the dense imploding core. They escape only by the relatively slow process of diffusion. As the core matter is crushed to high density, the Fermi energy of the thermalized electrons and neutrinos rises. Their pressure, together perhaps with the short-range repulsion between nucleons, resists further compression.

The infalling core material rebounds from the stiffened core sending outward a shock wave originating somewhere in the core interior. As the shock travels outward, its energy is dissipated by neutrino losses and by photodisintegration of all nuclei in its path. The shock stalls at a few hundred kilometers from the stellar center.

When the stellar material above the region occupied by the core prior to its implosion is no longer supported by the core, a decompression wave travels outward at the speed of sound in the diffuse stellar material of the

[4]For massive stars the red giant stage is sometimes referred to as supergiant.

red giant, and freefall of this material commences. The signal takes a long time to reach the edge of the star compared to the time from the core implosion to shock rebound and its subsequent stall.

The freefalling material is arrested as it meets the stalled shock front turning the latter into an accretion shock. The infalling matter heats the region of the accretion shock, and at the same time its momentum and mass exert an inward-directed pressure gradient.

A rarefied bubble region develops between the high-density core and the accreting shock front. Neutrino pairs diffusing from the hot interior, annihilate, heat, and expand the bubble. Through a complex (and not completely understood) interplay of convection and neutrino heating, a fraction (less than one percent) of the immense gravitational binding energy of the neutron star is transported to the accretion front. It is this small fraction which provides the kinetic energy for the ejection of all but the core of the progenitor star in a *supernova* explosion.

An elementary calculation that we shall shortly do reveals that the energy release of the neutron star (foreseen many years ago by Baade and Zwicky (1934) [1] as the engine driving supernovae) is $\sim 10^{53}$ ergs. It has taken some thirty years since the early work of Colgate and White (1966) [27] to arrive at a partial understanding of how a small fraction of this energy release, not much more nor less than 1/100, is so reliably converted to the kinetic energy of ejection (see especially Colgate in [28]).

For those stellar evolutions that end in a supernova explosion, the hot collapsed core or *protoneutron* star, with temperature of tens of MeV, loses its trapped neutrinos over an interval of some seconds and cools to an MeV or less [29]. At that point the collapsed core has reached its final equilibrium composition of neutrons, protons, hyperons, leptons, and possibly quarks. Thus is born a *neutron star* of radius about ten kilometers and average density 10^{14} times greater than that of earth. The star continues to cool for millions of years by the slow diffusion of photons to the surface and their radiation into space.

The bulk of the star blown off in the explosion, the *supernova remnant*, expands outward at great velocity (10,000 km/s) sweeping up interstellar gas. The remnant is visible at all wavelengths between radio and X rays, signifying the richness of the processes taking place in the ejecta and between ejecta and the interstellar medium, including molecular clouds. Only in some cases have associations between supernova remnants and *pulsars*, rotating magnetized neutron stars, been made. The remnants are visible for only about 10^4 to 10^5 years; pulsars are active for $\sim 10^8$ years or more.

For some unknown fraction of massive collapsing stars, the explosion is believed to fail or to fail to eject sufficient infalling material. The progenitor star therefore continues its *prompt* gravitational collapse to a black hole of mass about equal to the presupernova star ($> 8M_\odot$). This is so because there is a maximum mass called the Oppenheimer–Volkoff mass limit that can be sustained against gravitational collapse by the pressure of degenerate

neutrons and their repulsive interaction. Although not many neutron star masses are known, they appear to be clustered around $1.4M_\odot$, close to the Chandrasekhar limit for a degenerate iron core which undergoes implosion at the end of the luminous stage. If the limit for neutron star masses is not far above this, only a small amount of accretion onto the collapsed core will push it beyond the limit.

There is an additional mechanism for *delayed* collapse after formation of a protoneutron star and ejection in a supernova of most of the star. Some of the nucleons and high energy electrons in the protoneutron star can find a lower energy state as the last of the neutrinos are lost. This phenomenon is *hyperonization*, a process analogous to neutronization, in which the pressure of neutrons and protons is diminished by their conversion to hyperons [30]. Hyperonization may bring about the collapse of stars hovering near the limiting mass [31].

Thus, continued gravitational collapse can occur under several circumstances. Prompt collapse will result if the explosion fails altogether, creating a *black hole* having the approximate mass of the progenitor, more than $8M_\odot$ and perhaps up to $50M_\odot$. Delayed collapse may occur if the protoneutron star is close to the mass limit even if an explosion does eject most of the progenitor star (Section 9.7). In the second case, a low mass black hole ($\sim 1.5M_\odot$) will be created. Black holes of about this mass can also be created in the *accretion-induced collapse* of neutron stars in binary systems.[5] Accretion is a slow process. The surface of the neutron star will be heated by infalling material. When the infall rate is such that the radiation pressure from the hot surface counterbalances the gravitational force acting on the infalling material, a limit is reached. It is known as the Eddington limit.

Another type of black hole deserves mention. It is not the end point in the evolution of a single star, but rather is thought to be formed by the condensation of a dense *star-cluster* [32]. Such supermassive black holes as these are probably the maelstroms of *active galactic nuclei.*

Once formed, isolated neutron stars and white dwarfs will live almost unchanged forever. They will slowly cool, and their magnetic fields will decay. Pulsars will eventually become invisible, their emission terminated when the magnetic field becomes too weak. However the internal baryon constitution of neutron stars will be frozen within a few seconds of birth, once the temperature has fallen below a few MeV. White dwarfs will become crystals after cooling for billions of years, when their temperature falls below the lattice energy. There is no reason other than an encounter with another star that they should not endure forever as dead stars.

Let us briefly consider another perspective. Of all astrophysical phenom-

[5]Compact stars in binary systems can slowly accrete matter from a less dense companion. Accretion onto a neutron star or white dwarf near their respective mass limits can cause collapse to a black hole or white dwarf, respectively.

ena, none are more essential to life as we know it than the evolution of stars and the eventual explosion of some of them in supernovae. Only a few of the lightest elements were produced during the primordial nucleosynthesis in the big bang, none heavier then ^{7}Li [33, 34]. Other elements, up to iron, are synthesized by thermonuclear reactions during the 10^7 year evolution of massive stars, the heavier of these in the last few days of the life of the presupernova star. The heaviest elements are synthesized in supernovae explosions [26].

We ourselves (like the earth and all life on it) are made in large part from the material of earlier generations of stars. Even now, 10^{10} years after the big bang and a thousand generations of massive stars latter, the abundance of elements is still dominated by hydrogen. Nevertheless, the abundance of elements changes slightly with each succeeding stellar generation. The earliest and oldest stars contain negligible amounts of the elements heavier than helium. Younger ones are richer in heavier elements, referred as their *metallicity*. The lowest energy state of nucleons and nuclei is ^{56}Fe. This is the ground state toward which the universe is evolving on an unimaginably long timescale. It is interesting to note, that since the extinction of the dinosaurs 7×10^7 years ago, seven generations of massive stars have been born and died.

3.2 Objective

In the last chapter we saw that, in our universe, populated by massive objects, galaxies, stars and so on, spacetime is curved. This fact, so amazing because of our acquaintance with Euclidean geometry and its apparent accuracy in our vicinity, was arrived at by pursuing the underlying meaning of the equivalence of inertial and gravitational masses. From Schwarzschild's solution to Einstein's equations, we learned the metric of this curved spacetime in the empty space outside a static star.

The interior problem is the central concern of this book, and it is rather more delicate. We are accustomed to thinking of matter in flat spacetime, in terms of the Special Theory of Relativity. Our theories of nuclear matter are worked out in such a frame or even in flat space. By computing properties of matter in flat spacetime (the equation of state for example), a question of principle must be addressed when the matter resides in strong gravitational fields. Is the local inertial (Lorentz) frame surrounding each spacetime point in the star sufficiently large to justify solving the equations of motion for matter in flat spacetime and, constructing from the solution, the equation of state and the energy-momentum tensor for the relevant densities in the star? If not, we would have to solve the fully coupled problem of gravity simultaneously with the equations of motion containing the general metric functions and the matter and radiation fields (2.220, 2.221).

In this chapter we introduce essential material and concepts for under-

standing the constitution of compact stars and the various forms in which they may be realized in nature. In the process we answer the question of principle raised in the preceding paragraph. Gravitational units and their relation to the units that are convenient in the nuclear and particle physics of dense matter are introduced. We take the occasion to estimate the mass, baryon number, and radius of neutron stars. Certain general properties of stars and gravity are discussed, including charge neutrality and gravitational redshift. Simple models of white dwarfs are developed and then improved.

In this chapter elementary models of neutron stars are introduced beginning with the most basic—a free Fermi gas of nucleons. In the previous chapter we commented on a maximum or limiting mass of compact stars imposed by the nature of gravity. In the present chapter we show that, even if composed of an incompressible medium, a relativistic star has a maximum mass above which it is unstable to collapse to a black hole.

An upper bound on the limiting mass of neutron stars is obtained from very general considerations and independently of particular theories of dense matter. The limiting mass is important in distinguishing black hole candidates of a few solar masses from neutron stars. Finally, we present a brief section on black holes. Detailed studies of neutron and other compact stars, such as hyperon stars, quark-neutron hybrid stars, and strange stars, await our development of a theory of dense charge-neutral matter in this and later chapters.

3.3 Gravitational Units and Neutron Star Size

A compact star near the limit of collapse to a black hole has a higher density than any other star. Such a star is referred to as a neutron star. We want to show that the gravitational field (which in General Relativity is the collection of metric functions $g_{\mu\nu}$) changes by an infinitesimal amount over the distance between nucleons in such a star—and hence for all stars. If this is true, and it is as we shall show, it means that we can solve the problem of the matter fields in flat (Minkowski) spacetime as is customary in treating problems having to do with experiments under conditions such as those on the earth.

It is convenient to compute in gravitational units $G = 1 = c$:

$$\begin{aligned} 1 = c &= 2.9979 \times 10^{10}\ \mathrm{cm/s}\,, \\ 1 = G &= 6.6720 \times 10^{-8}\ \mathrm{cm}^3\ \mathrm{g}^{-1}\ \mathrm{s}^{-2}\,. \end{aligned} \tag{3.1}$$

These definitions can be treated as equations so that, for example, we have

$$\begin{aligned} 1\ \mathrm{s} &= 2.9979 \times 10^{10}\ \mathrm{cm}\,, \\ 1\ \mathrm{g} &= 7.4237 \times 10^{-29}\ \mathrm{cm}\,, \end{aligned}$$

$$
\begin{aligned}
1\ \mathrm{s}^{-2} &= 1.4988 \times 10^{7}\ \mathrm{g/cm}^{3}\,, \\
1\ \mathrm{erg} = 1\ \mathrm{g\ cm}^{2}\ \mathrm{s}^{-2} &= 8.2601 \times 10^{-50}\ \mathrm{cm}\,, \\
1\ \mathrm{g/cm}^{3} &= 7.4237 \times 10^{-19}\ \mathrm{km}^{-2}\,.
\end{aligned} \tag{3.2}
$$

In particular, note in this last equation that energy density is expressed in inverse squared kilometers. Other useful units are

$$
\begin{aligned}
\mathrm{MeV} &= 1.6022 \times 10^{-6}\ \mathrm{erg} = 1.3234 \times 10^{-55}\ \mathrm{cm}\,, \\
&= 1.7827 \times 10^{-27}\ \mathrm{g} = 1.1605 \times 10^{10}\ \mathrm{K}\,, \\
\hbar c &= 197.33\ \mathrm{MeV\ fm}\,, \\
e^{2} &= 1.4400\ \mathrm{MeV\ fm}\,,
\end{aligned} \tag{3.3}
$$

from which we derive

$$
\mathrm{MeV/fm}^{3} = 1.7827 \times 10^{12}\ \mathrm{g/cm}^{3}\,. \tag{3.4}
$$

In nuclear and particle physics, it is useful to use units chosen so that $\hbar = c = 1$. Then

$$
1/\mathrm{fm}^{4} = 197.33\ \mathrm{MeV/fm}^{3}\,. \tag{3.5}
$$

These are both units of energy density and pressure, and both are suitable for stellar quantities, especially at nuclear and supernuclear densities. In the astrophysical literature, energy density is frequently expressed in $\mathrm{g/cm}^3$ and pressure in $\mathrm{dyne/cm}^2$ (dyne=erg/cm). It is therefore useful to have on hand the conversion factors

$$
\begin{aligned}
1/\mathrm{fm}^{4} &= 3.5178 \times 10^{14}\ \mathrm{g/cm}^{3}\,, \\
&= 3.1616 \times 10^{35}\ \mathrm{dyne/cm}^{2}\,.
\end{aligned} \tag{3.6}
$$

Mixed units, which are useful in star calculations, are obtained by combining (3.5) with the value of MeV in cm,

$$
\begin{aligned}
1/\mathrm{fm}^{4} &= 2.6115 \times 10^{-4}\ /\mathrm{km}^{2}\,, \\
\mathrm{MeV/fm}^{3} &= 1.3234 \times 10^{-6}\ /\mathrm{km}^{2}\,.
\end{aligned} \tag{3.7}
$$

The unit on the right side is appropriate for expressing the pressure and energy density when solving the Oppenheimer–Volkoff equations. For example, the radial coordinate in integrals such as (2.199) can be conveniently chosen as kilometers or a fraction or multiple thereof. The integrand involving the energy density in the above units will always remain within a few orders of unity. The mass will be expressed in km and is easily compared with the solar mass

$$
M_{\odot} = 1.4766\ \mathrm{km} = 1.989 \times 10^{33}\ \mathrm{g} = 1.116 \times 10^{60}\ \mathrm{MeV}\,. \tag{3.8}
$$

TABLE 3.2. Mass, radius, Schwarzschild radius, and average density of some typical bodies (with all numbers rounded to one significant figure). Nominal neutron star = N.s., white dwarf (Sirius B) = W.d.

Name	$M/M_\odot$	R (km)	r_S (km)	$\overline{\rho}$ (g/cm^3)
N.s.	2	10	6	5×10^{14}
W.d.	1	5400	3	3×10^6
Sun	1	7×10^5	3	1.4
Jupiter	10^{-3}	7×10^4	3×10^{-3}	1.3
Earth	3×10^{-6}	6000	9×10^{-6}	5.5

We have noted that the Schwarzschild metric becomes singular at $r = r_S \equiv 2M$. For actual stars this radius is interior to the star itself where the Schwarzschild solution does not hold and the singularity therefore does not exist. However, for a neutron star, the Schwarzschild radius is not deep within the star as compared to other heavenly bodies as shown in Table 3.2. But in the special case where the star lies within its "gravitational radius", it must be a black hole.

Next we estimate the mass and radius of a star near the limit of gravitational collapse having $R = 2M$. This will be an estimate of the limiting or maximum mass possible for a neutron star. Assume that gravity packs nucleons up to their repulsive cores, say $r_0 \approx 0.5 \times 10^{-13}$ cm. Then

$$R \approx r_0 A^{1/3}, \quad M \approx Am, \tag{3.9}$$

where A is the number of baryons in the star and m is their mass,

$$m \approx 939 \text{ MeV} = 1.7 \times 10^{-24} \text{ g} = 1.2 \times 10^{-52} \text{ cm}. \tag{3.10}$$

Hence, substituting (3.9) into the equation $R = 2M$, we find

$$A^{2/3} = r_0/(2m) = 1.9 \times 10^{38}. \tag{3.11}$$

Putting this result back into the expressions for radius and mass, we have

$$A = 2.6 \times 10^{57},$$
$$R = r_0 A^{1/3} = 7 \text{ km},$$

and

$$M = R/2 = 3.5 \text{ km} = 2.3 M_\odot. \tag{3.12}$$

Here we have an estimate of the baryon number, radius, and mass of a star at the limit. In Fig. 3.1 the baryon number is plotted as a function of

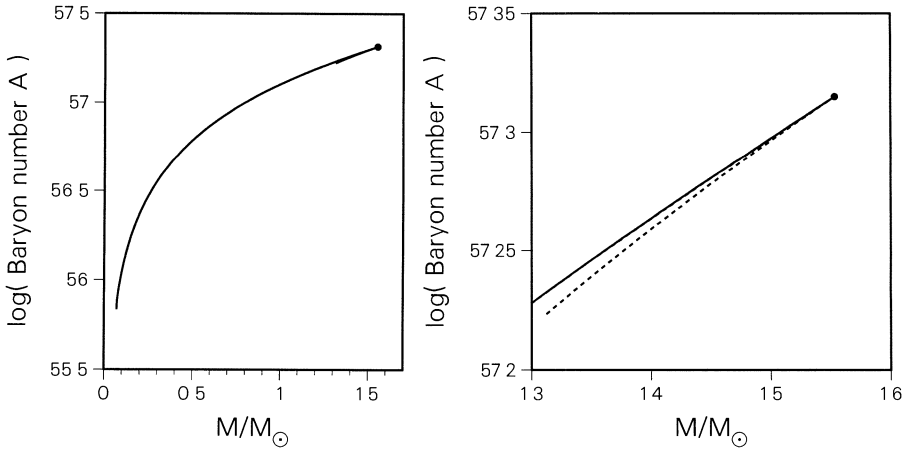

FIGURE 3.1. Total number of baryons vs. mass for neutron stars. Right figure is an enlargement in the vicinity of the maximum mass and baryon number. See Chapter 5 for details. (K=240 MeV, $m^\star_{\rm sat} = 0.78$, $x_\sigma = 0.6$).

stellar mass for a model sequence of neutron stars. Later in this chapter we discuss how this model sequence can be calculated.

Because the matter at the edge of the star will be less compacted than at the center, we expect a somewhat larger radius and smaller mass, say

$$M \approx 2M_\odot, \quad R \approx 10 \text{ km}. \tag{3.13}$$

The average density of such an object is

$$\bar{\epsilon} = 10^{15} \text{ g/cm}^3. \tag{3.14}$$

It is interesting to compare this result with the density of normal symmetric nuclear matter. Taking the average of

$$m_n = 939.57 \text{ MeV}, \quad m_p = 938.28 \text{ MeV}, \tag{3.15}$$

and using the saturation baryon density and binding per nucleon of nuclear matter obtained from the large A-limit of the droplet model of nuclear masses,

$$\rho_0 = 0.153 \text{ baryons/fm}^3, \quad -B/A = 16.3 \text{ MeV}, \tag{3.16}$$

we get for the energy density of normal symmetric nuclear matter

$$\epsilon_0 = 141 \text{ MeV/fm}^3 = 2.51 \times 10^{14} \text{ g/cm}^3. \tag{3.17}$$

The above crude estimate of the gross properties of a compact star near the limit of gravitational collapse suggests that the average density is about four times nuclear matter density. The density of the star near the mass limit is supernuclear. Also a star must be charge neutral because the repulsive Coulomb force for an infinitesimal charge on the star will expel particles of like charge. Therefore neutrons will be the majority population—hence, the name "neutron" star.

We can crudely estimate the gravitational energy for the above approximately uniform density star with nominally two solar masses and a 10-km radius. Using (2.199) we have,

$$\begin{aligned} M(r) &= \frac{4\pi}{3} r^3 \bar{\epsilon}, \qquad M = M(R), \\ E_G &\approx \int_0^R \frac{M(r)\, dM(r)}{r} = \int_0^R \frac{M(r)(4\pi r^2 dr \bar{\epsilon})}{r} = \frac{3}{5}\frac{M^2}{R} \\ &= 0.54 \text{ km} = 6.5 \times 10^{53} \text{ erg} = 7.3 \times 10^{32} \text{ g} \\ &= 4.1 \times 10^{59} \text{ MeV}. \end{aligned} \tag{3.18}$$

So the gravitational energy is a significant fraction of the total gravitational mass of the star, namely, 0.54/3 =0.18, or 18% for a two solar mass star ($M_\odot = 1.5$ km). For the above number of nucleons, it amounts to a gravitational energy of 157 MeV per nucleon. This is a factor ten times larger than the binding of nuclear matter. How can this be so since the strong force that binds nuclei is so much stronger than the weakest force we know, the gravitational? The answer lies in their ranges. The nuclear force acts only on neighbors that lie within its range, but each particle in the star feels the gravitational force of all others.

From the absolute limit on M/R of a stable star derived in Section 3.12, we can find an upper limit on the binding of a star relative to its mass. It is $(3/5)(M/R) < 4/15$ or 27 %. The import of these large bindings is that the energy released in a supernova event is large compared to that produced in thermonuclear fusion reactions during the entire lifetime of the star.

3.4 Partial Decoupling of Matter from Gravity

In nuclear and particle physics, we do not usually think of the matter Lagrangian and matter field equations as depending on the metric because we usually ignore gravity. In this event the metric tensor is the diagonal, constant, Minkowski metric $\eta_{\mu\nu}$ (2.6). For example, the Dirac equation for a nucleon contains the scalar product $\gamma_\mu \partial^\mu$, and the Lagrangian for a scalar meson contains $\partial_\mu \phi \partial^\mu \phi$. But these are merely shorthand notations that avoid the necessity of writing the Minkowski metric explicitly in the scalar product of four-vectors, $\gamma_\mu \partial^\mu = \eta_{\mu\nu}\gamma^\nu \partial^\mu$. They are correct when the metric $g_{\mu\nu}$ can be justifiably replaced by the Minkowski metric of a Lorentz frame.

However, this can be done only in a sufficiently small locality, the smallness of which depends on the curvature of spacetime. It is not possible to erect a global Lorentz frame. The differential equations for the gravitational fields, of which the $g_{\mu\nu}(x^\alpha)$ are the generalizations of the Newtonian gravitational potential, and those of the matter and radiation fields are therefore coupled in general (2.220,2.221).

For applications in strong gravitational fields we need to determine whether it is justified to solve the matter equations of nuclear and particle physics in flat spacetime. For stellar structure, this amounts to ascertaining the relevance of an equation of state for neutron star structure (and hence for all stars), one that is derived in a Lorentz frame. Let us put the mass and radius of a star near the limit of gravitational collapse into the metric for the space outside a star (2.185). We use the fact that, at the origin, $g_{11} = -1$ (2.203) to obtain

$$\frac{g_{11}(R)}{g_{11}(0)} = \left(1 - \frac{2M}{R}\right)^{-1} = \left(1 - \frac{6}{10}\right)^{-1} = 10/4\,. \tag{3.19}$$

The metric changes by a factor 2.5 over the dimension of the star. It changes by $2r_0/R = 2A^{-1/3} \approx 10^{-19}$ of this over the spacing of nucleons in the star. The change in the metric is negligible over a distance spanning many times the internucleon spacing and defines the extent of local inertial frames. So, in solving the field equations for matter, we make a negligible error for neutron stars by solving them in the absence of gravity (that is, in flat spacetime). We can then construct the energy-momentum tensor which is diagonal in a comoving Lorentz frame (2.33):

$$T^{\mu\nu} = \begin{pmatrix} \epsilon & 0 & 0 & 0 \\ 0 & p & 0 & 0 \\ 0 & 0 & p & 0 \\ 0 & 0 & 0 & p \end{pmatrix}. \tag{3.20}$$

By means of the principle of general covariance, we can then immediately write the corresponding tensor in an arbitrary gravitational field (Section 2.8.4). This contains, of course, the metric tensor, which is the gravitational field. Putting the general energy-momentum tensor (2.188) into Einstein's field equation (2.164), we find how matter is arranged under the influence of gravity and how in turn it shapes the gravitational fields $g_{\mu\nu}(x)$.

3.5 Equations of Relativistic Stellar Structure

In Chapter 2 we saw that, for a static isotropic star, Einstein's equations take a special form (2.199 2.212), derived first by Oppenheimer and Volkoff. By rewriting them we can see the Newtonian part and arrive at an inter-

pretation of them that is quite instructive.

$$4\pi r^2 dp(r) = -\frac{M(r)dM(r)}{r^2}$$
$$\left(1+\frac{p(r)}{\epsilon(r)}\right)\left(1+\frac{4\pi r^3 p(r)}{M(r)}\right)\left(1-\frac{2M(r)}{r}\right)^{-1}, \tag{3.21}$$
$$dM(r) = 4\pi r^2 \epsilon(r)\, dr\,. \tag{3.22}$$

The interpretation is very simple. Think of a shell of matter in the star of radius r and thickness dr. The second equation gives the mass energy in this shell. The pressure of matter exterior to the shell is $p(r)$ and interior to it $p(r) + dp(r)$. The left side of the first equation is the net force acting outward on the surface of the shell by the pressure difference $dp(r)$, and the first factor on the right side is the attractive Newtonian force of gravity acting on the shell by the mass interior to it. The remaining three factors are the exact corrections for general relativity. So these equations express the balance at each r between the internal pressure as it supports the overlaying material against the gravitational attraction of the mass-energy interior to r. They are the equations of hydrostatic equilibrium in general relativity.

Why did the equations for stellar structure lead us to the equation for hydrostatic equilibrium? Because they were built in by the condition that each fluid element is at rest in the star (2.195).

The equation of state $p = p(\epsilon)$ is the manner in which matter enters the equations of stellar structure. Otherwise they are completely specified, and their correctness is confirmed by the observational tests of general relativity. The most impressive of these are concerned with the Hulse–Taylor pulsar binary [35], known by its celestial coordinates as 1913+16 and studied with great care since its discovery in 1974 [4, 36, 37]. The orbit's orientation precesses at a rate of more than 4 degrees per year compared with the general relativistic contribution to the precession of Mercury, the former classic confirmation, which is only 43 seconds per century!

Einstein's gravitational radiation prediction, which affects the orbital motion of the binary pulsar pair causing the orbit to decay, is confirmed to less than one percent [4]. All other variants of Einstein's theory of gravitation are ruled out at this level of accuracy. At the measured rate of decay of the orbit due to the radiation of gravity waves, the two members of the binary will collide in about 10^8 years. While this is a long time, it is to be compared with the galaxy age of 10^{10} years. Collisions of compact stars are of possible importance to the question of strange quark nuggets as cosmic radiation, which we discuss in Chapter 10.

Newtonian stellar structure is obtained as a special case of the Oppenheimer–Volkoff equations equations by dropping the last three factors in (3.21). In Newtonian stars, ϵ is dominated by the rest mass of the baryons which however does not contribute to the pressure. The first and second

terms of the second line of (3.21) are close to unity for the same reason therefore, namely, that $p << \epsilon$. As noted in the first chapter, the last term is always positive for stars. Indeed for stars such as our sun, $2M/R = 4.3 \times 10^{-6}$, and so the last factor is also unity for Newtonian stars.

It is a particularly notable feature of the Oppenheimer–Volkoff equations that the pressure appears together with the energy density in sharpening the pressure gradient in a star, compressing the matter, and reducing the radius. As a consequence, no matter how large the pressure may be, it ultimately cannot prevent the collapse of stars whose mass exceeds what is referred to as the limiting mass (section 2.8.6).

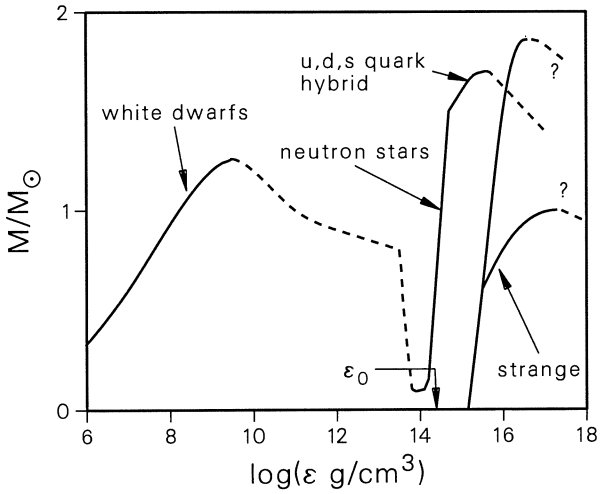

FIGURE 3.2. Schematic illustration of the solution of the O–V equations over a broad range of central densities. Hypothetical strange stars are also shown (see Chapter 10). Solid lines show stable configurations. See discussion of stability in text (Section 3.9.5).

The Oppenheimer–Volkoff equations can be integrated from the origin with the initial conditions that $M(0) = 0$ (since near $r = 0$ we may write $M(r) = (4/3)\pi r^3 \epsilon(0)$), and an arbitrary value for the central energy density $\epsilon(0)$, until the pressure $p(r)$ becomes zero. Zero pressure can support no overlying material against the gravitational attraction exerted on it from the mass within and so marks the edge of the star. The point R where the pressure vanishes defines the radius of the star and $M(R)$ its gravitational mass.

For a given equation of state, there is a unique relationship between

the stellar mass and central density $\epsilon(0)$. Thus, for each possible equation of state, there is a unique *sequence* of stars parameterized by the central density or, equivalently, the central pressure. For a vast range of densities spanning many orders of magnitude, a sequence of stars from white dwarfs to neutron stars is shown in Fig. 3.2.

At central densities about 10^8 times the density of iron here on Earth exists the famous class of stars called white dwarfs. They consist of isotopes from hydrogen to carbon and oxygen with possible admixtures of some heavier ones. All atoms, save at the surface, are ionized by the high compression. As the mass approaches about $M_\odot$, depending on the particular equation of state used to describe the matter of white dwarfs, they become unstable.

Stable dwarfs are supported against gravitational collapse by the pressure of degenerate electrons. This refers to a situation for which the temperature is much smaller than the Fermi energy of the electrons, so that they essentially fill all momentum states allowed by the Pauli principle up to the Fermi surface. However, with increasing white dwarf mass (and therefore central density and pressure), the electron Fermi energy rises. A point is reached at which it becomes energetically more favorable for electrons to be captured by protons. The supporting pressure of the relativistic electrons is lost, and a region of a few decades in central energy follows in which no stable stars exist in the sequence from white dwarfs to neutron stars.

The Fermi pressure of degenerate neutrons reestablishes stability against collapse for the lightest neutron stars. For more massive stars with higher densities, the repulsive nuclear force adds additional resistance to compression.

Neutron stars are denser by far than white dwarfs. Neutron stars are 5 to 10 times more dense at their centers than the nuclei of atoms ($\rho_0 \sim 2.5 \times 10^{14}$ g/cm^3). The density falls from its high central value to the density of of solid iron (7.85 g/cm^3) at the surface, some fifteen orders of magnitude.

It should be clear (but well worth emphasizing) that neutron stars are held together by gravitational attraction, not by the nuclear force. After all, nuclei themselves are stable only for $A \lesssim 250$ and neutron matter not at all. Indeed, except possibly for the very lightest neutron stars, gravity has compacted the neutron matter so severely that the most important part of the nuclear force is the repulsion. If gravity were switched off, a neutron star would explode!

As remarked above, the edge of a star occurs at the point where $p(R) = 0$. Frequently, one assumes that the pressure goes to zero as the energy density. But in cold matter on the nuclear scale, nucleons that are condensed into nuclei are of lower energy than a gas of nucleons. Material made of nuclei, like iron or carbon, has zero pressure. So in compact stars the edge of the star occurs at a finite energy density corresponding more or less to the laboratory density of whatever nuclei occur in the edge of the star. As we

will discuss later, the prevalent species will depend on the progenitor star in the case of a white dwarf. The dominant species will be iron atoms in a Coulomb lattice in the case of a neutron star (density ~ 7.85 g/cm^3). We shall discuss this in Section 3.10 in connection with the equation of state of subnuclear matter.

3.6 Electrical Neutrality of Stars

The repulsive Coulomb force acting on any charged particle of the same sign as the net charge on a star will overwhelm the gravitational attraction acting on the additional particle, and it will be expelled unless the net charge on the star lies below a certain minimum value which we wish to calculate. Therefore we must have

$$\frac{(Z_{\text{net}}\bar{e})e}{R^2} \leq \frac{GMm}{R^2} < \frac{G(Am)m}{R^2}\,, \tag{3.23}$$

where Z_{net}, R, M, are the net charge on the star, its radius, and mass and m and e the mass of a proton and its charge. The number of baryons in the star is denoted by A, so that we have $M < Am$, that is, the mass of the star, because of its gravitational binding, is less than the mass of the baryons distributed to infinity. Hence (in gravitational units),

$$Z_{\text{net}}/A < (m/e)^2\,. \tag{3.24}$$

A net charge larger than the above value would not allow any additional charged particle of the same sign to be gravitationally bound.

We evaluate $(m/e)^2$ for a proton. In that case using (3.3),

$$\left(\frac{m}{e}\right)^2 \sim \frac{(938\ \text{MeV})^2}{1.44\ \text{MeV fm}} \sim 10^{-36}\,. \tag{3.25}$$

Hence,

$$Z_{\text{net}} < 10^{-36}A\,. \tag{3.26}$$

This is the limit on the net positive charge. If the star had a net negative charge, we could similarly compute its limit considering the balance of Coulomb and gravitational forces on an added electron. The limit would be reduced by the factor m_e/m.

We conclude that the net charge per nucleon (and therefore the average charge per nucleon on any star) must be very small, essentially zero. However the number of charges of equal and opposite sign is not at all limited. It will be important in another context to note that the above condition on net charge on a star is a global one and not a local one. The above result places no restriction on the value of the charge density as a function of location in the star, so long as it integrates to the small value derived above.

3.7 "Constancy" of the Chemical Potential

Let us recall several thermodynamic relationships. The pressure is defined as

$$p = -\frac{\partial E}{\partial V}, \tag{3.27}$$

taken at constant entropy, where E is the energy and V the volume. For the present, we consider stars that are cold on the nuclear scale. The energy density and baryon number density are

$$\epsilon = E/V,$$

and

$$\rho = A/V, \tag{3.28}$$

where A is the number of conserved baryons in the star. Suppose the equation of state is known in the form

$$p = p(\rho), \qquad \epsilon = \epsilon(\rho), \tag{3.29}$$

from which ρ can always be eliminated, if desired, to provide $p = p(\epsilon)$. Now we can write

$$p = -\frac{\partial(\epsilon/\rho)}{\partial(1/\rho)} = \rho^2 \frac{\partial}{\partial\rho}\left(\frac{\epsilon}{\rho}\right) = \rho\mu - \epsilon, \tag{3.30}$$

where

$$\mu \equiv \frac{d\epsilon}{d\rho} \tag{3.31}$$

is the baryon chemical potential. From the relationship above between p and μ, we find

$$\frac{dp}{d\rho} = \rho\frac{d\mu}{d\rho}. \tag{3.32}$$

The Oppenheimer–Volkoff equation in the form (2.215) can be written

$$-\int_r^{r'} d\nu = \int_r^{r'} \frac{dp}{p+\epsilon} = \int_r^{r'} \frac{d\mu}{\mu}, \tag{3.33}$$

where $r < r' < R$, with R the radius of the star. Since r and r' are otherwise arbitrary, we obtain

$$\mu(r)e^{\nu(r)} = \mu(r')e^{\nu(r')} = \text{ constant} \tag{3.34}$$

This shows that the baryon chemical potential at any depth in a star, corrected by the factor $e^{\nu(r)}$, is a constant. (A theorem for an arbitrary

number of chemical potentials of independent components has been proven by Kodama [38].) The correction factor for energy is the inverse of the gravitational time dilation factor we will encounter in the next section.

At the stellar surface, p necessarily vanishes. Let us think what the surface material of a 'neutron' star made from the processed material of an evolved star could be. Surely the lowest energy equilibrium state ($p = 0$) of hadronic matter is Fe^{56} which is the end point of fusion reactions in presupernova stars. In its equilibrium state (lattice of Fe^{56} atoms), $p = 0$. Iron therefore forms the surface of neutron stars. From (3.28,3.30), we find that

$$\frac{E}{A} = \left(\frac{\epsilon}{\rho}\right)_0 = \mu_{\mathrm{Fe}} \,. \tag{3.35}$$

Hence, we obtain

$$\mu_{\mathrm{Fe}} \approx \frac{1}{56}\, m(\mathrm{Fe}^{56}) = 930.54 \text{ MeV}\,, \tag{3.36}$$

where $m(\mathrm{Fe}^{56})$ is the mass of the iron atom and we have ignored small energies associated with the molecular forces of the solid. Consequently, anywhere in the star it must be true that

$$\mu(r)e^{\nu(r)} = \mu_{\mathrm{Fe}}\left(1 - \frac{2M}{R}\right)^{1/2} . \tag{3.37}$$

This is not a condition that has to be imposed on the solution of the Oppenheimer–Volkoff equation. Rather it is the way that matter is arranged by gravity. From (3.34) we learn that, in the equilibrium configuration of the star, a particle can be brought from infinity to any point in the star, with the same gain in gravitational energy. In fact, (3.34) holds not only for the chemical potential, but also for the temperature at various points in a star in equilibrium. Thermal equilibrium does not correspond to $T =$ constant but to $T(r)e^{\nu(r)} =$ constant (cf. [39] p. 263).

3.8 Gravitational Redshift

The dilation in time, measured by observers in relative uniform motion, is familiar from the Special Theory of Relativity. Such an effect of a different origin holds also for stationary observers in a static gravitational field located at positions of different gravitational potential.

3.8.1 Integrity of an atom in strong fields

Consider the question of gravitational effects in the context of comparing spectral lines of atoms located on distant stars with those of atoms located

on earth. In Chapter 2 we have seen that, once a photon is emitted, its frequency will be shifted if it moves from one place to another having different gravitational fields. But is the internal structure of the atom itself unaffected by the gravitational field in which it is located, especially if the field is very strong? Can a local Lorentz frame be erected that encompasses the extent of the atom? We answer the question in two ways. First we consider the change in the metric across the diameter of the atom located on the surface of a massive star. From (2.184) we have

$$\begin{aligned} \delta g_{00} &\equiv g_{00}(R+r) - g_{00}(R-r) \\ &= \frac{4Mr}{R^2 - r^2} \approx \frac{4Mr}{R^2} < \frac{16}{9}\frac{r}{R}, \end{aligned} \tag{3.38}$$

where the limiting value (3.132) of $M/R < 4/9$ for any star satisfying the Oppenheimer–Volkoff equations has been used. For r we take the Bohr radius,

$$r_{\text{Bohr}} = \frac{\hbar^2}{m_e e^2} \approx 0.52918 \times 10^{-8}\ \text{cm}, \tag{3.39}$$

and for the star a nominal radius of ten kilometers (as for a neutron star since this is the type of star for which M/R is greatest), $R = 10^6$ cm and find

$$\delta g_{00} \sim 10^{-14}. \tag{3.40}$$

Likewise the change of the radial metric across the atom is very small. The gravitational fields being constant to high precision over the extent of the atom, (or molecule or nucleus), a local inertial frame that covers it can be erected and the laws of the Special Theory of Relativity hold for the atom on the star as for the like atom on earth.

While the above result answers the question of the integrity of the internal workings of an atom, even in the strongest gravitational fields of stable stars, it is interesting to address the question in a different way by comparing the change in the acceleration due to gravity across the diameter of the atom with the acceleration of the electron in the atom by the Coulomb force. The (Newtonian) acceleration due to gravity at the surface of a star is (3.139)

$$g_\star = \frac{M}{R^2} \leq \frac{4}{9}\frac{1}{R}. \tag{3.41}$$

Again, taking $R = 10^6$ cm and $1 = c = 3 \times 10^{10}$ cm/s, we have

$$g_\star < \frac{4}{9} \times 10^{-6}\left(\frac{\text{s}}{\text{cm}}\right)^2 \frac{\text{cm}}{\text{s}^2} = 4 \times 10^{14}\ \text{cm/s}^2. \tag{3.42}$$

(Notice how we have converted back from units with $c = 1$ in which acceleration is expressed in units of inverse length or, equivalently, inverse time

to ordinary units of cm/s^2.) The difference of the acceleration across the dimension of the atom is

$$\delta g_\star = \frac{M}{(R-r)^2} - \frac{M}{(R+r)^2} \approx \frac{4r}{R} g_\star \,. \tag{3.43}$$

We obtain

$$\delta g_\star \approx 2 \times 10^{-14} g_\star = 8 \text{ cm/s}^2 \,. \tag{3.44}$$

By comparison, the acceleration of the electron in a helium atom in a Bohr orbit is

$$a = \frac{1}{m_e} \frac{e^2}{r_{\text{Bohr}}^2} \approx \frac{1.44 \text{ MeV fm}}{0.5 \text{ MeV}(\frac{1}{2} 10^{-8} \text{ cm})^2} \approx 10^{25} \text{ cm/s}^2 \,. \tag{3.45}$$

So the acceleration experienced by the electron in the hydrogen atom is $\sim 10^{24}$ times larger than the change in the gravitational acceleration across the orbit when the atom is located on the surface of the star. It is also much larger than the gravitational acceleration at the surface of the star. Again we reach the conclusion that even the strongest gravitational fields on stars cannot affect the workings of an atom (much less a nucleus).

3.8.2 Redshift in a general static field

Now consider an idealized situation in which we have an observer at a great distance from a static star and from every other body and at rest with respect to the star. The gravitational field is therefore static. Let the mass and radius of the star be M and R. Let two identical atoms be located, one at the surface of the star and the other with the distant observer whose location we shall denote by ∞. For later simplicity, but by no means essential, let the center of the star, the atom on its surface, and the distant observer lie along the same line. Think of the emission of a photon as corresponding to a wave train. The two ends of a cycle, or equivalently, successive wave crests emanating from the source, correspond to neighboring spacetime events.

Having shown that a local inertial frame can be erected that encompasses the atom, choose one for which the atom is at rest. Then,

$$d\tau_{\text{a}} = \sqrt{\eta_{00}}\, d\xi_a^0 = d\xi_a^0 \tag{3.46}$$

is the invariant interval of emission from the atom (subscript "a") and is equal to the coordinate time $d\xi_a^0$ between wave crests in this local inertial frame. This relationship holds in the strong field of the star as at the location ∞ of the observer, as proven above. In an arbitrary gravitational field, the spacetime interval dx^μ between crests is governed by

$$d\tau_{\text{a}} = (g_{\mu\nu} dx^\mu dx^\nu)^{1/2} \,. \tag{3.47}$$

In particular, for the atom at rest on the surface of the star,

$$d\tau_{\rm a} = \sqrt{g_{00}(R)}\, dx^0 \tag{3.48}$$

gives the coordinate time interval dx^0 between crests in the gravitational field at R. But light propagates in the radial direction in the static field according to

$$d\tau^2 = 0 = g_{00}(r)dt^2 - g_{11}(r)dr^2\,. \tag{3.49}$$

Therefore,

$$\Delta t = t_\infty - t_R = \int_R^\infty \Big(\frac{g_{11}(r)}{g_{00}(r)}\Big)^{1/2} dr \tag{3.50}$$

is the constant transit time for each wave crest to travel from R to ∞. Hence the coordinate interval dx^0 at R governed by (3.48) is also the coordinate interval between wave crests arriving at ∞ from R. Therefore, the stationary observer with his apparatus at the location denoted by ∞ measures the proper time interval between crests arriving from the star,

$$d\tau_{\rm a'} = \sqrt{g_{00}(\infty)}\, dx^0 \tag{3.51}$$

(say by a process analogous to the inverse of (3.46)).

Denote a spacetime event associated with the distant observer by x'^μ. Similarly to (3.48), we have

$$d\tau_{\rm a} = \sqrt{g_{00}(\infty)}\, dx'^0\,, \tag{3.52}$$

as the equation that governs the coordinate time dx'^0 for emission from the like atom at rest at the location of the observer, because (3.46) holds equally at both locations. The proper time between crests (multiplied by c) gives the wavelength of the light or the reciprocal of the frequency. So we can compare the frequency $\omega(R)$ of the photon arriving from the surface R of the star, as measured by the observer at ∞ with that of the photon emitted by the like atom located with the observer, namely, $\omega(\infty)$. Using (3.51) and (3.52), respectively,

$$\frac{\omega(R)}{\omega(\infty)} = \frac{d\tau_{\rm a}}{d\tau_{\rm a'}} = \frac{dx'^0}{dx^0} = \Big(\frac{g_{00}(R)}{g_{00}(\infty)}\Big)^{1/2}\,, \tag{3.53}$$

where, in the last step, we eliminated $d\tau_{\rm a}$ between (3.48) and (3.52). Thus, as observed at ∞, the photon arriving from the atom located on the surface of the star has a lower frequency

$$\omega(R) = e^{\nu(R)}\, \omega(\infty) = \sqrt{1 - 2M/R}\, \omega(\infty) \tag{3.54}$$

than the photon from the identical atom located at ∞. The light is red shifted. Conversely, if a photon fell from ∞ to the surface of the star and

was observed there and compared with a photon from a like atom on the star surface, it would be found that the photon from the distant location had been blue shifted. We have introduced the Schwarzschild metric valid for a static spacetime outside a spherical star. Otherwise we could keep the expressions in terms of the general metric functions.

The result above can be stated in terms of clocks: time flows more slowly at R than at ∞. For an isolated static spherical star, the gravitational time dilation factor is $e^{-\nu(R)}$.

The conventionally defined gravitational redshift is the fractional change between observed and emitted wavelengths compared to emitted wavelength:

$$z \equiv \frac{\Delta\lambda}{\lambda_{\rm e}} = \frac{\lambda_{\rm o}}{\lambda_{\rm e}} - 1 = \frac{\omega_{\rm e}}{\omega_{\rm o}} - 1\,, \tag{3.55}$$

or, in this case,

$$z = \frac{\omega(\infty)}{\omega(R)} - 1 = \left(1 - \frac{2M}{R}\right)^{-1/2} - 1\,. \tag{3.56}$$

It is worth noting that the limit $2M/R < 8/9$ for any star obeying the Oppenheimer–Volkoff equations gives $z < 2$ as the maximum gravitational redshift of a stable star. In Fig. 3.3 we show the gravitational redshift of light emitted at the surface of neutron stars belonging to several model sequences.

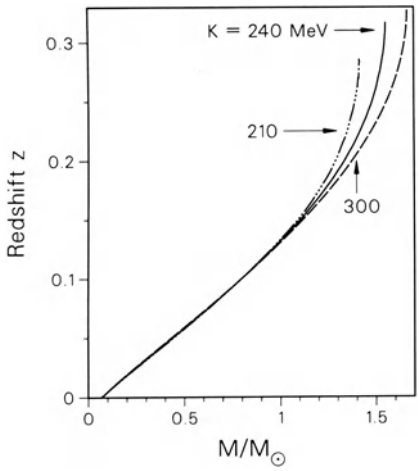

FIGURE 3.3. Surface gravitational redshift of several model neutron star sequences. See Chapter 5 for more details.

The maximum gravitational redshift of light emitted from a stable star is enormously different from that from just outside the horizon of a black hole. For the star, it is $z < 2$, but it tends to infinity for the black hole, as the atom approaches the Schwarzschild radius.

We can apply (3.53) to the situation discussed in section 2.3.1, a photon climbing up the constant weak gravitational field of the earth over a limited height h over which the acceleration due to gravity is nearly constant. The Newtonian potential is $V(r) = -M/r$ and its relationship to g_{00} was derived in Section 2.4.3:

$$\begin{aligned} \frac{\omega(R)}{\omega(R+h)} &= \left(\frac{g_{00}(R)}{g_{00}(R+h)}\right)^{1/2} \approx 1 - V(R+h) + V(R) \\ &\approx 1 - \frac{M}{R^2}\, h = 1 - gh\,. \end{aligned} \tag{3.57}$$

That is, the frequency of the photon emitted from the atom on the surface of the earth R compared at $R+h$ with a photon from a like atom at that location is

$$\omega(R) = (1 - gh)\, \omega(R+h)\,, \tag{3.58}$$

in agreement with the earlier weak field result. Noting that for Earth,

$$M_\oplus = 5.977 \times 10^{27}\ \mathrm{g} = 0.4438\ \mathrm{cm}, \qquad R_\oplus = 6.371 \times 10^8\ \mathrm{cm}\,, \tag{3.59}$$

we see that the Newtonian approximation is well justified.

3.8.3 Comparison of emitted and received light

The derivation above was carried out from the point of view of a hypothetical experiment: comparison of light received from a distant star with light from a laboratory source. Frequently, a simpler derivation of the redshift is given which simply compares (as the theorist can do) the frequencies of light emitted from an atom on the surface of the star and its frequency as received by a distant observer. The proper time corresponding to adjacent wave crests on the star was given by (3.48) which we now refer to with the subscript "e" for emitted,

$$d\tau_{\mathrm{e}} = \sqrt{g_{00}(R)}\, dx^0\,. \tag{3.60}$$

As shown above, the coordinate time taken for each wave crest to propagate from the emission location to the observer's location is the same in a static field. So the observer measures the proper time

$$d\tau_{\mathrm{o}} = \sqrt{g_{00}(\infty)}\, dx^0\,. \tag{3.61}$$

The inverse is proportional to the frequency, so the ratio of the observed to emitted frequencies is

$$\frac{\omega_{\mathrm{o}}}{\omega_{\mathrm{e}}} = \left(\frac{g_{00}(R)}{g_{00}(\infty)}\right)^{1/2}, \tag{3.62}$$

in agreement with the above.

3.8.4 Measurements of M/R from redshift

The potential usefulness of redshift measurements for compact stars is immediately evident from (3.54) in that it permits a determination of M/R. If either M or R is known from other measurements, say the mass from observations on a binary system, then the other quantity is known. So far, an independent measurement of, say M, has not been made for which a redshift measurement has also been made. Of course in comparing the two frequencies, one from the distant star, the other from an earth bound atom, one cannot a priori be sure one is comparing atoms. The identification would be more positive if several transition lines were observed and they all had the same ratio when compared to the atom on earth. There are about 30 known X-ray pulsars for which tentative spectral identifications have been made.

3.9 White Dwarfs and Neutron Stars

> "Chandrasekhar ... has shown that a star of a mass greater than a certain limit remains a perfect gas.... The star has to go on radiating and radiating, and contracting and contracting until, I suppose ... gravity becomes strong enough to hold in the radiation, and the star can at last find peace [as a black hole].
>
> I felt driven to the conclusion that this was almost a *reductio ad absurdum*.... I think there should be a law of nature to prevent a star from behaving in this absurd way."
>
> *A. Eddington*, 1935 [40]

> "It is clear from this [above] statement that Eddington fully realized, already in 1935, that given the existence of an upper limit to the mass of degenerate configurations, one must contemplate the possibility of gravitational collapse leading to the formation of what we now call black holes. But he was unwilling to accept a conclusion that he so presciently drew."
>
> *S. Chandrasekhar*, 1982 [41]

3.9.1 Overview

After sufficient time, a star, either a white dwarf or neutron star, will become cold on the nuclear scale. Ideally, it will be in the lowest energy state, and the neutrinos and photons produced by the reactions in achieving the lowest state, such as

$$e^- + p \to n + \nu\,,$$
$$n \to p + e^- + \bar{\nu}\,,$$

$$\bar{\nu} + \nu \rightarrow 2\gamma \tag{3.63}$$

will have escaped from the star. Once the star has dropped in temperature below an MeV ($= 1.1605 \times 10^{10}$ K), we may say that it is cold for the purpose of computing the energy and pressure, but the temperature is still very high compared to the neutrino masses (presumably zero or very small), so they have velocity sufficient to escape. Typical white dwarf surface temperatures are less than a few times 10^4 K with interior temperatures of $10^6 - 10^7$ K, while neutron stars are born very hot, of the order of 10^{10} K, but cool rapidly, reaching 10^8 K in a month and 10^6 K in less than a million years. White dwarfs have radii typically of a few thousand kilometers, while we estimated that neutron stars have radii of around 10 km. White dwarfs are about the smallest faintest stars that are visible in the optical spectrum. Neutron stars make their presence known in the radio spectrum as pulsars, highly magnetized rotating bodies.

Because of their low luminosity (generally several orders of magnitude less than the sun's) known white dwarfs lie in the immediate neighborhood of the sun (100 pc).[6] By comparison, the disk diameter of the Milky Way galaxy is 30,000 pc. White dwarf masses are sharply peaked around $0.6 M_\odot$ though Sirius B has an accurately determined mass $M = 1.053 \pm 0.028 M_\odot$. The largest known mass is $1.52 M_\odot$ (WD 1143+321), and the smallest is $0.33 M_\odot$ (WD 0349+27). The latter are deduced from gravitational redshifts [42] and are less certain. Known pulsars are also distributed around the sun, close to the galactic plane, and some are known at distances of more than 15 kpc. Few mass measurements have been made, and only four have high accuracy. The some 20 presently known masses have their maximum likelihood values in the range 1 and 1.8 $M_\odot$, but the error bars would admit pulsars of masses 0.6 to 2.6 $M_\odot$.

White dwarfs are born under relatively quiescent circumstances, the remnants of a nonexplosive evolution of fairly modest stars of mass up to seven or so solar masses, which comprise most of the stars in the Milky Way galaxy. What remains of the core after the bulk of the star has expanded into a planetary nebula becomes a white dwarf. Dwarf progenitor stars, because of their low mass (unlike the progenitors of neutron stars), have not completed the chain of fusion reactions up to the most bound nucleus, ^{56}Fe. They are therefore composed of matter that is not in its lowest energy state. They are too cold to ignite the nuclear reactions that would bring them there. However, even when cold and crystalline, white dwarfs may evolve on a very long timescale through zero temperature nuclear reactions in which lattice vibrations yield a small but finite probability of Coulomb barrier tunneling, a process known as a pycnonuclear reaction, which produces some heavier elements [43, 44]. However, the composition

[6] A parsec is the distance at which a star is observed with a parallax of 1 sec of arc. 1 parsec (pc) = 3.26 ly (light years) = 3.09 10^{13} km.

is essentially determined at birth.

Because of the circumstances of their birth, white dwarfs are not members of a single sequence corresponding to a unique equation of state. Rather, according to its individual history, each white dwarf is an equilibrium stellar configuration corresponding to an equation of state describing the particular composition attained in the thermonuclear burning of its progenitor (mostly He, C and O) together with an atmosphere that is the remnant of the vibrations of the envelope that became unstable and formed the planetary nebula.

On the other hand, neutron stars are born in enormous explosions—supernovae—that occur in the last few moments in the evolution of stars more massive than about $8M_\odot$. In their cores, thermonuclear combustion has proceeded through to iron. Neutron stars are therefore composed of matter that has been fully processed to extract all available energy. At each density in their interiors, matter is in its ground state, consistent with charge neutrality.

3.9.2 Fermi-Gas equation of state for nucleons and electrons

As a first orientation that will bring out some of the relationships and contrasts between white dwarfs and neutron stars and also serve to illustrate some of the principles involved in any calculation of compact stellar structure, we consider an idealization in which both types of stars are members of a sequence belonging to a particularly simple equation of state. The equation of state will describe a gas of noninteracting neutrons, protons, and electrons in such proportions at each baryon number density that the gas has its lowest possible energy. Such a situation is referred to as beta equilibrium or simply equilibrium. The neutrons will neither beta decay nor will the inverse reaction—electron capture on a proton—occur. In addition, we must demand that the minimum energy be found subject to the condition of charge neutrality.

Since neutrons, protons, and electrons are all fermions (particles of half odd-integer spin), they obey the Pauli exclusion principle—not more than one fermion can occupy a given quantum state. In this section we deal with a degenerate ideal Fermi gas. Ideal in this context means that interactions are ignored. Degenerate means that all quantum states up to a given energy, called the Fermi energy, are occupied. This means that, in summing the occupation of the states (which in the absence of interactions are momentum eigenstates) or in summing over the energies of the occupied states, we need to integrate over momentum states (recall box normalization), so that we have

$$\frac{1}{L^3}\sum_{\boldsymbol{k}}\cdots \longrightarrow \int \frac{d^3k}{(2\pi)^3}\cdots = \frac{1}{2\pi^2}\int k^2\,dk\cdots . \tag{3.64}$$

The last equality holds provided the integrand depends only on the magnitude of the wave number $k = |\boldsymbol{k}|$ as is usual. Particle momentum p and wave number are related in the usual way: $p = \hbar k$. But since we set $\hbar = 1 = c$, we refer to k as momentum. Its unit is inverse length. In numerical calculations it is also advantageous to convert mass to inverse length by dividing by $\hbar c = 197.33$ MeV-fm.

The assumption of degeneracy is valid for low temperatures (much less than the Fermi energy, $T << E_F = (k_F^2 + m^2)^{1/2}$). For electrons, $E_F > m_e = 0.511$ MeV $\sim 6 \times 10^9$ K, while the internal temperature of white dwarfs is $\sim 10^6$ to 10^7 K. So the Fermi energy of electrons (and therefore also nucleons) easily satisfies the degeneracy condition.

Each fermion type (n, p, e) contributes to the energy density, pressure, and number density according to

$$\begin{aligned} \epsilon &= \frac{\gamma}{2\pi^2}\int_0^k \sqrt{k^2+m^2}\, k^2\, dk\,, \\ p &= \frac{1}{3}\frac{\gamma}{2\pi^2}\int_0^k \frac{k^2}{\sqrt{k^2+m^2}}\, k^2\, dk\,, \\ \rho &= \frac{\gamma}{2\pi^2}\int_0^k k^2 dk\,, \end{aligned} \tag{3.65}$$

where γ denotes the degeneracy of each momentum state. The degeneracy is 2 for each particle type corresponding to the two spin projections $\pm 1/2$. The upper limit on the integrals stands for the Fermi momentum, sometimes denoted by k_F. For the simplicity of the appearance of formulae to follow, we call it simply k, or k_p when we have to distinguish proton Fermi momentum from others. According to the units just described, ϵ and p can be conveniently computed in units $1/\text{fm}^4$. They can be converted to MeV/fm^3 by multiplying by $\hbar c$ or still other units by using the conversion factors described in Section 3.3.

The integrals can be carried out in closed form using the results of Ref. [45], pp. 86 and 87:

$$\begin{aligned} &\textstyle\int_0^k \sqrt{k^2+m^2}\, k^2\, dk = \\ &\tfrac{1}{4}\big[k(k^2+m^2)^{3/2} - \tfrac{1}{2}m^2 k\sqrt{k^2+m^2} - \tfrac{1}{2}m^4 \ln\big(\tfrac{\sqrt{k^2+m^2}+k}{m}\big)\big]\,, \\ &\textstyle\int_0^k \frac{k^4}{\sqrt{k^2+m^2}} dk = \\ &\tfrac{1}{4}\big[k^3\sqrt{k^2+m^2} - \tfrac{3}{2}m^2 k\sqrt{k^2+m^2} + \tfrac{3}{2}m^4 \ln\big(\tfrac{\sqrt{k^2+m^2}+k}{m}\big)\big] \quad . \end{aligned} \tag{3.66}$$

It can be verified that the pressure written above obeys the usual thermodynamic relationship,

$$p = \rho^2 \frac{\partial}{\partial \rho}\frac{\epsilon}{\rho}\,. \tag{3.67}$$

As the contribution of each fermion type (of degeneracy $\gamma = 2$), we find

$$\begin{aligned} \epsilon &= \frac{1}{4\pi^2}\left[\mu k(\mu^2 - \frac{1}{2}m^2) - \frac{1}{2}m^4 \ln\left(\frac{\mu + k}{m}\right)\right], \\ p &= \frac{1}{12\pi^2}\left[\mu k(\mu^2 - \frac{5}{2}m^2) + \frac{3}{2}m^4 \ln\left(\frac{\mu + k}{m}\right)\right], \\ \rho &= \frac{k^3}{3\pi^2}, \end{aligned} \tag{3.68}$$

where

$$\mu = (m^2 + k^2)^{1/2} \tag{3.69}$$

is the Fermi energy (sometimes referred to as the chemical potential) and k the Fermi momentum. We could eliminate k in favor of ρ in the above equations, yielding $\epsilon(\rho)$ and $p(\rho)$.

Continuing our calculation of the equation of state, we want to minimize the total energy density of neutrons, protons, and electrons $\epsilon(\rho_n, \rho_p, \rho_e) = \epsilon(\rho_n) + \epsilon(\rho_p) + \epsilon(\rho_e)$ at fixed baryon density $\rho = \rho_n + \rho_p$ and subject to the condition of charge neutrality $\rho_p = \rho_e$. This can be done by the method of Lagrange multipliers [46]. Construct a new function from the one we wish to extremize and the two constraint equations:

$$F(\rho_n, \rho_p, \rho_n) \equiv \epsilon(\rho_n, \rho_p, \rho_n) + \alpha(\rho - \rho_n - \rho_p) + \beta(\rho_e - \rho_p)\,.$$

For arbitrary variations of the three particle densities we require that

$$\frac{\partial F}{\partial \rho_n} = 0, \qquad \frac{\partial F}{\partial \rho_p} = 0, \qquad \frac{\partial F}{\partial \rho_e} = 0\,.$$

Using the integral expressions for ϵ, we have

$$\frac{\partial \epsilon}{\partial \rho_n} = \frac{\partial \epsilon}{\partial k}\frac{\partial k}{\partial \rho_n} = \sqrt{k_n^2 + m_n^2}, \qquad \text{etc.} \tag{3.70}$$

Therefore the above conditions on F yield

$$\begin{aligned} \alpha &= \sqrt{k_n^2 + m_n^2} \equiv \mu_n, \\ \alpha + \beta &= \sqrt{k_p^2 + m_p^2} \equiv \mu_p, \\ -\beta &= \sqrt{k_e^2 + m_e^2} \equiv \mu_e\,. \end{aligned} \tag{3.71}$$

Eliminating the Lagrange multipliers, we obtain

$$\mu_e + \mu_p = \mu_n\,, \tag{3.72}$$

where the chemical potentials were defined above. Since μ_e is the electron chemical potential, it corresponds to unit negative electric charge while μ_n corresponds to unit baryon charge without electric charge (i. e., neutron).

The expression of chemical equilibrium (3.72) will recur in more general terms many times. It ensures that the particle levels are filled to such a point that no energy can be extracted from the gas by a neutron undergoing a beta decay or a proton an inverse beta decay. Of course all levels are Fermi-blocked below the Fermi energies. Of particular note in the above result is that the chemical potentials of three types of particles can all be expressed in terms of the two (Lagrange multipliers) associated with the conservation laws, namely, baryon number and electric charge conservation. The system is said to have three components of which only two are independent.

As an aside, we remark that the conclusion concerning the possibility of expressing the chemical potentials for m substances in equilibrium in terms of the chemical potentials of the n independent components (or as we shall often say, conserved charges) is not restricted to free particles as in the above example. In general the problem is to find the minimum of, say the Gibbs free energy Φ, subject to the subsidiary conditions that express the conservation of the independent components (charges). The problem is therefore of the same kind as solved above. The simple expressions for the chemical potentials (3.69) will not hold. But we will still have $\mu_i = (\partial\Phi/\partial N_i)_{P,T}$, and the derivation will go through as above.

There is an alternate way of deriving the relation of the chemical potentials for the m substances in terms of those for the independent components. It consists of writing down all of the expressions for the possible chemical transformations in the form $\nu_i A_i = 0$, where the ν_i are positive or negative (and not necessarily integers, as in the case of quarks) and the A_i are the chemical symbols. One then replaces the chemical symbols by the chemical potentials. If several chemical transformations are possible, there is an equation for each and the resulting relationships between the chemical potentials allows one to express the chemical potentials of all components in terms of the independent ones alone (see Chapter X of ref. [47]).

Pursuing our search for the minimum of the total energy at fixed density subject to charge neutrality, we note that the Fermi momenta of nucleons and the baryon density ρ are related by

$$\frac{1}{3\pi^2}(k_n^3 + k_p^3) = \rho\,. \tag{3.73}$$

The condition of charge neutrality can be written

$$k_p = k_e\,. \tag{3.74}$$

These two equations together with (3.72) can be used to determine the k_n, k_p, and k_e such that the energy is minimized subject to the stated conditions. We now analyze how they may be solved.

Suppose $k_p = 0$. Then we obtain

$$k_n^2 = (m_p + m_e)^2 - m_n^2 < 0\,, \tag{3.75}$$

where the values of neutron and proton masses were written earlier and $m_e = 0.51100$ MeV. So there is no real solution, and we conclude that k_p is always finite. Next try $k_n = 0$. We find

$$\begin{aligned} k_p^2 = \left(\frac{m_p^2 + m_n^2 - m_e^2}{2m_n}\right)^2 - m_e^2 &= 1.4269 \text{ MeV}^2 \\ &= 3.6644 \times 10^{-5} \text{ fm}^{-2} . \end{aligned} \tag{3.76}$$

This is the smallest value of k_p for which k_n can be finite. Below the density

$$\rho = \frac{k_p^3}{3\pi^2} = 7.4919 \times 10^{-9} \text{ fm}^{-3} \tag{3.77}$$

or below the energy density

$$\epsilon \sim \rho m_p = 3.56 \times 10^{-8} \text{ fm}^{-4} = 1.25 \times 10^7 \text{ g/cm}^3 , \tag{3.78}$$

a charge neutral Fermi gas in equilibrium is an equal mixture of protons and electrons with no neutrons. Below this neutron threshold, we have simply

$$k_p = (3\pi^2\rho)^{1/3}, \qquad k_e = k_p, \qquad k_n = 0 , \tag{3.79}$$

and the energy density and pressure can be computed from (3.68).

Above the neutron threshold, we can use the equation for fixed baryon density to write

$$k_n = (3\pi^2\rho - k_p^3)^{1/3} \tag{3.80}$$

together with the condition of charge neutrality to obtain an equation in k_p alone:

$$(k_p^2 + m_e^2)^{1/2} + (k_p^2 + m_p^2)^{1/2} = \left((3\pi^2\rho - k_p^3)^{2/3} + m_n^2\right)^{1/2} . \tag{3.81}$$

This can be solved numerically for k_p for any ρ, and then the corresponding k_n. The total energy density and pressure can then be calculated.

It is of some interest to look at the above equation in the ultrarelativistic regime where we ignore all masses. Then one obtains

$$\rho_p \to \frac{1}{8}\rho , \tag{3.82}$$

that is, ignoring the existence of all other baryon types, the asymptotic proton density is one-eighth of the baryon density. One can also easily show in the same limit that this fraction is approached from below. For this reason it is sometimes thought that neutron stars are composed mostly of neutrons. Such an assumption is frequently used in calculations of neutron star properties, for example masses, transport coefficients or cooling rates. However, besides other baryon species, the above model ignores an

important property of nuclear matter, the energetic preference for an equal number of neutrons and protons, modulo effects of the Coulomb force. This is often referred to as the preference for isospin symmetry, about which we shall elaborate in the next chapter. So within the overriding constraint of charge neutrality, we anticipate that the composition of neutron stars will be very rich in baryon species [48, 49]. We will elaborate in detail on this important topic in Chapter 5.

While the above formulae for energy density and pressure (3.68) are exact expressions for the equation of state within the limitations of the Fermi gas model, they are a poor basis for numerical computation in the case that a particle momentum is very small compared to its mass. In this case we must derive the nonrelativistic limits of the exact expressions and use them to compute the contributions to the energy density and pressure.

3.9.3 High- and low-density limits

For both the numerical reason mentioned above and for the sake of an interesting partially analytic discussion of white dwarfs as polytropes (which we shortly define), we derive the high- and low-density limits of the exact Fermi gas expressions (3.66). The high-density limit $k >> m$, which may also be called the relativistic limit if m is not ignored or the ultrarelativistic limit if it can be. The results are

$$\epsilon \approx \frac{1}{4\pi^2}\left[k^4 - \tfrac{1}{2}m^4 \ln\frac{2k}{m}\right],$$

and

$$p \approx \frac{1}{12\pi^2}\left[k^4 + \tfrac{3}{2}m^4 \ln\frac{2k}{m}\right]. \tag{3.83}$$

The logarithmic terms are small compared to k^4 in the ultrarelativistic limit, so we have

$$\epsilon \to 3p \approx \frac{1}{4\pi^2}(3\pi^2\rho)^{4/3} \quad \text{(high density, } k >> m\text{)}, \tag{3.84}$$

where ρ here is the density of the fermion type considered.

The low-density expansion can easily be found directly from the integral expressions by expanding in k/m:

$$\epsilon \approx \frac{m^4}{\pi^2}\left[\frac{1}{3}\left(\frac{k}{m}\right)^3 + \frac{1}{10}\left(\frac{k}{m}\right)^5 - \frac{1}{56}\left(\frac{k}{m}\right)^7 + \frac{1}{144}\left(\frac{k}{m}\right)^9\right],$$

and

$$p \approx \frac{m^4}{3\pi^2}\left[\frac{1}{5}\left(\frac{k}{m}\right)^5 - \frac{1}{14}\left(\frac{k}{m}\right)^7 + \frac{1}{24}\left(\frac{k}{m}\right)^9\right]. \tag{3.85}$$

For very low density, the nonrelativistic approximation involves the terms to k^5 only. When written in terms of ρ, they appear as

$$\epsilon \approx \rho m + \frac{(3\pi^2\rho)^{5/3}}{10\pi^2 m},$$

and

$$p \approx \frac{(3\pi^2\rho)^{5/3}}{15\pi^2 m} \quad \text{(low density, } k << m\text{)}. \tag{3.86}$$

Notice that the term in ϵ proportional to ρ does not contribute to the pressure. (See (3.67).) These are the contributions of each fermion type to the equation of state.

Of course 'low' and 'high' density have different meanings for electrons and nucleons. For example, in the domain $m_e < k_e = k_p < m_p$, the electrons are relativistic ($k_e > m_e$), but the protons are nonrelativistic ($k_p < m_p$). This has to be kept in mind in computing an equation of state over a wide range of densities for n, p, e in equilibrium.

The equation of state of this Fermi gas model is shown in Fig. 3.4. The kink at $\epsilon \approx 10^7$ g/cm^3 marks the neutron threshold. Below this, the gas is an equal mixture of protons and electrons. Above, it rapidly becomes dominated by neutrons. The flat region in pressure corresponds simply to the fact that the increase in density in this region is accounted for by low-momentum (threshold) neutrons.

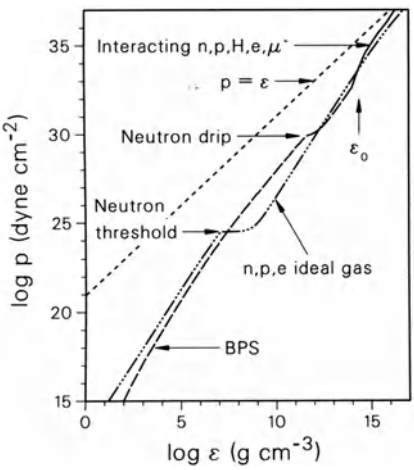

FIGURE 3.4. Charge neutral Fermi gas equation of state of n, p and e in beta equilibrium. Flat pressure region corresponds to neutron threshold. For comparison the BPS equation of state (see Section 3.10) is also shown, corresponding to the lowest energy state of nuclei located in a lattice with electrons in the interstices. The kink in this equation of state at $\epsilon \approx 4.3 \times 10^{11}$ g/cm^3 is the density at which free neutrons drip from the nuclei. Also shown are a high-density equation of state of hyperonized matter and the limit $p = \epsilon$.

3.9.4 Polytropes and Newtonian white dwarfs

The results above for an ideal gas equation of state could serve to provide a crude model of white dwarf structure. However what we have derived above can be used for an improved description that recognizes that white dwarfs do not consist of a gas of nucleons and electrons, but rather that the nucleons are clumped in nuclei, such as ^{4}He, ^{12}C, and ^{16}O .

For charge neutrality, we require $\rho_p = \rho_e$ or, equivalently, $k_p = k_e$. Let us recall that charge neutral matter consists only of protons and electrons below a certain nucleon density. The momentum corresponding to the neutron threshold is (3.76)

$$k_e = k_p = 0.00605 \text{ fm}^{-1} \quad \text{(neutron threshold)}. \tag{3.87}$$

This compares with the electron and proton masses of

$$\begin{aligned} m_e &= 0.511 \text{ MeV } = 0.511/197 \text{ fm}^{-1} = 0.00259 \text{ fm}^{-1}, \\ m_p &= 4.76 \text{ fm}^{-1}. \end{aligned} \tag{3.88}$$

Therefore, far below the threshold, electrons are nonrelativistic. From (3.86) find that the electron pressure is much greater than that of the protons,

$$\frac{p_e}{p_p} = \frac{m_p}{m_e} >> 1, \quad (k_e << m_e). \tag{3.89}$$

Neutron threshold is in the relativistic domain of the electrons since $k_e > m_e$. Above the threshold up to the interesting condition that neutron and proton densities are equal (as in nuclei), electrons are relativistic, and nucleons are nonrelativistic, $k_n,\ k_p << m_p$. For relativistic electrons refer to (3.86) and (3.84) to find

$$\frac{p_e}{p_p} = \frac{5}{4}\frac{m_p}{k_e} >> 1, \quad m_e << k_e << m_p. \tag{3.90}$$

The two equations above show that, in the white dwarf domain,

$$k_p \text{ and } k_n << m_p \quad \text{(white dwarf domain)}. \tag{3.91}$$

Electrons—whether nonrelativistic or relativistic—contribute virtually all the pressure while the nucleons contribute virtually all the energy density. Fowler was the first to recognize that white dwarfs are supported against gravitational collapse by the pressure of degenerate electrons [50].

We discussed above the domain up to the point where neutron and proton densities are about equal. However, because of the short-range attraction between nucleons, a dilute gas of nuclei is a lower energy state than a dilute gas of neutrons, protons, and electrons. We will return to this subject in a more exacting way. In the meanwhile it is worth pursuing the present model, modifying the idealized results in a physically motivated ad hoc manner, namely, as a dilute gas of nuclei and electrons. This is straightforward because we have just seen that the nucleons do not contribute appreciably to the pressure. It is only their rest energy that is important. We can therefore consider that the nucleons are bound in nuclei and write, for the energy density,

$$\epsilon = \rho_e m_N \nu, \tag{3.92}$$

where we now take m_N as the nominal nucleon mass in a nucleus, whether proton or neutron, and define ν as the number of nucleons per electron:

$$\nu = (\rho_p + \rho_n)/\rho_e \,. \tag{3.93}$$

In the discussion of the preceding section, ν was to be determined by the equilibrium condition for a neutral Fermi gas of nucleons and electrons. In this section it is a parameter used to represent the nucleon-electron ratio of the dominant nuclear species in particular white dwarfs, such as He, C, or O. For each of these, $\nu = 2$. We note that, from its definition, we can write

$$\rho_n = \rho_p(\nu - 1) \tag{3.94}$$

so that, since the neutron threshold occurs at nonzero proton density, we have $\nu \geq 1$.

In the white dwarf domain (3.91), it is easy to confirm that the electron pressure is always less than the electron energy density which itself is small compared to the rest mass density of the nucleons, namely,

$$\begin{aligned} \frac{p_e}{\epsilon_e} = \frac{1}{5}\left(\frac{k_e}{m_e}\right)^2 << 1\,, \qquad & k_e < m_e\,, \\ \frac{p_e}{\epsilon_e} = \frac{1}{3}\,, \qquad & k_e > m_e\,. \end{aligned} \tag{3.95}$$

Consequently, energy density dominates pressure, and we can write

$$p << \epsilon, \qquad 4\pi r^3 p << M(r), \qquad \frac{2M(r)}{r} << 1\,, \tag{3.96}$$

These inequalities assure that the Newtonian approximation to (3.21) is valid. The last of the inequalities follows from the fact that no region of a star can lie within its Schwarzschild radius [22]. It is also apparent that the pressure would not be monotonic unless the last inequality holds. Considering that the pressure at r supports all material above r, pressure should be monotonic increasing from the edge to the center of the star. The middle inequality follows from the first: (rearrange $M(r) \sim (4\pi/3)r^3\bar{\epsilon}$ to read $4\pi r^3 p \sim 3(p/\bar{\epsilon})M(r) << M(r)$).

Divide what remains of (3.21) after the Newtonian approximation by ϵ, differentiate by r, and combine with (3.22) to obtain

$$\frac{d}{dr}\left(\frac{r^2}{\epsilon}\frac{dp}{dr}\right) = -4\pi r^2 \epsilon\,. \tag{3.97}$$

This is the equation that governs the structure of a Newtonian star. As remarked earlier, for a given equation of state, there is a one-parameter family of stars (sometimes referred to as a sequence), for which the central energy density $\epsilon_c \equiv \epsilon(0)$ is a convenient means of parameterizing the continuum of stars belonging to the sequence.

We now derive a white dwarf sequence. The equation of state can be approximated by the following form in the white dwarf domain (3.91),

$$p = K\epsilon^{\gamma}\,, \tag{3.98}$$

as we shall shortly see. A star whose equation of state is approximated by such a simple form is known as a polytrope. Polytropes are interesting as approximate models of stars because more than the usual amount of work can be done analytically.

Boundary conditions for (3.97) can be found easily. Taking $r \to 0$ in (3.97) shows that, for finite $\epsilon(0)$, we must have $p'(0) = 0$. For a polytrope, $p' = \gamma(\epsilon'/\epsilon)p$ which shows that, for $\epsilon(0) \neq 0$, we must have $\epsilon'(0) = 0$. Summarizing, the boundary conditions on (3.97) are

$$\epsilon(0) = \epsilon_c, \qquad \epsilon'(0) = 0\,. \tag{3.99}$$

By transforming variables from r, ϵ to ξ, θ, we get a universal equation for polytropes parameterized by the polytropic index γ. The transformation is

$$r = \Big(\frac{K\gamma}{4\pi(\gamma-1)}\Big)^{1/2} \epsilon_c^{\frac{\gamma-2}{2}}\,\xi, \qquad \epsilon = \epsilon_c\,\theta^{\frac{1}{\gamma-1}}, \qquad p = K\,\epsilon_c^{\gamma}\,\theta^{\frac{\gamma}{\gamma-1}}\,, \tag{3.100}$$

and the result is the *Lane–Emden* equation of index $(\gamma-1)^{-1} = n$,

$$\frac{1}{\xi^2}\frac{d}{d\xi}\xi^2\frac{d\theta}{d\xi} + \theta^{\frac{1}{\gamma-1}} = 0\,. \tag{3.101}$$

The boundary conditions corresponding to (3.99) are

$$\theta(0) = 1, \qquad \theta'(0) = 0\,. \tag{3.102}$$

The Lane–Emden equation can be numerically integrated for various γ. It is easily verified that, for $\gamma > 6/5$, the Lane–Emden function $\theta(\xi)$ is monotonic decreasing with increasing argument (radius), as would be required of the pressure and energy density in a static star. The first zero occurs at a finite argument, call it ξ_1:

$$\theta(\xi_1) = 0\,. \tag{3.103}$$

Since this is the point where the pressure has fallen monotonically to zero, (3.100), ξ_1 marks the edge of the star. From the equations for the transformation of variables (3.100), the stellar radius is

$$R = \Big(\frac{K\gamma}{4\pi(\gamma-1)}\Big)^{1/2} \epsilon_c^{\frac{\gamma-2}{2}}\,\xi_1\,. \tag{3.104}$$

The mass is given by (3.22) as

$$M = \int_0^R 4\pi^2\epsilon(r)\,dr = 4\pi\epsilon_c^{(3\gamma-4)/2}\Big(\frac{K\gamma}{4\pi(\gamma-1)}\Big)^{3/2}\int_0^{\xi_1}\xi^2\theta^{\frac{1}{\gamma-1}}\,d\xi\,. \tag{3.105}$$

Using the Lane–Emden equation, the integral is easily evaluated:

$$\int_0^{\xi_1} \xi^2 \theta^{\frac{1}{\gamma-1}}\, d\xi = -\int_0^{\xi_1} \frac{d}{d\xi}\xi^2 \frac{d\theta}{d\xi}\, d\xi = -\xi_1^2 \theta'(\xi_1)\,. \tag{3.106}$$

Hence, the mass is found as

$$M = 4\pi\epsilon_c^{(3\gamma-4)/2}\Big(\frac{K\gamma}{4\pi(\gamma-1)}\Big)^{3/2}\xi_1^2|\theta'(\xi_1)|\,. \tag{3.107}$$

Thus, for a specific polytropic sequence, the mass and radius have the relationship

$$R \sim M^{(\gamma-2)/(3\gamma-4)}\,. \tag{3.108}$$

We return to these results after discussing the stability of stars.

3.9.5 Stability

Solutions of the Oppenheimer–Volkoff equations correspond to stellar configurations that are in hydrostatic equilibrium. This is clear from their derivation. Equilibrium does not assure stability. Equilibrium configurations may correspond either to a maximum or to a minimum in the energy for which one may think of compaction as the coordinate carrying one to the other. (Look ahead to the solid line in Fig. 9.16 as an example where, for a certain range in baryon number of the star, there are two equilibrium solutions, one at higher energy than the other.) In general, the determination of stability is a difficult and specialized topic which we do not take up here in detail.

It has been established convincingly that, along the continuum of equilibrium configurations corresponding to an equation of state satisfying the condition of *microscopic* stability of matter $dp/d\rho \geq 0$ (Le Chatelier's principle), there are two regions of compact stars where the configurations are stable. These are the white dwarf and neutron star regions. Between them there is an unstable region many orders of magnitude in central density, as shown in Fig. 3.2.

Stars in the unstable region between white dwarfs and neutron stars are subject to vibrational modes that will either cause their disassembly or else their collapse to neutron stars. At densities below the white dwarf region, there is a long region of instability for cold objects until one reaches other stable bodies, such as brown dwarfs and planets. However, above the stable neutron star sequence, there are no additional regions of stability. The physical reasons for this are discussed in Section 8.5.

It can be proved that, along the sequence of equilibrium configurations of the Oppenheimer–Volkoff equations, perfect fluid stars can pass from stability to instability with respect to any radial mode of oscillation only

at a value of the central density at which the equilibrium mass is stationary,

$$\frac{\partial M(\epsilon_c)}{\partial \epsilon_c} = 0\,. \tag{3.109}$$

This is a key result in the discussion of stability. Moreover, the baryon number of an equilibrium star is stationary at the same central densities as the mass. These and many other interesting theorems can be found in Ref. [23], Ch. 5 and 7 and Appendices B and C of that reference.

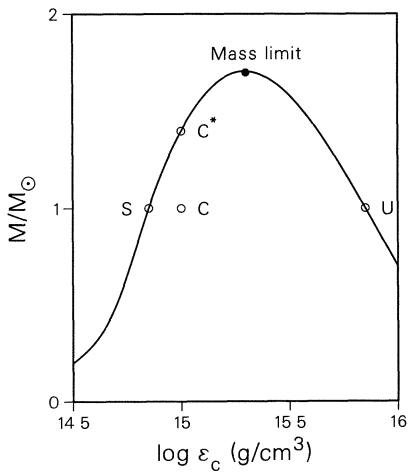

FIGURE 3.5. Schematic of solution of the Oppenheimer–Volkoff equations in a region of increasing and decreasing mass as function of central density. Hydrostatically stable configurations have positive slope so the stable region ends at 'mass limit'. See the discussion in the text.

Although the proofs of theorems concerning the passage from stability to instability of the succession of vibrational modes with ever higher nodal structure for configurations with central densities higher than neutron stars are not included in this book, it is easy and instructive to rationalize a *necessary* condition for stability. For this purpose refer to Fig. 3.5 for a depiction of a sequence of stars in the vicinity of a maximum. Suppose an equilibrium solution S is perturbed so that the central density ϵ_c is increased; the star is displaced to C (compressed). The equilibrium star with this new central density lies in mass at C*. The star at C therefore has a deficit of mass with respect to the equilibrium configuration, a deficit such that gravity underbalances the increased central pressure corresponding to the increased density at C, as compared to the equilibrium configuration of the star of this mass that lies at S. The forces acting on the matter of the star will therefore act to return it toward S. A similar argument shows that, if the star at S undergoes a perturbation that decreases its central density, the forces acting on the matter of the star will act to return it to S.

Going through a similar analysis of the star U on the decreasing curve of M vs. ϵ_c, we arrive straightforwardly at the conclusion that, if U is either

compressed or decompressed by a radial perturbation, the forces acting on the perturbed star will act to drive it further from U, that is to say, equilibrium configurations must satisfy

$$\frac{\partial M(\epsilon_c)}{\partial \epsilon_c} > 0 \quad \text{(necessary condition for stability)}. \tag{3.110}$$

This is a necessary but not sufficient condition for stability .

With regard to polytropes, we recall that the mass given by (3.107) is an increasing function of ϵ_c for $\gamma > 4/3$, is stationary at $\gamma = 4/3$, and is a decreasing function for $\gamma < 4/3$. So a necessary condition for the stability of polytropes is

$$\gamma > 4/3, \quad \text{(necessary condition for stability of polytropes)}. \tag{3.111}$$

The maximum in the mass is known as the mass limit, or limiting mass. It always exists in the white dwarf and neutron star sequences, but for different reasons to be discussed in Section 3.9.8.

3.9.6 Nonrelativistic electron region

As noted above, the white dwarf region (3.91) itself can be discussed in terms of two regions according to whether k_e is greater or less than the electron mass. In both cases the energy density is dominated by the rest-mass density of the nucleons.

Even in the region $k_p = k_e << m_e << m_p$ it is the electron pressure that dominates over the proton pressure. Neutrons are altogether absent in this region (in the Fermi gas model of the equation of state) because, as shown above, the value of k_e at the neutron threshold is larger than m_e. So it is required that $\nu = 1$. From (3.92), we may write

$$k_e = \left(\frac{3\pi^2\epsilon}{m_N\nu}\right)^{1/3}, \tag{3.112}$$

from which we obtain from (3.86) an expression for the pressure as

$$p = K\epsilon^\gamma, \quad K = \frac{1}{15\pi^2 m_e}\left(\frac{3\pi^2}{m_N\nu}\right)^\gamma, \quad \gamma = 5/3. \tag{3.113}$$

From the solution of (3.101), $\xi_1 = 3.65$ and $-\xi_1^2\theta'(\xi_1) = 2.71$ for $\gamma = 5/3$, we find

$$M = 2.79\,\nu^{-2}\left(\frac{\epsilon_c}{\epsilon_k}\right)^{1/2} M_\odot, \quad \text{(for } \gamma = 5/3), \tag{3.114}$$

where $\epsilon_k = \rho_k m_N \nu$ and $\rho_k = m_e^3/(3\pi^2)$ are the densities corresponding to $k_e = m_e$. We cannot say precisely what the inequality $k_e << m_e$ implies

about ϵ_c/ϵ_k, save that it is less than unity. However, we do understand that we are dealing with the lighter white dwarfs.

In the $\gamma = 5/3$ range of white dwarfs, the mass is an increasing function of central density, and the radius (3.104) is a decreasing function (for any $\gamma < 2$). A decrease of radius with an increase of mass is quite a general property of degenerate stars, and the physical reason is simple. The gravitational attraction grows as the mass increases, causing a greater compaction of the star.

3.9.7 Relativistic electron region: asymptotic white dwarf mass

For the high-density limit, we find k_e from (3.92) and hence from (3.84) the pressure

$$p = K\epsilon^\gamma, \qquad K = \frac{1}{12\pi^2}\left(\frac{3\pi^2}{m_N\nu}\right)^\gamma, \qquad \gamma = 4/3\,. \tag{3.115}$$

This is the equation of state in the limit of ultrarelativistic electrons throughout the star. In this limit we see that the mass (3.107) is independent of central density and the radius (3.9.4) tends to zero, as $\gamma \to 4/3$. The value of the unique mass, given in terms of the solution of the Lane–Emden equation $\xi_1 = 6.90$, $-\xi_1^2\theta'(\xi_1) = 2.02$, for $\gamma = 4/3$ is composition-dependent and given by

$$M = 5.87\,\nu^{-2}M_\odot\,, \qquad \text{for } \gamma = 4/3\,. \tag{3.116}$$

This is the famous Chandrasekhar mass limit for white dwarfs. To estimate its numerical value, we note that the region

$$m_e << k_e = k_p << m_p \tag{3.117}$$

is well above the neutron threshold. Therefore we can contemplate approximately equal numbers of neutrons and protons (as in ^{4}He, ^{12}C, and ^{16}O of which real white dwarfs are made). Then from (3.116) we find $M \approx 1.5M_\odot$. This is a rough estimate of the maximum white dwarf mass [51, 52].

We have thus learned that the sequence of white dwarfs beginning at low through to high density or correspondingly from $k << m_e$ to $k >> m_e$, has an equation of state in the two limits which are polytropes and that the polytropic index falls from $\gamma = 5/3$ to $4/3$ along the sequence of increasing density. This corresponds to a softening of the equation of state. Between the limits the equation of state can still be thought of as a polytrope but with γ a function of density ranging between the limits.

It is important to notice that the polytropic index reaches the value $\gamma = 4/3$ only as all electrons in the star become ultrarelativistic. In this limit the radius is zero and the density infinite. Along the sequence of

dwarfs of increasing density, the radius decreases as the mass increases toward the limiting value (3.116). The limit obtained by Chandrasekhar is an asymptotic limit. However the limit of real white dwarfs is of a different nature as discussed in the next section. The limiting mass of real white dwarfs is reached at finite density.

Chandrasekhar, while still a student, was the first to discover that there was a mass limit for completely degenerate configurations when one took account of special relativity in computing the equation of state. Limits to stellar masses had never been known before. It is not clear that Chandrasekhar fully understood the implication of his limit by enquiring of the ultimate fate of a star with mass above the limit. Eddington did grasp the implication—collapse to what we now call a black hole—but he dismissed it as absurd [40]. (See the quotations at the beginning of this section.)

Eddington was not alone in rejecting the notion of a black hole. Nor was he the first to conceive the notion. Some 150 years before Eddington's inference, the Rev. John Michell had conceived the possible existence of back holes, stars so dense that their light could not escape, and he explained it in a letter to Henry Cavendish dated November 27, 1783. However, the notion languished in the Philosophical Transactions of the Royal Society (London) [53] and never stimulated further interest (except possibly in Laplace, 1795).

It was not until the work of Oppenheimer and Snyder (1939) on continued gravitational collapse that the notion of black holes reappeared, and, even at that, it was not until the mid-1960s that intense interest in such objects emerged. Indeed, even John Wheeler, until the end of the 1950s, believed that other processes would intervene to prevent collapse of a star to a black hole. He was partially correct. Not all gravitational collapses result in the formation of black holes. Now we know that the fate of stars more massive than the Chandrasekhar limit is more varied and complicated than envisioned by Eddington. Much mass may be expelled in a planetary nebula or supernova. Even if the collapsing core is more massive than the limit for a white dwarf, the star may still be arrested in its collapse at the stage of a neutron star, and only if the collapsing object exceeds the limiting mass for neutron stars will it collapse forever beyond the Schwarzschild horizon.

Shortly after Chandrasekhar's pioneering work, Landau advanced a general argument for a maximum mass that the Fermi pressure of a degenerate gas of relativistic particles can sustain against gravity [54]. Landau's argument is based on fundamental constants. The maximum possible mass is of the order of a solar mass for either degenerate electrons or neutrons (see Ref. [23] for details). Landau's limit, based on the Fermi pressure of relativistic particles of unnamed type, was therefore a prediction of the limiting mass of white dwarfs and neutron stars.

Landau employed the Newtonian gravitational potential, and for Newtonian gravity there is no limiting mass in the sense of General Relativity. The limit obtained by Chandrasekhar is also Newtonian and, as we have seen, is

an asymptotic mass. Nevertheless, real white dwarfs do attain a mass limit along the sequence of equilibrium configurations but at finite density, as depicted in Fig. 3.6, and it is customarily called the Chandrasekhar limit. We will discuss the nature of the limit in the next section.

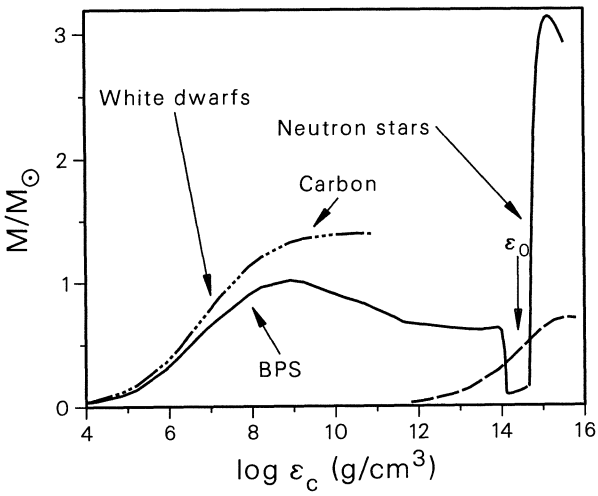

FIGURE 3.6. White dwarf sequences, one correspnding to the equation of state of BPS, the other to a pure Carbon white dwarf (see Section 3.10) and two neutron star sequences: the solid line corresponds to the causal limit equation of state (see Section 3.14), and the dashed to the charge-neutral ideal n,p,e gas in beta equilibrium.

3.9.8 Nature of limiting mass of dwarfs and neutron stars

We have seen that electrons become relativistic at a much lower density than nucleons and that the pressure of degenerate electrons, both non-relativistic and relativistic, establishes stable configurations called white dwarfs . These are Newtonian stars; general relativistic corrections are very small [55]. We also learned that the limiting mass of white dwarfs in the models that we have considered till now is attained only as an asymptotic limit at which the electrons are ultrarelativistic and the density is infinite. This leaves little room for neutron stars.

The dilemma is resolved by noting that, even in the more realistic model considered above in which nucleons reside in nuclei (page 88), the neutron–proton ratio was held fixed. However, an important process is neglected

in this approximation. As the electron Fermi energy increases, high-energy electrons are absorbed by protons—either free or in nuclei—in the inverse beta decay,

$$^{A}Z + e^{-} \longrightarrow {}^{A}(Z-1) + \nu\,. \tag{3.118}$$

The neutrinos diffuse to the edge of the star where, having the escape velocity, they depart. This process is also referred to as *neutronization.* Neutronization depletes the supporting electron pressure with increasing density, bringing the sequence of white dwarfs to an end at central densities of the order of 10^9 g/cm^3. Therefore the mass limit for white dwarfs has to do with their changing internal composition [56, 57]. This limit is unrelated to the limit for relativistic stars, discussed below. What is at issue for white dwarfs is an instability occasioned by electron capture of energetic electrons. Consequently, the white dwarf mass limit is not quite the one envisioned by Chandrasekhar which, as previously noted, is an asymptotic limit attained only at infinite density.

To complete our discussion of the the termination of the white dwarf sequence, we add that, if neutronization did not destabilize white dwarfs, the general relativistic instability discussed next would do so at a somewhat higher density [58].

White dwarf central densities range over about two orders of magnitude around 10^7 g/cm^3, (3.78). At a much higher density, the Fermi pressure of nucleons (assisted by the short-range repulsion between them) establishes a second sequence of stable configurations, the neutron stars. Neutron star densities can be estimated by finding the neutron number density corresponding to, say the point of transition from nonrelativistic to relativistic neutrons, $k_n = m_n$. In this case $\epsilon \sim \rho_n m_n \sim (1/(3\pi^2))m_n^4 = 6{\times}10^{15}$ g/cm^3.

In contrast to the neutronization instability of white dwarfs, gravitational collapse of a neutron star to a black hole or any relativistic star of sufficiently high mass concentration cannot be evaded by any conceivable form of matter, not even "incompressible" matter, as has been clearly argued by Harrison, Thorne, Wakano, and Wheeler [23]. They refer to the "no escape from collapse" in this connection. Collapse of relativistic stars is intrinsic to the structure of Einstein's theory. It has to do with the fact that pressure, which in Newtonian stars resists collapse, in General Relativity ultimately makes collapse inevitable since it appears together with energy density as a source of gravitational attraction in the Oppenheimer–Volkoff equation (2.212). (Recall Section 2.8.6.) Indeed in Section 3.12 we will see that even in the idealization of incompressible matter, there is a limit to the mass and radius of the star that depends simply on the assumed density of the incompressible medium! In general, compact relativistic stars have a mass limit that occurs at a finite central density. The particular value of the mass limit depends on the equation of state but its existence does not.

3.9.9 Degenerate ideal gas neutron star

In our study of the Fermi gas equation of state for nucleons and electrons in beta equilibrium, we learned that at high baryon density the proton fraction approaches one-eighth from below. To a first approximation, charge-neutral matter at densities above the white dwarf domain is pure neutron matter.

After the first few minutes of birth, a neutron star is very cold on the nuclear scale so that in the ideal gas model a neutron star is supported solely by the Fermi pressure of the degenerate neutrons, just as white dwarfs are supported by the pressure of degenerate electrons. Oppenheimer and Volkoff [59] were the first to investigate the structure of neutron stars, and they did so by assuming that the star was composed of noninteracting relativistic neutrons.

The numerical solution of the Oppenheimer–Volkoff equations for the structure of relativistic stars yielded a limiting mass of $\approx 0.72 M_\odot$ and a radius of ≈ 9.6 km [59]. This is an interesting result for the following reason. We know that nuclear forces, especially the repulsive components, will become important at densities higher than the equilibrium density of nuclear matter. The nuclear force therefore provides additional resistance to gravitational collapse beyond that provided by the neutron Fermi pressure. So the Oppenheimer and Volkoff result establishes a value of the maximum mass of neutron stars that is close to a lower bound. The ideal gas of nucleons and electrons that we developed earlier in Section 3.9.2 is an even softer equation of state. It allows the pressure of neutrons at the top of their Fermi sea to be relieved by decay to protons and electrons (always in a charge-neutral equilibrium admixture). The limiting mass in this case is $0.7 M_\odot$.

For real neutron stars, the nuclear force is decisive in establishing the limiting mass and how high it lies above the lower bound just discussed. In Section 3.14 we estimate the maximum amount by which the nuclear force can raise the mass limit above that established by the pressure of a degenerate ideal gas of nucleons and leptons.

The short-range repulsion of the nuclear force stiffens the equation of state compared to that of an ideal gas. By "stiffer" it is meant that at given energy density the pressure is higher in comparison with a "softer" equation of state. The stiffest equation of state that is compatible with the notion of causality is one for which the speed of sound is the light speed. This is not a unique definition because the limit on the sound speed is given by a derivative $\sqrt{dp/d\epsilon}$ which allows any normalization of the equation of state. However, for the purpose of describing neutron stars, the equation of state should match smoothly to a low-density equation of state. This selects a normalization. We refer to an equation of state at the causal limit at high density and normalized in the above manner near nuclear saturation density as a causal limit equation of state. Such an equation of state provides the most resistance to collapse and therefore yields an upper bound on the

limiting mass which is $\approx 3.2 M_\odot$ (see Section 3.14). For the two extremes of soft and stiff equations of state, Fig. 3.6 compares the corresponding neutron star sequences. The limiting mass of neutron star models based on realistic equations of state will lie between the two extremes.

3.10 Improvements in White Dwarf Models

3.10.1 Nature of matter at dwarf densities

A number of the principles involved in the structure of compact stars have been encountered in the above simple model of a degenerate Fermi gas of free neutrons, protons, and electrons in equilibrium. The major objection that can be raised against it as far as white dwarfs are concerned is that at densities below that of normal nuclei—and white dwarfs lie far below—it is energetically more favorable for nucleons to clump together into nuclei so as to exploit the short-range attractive nuclear force than to be uniformly dispersed at lower density [23, 60, 61].

A white dwarf spans an enormous range of densities from its center to its surface. For example, Sirius B ($M = 1.053 M_\odot$, $R = 5,400$ km) has an average density of

$$\bar{\epsilon} = M/\left(\frac{4}{3}\pi R^3\right) = \frac{1.053 \times 1.477 \text{ km}}{(4\pi/3)(5,400)^3 \text{ km}^3} = 2.35 \times 10^{-12} \text{ km}^{-2}$$
$$= 3.17 \times 10^6 \text{ g/cm}^3 = 4.03 \times 10^5 \epsilon_{\text{Fe}} = 1.26 \times 10^{-8} \epsilon_0 . \quad (3.119)$$

(Iron density is denoted by ϵ_{Fe}, and nuclear density by ϵ_0.) The central density is even higher than the average. The character of matter varies appreciably in this vast range of densities. For white dwarfs the constitution of matter is also very much influenced by the progenitor star and the extent of nuclear burning in it.

Unlike neutron stars, white dwarfs are not the remnants of progenitors in which nuclear fusion reactions have been driven to the iron end point under the relentless pressure of gravity (Recall page 81). In the low mass progenitors up to 7 or 8 $M_\odot$, nuclear combustion ceases at some intermediate element, so that dwarfs are composed mostly of ^{4}He, ^{12}C, or ^{16}O in some mixture. While such a composition is not the lowest possible energy state, the lowest energy state is not always attainable in a finite time. The most favored state energetically is actually not achieved in white dwarfs. White dwarfs are much more individualistic (depending on the details of the evolution of the particular progenitor) than they would be if the nuclear burning proceeded through to iron, as in the cores of massive stars prior to their collapse to neutron stars or black holes [60, 62].

The pressure is zero at the edge of a dwarf, and the energy density is low. Whatever elements are present are there in their normal atomic state,

generally arranged in a lattice to minimize the Coulomb energy. As the density increases in the direction of the center, the atoms become partially and then totally ionized, and the electrons become relativistic toward the center of the star. As we have already learned, the degenerate electrons provide virtually all the supporting pressure against collapse while the ponderous nuclei provide little pressure but almost all the mass. We shall develop an equation of state and solve the equations for stellar structure of C and O white dwarfs in the next section.

Notwithstanding that white dwarfs are not the products of complete nuclear combustion, they have been treated as such in several important works. The approximation is certainly better than treating dwarfs as composed of an ideal Fermi gas of nucleons and electrons. It is appropriate to discuss these works at this point.

Matter that has been fully processed by nuclear combustion, so that all available energy has been extracted at each density, is hadronic matter in its ground state, often referred to as "cold catalyzed matter" [23]. At zero pressure, such matter is composed of atoms with the most strongly bound nucleus, ^{56}Fe, arranged in a Coulomb lattice. At increasing density, the atoms become progressively more ionized, and the electrons fill the interstices. A Coulomb lattice arrangement of nuclei in the electron gas minimizes the energy.

At higher density (such that the electron chemical potential is large enough to induce inverse beta decay (3.118)), a lower energy state is achieved through the capture of energetic electrons by nuclei. Neutrinos and photons produced diffuse out of the star, thus lowering its energy. The nuclei become increasingly neutron-rich by this neutronization process. Neutronization sets in at a density for which the electron chemical potential, or fermi energy $\mu_e \equiv \sqrt{m_e^2 + k_e^2}$, equals the threshold for the reaction. We take the proton-neutron mass difference $Q \sim -1$ MeV for the threshold. The threshold density for neutronization is therefore $(Q^2 - m_e^2)^{3/2}/(3\pi^2)\nu m_N \sim 9 \times 10^6$ g/cm^3. (We have taken the baryon electron ratio ν as 2 and m_N, the typical energy of a nucleon in a nucleus, as 930 MeV.)

At densities as high as $\sim 4\times10^{11}$ g/cm^3, the most weakly bound neutrons drip out of the nuclei, and a gas of neutrons and electrons occupies the interstices. The drip density is high compared to the highest density in stable white dwarfs, but occurs in the crust of neutron stars. Therefore the Carbon sequence of dwarfs shown in Fig. 3.6 cannot be correct as this density is approached.

At still higher density around the saturation density of nuclear matter $\epsilon_0 = 2.51 \times 10^{14}$ g/cm^3 (3.17), nuclei disassemble into a uniform charge-neutral mixture of baryons and leptons. This is what we refer to as *neutron star matter*, nuclear matter that is charge-neutral and in its lowest energy state compatible with that constraint. It contains as many baryon species at each density as is required for equilibrium so that no particle transfor-

mations by beta decay or otherwise will take place. Neutron star matter at densities above about $\epsilon_0/2$ is discussed in much detail in the following two chapters and is used to describe the interiors of neutron stars. The subsaturation region described above serves to define the equation of state in the crust.

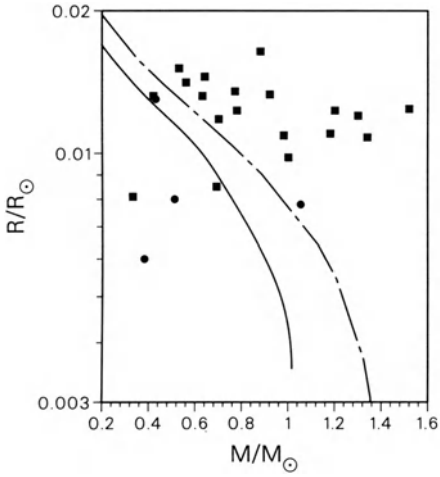

FIGURE 3.7. White dwarf radii and masses compared to the star sequence of the BPS equation of state (solid curve) representing equilibrium matter at each density. Also for carbon white dwarfs (dashed curve). ($R_\odot \approx 7 \times 10^5$ km.)

A number of authors have contributed to the calculation of the equation of state for cold catalyzed matter in various density domains below nuclear saturation: Feynman–Metropolis–Teller from 15 to 10^4 g/cm^3, Chandrasekhar upwards to 10^7 g/cm^3, Harrison–Wheeler–Wakano to 10^{12} g/cm^3, Bonche–Negele–Vautherin to 10^{13} g/cm^3. The compendium of results cited above are sometimes referred to as the Harrison–Wheeler (HW) equation of state [23].

There is another compendium involving detailed calculation at subnuclear densities by Bethe–Baym–Pethick–Sutherland–Siemens [63, 61, 64], often referred to as the BPS equation of state. Both of these papers, as remarked earlier, describe matter in its cold catalyzed state, that is, in the absolute ground state of charge-neutral hadronic matter. For both, the pressure becomes zero at the density of iron, the most bound state of low density matter.

Both equations of state are suitable for the description of the envelope of neutron stars, which are the product of progenitor stars sufficiently massive as to have sustained nuclear burning to the iron end point. Since zero pressure establishes the edge of a star, the surface of a neutron star is iron. A degenerate star has no atmosphere in the sense of the various gases that make up the earth's atmosphere.

As remarked above, the equation of state corresponding to cold catalyzed

matter is not the best description of white dwarf material which is the product of stars whose burning stops at helium, carbon, or oxygen. As such, dwarfs do not belong to a single sequence of stars having the same equation of state. This is perhaps the inference to be drawn from Fig. 3.7 which shows radii and masses of observed white dwarfs [42] and shows a curve corresponding to the BPS equation of state representing matter in its ground state at each density. Also shown is a sequence of carbon white dwarfs which we discuss in the next section and which was qualitatively described above. The BPS equation of state yields a white dwarf mass limit of $\sim 1M_\odot$ while a C white dwarf (closer to an accurate description of a real dwarf) has a limit $\sim 1.4M_\odot$ (see Fig. 3.6).

Except in certain instances, the mass and radius 'measurements' shown in Fig. 3.7 are highly model-dependent. Gravitational redshift measurements establish a relationship between mass and radius for a given star. The radius of a white dwarf is generally inferred from its luminosity and models of the stellar atmosphere, which presumably give a rough estimate but not likely an accurate one. Therefore both mass and radius depend on the atmospheric model.

3.10.2 Carbon and oxygen white dwarfs

White dwarfs constitute the final form into which stars of a few solar masses evolve. Mass loss occurs during their evolution. Because of their low mass, thermonuclear reactions do not burn through to iron, but terminate at lighter nuclei, helium, carbon, or oxygen. An equation of state corresponding to fully catalyzed matter is therefore not quite an accurate description. Here we do a simple calculation of the equation of state of dwarfs that consist of a single nuclear species. More accurate calculations for such white dwarfs were done many years ago by Hamada and Salpeter [60].

Except at the very lowest densities of dwarfs, atoms are compressed to the point that nuclei are fully ionized. Therefore, to lowest approximation, we consider a fully ionized nuclear species immersed in a background of uniform density electrons. The positively charged nuclei will arrange themselves into a lattice with the nuclei at the lattice sites so as to minimize the Coulomb energy. We approximate this situation in the way suggested by Wigner and Seitz, that is, by considering a sphere surrounding each nucleus and touching the neighboring spheres. Each sphere containing a nucleus and its electrons will be neutral. To a good approximation there is no interaction between spheres. We consider one of them.

Most of the mass is contributed by the nuclei, whereas most of the pressure by the electrons (Section 3.9.4). The energy in each sphere consists of the nuclear mass, the electron mass and kinetic energy, the energy of Coulomb repulsion among the electrons, and the attractive Coulomb energy between the electron sea and the nuclei. The Wigner–Seitz approximation will be reasonable as long as the nuclear volume is much smaller

than the volume of the cell which itself should be smaller than the atom.

The Coulomb energy needed to assemble the electrons into the cell of radius R is a familiar calculation. We need to integrate the interaction between the charge within the radius r and the charge in a shell at r of thickness dr,

$$E_{\text{self}} = e^2 \int_0^R \frac{1}{r}\Big(\frac{4\pi r^3}{3}\rho_e\Big) \cdot \Big(4\pi r^2\, dr\, \rho_e\Big) = \frac{3}{5}\frac{(Ze)^2}{R}\,, \tag{3.120}$$

where the electron number density is given by

$$Z = V\rho_e\,, \qquad V = \frac{4\pi}{3}R^3\,, \tag{3.121}$$

with Z the atomic number of the nucleus and therefore the electron number per cell. The electron gas will have an attractive interaction with the nucleus at the center of the cell,

$$E_{\text{int}} = -\int \frac{1}{r}(Ze)(4\pi r^2\, dr\, e\rho_e) = -\frac{3}{2}\frac{(Ze)^2}{R}\,. \tag{3.122}$$

Adding these we get the lattice energy

$$E_{\text{lat}} = -\frac{9}{10}\frac{(Ze)^2}{R}\,. \tag{3.123}$$

Eliminating R from the expression in favor of V, we have the lattice contribution to the pressure,

$$p_{\text{lat}} = -\frac{\partial E_{\text{lat}}}{\partial V} = -\frac{3}{10}\Big(\frac{4\pi}{3}\Big)^{1/3} Z^{2/3}\, e^2 \rho_e^{4/3}\,. \tag{3.124}$$

To compute the equation of state in the present approximation for a pure nuclear species, we may choose a baryon density ρ for which case the cell radius R is given by

$$A = \frac{4}{3}\pi R^3 \rho\,, \tag{3.125}$$

where A is the atomic number of the nuclear species (total nucleon number) and Z its proton number. For such a chosen density ρ, the electron density is $\rho_e = (Z/A)\rho$. We treat the free electrons as a Fermi gas with wave number

$$k_e = (3\pi^2\rho_e)^{1/3} = \Big(3\pi^2\frac{Z}{A}\rho\Big)^{1/3}\,, \tag{3.126}$$

and we denote the corresponding energy density and pressure by $\epsilon_e(k_e)$ and $p_e(k_e)$. We can compute these from (3.68, 3.84, 3.85) as the numerics dictate. The mass of the nuclei we take from experiment. These masses are typically measured as atomic masses, so we subtract the electron rest

masses, but we ignore their atomic bindings. The energy density is $\epsilon = E_{\text{total}}/V$ with the volume $V = A/\rho$. So the energy density and pressure are

$$\begin{aligned} \epsilon(\rho) &= \frac{\rho}{A}\Big(M(A,Z) - Zm_e - \frac{9}{10}\frac{(Ze)^2}{R}\Big) + \epsilon_e(k_e)\,, \\ p(\rho) &= p_e(k_e) - \frac{3}{10}\Big(\frac{4\pi}{3}\Big)^{1/3} Z^{2/3} e^2 \rho_e^{4/3}\,. \end{aligned} \tag{3.127}$$

In the above, $M(A,Z)$ denotes the atomic mass. For example,

$$\begin{aligned} M(^4\text{He}) = 4.00260326U, \quad M(^{12}\text{C}) = U, \\ M(^{16}\text{O}) = 15.99491502U, \quad U = 931.504\ \text{MeV}\,. \end{aligned} \tag{3.128}$$

The above equation of state cannot be valid beyond the density at which high energy electrons are captured by protons in the nuclei. We have already discussed how the white dwarf sequences are terminated by a diminuation of the supporting electron pressure by inverse beta decay. To account for this process, one should evaluate the difference in energies (3.127) between a medium composed of either the nuclear species (A,Z) or (A,Z-1) to find which is the lower and at what density.

To estimate the lower density range at which the approximation of fully ionized nuclei is valid, we may compare the Bohr radius of the inner orbit of the atomic species we have in mind with the cell radius which depends on the nucleon density, as in the relationship written above between A and the volume of the cell. For simplicity let $2Z \approx A$, which is exact in the case of He, C, and O stars. The two radii are

$$r_Z = r_{\text{Bohr}}/Z = \frac{\hbar^2}{m_e Z e^2}, \qquad R = \Big(\frac{3Z}{2\pi\rho}\Big)^{1/3}. \tag{3.129}$$

The first is large compared to the last for baryon densities that satisfy

$$\rho > \frac{3Z^4}{2\pi}\frac{1}{r_{\text{Bohr}}^3} \tag{3.130}$$

or energy densities

$$\epsilon > \rho U = 5.4 Z^4\ \text{g/cm}^3\,. \tag{3.131}$$

The results are very similar for He, C, and O white dwarfs. In Fig. 3.7 we show the mass–radius relationship for carbon white dwarfs for an equation of state as computed in the manner described above. We note that the mass limits for the BPS and C equations of state are, respectively $\sim 1M_\odot$ and $\sim 1.4M_\odot$.

The data on mass and radius of observed white dwarfs lies mostly to the right of the region where the two different types of dwarf sequences lie. Two types of measurements are shown. The circles show measurements

from binaries (giving M) combined with redshift measurements (giving M/R) and are rather accurate. The squares are probably much less certain. Again, they involve the redshift measurement but the other independent determination, this time of radius, is obtained through the less certain chain involving color and flux, distances as measured by parallax, and model atmospheres [42, 65].

There appear to be problems of two kinds in the comparison with theory. To begin, we note that the two curves should rather accurately bracket the theoretical expectations for cold dwarfs. The BPS curve, corresponding as it does to an equation of state of a nuclear lattice of varying species depending on density together with electrons, represents stars in the lowest energy state of hadronic matter in the density range of white dwarfs (cold catalyzed matter). It should yield a sequence of dwarfs more compacted than can be realized in nature given the evolution of the progenitors that produce white dwarfs. The carbon equation of state represents a lattice of carbon nuclei with free electrons. It is appropriate to a white dwarf produced before the end point of nucleosynthesis is reached in the evolution of its progenitor.

As remarked earlier, essentially the same result for the equation of state is obtained for pure He and O stars as for C. The reason is simply that the result can be thought of as that of a polytrope with an electron to nucleon fraction of 1/2, and with the polytropic index changing continuously from the nonrelativistic value (5/3) to relativistic (4/3) from low to high density. So the equations of state differ only in the small lattice energy and pressure in going from He to O. The import of this note is that all cold white dwarfs should lie in the band between the two curves of Fig. 3.7. They clearly do not. As discussed, mass measurements for most white dwarfs are not directly made as for binaries but depend strongly on model-dependent inferences about the radii. Since the equation of state is derived in a physically dependable regime, the inferred mass or radius determinations or both are most likely inaccurate.

3.11 Stellar Sequences from White Dwarfs to Neutron Stars

An approximate overall picture of the relative densities of white dwarfs and neutron stars is shown in Fig. 3.6, where the mass as a function of the central density is plotted. The BPS equation of state is used for white dwarfs up to the central density just above normal nuclear density marked as ϵ_0. The equations of state for He, C, or O white dwarfs or any mixture of these elements would each yield a somewhat different sequence with maximum masses as high as $1.4M_\odot$. As explained earlier, white dwarfs do not correspond to a single sequence because of the individuality conferred

on them by the particular evolution of their progenitors (page 81).

White dwarfs become unstable beyond the Chandrasekhar mass because the chemical potential of the increasingly relativistic electrons rises along the sequence of increasing central density to the point where electron capture by protons (inverse beta decay) yields an energetically more favorable composition. Loss of electron pressure terminates the stable sequence of white dwarfs. This occurs at a central density of about 10^9 g/cm^3 in the case of the BPS equation of state and about 6×10^9 g/cm^3 for C dwarfs.

Stability is not regained along the sequence until, with increasing density, the pressure of degenerate neutrons provides sufficient support against gravity, initiating the stable neutron star sequence. This sequence begins at densities slightly lower than the density of symmetric nuclear matter.

The distributions of mass-energy in two white dwarfs of the sequence are shown in Fig. 3.8, one near the mass limit of the BPS equation of state, the other a very light dwarf. The decrease of radius of the star with increasing mass—characteristic of degenerate gravitationally bound objects—is apparent, as is the very flat energy profile in the stellar interior.

Two extreme neutron star sequences are shown in Fig. 3.6. The sequence with maximum mass $\sim 3.1 M_\odot$ corresponds to a choice of equation of state that maximizes the limiting mass subject only to very general constraints on the equation of state —the causal limit equation of state. It will be discussed in connection with an upper bound on neutron star masses (Section 3.14) and is a very stiff equation of state. The other sequence with limiting mass $\sim 0.7 M_\odot$ corresponds to the soft equation of state developed earlier in this chapter, an ideal gas of neutrons, protons, and electrons that is charge-neutral and in beta equilibrium. Because the Fermi pressure is the only agent of resistance to compression, this result constitutes a lower bound on the mass limit of neutron stars.

Nuclear forces with their short-range repulsion will stiffen the equation of state and increase the limiting mass. Nuclei are bound by the attraction of the nuclear force and have a saturation density that is nearly the same in all nuclei because of the short-range repulsion. In contrast, neutron stars are bound by gravity, and the density is so high that nucleons experience a net repulsion from their interaction with others. Indeed the energy required to compress nucleons to the density found in the cores of neutron stars is 200–300 MeV per nucleon (cf. Fig. 4.2); the nuclear force reduces the binding of neutron stars. In Chapter 5, we will study sequences of neutron stars corresponding to equations of state which respect certain key nuclear properties.

The distribution of mass-energy in the limiting mass neutron stars of these two extreme sequences are shown in Fig. 3.9. The ideal gas stars near the limiting mass have central densities higher by almost a factor of three than those of the stiff equation of state. They also are much more compacted because of their soft equation of state. The profiles of realistic models generally fall between these extremes. In any case, the envelope of

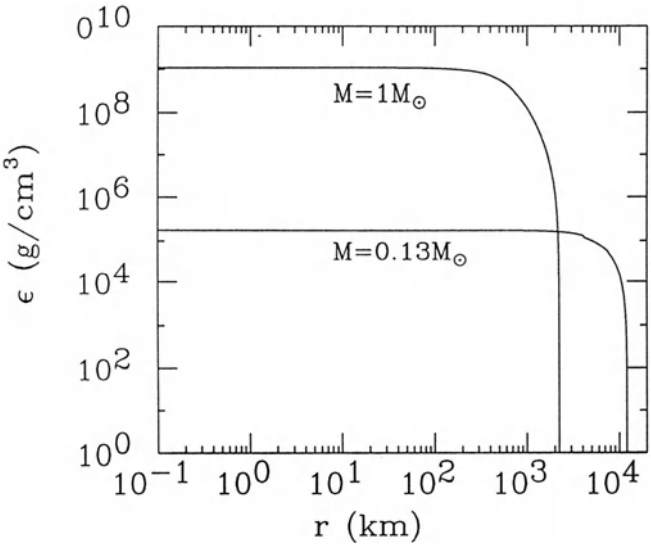

FIGURE 3.8. Mass-energy distribution in two white dwarfs of the BPS equation of state. [66]

the star, comprising densities less than nuclear, is thin. Lighter stars in each sequence, those with lower central densities, have larger radii and the envelope is thicker.

3.12 Star of Uniform Density

In general the equations of stellar structure have to be integrated numerically for realistic equations of state. However there is one analytic case of particular interest because it provides a limiting value of M/R that coincides with the absolute limit for any static star satisfying the Oppenheimer–Volkoff equations. A rigorous analysis yields the result

$$\frac{2M}{R} < \frac{8}{9}, \tag{3.132}$$

independent of the equation of state. It depends only on the structure of the relativistic equations for hydrostatic equilibrium and was obtained by Weinberg [14].

Not surprisingly, the special case that yields the same limit is a star of uniform energy density. The matter of such a star is obviously hypothetical and unphysical because it must be incompressible to maintain a constant density. On the other hand, the idealization is interesting because the energy distribution in neutron stars near their maximum mass limit is rather

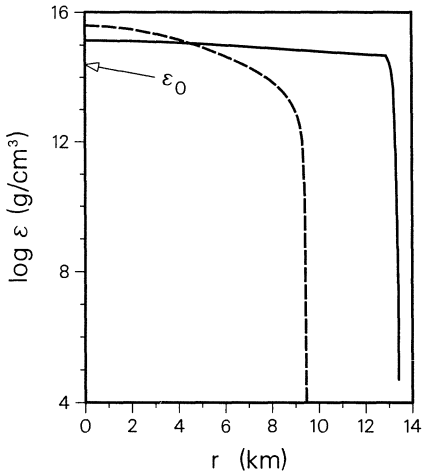

FIGURE 3.9. Mass-energy distribution in the maximum mass neutron stars of the two sequences of Fig. 3.6

uniform, though certainly not constant, as we shall see later when treating realistic equations of state. But most importantly, the idealization illustrates that, even in the hypothetical case of incompressible matter, there is a limit on the maximum possible mass of a stable, compact, relativistic configuration. This interesting and instructive idealization was proposed and solved by K. Schwarzschild (see ref. [67]).

For a star of uniform energy density, say ϵ_0, from (2.199) we have

$$\begin{aligned} M(r) &= \frac{4\pi}{3}\epsilon_0 r^3 , \\ M &= \frac{4\pi}{3}\epsilon_0 R^3 . \end{aligned} \tag{3.133}$$

The equation for hydrostatic equilibrium (2.212) now reads

$$\frac{dp}{dr} = -\frac{4\pi r}{3}\frac{\big(p(r)+\epsilon_0\big)\big(3p(r)+\epsilon_0\big)}{1-8\pi\epsilon_0 r/3} . \tag{3.134}$$

Although the energy density (by the hypothesis of incompressibility) is constant, the pressure varies throughout the star, and the central value is larger the larger the radius (and therefore the larger the mass of the object). Rearrange the above equation as

$$-\int_r^R \frac{dp}{(p+\epsilon_0)(3p+\epsilon_0)} = \frac{4\pi}{3}\int_r^R \frac{r\,dr}{1-8\pi\epsilon_0 r^2/3} . \tag{3.135}$$

Integrating and remembering that the edge of the star is defined by $p(R) = 0$, we easily find

$$\frac{p(r)+\epsilon_0}{3p(r)+\epsilon_0} = \sqrt{\frac{1-2M/R}{1-2Mr^2/R^3}} . \tag{3.136}$$

Solve to find

$$p(r) = \epsilon_0 \left[\frac{\sqrt{1-2M/R} - \sqrt{1-2Mr^2/R^3}}{\sqrt{1-2Mr^2/R^3} - 3\sqrt{1-2M/R}} \right] . \tag{3.137}$$

The central pressure of the star p_c can be obtained now by setting $r = 0$. Solve the resulting equation (3.136) for $2M/R$:

$$\frac{2M}{R} = 1 - \left(\frac{p_c + \epsilon_0}{3p_c + \epsilon_0} \right)^2 . \tag{3.138}$$

The larger the radius of a uniform density star, the more massive it is, and the higher the central pressure must be to support this mass. Take the limit of large p_c, but short of infinity. We find

$$\frac{2M}{R} < 1 - \left(\frac{1}{3}\right)^2 = \frac{8}{9} , \tag{3.139}$$

which as we noted previously is the absolute limit for any static star.

We can easily compute the corresponding radius and mass for the uniform density model. From (3.133) we obtain

$$\frac{4\pi}{3}\epsilon_0 = \frac{M}{R^3} = \frac{M}{R}\frac{1}{R^2} , \tag{3.140}$$

from which there follows

$$\begin{aligned} R_{\rm lim} &= \left(3\pi\epsilon_0\right)^{-1/2} , \\ M_{\rm lim} &= \frac{4}{9} R_{\rm lim} . \end{aligned} \tag{3.141}$$

The above is the limiting mass for stars made of incompressible matter whose energy density is ϵ_0. Others in the sequence have smaller mass, radius, and lower central pressure. The existence of such a limit is intrinsic to the General Theory of Relativity, as discussed in Section 2.8.6, and is absent from Newtonian theory.

It is also of interest to note a more stringent condition on $2M/R$. If matter is such that $p < \epsilon$ (believed to be the case), then (3.138) yields

$$\frac{2M}{R} < \frac{3}{4} . \tag{3.142}$$

The opposite situation $p > \epsilon$ is referred to as ultrabaric matter. Since the energy density of baryonic matter at low pressure is dominated by the rest mass of the baryons, we know that any realistic equation of state must be in the domain $p < \epsilon$ at low pressure (at zero pressure there remains the mass of the baryons). If the equation of state satisfies the so-called causality condition $dp/d\epsilon < 1$, it cannot cross into the ultrabaric region. However, whereas the 8/9 limit can be shown to depend only on the structure of

the Oppenheimer–Volkoff equations and the nonsingularity of the pressure, the above limit of 3/4 is derived explicitly for a uniform density star. It is therefore not as secure as the 8/9 limit. However, it lies very close to a limit of 0.78 obtained by Bondi [68] under the reasonable assumptions concerning the equation of state: $\epsilon > 0$, $p > 0$, and $dp/d\epsilon < 1$.

3.13 Baryon Number of a Star

It is particularly obvious how theorem (2.140) can be applied to a static star to find its baryon number and its binding energy compared to the energy of the dispersed baryons. Let j^μ denote the conserved baryon number current. To find the proper baryon number density, that is, the number density in a local inertial frame of the star at r, we need to evaluate

$$\rho(r) = u_\mu j^\mu = \sqrt{g_{00}(r)}j^0(r) = e^{\nu(r)}j^0(r)\,, \tag{3.143}$$

where, as in (2.195), u^μ is the fluid four-velocity. In Section 2.5.4 we learned that $\sqrt{-g}\,d^4x$ is the invariant volume element. For the Schwarzschild metric we have

$$\sqrt{-g} = e^{\nu(r)+\lambda(r)}\,r^2\,\sin\theta\,. \tag{3.144}$$

Using (2.140) for the total baryon number of the star we obtain

$$A = 4\pi\int_0^R e^{\lambda(r)}r^2\rho(r)\,dr = 4\pi\int_0^R\left(1-\frac{2M(r)}{r}\right)^{-1/2}r^2\rho(r)\,dr\,. \tag{3.145}$$

From whatever theory that provided the equation of state, we know $\rho(r)$ for any $p(r)$ or $\epsilon(r)$. We can therefore integrate the above equation concurrent with the Oppenheimer–Volkoff equations. Thus, the total number of baryons in a star can be computed.

Later we shall be interested in a description of neutron stars in which not only the neutron and proton are present, but also higher mass baryons. This is likely to be the case in the dense interior where the neutron chemical potential may exceed the masses of other baryons, such as the Λ. We will encounter this in Chapter 5. The proper[7] density of each species in the stellar model at a point r can be found by reference to the particle composition of the calculated equation of state associated with the energy density or pressure for that point. Their total number in the star is given by a formula analogous to the one above.

Fig. 3.10 shows an example of the metric function $e^{\lambda(r)} = \sqrt{-g_{11}(r)}$ that appears in the integral above. In Fig. 3.11 we take the opportunity

[7] *Proper* density is used to denote the density in a local inertial frame at the specified point in the gravitational field.

of comparing the gravitational masses of neutron stars with the masses of equivalent numbers of neutrons dispersed at rest at infinity, $M_A = Am_n$. The mass M_A is sometimes called the baryon mass of the star. By reading the mass difference from the graph at the limiting mass star and its baryon number from Fig. 3.1, one can find that the binding per neutron is about 100 MeV. This compares with our classical estimate of 160 MeV from (3.18). The latter refers only to the gravitational attraction and does not include the repulsive Fermi energy and nuclear compression energy.

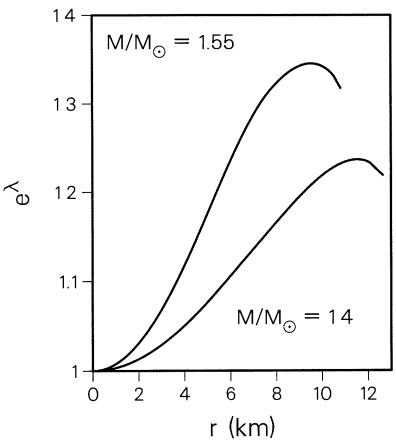

FIGURE 3.10. Metric function interior to neutron stars of two masses. The larger is at the mass limit. See Chapter 5 for details. (K=240 MeV, $m^\star = 0.78m$, $x_\sigma = 0.6$).

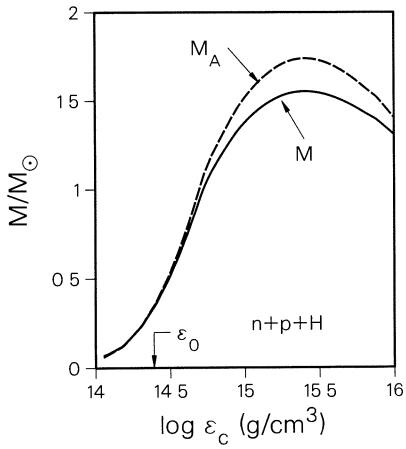

FIGURE 3.11. For the same case as Fig. 3.10, the gravitational mass M is compared with the mass of the corresponding number of neutrons dispersed at rest to infinity M_A.

The baryon mass is usually less than the gravitational mass and always less for configurations near the limiting mass. However, less massive neutron stars have a higher mass than that of the individual baryons dispersed to infinity as shown in Fig. 3.12 where the binding energy per nucleon, $B/A = (M_A - M)/A$ is plotted. These stars have even higher gravitational mass as compared to the mass of the equivalent baryon number assembled in the form of iron nuclei at infinity. Nevertheless, even in the case in which a star is not bound with respect to a simultaneous removal of all constituents to infinity, it is bound with respect to removal of single nucleons (or groups of nucleons but not all nucleons). The reason for this is the long-range attraction of all the remaining nucleons in the star. From page 73 the

energy of a nucleon in the star is $m(1-2M/R)^{1/2} =$ constant which is less than m.

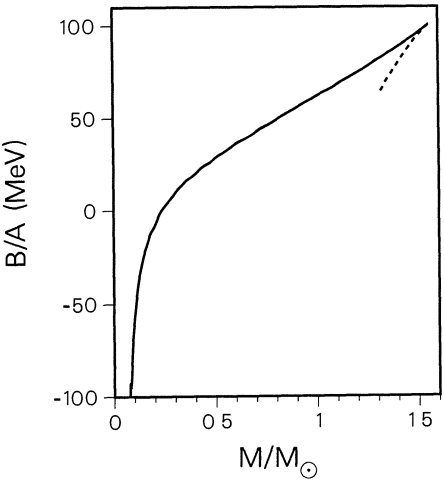

FIGURE 3.12. Binding energy per baryon of a neutron star sequence. The dashed line represents the unstable configurations with central densities higher than that of the limiting mass star. Note the negative binding for stars with $M < 0.2M_\odot$. Calculational details are in Chapter 5. Same case as in Fig. 3.10.

It may be relevant to observe that there may exist no creation mechanism for low-mass neutron stars having small or negative binding, even though they are stable in the sense discussed above. A large release of binding energy is required to eject most of the progentior star and evade the formation of a black hole. This observation may account for the apparent absence of low-mass neutron stars (say less than $1M_\odot$).

3.14 Bound on Maximum Mass of Neutron Stars

The Rev. John Michell explained to the Royal Society (London) in 1783 that if stars should exist whose light could not reach us (black holes), nonetheless, their presence may be revealed by their gravitational effect on luminous companion stars [53]. This is precisely how one attempts to identify black holes in the few solar mass range. There are a few such candidates [69, 70, 71]. However, it is necessary to be able to distinguish between a black hole candidate and a neutron star which would also in general be invisible to us (unless detected by pulsed radiation). This problem and the direction of its solution were recognized by Zwicky [72] and Ruffini [73].

In the General Theory of Relativity a maximum mass star with central density a few times nuclear density exists above which there are no stable configurations, no matter what the equation of state. We have seen that even if matter were to become incompressible at a certain density, a maximum mass still would exist (Section 3.12). If a compact star, unseen except by its gravitational effects on a luminous companion star, is detected and its mass is inferred to be greater than the limiting mass of neutron stars,then the alternative appears to be that it is a black hole. To

place such an identification on the firmest ground, the theoretical limiting neutron star mass must be established in a manner that does not depend sensitively on any details of the equation of state; for we do not know it with confidence in the high-density domain.

Rhoades and Ruffini attempted to obtain a limit free of any but very general and accepted assumptions. They were (1) The equations of stellar structure that follow from General Relativity are valid; (2) The matter of which stars are made is stable against local spontaneous expansion or contraction from equilibrium, (Le Chatelier's principle). The principle can be expressed in terms of the equation of state as $dp/d\epsilon \geq 0$ (the pressure must rise as the density or at least remain constant as in the mixed phase of a first-order phase transition in a single-component substance); (3) In the absence of dissipation, disturbances propagate with speed $\sqrt{dp/d\epsilon} < 1$ (referred to as the causal constraint); (4) The high density equation of state satisfying the above constraints matches continuously to a low-density equation of state.

For the maximum mass star, the energy profile, as a function of distance from the center, falls very rapidly to zero at the edge of the star, and very little mass is contained in the thin envelope of low-density matter. So the dependence on a specific choice for the low-density domain is weak.

It is fairly obvious (and will become abundantly clear in our later studies) that the stiffer the equation of state (meaning the higher the pressure as a function of density) the greater the limiting mass. A high-density equation of state that is at its causal limit will support a greater limiting mass than softer ones. Any density range of matter $\epsilon_1 < \epsilon < \epsilon_2$ for which $dp/d\epsilon$ vanishes is excluded from a star since the Oppenheimer–Volkoff equations inform us that the pressure is a monotonically decreasing function of the distance from the center. This is a well known property of the atmosphere of the earth. The pressure of matter at any radius must support the matter above it against the gravitational attraction of all that lies within. Therefore a constant pressure region in the equation of state contributes nothing to stellar masses. The matter described by such a region, usually a mixed phase, is totally absent from a star. The equation of state at higher density $\epsilon > \epsilon_2$ beyond such a constant pressure region is obviously softer than one that increases with density at ϵ_1. So for the purpose of obtaining an upper bound on the maximum mass, we may consider only equations of state that increase monotonically with density.

Accordingly, let us adopt the BPS equation of state for the low-density domain and match it continuously in density and pressure to an equation of state that is at the causal limit. Let the matching point be denoted by a subscript "f". Then the energy density and pressure given by

$$\epsilon(\rho) = \tfrac{1}{2}\left[\epsilon_f - p_f + (\epsilon_f + p_f)\left(\frac{\rho}{\rho_f}\right)^2\right]$$

and

$$p(\rho) = \epsilon(\rho) - \epsilon_f + p_f, \qquad \rho \geq \rho_f\,, \tag{3.146}$$

obey the thermodynamic relationship $p = \rho^2 \partial(\epsilon/\rho)/\partial\rho$. It is obviously at the causal limit $dp/d\epsilon = 1$, and it is equal to $(\epsilon_f,\ p_f)$ at ρ_f.

There remains the choice of matching density below which a specific equation of state is chosen, in this case BPS. There will be some sensitivity to this choice, and we need to explore it. Let us write the causal limit equation of state as

$$p = \epsilon - a, \qquad a \equiv \epsilon_f - p_f\,. \tag{3.147}$$

Now note that the Oppenheimer–Volkoff equations

$$\begin{aligned} \frac{dp}{dr} &= -\frac{\big(p(r) + \epsilon(r)\big)\big(M(r) + 4\pi r^3 p(r)\big)}{r\big(r - 2M(r)\big)}\,, \\ dM(r) &= 4\pi r^2 \epsilon(r)\, dr\,, \end{aligned} \tag{3.148}$$

have the same form in the scaled variables,

$$\overline{p} = p/a, \qquad \overline{\epsilon} = \epsilon/a, \qquad \overline{r} = \sqrt{a}\, r, \qquad \overline{M} = \sqrt{a}\, M\,. \tag{3.149}$$

If the above causal limit equation of state held for all densities, there would be perfect scaling, i.e., once the Oppenheimer–Volkoff equations were solved for a particular a and the mass and radius of the limiting star determined, the corresponding limiting values for any other a would be

$$R(a') = \sqrt{a/a'}\, R(a), \qquad M(a') = \sqrt{a/a'}\, M(a)\,. \tag{3.150}$$

However, since we use the causal limit equation of state only for $\rho > \rho_f$, there is a thin envelope of matter with $\rho < \rho_f$ overlying the major part of the star. This envelope does not obey the scaling rule, but it contributes little in mass or radius, and this statement will be more accurate the smaller ρ_f. On the other hand, the equation of state is certainly not at the causal limit at densities as low as the saturation density of nuclear matter $\rho_0 = 0.153\ \mathrm{fm}^{-3}$ or, equivalently, $\epsilon_0 \approx 2.5\ 10^{14}\ \mathrm{g/cm}^3$. So the matching density ought to be chosen larger than this value.

By numerical integration of the Oppenheimer–Volkoff equations using as a matching density one of the grid points in the tabulation of BPS ($\rho_f = 0.2715\ \mathrm{fm}^{-3}$ which corresponds to $\epsilon_f = 4.636\ 10^{14}\ \mathrm{g/cm}^3 = 3.442\ 10^{-4}\ \mathrm{km}^{-2}$ and $p = 5.041\ 10^{-6}\ \mathrm{km}^{-2}$), we find

$$M = 3.14 M_\odot, \qquad R = 13.4\ \mathrm{km} \quad \text{(causal limit)}\,. \tag{3.151}$$

From the above numbers it is clear that in the vicinity of saturation density the energy density dominates over the pressure by two orders of magnitude so that to good approximation a is just the energy density at the matching point. More accurately,

$$a = 3.392\ 10^{-4}\ \mathrm{km}^{-2} = 4.569\ 10^{14}\ \mathrm{g/cm}^3\,.$$

So,

$$R(a') = 13.4\sqrt{\frac{4.569\ 10^{14}\ \mathrm{g/cm^3}}{a'}}\ \mathrm{km}\,,$$
$$M(a') = 3.14\sqrt{\frac{4.569\ 10^{14}\ \mathrm{g/cm^3}}{a'}}\ M_\odot\,. \tag{3.152}$$

If we were to choose the saturation density as matching density (as remarked above it would be hard to justify such a small value), we would get $4.3M_\odot$ for the theoretical upper bound of a neutron star mass. It is safe to conclude that neutron stars cannot have masses that exceed this value and probably cannot exceed the first estimate of $3.14M_\odot$. With the addition of any other constraints in the form of a realistic equation of state, the bound can only become smaller.

We conclude that the Rhoades–Ruffini bound on the maximum possible mass of a neutron star is a good one. Any compact object of mass greater than $\sim 3M_\odot$ cannot be a neutron star unless it is rotating at or very near its Kepler frequency (the frequency at which the centrifugal force is balanced by the gravitational force at the equator), in which case the mass bound could be increased by 10 to 20 % [74, 75].

For the purpose of identifying black hole candidates, it should be emphasized that the estimate of an upper bound on the mass limit must be conservative. On the other hand, we are also interested in neutron stars themselves in which case we should incorporate as much knowledge or physically motivated theoretical considerations as possible. These can only lower the bound. So actual neutron stars are likely to have masses that are less than the bound derived above, perhaps considerably less. We will study this question in the context of realistic constraints on the equation of state in Chapter 5.

One final note to this discussion. The line $p = \epsilon$ is often referred to as the causal limit, particularly in figures showing equations of state in the $p - \epsilon$ plane. This terminology suggests that equations of state below this line are all causal. This is not so. In (3.147) we see an example that lies below $p = \epsilon$ but is itself at the causal limit $dp/d\epsilon = 1$. What is true is that an equation of state that is at any point below $p = \epsilon$ cannot cross into the region above without having slope greater than unity, becoming therefore acausal. For these reasons, the region above $p = \epsilon$ is better referred to as ultrabaric, meaning simply $p > \epsilon$. Since cold, low-density matter, say iron, has mass but no internal pressure under normal conditions, it lies below the ultrabaric line, and, since causal equations of state (in the sense taken here) cannot cross this line, it is likely that $p < \epsilon$ holds in general.

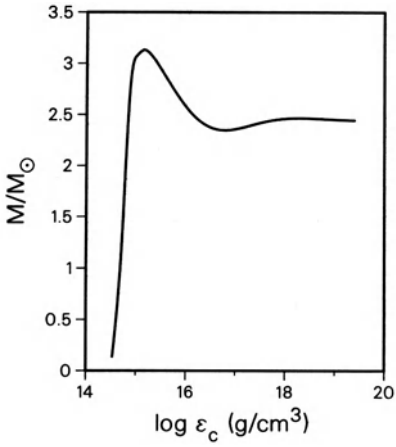

FIGURE 3.13. Stellar sequence with central densities from neutron stars and higher densities corresponding to the causal equation of state of Section 3.14. There are a denumerable infinity of turning points.

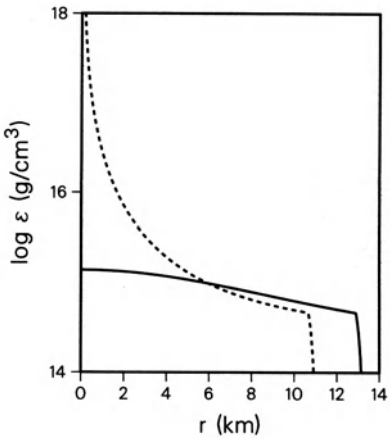

FIGURE 3.14. Mass-energy distribution of the two stars corresponding to the maxima of 3.13

3.15 Beyond Maximum-Mass Neutron Stars

The Oppenheimer–Volkoff equations provide the equilibrium configuration at each central star density corresponding to an equation of state of cold matter that spans a continuous density range. There are two ranges for which these configurations are stable (the mass-energy is a minimum with respect to radial perturbations). The white dwarfs form a stable sequence and are stabilized by the pressure of degenerate electrons. At higher density the neutron stars form a second stable sequence and are stabilized by the nucleon pressure and by the repulsion between nucleons at short range. Are there additional stable regions? We can think of no additional physical agent besides those mentioned that could reestablish equilibrium for stars of higher central density. We will discuss the physics of this remark in detail in Section 8.5 after we have encountered quark degrees of freedom.

In any case, as far as matter describable in terms of an equation of state from low (i.e., white dwarf densities) to arbitrarily high density is concerned, even if the equation of state is at the causal limit (such as the one described in the last section), additional stable regions do not exist. It is interesting that there are a denumerable infinity of star sequences that satisfy the necessary condition for stability (3.110) $dM/d\epsilon_c > 0$ for such

an equation of state. Fig. 3.13 illustrates two of them. Nevertheless, for those of the sequence with positive slopes that lie higher in central density than the neutron star sequence, the energy profile increases so steeply as the center of the star is approached that the star is unstable to acoustical vibrations, the lowest of which brings the central part of the star within its critical Schwarzschild radius. The core collapses, and then the rest of the star (with nothing to support it) follows [23].

A comparison is made in Fig. 3.14 between the mass-energy distribution of a stable neutron star at the Oppenheimer–Volkoff limit and that of the unstable star at the next maximum. The remarkably steep energy distribution in the second case is responsible for the instability described above and characterizes the distribution in all stellar configurations above the Oppenheimer–Volkoff limit for neutron stars. Despite the very early analysis of stability by Wheeler et. al. [23], suggestions of superdense stars continue to appear in the literature. The analysis referenced is for a particular simple analytic equation of state. We will return to this discussion when we have discussed quark stars in Chapter 8; the theorem proving the absence of stable configurations above the Oppenheimer–Volkoff limit must be completely general.

3.16 Black Holes

> "If there should really exist in nature any bodies, whose ... light could not arrive at us ... we could have no information from sight; yet, if any other luminous bodies should happen to revolve about them we might ... infer the existence of the central ones."
> *Rev. John Michell in a letter to Henry Cavendish, May 26, 1783* [53]

3.16.1 Interior and Exterior Regions

So far as is known the Rev. John Michell, a philosopher and scientist of some repute in his day, was the first person to conceive of a star from which light could not escape. He reasoned that gravity should act on light as it does on mass. According to his understanding, stars might exist for which light would not have the escape velocity. We now know that the velocity of light is a constant; it is its energy (frequency) that is diminished in its flight from a star. Nevertheless his conception was prescient. And as for the condition for confinement of light, consider the condition for the escape of a material body of mass m and velocity v from a star of mass M and radius R,

$$\tfrac{1}{2}mv^2 > \frac{GmM}{R}\,. \tag{3.153}$$

Letting $v \to c$ and using gravitational units, we find that the critical radius is $R = 2M$!

Now let us turn again to General Relativity. We have seen that Schwarzschild's solution to Einstein's equations in the region outside a static spherical star becomes singular at

$$r = r_S \equiv 2M\,. \tag{3.154}$$

If the star is enclosed by the Schwarzschild radius, it is a black hole. The spherically symmetric field described by Schwarzschild means that such a black hole is nonrotating; it is often referred to as a Schwarzschild black hole. As we shall see in Chapter 7, the field of a rotating star is not described by the Schwarzschild solution.

The collapse of a star to a black hole was first discussed in the General Theory of Relativity by Oppenheimer and Snyder [18]. There are currently two classes of black holes of intense observational activity, objects of a few solar masses, the compact accreting partners of low-mass, X-ray binaries (LMXB) and extremely massive objects of 10^7 to $10^{10} M_\odot$ in active galactic nuclei (AGN). The latter are probably ingesting stars of the surrounding galaxy by first reducing them to an accretion disk. In both cases, the radiation detected is thought to be produced by the accreting matter as it is heated by compression and friction while it spirals toward the hole. In the case of AGN's, radiation has been detected from X rays down to the infrared and probably includes gravitational radiation, though such has never been detected. The lighter black holes in binary systems are doing the same on a smaller scale.

While not of primary concern to us in this book, it is nonetheless interesting to understand more fully the meaning of the singular point in the Schwarzschild metric. Therefore we investigate the motion of a particle as it drops radially into a nonrotating black hole. Then two components of its four-velocity vanish, $u^2 = u^3 = 0$. The geodesic equation (2.70) for u^0—the equation of motion for a free particle in a gravitational field—is

$$\frac{du^0}{d\tau} = -\Gamma^0_{\alpha\beta} u^\alpha u^\beta = -2\Gamma^0_{10} u^1 u^0 = -2g^{00}\Gamma_{010} u^1 u^0\,. \tag{3.155}$$

We used the symmetry of $\Gamma^\lambda_{\mu\nu}$ in its lower indexes (2.71) to arrive at the factor 2. Because $g_{\mu\nu}$ is symmetric, from (2.80) we have $\Gamma_{010} = \frac{1}{2} g_{00,1}$. Hence, we obtain

$$\frac{du^0}{d\tau} = -g^{00} g_{00,1} u^1 u^0\,. \tag{3.156}$$

But

$$\frac{d\,g_{00}}{d\tau} = \frac{d\,g_{00}}{dr}\frac{dr}{d\tau} = g_{00,1} u^1\,, \tag{3.157}$$

so remembering that $g^{00} = 1/g_{00}$, (2.171), we arrive at

$$0 = g_{00}\frac{du^0}{d\tau} + u^0\frac{d\,g_{00}}{d\tau} = \frac{d}{d\tau}(g_{00}u^0) = 0\,. \tag{3.158}$$

Whence

$$g_{00}u^0 = C\,, \tag{3.159}$$

where C is a constant. Let the particle be dropped radially from rest with respect to the hole at $R > 2M$. Then $dr = d\theta = d\phi = 0$ at R and, from the formula for the invariant interval (2.184), we have $u^0(R) \equiv dt/d\tau = 1/\sqrt{g_{00}(R)}$, so that

$$C = \sqrt{g_{00}(R)} = \sqrt{1 - \frac{2M}{R}}\,. \tag{3.160}$$

From (2.39) we find

$$1 = g_{\mu\nu}u^\mu u^\nu = g_{00}(u^0)^2 + g_{11}(u^1)^2\,. \tag{3.161}$$

In the exterior region we have found $g_{00}g_{11} = -1$ from (2.184). Hence we have

$$g_{00} = C^2 - (u^1)^2\,, \tag{3.162}$$

or, using the explicit expression (2.182) for g_{00},

$$u^1 = -\Big(C^2 - 1 + \frac{2M}{r}\Big)^{1/2}\,, \tag{3.163}$$

where we have chosen the negative square root for the infalling particle. We now have expressions for u^0 and u^1 as functions of r. To get an expression between t and r, we use

$$\frac{dt}{dr} = \frac{dt/d\tau}{dr/d\tau} = \frac{u^0}{u^1} = -C\Big(1 - \frac{2M}{r}\Big)^{-1}\Big(C^2 - 1 + \frac{2M}{r}\Big)^{-1/2}\,. \tag{3.164}$$

We are interested in the behavior of t close to r_S. Introduce a new variable ρ defined by

$$r = 2M + \rho\,, \tag{3.165}$$

with $\rho << 2M$, and study the behavior of t for small ρ, keeping only leading terms in ρ:

$$\begin{aligned}\frac{dt}{dr} &= -C\Big(1 - \frac{2M}{2M+\rho}\Big)^{-1}\Big(C^2 - 1 + \frac{2M}{2M+\rho}\Big)^{-1/2}\\ &\approx -\frac{2M}{\rho} = -\frac{2M}{r-2M}\,.\end{aligned} \tag{3.166}$$

Integrating, we get

$$t = -2M \ln\Big(\frac{r}{2M} - 1\Big) + \text{ constant}. \tag{3.167}$$

From this result we see that, as the particle approaches the Schwarzschild radius $r \to r_S \equiv 2M$, the time $t \to \infty$. An external observer at rest with respect to the star observes that the particle takes an infinite time to reach the Schwarzschild radius. For any process taking place on the particle (including the emission of light), the time to do so will appear to an exterior stationary observer to approach infinity as the particle approaches r_S. Light emitted from the particle will tend to be infinitely red shifted as seen by an exterior observer!

On the other hand, in a frame falling freely with the particle, we have $d\tau = dt$. So,

$$\frac{dt}{dr} = \frac{d\tau}{dr} = \frac{1}{u^1} = -\Big(C^2 - 1 + \frac{2M}{r}\Big)^{-1/2}. \tag{3.168}$$

As $r \to r_S$, $dt/dr \to -1/C$. An observer falling with the particle measures a finite time lapse for the particle to reach the Schwarzschild radius. Thus, there is no singularity in spacetime (the singularity being in the metric for which a transformation could be made to new coordinates with a non-singular metric). If the Schwarzschild radius lies outside a star, it separates space into distinctly different regions. From outside $r = r_S \equiv 2M$, one cannot see a particle drop into the hole. Neither can any particle or light escape from inside the Schwarzschild radius, as we shall see shortly. The Schwarzschild radius is sometimes referred to as the Schwarzschild horizon.

An external observer is unable to obtain any signal of what might happen within the Schwarzschild radius. Only the imprint of the mass is left on the external geometry in the case of a Schwarzschild black hole. In general two other attributes of a black hole leave their imprint on the external geometry: electric charge and angular momentum. The field produced by a rotating or charged star is different from that of Schwarzschild. We discuss rotating stars in Chapter 6.

3.16.2 No statics within

To further analyze the nature of the singularity, let us define a new time coordinate due to Eddington and Finkelstein whose form is suggested by (3.167):

$$t' = t + 2M \ln\Big|\frac{r}{2M} - 1\Big|. \tag{3.169}$$

Under this transformation, the Schwarzschild metric has no singularity as $r \to r_S$. (The second term cancels the singularity in (3.167)). There are

other coordinate transformations as well that are nonsingular at the horizon. We see that the Schwarzschild singularity is a coordinate singularity.

We now study the behavior of null cones with vertices at different spacetime points both far from r_S, near, and inside. The null cones (or light cones) are the hypercones in four-dimensional spacetime connecting an event at the vertex of a cone to neighboring events between which a light signal can propagate. Light rays travel into the future of the vertex event on those cones opening toward $+t$. Timelike geodesics ($d\tau^2 > 0$)—the paths followed by material particles that pass through the vertex of a cone—lie within the cone. Events in the past of the vertex event lie on or inside the cone opening in the opposite direction.

It will be sufficient to study the behavior of the cones in the t-r plane, taking $d\theta = d\phi = 0$. From the Schwarzschild expression for the proper time (2.184), the equation for the future cone of events at r is

$$\left(1 - \frac{2M}{r}\right) dt^2 = \left(1 - \frac{2M}{r}\right)^{-1} dr^2 . \tag{3.170}$$

Transforming to the new time coordinate, we get

$$0 = \left(1 - \frac{2M}{r}\right)\left(\frac{dt'}{dr}\right)^2 - \frac{4M}{r}\left(1 - \frac{2M}{r}\right)\left|1 - \frac{2M}{r}\right|^{-1}\left(\frac{dt'}{dr}\right) - \left(1 + \frac{2M}{r}\right) . \tag{3.171}$$

The solutions are

$$\frac{dt'}{dr} = -1 \quad \text{and} \quad \left(1 + \frac{2M}{r}\right) / \left(1 - \frac{2M}{r}\right) . \tag{3.172}$$

So one side of the cone (closest to the star) always has slope -1 and the other has a slope that depends on the position of the event location of the cone. We can write the equation for the latter as

$$(r_0 - r_S)\, dt' = (r_0 + r_S)\, dr , \tag{3.173}$$

where r_0 is used to define the r coordinate at the vertex of the cone.

Far away from the Schwarzschild radius, the side of the cone that is remote from the black hole has slope $+1$. Therefore the geodesic path of a light ray or particle that is far from the horizon can lead away or toward the black hole. These distant cones have axes parallel to the time axis or, more accurately, as the distance from the star approaches infinity they approach a parallel orientation. At event points closer to r_S, the cones tilt toward the star and have narrower opening angles. The cone with vertex at $r_0 = r_S$ has one side parallel to the t' axis and the other pointing to smaller r, always with slope -1. Therefore a particle located at r_S, or interior to it, can only fall into the hole. Light emitted from the horizon can at best either circle the hole or fall in, but cannot escape.

The future cones of particles or photons already in the hole point only inward. There is no possibility of escape nor even of remaining at a stationary distance from the origin. Within the Schwarzschild radius, there is no possibility of statics or equilibrium! A star that falls through its Schwarzschild radius continues to collapse to a singularity or at least until the Planck scale[8] at which the classical theory may be invalid. (The Planck density is about 10^{78} times the central density of the most massive neutron star.)

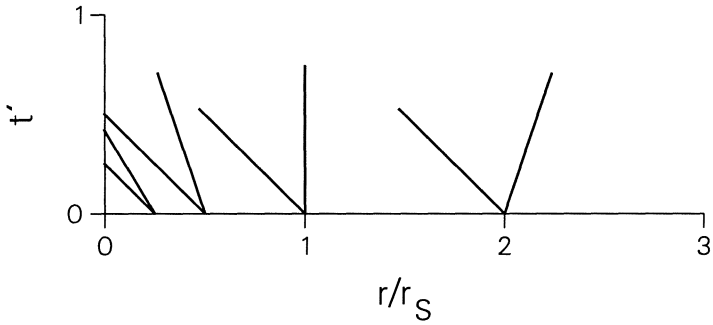

FIGURE 3.15. Future light cones at radial distances both inside and outside a black hole Schwarzschild radius $r_S \equiv 2GM$.

To summarize, distant light cones have an opening angle approaching $\pi/2$ as the distance from the black hole increases. The cones tilt toward the hole for events that are closer and their opening angles become smaller. Inside the Schwarzschild radius, both sides of the cone point to a smaller radius: world lines can lead only inward. A few such light cones are illustrated in Fig. 3.15. It should be noted that they are not related to each other but simply define the future light cone for each vertex point outside the black hole.

3.16.3 Black hole densities

Black holes are usually thought to have enormous densities. This is true of some. Those formed in the collapse of the degenerate cores of evolved stars have very high densities. Indeed, collapse continues to a singularity. We have seen that, within the horizon, all matter and even light can only fall inward. Collapse to the singularity is very rapid for solar mass stars

[8]Combinations of the Planck constant, the gravitational constant, and the speed of light define a Planck mass, length, and time. The first two define a density of 5×10^{93} g/cm^3. This can be compared to the central density of neutron stars $\sim 10^{15}$ g/cm^3. Therefore quantum gravity is of no relevance to compact, *stable* stars like neutron stars and white dwarfs.

but long for the collapse of a black hole having the mass of a galaxy. So it makes sense to enquire about the initial density of black holes of various masses.

Schwarzschild black holes are non-rotating stars whose radius satisfies $R < 2M$. The average density satisfies

$$\rho = M/\left(\frac{4\pi}{3}R^3\right) \geq \frac{3}{32\pi M^2}\,, \tag{3.174}$$

where (3.132) has been employed. Referring to the section on units (3.3), this can be expressed in the more convenient form,

$$\rho \geq \frac{1.8 \times 10^{16}}{(M/M_\odot)^2}\ \mathrm{g/cm^3}\,. \tag{3.175}$$

The Milky Way galaxy has a mass of about $10^{12} M_\odot$. The density of a black hole formed from its collapse need only be larger than 1.8×10^{-8} g/cm^3. The radius of the horizon is 3×10^{12} km—about a third of a light year.

4

Relativistic Nuclear Field Theory

4.1 Motivation

Matter and energy warp spacetime and in turn are shaped and moved by the curvature of spacetime. Accordingly, any theory of matter in the presence of strong gravitational fields should be examined within the context of curved spacetime. We are guaranteed by the equivalence principle that, at any spacetime point in a star, a local Lorentz frame can be erected. We found that, at the highest densities in a neutron star hovering at the verge of collapse to a black hole, the relative change in the metric over the average distance of baryons is exceedingly small ($\leq 10^{-19}$) (Section 3.4). Therefore, the extent of a local Lorentz frame in a neutron star is so large on the scale of particle spacings that we may treat the matter at a given density as if it were of infinite extent and neglect the energy associated with boundaries in comparison with the bulk energy. This establishes the frame in which we may work—a Lorentz frame—and the approximation in which we may work—the bulk approximation.

From a wealth of information on nuclei, we know that, at nuclear density (and for some density above), nuclei and nuclear matter are composed of protons and neutrons that interact through the nuclear force mediated by the exchange of mesons. In equilibrated hadronic matter at densities several times that of normal nuclear matter, the Fermi energy of the nucleons will be so large that it is energetically more favorable for some nucleons to transform to heavier baryon species through the electro-weak interaction. In this way the conserved baryon number is shared among a greater number of species of lower Fermi energy.

Some of the baryon and meson species and their quantum numbers are shown in Table 4.1. The most important baryons in neutron stars are the octet baryons, the lowest mass baryons of spin $\frac{1}{2}$. They comprise the nucleons and some of the hyperons, baryons that carry the strangeness quantum number. The most important mesons are the scalar σ, the spin one vector ω and the spin and isospin one vector-isovector $\boldsymbol{\omega}$. In the mean field approximation to the relativistic theory that will be used in this chapter, the above mesons mediate the interaction among baryons. The pion and kaon are of possible interest as condensates, but their mean values in the approximation in which we work vanish because they change parity and strangeness, respectively.

Hadrons—baryons and mesons—are not themselves the fundamental par-

TABLE 4.1. Baryon and meson states. Spin is J, isospin is I, baryon number is b, charge is q, and strangeness is s. The baryon octet comprises the baryons of spin $J = 1/2$.

	m (MeV)	J	I	b	q	s
N	939	1/2	1/2	1	0,1	0
Λ	1115	1/2	0	1	0	−1
Σ	1190	1/2	1	1	−1,0,1	−1
Ξ	1315	1/2	1/2	1	−1,0	−2
Δ	1232	3/2	3/2	1	−1,0,1,2	0
Ω	1673	3/2	0	1	−1	−3
σ	~ 800	0	0	0	0	0
ω	782	1	0	0	0	0
ρ	770	1	1	0	−1,0,1	0
π	139	0	1	0	−1,0,1	0
K^+	494	0	1/2	0	1	1
K^0	494	0	1/2	0	0	1
$\bar{K}^0$	494	0	1/2	0	0	−1
K^-	494	0	1/2	0	−1	−1

ticles they were once thought to be. We now know that they themselves are composed of quarks whose interactions are mediated by the exchange of gluons. So far as we know, the fundamental fields of nature are the quarks, leptons and gauge bosons (Tables 4.2 and 4.3).

The quarks and leptons are fermions of spin $\frac{1}{2}$. The theory that describes nature at this fundamental level is known as *quantum chromodynamics* (QCD). It is an unusual theory. Unlike quantum electrodynamics (QED), in which the force is mediated by photons that do not interact among themselves, the gluons mediating the strong force do interact. As a result,

TABLE 4.2. Quarks and leptons. Mass m in MeV, charge q in units of e.

		Quarks			Leptons		
Family	Flavor	name	m	q	name	m	q
I	1	u	~ 0	2/3	ν_e	0	0
	2	d	~ 0	−1/3	e	0.511	−1
II	3	c	1500	2/3	ν_μ	0	0
	4	s	150	−1/3	μ	106	−1
III	5	t	$\sim 10^5$	2/3	ν_τ	~ 0	0
	6	b	5000	−1/3	τ	1784	−1

TABLE 4.3. Gauge bosons. Mass m in GeV, charge q in units of e. The graviton is conjectured.

Force	Carrier	m	Spin	q
Gravity	graviton	0	2	0
EM	γ	0	1	0
Weak	W^+	81	1	0
	W^-	81	1	0
	Z^0	93	1	0
Strong	8 gluons	0	1	0

QCD is an almost intractable theory.

The most remarkable aspect of the theory is that quarks, which carry an attribute called *color* charge, can never appear in any combination that has color. There are three colors. An equal number of each form what is referred to as a *colorless* state. Physical states are colorless. A quark and antiquark of the same color also form a colorless state. Quarks are thus *confined* in the sense that they cannot be individually removed from a hadron and isolated. This contrasts with all other hierarchies of composite particles—molecules, atoms, nuclei—which can be separated into their constituents.

There are six *flavors* of quarks, each flavor associated with the mass of the quark. Baryons consist of three (valence) quarks of different color and various flavors. Mesons consist of a quark and antiquark of the same color and different flavor. The light quark flavors are called up, down, and strange. In Chapters 5 and 8 we shall see that these are the only flavors of possible significance in stars. The heavy flavors—charm, beauty and top—cannot be populated at the densities of stable, compact, stellar configurations (see Section 8.5). Of the leptons, only the electron and muon are of relevance to compact stars. The charge chemical potential or Fermi energy in neutron stars never becomes large enough to exceed the tau lepton mass, so the tau is absent (see Section 5.4.7).

Quantum chromodynamics is noted for the interaction coupling between quarks: it is strong at low density or momentum transfer, becoming weak at high density or high momentum transfer. The latter is referred to as *asymptotic freedom*. At very high hadronic density or at very high temperature, asymptotic freedom introduces a new phase of matter, one in which the quarks are not confined in individual hadrons but are free to explore a larger colorless region. This (locally) *deconfined* phase is called *quark matter*.

Quarks are almost free in the quark matter phase, though confined to a high-density or high-temperature region. Asymptotically, the description of this phase is simple. At the other extreme of low and moderate density (up to a few times nuclear density), a QCD description of matter is difficult to

achieve. No useful solution of QCD has been obtained for cold nuclear or neutron star matter, nor is one likely to be forthcoming in the foreseeable future.

As in many problems in physics, it is useful to isolate the degrees of freedom that are relevant at the scale under consideration. Hadrons represent the appropriate degrees of freedom with which to build an effective theory of nuclear matter up to the phase-transition density to quark matter (perhaps 3 to 10 nuclear density). Above the phase-transition density, the appropriate description is in terms of quarks. The quark phase and the phase transition will be discussed in Chapters 8, 9, and 10.

A Lorentz covariant theory of nuclear matter involving hadrons was proposed in its simplest form by Johnson and Teller [76], Duerr [77], in the mid-1950s and Walecka [78] in the mid-1970s. This theory describes the interaction between nucleons in matter through the two meson fields, the scalar σ and vector ω. We refer to this theory as the $(\sigma - \omega)$ nuclear field theory. It is not a fundamental theory inasmuch as it is not formulated in terms of the fundamental fields mentioned above. In many ways it is not as good a theory as the Schrödinger-based theory of nuclear physics.

Nuclei have been traditionally described by a Schrödinger-based nonrelativistic model, the shell model or various of its extensions. Shell models consist of a mean field in which nucleons are bound and a residual force through which they interact. One can compute the energy levels and properties of nuclei involving the active participation of at least a few nucleons. Recently, Monte Carlo techniques have been employed to extend the range of applicability of the shell model.

Nuclear field theory—particularly its extensions as discussed later in the chapter—is especially suitable for the description of neutron star matter. It does have its successes in describing rather well some single-particle properties of finite nuclei (cf. [79, 80, 81, 82, 83, 84, 85]). However it is the description of bulk matter that is relevant to neutron star structure, and the theory with the extensions we describe does well in this respect. For our purpose, relativistic nuclear field theory has several merits. It is automatically causal, whereas the equation of state computed in Schrödinger-based theories is not compelled to be. (It may be up to some density, but causality is not built into the structure of the theory.) Secondly, the coupling constants of relativistic nuclear field theory can be algebraically related to the bulk properties of nuclear matter. Thus the theory can be firmly anchored to the only information we have on high-density matter—(1) causality; (2) microscopic stability (Le Chatelier's principle, $dp/d\rho \geq 0$); (3) saturation properties of nuclear matter; and (4) at high density the asymptotic freedom of quarks.

Accordingly, our goal is to construct extensions of the above $(\sigma-\omega)$ model that will provide a relativistically covariant theory of dense hadronic matter, such as likely exists in neutron stars [49, 86, 87, 88]. The first part of this endeavor will be concerned with the important task of making firm contact

between the theory and five important properties near normal nuclear matter density. Two of these, the binding energy and saturation density, will normalize the equation of state at one point in the energy-density plane. Two others, the compression modulus and effective nucleon mass, assure that the extrapolation to higher density is correct in the vicinity of saturation. (This being so, we have some expectation that the extrapolation to greater extremes is reasonable, though we cannot say unique.) Finally the last nuclear matter property, the isospin symmetry energy coefficient, will assure that small extrapolations to isospin asymmetric systems (of which neutron star matter is an extreme) are correct.

We have no present measurements at extremes of density, isospin asymmetry, or temperature, though they are the object of current and planned experimentation in the field of relativistic nuclear collisions. So it is a special advantage of the theory being developed in this chapter that the coupling constants of the theory are *algebraically* related to the properties of matter at saturation and, within the framework of the particular theory, control its extrapolation in density and in isospin density. Thus the dependence of the properties of neutron stars, arising from the structure of the hadronic matter of which they are made, can be related directly to nuclear matter properties and their uncertainties. In addition the range of stellar properties associated with uncertainties in the nuclear matter properties can be assessed.

It will become clear that at higher densities nuclear matter will also be populated by higher mass baryons. Therefore, the second part of the development concerns the inclusion of other members of the baryon octet besides the neutron and proton. It is not possible to control this sector of the theory by the ground state properties of nuclear matter since only the nucleons populate that state. It will be possible to deduce some constraints on the coupling constants of the hyperons, but we will have to develop considerable additional material before this can be carried out in Section 5.4.3 [89].

The rapid accumulation of data on pulsars in recent years lends hope that real constraints on the equation of state will be obtained from these manifestations of neutron stars. Eventually, it may be possible to invert the process: from the properties of neutron stars deduce the equation of state. Indeed the inverse theorem has already been proved—that given a range of M and R measurements of neutron stars, a unique equation of state can be determined [90].

We use relativistic nuclear field theory for the description of the matter of compact stars up to the point of the phase transition to quark matter. We do not know empirically where this transition occurs. However, it can be computed for specific choices of theory of the confined and deconfined phases and will play an important role in the structure and composition of compact stars (Chapter 9).

We have already discussed a simple Fermi gas model of dense matter in

Section 3.9.2. Nuclear field theory is an extension which includes interactions of the baryons through the mean fields of certain mesons generated in a self-consistent way. In both cases the ground state is a *degenerate* state consisting of all particle momentum levels filled to the Fermi momentum. We begin by recalling certain pertinent elements of Lagrangian field theory. We introduce the Lagrangian of relativistic nuclear field theory, discuss how to compute solutions of the equations of motion in the mean-field approximation, and introduce the baryons of the octet appropriate to a description of dense matter.

After this summary of the Lagrangians and the equations of motion of fields of various quanta and their associated symmetries and conservation laws, we discuss nuclear matter properties as a prelude to their use as constraints on a field theory of nuclear matter. We construct our field theory in stages so as to be in accord finally with the five important properties of nuclear matter mentioned above. The spinor conventions of Bjorken and Drell [91] are used here. We also recall the operations of raising and lowering indices on contravariant and covariant vectors, derivatives of scalars as vectors, and the Minkowski metric tensor (2.3, 2.6, 2.15, 2.16).

4.2 Lagrange Formalism

The fields representing various particles may each be thought of as satisfying equations analogous to those derived for a continuous system obtained by a limiting process applied to a discrete mechanical system involving m degrees of freedom with m going to infinity [92]. Hamilton's principle states that the equations of motion are those for which the classical action is an extremum,

$$\delta S = 0, \qquad S = \int_{t_1}^{t_2} L\big[q, \dot{q}\big]\, dt\,, \tag{4.1}$$

where the Lagrangian depends on generalized coordinates of the system $q \equiv q_1, \cdots q_n$ and the velocities $\dot{q}$. By analogy we consider a Lagrangian *density* in the fields and their four-derivatives,

$$\mathcal{L} \equiv \mathcal{L}\big[\phi(x), \partial_\mu \phi(x)\big]\,, \tag{4.2}$$

where,

$$x \equiv x^\mu = (t, x, y, z), \qquad x_\mu = (t, -x, -y, -z)\,. \tag{4.3}$$

The Lagrangian is the spatial integral

$$L \equiv \int d\boldsymbol{r} \mathcal{L}\big[\phi(x), \partial_\mu \phi(x)\big]\,. \tag{4.4}$$

As with q, $\phi(x)$ may denote one or many fields. The Lagrangian density is a Lorentz scalar because we shall construct it only from scalar functions of the fields and their derivatives. Relativistic covariance is therefore manifest. The corresponding action then is

$$S = \int_{t_1}^{t_2} d^4x\, \mathcal{L}\big[\phi(x), \partial_\mu \phi(x)\big]\,. \tag{4.5}$$

The variation of the action is given by

$$\begin{aligned} \delta S &= \int_{t_1}^{t_2} d^4x \left\{ \frac{\partial \mathcal{L}}{\partial \phi}\delta\phi + \frac{\partial \mathcal{L}}{\partial(\partial_\mu \phi)}\delta(\partial_\mu \phi) \right\} \\ &= \int_{t_1}^{t_2} d^4x \left\{ \Big(\frac{\partial \mathcal{L}}{\partial \phi} - \partial_\mu \frac{\partial \mathcal{L}}{\partial(\partial_\mu \phi)} \Big)\delta\phi + \partial_\mu \Big(\frac{\partial \mathcal{L}}{\partial(\partial_\mu \phi)}\delta\phi \Big) \right\} \\ &= \int_{t_1}^{t_2} d^4x \Big(\frac{\partial \mathcal{L}}{\partial \phi} - \partial_\mu \frac{\partial \mathcal{L}}{\partial(\partial_\mu \phi)} \Big)\delta\phi(x)\,. \end{aligned} \tag{4.6}$$

The variations of the fields are taken as arbitrary save that they vanish at the end points. So the extremal condition is satisfied if

$$\frac{\partial \mathcal{L}}{\partial \phi(x)} - \partial_\mu \frac{\partial \mathcal{L}}{\partial(\partial_\mu \phi)} = 0\,. \tag{4.7}$$

This is the Euler–Lagrange equation for the field $\phi(x)$. If $\mathcal{L}$ depends on several fields, there is one such equation for each.

If the Lagrangian is a Lorentz scalar, then the equations of motion of the theory are Lorentz covariant. So we require that the the Lagrangian be a scalar, $\mathcal{L}'(x') = \mathcal{L}(x)$. By finding certain symmetries in nature (such as the observation that nuclei tend to be most strongly bound when $N = Z$, suggesting that the nuclear force favors isospin symmetric configurations), we can be guided to the construction of a sensible Lagrangian. The symmetry of the action of gravity on all bodies, no matter their composition, was of profound influence on Einstein's discovery of General Relativity as was the logical necessity of the covariance of the laws of nature to changes in the frame of reference or location in the universe. We will be guided here by the conservation laws and symmetries we know of in constructing a sensible nuclear field theory. We first consider symmetries before studying any particular fields and their Lagrangians.

4.3 Symmetries and Conservation Laws

The construction of a scalar Lagrangian from the fields of the quanta we wish to describe, such as the scalars $\phi^2(x)$ or $\partial_\mu \phi(x)\, \partial^\mu \phi(x)$ constructed from a scalar field $\phi'(x') = \phi(x)$, suggests at once that the Lagrangian will

be invariant in form to certain types of *manifest*, continuous, symmetry transformations. For example, if $\phi(x)$ is a complex field, the above scalars would be bilinear in the field and its complex conjugate. The two types of terms are obviously each invariant to a global phase transformation, $\phi(x) \to e^{i\epsilon}\phi(x)$. Such an invariance will be seen to correspond to an additive attribute which is conserved, such as charge.

The invariances and associated symmetry transformations are of various types. There are symmetries associated with spacetime, referred to as *external symmetries*, and there are *internal symmetries*, such as phase transformations. Internal symmetries may depend on x, in which case they are referred to as *local*, or may be independent of x and referred to as *global*.

Invariances under local transformations are of central importance to the theory of the fundamental fields mentioned earlier, but they play no role in our work at the level of effective fields for composite particles. Likewise, we shall be interested in manifest symmetries but not hidden symmetries [93, 94].

4.3.1 Internal global symmetries

We work first on an abstract and general level of internal global symmetries and look later at the specific fields that we shall need in a theory of nuclear matter. Consider a number n of fields $\phi_1(x), \phi_2(x), \cdots \phi_n(x)$ some of which may refer to different charge or isospin states of particles of particular mass. We do not need to specify whether they are Fermi or Bose fields. Consider an internal, infinitesimal, continuous transformation (finite transformations can be built from a number of infinitesimal ones):

$$\phi_i'(x) = \phi_i(x) + \lambda_j F_i^j \left[\phi_1(x), \cdots \phi_n(x)\right] . \tag{4.8}$$

F characterizes the transformation and may mix some of the fields. The λ_j are infinitesimal parameters that are spacetime-independent. Suppose a particular $\mathcal{L}$ is found to be invariant to a continuous symmetry transformation defined by a particular set of F_i^j. Its variation with respect to the parameters of the transformation must therefore vanish. To find the consequence, examine the formal expression for the variation,

$$\delta\mathcal{L} = \frac{\partial\mathcal{L}}{\partial\phi_i}\delta\phi_i + \frac{\partial\mathcal{L}}{\partial(\partial_\mu\phi_i)}\delta(\partial_\mu\phi_i) . \tag{4.9}$$

Since $\delta\phi_i = \lambda_j F_i^j$ and

$$\delta(\partial_\mu\phi_i) = \partial_\mu(\delta\phi_i) = \lambda_j \partial_\mu F_i^j , \tag{4.10}$$

then

$$\delta\mathcal{L} = \Big(\frac{\partial\mathcal{L}}{\partial\phi_i}F_i^j + \frac{\partial\mathcal{L}}{\partial(\partial_\mu\phi_i)}\partial_\mu F_i^j\Big)\lambda_j . \tag{4.11}$$

Employing the Euler–Lagrange equations for the fields in the first term, we obtain

$$\begin{aligned}\delta\mathcal{L} &= \Big(F_i^j\partial_\mu\frac{\partial\mathcal{L}}{\partial(\partial_\mu\phi_i)}+\frac{\partial\mathcal{L}}{\partial(\partial_\mu\phi_i)}\partial_\mu F_i^j\Big)\lambda_j \\ &= \partial_\mu\Big(\frac{\partial\mathcal{L}}{\partial(\partial_\mu\phi_i)}F_i^j\Big)\lambda_j\,. \end{aligned} \tag{4.12}$$

Hence, if $\mathcal{L}$ is invariant to the transformation, then $\delta\mathcal{L} = 0$. Since the parameters λ_j are arbitrary, the set of n four-vectors

$$J_j^\mu(x) \equiv \frac{\partial\mathcal{L}}{\partial(\partial_\mu\phi_i)}F_i^j\,, \tag{4.13}$$

satisfies

$$\partial_\mu J_j^\mu = 0, \qquad (j = 1, 2, \cdots n)\,. \tag{4.14}$$

Divergenceless four-vectors J^μ following from an invariance of the Lagrangian are referred to as Noether currents [95]. Because their four-divergences are zero, each current is conserved. Conservation of a divergenceless four-vector is proved quite simply. Write out in full the divergence (where for the moment we suppress the field identifier j):

$$0 = \partial_\mu J^\mu = \partial_0 J^0 + \partial_k J^k = \frac{\partial J^0}{\partial t} + \nabla\cdot\boldsymbol{J}\,. \tag{4.15}$$

This is the *continuity equation*. Integrate it over a 3-volume containing the system and use Gauss' theorem,

$$\frac{\partial}{\partial t}\int_V J^0\,d\boldsymbol{r} = -\int_V \nabla\cdot\boldsymbol{J}\,d\boldsymbol{r} = -\int_S \boldsymbol{J}\cdot d\boldsymbol{S}\,. \tag{4.16}$$

Since the system is contained within V, the current S crossing the boundary is zero. Therefore the surface integral vanishes. Consequently the time derivative on the left side is zero and we have the conserved charges

$$Q_j = \int_V J_j^0\,d\boldsymbol{r} \tag{4.17}$$

which are constant in time. The invariance of $\mathcal{L}$ to continuous internal symmetries implies the existence of conserved charges. This result will be of use to us in the sequel.

4.3.2 Spacetime symmetries

Physical theories in flat spacetime ought to be Lorentz covariant. Our choice for $\mathcal{L}$ must therefore be a Lorentz scalar. As such, the Lagrangian has certain spacetime symmetries or invariances, such as rotation or translation of

the spacetime coordinates. We consider the second—an infinitesimal translation,

$$x'^{\mu} = x^{\mu} + \epsilon^{\mu} . \tag{4.18}$$

The corresponding change in $\mathcal{L}$ can be written

$$\begin{aligned} \delta\mathcal{L} &\equiv \mathcal{L}\big[\phi(x^{\nu}+\epsilon^{\nu}),\, \partial_{\mu}\phi(x^{\nu}+\epsilon^{\nu})\big] - \mathcal{L}\big[\phi(x^{\nu}),\, \partial_{\mu}\phi(x^{\nu})\big] \\ &= \epsilon^{\mu}\frac{\partial\mathcal{L}}{\partial x^{\mu}} = \epsilon^{\mu}\partial_{\mu}\mathcal{L} = \epsilon_{\nu}\partial^{\nu}\mathcal{L} . \end{aligned} \tag{4.19}$$

We made a Taylor expansion in the first term on the right and kept terms to first order in ϵ to obtain the second line.

Alternately, since $\mathcal{L}$ depends only on ϕ and $\partial_{\mu}\phi$ and not explicitly on x^{μ}, we also may write the change as

$$\delta\mathcal{L} = \frac{\partial\mathcal{L}}{\partial\phi}\delta\phi + \frac{\partial\mathcal{L}}{\partial(\partial_{\mu}\phi)}\delta(\partial_{\mu}\phi) , \tag{4.20}$$

where, just as for $\delta\mathcal{L}$, we write

$$\begin{aligned} \delta\phi &\equiv \phi(x^{\nu}+\epsilon^{\nu}) - \phi(x^{\nu}) = \epsilon^{\nu}\partial_{\nu}\phi = \epsilon_{\nu}\partial^{\nu}\phi , \\ \delta(\partial_{\mu}\phi) &= \partial_{\mu}\,\delta\phi = \epsilon^{\nu}\partial_{\mu}\partial_{\nu}\phi = \epsilon_{\nu}\partial_{\mu}\partial^{\nu}\phi . \end{aligned} \tag{4.21}$$

The Lagrangian variation then is

$$\delta\mathcal{L} = \Big(\frac{\partial\mathcal{L}}{\partial\phi}\partial^{\nu}\phi + \frac{\partial\mathcal{L}}{\partial(\partial_{\mu}\phi)}\partial_{\mu}\partial^{\nu}\phi\Big)\epsilon_{\nu} . \tag{4.22}$$

Use the Euler–Lagrange equation to replace the first term and find

$$\delta\mathcal{L} = \partial_{\mu}\Big(\frac{\partial\mathcal{L}}{\partial(\partial_{\mu}\phi)}\partial^{\nu}\phi\Big)\epsilon_{\nu} . \tag{4.23}$$

Now we have two expressions for the variation in $\mathcal{L}$ under a translation of coordinates. Equating them yields

$$\partial_{\mu}\Big(\frac{\partial\mathcal{L}}{\partial(\partial_{\mu}\phi)}\partial^{\nu}\phi\Big)\epsilon_{\nu} = \epsilon_{\nu}\partial^{\nu}\mathcal{L} = \epsilon_{\nu}\eta^{\mu\nu}\partial_{\mu}\mathcal{L} \tag{4.24}$$

or

$$\partial_{\mu}\Big(\frac{\partial\mathcal{L}}{\partial(\partial_{\mu}\phi)}\partial^{\nu}\phi - \eta^{\mu\nu}\mathcal{L}\Big)\epsilon_{\nu} = 0 . \tag{4.25}$$

Since this holds for arbitrary translations ϵ_{ν} we have

$$\partial_{\mu}\mathcal{T}^{\mu\nu} = 0, \qquad (\nu = 0, 1, 2, 3) , \tag{4.26}$$

where

$$\mathcal{T}^{\mu\nu} \equiv \frac{\partial \mathcal{L}}{\partial(\partial_\mu \phi)} \partial^\nu \phi - \eta^{\mu\nu} \mathcal{L} \tag{4.27}$$

is the energy-momentum tensor of the theory. It is a tensor as can be seen from its structure (recall (2.6,2.57,2.59, 2.62)). Also it is straightforward to demonstrate explicitly that $\mathcal{T}^{\mu\nu}$ transforms as a Lorentz tensor.

Because of the vanishing divergence of the energy-momentum tensor, there are four conserved four-currents and their associated "charges". The vanishing divergence gives the continuity equations

$$\partial_0 \mathcal{T}^{0\nu} + \partial_k \mathcal{T}^{k\nu} = 0 . \tag{4.28}$$

Integrating over a 3-volume containing the fields so that there is no current across the boundary (or assuming the fields vanish at infinity) and using Gauss' theorem we find four time-constant "charges" which are the integrals over the volume of $\mathcal{T}^{0\nu}, \nu = 0, \cdots 3$.

What are these four currents, and what are the conserved quantities that correspond to the vanishing of their divergence? Recall from classical mechanics the definition of the canonical momentum corresponding to a generalized coordinate, in this case ϕ:

$$\pi(x) = \frac{\partial \mathcal{L}}{\partial(\partial_0 \phi)} . \tag{4.29}$$

The Hamiltonian density is

$$\mathcal{H} = \pi\, \partial^0 \phi - \mathcal{L} = \frac{\partial \mathcal{L}}{\partial(\partial_0 \phi)} \partial^0 \phi - \mathcal{L} . \tag{4.30}$$

This is the (00) component of $\mathcal{T}^{\mu\nu}$. Its integral over three-space is the Hamiltonian

$$H = \int_V d\boldsymbol{r}\, \mathcal{T}^{00} , \tag{4.31}$$

and its value is the energy. It is one of the four constants that follows from the vanishing divergence of $\mathcal{T}^{\mu\nu}$.

The corresponding spacelike components,

$$P^k = \int_V d\boldsymbol{r}\, \mathcal{T}^{0k}, \qquad (k = 1, 2, 3), \tag{4.32}$$

are the remaining conserved quantities. Together with H they form a conserved four-vector, namely, the energy-momentum vector. Therefore we have the Lorentz scalar (2.13)

$$P_\mu P^\mu = E^2 - \boldsymbol{P}^2 = M^2 = \text{ invariant} , \tag{4.33}$$

with M the invariant length of

$$P^\mu = (E, \boldsymbol{P}) . \tag{4.34}$$

4.4 Boson and Fermion Fields

4.4.1 Uncharged and charged scalar fields

The simplest example of a field—one of those that will form a part of nuclear field theory—is the uncharged scalar field which we denote by $\sigma(x)$. Consider the Lagrangian

$$\mathcal{L}_\sigma = \tfrac{1}{2}(\partial_\mu\sigma\partial^\mu\sigma - m_\sigma^2\sigma^2) \ , \tag{4.35}$$

where m_σ denotes the meson mass. The Euler–Lagrange equation of this Lagrangian is the Klein–Gordon equation for a free spin-zero meson of the indicated mass,

$$(\Box + {m_\sigma}^2)\sigma(x) = 0\,, \tag{4.36}$$

where $\Box = \partial_\mu\partial^\mu$. With the usual operator substitutions for energy and momentum,

$$E \to i\frac{\partial}{\partial t}, \qquad \boldsymbol{P} \to -i\nabla\,, \tag{4.37}$$

the Klein–Gordon equation represents

$$E^2 = P^2 + {m_\sigma}^2\,. \tag{4.38}$$

The Lagrangian written above has the space symmetries of any Lorentz scalar Lagrangian and therefore an energy-momentum tensor of the form derived above; however it has no internal symmetries.

A scalar Lagrangian that does have an internal symmetry is one representing two scalar mesons of the same mass,

$$\mathcal{L}(\sigma_1,\sigma_2) = \tfrac{1}{2}(\partial_\mu\sigma_1\partial^\mu\sigma_1 - m_\sigma^2\sigma_1^2) \ + \tfrac{1}{2}(\partial_\mu\sigma_2\partial^\mu\sigma_2 - m_\sigma^2\sigma_2^2) \ . \tag{4.39}$$

The symmetry becomes apparent if we define the complex field

$$\sigma = \big(\sigma_1 + i\sigma_2\big)/\sqrt{2}\,. \tag{4.40}$$

Then the Lagrangian can be rewritten

$$\mathcal{L}(\sigma_1,\sigma_2) = \partial_\mu\sigma^*\partial^\mu\sigma - m_\sigma^2\sigma^*\sigma \tag{4.41}$$

and is clearly invariant to the phase transformation

$$\sigma(x) \to e^{iq\lambda}\sigma(x) \ , \qquad \sigma^*(x) \to e^{-iq\lambda}\sigma^*(x)\,, \tag{4.42}$$

where λ is a continuous variable and we interpret q as the charge of the field, the reason for which will become apparent. The $\sigma(x)$, $\sigma^*(x)$ can be written in terms of the original fields,

$$\begin{aligned} \sigma_1 &\to \sigma_1\cos(q\lambda) - \sigma_2\sin(q\lambda)\,, \\ \sigma_2 &\to \sigma_2\cos(q\lambda) + \sigma_1\sin(q\lambda)\,. \end{aligned} \tag{4.43}$$

The above equations correspond to a rotation around the 3-axis in the space $(\sigma_1, \sigma_2, \sigma_3)$. The analogy of rotation will be useful later. For an infinitesimal λ, we can write the above phase transformation as

$$\delta\sigma = iq\lambda\sigma\,. \tag{4.44}$$

or, in terms of the original fields,

$$\sigma_1 \to \sigma_1 - q\lambda\sigma_2\,, \qquad \sigma_2 \to \sigma_2 + q\lambda\sigma_1\,. \tag{4.45}$$

From the general notation (4.8), we read

$$F_1^2 = -q\sigma_2, \qquad F_2^1 = q\sigma_1, \qquad F_1^1 = F_2^2 = 0\,. \tag{4.46}$$

It is important to note that the invariance of $\mathcal{L}$ involves only one continuous infinitesimal λ so (4.12) defines a single conserved current which is the sum of two terms:

$$\begin{aligned} J^\mu &= q\Big(\frac{\partial\mathcal{L}}{\partial(\partial_\mu\sigma_1)}\sigma_2 + \frac{\partial\mathcal{L}}{\partial(\partial_\mu\sigma_2)}\sigma_1\Big) = q\big(\sigma_1\partial^\mu\sigma_2 - \sigma_2\partial^\mu\sigma_1\big) \\ &= q(\boldsymbol{\sigma}\times\partial^\mu\boldsymbol{\sigma})_3\,, \end{aligned} \tag{4.47}$$

or, in terms of the complex field,

$$J^\mu = -iq\big(\sigma^*\partial^\mu\sigma - \sigma\partial_\mu\sigma^*\big)\,. \tag{4.48}$$

From the general results of Section 4.3.1, this four-vector is divergenceless and corresponds to a conserved current. From the application of Gauss' theorem there follows the conservation of charge within the volume containing the system.[1]

4.4.2 Uncharged and charged vector fields

Now consider a Lorentz vector field ω_μ for a meson of mass m_ω. The notation is chosen to correspond with the neutral omega meson of spin and parity 1^-. Define

$$\omega_{\mu\nu} = \partial_\mu\omega_\nu - \partial_\nu\omega_\mu \tag{4.49}$$

as in electromagnetic theory. A scalar that involves second derivatives and a mass term is

$$\mathcal{L}_\omega = -\tfrac{1}{4}\omega_{\mu\nu}\omega^{\mu\nu} + \tfrac{1}{2}m_\omega^2\omega_\mu\omega^\mu\,. \tag{4.50}$$

[1]Note that in (4.47), it may at first appear that a factor $\frac{1}{2}$ has been omitted because of the presence of this factor in $\mathcal{L}(\sigma_1, \sigma_2)$. However, note that $\partial_\mu\sigma\partial^\mu\sigma = \eta^{\mu\nu}\partial_\mu\sigma\partial_\nu\sigma$. So the derivative with respect to $\partial_\alpha\sigma$ is $2\partial^\alpha\sigma$.

The Euler–Lagrange equation is

$$(\Box + m_\omega^2)\omega_\mu - \partial_\mu \partial^\nu \omega_\nu = 0 \tag{4.51}$$

which is the Proca equation. Its divergence is

$$(\Box + m_\omega^2)\partial^\mu \omega_\mu - \Box \partial^\nu \omega_\nu = 0 \tag{4.52}$$

from which follows

$$m_\omega^2 \partial^\mu \omega_\mu = 0\,. \tag{4.53}$$

Since the mass is not zero, the field must be divergenceless. For free omega mesons, each of the four Lorentz components of ω_μ satisfies a Klein–Gordon equation,

$$(\Box + m_\omega^2)\omega_\mu = 0\,. \tag{4.54}$$

Next we would like to describe the charged triplet of rho mesons $\rho^0, \rho^\pm$ which have the same spin and parity as the omega meson. Therefore they should be described as Lorentz vector fields which we denote by

$$\boldsymbol{\rho}^\mu \equiv (\rho_1^\mu, \rho_2^\mu, \rho_3^\mu)\,. \tag{4.55}$$

From these we can form one real and two complex fields as for the pair of scalar fields, one the complex conjugate of the other. Therefore, the scalar Lagrangian for free rho mesons,

$$\mathcal{L}_\rho = -\tfrac{1}{4}\boldsymbol{\rho}_{\mu\nu}\cdot\boldsymbol{\rho}^{\mu\nu} + \tfrac{1}{2}m_\rho^2 \boldsymbol{\rho}_\mu \cdot \boldsymbol{\rho}^\mu\,, \tag{4.56}$$

has the same phase invariance as for complex scalar fields constructed from two of the fields, say 1 and 2:

$$\rho_\pm^\mu = \frac{1}{\sqrt{2}}(\rho_1^\mu \pm i\rho_2^\mu)\,. \tag{4.57}$$

Equivalently, it is invariant to a rotation about 3. There is also an invariance having to do with a general rotation in the space of the three fields. This is an isospin rotation to which $\mathcal{L}_\rho$ is manifestly invariant, consisting as it does of scalar products in the three vectors constructed from $\boldsymbol{\rho}_\mu$. Such a rotation can be written

$$\boldsymbol{\rho}_\mu \to \boldsymbol{\rho}_\mu + \boldsymbol{\Lambda} \times \boldsymbol{\rho}_\mu\,, \tag{4.58}$$

where $\boldsymbol{\Lambda}$ is an infinitesimal vector in isospin space. We can also write the vector product explicitly as

$$\boldsymbol{\rho}_\mu \to \boldsymbol{\rho}_\mu + \epsilon_{ijk}\Lambda_j \rho_{k\mu}\,, \tag{4.59}$$

where ϵ_{ijk} is antisymmetric under interchange of any two indices and symmetric under cyclic permutations,

$$\epsilon_{ijk} = -\epsilon_{ikj} = \epsilon_{kij}\,. \tag{4.60}$$

According to our general notation (4.8), the transformation may be characterized by

$$F_i^j = \epsilon_{ijk}\rho_{k\mu}\,. \tag{4.61}$$

Therefore, according to the general theorem on Noether currents,

$$I_j^\nu = \frac{\partial \mathcal{L}_\rho}{\partial(\partial_\nu \rho_{i\mu})}\rho_{k\mu}\epsilon_{ijk} \tag{4.62}$$

or

$$\boldsymbol{I}^\nu = \boldsymbol{\rho}_\mu \times \frac{\partial \mathcal{L}_\rho}{\partial(\partial_\nu \boldsymbol{\rho}_\mu)} = \boldsymbol{\rho}_\mu \times \boldsymbol{\rho}^{\nu\mu} \tag{4.63}$$

is a Lorentz four-current, the isospin current of the rho field. Each component of this current is a three-vector in isospin space. The charge current is easily obtained as the isospin 3-component multiplied by the charge q,

$$J^\nu = q\big(\boldsymbol{\rho}_\mu \times \boldsymbol{\rho}^{\nu\mu}\big)_3 \tag{4.64}$$

which follows by taking $\Lambda = (0, 0, \lambda)q$.

Just as for the omega field, we can show from the Euler–Lagrange equations that the massive rho field must be divergenceless. The equations of motion then reduce to

$$\big(\Box + m_\rho^2\big)\boldsymbol{\rho}^\mu = 0\,. \tag{4.65}$$

4.4.3 Dirac fields

The solutions of the Klein–Gordon equations are single-component fields and cannot describe a spin-1/2 particle. Dirac (1928) sought an equation that is linear in all derivatives so as to give equal treatment to space and time and whose energy for a free particle satisfies the relationship [96]

$$H^2\psi(x^\mu) = (\boldsymbol{p}^2 + m^2)\psi(x^\mu)\,. \tag{4.66}$$

Therefore he wrote

$$H\psi = \big(-i\boldsymbol{\alpha}\cdot\nabla + \beta m\big)\psi = i\frac{\partial\psi}{\partial t}\,, \tag{4.67}$$

where $\boldsymbol{\alpha}$ and β are as yet undetermined. If H is to be hermitian, then so must $\boldsymbol{\alpha}$, β. Squaring and comparing with the previous equation leads at

once to[2]

$$\begin{aligned} &\alpha_i\alpha_j + \alpha_j\alpha_i = 2\delta_{ij}\,, \\ &\alpha_i\beta + \beta\alpha_i = 0\,, \\ &\alpha_{(i)}^2 = \beta^2 = 1\,. \end{aligned} \tag{4.68}$$

A particular representation is

$$\boldsymbol{\alpha} = \begin{pmatrix} 0 & \boldsymbol{\sigma} \\ \boldsymbol{\sigma} & 0 \end{pmatrix}, \qquad \beta = \begin{pmatrix} I & 0 \\ 0 & -I \end{pmatrix}, \qquad I = \begin{pmatrix} 1 & 0 \\ 0 & 1 \end{pmatrix} \tag{4.69}$$

where the σ_i are the Pauli 2×2 matrices and I is the identity matrix. Consequently ψ is a four-component spinor.

In the above and original form, the Dirac equation is not manifestly Lorentz covariant. To make covariance manifest, we define new matrices,

$$\gamma^\mu = (\gamma^0, \gamma^1, \gamma^2, \gamma^3), \qquad \gamma^0 = \beta, \qquad \gamma^i = \beta\alpha_i\,. \tag{4.70}$$

Then the Dirac equation can be written in the compact and manifestly covariant form

$$(i\gamma_\mu\partial^\mu - m)\psi = 0\,. \tag{4.71}$$

A notation of convenience is

$$\not{A} \equiv \gamma_\mu A^\mu = \gamma^\mu A_\mu \tag{4.72}$$

so that the Dirac equation can be written even more compactly as

$$(i\not{\partial} - m)\psi = 0\,. \tag{4.73}$$

The gamma matrices satisfy a number of rules of which some are important to us:

$$\gamma^\mu\gamma^\nu + \gamma^\nu\gamma^\mu = 2\eta^{\mu\nu} = 2\begin{pmatrix} 1 & 0 & 0 & 0 \\ 0 & -1 & 0 & 0 \\ 0 & 0 & -1 & 0 \\ 0 & 0 & 0 & -1 \end{pmatrix}, \tag{4.74}$$

where $\eta^{\mu\nu}$ is the Minkowski metric tensor of flat spacetime. This tells us, for example, that $\gamma_0^2 = 1$, $\gamma_{(i)}^2 = -1$.

From the foregoing it follows that

$$\gamma_0 = \gamma_0^\dagger, \qquad \boldsymbol{\gamma}^\dagger = (\beta\boldsymbol{\alpha})^\dagger = \boldsymbol{\alpha}\beta = -\beta\boldsymbol{\alpha} = -\boldsymbol{\gamma}\,, \tag{4.75}$$

or more compactly,

$$\gamma_0\gamma_\mu^\dagger\gamma_0 = \gamma_\mu\,. \tag{4.76}$$

[2]We use brackets around repeated indices that are not summed.

The adjoint Dirac equation is,

$$-i\partial^\mu \psi^\dagger \gamma_\mu^\dagger - m\psi^\dagger = 0\,. \tag{4.77}$$

Upon defining the *Dirac adjoint* spinor,

$$\overline{\psi} \equiv \psi^\dagger \gamma_0\,, \tag{4.78}$$

we can write the adjoint equation as

$$i\partial^\mu \overline{\psi}\gamma_\mu + m\overline{\psi} = 0\,. \tag{4.79}$$

The Lagrangian that yields Dirac's equation is

$$\mathcal{L} = \overline{\psi}(i\partial\!\!\!/ - m)\psi \tag{4.80}$$

since the Euler–Lagrange equation yields simply

$$0 = \partial\mathcal{L}/\partial\overline{\psi} = (i\partial\!\!\!/ - m)\psi\,. \tag{4.81}$$

The Lagrangian is invariant to a continuous phase transformation,

$$\psi \to e^{-i\lambda}\psi = \psi - i\lambda\psi + O(\lambda^2)\,. \tag{4.82}$$

In terms of our general formulation of transformation of fields (4.8) we have $F = -i\psi$ so that there is a divergenceless four-current,

$$\partial_\mu j^\mu = 0. \tag{4.83}$$

There is therefore a conserved (divergenceless) baryon current,

$$j^\mu = \frac{\partial\mathcal{L}}{\partial(\partial_\mu\psi)}F = \overline{\psi}\gamma^\mu\psi\,. \tag{4.84}$$

The time component is

$$j^0 = \overline{\psi}\gamma^0\psi = \psi^\dagger\psi \tag{4.85}$$

which is the baryon density. We shall frequently denote it as ρ. According to the earlier analysis it is a constant in time for any system into or out of which there is no net flow of nucleons. So a particle satisfying the free Dirac equation is conserved. Nucleon decay, if it occurs, has a time-scale on the order of the lifetime of the universe.

4.4.4 Neutron and proton

According to the rationale stated in the introduction, we take the neutron and proton to be Dirac particles of the same mass m. The Lagrangian for the pair is

$$\mathcal{L} = \overline{\psi}_p(i\partial\!\!\!/ - m)\psi_p + \overline{\psi}_n(i\partial\!\!\!/ - m)\psi_n\,. \tag{4.86}$$

Combine the four-component spinors into a single eight-component spinor

$$\psi \equiv \begin{pmatrix} \psi_p \\ \psi_n \end{pmatrix}, \tag{4.87}$$

and write

$$\mathcal{L} = \overline{\psi}(i\partial\!\!\!/ - m)\psi\,. \tag{4.88}$$

Let $\boldsymbol{\tau} = (\tau_1, \tau_2, \tau_3)$ denote the 2×2 Pauli isospin matrices, and let $\Lambda = (\Lambda_1, \Lambda_2, \Lambda_3)$ be an arbitrary constant vector in isospin space. The Lagrangian is manifestly invariant to the continuous phase transformation

$$\psi \to e^{-i\boldsymbol{\tau}\cdot\boldsymbol{\Lambda}/2}\psi\,. \tag{4.89}$$

A finite rotation can be built from infinitesimal ones. Taking the $\boldsymbol{\Lambda}$ to have infinitesimal components

$$\delta\psi = -\frac{i}{2}\boldsymbol{\Lambda}\cdot\boldsymbol{\tau}\psi = \boldsymbol{\Lambda}\cdot\boldsymbol{F}, \qquad \boldsymbol{F} = -\frac{i}{2}\boldsymbol{\tau}\psi\,, \tag{4.90}$$

we find

$$\frac{\partial\mathcal{L}}{\partial(\partial_\mu\psi)} = \overline{\psi}i\gamma^\mu\,. \tag{4.91}$$

By the general method (4.13) given earlier, the conserved *isospin* current of the nucleons results in

$$\boldsymbol{I}^\mu = \tfrac{1}{2}\overline{\psi}\gamma^\mu\boldsymbol{\tau}\psi\,. \tag{4.92}$$

Since τ_3 has the representation

$$\tau_3 = \begin{pmatrix} 1 & 0 \\ 0 & -1 \end{pmatrix}, \tag{4.93}$$

we find the 3-component as

$$\begin{aligned} I_3^\mu &= \tfrac{1}{2}\overline{\psi}\gamma^\mu\tau_3\psi\,, \\ I_3^0 &= \tfrac{1}{2}(\psi_p^\dagger\psi_p - \psi_n^\dagger\psi_n) \to \begin{cases} -\frac{1}{2}\rho_n & \text{for neutrons} \\ +\frac{1}{2}\rho_p & \text{for protons} \end{cases}, \end{aligned} \tag{4.94}$$

with ρ_n and ρ_p the neutron and proton densities.

The Lagrangian is also invariant to the phase transformation

$$\psi \to e^{-i\Lambda q(1+\tau_3)/2}\psi\,. \tag{4.95}$$

Following the familiar construction, we have the conserved current

$$J^\mu = q\overline{\psi}\gamma^\mu\frac{1+\tau_3}{2}\psi\,. \tag{4.96}$$

We find

$$J^\mu = q\overline{\psi}_p\gamma^\mu\psi_p, \qquad J^0 = q\psi_p^\dagger\psi_p\,, \tag{4.97}$$

which have the appearance of a charge current and density.

4.4.5 Electromagnetic field

We introduced the nucleon charge current above but have not so far formally introduced the electromagnetic field. We do so now. The Lagrangian for the free electromagnetic field is

$$\mathcal{L}_{\rm em} = -\tfrac{1}{4} A_{\mu\nu} A^{\mu\nu} \,, \tag{4.98}$$

where

$$A_{\mu\nu} = \partial_\mu A_\nu - \partial_\nu A_\mu \,, \tag{4.99}$$

A^μ is the Lorentz vector

$$A^\mu = (V, \boldsymbol{A}) \,, \tag{4.100}$$

and V and $\boldsymbol{A}$ the scalar and vector potentials of electromagnetic theory. It is not our purpose to review electromagnetic theory here but only to recall those aspects appropriate to the interpretation of charge on the spinor and complex fields described above. We recall the "minimal" prescription for electromagnetic interactions in quantum mechanics, $p^\mu \to p^\mu - qA^\mu$, or since $p^\mu = i\partial^\mu$ (recall (2.57)),

$$\partial^\mu \to \partial^\mu + iqA_\mu \equiv \mathcal{D}^\mu \,. \tag{4.101}$$

Accordingly, for the spinor field, we introduce the combined Lagrangian

$$\begin{aligned} \mathcal{L} &= \overline{\psi}_p \big(i\gamma_\mu \mathcal{D}_\mu - m\big)\psi_p - \tfrac{1}{4} A_{\mu\nu} A^{\mu\nu} \\ &= \overline{\psi}_p \big(i\not{\partial} - m\big)\psi_p - \tfrac{1}{4} A_{\mu\nu} A^{\mu\nu} - A_\mu J^\mu \,, \end{aligned} \tag{4.102}$$

where J^μ is the same current referred to above as the charge current of the nucleons.

Similarly, say for the complex scalar field (4.39),

$$\begin{aligned} \mathcal{L} &= (\mathcal{D}^\mu \sigma)^\dagger (\mathcal{D}_\mu \sigma) - m\sigma^\dagger \sigma - \tfrac{1}{4} A_{\mu\nu} A^{\mu\nu} \\ &= \mathcal{L}(\sigma_1, \sigma_2) - \tfrac{1}{4} A_{\mu\nu} A^{\mu\nu} \\ &\quad + iqA_\mu \big(\sigma \partial^\mu \sigma^* - \sigma^* \partial^\mu \sigma\big) + q^2 A^2 \sigma^* \sigma \,. \end{aligned} \tag{4.103}$$

This result can also be written

$$\begin{aligned} \mathcal{L} &= \mathcal{L}(\sigma_1, \sigma_2) - \tfrac{1}{4} A_{\mu\nu} A^{\mu\nu} \\ &\quad - \frac{q}{2} A_\mu \big(\sigma_2 \partial^\mu \sigma_1 - \sigma_1 \partial^\mu \sigma_2\big) + \tfrac{1}{2} q^2 A^2 (\sigma_1^2 + \sigma_2^2) \,. \end{aligned} \tag{4.104}$$

We can now compute the conserved current

$$\begin{aligned} J^\mu &= q\big(\sigma_1 \partial^\mu \sigma_2 - \sigma_2 \partial^\mu \sigma_1\big) + q^2 A^\mu (\sigma_1^2 + \sigma_2^2) \\ &= -iq\big[\sigma^* (\mathcal{D}^\mu \sigma) - \sigma (\mathcal{D}^\mu \sigma)^*\big] \,. \end{aligned} \tag{4.105}$$

In contrast to the case of the Dirac field which, in interaction with the electromagnetic field, had the same current as for the free Dirac field, we see here an addition to the free current of the meson fields. It arises because of the additional derivatives. Note that it is quadratic in the charge and that the interaction Lagrangian has also a quadratic charge term. We remark on the quadratic coupling in electromagnetic theory because we shall encounter quadratic coupling in a different context in Section 4.9.

4.5 Properties of Nuclear Matter

We wish to anchor our description of the dense matter of neutron stars to what is known empirically about bulk nuclear matter. In practice this knowledge concerns the properties of symmetric nuclear matter at saturation density, that is, at the density at which the pressure is zero and at which the matter would remain static if not disturbed.

Uniform infinite symmetric matter is an idealization; nevertheless it is an idealization which has very definite properties related to finite nuclei. The history of the notion goes back to Weizsacker and the liquid drop model of the nucleus. All we need to know of the details of the model (much refined in recent years and which now correlates thousands of data on nuclear masses and other bulk properties) is that it seeks to characterize the energy of a nucleus by its atomic and proton numbers A and Z.

The basic property of nuclei or nuclear matter is that they are saturated systems. The reason for this lies in the strong repulsion of the nuclear force at a short distance. Saturation means that, as more nucleons are added to nuclei, the density of the central region remains essentially constant. This is why the nuclear radius is given by $R = r_0 A^{1/3}$ where $r_0 =$ constant and A is the atomic number. So the energy density is approximately a constant. Accordingly, we can write the volume energy of a nucleus as the energy density of symmetric matter at normal density ϵ_0 times the volume. This should be modified by the empirical fact that nuclei with neutron number N close to proton number Z are more tightly bound than their neighbors, altered by the increasing importance of the Coulomb repulsion at higher Z which shifts the energy minimum to nuclei with increasing $(A-Z)/Z = N/Z$ to those with a greater neutron fraction. The well-known valley of beta stability emphasizes the preference for isospin symmetry of the underlying nuclear force and the nucleon kinetic energy.

In addition to the above contributions to the energy, there will be a surface energy, also repulsive. This contribution arises because nucleons at the surface interact with fewer neighbors and so feel less attraction than those in the interior. Surface energy will be proportional to the surface area. There will also be a repulsive Coulomb energy because of the protons. It can be calculated in the same manner as the gravitational energy of a star (3.18).

From the above contributions, we can write the total mass of a nucleus approximately as

$$M(A,Z) = A\left[\frac{4}{3}\pi r_0^3\epsilon_0 + a_{\rm sym}\left(\frac{N-Z}{N+Z}\right)^2\right] + 4\pi r_0^2 A^{2/3}\epsilon_{\rm surf} + \frac{3}{5}\frac{e^2Z^2}{r_0A^{1/3}}. \tag{4.106}$$

This formula is sometimes referred to as the semiempirical mass formula or, with its more recent elaborations, the droplet model of nuclear masses. Subtracting $(A-Z)m_n+Zm_p \approx Am$ would give the total binding energy. In actual practice there are many additional effects with unknown coefficients. These are incorporated in the best fit of the parameters of the more general formula to thousands of data on nuclear masses [97]. We need not dwell on this. The point is that the binding energy per nucleon B/A is a series in various powers of $1/A$ including the zeroth power. Therefore certain terms become more important with increasing A, and, in the limit, just the volume term (the constant term in B/A) survives. In this way (based on a wealth of information on finite nuclei) one discovers the binding energy per nucleon of infinite, symmetric, nuclear matter and the symmetry energy coefficient:

$$B/A = -16.3 \text{ MeV}, \qquad a_{\rm sym} = 32.5 \text{ MeV}. \tag{4.107}$$

The radius parameter $r_0 = 1.16$ fm in the relationship between the nuclear radius and its atomic number $R = r_0A^{1/3}$ is obtained by an analysis of electron-nucleus scattering in terms of density distributions [98]. The equilibrium value of the nucleon number density is related to r_0 by

$$\rho_0 = \left[(4\pi/3)r_0^3\right]^{-1} = 0.153 \text{ fm}^{-3}. \tag{4.108}$$

A parameter equivalent to the saturation density is the Fermi momentum common to neutrons and protons in symmetric matter at saturation. Density and Fermi momentum are related through

$$\rho_0 = 4\int_0^{k_F}\frac{d\boldsymbol{k}}{(2\pi)^3} = \frac{2k_F^3}{3\pi^2}, \tag{4.109}$$

where 4 is the spin-isospin degeneracy of the nucleon momentum states. We find

$$k_F = 1.31 \text{ fm}^{-1}. \tag{4.110}$$

In terms of an equation of state $\epsilon(\rho)$, the binding energy per nucleon is related to the equilibrium values of the saturation energy density ϵ_0 and baryon number density ρ_0 by

$$\frac{B}{A} = \left(\frac{\epsilon}{\rho}\right)_0 - m. \tag{4.111}$$

The subscript "0" denotes evaluation at the saturation density of nuclear matter and $m = 938.93$ MeV $= 4.7582$ fm^{-1} is the average of the neutron and proton masses. Thus, we learn the energy density at saturation:

$$\epsilon_0 = 141 \text{ MeV/fm}^3 . \tag{4.112}$$

The binding energy per nucleon and nucleon number density at saturation will serve to fix two coupling constants of the theory. Any theory of matter that is intended to describe neutron stars should be anchored to these minimal constraints. Our first example of a nuclear field theory will do just that (and no more).

We note some of the additional important constraints. In Section 3.6 we have shown that stars must be electrically neutral. This means that neutron stars to first approximation are composed of neutrons. They are therefore highly isospin asymmetric. On the other hand, the short-range nuclear force together with the Fermi energies of the isospin-carrying baryons energetically prefer isospin symmetric configurations. So the constraint of charge neutrality that neutron star matter must obey if it is to be gravitationally bound in its lowest energy state exacts the price of a high isospin energy. Consequently, it is important that the theory of matter should correctly reflect the isospin symmetry energy. That is done by extracting it from the semiempirical mass formula above. From (4.106) the symmetry energy coefficient is related to the equation of state $\epsilon(\rho)$ by

$$a_{\text{sym}} = \frac{1}{2}\left(\frac{\partial^2(\epsilon/\rho)}{\partial t^2}\right)_{t=0}, \qquad t \equiv (\rho_n - \rho_p)/\rho . \tag{4.113}$$

To evaluate these expressions, the energy density and number density must be expressed in terms of k_n and k_p, the neutron and proton Fermi momenta. After evaluation of the expression, they are then set equal to the common value k_F of symmetric matter.

The compression modulus K which defines the curvature of the equation of state $\epsilon(\rho)/\rho$ at ρ_0 is another important contact with empirical knowledge. Its value will obviously be reflected in the high-density behavior of the equation of state though, of course, not uniquely. The larger the value of K, the more steeply the equation of state will increase with density. The high-density behavior is generally referred to as the "stiffness" or "softness" of the equation of state. These are relative terms referring to whether or not $\epsilon(\rho)$ increases rapidly with ρ. The stiffness will directly influence the maximum mass of the neutron star sequence belonging to the equation of state.

The compression modulus at saturation also enters the mass formula, but the dependence is rather weak. The giant monopole excitation in nuclei (an excitation that corresponds to a collective radial or "breathing" mode) ought to be the most direct measure of this important parameter, though its extraction from experiment is not without its ambiguities. The compression

modulus likely lies in the range 200 – 300 MeV [99, 100, 101, 102, 103], although recent evidence from a large body of nuclear data suggests that a value $K = 234$ MeV is preferred [104]. The compression modulus is related to the equation of state through

$$K = \left[k^2 \frac{d^2}{dk^2}\left(\frac{\epsilon}{\rho}\right)\right]_{k_F} = 9\left[\rho^2 \frac{d^2}{d\rho^2}\left(\frac{\epsilon}{\rho}\right)\right]_{\rho=\rho_0} . \tag{4.114}$$

Finally, the nucleon effective mass in matter is also relevant. It plays a role somewhat like the compression modulus as regards the high-density behavior of the equation of state. This is so because the equation of state will contain, among other terms, a sum of $[k^2 + m^{\star 2}(k_f)]^{1/2}$ over those nucleon momentum states that lie below the Fermi momentum k_f at the considered density (not necessarily saturation). The quantity $m^\star(k_f)$ is the effective nucleon mass in the medium and (perhaps not surprisingly as we shall see explicitly later) it depends on the Fermi momentum, or equivalently, the density of the matter. Therefore, the above mentioned sum will clearly influence the "stiffness" of the equation of state and hence, as with K, will have a direct bearing on the maximum mass that the equation of state can support against gravity. Our theory should make contact with what is known empirically about K and $m^\star$.

The effective mass at saturation density is not precisely known. According to the particular type of data and its analysis, the effective mass is defined in various ways. The value of the isoscalar component of the mean field can be derived from a nonrelativistic analysis of scattering of neutrons from Pb nuclei and is found to lie in the range [105, 106, 107]

$$m_S^\star/m \approx 0.74 \text{ to } 0.82 . \tag{4.115}$$

This is not the "Dirac effective mass" which appears in nuclear field theory. It can be identified approximately as the Landau effective mass [102, 107] which in turn is related to the Dirac effective mass of nuclear field theory through

$$m_S^\star \approx m_L^\star = \left(\frac{k}{\partial\epsilon(k)/\partial k}\right)_{k_F} = (m^{\star 2} + k_F^2)^{\frac{1}{2}} , \tag{4.116}$$

where

$$m^\star \equiv m^\star(k_F) \tag{4.117}$$

is the nucleon effective mass $m^\star$ (Dirac mass) at saturation density and k_F is the corresponding Fermi momentum. Consequently, the range expected for the Dirac effective mass at saturation density is

$$m^\star/m \approx 0.7 \text{ to } 0.8 . \tag{4.118}$$

A remarkable fact about nuclei (in addition to their being saturated systems) is that, to a good approximation, a nucleus behaves as if it were composed of almost independent nucleons moving in a mean field, despite the strong interaction between them in vacuum. Unlike the situation with atoms (where a massive nucleus provides the Coulomb mean field in which the electrons move) the above property of nuclei by no means follows in an obvious way from the nuclear force. It follows, instead, from an intricate interplay between the Pauli exclusion principle, the strong short-range repulsive part of the interaction between nucleons, and the moderate strength of the long-range attractive part of the interaction [108, 109]. For a two-body system, the long-range attractive part is just strong enough to bind the deuteron, but without a bound excited state.

4.6 The $\sigma - \omega$ Model

We introduce nuclear field theory by considering the original version of Johnson and Teller [76], Duerr [77], and Walecka [78]. It is based on the fields of four particles: the nucleons, a scalar meson, and the omega vector meson. The Lagrangian must be a Lorentz scalar, but that in and of itself does not uniquely define the form of the interaction between nucleons and the meson fields. It does, however, commend the so-called Yukawa coupling because, in the static limit, one boson exchange of these mesons leads to a Yukawa potential.

We want the Lagrangian to be a Lorentz scalar. Therefore the scalar meson is coupled to the baryon *scalar* density $\overline{\psi}\psi$ and the vector meson to the baryon four-current $\overline{\psi}\gamma^\mu\psi$ by contraction. The interaction Lagrangian can therefore be written

$$\mathcal{L}_{\text{int}} = g_\sigma\, \sigma(x)\, \overline{\psi}(x)\psi(x) - g_\omega\, \omega_\mu(x)\, \overline{\psi}(x)\gamma^\mu\psi(x)\,, \tag{4.119}$$

where $x \equiv x^\mu \equiv (t, x, y, z)$. The choice of signs of both terms is arbitrary and made in hindsight so that the mean values of the fields are positive numbers. Now, adding the free Lagrangians for nucleons and mesons, we obtain for the total Lagrangian

$$\begin{aligned} \mathcal{L} \;=\; & \overline{\psi}\Big[i\gamma_\mu(\partial^\mu + ig_\omega\omega^\mu) - (m - g_\sigma\sigma)\Big]\psi \\ & + \tfrac{1}{2}(\partial_\mu\sigma\partial^\mu\sigma - m_\sigma^2\sigma^2) - \tfrac{1}{4}\omega_{\mu\nu}\omega^{\mu\nu} + \tfrac{1}{2}m_\omega^2\omega_\mu\omega^\mu\,. \end{aligned} \tag{4.120}$$

The Euler–Lagrange equations in the presence of the interactions follow as

$$(\Box + {m_\sigma}^2)\sigma(x) = g_\sigma\, \overline{\psi}(x)\psi(x)\,, \tag{4.121}$$

$$(\Box + m_\omega^2)\omega_\mu(x) - \partial_\mu\partial^\nu\omega_\nu(x) = g_\omega\, \overline{\psi}(x)\gamma_\mu\psi(x)\,. \tag{4.122}$$

Because of nucleon conservation (the divergenceless of the baryon current (4.83)), we have $\partial^\mu \omega_\mu = 0$ for the massive vector field as in 4.52. The Euler–Lagrange equations for the nucleons are

$$\Big[\gamma_\mu\big(\partial^\mu - g_\omega \omega^\mu(x)\big) - \big(m - g_\sigma \sigma(x)\big)\Big]\psi(x) \;=\; 0. \tag{4.123}$$

The above three-coupled, nonlinear differential equations are clearly complicated.

We now introduce an approximation known as the *relativistic mean-field approximation*. The system we are interested in is static uniform matter in its ground state. We replace the meson fields by their mean values in this state, $\sigma \to \langle\sigma\rangle$, and $\omega_\mu \to \langle\omega_\mu\rangle$. These mean values are to be computed from the above equations with the mean nucleon source currents on the right side evaluated in the ground state of matter. In static uniform matter, the source currents $\overline{\psi}\psi$ and $\overline{\psi}\gamma^\mu\psi$ are independent of x. So then are the mean meson fields. As a consequence, the Euler–Lagrange equations reduce to the simpler form

$$\begin{aligned} m_\sigma^2 \sigma &= g_\sigma \langle\overline{\psi}\psi\rangle\,, \\ m_\omega^2 \omega_0 &= g_\omega \langle\psi^\dagger\psi\rangle\,, \\ m_\omega^2 \omega_k &= g_{\omega B} \langle\overline{\psi}\gamma_k\psi\rangle\,. \end{aligned} \tag{4.124}$$

We shall discuss shortly how the ground state expectations of the nucleon currents, $\langle\overline{\psi}\psi\rangle$, etc., can be evaluated.

Instead of renaming the mean meson values, we retain their old names, but now without indicating an x dependence. For the nucleons we have

$$\Big[\gamma_\mu(\partial^\mu - g_\omega \omega^\mu) - (m - g_\sigma \sigma)\Big]\psi(x) \;=\; 0\,, \tag{4.125}$$

wherein the *mean* meson fields now appear. Since, in the mean-field approximation of uniform static matter, the nucleon fields satisfy an equation with no x-dependent terms, these fields are momentum eigenstates which we write as

$$\psi(x) = \psi(k)\, e^{-ik\cdot x} \tag{4.126}$$

where

$$k \cdot x \equiv k_\mu x^\mu = k_0 t - \boldsymbol{k}\cdot\boldsymbol{r}\,. \tag{4.127}$$

Then we obtain

$$\Big[\gamma_\mu(k^\mu - g_\omega \omega^\mu) - (m - g_\sigma \sigma)\Big]\psi(k) \;=\; 0\,. \tag{4.128}$$

The quantity in the square bracket is a matrix and ψ is an eight-component spinor (4.87). Comparison with the Dirac equation we encountered

earlier suggests the definitions,

$$K_\mu = k_\mu - g_\omega \omega_\mu \,, \tag{4.129}$$

$$m^\star(\sigma) = m - g_\sigma \sigma \,. \tag{4.130}$$

It is typical of theories with scalar mesons that the Fermion mass is altered in the above way. We call $m^\star$ the effective mass or sometimes the Dirac effective mass especially when we need to distinguish it from effective masses of nonrelativistic theories. Note that the scalar field acts to reduce the effective nucleon mass.

With the above definitions, the Dirac equation can be rewritten

$$(\not{K} - m^\star)\psi(K) \;=\; 0 \,. \tag{4.131}$$

The Dirac eigenvalues can be found as usual by rationalizing the Dirac operator. Multiply by $\not{K}+m^\star$, and use the properties of the gamma matrices to find

$$\begin{aligned}(\not{K} + m^\star)(\not{K} - m^\star) &= \not{K}\not{K} - m^{\star 2} = \gamma_\mu K^\mu \gamma_\nu K^\nu - m^{\star 2} \\ &= K^\mu K^\nu \frac{\gamma_\mu\gamma_\nu + \gamma_\nu\gamma_\mu}{2} - m^{\star 2} = K_\mu K^\mu - m^{\star 2} \,. \end{aligned} \tag{4.132}$$

The result is

$$(K_\mu K^\mu - m^{\star 2})\psi(K) = 0 \,. \tag{4.133}$$

Since the operator has now become a number that multiplies $\psi(K)$ to give zero, that number must be zero. We obtain

$$K_0 = \sqrt{\boldsymbol{K}^2 + m^{\star 2}} \,. \tag{4.134}$$

Let us denote the timelike component by

$$e(\boldsymbol{k}) \equiv k_0(\boldsymbol{k}) = K_0 + g_\omega \omega_0 \,. \tag{4.135}$$

Hence the nucleon eigenvalues of momentum $\boldsymbol{k}$ for particle and antiparticle are

$$e(\boldsymbol{k}) \;=\; E(\boldsymbol{k}) + g_\omega \omega_0 \,, \tag{4.136}$$

$$\bar{e}(\boldsymbol{k}) \;=\; E(\boldsymbol{k}) - g_\omega \omega_0 \,, \tag{4.137}$$

with

$$E(\boldsymbol{k}) \;=\; \sqrt{(\boldsymbol{k} - g_\omega \boldsymbol{\omega})^2 + (m - g_\sigma \sigma)^2} \,. \tag{4.138}$$

Now we have the form of the Dirac momentum eigenvalues expressed in terms of the mean meson fields σ and ω^μ. But we must still find their values using the equations of motion (4.124, 4.128). This obviously poses

a self-consistency problem since the mean meson fields are given in terms of the ground state expectation values of the baryon currents whose eigenvalues are given in terms of the mean meson fields themselves. To give full expression to the problem, we have to obtain explicit expressions for the baryon currents appearing in (4.124).

An obvious (but not necessarily economical) means of constructing the ground state expectation values of the nucleon currents is to construct the nucleon spinors first. This can be done since the Dirac equation has the same form as the free equation; only the four-momentum and mass are shifted by the mean meson field values. Then the currents can be constructed with the spinors by matrix multiplication and summation over occupied nucleon states.

However, there is a more economical way of evaluating the ground state expectation values which avoids the unnecessary construction of the spinors as an intermediate step. This is the method we shall use. A single-nucleon state is characterized in this theory by the momentum $\boldsymbol{k}$ and the spin and isospin projection which we denote together by κ. Of course, each neutron and proton momentum state can have one of two spin projections $\pm 1/2$. Let us denote by a round bracket the expectation value of an operator in a single-particle state, $(\overline{\psi}\Gamma\psi)_{\boldsymbol{k}\kappa}$. The expectation value of an operator in the ground state of the many-nucleon system is obviously

$$\langle\overline{\psi}\Gamma\psi\rangle = \sum_{\kappa}\int \frac{d\boldsymbol{k}}{(2\pi)^3}(\overline{\psi}\Gamma\psi)_{\boldsymbol{k}\kappa}\Theta[\mu - e(\boldsymbol{k})]\,, \tag{4.139}$$

where the sum on κ is understood to be over the spin-isospin states of the occupied momentum states and $\Theta(x)$ is a step function which is unity for $x \geq 0$ and zero otherwise. We denote the Fermi energy by μ. We also refer to it as the chemical potential. The ground state expectation values (4.139) are momentum integrals over the filled states of the single-particle expectations in such momentum states; the integral is from zero up to that value of $\boldsymbol{k}$ for which the eigenvalues $e(\boldsymbol{k})$ lie below the chemical potential μ, i.e., up to some designated energy.

The above formulation in terms of the three-vector $\boldsymbol{k}$ allows for the Fermi surface prescribed by $e(\boldsymbol{k}) = \mu$ to be nonspherical in momentum space; however, our applications will always involve spherical Fermi surfaces. (Nonspherical Fermi surfaces occur in the theory of pion condensation in a many-body system because of the p-wave interaction [110].)

How are the single-particle expectation values appearing in expression (4.139) to be found? The operator, denoted by Γ, appearing in the integral is generally to be found also in the Dirac Hamiltonian. Use the Dirac equation (4.128), and remember that $\gamma_\mu k^\mu = \gamma_0 k_0 - \boldsymbol{\gamma}\cdot\boldsymbol{k}$. Isolate k^0, and find *the Dirac Hamiltonian*:

$$H_D = \gamma_0\Big[\boldsymbol{\gamma}\cdot\boldsymbol{k} + g_\omega\,\gamma_\mu\omega^\mu + m^\star\Big]\,. \tag{4.140}$$

Now, take the expectation in a single-nucleon momentum state as defined above:

$$(\psi^\dagger H_D \psi)_{\boldsymbol{k}\kappa} = K_0(\boldsymbol{k}) = E(\boldsymbol{k}) + g_\omega \omega_0 \,. \tag{4.141}$$

In the present example, note that the right side is independent of the spin-isospin projection label κ, i.e., the momentum states are degenerate with occupation 4. It need not be so in more complicated applications.

Now take a derivative of the left side of (4.141) with respect to any variable ζ in the Hamiltonian,

$$\frac{\partial}{\partial \zeta}(\psi^\dagger H_D \psi)_{\boldsymbol{k}\kappa} = (\psi^\dagger \frac{\partial H_D}{\partial \zeta} \psi)_{\boldsymbol{k}\kappa} + k_0(\boldsymbol{k}) \frac{\partial}{\partial \zeta}(\psi^\dagger \psi)_{\boldsymbol{k}\kappa} \,. \tag{4.142}$$

Because $\psi(\boldsymbol{k})$ is an eigenfunction, only the first term on the right survives. Use this result from now on in taking derivatives of (4.141). First take a derivative of the above equation (4.141) with respect to ω_0. This yields, immediately, the normalization

$$(\psi^\dagger \psi)_{\boldsymbol{k}\kappa} = 1 \,. \tag{4.143}$$

Then from (4.139) we have the baryon density,

$$\rho = \langle \psi^\dagger \psi \rangle = 4 \int_0^{\boldsymbol{k}} \frac{d\boldsymbol{k}}{(2\pi)^3} \Theta[\mu - e(\boldsymbol{k})] \,. \tag{4.144}$$

This is an expected and trivial result, especially when the Fermi surface is a sphere. Then the Θ function is unity for levels below $e(\boldsymbol{k}) \leq \mu$, and the expression for the density becomes the usual expression.

In like manner, we can compute other expectation values which are not so trivial. Take a derivative with respect to k^i:

$$(\overline{\psi} \gamma^i \psi)_{\boldsymbol{k}\kappa} \equiv \frac{\partial}{\partial k^i} E(\boldsymbol{k}) \,. \tag{4.145}$$

Hence, the nucleon current is

$$\begin{aligned} \langle \overline{\psi} \gamma^i \psi \rangle &= 4 \int \frac{d\boldsymbol{k}}{(2\pi)^3} \left(\frac{\partial}{\partial k^i} E(\boldsymbol{k}) \right) \Theta(\mu - e(\boldsymbol{k})) \\ &= 4 \int \frac{dk^i \, dk^j \, dk^k}{(2\pi)^3} \left(\frac{\partial}{\partial k^i} E(\boldsymbol{k}) \right) \Theta(\mu - e(\boldsymbol{k})) \\ &= 4 \int \frac{dk^j \, dk^k}{(2\pi)^3} \int dE(k^j, k^k) = 0 \,. \end{aligned} \tag{4.146}$$

The integral is over the occupied momentum states (meaning over some volume in the momentum space) which is a sphere if $e(\boldsymbol{k})$ depends only on $|\boldsymbol{k}|$, and otherwise is some other closed region. The integral above vanishes

because $E(\boldsymbol{k})$ equals the constant $\mu - g_\omega\,\omega_0$ everywhere on the boundary of the surface of the region of integration. Therefore the integral over dE is the difference of two equal numbers. As a consequence of the vanishing of the baryon current (a result intuitively expected inasmuch as we are dealing with the ground state of uniform static matter), we see from the equations of motion that the space components ω^i vanish. As a further consequence, the region of occupied momentum space is a sphere. The Dirac eigenvalues can then be written more simply as

$$e(k) = g_\omega\omega_0 + E(k), \qquad E(k) = \sqrt{k^2 + (m - g_\sigma\sigma)^2}\,, \tag{4.147}$$

and the density as

$$\rho \equiv \langle\psi^\dagger\psi\rangle = 4\int_0^k \frac{d\boldsymbol{k}}{(2\pi)^3} = \frac{2k^3}{3\pi^2}\,. \tag{4.148}$$

This is sometimes referred to as the *vector* density in contrast to the *scalar* density which we take up next. The vector density is the Lorentz time component of the conserved baryon current (4.84) and is simply the baryon density.

We make a special note here. Because of the isotropy of the momentum space for the ground state just proven, the upper limit on momentum integrals (the Fermi momentum at the desired density) will be denoted just by k and the corresponding density for symmetric nuclear matter given by (4.148). The Fermi energy is therefore given by $\mu \equiv e(k)$.

Finally, we need the scalar density $\langle\overline{\psi}\psi\rangle$. Take a derivative of (4.141) with respect to m:

$$(\overline{\psi}\psi)_{\boldsymbol{k}\kappa} = \frac{\partial E(k)}{\partial m}\,. \tag{4.149}$$

The result is

$$\rho_s \equiv \langle\overline{\psi}\psi\rangle = \frac{2}{\pi^2}\int_0^k k^2 dk \frac{m - g_\sigma\,\sigma}{\sqrt{k^2 + (m - g_\sigma\,\sigma)^2}}\,. \tag{4.150}$$

The above technique is quite powerful because it can be used to evaluate the expectation value of any operator that appears in the Dirac Hamiltonian without going through the intermediate step of constructing the Dirac spinors. In some applications the explicit construction is awkward.

Assembling the results just obtained, we find that the equations of motion now have the explicit forms

$$g_\sigma\sigma = \left(\frac{g_\sigma}{m_\sigma}\right)^2 \frac{2}{\pi^2}\int_0^k k^2 dk \frac{m - g_\sigma\,\sigma}{\sqrt{k^2 + (m - g_\sigma\,\sigma)^2}}\,, \tag{4.151}$$

$$g_\omega\omega_0 = \left(\frac{g_\omega}{m_\omega}\right)^2 \rho\,, \tag{4.152}$$

$$m_\omega^2\omega_k = 0\,. \tag{4.153}$$

The last two are trivial, but the first expresses a self-consistency condition on the scalar field since it appears in a transcendental equation. It will be noticed that, regarded as equations in $g_\sigma\sigma$ and $g_\omega\omega$, the solutions depend on the coupling constants and meson masses only through the ratios g_σ/m_σ and g_ω/m_ω. This is true in general at the mean-field level for infinite nuclear matter. It is also true for the rho meson which we discuss shortly. Only for finite nuclei do the field equations and nuclear properties become dependent on the individual values of coupling constants and meson masses. These two ratios (and others that we encounter later) may be taken as the parameters of the theory. They should be chosen so that the saturation density and binding per nucleon of the theory are in accord with the empirical values discussed in Section 4.5.

The schematic behavior of the solution $g_\sigma\sigma$ of (4.151) is easy to discern. At low nucleon density where k is small, the integral must be small and tend to zero. In fact it is easy to see that the scalar density approaches the nucleon density ρ for small k or ρ. At the other limit, as the density or k increases, the solution for $g_\sigma\sigma$ increases. But if it approaches m, the right side will become small, even for large k. So, at high density, the solution approaches but does not reach m. More precisely,

$$g_\sigma\sigma \to m\left(\frac{g_\sigma k}{m_\sigma \pi}\right)^2 \left[1 + \left(\frac{g_\sigma k}{m_\sigma \pi}\right)^2\right]^{-1} . \tag{4.154}$$

Therefore, the effective mass $m^\star = m - g_\sigma\sigma$ has the vacuum value m at small density and it goes to zero in the limit at high density. The fact that the scalar density can be approximated by the density is useful in numerically solving the theory.

In the above expression for the eigenvalue (4.147), we can see the roles played by the scalar and vector mesons. The Lorentz time component of the vector meson shifts the eigenvalue of given k to ever higher energy as the density increases (4.152), whereas the scalar meson tends to reduce it by reducing the effective mass as the nucleon density increases from zero. In consequence (as we shall see), there is a density at which the energy per nucleon becomes a minimum. That density is the saturation density, and, from the energy density at that point, we can find the saturation binding per nucleon through (4.111).

To compute the equation of state, we turn to the energy-momentum tensor (4.27) whose expectation value in the rest frame of the matter is diagonal (2.33) and has as elements the energy density and the pressure [111]. Using the Lagrangian of the present theory (4.120), we find

$$\begin{aligned} \epsilon &= -\langle\mathcal{L}\rangle + \langle\overline{\psi}\gamma_0 k_0\psi\rangle , \\ p &= \langle\mathcal{L}\rangle + \frac{1}{3}\langle\overline{\psi}\gamma_i k_i\psi\rangle , \end{aligned} \tag{4.155}$$

where we have used $i\partial_\nu\psi = k_\nu\psi$ and the fact that the meson fields are spacetime-independent. (The factor 1/3 appears in the above equation for

p because each of the three diagonal spacelike components of the energy-momentum tensor involves the corresponding $\gamma_i k_i$ (i unsummed). By summing these equal diagonal elements, we have to divide by three.) Employing the equations of motion for the Dirac field, the term in that field drops out, and we have simply

$$\langle \mathcal{L} \rangle = -\tfrac{1}{2} m_\sigma^2 \sigma^2 + \tfrac{1}{2} m_\omega^2 \omega_0^2 \,. \tag{4.156}$$

The second term in ϵ appearing in (4.155) is the contribution of the occupied nucleon momentum states each of whose eigenvalues we derived above. From (4.139) we have

$$\begin{aligned} \langle \overline{\psi} \gamma_0 k_0 \psi \rangle &= \frac{2}{\pi^2} \int_0^k k^2 \, dk \, e(k) \\ &= g_\omega \omega_0 \, \rho + \int_0^k k^2 \, dk \sqrt{k^2 + (m - g_\sigma \, \sigma)^2} \\ &= m_\omega^2 \omega_0^2 + \frac{2}{\pi^2} \int_0^k k^2 \, dk \sqrt{k^2 + (m - g_\sigma \, \sigma)^2} \,. \end{aligned} \tag{4.157}$$

The equation of motion for ω_0 (4.152) and the expression of the baryon density in terms of k were used to rewrite the first term. To evaluate the remaining expectation, we have

$$(\overline{\psi} \gamma \psi)_{\boldsymbol{k}_\kappa} = \frac{\partial E(\boldsymbol{k})}{\partial \boldsymbol{k}} \,, \tag{4.158}$$

whence

$$\langle \overline{\psi} \boldsymbol{\gamma} \cdot \boldsymbol{k} \psi \rangle = \frac{2}{\pi^2} \int_0^k \frac{k^4}{\sqrt{k^2 + (m - g_\sigma \, \sigma)^2}} \, dk \,. \tag{4.159}$$

Now, assemble the contributions to the energy density and pressure,

$$\epsilon = +\tfrac{1}{2} m_\sigma^2 \sigma^2 + \tfrac{1}{2} m_\omega^2 \omega_0^2 + \frac{2}{\pi^2} \int_0^k \sqrt{k^2 + (m - g_\sigma \, \sigma)^2} \, k^2 \, dk \,. \tag{4.160}$$

The pressure is given by

$$p = -\tfrac{1}{2} m_\sigma^2 \sigma^2 + \tfrac{1}{2} m_\omega^2 \omega_0^2 + \frac{1}{3} \frac{2}{\pi^2} \int_0^k k^4 \, dk / \sqrt{k^2 + (m - g_\sigma \, \sigma)^2} \,. \tag{4.161}$$

In both of these expressions, the first terms are contributions from the meson fields whose mean values are given above, and the integrals are over the occupied nucleon momentum states. The equation of state is here in the form $\epsilon = \epsilon(\rho)$, $p = p(\rho)$ since k, σ and ω are in that form. If needed, ρ could be eliminated numerically to yield $p = p(\epsilon)$ or its inverse.

We have seen that $g_\sigma \sigma$ is bounded by the nucleon mass, whereas, according to (4.152), the vector field grows as the baryon density. Since $\rho \sim k^3$, the vector term in both ϵ and p dominate at high density, and $p \to \epsilon$ from below. A disturbance of the medium propagates at speed $(dp/d\epsilon)^{1/2}$ [112], so the theory is causal.

The above explicit formula for the pressure was found using the energy-momentum tensor. One might wonder how it accords with the definition, $p = -\partial E/\partial V$. Divide both E and V (volume) by conserved particle number N. Then find

$$p = \rho^2 \frac{\partial(\epsilon/\rho)}{\partial \rho} . \tag{4.162}$$

One can prove algebraically that the above operation yields p in the explicit form written. Clearly, it is more advantageous to have explicit algebraic expressions than to have to take a numerical derivative in computing an equation of state.

The expressions for the equation of state are now at hand. To evaluate ϵ and p as functions of nucleon density ρ, we must solve (4.151) numerically, say for a set of values of k. Because the $(\sigma - \omega)$ theory has two parameters, the saturation density and binding energy per nucleon can be fitted exactly. The other relevant parameters do not agree well with the empirical values noted earlier. In particular, the compression modulus computed for the equation of state at saturation is $K \approx 550$ MeV, roughly a factor of two to three times larger than it should be according to the empirical range discussed in Section 4.5. The Dirac effective nucleon mass at saturation is $m^\star/m \equiv m - g_\sigma \sigma_0 \approx 0.5$. This is in poor agreement with the empirical range (4.118). At saturation both of these properties affect the high-density behavior of the equation of state, so we cannot expect that this simple model will extrapolate well to the high-density domain of symmetric matter.

Moreover, the symmetry energy coefficient is in poor accord with observation. After some calculation, one finds that the symmetry energy coefficient is related to the equation of state (4.113) by

$$a_{\rm sym} = \frac{k_F^2}{6(k_F^2 + m^{\star 2})^{1/2}} . \tag{4.163}$$

The derivation follows along the lines of Section 4.9. In our discussion of nuclear matter properties, we saw that the normal nuclear matter density implies $k_F = 1.31$ fm^{-1} and that the effective mass at saturation density falls within a fairly narrow range. In particular we take $m^\star = 0.75m = 3.5686$ fm^{-1}. This yields $a_{\rm sym} = 14.8$ MeV compared to an empirical value of 32.5 MeV.

In consequence of the above deficiencies, the model is not expected to extrapolate well to the asymmetric matter of neutron stars. Moreover, it yields a weakly bound state for pure neutron matter for which there is no evidence. (In this connection, see also Section 4.13.)

The main merit of the model from our point of view is that it has provided the opportunity of introducing, in a simple context, the techniques that will be employed in improvements to nuclear field theory. We are now in a position to take them up.

4.7 Stationarity of Energy Density

Let us reconstruct the energy density from (4.155) before employing the Euler–Lagrange equation for ω_0 (4.152) to simplify the result. It is

$$\begin{aligned}\epsilon &= \tfrac{1}{2}m_\sigma^2\sigma^2 - \tfrac{1}{2}m_\omega^2\omega_0^2 \\ &\quad + \frac{2}{\pi^2}\int_0^k \left[g_\omega\omega_0 + \sqrt{k^2 + (m - g_\sigma\,\sigma)^2}\right] k^2\,dk\,. \end{aligned} \tag{4.164}$$

Let us evaluate the condition that ϵ above is stationary with respect to ω_0 for fixed baryon density ρ (or, equivalently, fixed k). We immediately get the field equation for ω_0, namely, (4.152). Similarly for the scalar field. So the field equations are the conditions that the energy density be stationary at fixed baryon density:

$$\left(\partial\epsilon/\partial\omega_0\right)_{k=\text{const}} = \left(\partial\epsilon/\partial\sigma\right)_{k=\text{const}} = 0\,. \tag{4.165}$$

4.8 Model with Scalar Self-Interactions

We have seen that a field theory with only two meson fields, a scalar and vector, can yield the saturation phenomenon characteristic of nuclear matter and nuclei. Because it reduces the effective nucleon mass, the scalar meson contributes a reduction in the energy per nucleon near saturation, and the vector meson contributes repulsion. The repulsion grows with density whereas the attraction saturates so that a balance is reached at which the binding energy is a minimum. This is the equilibrium or saturation point that occurs at the saturation density and binding energy. However, other properties of the model—the compression modulus, the effective nucleon mass and the symmetry energy—were in poor agreement with the empirical values.

Here we study an extension of the theory due to Boguta and Bodmer [113], the main purpose of which is to bring the compression modulus and nucleon effective mass at saturation under control. (For another approach see [114].) Self-interactions of the scalar field are introduced:

$$U(\sigma) = \tfrac{1}{3}bm(g_\sigma\sigma)^3 + \tfrac{1}{4}c(g_\sigma\sigma)^4\,, \tag{4.166}$$

where m is a nominal nucleon mass and is introduced only to make the constants b and c dimensionless and m is taken throughout in this formula

to be 938 MeV. We noted above that g_σ is dimensionless and σ has the same dimension as m, which we have chosen to express in units of 1/fm with $\hbar c = 197.33$ MeV-fm. So the units of U are energy density, as is $\mathcal{L}$.

$$\begin{aligned}\mathcal{L} &= \overline{\psi}\Big[i\gamma_\mu(\partial^\mu + ig_\omega\omega^\mu) - (m - g_\sigma\sigma)\Big]\psi + \tfrac{1}{2}(\partial_\mu\sigma\partial^\mu\sigma - m_\sigma^2\sigma^2) \\ &\quad - \tfrac{1}{4}\omega_{\mu\nu}\omega^{\mu\nu} + \tfrac{1}{2}m_\omega^2\omega_\mu\omega^\mu - \tfrac{1}{3}bm(g_\sigma\sigma)^3 - \tfrac{1}{4}c(g_\sigma\sigma)^4 . \qquad (4.167)\end{aligned}$$

The Euler–Lagrange equation for the scalar field is now

$$\begin{aligned}g_\sigma\sigma &= \left(\frac{g_\sigma}{m_\sigma}\right)^2\left[\frac{2}{\pi^2}\int_0^k k^2 dk \frac{m - g_\sigma\sigma}{\sqrt{k^2 + (m - g_\sigma\sigma)^2}}\right. \\ &\quad \left. - bm(g_\sigma\,\sigma)^2 - c(g_\sigma\,\sigma)^3\right]. \qquad (4.168)\end{aligned}$$

The other field equations would be unaffected by the addition of $U(\sigma)$ to $\mathcal{L}$. We reproduce them here for completeness:

$$g_\omega\omega_0 = \left(\frac{g_\omega}{m_\omega}\right)^2 \rho , \qquad (4.169)$$

$$m_\omega^2\omega_k = 0 , \qquad (4.170)$$

$$\Big[\gamma_\mu(k^\mu - g_\omega\omega^\mu) - (m - g_\sigma\sigma)\Big]\psi(k) = 0 . \qquad (4.171)$$

The (Dirac) effective mass, as before, is

$$m^\star(\sigma) = m - g_\sigma\sigma , \qquad (4.172)$$

with $m^\star$ denoting its value at saturation density. The Dirac momentum eigenvalues are of the same form as before (4.147).

As seen in the earlier result (4.155), the energy density and pressure have contributions $\mp\langle\mathcal{L}\rangle$ so the modifications to the previous results for energy density and pressure are $\pm U(\sigma)$:

$$\begin{aligned}\epsilon &= \tfrac{1}{3}bm(g_\sigma\sigma)^3 + \tfrac{1}{4}c(g_\sigma\sigma)^4 + \tfrac{1}{2}m_\sigma^2\sigma^2 + \tfrac{1}{2}m_\omega^2\omega_0^2 \\ &\quad + \frac{2}{\pi^2}\int_0^k \sqrt{k^2 + (m - g_\sigma\sigma)^2}\, k^2\, dk , \\ p &= -\tfrac{1}{3}bm(g_\sigma\sigma)^3 - \tfrac{1}{4}c(g_\sigma\sigma)^4 - \tfrac{1}{2}m_\sigma^2\sigma^2 + \tfrac{1}{2}m_\omega^2\omega_0^2 \\ &\quad + \frac{1}{3}\frac{2}{\pi^2}\int_0^k \frac{k^4\, dk}{\sqrt{k^2 + (m - g_\sigma\sigma)^2}} . \qquad (4.173)\end{aligned}$$

(All momentum integrals of the theory can be found in standard tables [45] but for display, the formulae are shorter and more transparent in meaning when left as integrals.)

In deriving the above expression, the field equation of the rho meson was used with the result

$$\tfrac{1}{2}{m_\omega}^2\omega_0^2 = \tfrac{1}{2}\left(\frac{g_\omega}{m_\omega}\right)^2\rho^2 . \tag{4.174}$$

What is particularly interesting about the above extension of the previous $(\sigma - \omega)$ model is that there are two additional coupling constants. This allows the values of the two additional properties of symmetric nuclear matter, the compression modulus K and the effective nucleon mass $m^\star$ at saturation, to be reproduced by the theory. As explained previously, both are important as concerns the high-density behavior of the equation of state.

4.8.1 Algebraic determination of the coupling constants

It is perhaps surprising that the four coupling constants g_σ/m_σ, g_ω/m_ω, b, and c, can be found algebraically in terms of the four empirical quantities ρ, B/A, K, and $m^\star$ at nuclear saturation. While the algebra is more involved than is worth reproducing here in detail, we indicate the necessary steps and results since the existence of an algebraic solution for the couplings makes the theory especially well defined in terms of the nuclear bulk properties. So far as we are aware, this fact has not been known before.

First, using the expression for the energy density, take a derivative with respect to ρ to find

$$\begin{aligned}\frac{d\epsilon}{d\rho} &= \frac{d\sigma}{d\rho}\left(m_\sigma^2\sigma + \frac{dU}{d\sigma} - g_\sigma\frac{2}{\pi^2}\int\frac{m - g_\sigma\sigma}{\sqrt{k^2 + (m - g_\sigma\sigma)^2}}k^2\,dk\right)\\ &\quad + g_\omega\omega_0 + \sqrt{k^2 + (m - g_\sigma\sigma)^2}\,.\end{aligned} \tag{4.175}$$

The quantity in the parenthesis vanishes identically by virtue of the scalar field equation (4.151). So the derivative $d\epsilon/d\rho$ at saturation is equal to the Fermi energy which we have called μ. We have

$$\mu \equiv g_\omega\omega_0 + \sqrt{k^2 + m^{\star 2}} = \frac{d\epsilon}{d\rho}\,, \tag{4.176}$$

where all quantities, ω_0, ρ, k, $m^\star, \ldots$, are evaluated at saturation density. This will be the case throughout the remainder of this derivation. At saturation, the function ϵ/ρ has a minimum as a function of ρ. So we require

$$0 = \frac{d}{d\rho}\frac{\epsilon}{\rho} = \frac{1}{\rho}\left(\frac{d\epsilon}{d\rho} - \frac{\epsilon}{\rho}\right), \qquad \text{(at saturation)}\,, \tag{4.177}$$

from which we find

$$\frac{\epsilon}{\rho} = \frac{d\epsilon}{d\rho} = \mu \qquad \text{(at saturation)}\,. \tag{4.178}$$

So, from the relations developed,

$$m + \frac{B}{A} \equiv \frac{\epsilon}{\rho} = \left(\frac{g_\omega}{m_\omega}\right)^2 \rho + \sqrt{k^2 + m^{\star 2}} \qquad \text{(at saturation)}\,, \tag{4.179}$$

where the Fermi momentum at saturation k is related to the density in the usual way:

$$\rho = 2k^3/(3\pi^2)\,. \tag{4.180}$$

Next take a second derivative of ϵ/ρ using (4.177), and find at saturation density

$$\frac{d^2}{d\rho^2}\frac{\epsilon}{\rho} = \frac{1}{\rho}\frac{d^2\epsilon}{d\rho^2} = \frac{1}{\rho}\frac{d\mu}{d\rho}\,. \tag{4.181}$$

We have seen in (4.114) an expression for the compression modulus and are now able to write

$$K = 9\rho\frac{d\mu}{d\rho}\,. \tag{4.182}$$

From the expression for μ above, we have

$$\frac{d\mu}{d\rho} = \left(\frac{g_\omega}{m_\omega}\right)^2 + \frac{1}{E(k)}\left(k\frac{dk}{d\rho} - m^\star g_\sigma \frac{d\sigma}{d\rho}\right), \tag{4.183}$$

where,

$$E(k) = \sqrt{k^2 + m^{\star 2}}\,, \tag{4.184}$$

as defined before. To evaluate the derivative of σ, use the field equation. Substitute the result in the above equation and that result in the above expression for K at saturation. After some calculation obtain

$$\begin{aligned} K = {} & \left(\frac{g_\omega}{m_\omega}\right)^2 \frac{6k^3}{\pi^2} + \frac{3k^2}{E(k)} \\ & - \frac{6k^3}{\pi^2}\left[\frac{m^\star}{E(k)}\right]^2 \left(\frac{g_\sigma}{m_\sigma}\right)^2 \left\{1 + \left(\frac{g_\sigma}{m_\sigma}\right)^2 \left[\frac{d^2U}{d(g_\sigma\sigma)^2} + \frac{2}{\pi^2}\int \frac{k^4\,dk}{E^3(k)}\right]\right\}^{-1}. \end{aligned} \tag{4.185}$$

Note that we know the scalar field strength at saturation, $g_\sigma\,\sigma = m - m^\star$ since $m^\star$ is one of the empirical data whose range is known. So the above equation has only (g_σ/m_σ), b, and c as unknowns. Two additional equations in the same unknowns are the scalar field equation (4.168) and the equation for the energy density (4.173) whose value is known from

$$\epsilon = \rho(m + B/A), \qquad B/A = -16.3 \text{ MeV}\,, \tag{4.186}$$

as in (4.107,4.108). So we have three equations in the three unknowns just mentioned which are all of the form

$$\alpha_i(m_\sigma/g_\sigma)^2 + \beta_i b + \gamma_i c = \delta_i, \qquad i = 1,2,3\,, \tag{4.187}$$

where in each case the coefficients $\alpha, \beta, \gamma, \delta$ are calculable constants given in terms of the saturation properties. We note that all of the momentum integrals appearing in the coefficients can be evaluated in closed form by reference to a table of standard integrals [45]. Thus all four couplings can be determined *algebraically* from the four nuclear saturation properties after which the equation of state for symmetric nuclear matter can be computed.

We show how to express the solution in one possible way. To yield numbers, all quantities must be expressed in a consistent set of units. In this connection a note on dimensions that are useful in nuclear physics is provided in Section 4.14. Thus energies and momenta will be expressed in inverse fermis. The vector coupling is obtained simply from (4.179):

$$\left(\frac{g_\omega}{m_\omega}\right)^2 = \frac{m + B/A - \sqrt{k^2 + m^{\star 2}}}{\rho}\,. \tag{4.188}$$

All quantities on the right side are provided by the saturation properties of nuclear matter. The coefficients in (4.187) are

$$\begin{aligned}
\alpha_1 &= K - \left(\frac{g_\omega}{m_\omega}\right)^2 \frac{6k^3}{\pi^2} - \frac{3k^2}{\sqrt{k^2 + m^{\star 2}}}\,,\\
\beta_1 &= 2(m - m^\star)\alpha_1\,,\\
\gamma_1 &= 3(m - m^\star)^2\alpha_1\,,\\
\delta_1 &= -\alpha_1 I_1 - \frac{6k^3}{\pi^2}\left(\frac{m^\star}{\sqrt{k^2 + m^{\star 2}}}\right)^2,
\end{aligned} \tag{4.189}$$

$$\begin{aligned}
\alpha_2 &= \tfrac{1}{2}(m - m^\star)^2\,,\\
\beta_2 &= \tfrac{1}{3}m(m - m^\star)^3\,,\\
\gamma_2 &= \tfrac{1}{4}(m - m^\star)^4\,,\\
\delta_2 &= \rho(m + B/A) - I_2 - \tfrac{1}{2}\left(\frac{g_\omega}{m_\omega}\right)^2 \rho^2\,,
\end{aligned} \tag{4.190}$$

$$\begin{aligned}
\alpha_3 &= m - m^\star\,,\\
\beta_3 &= m(m - m^\star)^2\,,\\
\gamma_3 &= (m - m^\star)^3\,,
\end{aligned}$$

and

$$\delta_3 = I_3\,. \tag{4.191}$$

For convenience, we have expressed the integrals in algebraic form and defined

$$\begin{aligned}
x &= k/m^\star\,, \\
t &= \sqrt{1+x^2}\,, \\
I_1 &= \frac{2}{\pi^2} m^{\star 2}[\tfrac{1}{2}xt + \frac{x}{t} - \tfrac{3}{2}\ln(x+t)]\,, \\
I_2 &= \frac{2}{\pi^2} m^{\star 4}\tfrac{1}{4}[xt^3 - \tfrac{1}{2}xt - \tfrac{1}{2}\ln(x+t)]\,, \\
I_3 &= \frac{2}{\pi^2} m^{\star 3}\tfrac{1}{2}[xt - \ln(x+t)]\,.
\end{aligned} \tag{4.192}$$

The solution can be expressed as

$$\begin{aligned}
c &= \frac{(\alpha_3\beta_1 - \alpha_1\beta_3)(\alpha_2\delta_1 - \alpha_1\delta_2)(\alpha_2\beta_1 - \alpha_1\beta_2)(\alpha_3\delta_1 - \alpha_1\delta_3)}{(\alpha_3\beta_1 - \alpha_1\beta_3)(\alpha_2\gamma_1 - \alpha_1\gamma_2)(\alpha_2\beta_1 - \alpha_1\beta_2)(\alpha_3\gamma_1 - \alpha_1\gamma_3)}\,, \\
b &= \frac{(\alpha_2\delta_1 - \alpha_1\delta_2) - (\alpha_2\gamma_1 - \alpha_1\gamma_2)}{\alpha_2\beta_1 - \alpha_1\beta_2} c\,, \\
\left(\frac{g_\sigma}{m_\sigma}\right)^2 &= \frac{\alpha_1}{\delta_1 - \gamma_1 c - \beta_1 b}\,.
\end{aligned} \tag{4.193}$$

Looking ahead to the section on the isospin force and the symmetry energy, we can write the coupling of the rho meson (4.216) as

$$\left(\frac{g_\rho}{m_\rho}\right)^2 = \frac{8}{\rho}\left[a_{\rm sym} - \frac{k^2}{6\sqrt{k^2+m^{\star 2}}}\right]. \tag{4.194}$$

Notice that the three ratios g/m have the dimension of fermis and b and c are dimensionless.

We are now in a position to describe all five important bulk properties of nuclear matter, both symmetric and asymmetric. The five coupling constants of the theory, g_σ/m_σ, g_ω/m_ω, g_ρ/m_ρ, b, and c are defined algebraically in terms of the five saturation properties of symmetric nuclear matter, B/A, ρ_0, $a_{\rm sym}$, K, and $m^\star$. The field equations of the same Lagrangian with the couplings so obtained can be solved with subsidiary constraints appropriate to charge-neutral, beta-stable matter suitable for neutron star structure as described in Chapter 5. The algebraic connection makes it convenient to explore the effects of uncertainties in the saturation properties on neutron star structure (albeit in the particular theory of this chapter).

4.8.2 Symmetric nuclear matter equation of state

In the discussion of nuclear matter properties, it was found that the binding energy and saturation density are well known but that the compression

modulus K and the value of the nucleon effective mass $m^\star$ at saturation are known only within a range. It is interesting to see the uncertainty in the equation of state of symmetric nuclear matter that corresponds to the uncertainty in the above two data. This is shown in Fig. 4.1. Considering that it is the binding energy per nucleon that is shown (measured in reference to the nucleon mass (4.111)), the uncertainty does not seem too great, although we shall see that it is reflected in a considerable range in neutron star masses and baryon populations.

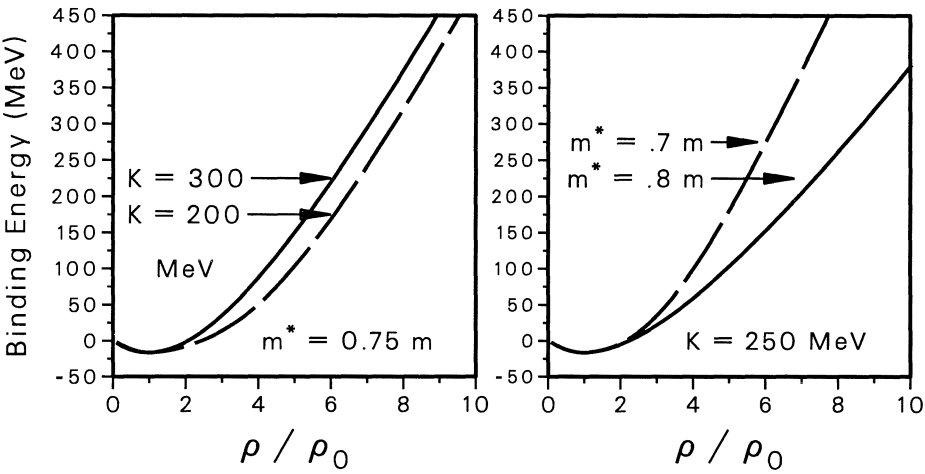

FIGURE 4.1. Equation of state for symmetric nuclear matter for two values of K at fixed $m^\star$ and vice versa. The range of both properties is within the experimental bounds.

As expected, the higher the compression modulus, the steeper (or stiffer) the equation of state at high density. In contrast, the smaller the value of the effective nucleon mass at saturation, the stiffer the equation of state. Since the simple $\sigma - \omega$ model discussed as a first example has both too high a K and too small an $m^\star$ (both lie outside the empirical range), the model has an extremely stiff equation of state (both effects act in the same direction).

4.8.3 Negative self-interaction

The coupling constants corresponding to a selection of nuclear matter properties in the range determined by experiment are shown in Table 4.4. The constant c is negative for several entries. From the expression for the energy density, this permits the energy to become unbounded from below for

a large enough scalar field. This would certainly be a fatal problem for a quantum field theory. Some authors consider this unacceptable even for an effective theory. We take the view that the theory is an effective theory of composite particles, not of fundamental ones. Further, the field equations provide an equation of state which is well behaved in the density region for which a theory based on composite hadrons is plausible.

By choosing the coupling constants so that the saturation properties of nuclear matter are well reproduced by theory, a reasonable behavior of the equation of state is assured in the vicinity of saturation. By continuity, a plausible extrapolation in density and isospin density can also be made when the coupling constants are chosen as above to describe the important properties of nuclear matter at saturation. We shall therefore be interested in the behavior of the theory as a function of density along the trajectory in the field variables that are specified by the Euler–Lagrange equations.

It is evident from Fig. 4.1 that, for the small negative values corresponding to the combinations of matter properties considered realistic, the equation of state is well behaved, even at ten times saturation density. This is certainly at or beyond the range of validity of any theory or model based on (composite) hadrons. However, whenever negative c is encountered, the equation of state should be checked for normal behavior in the interesting region from zero to a few times nuclear density. In the corresponding neutron star models, as we shall see in the next chapters, the central density of even the limiting mass star does not extend as high as ten times the saturation density of nuclei.

TABLE 4.4. Coupling constants that yield binding $B/A = -16.3$ MeV, saturation density $\rho_0 = 0.153$ fm^{-3}, and symmetry energy coefficient, $a_{sym} = 32.5$ MeV for saturated nuclear matter with the compression K and effective mass $m^\star$ listed below.

K MeV	$m^\star/m$	$(g_\sigma/m_\sigma)^2$ fm^2	$(g_\omega/m_\omega)^2$ fm^2	$(g_\rho/m_\rho)^2$ fm^2	b $\times 100$	c $\times 100$
200.	0.70	12.684	7.148	4.410	0.5610	−0.6986
200.	0.75	11.299	5.696	4.656	0.8784	−1.0098
200.	0.80	9.926	4.233	4.876	1.4602	−1.2412
250.	0.70	12.230	7.148	4.410	0.4312	−0.4103
250.	0.75	10.727	5.696	4.656	0.6275	−0.3409
250.	0.80	9.134	4.233	4.876	0.8804	0.6917
300.	0.70	11.785	7.148	4.410	0.2948	−0.1071
300.	0.75	10.177	5.696	4.656	0.3601	0.3722
300.	0.80	8.403	4.233	4.876	0.2480	2.7997

4.9 Introduction of Isospin Force

It was seen above how the four properties of nuclear matter at saturation can be accounted for in the theory by adding self-interaction terms for the scalar field. The compression modulus and effective mass are especially relevant to the high-density extrapolation. The binding energy and saturation density serve to normalize the equation of state. Since we wish an equation of state for neutron star matter, the theory must be extended to incorporate an isospin restoring interaction, that is, a component in the nuclear interaction that yields an effect such as seen in the empirical mass formula (4.106).

The expression for the energy density (4.173) taken with (4.169) suggests the solution. The vector meson has as its source the (vector) nucleon density, and the energy density is quadratic in this density. We need to introduce a meson that has as its source the 3-component of isospin and expect as a result a term in the energy density that is quadratic in the deviation from isospin symmetry, that is, quadratic in the 3-component of the isospin density.

We have encountered the rho meson in (4.55), a triplet of mesons of the same mass and charges (0, ± 1), which form an isospin triplet with isospin current (4.63). We need to couple this triplet to the isospin of the nucleon given by (4.92) in such a way that a scalar is formed. It also has to be done in such a way as to involve the total conserved isospin current of the Lagrangian.

Recalling the isospin current of nucleon and rho fields (4.92 4.63), we tentatively consider the sum of these two as the isospin current of the combined theory and add an interaction term $\boldsymbol{\rho}_\mu \cdot \boldsymbol{I}^\mu$ to the Lagrangian. However, the contribution of the rho meson to this current contains the derivative of the field, and, from the general expression of the Noether current (4.13), this would itself make a contribution to the current. So the rho meson must contribute an additional piece as a result of its interaction with the isospin current. Let us see what it is.

For this purpose we need only consider the rho meson contribution to the current for which the interaction Lagrangian is

$$\mathcal{L}_{\text{int}} = -g_\rho \boldsymbol{\rho}^\nu \cdot (\boldsymbol{\rho}^\mu \times \boldsymbol{\rho}_{\nu\mu}) = -g_\rho (\boldsymbol{\rho}^\nu \times \boldsymbol{\rho}^\mu) \cdot \boldsymbol{\rho}_{\nu\mu} \,. \tag{4.195}$$

Now use (4.13) to compute the contribution of this piece of $\mathcal{L}$ to the current, and find $2g_\rho(\boldsymbol{\rho}^\nu \times \boldsymbol{\rho}^\mu) \times \boldsymbol{\rho}_\mu$. So the total conserved isospin current is

$$\boldsymbol{I}^\nu = \tfrac{1}{2}\overline{\psi}\gamma^\nu \boldsymbol{\tau}\psi + \boldsymbol{\rho}_\mu \times \boldsymbol{\rho}^{\nu\mu} + 2g_\rho(\boldsymbol{\rho}^\nu \times \boldsymbol{\rho}^\mu) \times \boldsymbol{\rho}_\mu \,. \tag{4.196}$$

Correspondingly, the interaction part of the Lagrangian is

$$\mathcal{L}_{\text{int}} = -g_\rho \boldsymbol{\rho}_\nu \cdot \boldsymbol{I}^\nu \,. \tag{4.197}$$

(The Lagrangian will now involve the square of the coupling constant as in the case of the coupling of a scalar field to the electromagnetic.) The above interaction will modify the Dirac equation and the free equation of the rho meson. The modification of the Dirac equation is the addition of the term

$$\frac{\partial \mathcal{L}_{\text{int}}}{\partial \overline{\psi}} = -\frac{g_\rho}{2}\gamma_\nu \boldsymbol{\rho}^\nu \cdot \boldsymbol{\tau}\psi\,. \tag{4.198}$$

This will alter the eigenvalues in a way analogous to that of the vector-isoscalar (omega) meson.

Now we remark that the presence of any field costs energy. Only those fields which will have nonvanishing mean values in the ground state of matter at a given density must be there. For example, in matter of a given baryon density, the σ and ω_0 fields must have finite mean values because they are solutions to equations with nonvanishing baryon densities as sources (4.168, 4.169). But a vanishing mean field is a possible solution to the free field equation, and thereby the energy is lowered. Otherwise there would be a positive term of the form $(\frac{1}{2})m_\phi^2\phi^2$ present in the energy density. So a nonvanishing baryon density requires the presence of those meson fields which are coupled to the various baryon densities (scalar, vector, isovector ...), but the condition that the matter be in its ground state at any prescribed baryon density assures that all other meson fields must vanish.

Now apply this reasoning to the rho meson. The ground state is assumed to be a degenerate fermion state with eigenvalues modified by the mean meson fields encountered earlier. These momentum states of neutron and proton are filled pairwise to the Fermi level, so the ground state has definite charge, spin and parity. Since the first two components of the isospin vector $\boldsymbol{\rho}$ can be written as a combination of the raising and lowering operators for charged rho mesons (4.57), their (diagonal) ground state expectation values vanish.

The implications of the foregoing remarks are severalfold: (1) Only the isospin 3-component of the $\boldsymbol{\rho}^\mu$ field has finite mean value, i.e., the neutral rho meson ρ_3^μ. (2) The Lorentz three-current part must vanish in the static ground state of matter, just as for the omega meson, leaving only ρ_3^0. (The subscript is for the 3-component of isospin and the superscript is the Lorentz time component.) (3) Although formally the isospin current is (4.196), all that survives as a result of the above conditions is the nucleon contribution. As a result, the equations for the mean values of the rho meson and the Dirac equation are

$$g_\rho \rho_3^0 = \tfrac{1}{2}\left(\frac{g_\rho}{m_\rho}\right)^2 \langle \overline{\psi}\gamma^0\tau_3\psi\rangle = \left(\frac{g_\rho}{m_\rho}\right)^2 \tfrac{1}{2}(\rho_p - \rho_n)\,, \tag{4.199}$$

$$g_\rho \rho_3^k = \tfrac{1}{2}\left(\frac{g_\rho}{m_\rho}\right)^2 \langle \overline{\psi}\gamma^k\tau_3\psi\rangle = 0\,, \tag{4.200}$$

$$\left[\gamma_\mu(k^\mu - g_\omega\omega^\mu - \tfrac{1}{2}g_\rho\tau_3\rho_3^\mu) - (m - g_\sigma\sigma)\right]\psi(k) \;=\; 0\,. \quad (4.201)$$

In the first of these equations, $\frac{1}{2}\rho_p$ and $-\frac{1}{2}\rho_p$ are the isospin densities of the proton and neutron, where $\rho_{p,n}$ are the number densities. In the source for the 3-vector part of the rho meson field, the operator τ_3 produces a factor of ± 1 and leaves $\langle\overline{\psi}\gamma^k\psi\rangle$ which vanishes as we proved earlier (4.146). So if we intend to solve the problem at the mean field level, we do not need the full isospin current derived above but only the baryon part of it.

The Dirac eigenvalues can be obtained by rationalizing the Dirac operator as before and are

$$e_{I_3}(k) = g_\omega\omega^0 + g_\rho\rho_3^0 I_3 + E(k), \qquad E(k) = \sqrt{k^2 + (m - g_\sigma\sigma)^2}\,, \quad (4.202)$$

where I_3 is the isospin of the proton $(1/2)$ or neutron $(-1/2)$. In contrast to the earlier models, the rho meson lifts the isospin degeneracy of the baryons and shifts them up or down according to the sign of $\rho_3^0 I_3$ for a given baryon species. We will discuss this effect further in connection with neutron star matter. For the moment let us note that the sign of ρ_3^0 is determined from the Euler–Lagrange equation (4.199). There we see that the the sign of the isospin projection of the dominant species determines the sign. An added particle having the same sign of I_3 as the dominant species will have its eigenvalue shifted upward, and of opposite sign, downward. In the first case we can say the species is isospin-unfavored; in the other, favored. Clearly, for a neutron star, baryons with the same isospin projection as the neutron are isospin-unfavored.

Because the isospin interaction lifts the degeneracy of the Dirac eigenvalues, the sum on the spin-isospin label κ in the expression for the expectation value of any operator (4.139) will not yield simply the factor 4 but rather a factor 2 (for the two spin projections), and the sum on isospin projection will remain to be done explicitly.

Now the expectation of the Lagrangian has the addition of the field energy of the rho meson as well as the contributions of the scalar self-interactions represented by U,

$$\langle\mathcal{L}\rangle = -\tfrac{1}{2}m_\sigma^2\sigma^2 + \tfrac{1}{2}m_\omega^2\omega_0^2 + \tfrac{1}{2}m_\rho^2\rho_{03}^2 - \tfrac{1}{3}bm(g_\sigma\sigma)^3 - \tfrac{1}{4}c(g_\sigma\sigma)^4\,, \quad (4.203)$$

while the energy density and pressure are given by the general expressions as before,

$$\epsilon \;=\; -\langle\mathcal{L}\rangle + \langle\overline{\psi}\gamma_0 k_0\psi\rangle\,, \quad (4.204)$$

$$p \;=\; \langle\mathcal{L}\rangle + \frac{1}{3}\langle\overline{\psi}\gamma_i k_i\psi\rangle\,, \quad (4.205)$$

with

$$\langle\overline{\psi}\gamma_0 k_0\psi\rangle \;=\; \sum_\kappa \int \frac{d\boldsymbol{k}}{(2\pi)^3}(\overline{\psi}\gamma_0 k_0\psi)_{\boldsymbol{k}\kappa}\Theta[\mu - e_{I_3}(k)]$$

$$
\begin{aligned}
&= \frac{1}{\pi^2}\sum_{I_3}\int_0^k k^2\,dk\, e_{I_3}(k)\Theta[\mu - e_{I_3}(k)] \qquad (4.206)\\
&= \frac{1}{\pi^2}\int_0^{k_p} k^2\,dk\Big[g_\omega\omega^0 + \tfrac{1}{2}g_\rho\rho_3^0 + \sqrt{k^2+(m-g_\sigma\sigma)^2}\Big]\\
&\quad + \frac{1}{\pi^2}\int_0^{k_n} k^2\,dk\Big[g_\omega\omega^0 - \tfrac{1}{2}g_\rho\rho_3^0 + \sqrt{k^2+(m-g_\sigma\sigma)^2}\Big].
\end{aligned}
$$

Put this result in the expression for ϵ, and find its stationary point with respect to variations in the ρ_{03} field. Thus obtain the field equation for the rho field. Hence the field equation expresses the stationarity of the energy density at fixed neutron and proton densities. An analogous result was obtained in Section 4.7:

$$
\left(\partial\epsilon/\partial\rho_{03}\right)_{k_n,k_p=\text{const}} = 0\,. \qquad (4.207)
$$

Because the systems of interest are isospin asymmetric, we have separate Fermi energies for proton and neutron. Their densities are

$$
\rho_p = 2\int_0^{k_p}\frac{d\boldsymbol{k}}{(2\pi)^3} = \frac{k_p^3}{3\pi^2} \qquad (4.208)
$$

and a similar expression for neutrons.

Now use the field equations to get the simpler expression

$$
\begin{aligned}
\langle\overline{\psi}\gamma_0 k_0\psi\rangle &= m_\omega^2\omega_0^2 + {m_\rho}^2\rho_{03}^2 + \frac{1}{\pi^2}\Bigg[\int_0^{k_p} k^2\,dk\sqrt{k^2+(m-g_\sigma\sigma)^2}\\
&\quad + \int_0^{k_n} k^2\,dk\sqrt{k^2+(m-g_\sigma\sigma)^2}\Bigg]. \qquad (4.209)
\end{aligned}
$$

Gather together this material to find the energy density and pressure,

$$
\begin{aligned}
\epsilon &= \tfrac{1}{3}bm(g_\sigma\sigma)^3 + \tfrac{1}{4}c(g_\sigma\sigma)^4 + \tfrac{1}{2}m_\sigma^2\sigma^2 + \tfrac{1}{2}m_\omega^2\omega_0^2 + \tfrac{1}{2}{m_\rho}^2\rho_{03}^2\\
&\quad + \frac{1}{\pi^2}\left[\int_0^{k_p}\sqrt{k^2+(m-g_\sigma\sigma)^2}\,k^2\,dk + \int_0^{k_n}\sqrt{k^2+(m-g_\sigma\sigma)^2}\,k^2\,dk\right],\\
p &= -\tfrac{1}{3}bm(g_\sigma\sigma)^3 - \tfrac{1}{4}c(g_\sigma\sigma)^4 - \tfrac{1}{2}m_\sigma^2\sigma^2 + \tfrac{1}{2}m_\omega^2\omega_0^2 + \tfrac{1}{2}{m_\rho}^2\rho_{03}^2\\
&\quad + \frac{1}{3}\frac{1}{\pi^2}\left[\int_0^{k_p}\frac{k^4\,dk}{\sqrt{k^2+(m-g_\sigma\sigma)^2}} + \int_0^{k_n}\frac{k^4\,dk}{\sqrt{k^2+(m-g_\sigma\sigma)^2}}\right]. \qquad (4.210)
\end{aligned}
$$

Recall that the earlier models of this chapter had an isospin symmetry energy arising only from a difference in the Fermi energies of neutrons and protons in the event of unequal numbers of these species (4.163). We saw that the Fermi energy contribution could account for only about one-half

the observed value of 32.5 MeV for the symmetry energy coefficient. We have now introduced the rho meson for the reason described above; it will introduce an additional restoring energy that favors isospin symmetry as manifested in the valley of beta stability in nuclear physics. This restoring term is the ρ_{03}^2 term in the energy density which, according to the equation for the rho field (4.199), produces a quadratic term in the deviation from isospin symmetry and so favors symmetric systems.

We sketch how to compute the symmetry energy of the theory so as to relate the new coupling constant g_ρ to the empirical value of the symmetry energy. Look at that part of the energy per nucleon that depends on the asymmetry between proton and neutron contributions. It can be written with the aid of the field equation for the rho meson as

$$\begin{aligned} \frac{E_s}{A} &= \frac{\epsilon_s}{\rho} = \frac{1}{8}\left(\frac{g_\rho}{m_\rho}\right)^2 \rho t^2 + \frac{1}{\rho}\frac{1}{\pi^2}\left[\int_0^{k_p} k^2\, dk \sqrt{k^2 + (m - g_\sigma \sigma)^2}\right. \\ &\quad \left. + \int_0^{k_n} k^2\, dk \sqrt{k^2 + (m - g_\sigma \sigma)^2}\right], \end{aligned} \tag{4.211}$$

where

$$t \equiv (\rho_n - \rho_p)/\rho, \qquad \rho = \rho_n + \rho_p. \tag{4.212}$$

It is worth commenting that the coupling of the rho meson to the isospin current leads to a contribution in the symmetry energy per nucleon E_s/A proportional to ρ. Such a dependence does not appear in nonrelativistic, Schrödinger-based approaches based on two- and three-body potentials [115]. In the present model, the interaction part of the isospin symmetry term comes exclusively from the coupling between the isospin current and rho meson. We need a coupling constant $(g_\rho/m_\rho)^2$ about twice as large as expected from the rho decay into two pions [79].

The symmetry energy coefficient is the coefficient of the quadratic term in t in the energy per nucleon:

$$a_{\text{sym}} = \frac{1}{2}\left[\frac{\partial^2(\epsilon/\rho)}{\partial t^2}\right]_{t=0}. \tag{4.213}$$

We write the nucleon Fermi momenta in terms of t and

$$k_F \equiv \left(\frac{3\pi^2 \rho_0}{2}\right)^{1/3}, \tag{4.214}$$

namely,

$$k_n = k_F(1+t)^{1/3}, \qquad k_p = k_F(1-t)^{1/3}. \tag{4.215}$$

We now take the indicated derivatives at a constant total baryon number density $\rho = \rho_n + \rho_p$. After some algebra, the result is

$$a_{\text{sym}} = \left(\frac{g_\rho}{m_\rho}\right)^2 \frac{k_F^3}{12\pi^2} + \frac{k_F^2}{6(k_F^2 + m^{\star 2})^{1/2}} = 32.5 \text{ MeV}. \tag{4.216}$$

This expression allows one to evaluate the coupling constant of the ρ meson. There are two parts to the symmetry energy coefficient. The first arises from the explicit coupling between the nucleon isospin and the rho meson; the second from the kinetic energy when there is a relative displacement of the Fermi energies of proton and neutron. The two parts contribute about equally to the empirical value.

4.10 Inclusion of the Octet of Baryons

Our goal is to find a relativistically covariant theory of dense hadronic matter, such as likely exists in neutron stars. In the foregoing we have constrained the theory by what is known empirically about the properties of matter near normal nuclear matter density. Our constraints normalize the equation of state at one point in the energy-density plane, assure that the extrapolation to higher density or isospin asymmetric matter in the vicinity of saturation is correct, and give some expectation that the extrapolation to greater extremes is reasonable. The only certain knowledge above saturation is that the equation of state is causal and obeys Le Chatelier's principle ($dp/d\epsilon \geq 0$).

There remains a further extension of the theory that pertains uniquely to matter at high-energy density, be it cold, dense matter, or hot matter of any baryon density. It is clear from the relationship written earlier between baryon density and Fermi momentum or Fermi energy that, as the density is increased, the Fermi energy will increase and ultimately exceed the masses of the heavier baryons. This statement is made in the framework of a free Fermi gas, but it is also valid in an interacting system, provided we simply refer to the eigenenergies of the baryons in the medium. When the Fermi energy of the occupied baryon states rises above the eigenenergies of other species, the energy and pressure of the system will be lowered by conversion of some of the baryons to the other species. The generalization of relativistic, mean-field theory to include higher mass baryons was first implemented by Garpman, Glendenning, and Karant [116]. We need to discuss carefully the method of arriving at an equilibrium balance of baryon species in dense matter.

The theory developed in the foregoing is well suited to incorporating additional baryon species. The most important are the remaining members of the lowest baryon octet, the hyperons Λ, Σ, Ξ. Because of the charge neutrality of stars and the interaction with the rho meson, we must distinguish the various isospin and charge states. We do this by affixing a subscript B to Fermi momenta, isospin projections, masses and so on. Therefore the case of nucleons with different isospin projection is but a special case and readily generalized.

TABLE 4.5. The octet baryons, their spin J, isospin projection I_3, charge q, and strangeness s

	m (MeV)	J	I_3	q	s
N	939	1/2	1/2	1	0
			−1/2	0	0
Λ	1115		0	0	−1
Σ	1190		1	1	−1
			0	0	−1
			−1	−1	−1
Ξ	1315		1/2	0	−2
			−1/2	−1	−2

A suitable generalization of the Lagrangian is [49, 86, 87]

$$\begin{aligned}\mathcal{L} \;=\; & \sum_B \overline{\psi}_B(i\gamma_\mu\partial^\mu - m_B + g_{\sigma B}\sigma - g_{\omega B}\gamma_\mu\omega^\mu - \tfrac{1}{2}g_{\rho B}\gamma_\mu\boldsymbol{\tau}\cdot\boldsymbol{\rho}^\mu)\psi_B \\ & + \tfrac{1}{2}(\partial_\mu\sigma\partial^\mu\sigma - m_\sigma^2\sigma^2) - \tfrac{1}{4}\omega_{\mu\nu}\omega^{\mu\nu} + \tfrac{1}{2}m_\omega^2\omega_\mu\omega^\mu \\ & - \tfrac{1}{4}\boldsymbol{\rho}_{\mu\nu}\cdot\boldsymbol{\rho}^{\mu\nu} + \tfrac{1}{2}m_\rho^2\boldsymbol{\rho}_\mu\cdot\boldsymbol{\rho}^\mu - \tfrac{1}{3}bm_n(g_\sigma\sigma)^3 - \tfrac{1}{4}c(g_\sigma\sigma)^4 . \qquad (4.217)\end{aligned}$$

The spinor for the baryon species B, one of those listed in Table 4.5, is denoted by ψ_B. A difficulty arises. Only nucleons are present in hadronic matter near saturation density, and their coupling constants to the meson fields can be related to nuclear matter properties, as discussed above. However, the hyperons can populate matter only at high density. They do not affect the ground state properties. Nevertheless, meaningful constraints on their couplings can be obtained [89]. We discuss them after the necessary groundwork has been laid in Section 5.4.3.

The Euler–Lagrange equations follow from the above Lagrangian. In the mean-field approximation, the Dirac equations in uniform matter for each species B are

$$\Big[\gamma_\mu(k^\mu - g_{\omega B}\omega^\mu - \tfrac{1}{2}g_{\rho B}\boldsymbol{\tau}\cdot\boldsymbol{\rho}^\mu) - (m_B - g_{\sigma B}\sigma)\Big]\psi_B(k) = 0\,, \qquad (4.218)$$

where the meson mean fields are the scalar, vector, and isovector σ, ω, ρ . The eigenvalues of particle and antiparticle can be found as

$$e_B(k) = g_{\omega B}\omega_0 + g_{\rho B}\rho_{03}I_{3B} + \sqrt{k^2 + (m_B - g_{\sigma B}\sigma)^2}\,, \qquad (4.219)$$

$$\overline{e}_B(k) = -g_{\omega B}\omega_0 - g_{\rho B}\rho_{03}\overline{I}_{3B} + \sqrt{k^2 + (m_B - g_{\sigma B}\sigma)^2}\,, \qquad (4.220)$$

where I_{3B} is the isospin 3-component for baryon B. We have explicitly used the fact (derived in Section 4.9) that only the isospin 3-component of the

rho field survives in the mean-field approximation and that the Lorentz three-current part of both the omega and rho fields vanishes in the static ground state of matter. The meson field equations in uniform static matter (in which space and time derivatives can be dropped) are

$$\omega_0 = \sum_B \frac{g_{\omega B}}{m_\omega^2} \rho_B \,, \tag{4.221}$$

$$\rho_{03} = \sum_B \frac{g_{\rho B}}{m_\rho^2} I_{3B} \rho_B \,, \tag{4.222}$$

$$\begin{aligned} m_\sigma^2 \sigma &= -b m_n g_\sigma (g_\sigma \sigma)^2 - c g_\sigma (g_\sigma \sigma)^3 \,, \\ &\quad + \sum_B \frac{2J_B+1}{2\pi^2} g_{\sigma B} \int_0^{k_B} \frac{m_B - g_{\sigma B}\sigma}{\sqrt{k^2 + (m_B - g_{\sigma B}\sigma)^2}} k^2 \, dk \end{aligned} \tag{4.223}$$

We use the notation $g_\sigma \equiv g_{\sigma N}$, etc., for brevity in denoting the nucleon couplings.

The energy density and pressure can be found in the now familiar manner. They are

$$\begin{aligned} \epsilon &= \tfrac{1}{3} b m_n (g_\sigma \sigma)^3 + \tfrac{1}{4} c (g_\sigma \sigma)^4 + \tfrac{1}{2} m_\sigma^2 \sigma^2 + \tfrac{1}{2} m_\omega^2 \omega_0^2 + \tfrac{1}{2} m_\rho^2 \rho_{03}^2 \\ &\quad + \sum_B \frac{2J_B+1}{2\pi^2} \int_0^{k_B} \sqrt{k^2 + (m_B - g_{\sigma B}\sigma)^2} \, k^2 \, dk \end{aligned} \tag{4.224}$$

$$\begin{aligned} p &= -\tfrac{1}{3} b m_n (g_\sigma \sigma)^3 - \tfrac{1}{4} c (g_\sigma \sigma)^4 - \tfrac{1}{2} m_\sigma^2 \sigma^2 + \tfrac{1}{2} m_\omega^2 \omega_0^2 + \tfrac{1}{2} m_\rho^2 \rho_{03}^2 \\ &\quad + \frac{1}{3} \sum_B \frac{2J_B+1}{2\pi^2} \int_0^{k_B} k^4 \, dk / \sqrt{k^2 + (m_B - g_{\sigma B}\sigma)^2} \,. \end{aligned} \tag{4.225}$$

These are functions of the baryon density ρ through the dependence on the Fermi momenta. Together they are frequently referred to as the equation of state.

The above equations are not complete when the density is high enough that baryon species beyond the nucleons are populated. It is necessary to supplement the field equations by subsidiary constraints appropriate to the state of matter in which one is interested. Such a state will be characterized by specified values of conserved quantities such as the baryon number, the charge, and strangeness densities,

$$\begin{aligned} \rho_B &= (2J_B+1) b_B k_B^3 / (6\pi^2) \,, \\ Q_B &= (2J_B+1) q_B k_B^3 / (6\pi^2) \,, \end{aligned}$$

and

$$S_B = (2J_B+1) s_B k_B^3 / (6\pi^2) \,. \tag{4.226}$$

The total densities are

$$\rho = \sum_B \rho_B, \quad q = \sum_B Q_B, \quad S = \sum_B S_B \,. \tag{4.227}$$

These conserved charges will have the values determined in the preparation of the system. For example, if we want to describe high-density matter obtained by compressing symmetric nuclear matter on a short time scale compared to the weak interaction scale (as for a nuclear collision), then we want a solution with $q = \rho/2$, $S = 0$ at all chosen baryon densities ρ. This constraint can be implemented through the use of Lagrange multipliers as in Section 3.9.2.

Let the strangeness chemical potential for positive unit strangeness be μ_K, and let μ_b and μ_q be the chemical potentials for unit positive baryon and electric charge. In general, the chemical potential of particle B with baryon charge b_B, electric charge q_B (in units of e), and strangeness s_B is given by

$$\mu_B = b_B\mu_b + q_B\mu_q + s_B\mu_K \,. \tag{4.228}$$

The Fermi momenta appearing in the expression for the conserved charges (4.227) are related to the chemical potentials (Fermi energies) through

$$\mu_B = e_B(k_B)\,, \tag{4.229}$$

where the eigenvalue $e_B(k)$ was written above. Now we have a system of nonlinear equations in the unknown meson field strengths, the three independent chemical potentials, and Fermi momenta which need to be solved simultaneously.

The above equations hold at zero temperature. Finite temperature results can be obtained in the usual manner by writing the partition function for the system and carrying out the appropriate manipulations [116, 117, 118]. The results may be simply stated. In all the expressions containing a sum over B, the sum is extended over antiparticles as well as particles since the former are thermally excited. The antiparticle quantum numbers—like baryon number, charge, isospin, and strangeness as well as their chemical potentials—are the negatives of the particles. A thermal factor has to be inserted and the momentum integrated. The thermal baryon and antibaryon densities are given, respectively, by

$$\rho_B = \frac{2J_B+1}{2\pi^2} b_B \int_0^\infty \Big(\exp[(e_B(k)-\mu_B)/T]+1\Big)^{-1} k^2\, dk \tag{4.230}$$

$$\bar{\rho}_B = \frac{2J_B+1}{2\pi^2} \bar{b}_B \int_0^\infty \Big(\exp[(\bar{e}_B(k)+\mu_B)/T]+1\Big)^{-1} k^2\, dk\,. \tag{4.231}$$

Similar expressions hold for the electric charge and strangeness densities. Note that ρ_B and $\bar{\rho}_B$ are defined as baryon charge densities so that, if there are antibaryons present, $\bar{\rho}_B$ will be negative. The thermal factor is also introduced into all the integrals over momentum in the scalar field equation above and in the expressions for pressure and energy density. At finite temperature other mesons than those driven by finite baryon currents will be thermally excited. Their contribution to the conserved charge, strangeness, and energy density can be added as in [117, 118].

4.11 High-Density Limit

Asymptotically for large baryon density, $p \to \epsilon$ is a feature of any theory having a vector meson interaction [119]. Examine the above expressions for ϵ and p using the field equations in the limit of large k_B. The mass terms in the integrals can be ignored. The σ field is bounded by the order of the baryon masses as can be inferred by an examination of its field equation. Indeed, when only the nucleons are considered, it is bounded by the nucleon mass as we showed explicitly. We find

$$\epsilon \to \tfrac{1}{2}\Big(\sum_B \frac{g_{\omega B}}{m_\omega}\rho_B\Big)^2 + \tfrac{1}{2}\Big(\sum_B \frac{g_{\rho B}}{m_\rho} I_{3B}\rho_B\Big)^2 + \sum_B \frac{2J_B+1}{2\pi^2}\frac{k_B^2}{4} \quad (4.232)$$

and

$$p \to \tfrac{1}{2}\Big(\sum_B \frac{g_{\omega B}}{m_\omega}\rho_B\Big)^2 + \tfrac{1}{2}\Big(\sum_B \frac{g_{\rho B}}{m_\rho} I_{3B}\rho_B\Big)^2 + \tfrac{1}{3}\sum_B \frac{2J_B+1}{2\pi^2}\frac{k_B^2}{4}\,. \quad (4.233)$$

The first two terms of both ϵ and p are identical and proportional to k^6. Consequently, p approaches ϵ from below because of the factor $1/3$ in the last term of p. Therefore the speed of sound $(dp/d\epsilon)^{1/2}$ is always less than the speed of light. The equation of state is causal at all densities.

The low-density limit of this theory is not of interest. At low density (below saturation density), the lowest state of matter is not a uniform gas of nucleons. Rather it is energetically more favorable for nucleons to clump together as nuclei and leave voids between them. We have discussed this limit in Section 3.10.2 and further in Section 5.3.7.

4.12 Effective vs. Renormalized Theory

It is evident that the point of view adopted in the preceding development is that nuclear field theory is to be solved in the mean-field approximation and with coupling constants fitted to nuclear properties. This is a common but not universal point of view. Some authors have insisted on renormalization. The presence of matter alters the vacuum by altering the masses of antiparticles. The filled fermi sea therefore shifts in energy with the density of fermions. However true this may be of a fundamental theory, we deal in compact stars with baryons. They are composite, not fundamental fields.

The question arises as to what meaning can be attached to renormalized baryon fields when in fact they are composites. Of course, if their substructure is ignored and they are thought of as fundamental, then expressions for the renormalization of the theory derived in the foregoing can be obtained. What we shall show here is that the renormalized theory and the mean-field approximation, derived in detail above, yield the same equation of state to high accuracy if the coupling constants are chosen to reproduce

the *five* nuclear matter properties that were emphasized above as important constraints on the theory [120, 86]. This being so, there seems little point in going through the renormalization procedure, at least as concerns the structure of stars.

For the purpose of demonstrating the above correspondence, we recall, without derivation, results that have been obtained elsewhere [121, 79]. With the inclusion of vacuum renormalization energies, the energy density is given by

$$\epsilon_{\rm RHA} = \epsilon_{\rm MFA} + V_N + V_\sigma \,. \tag{4.234}$$

The approximation which includes the vacuum renormalization is known as the relativistic Hartree approximation (RHA) [79]. The subscript "MFA" simply denotes the mean-field approximation derived above for any of the versions that include scalar self-interactions. In their absence, the V_σ term should be dropped throughout. The pressure is given in RHA by

$$p_{\rm RHA} = p_{\rm MFA} - V_N - V_\sigma \,. \tag{4.235}$$

The last two terms represent the contributions from renormalization of the scalar meson and nucleon, respectively, and are given by

$$\begin{aligned} V_\sigma &= \frac{m_\sigma^4}{(8\pi)^2}\Big[(1+\phi_1+\phi_2)^2\ln(1+\phi_1+\phi_2)\,, -(\phi_1+\phi_2) - \frac{3}{2}(\phi_1+\phi_2)^2\,, \\ &\quad -\frac{1}{3}{\phi_1}^2(\phi_1+3\phi_2) + \frac{1}{12}{\phi_1}^4\Big] \qquad (4.236) \\ V_N &= -\frac{m_n^4}{4\pi^2}\Big[(1-\chi)^4\ln(1-\chi) + \chi - \frac{7}{2}\chi^2 + \frac{13}{3}\chi^3 - \frac{25}{12}\chi^4\Big]\,, \qquad (4.237) \end{aligned}$$

where

$$\phi_1 = \frac{2bm_n g_\sigma^3\sigma}{{m_\sigma}^2}, \qquad \phi_2 = \frac{3cg_\sigma^4\sigma^2}{{m_\sigma}^2}, \qquad \chi = \frac{g_\sigma\sigma}{m_n}\,, \tag{4.238}$$

and m_n and m_σ are the nucleon and σ mass. The Euler–Lagrange equations are the same as before, except that the the equation for the sigma-field is modified by the derivative of the above renormalization terms. The sigma-field equation may be found in the usual way (as the Euler–Lagrange equation) or as a condition that the energy density is a minimum for fixed baryon density:

$$\begin{aligned} m_\sigma^2\sigma &= -bm_n g_\sigma(g_\sigma\sigma)^2 - cg_\sigma(g_\sigma\sigma)^3 - \frac{\partial}{\partial\sigma}[V_N + V_\sigma] \\ &\quad + \sum_B \frac{2J_B+1}{2\pi^2} g_{\sigma B}\int_0^{k_B} \frac{m_B - g_{\sigma B}\sigma}{\sqrt{k^2 + (m_B - g_{\sigma B}\sigma)^2}}\, k^2\, dk \qquad (4.239) \end{aligned}$$

The coupling constants for the two cases, MFA and RHA, that yield the nuclear matter properties listed in the caption are given in Table 4.6. The

binding energy per nucleon for symmetric nuclear matter and pure neutron matter are shown in Fig. 4.2. It is evident that, when the two theories are fitted to the same five data, the results are essentially the same [120, 86].

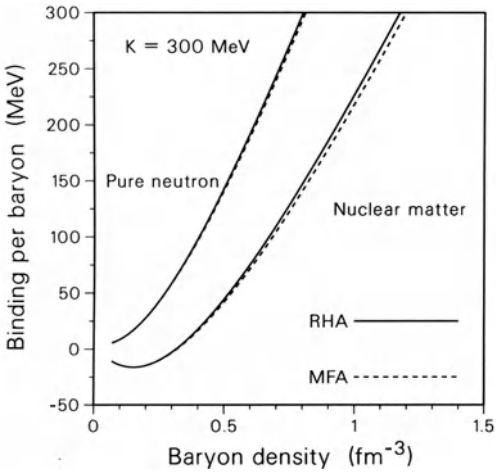

FIGURE 4.2. Binding energy of nuclear and pure neutron matter as a function of density computed with and without vacuum renormalization (denoted RHA and MFA, respectively). The corresponding nuclear matter properties are listed in Table 4.6 (From [86]).

4.13 Bound vs. Unbound Neutron Matter

We emphasize that the simple $(\sigma - \omega)$ model of Johnson and Teller [76], Duerr [77], and Walecka [78, 79] was used only as the starting point for the development of a more comprehensive, relativistic, mean-field theory. The simple model describes nuclear matter poorly. It is also unsuitable for the description of neutron stars, although it has been employed frequently for this purpose. We discussed one shortcoming earlier and have appropriately extended the simple model in Section 4.10.

However, there is another problem with the simple model; pure neutron matter has a minimum in the binding per nucleon as a function of density that lies at a slightly negative or positive value, depending on the parameters of the theory [79]. In the first case, neutron matter would be bound; in the second there would be a first-order phase transition between neutron matter near saturation density and a very diffuse gas of neutrons. We discuss the two cases separately.

4.13.1 Bound neutron matter

There is no terrestrial evidence that pure neutron matter is bound and stable against beta decay. If it were, bound uncharged nuclei ought to exist, possibly of high baryon number—high enough that surface and shell effects do not render them unstable. Moreover, the behavior of some pulsars suggests that neutron star matter is not bound by the nuclear force[3]. We now take up these issues.

If neutron matter is bound, then $p = 0$ at the equilibrium density. Zero pressure can support no overlying layer of matter against the attraction of gravity and so marks the surface of a star. Of course, the density at which neutron matter is bound in the simple model is close to the density at which symmetric matter is bound. Whether the difference is a few percent or even a factor of two or so makes no difference to our argument. Therefore the surface of the star (in the case of bound neutron matter) is near the saturation density of nuclear matter (of the order of 10^{14} g/cm^3). A neutron star built from such matter has a surface region that is therefore a nuclear *liquid.*

In contrast (as we discussed in Section 3.10.1), the region near the surface of a neutron star is thought to form a solid crust of material at subnuclear density, a Coulomb lattice of nuclei immersed in an electron gas. This would occur below the neutron drip density ($\sim 10^{11}$ g/cm^3) and all the way down to near zero pressure at the surface of the star. The solid region is important for the glitch phenomenon—irregular small discontinuities in the rotational period—observed in some pulsars. Since a purely liquid or gaseous star has no mechanism by which the moment of inertia of the star can undergo a sudden change, a solid region must be involved.

4.13.2 First-Order phase transition

In the case that the simple $(\sigma - \omega)$ model has a positive energy at the minimum in the binding energy curve for certain ranges of the coupling constants, a first-order phase transition exists between neutron liquid near saturation density (10^{14} g/cm^3) and a very low-density neutron gas. The constant pressure region is compressed to a point in the radial coordinate because the pressure is monotonic in a star, as in our atmosphere. The Oppenheimer–Volkoff equations or their Newtonian equivalent assure that this is so. The physical reason is quite simple. The weight of the overlying part of the star at any radial distance r from the center is counterbalanced by the internal pressure of matter at r. With increasing r, the

[3]The issue is not whether neutron stars are bound by the nuclear force; they are not. Through most of the star, the nucleons are compressed to a density at which they only exert repulsion on each other. The issue is whether there is a bound state of neutron matter at any density. If so, since an equilibrium state has $p = 0$, the density of the bound state would be that of the star's edge.

weight decreases and hence also the internal pressure required to support it in equilibrium.

Obviously, no region of constant pressure can exist in a star that is in hydrostatic equilibrium. As a consequence, if neutron matter did have a first-order phase transition near saturation density, the density profile of the star would have a discontinuity at the radial point corresponding to the constant pressure of the phase transition. At the interior edge of the discontinuity, the density of the star would be that of the nuclear liquid near saturation density. At the exterior edge, the star would have a thin layer of low-density nuclear gas. As in the case of a bound state, such a situation as this appears to be ruled out by the pulsar glitch phenomenon.

The surface features of neutron star models described above appear to be artificial and are likely the result of the low value of the symmetry energy of the simple model. We have noted that the $(\sigma - \omega)$ theory can account for only about 1/2 the empirical symmetry energy coefficient. Therefore the bound state (or phase transition between the high-density nuclear liquid and low-density nuclear gas predicted by the simple model) is a consequence of the small value of the symmetry energy coefficient.

When the rho meson is included with coupling constant chosen so that the theory reproduces the empirical symmetry energy, neutron matter is unbound as shown in Fig. 4.2. Nor is there an equilibrium phase between neutron liquid and gas at such a high isospin asymmetry. Consequently, stellar models will not have surface densities close to that of nuclear density (about 2.5×10^{14} g/cm^3), but, instead, will have the much lower density of solid iron (7.86 g/cm^3) for which the internal pressure is zero (see page 71).

As mentioned above, these effects have real consequences for pulsar glitching phenomena as well as for the cooling rate of neutron stars for which the outer layers are important. Therefore pulsar glitches make a strong case against the binding of neutron matter or even a minimum in the binding per neutron as a function of density.

TABLE 4.6. Nucleon-meson coupling constants, corresponding to $K = 300$ MeV, $B/A = -16.3$ MeV, $\rho_0 = 0.153$ fm^{-3}, $a_{sym.} = 32.5$ MeV, $m^*_{sat.}/m = 0.78$

	$(g_\sigma/m_\sigma)^2$ fm^2	$(g_\omega/m_\omega)^2$ fm^2	$(g_\rho/m_\rho)^2$ fm^2	b	c
MFA	9.031	4.733	4.825	0.003305	0.01529
RHA	9.249	4.732	4.823	0.005723	0.000601

4.14 Note on Dimensions

In nuclear and particle physics it is convenient to express length in the unit of a fermi (fm= 10^{-13} cm) because it is the order of the dimension of a nucleon, and a nucleus has a radius of a few of these units. It is also convenient to take $\hbar = c = 1$. The unit of $\hbar$ is $\hbar c = 197.33$ MeV-fm. The wave number (which we usually refer to as the momentum) is $k = p/\hbar$ and has the unit of inverse length. This is consistent with our use of it in relating the density and momentum eigenstates

$$\rho = \gamma \int \frac{d\boldsymbol{p}}{(2\pi\hbar)^3} = \gamma \int \frac{d\boldsymbol{k}}{(2\pi)^3} \tag{4.240}$$

with γ the degeneracy of the momentum states and ρ the particle number density in $1/\text{fm}^3$.

With such a choice of unit for k and since the relativistic energy of a free particle is given by $\sqrt{k^2 + m^2}$, we should use inverse length as the unit of mass and energy also. For example, we have

$$m \approx 939 \text{ MeV} = \frac{939}{197} \text{ fm}^{-1} = 4.77 \text{ fm}^{-1} \tag{4.241}$$

This means that energy density has the natural unit fm^{-4}, and pressure has the same unit. The conversion to units frequently used in astrophysics is given by (3.6). We call attention to the discussion of units surrounding the quoted equation.

The Lagrangian also has the unit of energy density, or, equivalently, fm^{-4}. Referring to (4.120) (in particular the Lagrangian of the scalar (or vector) meson), the mass term $m_\sigma^2 \sigma^2$ informs us that the dimension of the mean scalar and vector fields σ and ω_0 is $1/\text{fm}$. So the combination $m - g_\sigma \sigma$ informs us that the coupling constant is dimensionless, as with g_ω.

Of course, the choice made here to use length as the unit to express dimensions is not unique. Through $\hbar c = 197.33$ MeV, we could as well choose energy, as is frequently done.

4.15 Summary

In this chapter a relativistic nuclear field theory was developed, and a succession of improvements to the early version of the theory were introduced. We placed special emphasis on five important constraints on the theory that are bulk properties of symmetric nuclear matter. The theory was generalized to include the octet baryons, and in fact the generalization could extend over an arbitrary number of baryon types. Algebraic relationships were derived between the bulk properties of nuclear matter and the cou-

plings in the theory. With the addition of the Lagrangians for free leptons (electrons and muons), we will be in a position to develop the equation of state for neutron star matter—matter that is charge-neutral and in generalized beta equilibrium.

5

Neutron Stars

"I bow low. I have observed the apparition of a guest star. Its color was an iridescent yellow.... The land will know great prosperity."
Yang Wei-T'e, Imperial Astronomer of the Sung Dynasty, 1054.

"With all reserve we advance the view that supernovae represent the transition from ordinary stars into *neutron stars*, which in their final stages consist of closely packed neutrons."
W. Baade and F. Zwicky, 1933 [1].

5.1 Introduction

A year following Chadwick's 1932 discovery of the neutron, Baade and Zwicky conceived the notion of neutron stars in the course of their investigation of supernovae. What source other than the gravitational binding of a highly compact object formed from the central core of the presupernova star could release suddenly such an energy as renders stellar explosions visible[1] in daylight and hurls the stellar remnant of many solar masses into space at velocities of thousands of kilometers per second?

Compelling though the insight of Baade and Zwicky was or is to us now, no searches for neutron stars were mounted immediately following their paper. No one knew what to look for. A compact star made of "closely packed neutrons" would have to be degenerate; it could not generate energy after formation, but could only radiate its remaining store of heat over millions of years through the slow process of photon diffusion, just as for white dwarfs. But being so much smaller than white dwarfs, neutron stars would not be optically visible.[2] Other types of radiation did not appear

[1]The visible light represents about 1/100 of the energy deposited in the remnant, which in turn is but 1/100 of the total energy release, the bulk being carried by energetic neutrinos that diffuse out of the protoneutron star during the first few seconds of its life.

[2]Some pulsars can be observed optically, and a few radiate over a spectrum from high-energy gammas to radio frequencies. Pulsars are most frequently discovered at radio frequencies.

likely. Gravitational radiation by a pulsating rotating neutron star would be a fleeting phenomenon since the amplitude of vibrations giving rise to quadrupole or higher multipole mass transport would be rapidly damped.

In 1939, years before the discovery of pulsars, Oppenheimer and Volkoff [59] and Tolman [122] were the first to take seriously the question of the structure of the compact objects of Baade and Zwicky. They estimated their radius and maximum mass to be about ten kilometers and $\frac{3}{4}$ of a solar mass. A year later Woltjer estimated that the conservation of magnetic flux[3] in a star that contracts from a red giant to a neutron star could produce fields of 10^{12} gauss [123]. Such high fields led Pacini [124] to the prescient notion that energy could be fed from a highly magnetized rotating neutron star, as yet undiscovered, to the Crab nebula—whose expansion is known to be accelerating.

Meanwhile, Anthony Hewish at Cambridge had designed a radio telescope and auxiliary equipment with a short time response and an extended observing routine for the purpose of studying scintillation of point radio sources such as quasars. It was not the first radio telescope, but it was the first to have the above attributes which proved crucial to the discovery about to be made. Within a month his student, Jocelyn Bell, noticed the first indications of a persistent periodic source later measured to have a pulse period of 1.337 seconds. Thirty-four years after the suggestion of Baade and Zwicky that the power house driving a supernova must be the gravitational binding of a neutron star, Hewish, Bell, Pilkington, Scott, and Collins [125] published their discovery paper. They had detected a very small source of pulsed radio signal lying outside the solar system, presumably a condensed star, white dwarf, or neutron star. The first *pulsar* had been discovered.

Shortly thereafter, the Crab and Vela pulsars were discovered, and then some 250 others in the large surveys of the 1970s. The total number is now over 730. The last several hundred were discovered only in the last several years in radio surveys of the sky in both hemispheres made by several teams using the Jodrell Bank 76m, Parkes 64m, and the Arecibo 305m antennas.

Pulsars, so named because they are sources of periodic signals of great timing stability, are the astrophysical objects that are presumed to correspond to neutron stars. They are observed under a variety of circumstances, usually as isolated sources, but sometimes in binary orbit with another star (white dwarf or neutron star), in *X-ray binary* systems, and perhaps *γ-ray bursters* and, as recently realized, soft gamma-ray repeaters [126].

Although pulsars are assumed to be neutron stars, we shall not use the names as equivalent. The name pulsar is reserved for the astrophysical object having the property that it emits pulsed radiation. For very good

[3]Magnetic fields in stars are detected by measurements of the opposite circular polarization of spectral lines split by the Zeeman effect. Stars have fields ranging from a few to thousands of gauss and in white dwarfs of 10^8 gauss.

reasons, pulsars are believed to be neutron stars. Neutron star is reserved for the theoretical object, independent of its observation as a pulsar or for a very compact star that is not observed by its pulsed radiation but by other means. An example is the partner of the Hulse–Taylor pulsar, which is unobserved as a pulsar. Rather, its presence is known by the Doppler shift produced by the orbital motion on the timing of pulses received from the observed pulsar. The mass and orbital parameters derived from the observations require the invisible partner to be very compact so that it is almost certain to be a neutron star and not a white dwarf. The companion may also be a pulsar. If so, the earth is not on the cone swept out by the radio emission along the magnetic dipole as the star rotates.

It is fitting that mention should be made of early work on the theory of neutron stars. It is well known that in 1939 Oppenheimer and Volkoff [59] and Tolman [122] first derived the equations of relativistic stellar structure from Einstein's field equations and discovered the existence of a limit to the mass of stable degenerate relativistic stars. The small book by Harrison, Thorne, Wakano, and Wheeler [23] is broader in scope and of great importance today, quite aside from the evolutionary development of the field. These authors developed a rigorous framework in which to understand compact stars.

The interpretation of the 1967 discovery of the first pulsar by Hewish and Bell as a highly magnetized neutron star was already available in the paper of Pacini [124]. Following the discovery and independently of Pacini, Gold's paper [127] also provided a strong case for identifying the pulsar with a neutron star. Many authors, Canuto and his collaborators [128], Ruderman [129, 130, 131], Ostriker and Gunn [132, 133, 134], Pines and Shaham [135, 136, 137], and Alpar [138] contributed additional ideas to the subject.

The likely existence of hyperons in neutron stars was recognized by Cameron [139] and Ambartsumyan and Saakayan [140] who used a free Fermi gas to describe neutron star matter. Pandharipande [141] and Bethe and Johnson [142] introduced hyperons in a Schroedinger potential approach to interactions among the constituents as did Moszkowski [143]. Hyperon populations in neutron stars and their effect on a number of pulsar observables including the limiting mass have been emphasized by the author in a number of papers [49, 86, 87]. The vexing problem of connecting hyperon couplings to observables was addressed in [89]. These works also stressed the importance of constraining the theory by a number of nuclear matter properties [101, 102]. Hybrid stars—neutron stars with mixed phase hadronic and quark matter—were given their modern analysis by the author [144, 145]. In collaboration with Weber, the rotation of neutron star models built on modern equations of state (especially relativistic approaches) were extensively studied [146, 75] as well as rotation of strange stars with nuclear crusts [147, 148, 149, 66]. These and other researches are referenced in the following sections and chapters dealing with the many

facets of neutron stars. Several monographs on pulsars from the observational perspective are the classic "Pulsars" by Manchester and Taylor [150] and the recent "Pulsar Astronomy" by Lyne and Graham–Smith [151].

This chapter is divided into three parts. The first is concerned with the observed objects—pulsars—and the basis for their interpretation as neutron stars. We open the first part by recounting some of the important discoveries involving pulsars. Then we discuss the main observations made on these objects: pulse profiles, the range of observed periods and masses, pulsar ages as estimated from their rate of loss of rotational energy, why we know they are compact objects, supernova associations, and the apparent existence of two evolutionarily different pulsar populations.

We study the theory of neutron stars in the second part. The similarities and differences between nuclear matter and neutron star matter (charge neutral and in general equilibrium) are emphasized. We discuss how strangeness is created in neutron stars in the first few seconds of their birth. Chemical equilibrium in a star is discussed under the circumstance that neutrinos and photons diffuse out allowing net strangeness to be locked in. This sets the stage for an account in later chapters of the formation of low-mass black holes, of hybrid stars having quark populations, and strange stars composed entirely of quarks. We return briefly to a discussion of nuclear field theory and the subsidiary conditions needed for a description of *neutron star matter* as compared to symmetric nuclear matter. We are then in a position to compute neutron star models tightly constrained by hadronic interactions consistent with nuclear matter properties. Generic features of neutron stars are emphasized, especially the mass-radius relationship.

The constitution of neutron stars is the subject of the third part of the chapter. There we discuss the hyperonic composition of stars, their radial distribution, and how hyperons affect the star's limiting mass. We also examine how charge neutrality can be achieved among baryons in the core. (That hyperons and quarks can, under conditions of high density, replace electrons in neutralizing compact stars has ramifications for the core electrical conductivity and thereby for stellar magnetic fields and cooling rates.) Possible meson condensates, pion and kaon, are discussed.

5.2 Pulsars: The Observational Basis of Neutron Stars

5.2.1 Important pulsar discoveries

Pulsars are believed to be highly magnetized rotating neutron stars. An electromagnetic beam, typically at radio frequencies, is emitted along the magnetic axis with an angular spread typically of ten degrees. If an angular separation between the rotational and magnetic axes exists, the rotating

object is analogous to a lighthouse. If, as observers on earth, we lie on the cone swept out by the rotating star, we have a chance to observe it as a pulsed source. The range of the frequencies in the emitted signal in some pulsars, such as the Crab, is enormous, ranging from radio to optical to X rays to γ rays, but most pulsars (including all known millisecond pulsars) have been observed only at radio frequencies.

More than 700 pulsars have been found since the discovery by Hewish and Bell in 1967 of the pulsed signals of period 1.337 seconds from a source outside the solar system [125]. That source is now known as PSR 1919+21. Two additional pulsars were discovered shortly afterwards, the Crab [152] and the Vela Pulsar [153]. Both are found within supernova remnants, the Crab and Vela nebulae. Both have much shorter periods than the first pulsar discovered. The periods of 33 ms and 89 ms were decisive in identifying the pulsar objects as neutron stars rather than white dwarfs.

Several hundred of the pulsars known today were discovered in large surveys conducted in the 1970s at Arecibo, Jodrell Bank, Molonglo, and Greenbank. All but two of the presently known pulsars lie within our galaxy. One of the exceptions lies in the nearby Large Magellanic Cloud galaxy (PSR 0540-69) and the other in the Small Magellanic Cloud (PSR 0042-73). A large number of additional pulsars (about 200) have been discovered in the last several years as the result of a second generation of all-sky searches, from Parkes (Australia) covering the southern sky and Jodrell Bank (Cambridge) and Arecebo (Peurto Rico), the northern sky.

Of course we expect that other galaxies with populations of massive stars ($M > 8M_{\odot}$) also have pulsars in them, but they are too distant for detection of the dim signal.

A few pulsars are named, such as the Crab, because of the beautiful nebula which is the supernova remnant in which it lies. The supernova event, also named after the suggestive form of the remnant, was recorded in Chinese history in 1054 AD. However, most pulsars are designated by "PSR" (for pulsating source of radio) and by their celestial coordinates. Supernova are designated by the year in which they were first detected, together with a letter, a, b, ... aa, ab ..., to distinguish the order of discovery within the year, eg, SN 1987a.

In addition to the first pulsar discoveries of Hewish and Bell and the Crab and Vela, there are other discoveries of importance. Hulse and Taylor (1974) discovered the first pulsar (PSR 1913+16) in a binary system in which its partner is also a neutron star [35]. The orbital period of about eight hours is remarkably short and the precession of the orbit remarkably large (4.2 degrees per year) compared to the general relativistic precession of Mercury of 43 seconds per century.

The many careful measurements made on this system by Taylor and collaborators during the intervening years have provided singular tests of General Relativity under strong field circumstances (surface gravity for neutron stars is $M/R \sim 0.2$) [37, 36, 4]. So far, they provide the only evi-

dence of gravitational radiation whose effect is to damp the orbital motion. It is estimated that the two stars will collide in $\sim 10^8$ years. This system provides an unusual laboratory for studying General Relativity [154]. A very recent discovery by Wolszczan [155] of a close binary pulsar having a period of 27.9 ms. and with a highly elliptical orbit and short period of 10 hours, PSR 1534+12, promises to be even more rewarding as measurements accumulate over the years [154].

The fastest known pulsar so far is PSR 1937+21 discovered in 1982 by Backer. Kulkarni, Heiles, Davis, and Goss [156]. It has a period of 1.56 milliseconds, and it took great ingenuity to detect such rapid pulses given their dispersion by the interstellar medium (discussed later). It was the first millisecond pulsar to be discovered. Such rapid rotation of 650 times a second was quite astonishing. It was the first of a new class of pulsars that had been foreseen by Alpar, Cheng, Ruderman, and Shaham and by Bachus, Taylor, and Damashek as the result of spinup of a low-magnetic field neutron star by slow accretion from a Keplerian disk [157, 158]. The interpretation was soon confirmed by the discovery of a second millisecond pulsar ($P = 6.1$ ms), PSR 1953+29, by Boriakoff, Buccheri and Fauci in a 120 day orbit with a white dwarf [159].

The chance that the orbital plane of a pulsar and a companion would lie sufficiently close to the line of sight as to cause the pulsar to be eclipsed is small, but it has been observed for a 1.6 ms pulsar which is in an eight hour orbit with a white dwarf. The pulsar signal is obscured for about one-tenth of the orbital period, as discovered by Fruchter, Steinbring, and Taylor [160]. The importance of *globular clusters* as being rich in fast and binary pulsars has been supposed for some time, but this was spectacularly confirmed in a discovery of ten millisecond pulsars in 47Tucanae by Manchester, Lyne, Robinson, D'Amico, Bailles, and Lim in 1991 [161].

The first planets in orbit around a very old ($\sim 10^9$ yrs.) millisecond pulsar were discovered in 1992 by Wolszczan and Frail [162]. They are the first known planets outside the solar system. The Doppler shift in the pulsar signal caused by three planets—two earth-mass bodies and one moon-mass body—are shown in Fig. 5.1. The pulse arrival times of the other planets has been subtracted in each case.

The revolution in technology in the last few years is bringing to light many unusual phenomena. The closest (140 pc) and brightest pulsar (JO437-4715) was discovered by Bell, Bailes, Manchester, Weisberg and Lyne [164]. It has a period of 5.75 ms and is in a 5.74 day orbit with a low-mass white dwarf companion. A wind from the pulsar creates a bow shock in the interstellar medium as the binary pair passes through it at high velocity (Fig. 5.2).

So far, a binary system consisting of a neutron star and black hole has not been discovered, but such binaries likely exist. Indeed, one of the fascinations of astronomy and astrophysics is that whatever is allowed by the laws of physics does in all likelihood occur somewhere in the universe.

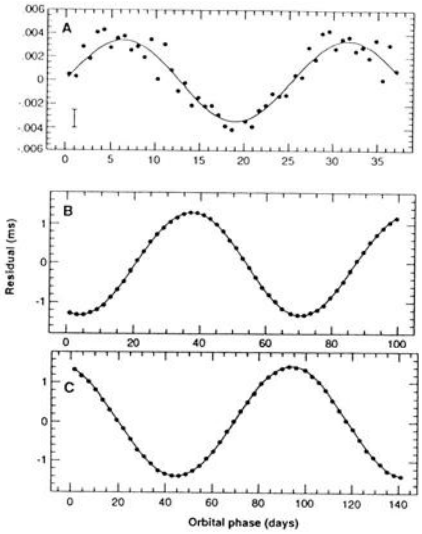

FIGURE 5.1. Timing residuals showing Doppler shift of three planets (effect of other two is subtracted in each case) in orbit with a neutron star [162, 163]. Reprinted with permission from *Science*, 264 (1994), 538. Copyright 1994 American Association for the Advancement of Science.

5.2.2 Pulsar periods

The periods of the pulsars, so far discovered, range from milliseconds to seconds with the mean period being about 0.7 s. Some of the periods are measured with enormous accuracy, as, for example, PSR 1913+16 (Hulse–Taylor pulsar) where 14 significant figures are known with an error of 1 in the last. The fastest pulsar presently known, PSR 1937+21, discovered as recently as 1982, has a (nominal) period of 1.56 ms [156]. As we shall discuss, neutron stars carry large magnetic fields. Since the magnetic axis would be coincident with the rotation axis only by accident, the rotation of the star causes a loss of rotational energy by magnetic dipole radiation. The rate of rotation therefore decreases with time, albeit very slowly. Consequently, the full accuracy of the measurement of the period can be given only with reference to the time of the measurement! The period of the above pulsar was

$$1.557\,806\,448\,872\,75 \;\pm 0.000\,000\,000\,000\,03 \text{ ms},$$

as of 29 November 1982 at 1903 UT [165]. The limit on the accuracy of the measurement is actually due to the precision of terrestrial time standards. Such precise timing provides a unique tool for studying certain astrophysical problems [166, 167]. As we shall soon see, the above period is

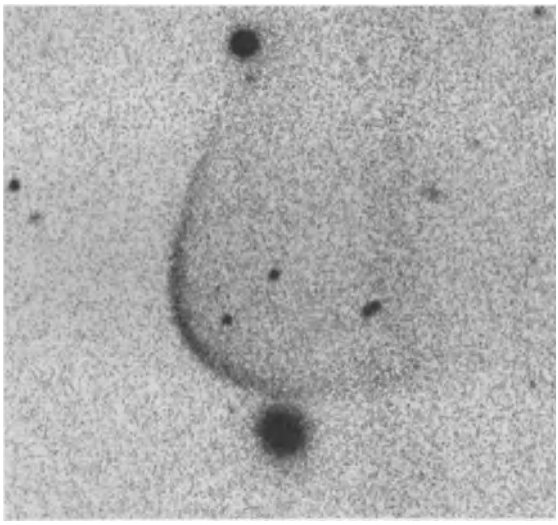

FIGURE 5.2. The bow shock of a fast pulsar and its white dwarf companion (visible just behind the shock front) as it ploughs through the interstellar medium. The H alpha line of hydrogen makes the shock visible. (Other objects are background stars.) Image courtesy of A. Fruchter and Cerro Tololo Inter-American Observatory.

attributable to rotation—more than 600 times per second—of a star having the mass of about our sun and a radius of about 10 km!

The present discovery rate of *millisecond pulsars* is accelerating with the discovery that globular clusters seem to have a high population of fast pulsars. There are some 150 globular clusters in our galaxy, distributed approximately spherically, to distances from the galaxy center equal to the radius of the disk. They are self-bound groups of 10^5 to 10^6 stars and the density of stars is about 1000 greater than that part of the galaxy that our sun occupies—and presumably any other typical part. These groups of stars are by their nature especially rich in fast pulsars [166], as attested to by the discovery referred to above in the globular cluster 47Tucanae [161]. However, most of the globular clusters are too distant for the detection of the weak pulsar signals. Those that are close enough will prove to be rich in phenomena associated with the fate of old pulsars: rebirth by mass and angular momentum accretion in binaries and eventual spin-up to millisecond pulsars. Doubtless, many surprises await.

5.2.3 Individual pulses and pulse profiles

What is referred to as the shape of a pulse (or integrated pulse) is actually the shape of individual pulses averaged over a hundred or more. It is the

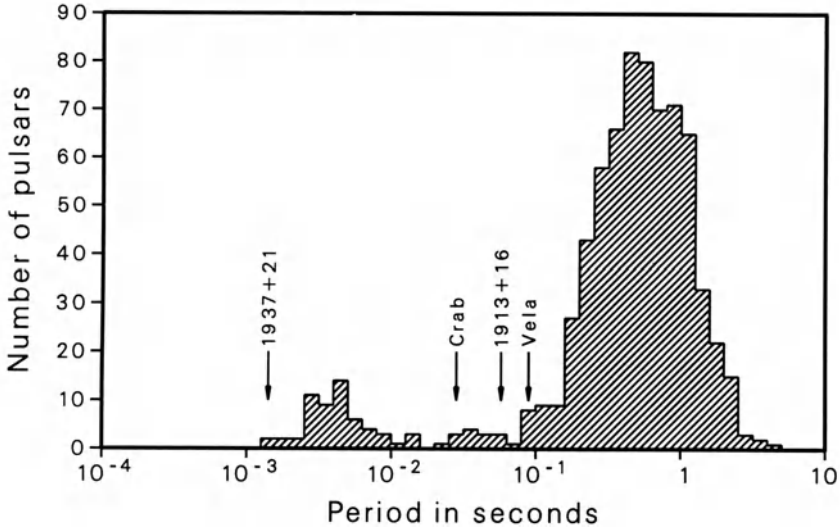

FIGURE 5.3. Distribution of periods for the presently known 736 pulsars, 50 of which have periods between 1.56 and 10 ms. The average period is 0.7 s. and the maximum is 5 s. There is a strong attenuation in sensitivity of radio surveys for periods below about 1 ms, as discussed in Section 5.2.4. (I am indebted to M. Bailes for supplying the data for this graph as of May 1996.)

integrated pulse profile that is stable in shape and timing and characteristic of an individual pulsar and which is different from that of other pulsars. Individual pulses, on the other hand, are highly variable in intensity, timing, and in subpulse structure, suggesting small, rapid changes in the conditions of the emission.

The pulse arrival time is generally reduced by an integral multiple of the period of the average pulse profile and is sometimes then referred to as the phase or longitude (with 360 degrees corresponding to a full rotation and continuous signal). For most pulsars the longitude of individual pulses is quite random within the longitude spanned by the integrated pulse.

For some few pulsars there are interesting systematics in individual pulses or subpulses [150]. Some show a slow drift in the longitude of a string of individual subpulses across the width of the integrated profile, returning to the original longitude and beginning the drift again. There is a quasi-periodicity associated with such *drifting*, the number of pulses within a string and the longitude of corresponding members of different strings being about the same, but not exactly. Still another class of pulsars exhibits a

phenomenon referred to as *mode switching*. A string of individual pulses occurs at or near a given longitude. Then the pulses switch to a neighboring longitude and then back. Approximately the same number of pulses occurs in either string, and they alternate between the two longitudes. A third phenomenon observed in some pulsars is that of *nulling*, a situation in which the signal is so weak or absent that it cannot be seen for some number of periods.

The phenomena of pulse drifting, nulling, and mode switching, characteristic of certain individual pulsars, are possibly associated with complicated electromagnetic phenomena at the surface and in the magnetosphere of the star. Curiously, an isolated freely precessing object with an emission in a direction fixed in the rotating star but offset from the angular momentum axis can exhibit all three phenomena according to the particular parameters—angle between the above axes, direction of observer, and so on [168].

5.2.4 Detection biases

For various reasons, including the beaming effect, the known population of pulsars represents a highly biased sample of the true pulsar population in our galaxy ($\approx 10^{11}$ stars). Most notable is the inverse-square law. Most known pulsars lie in the vicinity of the sun. The sun lies approximately 2/3 of the radius of the galaxy ($R_G = 15$ kps $\approx 49,000$ ly) from its center and near the galactic plane. Most known pulsars lie within a distance $R_G/3$ of the sun.

Distances are estimated in a variety of ways, parallax using Earth's orbital diameter as base line, associated supernova remnants, absorption or not of spectral lines by known hydrogen clouds, and by dispersion of the various wavelengths in the pulsed radio signal. Because of their interaction with the interstellar electrons, the longer wavelengths suffer a greater time delay in reaching us than the shorter. Having some knowledge of the distribution of electrons in the galaxy, one can infer the column height of intervening electrons from the dispersion of the various wavelengths in the pulsed signal [169]. When several types of measurements can be applied to the same pulsar, agreement within a factor of two is generally found. The total galactic population is believed to be something like 10^5 active pulsars [170].

Because of the dispersion of the radio signal within the chosen frequency band, there are practical limits on the detection of short periods set by compromises chosen for the large surveys [171]. For this reason the observed distribution of pulsar periods is not expected to accurately reflect the actual population. Even now there is a strong roll-off in sensitivity to periods below about 1 ms [172].

The signals from fast pulsars cannot be seen in the raw data. Each pulse contains a range of radio frequencies, each of which is subject to a different

time delay because of dispersion by the interstellar medium. So, although each pulse has a well-defined beginning and end at the location of the pulsar as the beam sweeps past our direction, the arrival times of different frequencies are spread out. This problem is most acute for short period pulsars.

The technique for detecting closely spaced pulses is first to store the pulses in bins according to their frequency at some chosen sampling rate. Each bin will contain a finite width of frequencies according to the cost and compromises that have to be made in designing the equipment. The frequencies in each bin will be subject to some as yet unknown average time delay depending on the density of dispersive electrons integrated over the distance the signal has traversed. The integral measuring the electron content between pulsar and observer is known as the dispersion measure (DM). Before the discovery of the pulsar, the dispersion measure is unknown. A dispersion measure is guessed, and the appropriate correction to the arrival time corresponding to each bin of the raw data is made. A fast Fourier transform is then used to determine if any periodicity can be found in the reconstructed signal. If not, another DM is tried, and the process repeated. This is continued until a periodic pulse is detected in the data, or (because one is not sure that there really does exist a pulsar in the direction being searched at a distance that can be observed, and no periodicity has yet been detected) one abandons the process in favor of a new search direction [166]. Clearly, compromises inherent in the detection equipment and in the cost of the analysis of the raw data (there is radio noise in all directions) impose a practical limit to the lowest detectable period of a given search.

Recently, a dozen or more millisecond pulsars have been discovered in globular clusters which are believed to have environments ideal for the incubation of fast pulsars as explained earlier. There, as soon as one discovery is made, the interstellar dispersion (DM) to that general location is determined. Correction of the data with DMs in its neighborhood much enhances the detection technique. In other words, globular clusters are especially favorable sites in which to discover fast pulsars.

5.2.5 Two populations of pulsars

It appears that there are two populations of pulsars. One corresponds to the distribution centered around a period of 0.7 s as in Fig. 5.3 which includes most pulsars presently known. These pulsars are usually isolated stars with strong magnetic fields $\sim 10^{12}$ to 10^{13} gauss. The other population consists of the millisecond pulsars in the lower tail of the distribution, more than half of which are in binaries and have weak fields $\sim 10^8$ to 10^9 gauss. Many are in globular clusters, though it is now believed that the field of the galaxy contains a population of millisecond pulsars that is comparable to the slower ones.

Pulsars are believed to be born with fairly short periods—spun-up by conservation of angular momentum during formation from the collapse of the white-dwarf-sized iron core of the progenitor star. They then evolve for a few million years through rotational energy loss toward smaller periods. During this epoch they are pulsars, though not necessarily visible to us on Earth through their radio emission.

Depending on a combination of the magnetic field strength and period, the pulsar beam turns off at some critical value of the product of small period and low field strength. Apparently insufficient energy to power the (little understood) radiation mechanism is fed to the magnetosphere by the rotating field. In any case, when the position of pulsars is plotted on a graph, having the field strength and period as axes, the result is quite striking. Active pulsars all lie to one side of an invisible line called the *death line* (see Fig. 5.4).

If the magnetic field is constant or decays very slowly on a timescale of a few million years, the trajectory of pulsars toward the death line will be at approximately constant field strength B. The Crab pulsar will reach the death line in a few million years. A pulsar can no longer be 'seen' when its beam turns off. However, the magnetic field of the neutron star presumably continues to decay slowly, so that with time it descends in the above type of plot with the period changing little.

The second population is believed to be more evolved than the first. Pulsars in the second population have passed through the first phase of evolution described above and have reached the death line. They are believed to have been involved in a binary system and have been spun up to millisecond periods by the coherent accretion of matter from a less dense companion during a late epoch in their lives. The magnetic field may also be partially destroyed in this epoch. Millisecond pulsars are sometimes referred to as "recycled" pulsars [166, 173]. (For an excellent detailed discussion of the whole subject of formation and evolution of binary and millisecond pulsars, see Bhattacharya and van den Heuvel [173]). It must be stressed that the origin of millisecond pulsars, as described above, is as yet not well substantiated.

Recycled pulsars are believed to be very old because some of the companions are white dwarfs. Their magnetic fields are much smaller than the first population by three or four orders of magnitude. The presently known second population is much smaller than the first. However, folding in detection biases, it is possible that the two populations are comparable.

5.2.6 Supernova associations with pulsars

Although we believe that neutron stars are born in the supernovae explosions of stars with masses in the range of about $8M_\odot$ or more, there are a few cases in which a positive association can be made. When this can be done, it is for young pulsars. The reason is easy to understand. Pulsars are

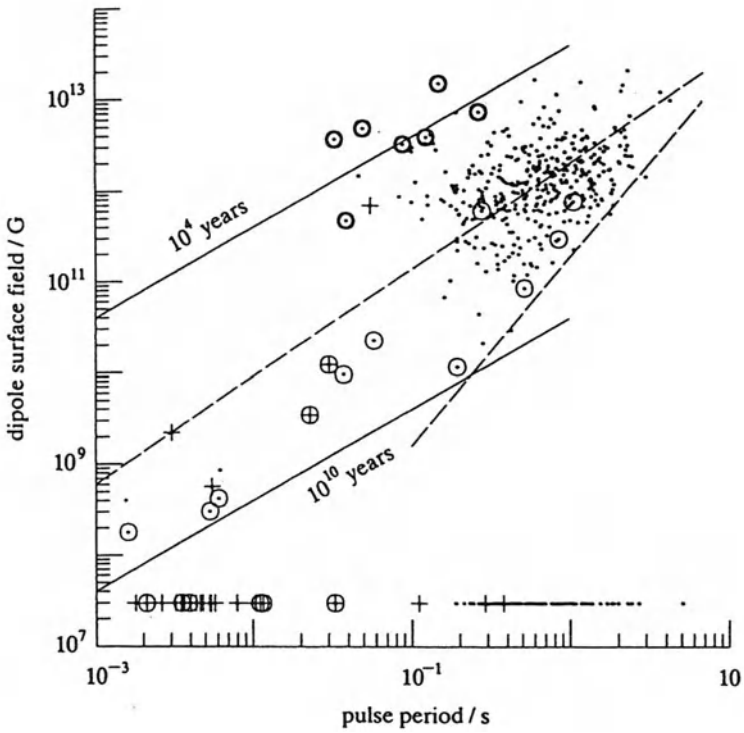

FIGURE 5.4. Magnetic fields of radio pulsars as a function of period. Most of the recently discovered millisecond pulsars do not appear here but would be located near the bottom left. Pulsars whose period derivative is not yet measured (see 5.3 for connection to magnetic field) are shown at the bottom. Double circles denote a supernova association, single circles denote binaries, and plus signs denote pulsars in globular clusters. The dashed line on the right is the "death line". Courtesy of S. Kulkarni [172] Reprinted by permission of Oxford University Press.

observed to have large velocities with an average value of 450 km/s [174]; one has been discovered with a velocity of 1200 km/s [126]. Consequently, older pulsars have moved a great distance from their birth place. The cause of the large velocities is not known. Moreover, not only have old pulsars moved away from their birth site, but old supernova remnants will have faded (over a time scale of the order of 10^4 to 10^5 yrs.) [175].

Another contributing factor to an 'apparent' discrepancy between pulsars and supernova remnants concerns the strength of the signal. As long as they are visible, supernova remnants are larger and stronger sources and therefore can be seen at distances greater than pulsars. The whole issue is a very subtle one with which observers are just coming to grips[174, 175].

A very interesting association occurs in PSR 1757-24 in which a high velocity pulsar with dipole age of about 10^4 years is interacting with the supernova remnant it is overtaking. The pulsar velocity is estimated as ≈ 2300 km/s [176]. The velocity of the remnant of the supernova explosion is also high[4] but is slowed by the interstellar gas that it picks up as it moves outward from the explosion site. The bulletlike passage of the pulsar is revealed in Fig. 5.5 by radio emission from the *remnant* stimulated by the passage of the pulsar. The supernova remnant likely had an initial velocity of 10^4 km/s. If it were not for the deceleration of the remnant as it sweeps up interstellar gas, the pulsar would never catch up. The dipole age is therefore an estimate of the time taken to do so.

5.2.7 Why pulsars are neutron stars

The pulsation of pulsars is interpreted as the period of their rotation, not vibration. Why? Gold cites the enormous energy radiated ($\sim 10^{38}$ erg/s for Crab), the spectacular rotational energy that can be stored by a compact star of dimension ~ 10 km, and the very large magnetic field to which a collapsed star would scale through conservation of flux of the progenitor star, all of which suggests that a rotating magnetized star is the source of such stable periodic signals as are observed [127]. To these reasons we can add that, since pulsars are observed here on earth through their electromagnetic radiation (generally using a radio telescope), we know that the pulsar is losing energy. Over time the amplitude of vibration is diminished by energy loss, but the frequency is not. For rotation, the frequency is damped. This is what is observed, as in the example shown in Fig. 5.6 for the Vela pulsar.

Although the period of pulsars is very stable by most normal standards, the periods do measurably change over time. Depending on the period, the rate of change can be determined by making observations over periods of days to weeks or months. Known pulsars have period rates of change falling in the range,

$$10^{-20} < \dot{P} < 10^{-12} \text{ s/s}. \tag{5.1}$$

Taking as typical a value of the exponent in the middle of the range, the change in period amounts to three seconds in 10^8 years. Also some pulsars exhibit sudden irregularly timed, small increases in rotational frequency which are referred to as *glitches*. The time between glitches can vary from months to years with the approximate rate and intensity being rather the

[4]Supernova ejecta can have velocities of 10,000 km/s or so. As a rough estimate, equate 1/100 of the gravitational energy of a neutron star (3.18) to the kinetic energy of ejecta of mass $\mathcal{M}$ to find for the velocity (in units of c) $v = \sqrt{(6M^2)/(500R\mathcal{M})}$. Thus we find a velocity of 8000 km/s for a $10M_\odot$ remnant if a $1M_\odot$ neutron star is formed.

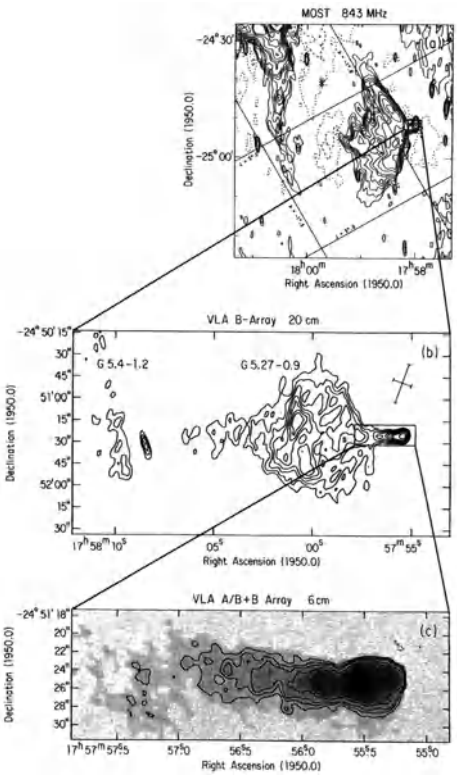

FIGURE 5.5. Radio image of a portion of a supernova remnant excited by the passage of a high-velocity pulsar, PSR 1757-24. Plate courtesy of D. Frail and S. R. Kulkarni [176]. (Reprinted with permission from *Nature*. Copyright 1991 Macmillan Magazines Limited.)

same for individual pulsars. The first such glitch phenomenon was observed in the Vela pulsar and, since then, glitches have been observed in many others. There is great individuality observed in glitch magnitude and recovery of period from pulsar to pulsar [178] and sometimes among glitches observed for the same pulsar [179]. Both the steady but slow change in period and the glitch phenomena are shown in Fig. 5.6.

Ordinary stars have magnetic fields ($\sim$ 100 gauss) and rotate. When they collapse from a radius of 10^6 km to 10 km, both the rotational frequency and field are scaled up by the conservation laws of angular momentum and magnetic flux. In the cataclysmic event that created the pulsar, there is no reason to expect that the axis of rotation and the direction of the magnetic field coincide [124]. The field is typically scaled to 10^{12} gauss. It exerts a strong torque on the rotating star and together with a 'wind' of relativistic

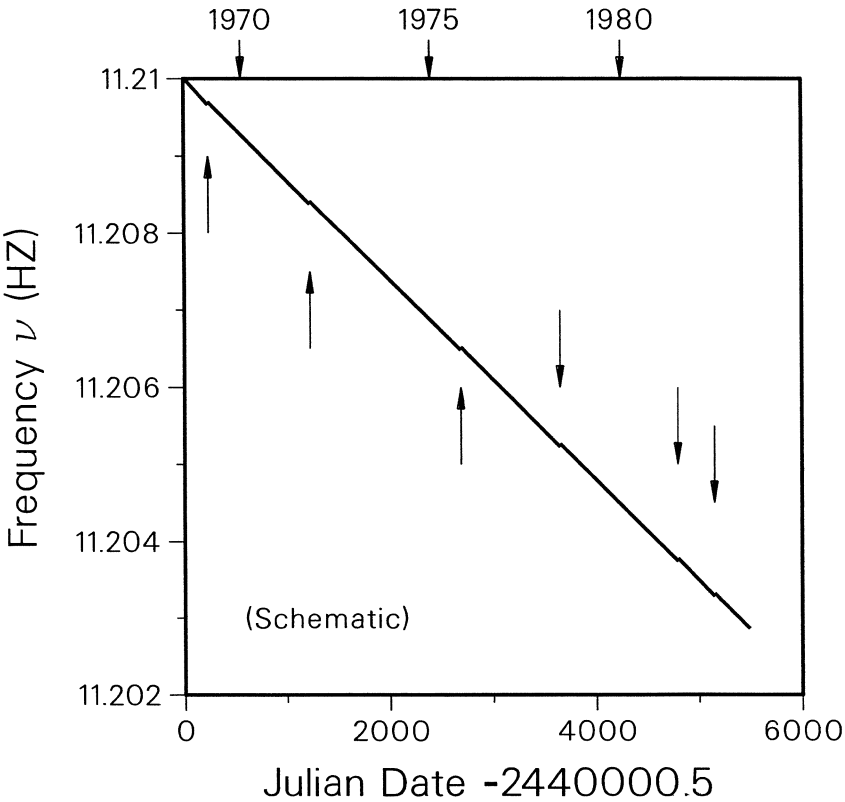

FIGURE 5.6. The slow variation of the rotational frequency of the Vela pulsar, $\dot{P} = 1.2503 \times 10^{-13}$ s/s. Also a number of "glitches" are seen in the time frame, thought to correspond to star quakes. (Courtesy of Cordes, Downs and Krause-Polstroff [177].)

particles [180] is thought to be responsible for the steady slow decrease in period.

There is other evidence of such strong fields. The remnant of the Crab supernova, some nine hundred years after the explosion, is both accelerating and radiating in radio, optical, and X-ray bands with an apparent energy input to the nebula of $\sim 10^{38}$ ergs/s. The most likely source of energy is the absorption of magnetic dipole radiation and relativistic particles from the fast pulsar within it (page 67 of Ref. [150]). Indeed, Hewish and Okaye in 1964 observed a radio emission from within the Crab nebula whose scintillation proved the presence of a compact source [181].

Energy balance implies about the same strength for the magnetic field

as quoted above from flux conservation:

$$10^{38}\ \text{ergs/s} = -\frac{dE}{dt} = -\frac{d}{dt}(\frac{1}{2}I\Omega^2) = \frac{2}{3}R^6B^2\Omega^4\sin^2\alpha\,, \tag{5.2}$$

where the last term [182] in the string of equalities is the rate of energy radiation by the rotating magnetic field (dipole). Here I is the moment of inertia of the pulsar, Ω its angular velocity, R its radius, B its surface magnetic field strength, and α the angle of inclination of the magnetic axis to the rotational axis. From the above relationship, we can write one between the magnetic field strength and the square root of the product $P\dot{P}$,

$$B = \sqrt{\frac{3I}{8\pi^2R^6\sin^2\alpha}P\dot{P}}\,. \tag{5.3}$$

Given the observed period and rate of change of period of the Crab pulsar ($P = (2\pi)/\Omega$),

$$P \sim \frac{1}{30}\ \text{s}, \qquad \dot{P} \sim 4\times 10^{-13}\ \text{s/s}\,, \tag{5.4}$$

and a canonical neutron star radius as estimated in (3.13), we find (taking $\sin\alpha = 1$),

$$I \sim 2\times 10^{45}\ \text{g cm}^2 \sim 150\ \text{km}^3\,, \qquad B \sim 3\times 10^{12}\ \text{gauss}\,,$$

and

$$E_{\text{rot}} \sim \frac{1}{2}I\Omega^2 \sim 4\times 10^{49}\ \text{ergs} \sim 2\times 10^{55}\ \text{MeV}\,. \tag{5.5}$$

Magnetic field in gauss is related to centimeters by

$$3.479\times 10^{24}\ \text{gauss cm} = 1\,, \tag{5.6}$$

where gravitational units are used. It is believed, but not understood, that radiation over a broad band of frequencies is emitted within some angular spread typically of 10 degrees along the magnetic axis [183, 184]. Given the rotation, one has a beacon which we see as pulses as the star rotates.

We can use the period of rotation to estimate the average energy density of a millisecond pulsar. For the star to hold together at its equator under the opposing forces of gravity and centrifuge, we must have

$$\zeta^2\frac{GmM}{R^2} > m\Omega^2R\,. \tag{5.7}$$

Hence, for the average density we require

$$\bar{\epsilon} = M/\left(\frac{4\pi}{3}R^3\right) > \frac{3\pi}{(\zeta P)^2} = 3.6\times 10^{14}\ \text{g/cm}^3\,, \tag{5.8}$$

where the last equality holds for a millisecond pulsar. The factor ζ is unity in Newtonian physics and is empirically found to be about 0.625 in General Relativity [185, 186]. Since the density of normal nuclear matter is $\epsilon_0 \approx 2.5 \times 10^{14}$ g/cm^3, we learn that the average density of a pulsar has to be about as large as nuclear density. We know from the Oppenheimer–Volkoff equations (3.21,3.22) that the pressure (and hence the energy density) are monotonically decreasing functions of the distance from the center; so the central density must be greater than the average. Since any net electric charge above an infinitesimal (3.26) would overwhelm the gravitational binding of the added charged particle, a neutron star must be charge-neutral and hence composed of neutrons, in large part. Therefore, pulsars must be neutron stars, or, more speculatively, another form of dense matter, such as strange quark matter which we discuss in Chapter 10.

The range of densities in neutron stars is enormous. At the edge, where the pressure is zero, the density is that of ordinary iron, the lowest energy state of hadronic matter. At the center it is $\sim 10^{15}$ g/cm^3. The density profiles of several neutron stars are shown in Fig. 5.7. They range in mass from the limiting mass of the equation of state to one of rather low mass. Notice that the central region in all cases is highly compacted and fairly constant, and the edge is very abrupt except for the lightest stars. The low-density crust of a light neutron star is thick, of the order of tens of kilometers. However, such low-mass neutron stars are probably not realized in nature. For a star of canonical $1.4M_\odot$ the crust—having densities below $\sim 10^{13}$ g/cm^3—is measured in hundreds of meters—certainly less than a kilometer (except in the lightest, and possibly non-existent, stars of a tenth or so solar mass). The kinks and wiggles that appear in Fig. 5.7 are not numerical inaccuracies but correspond to features of the equation of state. Four density regions, the source for, and the general nature of the equation of state in each are indicated in Table 5.1.

5.2.8 Pulsar masses

In theory, pulsars could have any one of a range of masses from something of the order of $0.1M_\odot$ to the limiting mass of the equation of state of nature. The lower limit corresponds to configurations that are sufficiently dense (near nuclear density), that the Fermi pressure of the nucleons reestablishes stability that was lost in the white dwarf family because of depletion of electron pressure due to neutronization with increasing stellar mass. The density at which neutron Fermi pressure reestablishes stability marks the beginning of the last family of stable compact stars more dense than white dwarfs— neutron stars (recall Fig. 3.6).

In Chapter 3 we have seen that the maximum mass of neutron stars would be about $3M_\odot$ if the high density equation of state were at the causal limit. For theories of matter that incorporate a knowledge of the properties of nuclear matter, the estimated limiting mass is lower, generally falling in

TABLE 5.1. Density regions needed to describe a neutron star: Surface, I and II; – Interior, III and IV

Region	Density g/cm^3	Nature of matter	Reference
I	$2 \times 10^3 < \rho < 1 \times 10^{11}$	crystalline: light metals	[23], [61]
II	$1 \times 10^{11} < \rho < 2 \times 10^{13}$	crystalline: heavy metals, relativistic electrons	[61], [187]
III	$2 \times 10^{13} < \rho < 3 \times 10^{14}$	relativistic nucleons, leptons	this work [49]
IV	$\rho > 3 \times 10^{14}$	relativistic nucleons, leptons hyperons, (pions) (quarks)	this work [49] [89] [188]

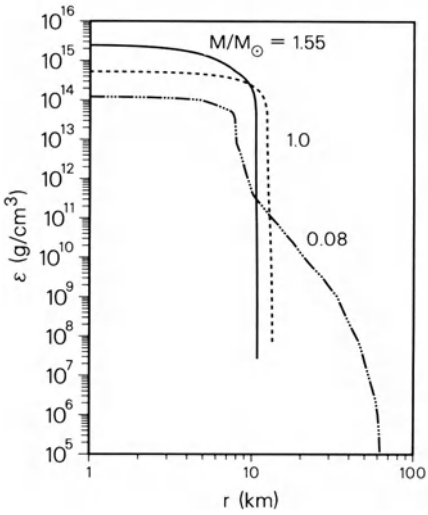

FIGURE 5.7. Energy density profile of several neutron stars. Here, the compression modulus is $K = 240$ MeV and the saturation value of the nucleon effective mass is $m^\star/m = 0.8$.

the range of 1.4 to 2.4 $M_\odot$, depending on the equation of state. We will see later in this chapter that realistic limits lie below $2M_\odot$ and more likely below $1.7M_\odot$. As remarked elsewhere, any theory must at least account for neutron stars as massive as the most massive observed pulsar. Knowledge of pulsar masses provides a very important constraint on theory.

From the point of view of discovering a pulsar near the limiting mass, it is unfortunate that nature prepares neutron stars in a particular way, namely,

in the collapse of the core of a massive star ($M > 8M_\odot$) that results in a supernova explosion. The core collapses due to instabilities that are triggered when the core mass attains approximately the Chandrasekhar mass, 1.4 to 1.5 $M_\odot$, the maximum mass that can be supported by the degenerate electron pressure corresponding to the lepton fraction prevalent in the core (see Section 3.9.7). The core has a radius of the order of 1000 km prior to collapse. The above mass range, augmented by perhaps $0.1M_\odot$ of material accreted during the supernova event, establishes the mass of the neutron star that will be produced at the end of collapse. Thus the creation mechanism is likely to produce neutron stars in a fairly limited range of masses. There may be no astrophysical means of producing the most massive neutron star that the equation of state of nature would support! So theory must have a limiting mass at least as large as the most massive observed pulsar.

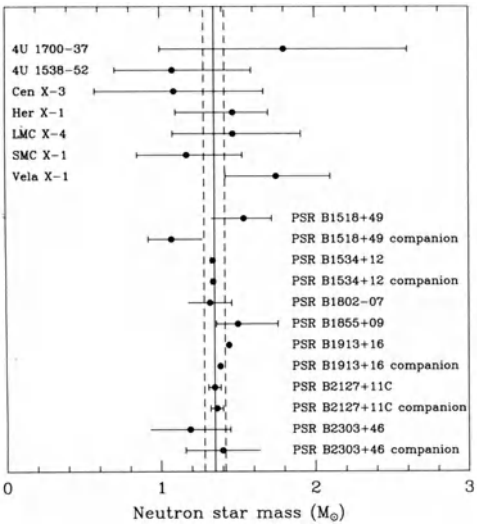

FIGURE 5.8. Compilation of presently known pulsar masses, courtesy of S. Thorsett [189]. (The graph contains additional unpublished data from Thorsett and Arzoumanian, from W. Deich, R. Sayer, and published data from Kaspi, Taylor, and Ryba, Astrophys. J. **428** (1994) 713.)

What do we know of masses? Of the some 730 pulsars that are known, there are mass measurements for about 20. Measurements are possible for binary systems. Those reported in the early work of Joss and Rappaport [190] have been improved in later work of Nagase [191] and by Thorsett et al. [189]. The most accurately measured masses are of the pair of neutron

stars in the famous Hulse–Taylor binary (PSR 1913+16). They are close in mass, and the most massive of the pair is $1.4411 \pm 0.0007 M_\odot$ [36, 154]. The most massive observed neutron star is possibly the X-ray pulsar, Vela X-1 (4U0900-40), with $M = 1.77^{+0.27}_{-0.21} M_\odot$ [191, 189]. Most are known only within large errors. Fig. 5.8 summarizes the present knowledge. The error bars would be consistent with an interpretation that presently known neutron stars have masses spanning the range $\sim 1.05 - 1.6 M_\odot$. Given the large error bars, it is not inconsistent with the evolutionary scenario to give weight to the lowest mass admitted by the error bars in the cases that lie above the Chandrasekhar mass. So taking account of the creation mechanism of neutron stars, observed masses may be smaller than the actual mass limit. In any case, with such a small sample of measured masses, we may not have detected the most massive neutron star, nor may we ever. Because the most massive neutron star may never be discovered—how would we recognize it?—theory is only constrained by the requirement that it provide a mass limit that exceeds known masses. Vela X-1 seems to establish for now that theory must be able to account for pulsars of mass at least as large as $1.5 - 1.6 M_\odot$. The more recent discoveries of millisecond pulsars, about half of which presently have binary companions, leads one to speculate that more mass measurements will be forthcoming in the not too distant future.

5.2.9 Pulsar ages

We have seen that pulsars must be very dense. They are therefore likely to be neutron stars, or possibly, as we will later discuss, hybrid stars (Chapter 9) or strange stars (Chapter 10). Neutron stars are born in the supernova explosions at the end point of the evolution of massive stars ($M \geq 8 M_\odot$). Initially the angular velocity of the progenitor star is set by conservation of the angular momentum of its core and the conditions accompanying its birth. Since pulsars do pulse because of their rotation, rotation will be damped by the loss of energy, a small part of which we see as pulses. The law that governs the decay of the rotation was written in (5.2) for magnetic dipole radiation. Other possible radiation is gravitational. Let us write, in general,

$$\dot{\Omega} = -K\Omega^n \tag{5.9}$$

where $n = 3$ for magnetic dipole electromagnetic radiation and $n = 5$ for quadrupole gravitational radiation. Taking $t = 0$ at birth and Ω_0 as the initial angular velocity, we can integrate the above equation to yield,

$$\begin{aligned} t &= \frac{1}{(n-1)K}\left[\frac{1}{\Omega^{n-1}} - \frac{1}{\Omega_0^{n-1}}\right] \\ &= -\frac{1}{n-1}\frac{\Omega}{\dot{\Omega}}\left[1 - \left(\frac{\Omega}{\Omega_0}\right)^{n-1}\right] \end{aligned} \tag{5.10}$$

TABLE 5.2. Pulsar braking indices

Name	n	Ref.
Crab	2.515 ± 0.005	[192, 193]
Vela	1.4 ± 0.2	[194]
1509-58	2.8 ± 0.2	[195, 196]
0540-69	2.01 ± 0.02	[197, 198, 199, 200]

After a long time, such that $\Omega << \Omega_0$, the above expression becomes independent of the initial frequency, and we get an estimate of the present age of the pulsar,

$$\tau = -\frac{1}{n-1}\frac{\Omega}{\dot{\Omega}} = \frac{1}{n-1}\frac{P}{\dot{P}}. \tag{5.11}$$

The "dipole" age is simply defined as,

$$\tau_{\text{dipole}} = \frac{1}{2}\frac{P}{\dot{P}}. \tag{5.12}$$

In Table 5.3 we show a range of pulsar ages as thus determined. That of the Crab is in fair agreement with recorded history.

Equation (5.10) can also be written as

$$P(t) = \left[P_0^{n-1} + (2\pi)^{n-1}(n-1)Kt\right]^{1/(n-1)} \tag{5.13}$$

where the initial period can be found from

$$P_0 = P\left[1 - (n-1)\frac{\dot{P}}{P}\tau\right]^{1/(n-1)} \tag{5.14}$$

in terms of the present values of $P, \dot{P}$, and the present age τ of the pulsar, if known as in the case of historic supernovae like the Crab. (The value of K can be determined from (5.9)). Thus, from (5.13), we can compute the time variation in a pulsar's period.

The index n is referred to as the braking index and is shown for several pulsars in Table 5.2. According to (5.9) it can be empirically determined if the second time derivative of the frequency is measured:

$$n = \frac{\Omega\ddot{\Omega}}{\dot{\Omega}^2}. \tag{5.15}$$

For the Crab pulsar as well as several others for which it is measured, the braking index is less than 3, the value expected for magnetic dipole radiation. A component of gravitational radiation in the energy loss would increase the effective braking index. An index less than 3 therefore indicates

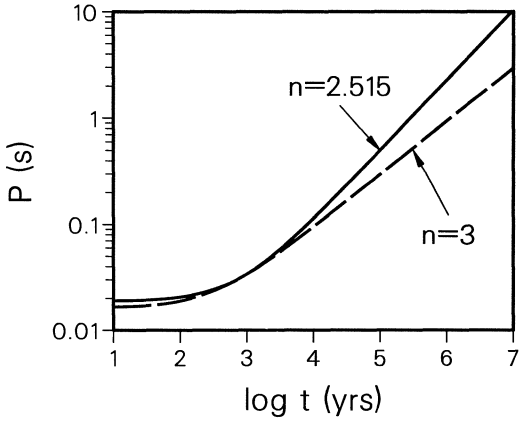

FIGURE 5.9. Evolution of Crab pulsar period as a function of time for the dipole braking index and the index measured (in this epoch).

an incomplete understanding of the rotational energy loss mechanism in pulsars, though certainly magnetic dipole is one component.

Using the data of Tables 5.2 and 5.3 for the Crab pulsar and (5.13,5.14), we show how the period is expected to evolve both for the pure magnetic dipole (n=3) and for the observed braking index in Fig. 5.9. (We used the historical age $\tau = 930$ yrs.) The inferred initial period of the Crab is ~ 0.018 s. The pulsar will likely have an active life (as a pulsar) for several million years. The behavior of the period with time is characteristically dominated by the first term in the bracket of (5.13) during which (short) time the period changes little. There is a transition epoch—the curved part of the graph—followed by a linear relationship between $\log(P)$ and $\log(t)$ with slope $1/(n-1)$. Clearly, a pulsar spends most of its life at a rotational period that is much longer than its initial value.

5.2.10 Evolution of the braking index[5]

The law for the rate of change of the pulsar period (5.9) is derived from the energy loss equation (5.2) under the assumption that the moment of inertia I is independent of rotational frequency. This is the assumption implicitly made in the literature and leads to the important 'dipole' age formula (5.11) for estimating the spin-down time or age of pulsars. The

[5]Unpublished work of N. K. Glendenning, S. Pie and F. Weber.

TABLE 5.3. Pulsars spanning the apparent range of ages

Name	P (s)	$\dot{P}$ 10^{-15} s/s	dipole age (yr)
Crab	0.033	422.7	1200
Vela	0.089	125.03	11,000
1913+16	0.059	0.009	10^8
1952+29	0.4266	.0019	3.6×10^9

same assumption lies behind the connection between the magnetic field strength B and the period and its time derivative (5.3).

However, the moment of inertia is not constant in time but responds to changes in rotational frequency, more or less according to the softness or stiffness of the equation of state and whether the stellar mass is small or large. We can show that this response reduces the value of the braking index in a frequency-dependent manner, even though the sole energy-loss mechanism is assumed to be pure magnetic dipole. Thus during any epoch of observation, the braking index will be measured to be less than 3 for dipole radiation. How much less for any given pulsar depends on its rotational frequency and, for different pulsars of the same frequency, on their mass and on their internal constitution.

To investigate for which frequencies the response of the moment of inertia substantially modifies the results (5.9 and 5.15), we rewrite (5.2) in greater generality:

$$\dot{E} = \frac{d}{dt}\left(\frac{1}{2}I\Omega^2\right) = -C\Omega^{n+1}\,. \tag{5.16}$$

We refer to this equation as the energy-loss equation, and it assumes for simplicity of exposition, that there is a single multipole. We refer to n in the above formula as the *intrinsic* (energy-loss) index. For magnetic dipole radiation ($n = 3$), one can read C from (5.2) as

$$C = (2/3)R^6B^2\sin^2\alpha\,. \tag{5.17}$$

When the frequency response of the moment of inertia is taken into account, (5.9) is replaced by

$$\dot{\Omega} = -K\Omega^n\left(1 + \frac{I'\Omega}{2I}\right)^{-1}, \tag{5.18}$$

where $I' \equiv dI/d\Omega$ and $K = C/I$. We realize that over any observational era, and even over much longer times, $I(\Omega)$ and its derivatives are essentially constant. *However* what is relevant is that I' is finite, and this fact changes the braking law from (5.9) to (5.18). Accordingly, for a given strength of

radiation process, $\dot{\Omega}$ is reduced for millisecond pulsars by the correction factor in (5.18). The estimate of B from (5.3) based on the assumption of constant I is altered to read,

$$B_{\text{new}} = B_{\text{old}}\left(1 + \frac{I'\Omega}{2I}\right)^{1/2}. \tag{5.19}$$

Equation (5.18) can be represented in the form of (5.9) by evaluating (5.15);

$$n(\Omega) = \frac{\Omega\ddot{\Omega}}{\dot{\Omega}^2} = n - \frac{3I'\Omega + I''\Omega^2}{2I + I'\Omega}. \tag{5.20}$$

From (5.20) it is clear that the *apparent* index $n(\Omega)$ depends on frequency and therefore time through the appearance of Ω, $I(\Omega)$ and the derivatives of I. The apparent index is independent of the strength of the constant C of the energy loss mechanism (5.16). The index $n(\Omega)$ reduces to the constant intrinsic value n when I is a constant. Otherwise it is less than n because the derivatives I' and I'' are positive (the moment of inertia increases with Ω and the centrifugal force grows with the equatorial radius). Therefore, the apparent braking index achieves its canonical value n of the energy loss equation (5.16) only at low enough frequencies. Its variation over time is very slow, the time scale being astronomical. So what one would observe over any observational era is a constant braking index $n(\Omega)$ less than that characteristic of the energy-loss mechanism n (5.16) even if the radiation were a pure multipole.

An expression for the moment of inertia of slowly rotating stars is well known (6.21). It is a constant and therefore inadequate for our purpose since we wish to study the braking index over the history of the star, including frequencies close to the Kepler limit.[5] Elsewhere, we derived an expression for the moment of inertia of a relativistic star that accounts for the centrifugal flattening as well as the dragging of local inertial frames that we will encounter in Chapter 6 [147, 201]. We use the referenced expression in our model calculations of the braking index.

For different equations of state describing the matter of a star (that is, for different stellar constitutions), the moment of inertia will respond differently to frequency and to mass of the star. The frequency response is shown for several stellar models in Fig. 5.10. The value of the apparent braking index is also shown in Fig. 5.10 for two pulsars of different mass. For definiteness the illustration is for magnetic dipole loss. Along each sequence the baryon number of the star is constant, as it should be. The braking index for magnetic dipole radiation clearly is not the constant $n = 3$

[5]The Kepler frequency of a star is the frequency at which the centrifugal force would overwhelm gravity at the equator.

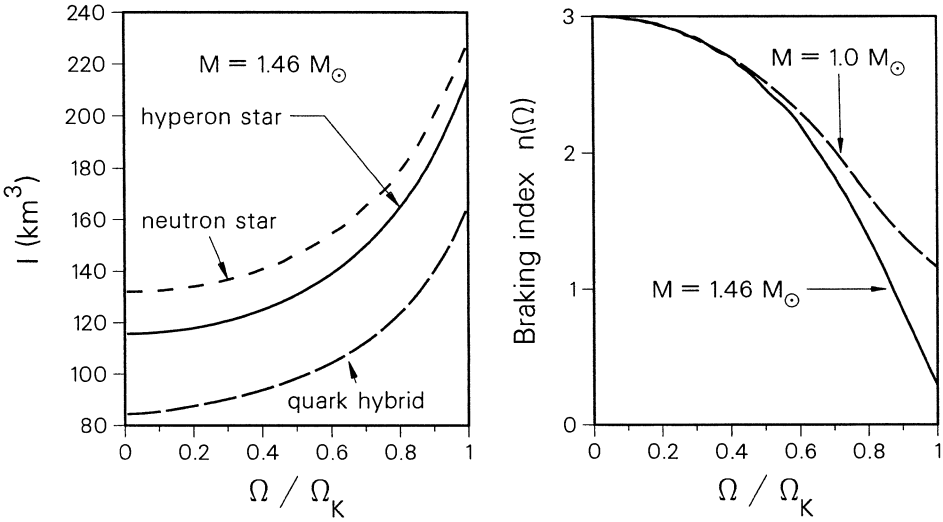

FIGURE 5.10. Moment of inertia (left panel) for several stellar models as a function of rotational frequency (in units of Kepler). Neutron star denotes a star with only neutrons protons and leptons in equilibrium. See later in this chapter for the meaning of hyperon star, and Chapter 9 for the meaning of hybrid star (quark matter core). Apparent braking index (right panel) for pure dipole ($n = 3$) as function of rotational frequency for stars of two different masses of the hyperon model. Masses indicated are for slow rotation. Meaning of parameters is discussed later in the chapter ($K = 240$ MeV, $m^\star/m = 0.78$, $x_\sigma = 0.6$). The fastest pulsar known, PSR 1937+21, lies at about $\Omega/\Omega_K = 0.7$ on the scale in the case of the hyperon model.

for high frequency pulsars. Over any observational era it may be smaller depending on frequency and on mass.

The age formula (5.11) that is so universally used in classifying stars for various purposes (glitch activity, two-pulsar populations, etc.) was derived under the assumption of constant moment of inertia *throughout* the entire life of the star. Clearly, it will give an incorrect answer for any pulsar that has had a frequency, during its history, that is a substantial fraction of its Kepler frequency. In general there is no analytic formula for the age, and for a pulsar that was a rapid rotor in any era, the age could only be obtained by integrating the energy-loss equation with a moment of inertia obtained from a model of the star and having an explicit dependence on the frequency.

Measurements of braking indices have been made for four pulsars. All are rather low-frequency pulsars (Table 5.2). As can be seen from the Fig. 5.10 the effect of the variation of the moment of inertia with Ω is very small for

slow rotation. Therefore, a measured braking index for these pulsars would essentially coincide with the intrinsic index of the energy-loss mechanism (5.16). In that case, for whatever reason, the only observed energy-loss indices are less than 3. If this is generally true then, for fast pulsars such that the effective index deviates substantially from the intrinsic one, the age formula (5.11) is not only wrong but could give a very large, even negative age .

5.3 Theory of Neutron Stars

Neutron stars are bound by gravity, not by the nuclear force. This statement may seem obvious to those with an astrophysical orientation rather than to those with a nuclear one. The nuclear force, after all, is the strong force, but it is short-ranged and so acts only on its near neighbors. The gravitational force is long-ranged and acts on all mass-energy. For large and dense enough objects, it is therefore the binding force. One can easily estimate the binding per nucleon due to gravity for a canonical neutron star as was done in Chapter 3 and find a gravitational energy of $\sim$ 160 MeV/A compared to the binding energy of nuclear matter at its saturation density of $\sim$ 16 MeV/A. Not only is there a factor of 10 in favor of the gravitational energy, but gravity compresses the matter of neutron stars so that the density lies far above the saturation density of nuclear matter. The nucleons do not feel attraction from their neighbors, but repulsion. In fact the energy required to compress nuclear matter to the density found at the center of the more massive neutron stars is 200–300 MeV per nucleon. The compression energy reduces the net binding energy of neutron stars near the mass limit to about 100 MeV per nucleon as compared to the energy of the nucleons dispersed to infinity.[6] (See Fig. 4.2 for compression energy.) So the nuclear force contributes negatively to the binding of neutron stars, but it shapes the equation of state which is uniquely related to the structure and constitution of the star.

5.3.1 Nuclear and neutron star matter: Similarities and differences

The idealized matter of the interior of nuclei and the matter of neutron stars have important similarities and differences. The similarities include the fact that they are composed of baryons and the densities are the same within an order of magnitude or less. The differences arise from two facts:

[6] Although the center of the star is more highly compressed than elsewhere, we learned in Section 3.7 that, in the equilibrium configuration of a star, no energy is gained or lost by moving a fluid element from one place to another in the star.

(1) Nuclei are bound by the isospin symmetric nuclear force (see Section 4.9), but neutron stars are bound by gravity. Hence, in nuclei it is true that $N \approx Z$. However, since the repulsive Coulomb force is so much stronger than the gravitational force that binds stars, the net charge in a star must be very small,

$$\frac{(Z_{\text{net}}e)e}{R^2} < \frac{G(Am)m}{R^2} \longrightarrow Z_{\text{net}} \sim |Z_p - Z_e| < 10^{-36}A, \tag{5.21}$$

where Z_p is the proton number and Z_e the electron number. As noted previously, the net charge on a star is essentially zero. Although Z_p need not be zero since the proton charge may can be neutralized by leptons, it is smaller than $A/2$. So nuclei tend to be symmetric in isospin whereas neutron stars are very asymmetric.

(2) There is another and profound difference arising from the weak interaction timescale, $\tau_{\text{weak}} \sim 10^{-10}$ seconds. Because of the high density of matter in neutron stars and the fact that baryons obey the Pauli principle, it is energetically favorable for nucleons at the top of the Fermi sea to convert to other baryons, including strange ones (hyperons) so as to lower the Fermi energies. The transformations do not violate strangeness conservation of the strong interactions because strangeness is conserved only on the strong interaction timescale, not on the weak. In the time it took to read the above sentence, strangeness conservation could be violated $\sim 10^{10}$ times. Even the timescale of core collapse in supernova is long compared to that of the weak interaction.

Thus strangeness is not conserved in astrophysical objects. Strangeness would not be conserved in stable nuclei either, but it is not energetically favorable to have hyperons in the ground state because their masses exceed the nucleon mass by more than the Fermi energy of the nucleons in a nucleus. Nuclear reactions, on the other hand, are so fast ($\sim 10^{-22}$ sec) that strangeness is conserved on their timescale. So the matter studied in nuclei or their reactions has zero net strangeness whereas neutron stars can and almost certainly do contain hyperons and have net strangeness.

In accordance with the above and a subsequent more detailed discussion, we shall mean by the phrase "neutron star matter" cold, charge-neutral, nuclear matter in its lowest energy state (meaning in general beta equilibrium). All baryons are populated as allowed by baryon conservation and charge neutrality in such proportion as to achieve the ground state of matter at a given baryon number density without regard to the strangeness quantum number.

These are the differences. Of course, the properties of such systems as the hot, symmetric, nonstrange matter produced in relativistic nuclear collisions and the cold, asymmetric, charge-neutral and strangeness-carrying matter of neutron stars are related in any comprehensive theory of matter. It is through relativistic nuclear field theory that we shall make the connection between them. This theory can be generalized to incorporate

nucleons and higher mass baryon states interacting through the exchange of mesons [116]. Its coupling constants can be fixed by properties of symmetric nuclear matter, as discussed in detail in Section 4.8.1. The theory also describes numerous properties of finite nuclei [202, 203, 204, 205]. It can be extended to finite temperature [116, 79]. It can be extrapolated to hot, dense matter and its composition (nucleons, deltas, and their excited baryon states) [116], and to dense neutron star matter [49, 86, 87, 206]. One and the same theory with fixed coupling constants describes

1. symmetric nuclear matter and the matter produced in high energy collisions when the field equations are solved subject to the constraints of *charge symmetry* ($q = \rho/2$) and *strangeness conservation* (in this case zero), and

2. neutron star matter when the field equations, supplemented as we shall discuss, by those of leptons, are solved subject to the constraints of *charge neutrality and generalized beta equilibrium.*

Therefore, we are able to conveniently characterize the neutron star matter equation of state by the compression modulus and other properties of the corresponding symmetric matter, by which the coupling constants are fixed, and shall always do so.

5.3.2 Chemical equilibrium in a star

To understand the nature of chemical equilibrium in a star, it is useful to note that the star evolves and that a cold neutron star is a possible ground state configuration. Many different reactions can occur during the evolution. Reactions between hadrons occur. Certain quantum numbers or particles, such as electric charge and baryon number, are conserved on a long timescale compared to the life of the star. However, any kaons produced in association with hyperons generally will decay on the electro-weak timescale and their products will end as leptons, photons, and neutrinos.

The neutrinos and photons diffuse to the surface and, having more than the escape velocity, leave the star, lowering its energy and causing a Pauli blocking of the hyperons produced in association with the kaons. This will proceed until the star reaches a degenerate state where further reactions are not possible. Therefore, strangeness is not conserved in a star, nor on any macroscopic timescale; a net strangeness carried by hyperons is achieved. At this stage the star is cold on the nuclear scale, (1 MeV $\sim 10^{10}$ K), and from the point of view of its hadronic and leptonic composition, it is essentially frozen. The timescale for reaching the frozen state is set by the neutrino diffusion time—about ten seconds.

Although cold, by which we mean 10^5 to 10^9 K, the star is still hot compared to the cosmic microwave background radiation of about 3 K. That is why there is a net radiation of photons and neutrinos. Photon

diffusion continues for millions of years. This is a brief statement of the situation [49]. We now discuss it in some detail.

It is generally understood that knowledge of the particular path that a body or substance may follow in reaching its equilibrium state is not needed to find that state. To find it, one needs to identify those components or attributes A_i that are conserved on a timescale longer than the lifetime of the star itself or the epoch during which it is observed and those that have a much shorter timescale [49]. We write the equations of transformation among the components. For example, bring all terms to the left of a reaction equation

$$\nu_i A_i = 0 \tag{5.22}$$

where the ν_i may be positive or negative (and are not necessarily integers, as, for example, in relationships involving quarks) and denote the number of independent components of type A_i. The same equations hold for the *chemical potentials* of the components with the 'chemical' symbols A_i replaced by the chemical potentials [47]. Thus we may write

$$\nu_i \mu_i = 0\,. \tag{5.23}$$

Any components that are not conserved on the timescale of the star are now set to zero. One then has relationships among the chemical potentials. There are as many *independent* chemical potentials as there are conserved components or attributes, or more generally 'charges' that are absolutely conserved, or conserved on a time long compared to the life of the star (or in a more restricted sense, over the epoch of observation). All others can be written in terms of them. This rule was derived in a special case in Section 3.9.2 by means of Lagrange multipliers.

Any neutrinos and photons produced in reactions during the deexcitation of the star from its hot beginning diffuse out. We are interested in the ground state after such diffusion has occurred and the star has attained its frozen state in which further reactions are forbidden because of Pauli blocking of the products of the reaction. Since the neutrino population is lost to the star, we must set its chemical potential to zero,

$$\mu_\nu = 0\,, \quad \text{(all types)}\,. \tag{5.24}$$

As already noted, the timescale of the electro-weak interaction is short in comparison to macroscopic scales so the strangeness quantum number, though conserved by the strong interaction, is not conserved on the scale of a star. There are therefore only two conserved 'charges' with their corresponding chemical potentials—those for baryon and electric charge number. The chemical potentials of all other constituents can be written in terms of these two.

Although, as mentioned above, it is not necessary to trace or enumerate all of the reactions by which the constituents transform, it is necessary to

know a sufficient number of them to establish the relationships between the chemical potentials. It is also interesting to discuss a few of them so as to elucidate how a star transforms from its state at birth to its ground state, the state to which it has evolved in all essentials at the time of any observation we may make on it [49]. In general this is the situation in which we are interested—evolved neutron stars. It would be a rare event indeed, and none are yet known, where observations can be made on a newly born neutron star.

Neutron stars evolve from an initially hot *protoneutron star*, bloated with neutrinos and photons, that forms in the collapse of a massive star following the ejection in a *supernova* of most of the progenitor star [29]. The energy carried off by the ejecta is a small fraction, of the order of a percent, of the energy that will be carried off shortly thereafter by neutrinos. The source of the energy is, of course, the gravitational binding energy of the neutron star (up to 100 MeV per nucleon (Fig. 3.12)). This initial protoneutron star is not isothermal and has interior temperatures of several tens of MeV (1 MeV $= 1.1065 \times 10^{10}$ K) and a high density, so that even neutrinos have a long diffusion time compared to the dynamical timescale of the collapse. Indeed, most of the neutrinos escape in about 10 seconds carrying off almost all of the binding energy, and the temperature falls rapidly to about 10 MeV in the interior and several MeV at the edge in 20 s. Thereafter the star cools by further neutrino emission, by X ray and later by photon emission, taking a few million years to fall to a surface temperature of 10^5 K [207, 208, 209]. There is still considerable controversy over what are the most relevant processes by which the cooling occurs.

In any case, the temperature has fallen in a short time to less than a MeV. This is cold on the nuclear scale. Before the end of this phase in the evolution of the star, the Fermi momenta of nucleons are high and the fermions are not yet degenerate, so that strong reactions, such as

$$N + N \longrightarrow N + \Lambda + K\,, \tag{5.25}$$

are possible. The associated kaon is free to decay unless it is driven by a phase transition to a condensed state (which we discuss later). Depending on the combination of protons and neutrons that are involved in the above reaction, all three charge states may be formed. Some of their decays are

$$K^0 \longrightarrow 2\gamma\,, \tag{5.26}$$

$$K^- \longrightarrow \mu^- + \nu\,, \tag{5.27}$$

$$\mu^- + K^+ \longrightarrow \mu^- + \mu^+ + \nu \longrightarrow 2\gamma + \nu\,. \tag{5.28}$$

As remarked, the star's energy is lowered by the leakage of the photons and neutrinos. Consequently, the Λ becomes Pauli-blocked, the reaction (5.25) becomes irreversible, and net strangeness is evolved [49]. Similar reactions involving other hyperons also may occur. Such processes continue

until the star has reached its ground state, the state in which the baryon populations are distributed among the various species so as to account for the least energy for the given number of baryons under the constraint of zero net charge. All photons and neutrinos have escaped. (By all we mean that the temperature has become so low and the degeneracy of the baryon Fermi seas is so complete that further reactions are not possible because of Pauli blocking.)

The only role played by the weak interactions is to allow reactions that cool the star. These reactions cause the negative strangeness of the kaons to be lost, i.e., to violate the strangeness conservation of the strong interaction. The baryon populations are determined by their masses, charges, isospin projections, and the strong interactions subject only to the constraints imposed by baryon conservation and charge neutrality of the star.

According to the preceding discussion, all particle chemical potentials can be written in terms of those for the conserved 'charges'—baryon and electric—which we denote by μ_n and μ_e. The subscripts stand for neutron and electron. For example, the reaction $n \leftrightarrow p + e^- + \overline{\nu}_e$ tells us

$$\mu_p = \mu_n - \mu_e \tag{5.29}$$

because, as remarked, the neutrino chemical potentials are zero in the evolved star. As the neutron density increases, so does that of protons and electrons. So, μ_e may attain the value of the muon mass, in which case it also will be populated. The equilibrium with respect to the reaction $e^- \leftrightarrow \mu^- + \nu_e + \overline{\nu}_\mu$ informs us that

$$\mu_{\mu^-} = \mu_e \,. \tag{5.30}$$

Given the kaon decay channels (5.28) in which all decay products diffuse out of the star, the kaon chemical potentials are

$$\begin{aligned} \mu_{K^0} &= 0, \\ \mu_{K^-} &= \mu_e, \end{aligned}$$

and

$$\mu_{K^+} = -\mu_e \,. \tag{5.31}$$

Equilibrium with respect to (5.25) coupled with the decay of the K^0 into gamma rays yields

$$\mu_\Lambda = \mu_n \,. \tag{5.32}$$

The chemical potentials of the other hyperons can be inferred in like manner. For example, a particular form of (5.25) pertaining to the Σ^+ is $n + n \leftrightarrow n + \Sigma^+ + K^-$ from which we learn that

$$\mu_{\Sigma^+} = \mu_n - \mu_e = \mu_p \,. \tag{5.33}$$

We have written only a few of the possible reactions among hadrons and leptons, in fact only a sufficient number so as to learn the relationship between their chemical potentials and the two independent ones, μ_n and μ_e, for baryon and (negative) electric charge. In general the chemical potential of any particle is a linear combination of these two, weighted by the baryon and electric charge carried by the particle,

$$\mu = b\mu_n - q\mu_e, \tag{5.34}$$

where b is the particle's baryon charge and q is its electric charge number (in units of $+e$). The strangeness chemical potential is zero, as discussed previously. From the above expression, the chemical potential for any particle—baryon, hadron, or quark, for example—can be written down immediately.

Since a particle type is populated only if its chemical potential exceeds its lowest energy state in the medium, we see that the only possibility for a kaon population is that μ_e exceeds the K^- effective mass in the medium. A first-order estimate is its vacuum mass, 494 MeV. The electron chemical potential can never reach this value. The reason is the following: The three charge states of the pions have the same chemical potentials, respectively, as those of the kaons. One can show this by writing down their decay modes or by using the general expression, (5.33). As the density of neutron star matter is increased from nuclear density, $\mu_e = \mu_n - \mu_p$ increases. If μ_e attains the value of the pion effective mass, negative pions will condense (being bosons they can, unlike the electrons, all occupy the same energy state). Thus, the electron chemical potential will saturate at the pion effective mass [49]. Thereafter the lepton populations will be frozen and the π^- population will maintain charge neutrality at higher densities. A further feature of the high-density domain that we will encounter in greater detail shortly is that, as charged hyperons become populated, it becomes energetically more favorable for charge neutrality to be achieved among baryon-carrying particles instead of pions or leptons.

5.3.3 Hadronic composition of neutron stars

Neutron stars, as their name implies, are not pure in neutrons as was first proposed. Charge neutrality is automatically respected by pure neutron matter, but this is not the lowest energy state of dense neutral matter. Some neutrons will beta decay until equilibrium between neutrons, protons, and electrons is reached. This is expressed by the relationship, $\mu_p = \mu_n - \mu_e$ among the chemical potentials (see (3.72)).

The chemical potentials grow with increasing density. Therefore, other thresholds are reached, and additional particle species are populated. In a Fermi gas model the thresholds are simply the masses of the particles. For example, the Λ hyperon, whose chemical potential is given by (5.32), will be in equilibrium in the star when the neutron chemical potential attains the value of the lambda mass ($m_\Lambda = 1115$ MeV) and will be one of its

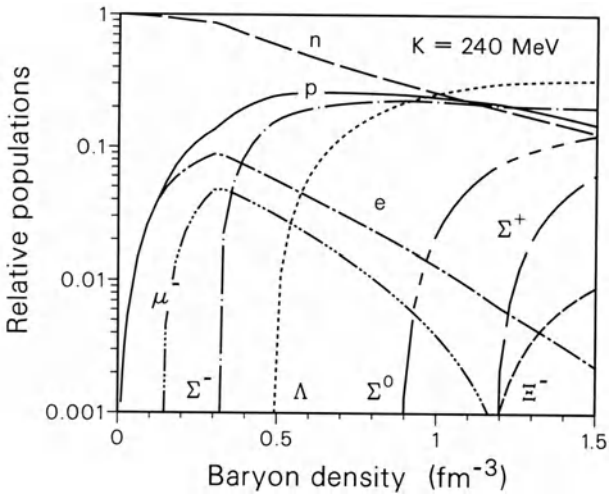

FIGURE 5.11. Populations of various particles in neutron star matter relative to the neutron as a function of density. The compression modulus of the corresponding symmetric nuclear matter is $K = 240$ MeV. The effective mass at saturation is $m^\star = 0.78m$ and hyperon couplings $x_\sigma = 0.6$ (Section 5.4.3). See also ref. [86].

constituents when $\mu_n > m_\Lambda$. In general the particle thresholds depend on the interactions as well, which we include in the sequel.

The isospin symmetry energy arising from the coupling of baryon isospin to the neutral rho meson is very important in this respect. Obviously it favors conversion of neutrons to baryons of opposite isospin projection, consistent of course with charge neutrality. For these reasons neutron star matter is very complex in composition and the Lagrangian used in nuclear field theory has to be generalized to include these complications [49, 86, 87, 206, 88].

The particle populations of a neutron star are shown in Fig. 5.11 when equilibrium is treated in the general manner described. For low density, one sees that charge-neutral uniform matter is almost pure in neutron, but with a small proton and electron admixture in equal numbers. With increasing density, the electron Fermi energy increases to the muon mass, and then the muon as well will be populated. As we discuss later, the pion may also condense. Hyperon thresholds are reached at densities beginning at about three times nuclear density, and become important components of neutron star matter with further increase in density.

Neutron stars therefore are not made of neutron matter but rather of hadronic matter in the lowest energy state consistent with charge neutrality.

We call this matter neutron star matter. Its baryonic composition depends on the density, as is easily understood from the foregoing discussion.

5.3.4 Neutron star matter

To describe the complex baryonic composition of neutron stars discussed above, the Lagrangian of hadronic matter must be sufficiently general as to accommodate not only neutrons and protons, as in nuclear matter, but also higher mass baryon states. A suitable generalization of the σ, ω, ρ theory, used to describe nuclear matter and finite nuclei, is [49, 87]

$$\begin{aligned}\mathcal{L} \;=\; & \sum_B \overline{\psi}_B (i\gamma_\mu \partial^\mu - m_B + g_{\sigma B}\sigma - g_{\omega B}\gamma_\mu \omega^\mu - \tfrac{1}{2} g_{\rho B}\gamma_\mu \boldsymbol{\tau}\cdot\boldsymbol{\rho}^\mu)\psi_B \\ & + \tfrac{1}{2}(\partial_\mu\sigma\partial^\mu\sigma - m_\sigma^2\sigma^2) - \tfrac{1}{4}\omega_{\mu\nu}\omega^{\mu\nu} + \tfrac{1}{2}m_\omega^2\omega_\mu\omega^\mu \\ & - \tfrac{1}{4}\boldsymbol{\rho}_{\mu\nu}\cdot\boldsymbol{\rho}^{\mu\nu} + \tfrac{1}{2}m_\rho^2\boldsymbol{\rho}_\mu\cdot\boldsymbol{\rho}^\mu - \tfrac{1}{3}bm_n(g_\sigma\sigma)^3 - \tfrac{1}{4}c(g_\sigma\sigma)^4 \\ & + \sum_\lambda \overline{\psi}_\lambda (i\gamma_\mu\partial^\mu - m_\lambda)\psi_\lambda\,. \end{aligned} \tag{5.35}$$

The first line is the sum of baryon Lagrangians and the interactions with the scalar, vector, and vector-isovector mesons (σ, ω, ρ). The baryon species are denoted by B. They are coupled to the $\sigma, \omega, \boldsymbol{\rho}$ mesons. The sum on B is over all the charge states of the baryon octet, $(p, n, \Lambda, \Sigma^+, \Sigma^-, \Sigma^0, \Xi^-, \Xi^0)$ as well as the Δ quartet (see table 4.5). However, the latter are not populated up to the highest density in neutron stars, nor are any other baryon states save those of the lowest octet, for reasons given elsewhere [49]. The baryon spinors are denoted by ψ_B, while $\overline{\psi}_B \equiv \psi_B^\dagger\gamma_0$ denotes the adjoint. (We use the conventions of [91].)

The second line of (5.35) contains the Lagrangians of the scalar and vector mesons, whose interactions with the baryons give rise, respectively, to attraction and short-range repulsion. The third line contains the Lagrangian for the isovector meson which couples to the isospin of baryons and gives rise to the charge symmetry energy. This line also contains self-interaction terms of the scalar field. The last line contains the Lagrangians for the leptons (electrons and muons) which are important agents in the charge neutrality of neutron star matter.

It is, of course, essential to keep track of the individual baryon charge states so that charge conservation can be enforced (zero in a star and one-half the baryon density in charge symmetric nuclear matter). How the theory can be solved in the mean-field approximation for the ground state of charge-neutral matter in general beta equilibrium (neutron star matter) is described fully in ref. [49].

When the Euler–Lagrange equations of (5.35) are solved by replacing the meson fields by their spacetime, constant, mean values and the nu-

cleon currents by the ground state expectation generated in the presence of the mean meson fields, one obtains the so called mean-field approximation (MFA). This was discussed in Chapter 4. It is in this approximation that nuclear field theory has been typically solved and applied. Henceforth the meson fields, σ, ω, ρ, denote these mean-field values.

The fermion field equations for uniform matter in momentum representation (4.126) are

$$(i\gamma_\mu k^\mu - m_B + g_{\sigma B}\sigma - g_{\omega B}\gamma_\mu\omega^\mu - \tfrac{1}{2}g_{\rho B}\gamma_\mu\tau_3\rho_3^\mu)\psi_B(k) = 0 \tag{5.36}$$

whose eigenvalues for particle and antiparticle can be found, as before, as

$$e_B(k) = g_{\omega B}\omega_0 + g_{\rho B}\rho_{03}I_{3B} + \sqrt{k^2 + (m_B - g_{\sigma B}\sigma)^2}\,, \tag{5.37}$$

$$\bar{e}_B(k) = -g_{\omega B}\omega_0 - g_{\rho B}\rho_{03}\overline{I}_{3B} + \sqrt{k^2 + (m_B - g_{\sigma B}\sigma)^2}\,. \tag{5.38}$$

We recall that the meson field equations for uniform static matter (in which space and time derivatives can be neglected) are

$$\omega_0 = \sum_B \frac{g_{\omega B}}{m_\omega^2}\rho_B\,, \tag{5.39}$$

$$\rho_{03} = \sum_B \frac{g_{\rho B}}{m_\rho^2} I_{3B}\rho_B\,, \tag{5.40}$$

$$\begin{aligned} m_\sigma^2\sigma &= -bm_n g_\sigma(g_\sigma\sigma)^2 - cg_\sigma(g_\sigma\sigma)^3 \\ &\quad + \sum_B \frac{2J_B+1}{2\pi^2} g_{\sigma B}\int_0^{k_B} \frac{m_B^\star(\sigma)}{\sqrt{k^2 + m_B^{\star 2}(\sigma)}}\,k^2\,dk\,, \end{aligned} \tag{5.41}$$

where $m_B^\star(\sigma) = m_B - g_{\sigma B}\sigma$ is the effective mass of baryon species B and it depends on σ. The baryon source currents have been replaced by their ground state expectation values; the ground state is defined as having the single-particle momentum eigenstates with eigenvalues given by (5.37) filled to the Fermi momentum. We will discuss shortly how the Fermi momenta of the various species B are to be found so that the system is in chemical equilibrium. In the above equations, I_{3B} is the isospin projection of baryon charge state B, and k_B is the Fermi momentum of species B. Only the timelike components of the vector fields and the isospin 3-component of the charged ρ field have nonvanishing values on account of the isotropy of nuclear matter and electric charge conservation, respectively, as found in (4.146).

The baryon number, charge, and strangeness densities of the various particle species read

$$\rho_B = (2J_B+1)b_B k_B^3/(6\pi^2)\,, \tag{5.42}$$

$$Q_B = (2J_B+1)q_B k_B^3/(6\pi^2)\,, \tag{5.43}$$

$$S_B = (2J_B+1)s_B k_B^3/(6\pi^2)\,. \tag{5.44}$$

The total baryon and charge densities, the latter of which must be effectively zero for a star, are

$$\rho = \sum_B \rho_B, \qquad q = \sum_B Q_B = 0\,. \tag{5.45}$$

The equation of state can be found as follows. Compute the ground state expectation value of the canonical stress-energy tensor

$$\mathcal{T}^{\mu\nu} = -g^{\mu\nu}\mathcal{L} + \sum_\phi \frac{\partial \mathcal{L}}{\partial(\partial_\mu \phi)} \partial^\nu \phi\,, \tag{5.46}$$

and compare with (3.20) to read the energy density and pressure. Employ the field equations to rewrite the energy density as

$$\begin{aligned} \epsilon \;=\; & \tfrac{1}{3} b m_n (g_\sigma \sigma)^3 + \tfrac{1}{4} c (g_\sigma \sigma)^4 + \tfrac{1}{2} m_\sigma^2 \sigma^2 + \tfrac{1}{2} m_\omega^2 \omega_0^2 + \tfrac{1}{2} m_\rho^2 \rho_{03}^2 \\ & + \sum_B \frac{2J_B + 1}{2\pi^2} \int_0^{k_B} \sqrt{k^2 + (m_B - g_{\sigma B}\sigma)^2}\, k^2\, dk \\ & + \sum_\lambda \frac{1}{\pi^2} \int_0^{k_\lambda} \sqrt{k^2 + m_\lambda^2}\, k^2\, dk\,. \end{aligned} \tag{5.47}$$

The pressure is given by

$$\begin{aligned} p \;=\; & -\tfrac{1}{3} b m_n (g_\sigma \sigma)^3 - \tfrac{1}{4} c (g_\sigma \sigma)^4 - \tfrac{1}{2} m_\sigma^2 \sigma^2 + \tfrac{1}{2} m_\omega^2 \omega_0^2 + \tfrac{1}{2} m_\rho^2 \rho_{03}^2 \\ & + \frac{1}{3} \sum_B \frac{2J_B + 1}{2\pi^2} \int_0^{k_B} k^4\, dk / \sqrt{k^2 + (m_B - g_{\sigma B}\sigma)^2} \\ & + \frac{1}{3} \sum_\lambda \frac{1}{\pi^2} \int_0^{k_\lambda} k^4\, dk / \sqrt{k^2 + m_\lambda^2}\,. \end{aligned} \tag{5.48}$$

The energy density and pressure are functions of baryon density ρ through the Fermi momenta k_B of each species.

The first step in the application of the above theory is to fix the five coupling constants g_σ, g_ω, g_ρ, b, and c. This has been discussed in the preceding chapter. They can be fixed by the saturation properties of nuclear matter, in particular, the binding per nucleon, the saturation baryon density, the effective mass of the nucleon at saturation, the compression modulus, and the symmetry energy coefficient. They can even be determined algebraically in terms of these five bulk nuclear properties, as shown there.

Here, we are interested in describing the structure of observable neutron stars, identified as pulsars. At birth, the temperatures of neutron stars are high, falling to 10^{10} to 10^{11} K in a few seconds. Thereafter, their cooling rate is slower, but they cool to insignificant temperatures on the nuclear scale within a minute. The epoch of observation is generally thousands to

several millions of years after formation. Still very hot by earthly standards (10^5 to 10^9 K), the star is cold on the nuclear scale of MeV ($= 1.16 \times 10^{10}$ K). We therefore take $T = 0$: the star's hadronic degrees of freedom are frozen.

A description of neutron star matter appropriate to a frozen star is obtained by imposing the conditions of charge neutrality and chemical equilibrium as discussed in Section 5.3.2. In general the chemical potential of particle i with baryon charge b_i and electric charge q_i (in units of e) is given by

$$\mu_i = b_i \mu_n + q_i \mu_q, \qquad \mu_K \equiv 0 \tag{5.49}$$

where μ_n and $\mu_q (\equiv -\mu_e)$ are the chemical potentials for unit positive baryon (neutron) number and positive unit electric charge. They correspond to the two conserved quantities in neutron star matter. The strangeness chemical potential is denoted by μ_K: it is zero because strangeness is not conserved on the timescale of the star. The above equation (5.49) is a generalization of (3.72). Chemical equilibrium can now be expressed in terms of the Dirac eigenvalues (5.37) as

$$\mu_B = e_B(k_B), \qquad B = 1, \cdots N\,. \tag{5.50}$$

These equations relate the Fermi momenta of the baryons to the two independent chemical potentials. For the negative leptons, the corresponding equations are

$$\begin{aligned} (m_{e^-}^2 + k_{e^-}^2)^{1/2} &= \mu_e\,, \\ (m_{\mu^-}^2 + k_{\mu^-}^2)^{1/2} &= \mu_\mu = \mu_e\,, \end{aligned} \tag{5.51}$$

and, for free negative pions,

$$(m_{\pi^-}^2 + k_{\pi^-}^2)^{1/2} = \mu_{\pi^-} = \mu_e\,. \tag{5.52}$$

The Fermi momenta in all cases are the positive real solutions when they exist and are otherwise zero.

Neutron star matter is thus obtained as the self-consistent solution to a system of coupled nonlinear equations in 7+N unknowns, as follows:

(1) three field equations for the meson fields (ω_0, ρ_{03}, σ) (5.39,5.40, 5.41)

(2) one equation for electrical neutrality (μ_q) (5.45)

(3) one equation for baryon density (μ_b) (5.45)

(4) two equations for lepton Fermi momenta, (k_e, k_μ) (5.51)

(5) N equations for the Fermi momenta of N baryon species in chemical equilibrium (k_n, k_p, $k_\Lambda, \ldots, k_{\Xi^-}, \ldots$) (5.50).

The system of nonlinear equations, such as described above, is generally difficult to solve. This accounts for the fact that most calculations of equations of state for neutron star structure approximate the star as either pure in neutrons, or else as involving beta equilibrium in the restricted sense of equilibrium among only neutrons, protons, and leptons. Approximations that omit the hyperons are not very useful in connection with the mass constraint on the equation of state. Nor do such approximations constitute a meaningful test of the theory by which the equation of state was found. (We shall show that an equation of state computed under generalized beta equilibrium derived in this chapter as compared to one for pure neutron matter, or even one that includes beta equilibrium among n, p, e^-, μ^-, yields substantially different results for the neutron star sequence.)

There are no means presently available to test the theory of dense neutron star matter. Eventually, connections to observables may be found through high-energy experiments on symmetric nuclear matter involving nuclear collisions. The theory developed here is not unique. However, it does have notable merits that any theory of dense matter should share. The present theory is relativistically covariant, and the nucleon-meson coupling constants are related to symmetric nuclear matter properties in a direct (and algebraic) way. Moreover, as we shall see, the coupling to hyperons can be constrained in a meaningful way. Importantly, the equation of state at higher density is connected to that near saturation through continuity and causality.

It is sometimes thought that neutron stars are so dense that nuclear matter properties are irrelevant. This is not so. Although the density at the center of a neutron star may be quite high, the central region contributes little to the mass on account of the volume element. We have found [102, 86] that the mean density is only three or so times nuclear density for the star at the mass limit, and even less otherwise, depending on how stiff or soft the equation of state is. In Fig. 5.12 we see that, for the most likely value of the compression modulus $K \sim 240$ MeV, only ten percent of a canonical 1.4-$M_\odot$ neutron star has density higher than $3\rho_0$. We therefore insist that a meaningful investigation of the possible constitution and properties of neutron stars can be accomplished only through a theory of matter that is causal, obeys Le Chatelier's principle, and that describes correctly (within the experimental uncertainties) the properties of matter at nuclear density.

Any theory of matter described by hadronic degrees of freedom is relevant around nuclear densities and up to some ill-defined upper limit where a description in terms of individual hadrons must break down. For the present, we assume that this density lies above the highest encountered in neutron star interiors. In Chapter 9 we shall consider a possible transition to a quark core in the more massive stars. This is an interesting transition, especially because of the Coulomb lattice structure of the coexistence phase of quark and nuclear matter [144, 145].

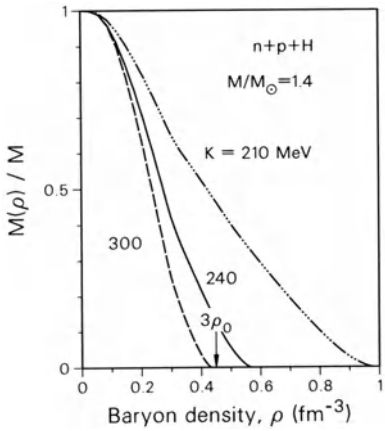

FIGURE 5.12. Fraction of mass of a 1.4-$M_\odot$ neutron star that is resident in matter at densities greater than the value of ρ shown on the x axis.

5.3.5 Hints for computation

Numerical solution of the above defined transcendental system of equations comprising the Euler–Lagrange equations and constraint equations expressing charge neutrality and equilibrium is carried out in the following way. At very low density, say 0.1ρ, the scalar density is approximately equal to the baryon density. One sees this by neglecting k compared to $m^\star$ in the field equation for the scalar field. This fact allows one to approximate the scalar field σ defined by (5.41) in terms of the baryon density (ignoring the small quadratic and cubic terms in σ). The ω_0 field is always given through its field equation (5.39) by the baryon density. At the low densities mentioned, neutron star matter is almost purely neutron, so that the ρ_{03} field is also given by the baryon density through (5.40). One can also approximate the two independent chemical potentials. In summary,

$$g_\sigma \sigma \approx \left(\frac{g_\sigma}{m_\sigma}\right)^2 \rho\,,$$

$$g_\omega \omega = \left(\frac{g_\omega}{m_\omega}\right)^2 \rho\,,$$

$$g_\rho \rho_{03} \approx -\left(\frac{g_\rho}{m_\rho}\right)^2 \frac{\rho}{2}\,,$$

$$\mu_n \approx m - g_\sigma \sigma + g_\omega \omega + g_\rho \rho_{03}\,,$$

and

$$\mu_e \approx .12 m \left(\frac{\rho}{\rho_0}\right)^{2/3}.$$

These five equations can be used to calculate an initial guess in a Levenberg–Marquardt (or similar) type of algorithm for finding the zero of a sum

of squares. For this purpose, move all terms of the three field equations and the two conservation equations for the electric charge density (zero) and baryon density to the left of the equations, square, and add. Embed in the algorithm the equations that define the Fermi momenta in terms of the field amplitudes and chemical potentials (5.50, 5.51), and solve for the nonzero Fermi momenta at each desired density. One has a solution for all of the unknowns listed above when the sum of squares of the mentioned equations is zero.

Repeat the above procedure for a neighboring density. Once one has obtained solutions at a succession of several low densities, use a spline to extrapolate each of the variables an additional increment in density. Use the extrapolated values as the next guess, and continue the process. Thus develop all of the unknowns as a function of baryon density up to the highest density likely to occur in a neutron star, which, as we shall see, is typically (6 to 8)ρ_0.

The complete solution of the theory above is characterized by the values of the quantities enumerated above, of which there are 7+N. The Fermi momenta can be equally represented by the populations of the particles they represent. These populations were shown in one case in Fig. 5.11. The meson field strengths and the two independent chemical potentials, μ_n and μ_e, are shown for the corresponding case in Fig. 5.13.

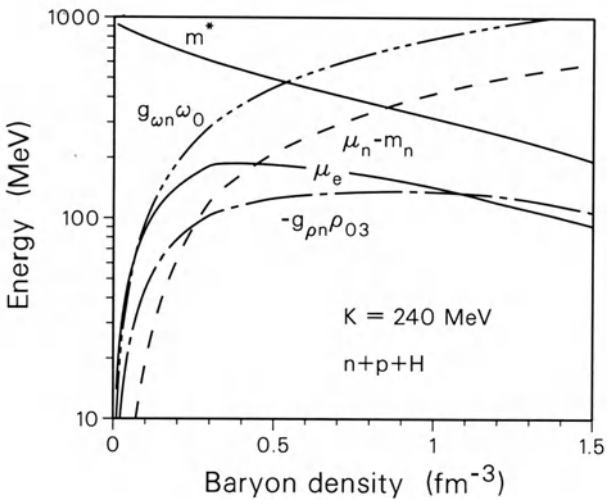

FIGURE 5.13. Solution of the theory for the field strengths and independent chemical potentials with the populations of particles shown in Fig. 5.11. See also ref. [86].

5.3.6 Isospin- and charge-favored baryon species

From the expression for the baryon eigenvalue (5.37) and the requirement of charge neutrality, we can understand the terms, additional to the mass, that determine the baryon thresholds as they appear in Fig. 5.11. We introduce the notion of charge-favored or unfavored and isospin-favored or unfavored [49].

We refer to a baryon species that has the same sign of electric charge as the charge-unfavored proton because it must appear together with a particle of opposite sign to maintain charge neutrality. Equivalently, the left side of (5.53) is reduced by the term $-q_B\mu_e$. From Fig. 5.13 we can learn the values of the various terms in any particular instance.

The isospin term $+g_{\rho B}\rho_{03}I_{3B}$ in the eigenvalue determines whether a species is isospin-favored or unfavored. From it we can write the threshold equation for a given species,

$$\mu_n - q_B\mu_e \geq g_{\omega B}\rho_{03}I_{3B} + m_B - g_{\sigma B}\sigma\,. \tag{5.53}$$

We can deduce what the sign of ρ_{03} will be in neutron star matter from (5.40) and the fact that charge neutrality will assure that the neutron is the dominant baryon species. Therefore the neutron (or any other baryon having the same isospin projection) is unfavored by the isospin-restoring term. Baryons having opposite sign of the isospin projection are favored because their presence will reduce the absolute value of ρ_{03} given by (5.40) and hence the quadratic isospin symmetry term $(\rho_{03})^2$ in the energy density (5.47).

5.3.7 Surface of neutron stars

The outer parts of a neutron star contribute little to its mass. However, the low-density domain of the stellar crust poses interesting physical problems which we briefly describe. We also need to supplement the equation of state of the higher density domain that was described earlier in this chapter.

Consider the surface of a neutron star where the pressure is zero. The condition is much like that on earth since one atmosphere of pressure is very little as concerns the structure of matter. Clearly, the nature of low-density neutron star matter is quite different from the uniform dense matter described by the theory of the preceding sections. Therefore, we need to know the equation of state for neutron star matter from zero pressure up to that pressure at which the individuality of nuclei is destroyed. This is the pressure range of white dwarfs, and so, the outer regions of neutron stars will consist of matter somewhat similar to that of white dwarfs described in Section 3.10.

An important distinction exists, however, between white dwarf matter and the matter in the crust of neutron stars. As discussed in Section 3.10, white dwarfs are the end point in the evolution of stars with mass up to

$\sim 5M_\odot$, which become unstable before nuclear burning to the most stable elements is reached. Neutron stars, on the other hand, are an end point (the other being a black hole) of the evolution of more massive stars which do complete nuclear burning to the most bound nuclei. As such, the relevant nature of the matter of neutron stars is what is referred to as *cold-catalyzed matter* [23], or in our terminology, *neutron star matter*. It is the lowest energy state of a neutral system at zero temperature, containing a large number of baryons A, and is the state to which the matter of a neutron star evolves as it cools by neutrino and photon emission.

The lowest energy form of matter at zero compression and in its lowest possible energy state is composed of solid Fe^{56}. Iron is the most stable element, and therefore has the lowest value for the energy per nucleon. Therefore, it is the lowest density matter of a neutron star and marks the star's edge because the pressure in solid iron is zero. In the solid at the stellar surface, some of the electrons will be in conduction bands. A little deeper into the star, the pressure will be higher, and the atoms will be compressed so that the nuclear spacings no longer leave room for the normal atomic structure—the atoms will be completely ionized. However, the nuclear forces will hold the nuclei together as individual entities. This state is preferred by the short-range nuclear forces to a uniform state of nuclear matter at subnuclear densities. The electrons will form an almost uniform medium in which the positively charged nuclei minimize the total energy by taking up lattice positions, as we studied in Chapter 3. At greater density, the most favored nuclear species will become more neutron rich. Detailed analysis of matter in this density range has been performed by a number of authors [61, 187, 210, 211, 212, 213].

Whereas we can speak of neutron star matter, as described by the theory of this chapter, as a quantum liquid of various relativistic baryons and leptons, the matter at lower density in the crust of the star is of crystalline form and is qualitatively described in Table 5.1 and in Section 3.10 Two useful tabulations of the equation of state of cold-catalyzed matter at low to moderate density can be found in refs. [23, 61] .

5.3.8 Reprise of white dwarfs to neutron stars

We recall from Section 3.9.7 that the Fermi pressure of the relativistic electrons supports white dwarfs. Due to the changing composition of matter with increasing density in the white dwarf domain shown in Fig. 3.6, this supporting pressure becomes insufficient at a certain density due to the inverse beta decay in which some of the electrons are absorbed by protons in the *neutronization* process, and the white dwarf sequence terminates as a result. Recall that the sign of $dM/d\epsilon_c$ changes at the points where hydrodynamic equilibrium changes between stable and unstable (see Section 3.9.5).

Stability is regained for a new family of stars at much higher central

density—the neutron stars—for which the Pauli principle for neutrons first yields a large enough Fermi pressure to oppose gravity. This is a qualitative statement of the onset of stability for neutron stars. (More precisely, the matter of which the very lightest stars are composed, in the approximate mass range $0.09 < M/M_\odot < 0.11$, is a Coulomb solid [61]. Therefore, the pressure is less than for free nucleons of the same energy density. Stability is deferred to a somewhat higher density. This is why the two neutron star sequences of Fig. 3.6 differ on the low-density side.) For stars whose central density is greater than nuclear density, the Fermi pressure is increasingly eclipsed in its role as the agent resisting collapse by the repulsion between baryons at short distances. The vector mesons cause the repulsion in our theory because they contribute a positive (repulsive) term to the energy density (5.47).

5.3.9 Development of neutron star sequences

Neutron stars are fully relativistic objects. Their structure cannot be derived save in the context of General Relativity. When the solution to the above neutron star matter problem (or any other purporting to describe such matter) is obtained, the equation of state $\epsilon = \epsilon(\rho), p = p(\rho)$ is available. One could eliminate ρ to express $p = p(\epsilon)$ or the inverse. The equations of stellar structure—the Oppenheimer–Volkoff equations— (3.21, 3.22) provide a one-parameter family of stellar models corresponding to any particular equation of state.

Several equations of state corresponding to different degrees of completeness with respect to the baryon types that are included in its derivation are illustrated in Fig. 5.14, and the resulting neutron star sequences are shown in Fig. 5.15. (We discuss this figure further in a later section.)

The Oppenheimer–Volkoff equations are easy to solve because they are simple, first-order, differential equations each with an initial condition, say, the central density $\epsilon(0) = \epsilon_c$ and $M(0) = 0$ at $r = 0$. The equations have to be integrated until the pressure becomes zero or until the pressure drops so precipitously with increasing r, that, effectively, the edge of the star has been reached. Then the radius R and the mass $M = M(R)$ for the chosen central density are known. Choosing a succession of increasing values for the central density corresponds to developing a *sequence* of stars of increasing mass, until the mass limit is reached.

From the solution of the Oppenheimer–Volkoff equations for given equation of state and chosen central density, one learns not only the corresponding stellar mass and radius, but, as a result of the numerical integration of the equations, one has the distribution of mass-energy for the particular stellar model. In addition one could, simultaneous with the solution of the structure equations, accumulate the baryon populations (3.145), the radial metric (2.203), and the time metric (2.214 or 2.216) as a function of the

radial coordinates. The equation for the moment of inertia (6.21) could be integrated at the same time.

One can learn additional things. The solution of the nuclear matter theory that provided the equation of state provides many other internal properties of the matter as a function of density, ϵ. For example, the baryon populations are available as a part of the solution, as are the meson fields and chemical potentials. So, having these quantities as a function of ϵ and knowing the distribution of energy density $\epsilon(r)$ as a function of Schwarzschild radius, one can immediately deduce the radial distributions of these other quantities in the star.

5.3.10 Mass as a function of central density

Neutron star sequences are most frequently represented by the relationship between stellar mass and central density. Several sequences are illustrated in this section that correspond to varying degrees of completeness of the underlying theory of the equation of state with respect to beta equilibrium.

First, we exhibit the effects on the equation of state of extending the description of the matter of neutron stars from pure neutron matter to matter that consists of additional baryon species in equilibrium. Figure 5.14 shows the pressure as a function of energy density. Notice that, with each addition of baryon species, the equation of state is softened for the reason that the Fermi pressure of neutrons and protons near the top of their Fermi seas is relieved by allowing them to hyperonize.

The corresponding results for neutron star masses is shown in Fig. 5.15. It is clear that gravity effectively exploits the softening of the equation of state at the higher density introduced by hyperonization. Figure 5.15 also illustrates a generic property of a stable sequence of neutron stars, a minimum and a maximum mass between which $dM/d\epsilon_c > 0$. Stability is lost when the slope becomes zero at either end of the sequence. Below the minimum mass, the configurations are unstable to radial oscillations that destroy them by dispersal. Beyond the maximum mass, gravity overwhelms all resistance to collapse. Stars beyond this point are unstable to an acoustical mode of vibration which so greatly elevates the density at the center of the star that a central region lies within its Schwarzschild radius. The star then would begin its collapse to a black hole. The central density of stable neutron stars lies between about one-half nuclear energy density and about ten times nuclear energy density ($\epsilon_0 \sim 2.5 \times 10^{14}$ g/cm^3), or 6 to 8 times normal baryon density.[7]

As depicted in Fig. 3.1, the baryon number reaches a maximum for the same configuration as has the maximum mass. For stars beyond the limiting mass, the baryon number decreases with increasing density until the next

[7]The energy density of compressed nuclear matter increases more rapidly than the baryon density because of repulsive energy.

turning point of the curve. Notice also that the stellar mass for a given baryon number is larger on the unstable sequence, as expected from its instability.

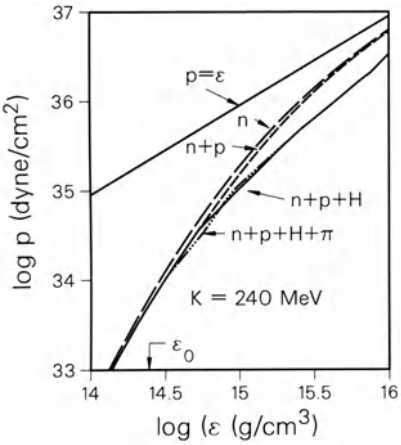

FIGURE 5.14. Compares the equation of state of pure neutron matter and of neutron star matter in which protons, protons and hyperons and lastly pions in addition are included. Here $K = 240$ MeV and $m^\star = 0.78$. Cf. [86].

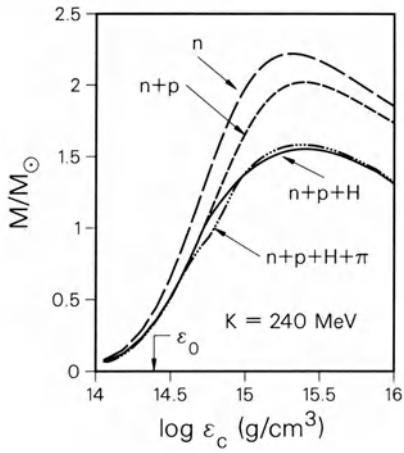

FIGURE 5.15. Neutron star masses for a purely neutron star, one in β equilibrium between neutrons, protons and leptons, one with hyperons in addition; finally, also pions. Here $K = 240$ MeV and $m^\star = 0.78$. Cf. [86].

5.3.11 Radius–Mass characteristic relationship

The most important representation of a neutron star sequence is its radius–mass relationship. It is uniquely related to the underlying equation of state [214]. While both mass and radius are so far not known for any pulsar, it is, in principle, possible to determine them in some cases. Masses can often be determined for a pulsar that is in binary orbit with a companion. In principle, radius determinations could be made through the measurement of the Doppler shift of known spectral transitions, or say, the annihilation of electron pairs. The Doppler shift determines M/R from (3.54), which provides the radius if the mass is known.

Neutron stars are degenerate Fermi systems—their matter can be com-

pressed without the generation of energy.[8] Degenerate stars possess a generic relationship between their mass and radius. Rather than being larger, high-mass degenerate stars are smaller than low-mass stars. The reason is simple. For low-mass stars, the gravitational attraction is weak and the corresponding stars large and diffuse. For the limiting-mass star, the gravitational attraction is strongest of all those in *stable* hydrostatic equilibrium, and the radius correspondingly, is smallest.[9] The limiting-mass star is the most compact of all. With slightly more compaction, it becomes unstable, collapsing to a black hole. The behavior of the radius vs. mass is illustrated in Fig. 5.16 for three different equations of state distinguished by the compression modulus of the corresponding symmetric nuclear matter. The general form of this radius–mass relationship is *generic* to compact stars that are bound by the gravitational force.

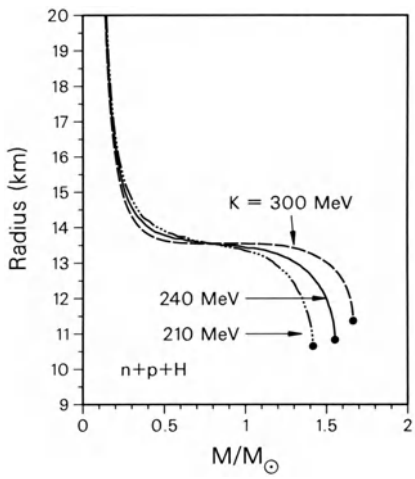

FIGURE 5.16. Radius–Mass relationship characteristic of (gravitationally bound) neutron stars for a selection of models having various compression moduli for the corresponding symmetric nuclear matter (and $m^\star = 0.78m$). In all cases the neutron star matter is in general beta equilibrium between neutrons, protons, hyperons, and leptons. [215]

An interesting theorem has been proven by Lindblom [90]. It is the solution of the inverse problem. Given a table of masses and radii of neutron stars, the equation of state that describes the matter of which they are made can be found over a range which is large or small depending on whether the table spans a sufficient range. Whether or not the theorem will prove to be useful in that respect depends on whether neutron stars can be produced

[8]Gravitational compression of pre-main or main-sequence stars, which can be described by an ideal gas equation of state, raises the temperature to the combustion point of ever heavier elements in thermonuclear reactions.

[9]This fact is of importance in connection with rotation. From (5.7) we see that the mass-shedding angular velocity (Kepler) is given by $\Omega_K \approx 0.625(M/R^3)^{1/2}$. Hence, the limiting mass-star in a sequence of degenerate stars can rotate most rapidly.

in astrophysical phenomena with a sufficient spread in mass and radii. At present the masses for those few cases that have been measured are fairly close, and no radius measurements exist.

5.4 Constitution of Neutron Stars

5.4.1 Limiting mass and the equation of state

We have already learned that there exists a maximum limiting mass that a neutron star can possess. Even in the idealized limit of *incompressible* matter, the structure of the Oppenheimer–Volkoff equations is such as to impose a limit above which gravity would bring about collapse (Section 3.12). In Fig. 3.6 we saw other examples of limiting mass in the sequence of neutron stars.

The qualitative statement that can be made is that the limiting mass of a model sequence of stars depends on the stiffness or softness of the equation of state. One equation of state is said to be stiffer than another if the pressure at every energy density (or energy per baryon) is greater for the one than the other. It is easily shown that the above statement implies and is implied by several other relationships, for example, the energy density and the energy per baryon are both greater at each baryon density for the stiffer equation of state.

The stiffer the equation of state, the larger the mass that can be sustained against collapse. In the figure just referred to (Fig. 3.6), two extreme cases were illustrated, one for which the equation of state was as stiff as allowed by the causal constraint $\partial p/\partial \epsilon \leq 1$. The limiting mass is just over $3M_\odot$. The other case corresponds to a very soft equation of state; it was assumed that dense matter consists merely of a free Fermi gas of neutrons, protons, and leptons in equilibrium. In this case only the Pauli exclusion principle provides the supporting (Fermi) pressure. The limiting mass is $\approx 0.7M_\odot$. We expect any realistic model involving nuclear forces to fall between these extreme cases because the central density corresponding to the maximum mass is so high that the strong, short-range repulsion between baryons dominates the longer range attraction. It therefore adds to the pressure. Indeed, repulsion dominates attraction in the core for densities not far above nuclear density and not far above the minimum mass star in the sequence.

If we knew precisely the equation of state of nature, then, from the Oppenheimer–Volkoff equations, we could simply compute the sequence of neutron stars. However, we have only imperfect theories of dense matter and for the foreseeable future, QCD will not provide the detail needed. So the inverse strategy is relevant—to attempt, from laboratory experiments and from observations on neutron stars, to infer information about the

equation of state and the high density behavior of matter and the stars made from it.

Having recognized that the limiting mass depends on the stiffness of the equation of state, the questions are then as follows. What makes the equation of state stiff or soft? What physical effects are the most important and must not be neglected in computing a model sequence of stars or in testing a particular theory of matter against what is known about them? We now take up these matters.

5.4.2 Beta equilibrium and symmetry energy

Neutron star models have been computed frequently under the simplifying assumption that the star is pure in neutrons. We have already discussed several defects of this assumption.

First, although satisfying the constraint of charge neutrality trivially, such a state of matter is an excited state. The neutron Fermi energy exceeds the sum of the eigenenergies in the medium of the proton and the free electron. Indeed, in Section 3.9.2 we found that, for a Fermi gas of neutrons, protons, and electrons, all are present in equilibrated charge-neutral matter except at extremely low density. (At very low-density, charge-neutral, baryonic matter consists solely of an equal number of protons and electrons.) So the pure neutron state is not in equilibrium as expressed by the equations of chemical equilibrium discussed above (Section 5.3.2 and (5.29)).

Second, we know that nuclear forces and Fermi energies favor isospin symmetry. The valley of beta stability of nuclear masses vividly expresses this (Section 4.5). In our theory, this preference is expressed through the rho meson and its repulsive contribution to the energy density, as displayed in (5.47) which (for nucleons only) is $(1/8)(g_\rho/m_\rho)^2(\rho_p - \rho_n)^2$. Isospin symmetry is clearly favored. In addition to the explicit preference of the nuclear force, the kinetic energy contribution (4.216) also favors symmetry.

Charge-neutral matter cannot satisfy the preference for isospin symmetry fully, and we understand that charge neutrality is an overriding constraint. The force that binds stars is the gravitational force. Above a certain small net charge per baryon, additional charged particles would not be bound. But treating the star as if it were purely neutron prevents neutron star matter from reaching its lowest energy state—the one that is charge-neutral and in beta equilibrium. As can be confirmed, neutral matter always has neutrons as the majority population in the density domain above nuclear density, but populations of protons, leptons, and hyperons are also present. This is even true of a Fermi gas.

If beta equilibrium were neglected, a stiffer equation of state would result than would otherwise be the case. Consequently, an overestimate of the limiting mass would be made as is shown in Fig. 5.15. Since a test of theory involves confirming that it can account for measured masses, the test is misleading if either beta equilibrium or the charge symmetry of

the nuclear force is neglected. So far we have discussed beta equilibrium in the usual sense of nuclear physics, the equilibrium between neutrons, protons, and electrons. For dense matter, we need to consider a generalized beta equilibrium that includes all relevant fermion species in the density domain of neutron stars. Doing so will further soften the equation of state of dense matter.

5.4.3 Hyperon stars

It has long been recognized that hyperons will be present in the dense cores of neutron stars [139, 140, 141, 142, 48, 49]. This is a consequence of the Pauli principle as follows. The weak interaction allows the conversion of some nucleons to hyperons which is energetically favorable in dense matter because the Fermi energy of the highest lying nucleons will otherwise exceed the mass of hyperons, less any associated interaction energy and plus the mass of leptons required by charge conservation. Since the conversion relieves the Fermi pressure exerted by the baryons, the equation of state is softened, and the maximum mass of the neutron star sequence is lowered. Said in an equivalent way, at a given baryon density, the energy of baryonic matter is lowered by sharing baryon number among as many fermion seas as are available.

The neglect of hyperons always leads to an overestimate of the maximum possible mass. However, the magnitude of the reduction has been difficult to quantify, and many works used a universal coupling of nucleons and hyperons to the meson fields, while others applied a reduction factor for the hyperons. Consequently, there has been considerable uncertainty concerning the effect of hyperons on the theoretical maximum mass [49, 86, 87, 88, 216]. It is the purpose of this section to show how (1) the binding of the Lambda hyperon in nuclear matter, (2) hypernuclear levels, and (3) a lower bound on the maximum possible neutron star mass can be used to narrow the uncertainty and thus arrive at a plausible estimate of the effect of general beta equilibrium on neutron star masses, particularly the limiting mass [89]. We recall that, according to present observations, it appears that the lower bound on the maximum neutron star mass is $\sim 1.5 M_{\odot}$.

Recent research on the role of hyperons in neutron stars has been done in the framework of relativistic nuclear field theory [49, 86, 87, 88, 216], the framework in which we work in this book and the same framework in which analysis of hypernuclear levels has been performed recently [217, 218, 219, 220]. The Lagrangian of the theory was derived and discussed in an earlier part of this chapter. There are five coupling constants in the Lagrangian that pertain to nuclear matter properties near saturation, as discussed in Chapter 4. They are determined *algebraically* by the properties of symmetric nuclear matter. Three of them determine the nucleon couplings to the scalar, vector, and vector-isovector mesons ($g_\sigma/m_\sigma, g_\omega/m_\omega, g_\rho/m_\rho$), and

two determine the scalar self-interactions (b, c). The nuclear properties that define their values are the saturation values of the binding, baryon density, symmetry energy coefficient, compression modulus, and nucleon effective mass. We explore their likely ranges.

The hyperon couplings are not relevant to the ground state properties of nuclear matter, but information about them can be gathered from levels in hypernuclei. We shall assume that all hyperons in the octet have the same coupling as the Λ. The hyperon couplings are expressed as a ratio to the above mentioned nucleon couplings,

$$x_\sigma = g_{H\sigma}/g_\sigma, \qquad x_\omega = g_{H\omega}/g_\omega, \qquad x_\rho = g_{H\rho}/g_\rho. \tag{5.54}$$

In most analysis of hypernuclei, the first two ratios are taken equal, and the third is not determined by Λ hypernuclei, since the Λ has zero isospin.

With the constraint $x_\sigma = x_\omega = x$, it was found that x must be small, in the range 0.21 to 0.4, by various authors [217, 218, 219, 220]. Under the above constraints, the maximum neutron star masses are too small [86, 216]. For $x = 0.21$ the maximum mass star is $1.02 M_\odot$ and for $x = 0.4$ it is $1.29 M_\odot$ if the nuclear matter value of the compression modulus is taken to be $K = 300$ MeV (which is at the upper end of plausible values). Such low mass values lie below that of the Hulse–Taylor binary pulsars which therefore rule out small couplings.

When the hypernuclear levels are analysed without the constraint of $x_\sigma = x_\omega$, large correlation errors are found for their values; their determination is highly uncertain, $\pm 100\%$ [219] and $\pm 55\%$ [220].

What we can do to resolve the discrepancy between data on hypernuclei and neutron star masses is to employ the accurately extrapolated value of the Λ hyperon binding in saturated nuclear matter [221]. This procedure avoids the idiosyncrasies of individual nuclear levels in favor of bulk nuclear matter, the stuff of which neutron stars are made (in its charge-neutral form, of course).

Now, we derive an expression for this binding. Recall the relationship (4.176) at saturation between the Fermi energy and the energy per nucleon of a self-bound system $e_F = (\epsilon/\rho)_0$ which is a special case of the Hugenholtz–Van Hove theorem [222]. The Fermi energy of the lowest Λ level is the $k = 0$ value of the Dirac eigenvalue of the theory (5.37),

$$e_\Lambda(k) = g_{\omega\Lambda}\omega_0 + (k^2 + m_\Lambda^{\star\,2})^{1/2}\,. \tag{5.55}$$

Therefore, for the binding energy of the lowest Λ level in nuclear matter from the above theorem, we obtain $(B/A)_\Lambda = e_\Lambda(0) - m_\Lambda$ or

$$\left(\frac{B}{A}\right)_\Lambda = x_\omega V + m_\Lambda^\star - m_\Lambda = x_\omega V - x_\sigma S, \tag{5.56}$$

where

$$S = g_\sigma \sigma = m - m^\star{}_{\text{sat.}}\,, \qquad V = g_\omega\,\omega_0 = (g_\omega/m_\omega)^2 \rho_0\,, \tag{5.57}$$

TABLE 5.4. Values of the hyperon to nucleon scalar and vector coupling compatible with the binding of -28 MeV for Λ hyperons in nuclear matter for two values of the nucleon (Dirac) effective mass at saturation density.

x_σ	x_ω	
	$m^\star = 0.70$	$m^\star = 0.78$
0.2	0.131	0.091
0.3	0.261	0.233
0.4	0.392	0.375
0.5	0.522	0.517
0.6	0.653	0.568
0.7	0.783	0.800
0.8	0.913	0.942
0.9	1.04	1.08
1.0	1.17	1.23

are the values of the scalar and vector field strengths for symmetric nuclear matter at saturation. These values can be obtained immediately from the saturation properties of nuclear matter (Section 4.5) and (4.179).

Equation (5.56) yields a continuous ambiguity in the pair of values x_σ, x_ω each pair of which yield the same Λ binding of -28 MeV. Combined with neutron star masses, the ambiguity is bounded from below by $M_{\max} \gtrsim 1.5 M_\odot$. Combined with the reasonable assumption that the hyperon coupling constants are less than those of the nucleon, based both on the observation that the lowest s-state nucleon is bound by approximately twice as much as the Λ hyperon and also on the basis of quark counting [143], the ambiguity is bounded from above; $x_\sigma < 0.9$ (see Table 5.4). It is even more stringently bounded from above from the fit to hypernuclear levels [220]. In the quoted work it was found that $x_\sigma = 0.46 \pm 0.26, x_\omega = 0.48 \pm 0.32$, so that we may take $x_\sigma < 0.72$.

The results of the analysis are shown in Fig. 5.17. Several curves of maximum neutron star mass as a function of x_σ are shown for a range of values of K and $m^\star$. The ambiguity in the empirical values of K lies in the range 240 to 300 MeV [100, 102, 103, 223]. In view of a recent analysis of nuclear saturation properties [104], the value $K = 240$ may be preferred. The effective (Dirac) nucleon mass at saturation density $m^\star/m$ lies in the range 0.7 to 0.78 and corresponds to the empirical, nonrelativistic, effective mass in the range 0.74 to 0.83, which, to a good approximation [107], has been identified as the Landau effective mass [120]. The related coupling constants are listed in Table 5.5.

Recall our discussion in Chapter 4. We regard nuclear field theory as an effective one. When c is negative, the solution of the field equations yields a well-behaved equation of state even though, regarded as a funda-

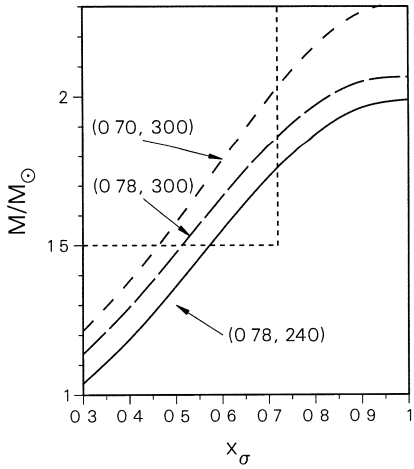

FIGURE 5.17. Maximum neutron star mass as a function of hyperon scalar coupling with vector coupling chosen so as to yield correct Λ binding in nuclear matter. Numbers in parentheses are $m^\star/m$ and K in MeV. [89]

TABLE 5.5. Coupling constants that yield binding $B/A = -16.3$ MeV, density $\rho = 0.153$ fm^{-3}, and symmetry energy coefficient, $a_{sym} = 32.5$ MeV for saturated nuclear matter with the compression K and effective mass $m^\star$ listed below.

K MeV	$m^\star/m$	$(g_\sigma/m_\sigma)^2$ fm^2	$(g_\omega/m_\omega)^2$ fm^2	$(g_\rho/m_\rho)^2$ fm^2	100b	100c
300	0.7	11.79	7.149	4.411	.2947	−.1070
300	0.78	9.148	4.820	4.791	.3478	1.328
240	0.78	9.927	4.820	4.791	.8659	−.2421
210	0.78	10.339	4.820	4.791	1.1078	−0.9751

mental theory, a negative value would be unsatisfactory, since the energy functional would be unbounded from below. With regard to the variation of the nuclear properties that determine the couplings, the equations of state corresponding to negative c are continuous with those having positive values.

The three curves of Fig. 5.17 span the range of uncertainty in K and $m^\star$. For each value of of x_σ, the value of x_ω is chosen to yield the Λ hyperon binding in saturated nuclear matter of -28 MeV. The correspondence is given in Table 5.4. We arbitrarily set $x_\rho = x_\sigma$. The choice is not sensitive; an alternative choice $x_\rho = x_\omega$ yields essentially the same results. The acceptable ranges of M and x_σ, as discussed above, lie in the boxed area in the upper left of the figure. For the hyperon to nucleon scalar coupling x_σ, we find a minimum allowable value of ~ 0.5 from the lower bound on the maximum neutron star mass. It is important to observe that this value is also consistent with the Λ binding in nuclear matter, while hy-

pernuclear levels yield a somewhat uncertain upper bound of ~ 0.72. The corresponding values of x_ω can be found in Table 5.4.

In Fig. 5.17 it will be noticed that the weaker the hyperon coupling, the lower the maximum mass star. A shift in baryon populations from nucleons to hyperons occurs only when the shift softens the equation of state. Therefore the lower stellar mass implies that the hyperons actually participate to a higher degree, the weaker their coupling. In fact, if the couplings of hyperons are reduced to zero (meaning that they are treated as a free Fermi gas), the limiting star mass lies about $\frac{1}{2}M_\odot$ below that corresponding to interacting hyperons [89]. This seemingly paradoxical behavior is easy to understand and has been explained in Ref. [86, 88]. High-density matter is dominated by the repulsion, not the attraction of the nuclear force. Since the coupling of the hyperons to the omega meson is weaker than that of the nucleons, the repulsion contributed by the omega field is weakened by the conversion of nucleons to hyperons.

As a final word on hyperon couplings, it is reasonable, but unproven, that all hyperons couple with the same strengths as the Λ, as assumed here. It would be very useful to have more experimental evidence on this question, say as to $\Sigma^{+,0,-}$ hypernuclei. Some theoretical work on hypernuclear levels in selected nuclei has been done as a possible guide [224, 225].

5.4.4 Limiting mass and hyperon populations

Now, we illustrate the important role of hyperons in softening the equation of state and reducing the limiting mass that would otherwise be computed if hyperons were neglected.

As standard values of nuclear properties, we choose $K = 240$ MeV, $m^\star/m = 0.78$ for symmetric nuclear matter, which we consider good empirical values [100, 102, 103, 223, 107]. The value of K is close to that found in a careful analysis by Myers and Swiatecki, namely, 234 MeV [104]. For hyperons we take the coupling $x_\sigma = 0.6$ (and corresponding x_ω) which falls in the middle of the range discussed above. Fig. 5.15 shows sequences of stars obtained under four different circumstances: (1) a purely neutron star, (2) one in which β equilibrium between neutrons protons and leptons is incorporated, (3) hyperons are included in the above, and (4) pion condensation, as described later, is also included. The parameters quoted above are used for the figures in this chapter unless otherwise noted.

For case (3) the populations in the maximum mass star are shown in Fig. 5.18. Integrated over the star, the baryon population is about 65% neutrons. Protons and hyperons appear with near equal populations of about 18% each. (Recall (3.145) for the integration.) In the inner 3 km of the star, hyperons are the dominant species. Thus, while neutrons comprise the largest part of the population, they are by no means dominant, as was originally conceived in the notion of a neutron star. Indeed, even very recent works neglect the contribution of hyperons, and their absence also modifies

the proton and lepton populations. We have seen the effect of hyperon populations on the limiting mass—it is a major effect. Likewise, models of neutron stars that omit the hyperon population give poor estimates of the cooling of neutron stars and their electrical conductivity.

Calculation of the temperature history of neutron stars is interesting and comparison of measurements of present temperatures can be made by use of the dipole lifetime or an historical lifetime together with a model for the initial protoneutron star which provides initial conditions for the temperature [226, 227]. Surface temperatures of some neutron stars have been measured, and theoretical models can be compared with these. Electrical conductivity cannot be directly measured. However, ohmic resistance influences the decay or persistence of the magnetic field of pulsars and also its location in the star.

We can gauge the contribution of hyperons to the determination of the star mass by reference to Fig. 5.15 where it is seen that they reduce the limiting mass by about $\frac{1}{2}M_\odot$, depending on the compression modulus and effective nucleon mass [228]. Within the uncertainty of their coupling as limited by the above considerations (boxed region), the hyperons place the limiting mass in the range $M/M_\odot \sim 1.5$ to 2. The more likely value of compression, $K \approx 240$ MeV, sets the range 1.5 to $1.7M_\odot$. The reduction is even greater than it seems at first because the least value of maximum mass that theory provides is that of noninteracting neutrons, i.e., a star supported solely by the Fermi pressure. This value is $\sim 0.7M_\odot$ [59].

Hyperon and proton fractions of the total baryon population of stars corresponding to three values of compression modulus are shown in Fig. 5.19. What is particularly noticeable is the steep rise in hyperon populations as the limiting mass is approached. The implication is that hyperons will be a strong component, up to 18%, in neutron stars if the true mass limit is $\sim 1.5M_\odot$. In fact this may be the case [229]. It is certainly the limit that fits most comfortably with the preferred value of $K = 240$ MeV and the role played by hyperons in softening the equation of state, as we have found. The strong dependence of hyperon populations on limiting mass can be traced, of course, to the higher central density of stars near the mass limit.

5.4.5 Compression modulus and effective nucleon mass

As has been already remarked, the stiffer the equation of state is, the more massive the limiting star of the corresponding one-parameter family of stars. We have also noted that the best known properties of symmetric matter are the binding energy and saturation density (Chapter 4). The symmetry energy coefficient is quite well known, while the effective nucleon mass at saturation density and the compression modulus are the least well known. At the same time, the latter two strongly influence the high-density

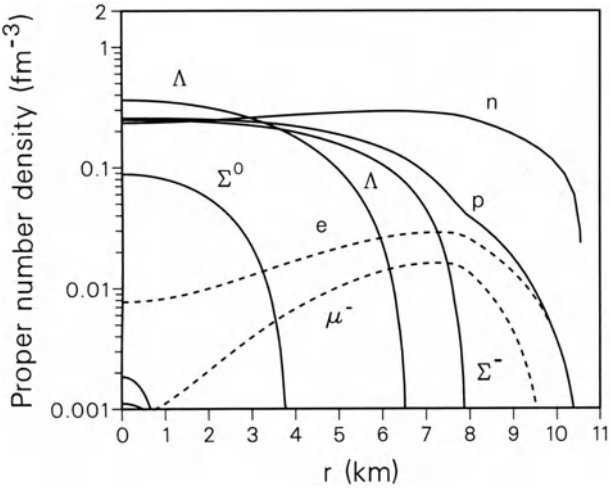

FIGURE 5.18. Composition of the maximum mass star for the case discussed in the text. See also [89].

behavior of the equation of state of symmetric matter, as we saw in Fig. 4.1. By extension, the effect shows up in neutron-rich, and neutron star matter. Recall that, by the latter phrase, we mean cold, charge-neutral uniform matter in general beta equilibrium. For one choice of nucleon effective mass at saturation, $m^\star/m = 0.78$, we show three neutron star sequences corresponding to the indicated values of the compression modulus of the corresponding symmetric nuclear matter in Fig. 5.20. The mass-energy distribution for $1.4M_\odot$ stars for the same three values of $K = 210$, 240, and 300 MeV are shown in Fig. 5.21. The inflection point in each curve signals the hyperon threshold, evident in the equation of state of Fig. 5.14. These figures show that the softer the equation of state is, the more compressed the star.

Rather than show a similar plot for a range of values of the effective nucleon mass, we summarize the situation with respect to the limiting mass as a function of the compression modulus at several values of the effective mass in Fig. 5.22. What we learn here is that, when hyperons are included in the equilibrium description of neutron star matter, a compression modulus as low as 210 MeV is only marginally acceptable.

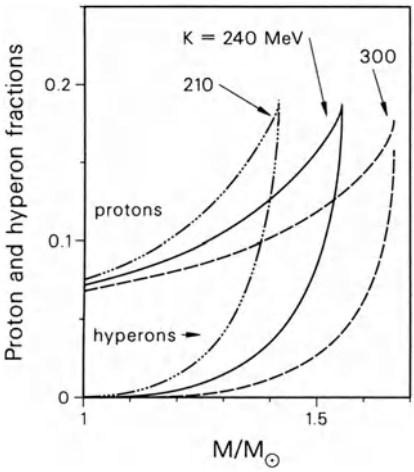

FIGURE 5.19. Proton and hyperon fraction of baryon number density for two values of the compression modulus. After [89].

5.4.6 Pion and kaon condensation

In Chapter 4 we have seen that the general form of the Euler–Lagrange equation for a meson field ϕ is

$$(\Box + m_\phi^2)\phi(x) = g_\phi \, \overline{\psi}(x)\Gamma_\phi\psi(x) \,. \tag{5.58}$$

The quantum numbers of certain mesons are such that the ground state expectation of the source current on the right-hand side vanishes identically in the mean-field approximation. This is so for the pion (spin-parity 0^-) and the kaon which carries strangeness. Only such off-diagonal source currents as $\langle\bar{\Lambda}\gamma_5 N\rangle$ appear on the right side as sources for the kaon, and they vanish in the *normal* ground state. If the source current vanishes, the meson field $\langle\phi\rangle$ vanishes so as to yield the lowest energy. Nevertheless, a different configuration of the fermion state might exist for which the source is finite. Such a situation is referred to as a condensate. Denote the current by $J = \overline{\psi}(x)\Gamma_\phi\psi(x)$ and the polarization operator or self-energy by

$$\Pi_\phi = -\lim_{\langle\phi\rangle\to 0} \frac{\langle J\rangle}{\langle\phi\rangle} \,. \tag{5.59}$$

The brackets denote expectation values with respect to the fermion configuration, typically the ground state. Threshold for condensation is the lowest fermion density at which the fermion state has undergone a structural change from the normal ground state that endows $\langle\phi\rangle$ with a finite value. We can write the following equation at threshold:

$$[-k_0^2 + \boldsymbol{k}^2 + m_\phi^2 + \Pi_\phi(k_0, \boldsymbol{k})]\langle\phi\rangle = 0 \,. \tag{5.60}$$

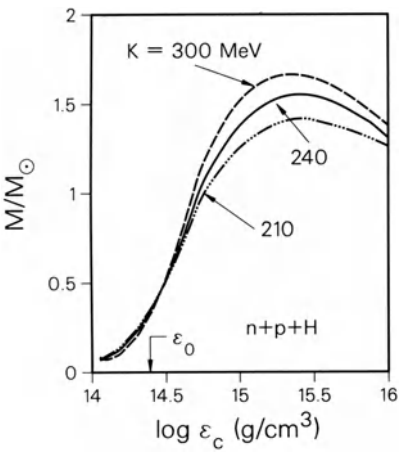

FIGURE 5.20. Neutron star sequences for three values of compression K labeled according to its value in symmetric nuclear matter. Normal nuclear matter density is labeled by ϵ_0. Hyperon couplings as in text [230].

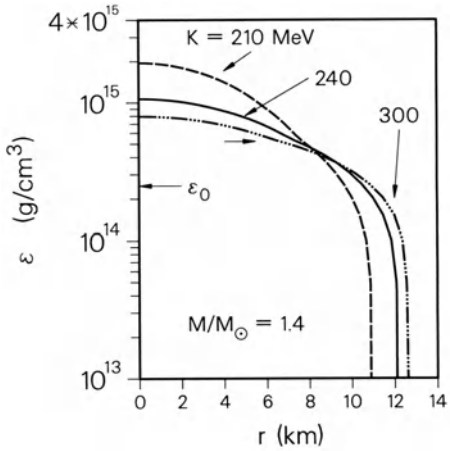

FIGURE 5.21. Mass-energy distributions of three $1.4M_\odot$ mass stars corresponding to the indicated values of K. They belong to the sequences of Fig. 5.20. Hyperon thresholds at a common density are visible by inflections shown by the arrow.

The condition for nonvanishing $\langle\phi\rangle$ is that the quantity in square brackets should vanish. The threshold for nonvanishing condensate $\langle\phi\rangle$ is the lowest density for which

$$-k_0^2 + \boldsymbol{k}^2 + m_\phi^2 + \Pi_\phi(k_0, \boldsymbol{k}) = 0 \tag{5.61}$$

has a solution for real $\boldsymbol{k}$ and $k_0 = \mu_\phi$. The field ϕ could stand for pion or kaon, and the chemical potential for the negatively charged mesons of these types is the electron chemical potential μ_e. We now discuss the plausibility of condensation of the lowest mass mesons that have vanishing source currents in the normal ground state of hadronic matter or, more particularly, in neutron star matter.

Pion condensation was a subject of much investigation a few years ago, especially for symmetric nuclear matter and nuclei, but pions are more likely to condense in neutron star matter. Condensation occurs in nuclear matter if the pion energy becomes degenerate with the normal state. This might happen if the interaction is attractive and strong enough. However, in neutron stars charge neutrality favors pion condensation. This is so because,

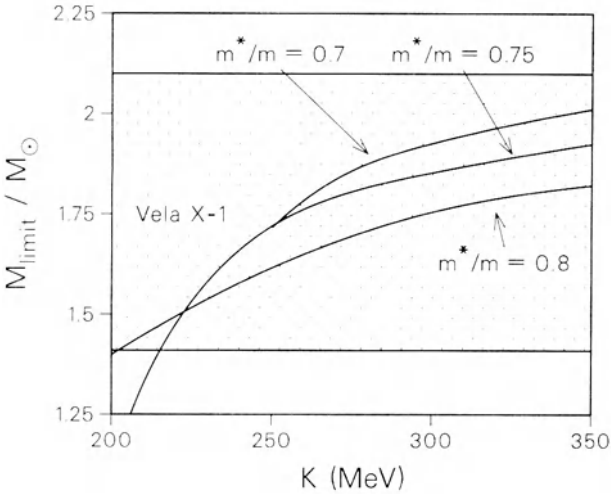

FIGURE 5.22. Limiting mass of various neutron star sequences as a function of the value of the compression modulus of symmetric nuclear matter for several values of the effective nucleon mass. Dotted area denotes uncertainties in Vela X-1 mass. From [102].

as a function of increasing density, neutrons at the top of the Fermi sea will decay to proton plus electron. The electrons are fermions and their Fermi level increases with further increase in density. When the electron chemical potential (Fermi energy) becomes equal to the effective pion mass (or self-energy) in the medium, it will be favorable thereafter for negative pions to play the role that the electrons had in preserving charge neutrality because they are bosons and can all condense in the lowest state. Thus, while $\mu_e = \mu_n - \mu_p$ is essentially zero in symmetric matter, it is positive in neutron star matter, thus favoring the π^- since $\mu_{\pi^-} = \mu_e$. On the other hand, the other charge states of the pion are excluded since $\mu_{\pi^+} = -\mu_e$ and $\mu_{\pi^0} = 0$. Similar remarks and relationships hold for the kaon, except that its participation seems less likely because of its greater mass [49].

If pions condense, the growth of the electron chemical potential with further increase in density is arrested at a value equal to the effective pion mass, as illustrated in Fig. 5.23. In this event the electron chemical potential cannot approach the mass of the negative kaon, which is greater than that of the pion, and so negative kaons cannot condense. Condensation of the other kaon states is even less likely, for the same reason given above, for the other charge states of the pion. This conclusion regarding kaon condensation is in contradiction to suggestions that kaons might condense at rather low density in nuclear or neutron matter [231]. The question of

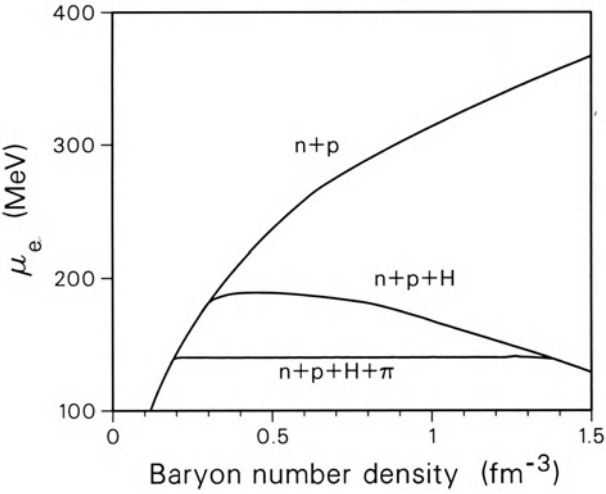

FIGURE 5.23. Electron chemical potential as a function of neutron star baryon number density for three cases as discussed in the text. (Adapted from [86].)

kaon condensation has been further studied in recent work [232] where kaon condensation occurs at an estimated density of three or four times nuclear.

However, as seen in Fig. 5.12, for the most likely value of $K \sim 240$ MeV, only ten percent of the matter of a canonical $1.4M_\odot$ neutron star has a density greater than $3\rho_0$. Research that takes the presence of hyperons as necessary for an adequate description of neutron star matter finds that their presence pushes the condensate density to a higher value than $4\rho_0$ or that it is absent at all densities [233, 234]. The reason is the same given above (Section 5.4.7) and years ago [49]: the growth of the electron chemical potential with increasing density is arrested by pion condensation or by the growth of hyperon populations, or both. Kaon condensation seems unlikely according to present theory. In any case, such a condensate cannot suppress the participation of hyperons or possibly quark matter in dense stars. The Pauli exclusion principle assures this because of the conservation of the baryon number of the star. At sufficiently high density the energy can be lowered by distributing baryon number over many fermi seas.

The electron chemical potential will saturate at the π^- self-energy if it is small enough (Fig. 5.23). It will remain essentially saturated through a range of density and then decrease as the hyperon populations grow and reduce the electron chemical potential. (Charge neutrality is achieved at higher density among the conserved baryon-carrying species. See next section.) The pion population at this point will be suppressed. So pion condensation, if it occurs (i.e., if the pion effective mass is small enough),

is an intermediate density phenomenon in neutron stars. This can be seen in Fig. 5.24. Pion condensation does not seem to have a large effect on neutron

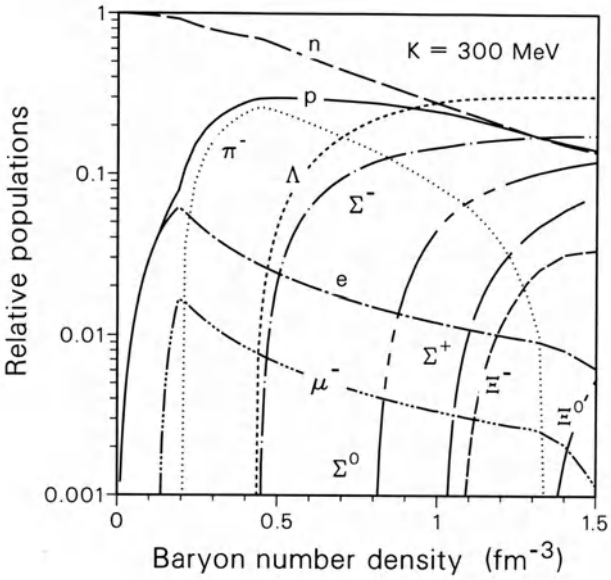

FIGURE 5.24. Populations of neutron star matter relative to that of the neutron in the case that pions of effective mass equal to their vacuum mass are admitted. [86].

star structure, an example of which can be seen in Fig. 5.15, although the effect is larger the softer the equation of state [228].

In the above calculations, the effective pion mass was taken to be the vacuum mass. This probably overestimates the role of the pion. In neutron star matter, the pion experiences a repulsive s-wave interaction which would increase its effective mass. It also experiences an attractive p-wave interaction which it must pay for by having a finite momentum. Our estimate of the effective mass due to the latter is ~ 200 MeV [235].

5.4.7 Charge neutrality achieved among baryons

We understand that neutron stars—indeed, any star—must have zero net charge (though this does not imply zero charge density, a fact that has interesting consequences, as we shall see in Chapter 9). The reason is that the star is bound by the long-range gravitational force and any net charge above an infinitesimal (5.21) would unbind additional charge. Let us imagine building up a neutron star, not as nature does in a supernova where the material is approximately symmetric in neutron and proton in the progenitor star, but rather building the star initially using neutrons and adding

more and more of them. This is a perfectly legitimate consideration as discovered many years ago in chemical thermodynamics since at this point we are interested in the final ground state and not the path by which it is attained.

What we would find is that even at modest density, the Fermi energy of the neutron at the top of the Fermi sea exceeds the energy of a proton, electron, and neutrino. In that case the neutron would inverse beta decay, and so for all high-lying neutrons until the system finds the equilibrium number of neutrons, protons, and electrons. Equilibrium occurs when the chemical potentials (or Fermi energies) obey the relationship $\mu_n = \mu_p + \mu_e$. (The neutrinos diffuse to the surface eventually and, being massless, escape, lowering the energy of the star.) If the only hadrons were neutrons and protons, then the electron chemical potential would increase with density as in Fig. 5.23. However, as the density of neutrons is increased, still higher thresholds are reached. If the effective mass of pions is taken as their vacuum mass, when the electron chemical potential attained that value, it would be energetically more favorable for pions to condense since they are bosons and can all occupy the same zero momentum state. The electron chemical potential would saturate at the pion effective mass as seen in Fig. 5.23, if that threshold falls below still a third one, that of the hyperons.

At some density, only about two or three times normal nuclear density, hyperons become energetically favorable. The electron chemical potential will then saturate as shown in Fig. 5.23 and will actually fall with increasing density. What is happening is that charge neutrality is now being achieved among the one class of particles that must be present by conservation of the number of baryons with which the star was formed [49]. Leptons, π^- or K^- are not needed for charge neutrality if it becomes energetically favorable for charge neutrality to be achieved among the conserved baryons (a definite number of which the star has had since birth).

We can formally state the basis for the phenomenon described above as follows: Lepton number is not conserved in a star (because of neutrino diffusion) and meson number is not conserved. We are assured by the Pauli principle that particles carrying the conserved baryon number will distribute themselves, at high density, among many species so as to lower the fermi energies. Therefore, baryons (or quarks) will tend to neutralize charge among themselves since the cost of their masses and fermi energies must be paid, but not those of leptons nor the masses of charged mesons. Leptons and charged mesons will in this way be quenched.

The phenomena discussed above can be seen in Fig. 5.11; the lepton populations decrease as the density of neutron star matter increases. This is a noteworthy phenomenon and, possibly, has implications for the cooling of neutron stars as well as their electrical conductivity, hence the decay rate of their magnetic fields and therefore their active lifetimes as pulsars.

In our opinion, the saturation of the electron chemical potential at the hyperon threshold for stars of canonical mass $1.44M_\odot$ (if it does not occur

at lower density because of condensation of pions) effectively rules out the importance of kaon condensation as well possible of pion condensation. As noted, only about 10% of their mass is comprised of matter greater than $\approx 3\rho_0$ (Fig. 5.12).

5.5 Tables of Equations of State

5.5.1 Low density

Following are tables of the equation of state of neutron star matter at subsaturation densities due to Harrison and Wheeler and BPS.

TABLE 5.6. Equation of state of Harrison and Wheeler. The first 27 entries are from [23]. The remainder were computed by Negele and Vautherin as quoted by Pandharipande, Pines, and Smith in Astrophys. J. 208 (1976) 550. (A number 3.5 +14 means 3.5×10^{14}.)

ρ (fm^{-3})	ϵ (g/cm^3)	p (dyne/cm^2)	ρ (fm^{-3})	ϵ (g/cm^3)	p (dyne/cm^2)
0.473 −14	7.86 + 0	1.01 + 9	0.602 −9	1.00 + 6	2.80 +22
0.475 −14	7.88 + 0	5.07 + 9	0.145 −8	2.41 + 6	1.21 +23
0.476 −14	7.90 + 0	1.01 +10	0.482 −8	8.00 + 6	8.96 +23
0.485 −14	8.06 + 0	5.07 +10	0.277 −7	4.61 + 7	6.50 +24
0.491 −14	8.15 + 0	1.01 +11	0.455 −7	7.56 + 7	1.21 +25
0.699 −14	1.16 + 1	1.21 +12	0.615 −6	1.02 + 9	3.18 +26
0.990 −14	1.64 + 1	1.40 +13	0.190 −5	3.15 + 9	1.74 +27
0.157 −13	2.60 + 1	4.41 +13	0.139 −4	2.32 +10	2.22 +28
0.272 −13	4.51 + 1	1.69 +14	0.415 −4	6.92 +10	8.50 +28
0.532 −13	8.82 + 1	8.46 +14	1.000 −3	1.00 +11	1.40 +29
0.127 −12	2.11 + 2	5.82 +15	0.200 −2	2.00 +11	3.14 +29
0.425 −12	7.05 + 2	7.23 +16	0.300 −2	4.01 +11	7.16 +29
0.693 −12	1.15 + 3	1.90 +17	0.400 −2	8.02 +11	1.04 +30
0.124 −11	2.06 + 3	5.61 +17	0.500 −2	1.00 +12	1.26 +30
0.300 −11	4.98 + 3	2.85 +18	0.600 −2	2.00 +12	2.12 +30
0.998 −11	1.66 + 4	2.45 +19	0.700 −2	4.01 +12	3.78 +30
0.500 −10	8.30 + 4	4.10 +20	0.800 −2	8.02 +12	8.53 +30
0.200 −9	3.31 + 5	4.46 +21	0.900 −2	1.00 +13	1.16 +31

TABLE 5.7. Equation of state of BPS

ρ (fm^{-3})	ϵ (g/cm^3)	p (dyne/cm^2)	ρ (fm^{-3})	ϵ (g/cm^3)	p (dyne/cm^2)
4.730 −15	7.861 + 0	1.010 + 9	9.976 −6	1.659 +10	1.425 +28
4.760 −15	7.900 + 0	1.010 +10	1.256 −5	2.090 +10	1.938 +28
4.910 −15	8.150 + 0	1.010 +11	1.581 −5	2.631 +10	2.503 +28
6.990 −15	1.160 + 1	1.210 +12	1.990 −5	3.313 +10	3.404 +28
9.900 −15	1.640 + 1	1.400 +13	2.506 −5	4.172 +10	4.628 +28
2.720 −14	4.510 + 1	1.700 +14	3.155 −5	5.254 +10	5.949 +28
1.270 −13	2.120 + 2	5.820 +15	3.972 −5	6.617 +10	8.089 +28
6.930 −13	1.150 + 3	1.900 +17	5.000 −5	8.333 +10	1.100 +29
6.295 −12	1.044 + 4	9.744 +18	6.294 −5	1.049 +11	1.495 +29
1.581 −11	2.622 + 4	4.968 +19	7.924 −5	1.322 +11	2.033 +29
3.972 −11	6.587 + 4	2.431 +20	9.976 −5	1.664 +11	2.597 +29
9.976 −11	1.654 + 5	1.151 +21	1.105 −4	1.844 +11	2.892 +29
2.506 −10	4.156 + 5	5.266 +21	1.256 −4	2.096 +11	3.290 +29
6.294 −10	1.044 + 6	2.318 +22	1.581 −4	2.640 +11	4.473 +29
1.581 −9	2.622 + 6	9.755 +22	1.990 −4	3.325 +11	5.816 +29
3.972 −9	6.588 + 6	3.911 +23	2.506 −4	4.188 +11	7.538 +29
5.000 −9	8.294 + 6	5.259 +23	2.572 −4	4.299 +11	7.805 +29
9.976 −9	1.655 + 7	1.435 +24	2.670 −4	4.460 +11	7.890 +29
1.990 −8	3.302 + 7	3.833 +24	3.126 −4	5.228 +11	8.352 +29
3.972 −8	6.590 + 7	1.006 +25	3.951 −4	6.610 +11	9.098 +29
7.924 −8	1.315 + 8	2.604 +25	4.759 −4	7.964 +11	9.831 +29
1.581 −7	2.624 + 8	6.676 +25	5.812 −4	9.728 +11	1.083 +30
1.990 −7	3.304 + 8	8.738 +25	7.143 −4	1.196 +12	1.218 +30
3.155 −7	5.237 + 8	1.629 +26	8.786 −4	1.471 +12	1.399 +30
5.000 −7	8.301 + 8	3.029 +26	1.077 −3	1.805 +12	1.638 +30
6.294 −7	1.045 + 9	4.129 +26	1.314 −3	2.202 +12	1.950 +30
7.924 −7	1.316 + 9	5.036 +26	1.748 −3	2.930 +12	2.592 +30
9.976 −7	1.657 + 9	6.860 +26	2.287 −3	3.833 +12	3.506 +30
1.581 −6	2.626 + 9	1.272 +27	2.942 −3	4.933 +12	4.771 +30
2.506 −6	4.164 + 9	2.356 +27	3.726 −3	6.248 +12	6.481 +30
3.972 −6	6.602 + 9	4.362 +27	4.650 −3	7.801 +12	8.748 +30
5.000 −6	8.313 + 9	5.662 +27	5.728 −3	9.612 +12	1.170 +31
6.294 −6	1.046 +10	7.702 +27	7.424 −3	1.246 +13	1.695 +31
7.924 −6	1.318 +10	1.048 +28	8.907 −3	1.496 +13	2.209 +31

5.5.2 High density

Following are equations of state for neutron star matter corresponding to nuclear properties identified in table 5.5. The octet of baryons comprises the composition of the matter which is in generalized beta equilibrium. The ratio of hyperon to nucleon coupling to the scalar meson field is denoted by x_σ. The corresponding coupling to the vector fields can be found in Table 5.4. Muons as well as electrons are included.

TABLE 5.8. Equation of state corresponding to $K = 240$ MeV, $m^\star/m = 0.78$, $x_\sigma = 0.6$

ρ (fm^{-3})	ϵ (g/cm^3)	p (dyne/cm^2)	ρ (fm^{-3})	ϵ (g/cm^3)	p (dyne/cm^2)
0.010	1.6758 +13	7.4377 +30	0.660	1.2571 +15	1.5479 +35
0.015	2.5141 +13	8.9843 +30	0.690	1.3224 +15	1.6825 +35
0.020	3.3529 +13	1.2123 +31	0.720	1.3884 +15	1.8239 +35
0.025	4.1911 +13	1.9243 +31	0.750	1.4550 +15	1.9723 +35
0.030	5.0301 +13	3.2767 +31	0.780	1.5224 +15	2.1277 +35
0.060	1.0074 +14	3.6507 +32	0.810	1.5904 +15	2.2903 +35
0.090	1.5151 +14	1.3499 +33	0.840	1.6591 +15	2.4601 +35
0.120	2.0279 +14	3.1938 +33	0.870	1.7284 +15	2.6372 +35
0.150	2.5471 +14	5.9384 +33	0.900	1.7985 +15	2.8187 +35
0.180	3.0735 +14	9.6207 +33	0.930	1.8692 +15	2.9981 +35
0.210	3.6075 +14	1.4377 +34	0.960	1.9406 +15	3.1802 +35
0.240	4.1500 +14	2.0302 +34	0.990	2.0126 +15	3.3665 +35
0.270	4.7019 +14	2.7477 +34	1.020	2.0853 +15	3.5571 +35
0.300	5.2630 +14	3.5979 +34	1.050	2.1586 +15	3.7528 +35
0.330	5.8336 +14	4.3403 +34	1.080	2.2325 +15	3.9536 +35
0.360	6.4112 +14	5.0478 +34	1.110	2.3070 +15	4.1601 +35
0.390	6.9958 +14	5.8246 +34	1.140	2.3822 +15	4.3719 +35
0.420	7.5872 +14	6.6820 +34	1.170	2.4580 +15	4.5894 +35
0.450	8.1859 +14	7.6277 +34	1.200	2.5344 +15	4.8009 +35
0.480	8.7920 +14	8.6647 +34	1.230	2.6114 +15	5.0020 +35
0.510	9.4052 +14	9.6875 +34	1.260	2.6890 +15	5.2021 +35
0.540	1.0025 +15	1.0735 +35	1.290	2.7670 +15	5.4035 +35
0.570	1.0652 +15	1.1831 +35	1.320	2.8456 +15	5.6068 +35
0.600	1.1285 +15	1.2984 +35	1.350	2.9247 +15	5.8129 +35
0.630	1.1925 +15	1.4199 +35	1.380	3.0043 +15	6.0222 +35

TABLE 5.9. Equation of state corresponding to $K = 210$ MeV, $m^\star/m = 0.78$, $x_\sigma = 0.6$

ρ (fm^{-3})	ϵ (g/cm^3)	p (dyne/cm^2)	ρ (fm^{-3})	ϵ (g/cm^3)	p (dyne/cm^2)
0.010	1.6752 +13	3.9994 +30	0.630	1.1807 +15	1.2170 +35
0.015	2.5131 +13	3.4326 +30	0.660	1.2436 +15	1.3225 +35
0.020	3.3510 +13	5.4699 +30	0.690	1.3071 +15	1.4339 +35
0.025	4.1890 +13	1.2938 +31	0.720	1.3712 +15	1.5515 +35
0.030	5.0273 +13	2.8451 +31	0.750	1.4358 +15	1.6757 +35
0.060	1.0069 +14	3.9881 +32	0.780	1.5009 +15	1.8067 +35
0.090	1.5147 +14	1.4359 +33	0.810	1.5667 +15	1.9446 +35
0.120	2.0278 +14	3.2931 +33	0.840	1.6330 +15	2.0899 +35
0.150	2.5471 +14	5.9640 +33	0.870	1.6999 +15	2.2426 +35
0.180	3.0733 +14	9.4446 +33	0.900	1.7674 +15	2.3941 +35
0.210	3.6068 +14	1.3837 +34	0.930	1.8355 +15	2.5436 +35
0.240	4.1478 +14	1.9208 +34	0.960	1.9042 +15	2.6953 +35
0.270	4.6973 +14	2.5623 +34	0.990	1.9733 +15	2.8502 +35
0.300	5.2552 +14	3.3149 +34	1.020	2.0430 +15	3.0087 +35
0.330	5.8216 +14	3.9817 +34	1.050	2.1131 +15	3.1717 +35
0.360	6.3940 +14	4.5742 +34	1.080	2.1839 +15	3.3396 +35
0.390	6.9723 +14	5.2160 +34	1.110	2.2551 +15	3.5125 +35
0.420	7.5559 +14	5.9208 +34	1.140	2.3269 +15	3.6867 +35
0.450	8.1458 +14	6.6966 +34	1.170	2.3991 +15	3.8357 +35
0.480	8.7414 +14	7.5499 +34	1.200	2.4718 +15	3.9751 +35
0.510	9.3433 +14	8.4437 +34	1.230	2.5448 +15	4.1095 +35
0.540	9.9512 +14	9.3173 +34	1.260	2.6182 +15	4.2384 +35
0.570	1.0564 +15	1.0222 +35	1.290	2.6920 +15	4.3491 +35
0.600	1.1183 +15	1.1171 +35	1.320	2.7659 +15	4.4414 +35

TABLE 5.10. Equation of state corresponding to $K = 300$ MeV, $m^\star/m = 0.78$, $x_\sigma = 0.6$

ρ (fm^{-3})	ϵ (g/cm^3)	p (dyne/cm^2)	ρ (fm^{-3})	ϵ (g/cm^3)	p (dyne/cm^2)
0.010	1.6770 +13	1.4536 +31	0.660	1.2733 +15	1.7555 +35
0.015	2.5163 +13	2.1180 +31	0.690	1.3405 +15	1.9058 +35
0.020	3.3559 +13	2.7070 +31	0.720	1.4084 +15	2.0630 +35
0.025	4.1957 +13	3.4288 +31	0.750	1.4770 +15	2.2272 +35
0.030	5.0357 +13	4.4907 +31	0.780	1.5463 +15	2.3984 +35
0.060	1.0084 +14	2.9325 +32	0.810	1.6165 +15	2.5766 +35
0.090	1.5159 +14	1.1633 +33	0.840	1.6873 +15	2.7620 +35
0.120	2.0283 +14	2.9844 +33	0.870	1.7589 +15	2.9545 +35
0.150	2.5472 +14	5.8863 +33	0.900	1.8313 +15	3.1506 +35
0.180	3.0737 +14	9.9578 +33	0.930	1.9044 +15	3.3459 +35
0.210	3.6089 +14	1.5355 +34	0.960	1.9782 +15	3.5445 +35
0.240	4.1538 +14	2.2168 +34	0.990	2.0526 +15	3.7474 +35
0.270	4.7093 +14	3.0465 +34	1.020	2.1278 +15	3.9552 +35
0.300	5.2760 +14	4.0295 +34	1.050	2.2037 +15	4.1682 +35
0.330	5.8529 +14	4.8527 +34	1.080	2.2803 +15	4.3864 +35
0.360	6.4383 +14	5.6934 +34	1.110	2.3575 +15	4.6099 +35
0.390	7.0317 +14	6.6156 +34	1.140	2.4354 +15	4.8394 +35
0.420	7.6333 +14	7.6290 +34	1.170	2.5140 +15	5.0744 +35
0.450	8.2436 +14	8.7380 +34	1.200	2.5933 +15	5.3083 +35
0.480	8.8620 +14	9.8832 +34	1.230	2.6732 +15	5.5328 +35
0.510	9.4886 +14	1.1022 +35	1.260	2.7537 +15	5.7570 +35
0.540	1.0122 +15	1.2207 +35	1.290	2.8348 +15	5.9830 +35
0.570	1.0764 +15	1.3448 +35	1.320	2.9165 +15	6.2119 +35
0.600	1.1413 +15	1.4752 +35	1.350	2.9988 +15	6.4440 +35
0.630	1.2070 +15	1.6120 +35	1.380	3.0817 +15	6.6798 +35

6

Rotating Neutron Stars

6.1 Motivation

Galaxies and the individual stars within them rotate, as evidenced by Doppler broadening of their spectral lines. The sun rotates rather slowly, with an equatorial speed of 2 km/s. Some stars rotate with equatorial speeds in excess of 400 km/s, close to the limit at which matter would be torn off by centrifugal force. When the core of a massive star collapses to produce a neutron star, conservation of angular momentum assures its enhanced rotation, sometimes rapid. Therefore, in this chapter we are interested in the effects of rotation on the structure and stability of relativistic stars and on spacetime.

As inhabitants of a solar system well described by Newtonian gravity, we have no experience of the effect of stellar rotation on the fabric of spacetime. It may be unexpected therefore that an observer in an inertial frame near a rotating star will himself be found to rotate around its center relative to the distant stars. He would require rockets or some other means of propulsion to stop his own rotation. The closer he approaches the star, the more rapidly he rotates. The rotation of local inertial frames has a real effect on the internal structure of rotating stars as is easily imagined. The effect of a rotating star on spacetime is referred to as the dragging of local inertial frames, or sometimes as the Lense–Thirring effect.

Rotation necessarily breaks spherical symmetry—a rotating star is centrifugally deformed and retains only axial symmetry. One might wonder whether the Kerr metric would serve. Although it possesses axial symmetry, the Kerr metric is appropriate for spacetime outside a black hole. It is formulated in terms of two parameters, the mass and angular momentum, which are otherwise unspecified. We are interested in calculating the mass and angular momentum of stars and must necessarily involve ourselves in their interior structure.

The angular velocity associated with dragging of local inertial frames is fundamental to rotation in gravity. We must therefore devote careful attention to its formulation. The frame-dragging frequency is largest at the center of a rotating star and falls to zero at great distances where spacetime becomes flat. Only after having the frame-dragging effect in hand are we prepared to take the next step, a derivation of the expression for the Kepler frequency—the frequency at which a rotating star would shed

matter at its equator.[1] We shall find that, rather than being a simple relation expressing the balance of gravitational and centrifugal forces as in Newtonian gravity (5.7), the Kepler frequency depends, in a complicated manner, on the internal structure of the star through the interior metric and the frame-dragging frequency. The Kepler frequency in General Relativity is expressed as a self-consistency condition that must be satisfied by the solution to Einstein's equations rather than a formula for that frequency.

The equilibrium configurations of rotating stars pose a more difficult problem than of nonrotating stars. Hartle and Thorne were the first to address the problem. They employed a perturbative approach [236, 237]. Extensive studies based on the method were reported both by the authors of the method and in later research [238, 146, 239, 240, 75]. For years the perturbative method was thought to be valid only for slow rotation. We now know, that supplemented by the self-consistency condition spoken of above, it is valid to frequencies up to Kepler [146, 239, 240, 75].

We employ the perturbative method supplemented by the self-consistency condition because of the greater insight it provides, compared to direct numerical solution. Direct numerical solutions, however, are more accurate [241]. Subsequent to the work of Hartle and Thorne, many authors obtained numerical solutions to Einstein's equations for rotating (but otherwise static) configurations [74, 185, 186, 242, 243].

A useful empirical formula for the Kepler frequency has been proposed by several authors [185, 186]. We show how its simple form can be justified using the general relativistic expression of the Kepler frequency and exhibit thereby another example of how rotation in General Relativity frequently produces nonintuitive results. We shall obtain properties of rotating stellar models for a wide variety of equations of state derived from both relativistic and nonrelativistic theories of matter and compare them to their nonrotating counterparts. We shall also compare the results of relativistic theories of matter and those based on Schrödinger approaches.

Finally, we briefly discuss the interesting topic of gravitational wave instabilities in rotating stars. Such instabilities may occur—especially in young hot stars—at frequencies below the Kepler frequency. If this happens, stable rotation at frequencies beyond the onset of instability is not possible. The star rapidly loses angular momentum to gravitational radiation until the instability is damped. If the gravitational wave instability occurs at a frequency above Kepler, it is irrelevant since the Kepler frequency sets the absolute limit; a stable star cannot attain a frequency higher than that at which it loses mass at the equator. These results are interesting in connection with the two populations of pulsars discussed in Chapter 5. The recycled population consists of old, cold stars for which gravitational

[1]The Kepler angular velocity is that possessed by a particle in stable circular orbit at the equator of a star, hence, the limit to rotation of the star itself. For brevity we frequently refer to angular velocity as frequency.

instabilities are moved to frequencies higher (sometimes above the Kepler frequency) than those of young, hot stars. In most stellar models, cold neutron stars can rotate more rapidly than hot ones.

6.2 Dragging of Local Inertial Frames

So far we have considered the simplest nontrivial form that Einstein's equations take—the form for static, spherically symmetric stars. In this case, the line element $d\tau^2 = g_{\mu\nu}dx^\mu dx^\nu$ has the general Schwarzschild form (2.169) possessing only diagonal elements.

It is evident that the line element for a rotating star cannot consist of only diagonal components. First of all, we expect the rotation to flatten the star more or less depending on the star's angular velocity. Spherical symmetry is thereby broken, but the star maintains axial symmetry. The star is assumed to be static in the sense that, although rotating, it is in uniform rotation and static in the corotating frame. Uniform rotation is the configuration that minimizes the total mass-energy at a specified baryon number and angular momentum [244].

The general expression for the line element for an axial symmetric spacetime has a form dictated by time-translational invariance and axial-rotational invariance:

$$\begin{aligned} d\tau^2 &= e^{2\nu(r,\theta)}\,dt^2 - e^{2\lambda(r,\theta)}\,dr^2 \\ &\quad - e^{2\alpha(r,\theta)}\left[r^2 d\theta^2 + r^2\sin^2\theta\big(d\phi - L(r,\theta)\,dt\big)^2\right]. \end{aligned} \tag{6.1}$$

The polar angle θ makes its appearance in the metric because of the centrifugal flattening of rotating stars and the rotation of inertial frames. We have chosen units $G = c = 1$, so that the term in (6.1) has the dimension of squared length, or, equivalently, squared time. The stellar radius can also be given in either of these units. (For example, the Sun has mass $M = 1.5$ km.) We therefore adopt the convention that time and distance intervals in the metric will be measured in some arbitrary length R, a typical neutron star radius. While this may seem a little eccentric, it will simplify later formulae considerably. Indeed, the line element itself will appear simpler because factors like r^2 and $r^2\sin^2\theta$ will not appear explicitly; they will be absorbed into the exponential functions appearing in the metric.

The general expression for the line element for an axial symmetric spacetime can now be written as

$$\begin{aligned} d\bar{\tau}^2 &= e^{2\nu(r,\theta)}\,d\bar{t}^2 - e^{2\lambda(r,\theta)}\,d\bar{r}^2 \\ &\quad - e^{2\mu(r,\theta)}d\theta^{\,2} - e^{2\psi(r,\theta)}\big(d\phi - \overline{L}(r,\theta)\,d\bar{t}\big)^2. \end{aligned} \tag{6.2}$$

Here $d\bar{r} \equiv dr/R$, $d\bar{t} \equiv dt/R$, $d/\tau/R$ and

$$\begin{aligned} e^{2\mu(r,\theta)} = (r/R)^2 e^{2\alpha(r,\theta)}, \quad e^{2\psi(r,\theta)} = \sin^2\theta\, e^{2\mu(r,\theta)}, \\ \overline{L}(r,\theta) = RL(r,\theta). \end{aligned} \tag{6.3}$$

We have written the line element so that it goes over to the Schwarzschild metric in case of spherical symmetry ($L \equiv 0,\ \alpha \equiv 0$). Throughout the chapter, we distinguish the metric functions from those of Schwarzschild by their angular dependence. The metric functions also depend implicitly on the angular velocity of the rotating star which the metric is designed to take into account.

By writing out the square in (6.2), one can identify the various components of the metric tensor. In particular, a new feature appears, a non-diagonal metric,

$$g_{t\phi} = g_{\phi t} = R^2\, e^{2\psi(r,\theta)} L(r,\theta)\,. \tag{6.4}$$

Such a term must appear because of the axial symmetry and the rotation about the azimuthal direction.

The structure of the axisymmetric star and the metric should be the same under a reversal of time as under a reversal of angular velocity. Then L can depend only on odd powers of the angular velocity Ω of the star, for under one transformation or the other, only one term in the squared expression in (6.2) would otherwise change. (Similarly, the other metric functions can have only even powers of Ω.) Hence, the function $L(r,\theta)$ has the form

$$L(r,\theta) = \omega(r,\theta) + O(\Omega^3)\,, \tag{6.5}$$

where ω is linear in Ω.

The quantity L (or to leading order, $\omega(r)$) has a most interesting and fundamental significance. It is the angular velocity of local inertial frames. Imagine, for example, that a particle is dropped from rest at a great distance. If the star were not rotating, the particle would fall toward the center of the star. But if the star is rotating, its freely falling path is not toward the center. The particle experiences an ever increasing drag in the direction of rotation of the star as it approaches. For this reason, $\omega(r)$ is referred to as the 'angular velocity of the local inertial frames'. The plural is used because the angular velocity depends on the distance r from the star. As we shall see, it is true that $\omega(r) \sim r^{-3}$ outside the star, so that at infinity spacetime is again flat and local inertial frames do not rotate about the star.

To prove the above assertion that $\omega(r)$ is the angular velocity of a freely falling particle (and hence that of the local inertial frames), we need some algebra combined with an earlier result. In (2.117) we proved that, if the metric is independent of ϕ, then a particle's trajectory conserves the covariant component of the velocity u_ϕ. We write the contravariant components as

$$\begin{aligned} u^\phi = g^{\phi\mu} u_\mu &= g^{\phi\phi} u_\phi + g^{\phi t} u_t\,, \\ u^t &= g^{tt} u_t + g^{t\phi} u_\phi\,. \end{aligned} \tag{6.6}$$

We imagined dropping a particle from rest at a great distance from the star. Therefore, all three contravariant velocity components of the particle are initially zero. Because u_ϕ is conserved, we may erect a local Lorentz frame in the vicinity of the point from which the particle is dropped. We have there and for all time on the particle's trajectory, $u_\phi = 0$. Moreover, since $u^t = dt/d\tau$ and $u^\phi = d\phi/d\tau$, we find

$$\frac{d\phi}{dt} = \frac{u^\phi}{u^t} = \frac{g^{\phi t}}{g^{tt}} \,. \tag{6.7}$$

We have the metric elements $g_{\mu\nu}$ which can be read off the general form for the line element of an axial symmetric static geometry. We need the inverse elements $g^{\mu\nu}$ since they appear in the above formula. The only off-diagonal elements belong to t and ϕ. We must invert that part of the covariant metric tensor

$$\begin{pmatrix} g_{tt} & g_{t\phi} \\ g_{\phi t} & g_{\phi\phi} \end{pmatrix} \tag{6.8}$$

that is not diagonal. The determinant is

$$D = g_{tt}g_{\phi\phi} - (g_{t\phi})^2 \tag{6.9}$$

and the inverse matrix

$$\begin{pmatrix} g^{tt} & g^{t\phi} \\ g^{\phi t} & g^{\phi\phi} \end{pmatrix} = \frac{1}{D}\begin{pmatrix} g_{\phi\phi} & -g_{t\phi} \\ -g_{\phi t} & g_{tt} \end{pmatrix} . \tag{6.10}$$

Hence, we find

$$\frac{d\phi}{dt} = \frac{-g_{\phi t}}{g_{\phi\phi}} = \frac{-R^2 e^{2\psi(r,\theta)}\omega(r)}{-R^2 e^{2\psi(r,\theta)}} \,. \tag{6.11}$$

Accordingly the particle coordinate ϕ obeys the equation

$$\frac{d\phi}{dt} = \omega(r) \,. \tag{6.12}$$

This is what we sought to prove: though dropped from rest at a great distance from a rotating star, the freely falling particle does not drop toward the star's center but is deflected. Since it is freely falling in the gravitational field, it defines local inertial frames, frames with rotational angular velocities $\omega(r)$ about the center of the star as measured by an observer at infinity at rest with respect to the star, hence the 'dragging of local inertial frames' by a rotating star. This is a remarkable and important effect of rotation not present in Newtonian gravity.

We asserted earlier that $\omega(r) \sim r^{-3}$. The constant of proportionality is more difficult to derive. We need to solve for the actual metric functions

appearing in (6.2) and use the results in (6.7). The problem divides into two parts: the interior and exterior problem, as in the case of the metric for a static spherical star. The solution of the exterior problem will provide the above asymptotic behavior of the dragging angular velocity. The solution of the interior problem will provide its form inside the star and the normalization of the exterior solution. We take up the internal problem in the next sections.

Dimensional analysis will inform us of the exterior behavior of $\omega(r,\theta)$ modulo the normalization. At great distance from the star, spacetime ought to become asymptotically flat and the dragging frequency ought to vanish, falling off as some power of $1/r$. It should also be proportional to the angular momentum[2] $J = I\Omega \sim MR^2\Omega$ carried by the star, the source of the effect.

We have become accustomed to using gravitational units, but for dimensional analysis must revert to the actual dimensions, because, for example, time and length have the same gravitational units and would be indistinguishable. Since G has units of $\mathrm{cm}^3/(\mathrm{g\ s}^2) = \mathrm{L}^3/(\mathrm{M\ T}^2)$, J has units $\mathrm{M\ L}^2/\mathrm{T}$, and ω has the unit $1/\mathrm{T}$ (where M,L,T stand for mass, length, and time), we can write

$$\omega \sim \frac{GJ^l}{c^m r^n} \sim \mathrm{L}^{3+2l-m-n}\,\mathrm{T}^{-2-l+m}\,\mathrm{M}^{-1+l}\,.$$

The powers are to be found by insuring that the right side has the same dimensions as the left. This gives the equations

$$\begin{aligned} l - 1 &= 0\,, \\ -2 - l + m &= -1\,, \\ 3 + 2l - m - n &= 0\,. \end{aligned}$$

The solution is $l = 1$, $m = 2$, and $n = 3$ which yields $\omega \sim GJ/(c^2 r^3)$ or, reverting to gravitational units,

$$\omega(r) \sim \frac{J}{r^3} = \frac{I}{r^3}\Omega\,, \qquad r \geq R\,. \tag{6.13}$$

As remarked earlier, $L(r,\theta)$ has to contain odd powers of Ω, and this is the leading order term. Observe that ω does not depend on θ to leading order.

Luminous stars are believed to rotate differentially. However, for compact stars, the viscosity is high enough to bring the star into uniform rotation on a short timescale compared to the life of the star[245]. Therefore, we assume that the star rotates uniformly with angular velocity Ω (as measured at infinity).

---

[2]We are only interested here in dimensions, so we write the classical expression for I.

Recall from Section 3.8 that clocks run at different rates according to the gravitational fields within which they reside. Therefore, neither the angular velocity $\Omega = d\phi/dt$ nor the angular velocities of the local frame $\omega(r)$ at r, as measured by a distant observer who is at rest in the asymptotic Lorentz frame, are the same as those measured by a local observer. Since clocks run more slowly on the surface or within a star than at infinity, an observer in a local inertial frame within the star at r would measure angular velocities larger than those measured by a distant observer by the factor $e^{-\nu(r,\theta)}$, the gravitational time dilation (3.54).

6.3 Interior Solution for the Dragging Frequency

Because of the rotation of the local inertial frames, the structure of a rotating star depends, in a complicated way, on its frequency. The centrifugal force acting on a fluid element of the star must depend not on Ω (as would be the case in Newtonian physics), but rather on the difference between the frequency Ω and the frequency $\omega(r)$ of the local inertial frame at the location of the fluid element:

$$\overline{\omega}(r) \equiv \Omega - \omega(r,\theta)\,. \tag{6.14}$$

The relative angular velocity is of prime interest. But it is difficult to obtain the equation that governs its behavior inside the star. Even for a spherically symmetric static star, a great deal of algebra is required to obtain the equations of stellar structure. Hartle [236] has obtained the relevant equation from the Einstein equation

$$G_\phi^{\ t} = 8\pi T_\phi^{\ t} \tag{6.15}$$

and we quote his result:

$$\frac{1}{r^4}\frac{d}{dr}\left(r^4 j\frac{d\overline{\omega}}{dr}\right) + \frac{4}{r}\frac{dj}{dr}\overline{\omega} = 0\,. \tag{6.16}$$

Observe that $\overline{\omega}$ depends only on r to lowest order in Ω, as noted previously.

The quantity $j(r)$ used above is defined in terms of the metric for a Schwarzschild star,

$$\begin{aligned} j(r) &\equiv e^{-(\nu+\lambda)} = e^{-\nu}\sqrt{1-2M(r)/r}\,, \qquad r<R\,, \\ j(r) &\equiv 1\,, \qquad r \geq R\,. \end{aligned} \tag{6.17}$$

After some algebra and use of (2.213), we obtain

$$\frac{dj}{dr} = -4\pi r(p+\epsilon)e^{-\nu}/\sqrt{1-2M(r)/r}\,. \tag{6.18}$$

From (6.16) integrated in the interval $(0, R)$, we have

$$\left(r^4 \frac{d\overline{\omega}}{dr}\right)_R = \int_0^R 4r^3 \frac{dj}{dr} \overline{\omega}\, dr\,. \tag{6.19}$$

Hence, according to (6.13), the angular momentum is

$$J = -\frac{2}{3} \int_0^R dr\, r^3 \frac{dj}{dr} \overline{\omega}\,, \tag{6.20}$$

where the proportionality constant has been set to 2/3 (the choice will become immediately clear from a comparison with the classical expression). From the results written above, we find the moment of inertia $I = J/\Omega$ of a slowly rotating star:

$$I = \frac{8\pi}{3} \int_0^R dr\, r^4 \frac{\epsilon + p}{\sqrt{1 - 2M(r)/r}} \frac{[\Omega - \omega(r)]}{\Omega} e^{-\nu}\,. \tag{6.21}$$

This expression is referred to as a "slowly rotating" result because (6.16) was obtained to lowest order in Ω which means that the structure equations of the star are, in this approximation, those of Oppenheimer–Volkoff for a spherically symmetric star. Notice the appearance in this expression of the factor $e^{-\nu}$ spoken of above that converts the difference of frequencies $\Omega - \omega(r)$, as it would be measured at infinity, to its value in a local inertial frame at r. (An expression for I valid through quadrupole deformations of the star has been obtained elsewhere [147].)

In Newtonian physics (valid if $2M/R << 1$) the dragging frequency does not exist. Since ϵ contains the rest mass of the particles in the star, it will be true that $p << \epsilon$. It can be seen that the above result then reduces to the classical value

$$I_{\text{classical}} = \frac{8\pi}{3} \int_0^R dr\, r^4 \epsilon\,. \tag{6.22}$$

At the edge of the star and beyond, the fundamental equation (6.16) for $\overline{\omega}$ becomes simply

$$\frac{d}{dr}\left(r^4 \frac{\overline{\omega}}{dr}\right) = 0\,, \qquad r \geq R\,, \tag{6.23}$$

which integrates to

$$\frac{d\overline{\omega}}{dr} = \frac{A}{r^4} \tag{6.24}$$

with A a constant. From the dimensional analysis above, A is proportional to the angular momentum J, namely, $A = 6J$. Next, integrate (6.24) to obtain

$$\Omega - \omega(r) \equiv \overline{\omega} = -\frac{A}{3r^3} + B\,, \qquad r \geq R\,. \tag{6.25}$$

Since ω vanishes far from the star, the constant B has the value $B = \Omega$. We can now write

$$\omega(r) = \frac{2J}{r^3} = \frac{2I}{r^3}\Omega\,, \qquad r \geq R\,. \tag{6.26}$$

The last equation together with the one for $\bar{\omega}(r)$ (6.16) provides a means of calculating the dragging angular velocity everywhere. The differential equation for $\bar{\omega}(r)$ can be integrated from $r = 0$ with an arbitrary choice of the central value $\overline{\omega}(0)$ and with vanishing slope. At the surface, the corresponding Ω and J are found by matching to the exterior solution:

$$J = \frac{1}{6}R^4\left(\frac{d\overline{\omega}}{dr}\right)_R\,, \qquad \Omega = \overline{\omega}(R) + \frac{2J}{R^3}\,. \tag{6.27}$$

It may be noticed from the linearity of the differential equation defining $\overline{\omega}(r)$ and the matching value at the surface of the star that $\overline{\omega}(r)/\Omega$ is a universal function for a given equation of state and value of the central density at the present level of approximation (namely, that a spherical star is set into rotation without any change in its structure). Therefore, we have

$$\omega(r)/\Omega = \omega'(r)/\Omega' \tag{6.28}$$

for a given member of a stellar sequence.

We show an example of the ratio of the frame-dragging frequency to the star frequency in Fig. 6.1. It is always less than unity and decreases monotonically with r. It reaches a value of ~ 0.6 at the star's center and has significant value throughout. Therefore, we can expect significant effects on the actual structure of a rotating star as Ω becomes larger, not merely because of the centrifugal flattening, but because it is taking place against the background of a radially dependent, frame-dragging frequency. It is therefore of some interest to understand in greater detail the statement that the effects of the centrifugal force depend on the star's frequency relative to those of the local inertial frames. We take this up shortly.

6.4 Kepler Angular Velocity in General Relativity

The condition for the balance of centrifugal and gravitational forces can be written in Newtonian gravity as

$$\frac{Mm}{R^2} = m\Omega^2 R\,. \tag{6.29}$$

The condition that a particle be in a stable circular orbit at the equator of a star (itself rotating or not) is found immediately. The particle has angular velocity

$$\Omega_c = \sqrt{\frac{M}{R^3}}\,, \qquad \text{(Newton)}\,, \tag{6.30}$$

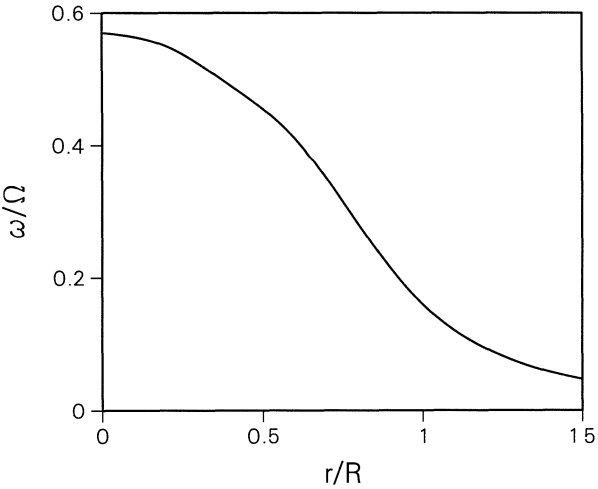

FIGURE 6.1. Ratio of frame-dragging angular velocity to the angular velocity of the star for the limiting-mass star of a typical equation of state (adapted from ref. [246]).

where the subscript 'c' denotes the classical balance of the two forces. Fluid elements at the equator of the star are dislodged at higher angular velocity. The Kepler angular velocity, which we refer to more briefly as the Kepler frequency, is an absolute limit for the rotation of a star.

A star may be subject to other instabilities at lower frequencies that prevent it from reaching rotational frequencies as high as the Kepler frequency. Theoretical instabilities that occur above the Kepler frequency are of no interest because the instability that occurs at the lowest frequency sets the limit.

The Newtonian expression (6.30) also holds for a body in stable orbit around the equator of a nonrotating star in General Relativity. This is not immediately evident. What is intuitively evident is that the expression for the Kepler frequency in the General Theory of Relativity for a rotating star must be more complicated than the above. First of all, we expect that a rotating star will become flattened to some degree and the metric of spacetime is determined by and in turn determines the configuration of mass-energy. Accordingly, the metric must in some way be involved. Moreover as we have just seen, the centrifugal force depends on the star's frequency relative to the frequency of the local inertial frames. Hence $\omega(R)$ must enter the expression also.

We now consider the Kepler angular velocity in General Relativity. First, let us repeat that we are interested in stars in uniform rotation and other-

wise static. They are therefore describable in a static axisymmetric spacetime for which the metric functions are independent of t and ϕ, as in (6.2). For a particle at the circumference ($dr = d\theta = 0,\ \theta = \pi/2$), we learn from the axisymmetric line element

$$1 = e^{2\nu}\left(\frac{dt}{d\tau}\right)^2 - R^2 e^{2\psi}\left(\frac{d\phi}{d\tau} - \omega\frac{dt}{d\tau}\right)^2 . \tag{6.31}$$

For the purpose of brevity, the arguments of the functions here and in the remainder of this section are omitted, though they are understood to be those of (6.2).

From $u^\phi = \Omega u^t$, where $u^\phi \equiv d\phi/d\tau$ and $u^t \equiv dt/d\tau$, one obtains $d\phi/d\tau = \Omega\, dt/d\tau$. Thus, the time component of the particle's four-velocity at the star's equator is given by

$$\frac{dt}{d\tau} = \frac{e^{-\nu}}{\sqrt{1-V^2}} \tag{6.32}$$

where

$$V \equiv e^{\psi-\nu} R\varpi \tag{6.33}$$

denotes the particle's orbital velocity ($u^r = u^\theta = 0$) relative to an observer with zero angular velocity in the ϕ direction.

Equation (6.33) expresses the star's rotational frequency in terms of V and the frame-dragging frequency which we rewrite as

$$\Omega_K = e^{\nu-\psi}\, V/R + \omega(R)\,. \tag{6.34}$$

However, it is most important to note that, unlike the Newtonian case, this result does not provide a formula for the Kepler angular velocity. Rather, it is a *self-consistency* condition that must be obeyed by Ω_K. This is so because the metric functions and the frame-dragging angular velocity $\omega(R)$ depend on Ω_K.

We need an expression for V to complete the above condition on Ω_K. Think of a particle at the Kepler frequency in circular orbit at the equator of the rotating axisymmetric star. As we have learned, geodesic paths are obtainable as the extremum of the proper time. However, in this case it is simpler to do the variation directly, rather than compute the relevant Christoffel symbols in the geodesic equation. Note that we seek a particle velocity on a circular orbit $r = R$ and $\theta = \pi/2$, so that the line element (6.31) can be written,

$$d\tau^2 = [e^{2\nu(r,\pi/2)} - e^{2\psi(r,\pi/2)} R^2(\Omega-\omega)^2]dt^2\,, \tag{6.35}$$

where according to (6.33) $d\phi - \omega\, dt = (\Omega-\omega)\, dt = (V/R)e^{(\nu-\psi)}\, dt$. We seek the extremal of

$$d\tau = \int_{t_1}^{t_2} \sqrt{e^{2\nu} - e^{2\psi}\,(\Omega-\omega)^2 R^2}\, dt\,, \tag{6.36}$$

where the variation vanishes at the end points $\delta r(t_1) = \delta r(t_2) = 0$. Note that the factor R^2 appears because of the reversion to the unbarred coordinate differentials introduced into (6.2). After some algebra, we obtain

$$\psi' e^{2\nu} V^2 - \omega' e^{(\psi+\nu)} V R - \nu' e^{2\nu} = 0\,. \tag{6.37}$$

Equation (6.37) constitutes a quadratic equation in the equatorial velocity V. Its solutions are

$$V_{\pm} = \frac{R\omega'}{2\,\psi'} e^{(\psi\,-\,\nu)} \pm \sqrt{\frac{\nu'}{\psi'} + \left(\frac{R\omega'}{2\,\psi'} e^{(\psi-\nu)}\right)^2}\,. \tag{6.38}$$

The solution V_+ corresponds to corotation which is the desired one in connection with the stability of the star to mass-shedding. The other solution corresponds to a counterrotating particle at its Kepler frequency. In General Relativity the Kepler frequency of a particle circulating at the equator of a rotating star depends on whether it is corotating or counterrotating.

To obtain the solution of the Einstein equations for a rotating star, equation (6.34) with the velocity given by V_+, (6.38), must be solved simultaneously with the stellar structure equations by means of a self-consistent iteration procedure in order to find the general relativistic Kepler frequency of a rotating stellar model of given central density and to find the structure of the star itself at the Kepler frequency[74, 75]. This self-consistency condition has not always been observed in the literature, especially in the applications of the Hartle–Thorne method, as first pointed out in Ref. [75].

6.5 Effect of Frame Dragging on Kepler Frequency

We learned above that the effect of rotation on a fluid element of a star depends not on the star's angular velocity Ω but on the angular velocity relative to that of the local inertial frames $\omega(r)$ [236, 237]. The literal meaning of this quarter-century-old true statement is that the dragging of the local inertial frames reduces the effects of the centrifugal force at the observed frequency Ω since $\omega(r)$ is in the same sense as Ω. From our classical understanding, that in turn implies that the frequency at which centrifugal disruption of a rotating star occurs is larger than the Kepler frequency of a particle in a stable circular orbit of the same radius around a nonrotating star of the same mass. We now show the opposite is true [201].

It has been found by comparing actual numerical solutions of Einstein's equations that the Kepler frequency of a rotating relativistic star is less than the classical value (6.30) rather than larger as intuitively expected. The empirical formula is of the form of (6.30), but reduced by a factor of

about 0.625, and is accurate to better than 10% [185, 186]. The empirical formula is very useful, for it allows one to deduce an accurate value of the Kepler frequency from the radius and mass of a nonrotating star. The latter are easily obtained from a solution to the Oppenheimer–Volkoff equations, whereas the general relativistic solution for a rotating star is more involved and computationally intensive. For this reason the empirical formula has been employed in a large number of papers as well as in this book (see 5.7).

From the self-consistent condition on the relativistic Kepler frequency, we can obtain a form similar to the empirical one with a reduction factor thus showing, in part, its origin. We are thus able to demonstrate analytically that centrifugal effects in strong fields are sometimes counterintuitive and in the process justify the empirical formula [201]. We will make a start on this proof here, where we can get an idea of the results and procedure without the apparatus needed for the full solution of a rotating star.

We recall that in writing (6.2) we have simplified the appearance of the line element by agreeing to measure certain of the differentials in units of R. We get our first estimate of the solution of (6.38) by approximating the metric of the rotating star which appears in this equation by the Schwarzschild metric. With the above note on units, we then compare (2.169) with (6.2) to find

$$R^2 e^{2\psi(r,\theta)} \approx r^2 \sin^2\theta\,. \tag{6.39}$$

Thus at the equator, we have

$$\psi' \approx 1/R\,. \tag{6.40}$$

Likewise, recall that

$$e^{2\nu(R,\theta)} \approx e^{2\nu(R)} = 1 - \frac{2M}{R}\,. \tag{6.41}$$

Using these approximations and (6.26) in (6.34) and (6.38), we are actually able to solve for the Kepler frequency. As an intermediate step in the algebra, we find

$$\Omega_K^2 + \omega(R)\Omega_K - 2\omega^2(R) = M/R^3\,. \tag{6.42}$$

Hence,

$$\Omega_K \approx \left[1 + \frac{\omega(R)}{\Omega_K} - 2\left(\frac{\omega(R)}{\Omega_K}\right)^2\right]^{-1/2} \sqrt{\frac{M}{R^3}}\,. \tag{6.43}$$

The ratio of frequencies is equal to the constant $\omega(R)/\Omega_K = 2I/R^3$. Thus we have obtained the form of the Newtonian answer with a prefactor that depends on the relative dragging frequency at the equator of the star. It is less than unity if $\omega(R)/\Omega_K < 1/2$. In Fig. 6.1 we saw that this is so. Nevertheless, it is the lowest order approximation and can be improved upon after development of more apparatus. Better approximations turn out to strengthen the conclusion—the prefactor is always less than unity [201].

6.6 Hartle–Thorne Perturbative Solution

The problem of stellar structure for static isotropic stars is solved in the manner of Oppenheimer–Volkoff, a solution we derived in detail. The expression for the proper time was diagonal. We also learned that, for a given equation of state, a one-parameter sequence of solutions exists that are usually characterized by differing central densities.

The situation is different for rotating stars. We shall also be interested in static[3] solutions that correspond, however, to a rotating star. In this case there are two off-diagonal metric components, so there is an additional coupled equation. Moreover, an altogether new element has entered—the dragging of the local inertial frames. Hence, in contrast to the situation for Schwarzschild stars, there is a continuum of solutions for given central densities corresponding to different rotational angular velocities.

The first rotating stellar models were obtained as a perturbative expansion in deviations from a spherical star [236, 237]. However Hartle and Thorne and succeeding authors who employed their method failed to impose the self-consistency condition discussed above and were not able to determine precisely the all-important Kepler frequency. The method is referred to as the "slow rotation" method. However, the precise meaning of "slow" (the frequency up to which the method is accurate) was not clarified until our recent research [146, 75, 240].

By comparison with direct integration of Einstein's equations for rotating stars, the perturbative method was found to be fairly accurate to periods of about $\frac{1}{2}$ millisecond. This is three times shorter than the presently fastest known pulsar. It is therefore a good approximation when augmented by the self-consistency condition. Highly accurate numerical methods have been developed and can be studied elsewhere. (See Ref. [241] and citations therein.) We pursue the perturbative approach since it will provide a means of improving the analysis of the effect of frame dragging on the Kepler frequency.

The perturbation expansion of the metric about spherical symmetry has the form

$$e^{2\lambda(r,\theta)} = e^{2\lambda}\left[1 + 2\,\frac{m_0 G + m_2 P_2(\cos\theta)}{r - 2M(r)}\right], \tag{6.44}$$

$$e^{2\nu(r,\theta)} = e^{2\nu}\left[1 + 2(h_0 + h_2 P_2(\cos\theta))\right], \tag{6.45}$$

$$e^{2\alpha(r,\theta)} = 1 + 2(v_2 - h_2)P_2(\cos\theta), \tag{6.46}$$

where m_0, m_2, h_0, h_2, and v_2 are functions of r and Ω and obey the equations derived by Hartle and Thorne [236, 237]. The function $P_2(\cos\theta)$ is a Legendre function. It is readily seen that in the first two metric functions,

[3]Static rotating stars are ones that are static in a corotating frame.

the first term is simply the Schwarzschild metric. The term with a subscript '0' is the monopole correction, and the term with subscript '2' the quadrupole correction (except for $e^{2\alpha(r,\theta)}$, where a transformation of the r coordinate that leaves the general form of the line element unaltered has been used to eliminate the monopole correction to this element) [236]. The perturbation functions need to be solved iteratively in connection with the self-consistency conditions (6.34,6.38).

Although we will not rewrite the basic equations derived by Hartle for the perturbation functions, it is relevant to our purpose here to note the exterior behavior of the monopole correction to the metric. It is given by

$$e^{2\nu} h_0(r) = -\frac{\Delta M}{r} + \frac{J^2}{r^4}, \qquad r > R. \tag{6.47}$$

Here ΔM is the mass-energy increase of the rotating star, and J is its angular momentum, as defined in terms of the Schwarzschild metric (6.21). Equation (6.41) now assumes the form

$$e^{2\nu(R,\theta)} \approx 1 - \frac{2M}{R} + \frac{2J^2}{R^4} \tag{6.48}$$

while at the monopole level of correction, $\psi(R,\theta)$ is unchanged from the previous approximation (6.39). Using these approximations to the metric in the self-consistency condition for the Kepler angular velocity in General Relativity, we obtain

$$\Omega_K^2 + \omega(R)\Omega_K - \omega^2(R) = M/R^3, \tag{6.49}$$

the solution of which is

$$\Omega_K \approx \left[1 + \frac{\omega(R)}{\Omega_K} - \left(\frac{\omega(R)}{\Omega_K}\right)^2\right]^{-1/2} \sqrt{\frac{M}{R^3}}, \tag{6.50}$$

where again, $\omega(R)/\Omega_K = 2I/R^3 =$ constant for a given member of the sequence, (6.28). Here M refers to the mass of the rotating star. The prefactor of this equation is always less than unity since $\omega(r) < \Omega$. Corrections through quadrupole confirm this conclusion. It is at the quadrupole level that a weak dependence on the equation of state enters [201]. This would account for the weak dependence of the empirical formula on the stellar model. Other details, including the effect of mass increase due to rotation and centrifugal flattening, can be found in Ref. [75].

6.6.1 Comparison of Perturbative and Numerical Solutions

We have mentioned above that two possibilities exist for computing rotating equilibrium stellar models in General Relativity—the method of Hartle and

Thorne, which provides an approximate solution of Einstein's equations up to and including quadrupole changes in the stellar configuration, and the numerical solution of Einstein's equations. We compare stellar properties for two equations of state (notation as in Table 6.2), in Table 6.1 and find agreement to better than 10%. The central frame-dragging angular velocity is denoted by ω_c and the ratio of rotational energy to gravitational energy by T/W. The equatorial velocity is denoted by $V_{\rm eq}$. The two equations of state used for the comparison and designated by "12" and "14" are specified in more detail in Table 6.2.

6.7 Imprint of Angular Momentum

We will not discuss rotating black holes but can mention that since

$$g_{t\phi} \approx \frac{2J}{r} \sin^2 \theta \,, \tag{6.51}$$

which follows from (6.4) in lowest order (i.e., taking $e^\alpha = 1$), we see that the imprint of the angular momentum of a black hole will remain in the gravitational field outside the horizon. Like its mass, its angular momentum is a property that can be measured from outside. Its electrical charge is also imprinted on the exterior metric, though we do not prove that here. It may be remarked that stars are neutral, in general, for the reason explained elsewhere.

TABLE 6.1. Comparison of the properties of rotating neutron stellar models calculated from Hartle's perturbative solution with those of the numerical solution of Einstein's equations [75]

EOS	Method	$\frac{M_{\rm rot}}{M_\odot}$	$\epsilon_c{}^a$	Ω_K	$R_{\rm eq}$ (km)	$\frac{\omega_c}{\Omega_K}$	$\frac{T}{W}$	$\frac{V_{\rm eq}}{c}$	e
12	Exact	0.77	0.63	0.542	15.1	0.27	0.10	0.27	0.72
	Hartle	0.77	0.66	0.570	13.7	0.23	0.08	0.26	0.71
	Exact	1.30	0.92	0.705	14.9	0.43	0.12	0.35	0.77
	Hartle	1.30	0.98	0.780	13.1	0.40	0.09	0.39	0.71
14	Exact	0.78	0.51	0.410	18.1	0.25	0.07	0.25	0.71
	Hartle	0.78	0.47	0.406	17.5	0.21	0.07	0.25	0.70
	Exact	1.29	0.77	0.570	16.9	0.40	0.09	0.38	0.74
	Hartle	1.29	0.75	0.606	15.6	0.34	0.08	0.35	0.70

[a] ϵ_c is measured in 10^{15} g/cm^3, Ω_K in 10^4 s^{-1}. The stellar eccentricity (defined in the text on page 264) is denoted by e.

TABLE 6.2. Nuclear equations of state used for the construction of models of general relativistic rotating neutron stars [75]

Label	EOS	Description[a]	Reference
	Relativistic field theoretical equations of state		
1	G_{300}	H, K=300	[86]
2	HV	H, K=285	[49, 247]
3	G_{B180}^{DCM2}	Q, K=265, $B^{1/4}=180$	[89, 145]
4	G_{265}^{DCM2}	H, K=265	[248]
5	G_{300}^{π}	H, π, K=300	[86]
6	G_{200}^{π}	H, π, K=200	[101]
7	Λ_{Bonn}^{00} + HV	H, K=186	[146]
8	G_{225}^{DCM1}	H, K=225	[248]
9	G_{B180}^{DCM1}	Q, K=225, $B^{1/4}=180$	[89, 145]
10	HFV	H, Δ, K=376	[247]
11	Λ_{HEA}^{00} + HFV	H, Δ, K=115	[146]
	Nonrelativistic potential model equations of state		
12	BJ(I)	H, Δ	[142]
13	WFF(UV_{14}+TNI)	NP, K=261	[115]
14	FP(V_{14}+TNI)	N, K=240	[249]
15	WFF(UV_{14}+UVII)	NP, K=202	[115]
16	WFF(AV_{14}+UVII)	NP, K=209	[115]
17	Pan(C)	H, Δ, K=60	[141]

[a] The following abbreviations are used: N=pure neutron matter, NP=neutrons, protons, and leptons in equilibrium concentrations, π = pion condensation, H=hyperons, neutrons, protons, and leptons, $\Delta = \Delta_{1232}$ resonance is populated, Q=quark-hadronic hybrid star, K=compression modulus in MeV, $B^{1/4}$=quark model bag constant in MeV.

6.8 Rotating Stars with Realistic Equations of State

In this section we review some results for a collection of mostly modern equations of state [75]. The references and ingredients are listed in Table 6.2, while Table 6.3 shows the corresponding properties of ordinary symmetric nuclear matter. There are two groups. The first is derived from relativistic theories and is causal at all densities. All of these models are of matter in general beta equilibrium, including nucleons, hyperons, and leptons, and in several cases, a phase transition to quark matter in the core of the star is included. Some are calculated in the relativistic mean-field theory studied in an earlier chapter (also known as the Hartree approximation [49, 247]) or in the Hartree–Fock approximation [247]. Others

contain the influence of "dynamical" (Brueckner-type) two-particle correlations that are connected with a two-body meson-exchange potential. These correlations are incorporated in the ladder (Λ) approximation [250] of the scattering T-matrix of two baryons in matter by employing the Bonn [251] and HEA [252] meson-exchange potentials as an input. The latter approximation is similar to the well-known relativistic Brueckner–Hartree–Fock method (see, for example, Refs. [79, 253, 254], and [255]). The essential difference between the Λ and the above mentioned Hartree–Fock approximation consists in the neglect of dynamical correlations in the latter case. More detail can be found in Ref. [75, 256].

The members of the second group are based on nonrelativistic theories and become acausal at some density within the limiting-mass star (except one of them). The density at which the equations of state become acausal is shown in the last column of Table 6.3. Several of the latter group are from publications that list no saturation properties of nuclear matter, like that of Bethe and Johnson and of Pandharipande. The latter author gives the compression modulus, and it is extraordinarily small—less than a third of what is believed to be the lower bound on empirically acceptable values ($K = 200 - 300$ MeV). They are included more for historical interest. As suggested by the 'description' column of Table 6.2, the equations of state are taken from a rather broad selection of theories that incorporate various effects, such as hyperon populations, pion condensation, and quark cores. Illustrations of these equations of state can be found in ref. [246].

6.9 Effect of Rotation on Stellar Structure

There have been a number of comparisons of the changes in various properties of the limiting stars of a nonrotating sequence and of a sequence rotating at the Kepler frequency. However, it is also interesting to compare the properties of a star of fixed baryon number A as it is spun up. We make the comparison for a star that has $M = 1.4M_\odot$ at zero rotation, and then compare the central density and the moment of inertia of the stars with the same A at various frequencies of rotation. What we find, as shown in Figs. 6.3 and 6.4 is that the change is most pronounced as the star closely approaches its Kepler frequency.

Tables 6.4 and 6.5 can be used to assess the effect of rotation on the masses, radii, and central densities of limiting-mass stars that are rotating at their Kepler frequencies. In particular, masses increase due to rotation typically by 10%, equatorial radii increase typically by 1.5–2 km and central densities decrease by about 20%. Moments of inertia increase by 15–20%. It is noteworthy that, at the Kepler frequency, the velocity at the equator is about $0.5c$. Eccentricities $e = \sqrt{1 - (R_p/R_{eq})^2}$ are rather uniform for all models at about 0.7. The frame-dragging angular velocity ω is an appreciable fraction of the Kepler angular velocity. It is 0.6–0.8 at the center and

TABLE 6.3. Nuclear matter properties of the equations of state of Table 6.2 [75]

Label	B/A (MeV)	ϱ_0 (fm^{-3})	K (MeV)	m^*/m	a_{sym} (MeV)	ϵ/ϵ_0 [a]
1	−16.3	0.153	300	0.78	32.5	–
2	−15.98	0.145	285	0.77	36.8	–
3	−16.0	0.16	265	0.796	32.5	–
4	−16.0	0.16	265	0.796	32.5	–
5	−16.3	0.153	300	0.78	32.5	–
6	−15.95	0.145	200	0.8	36.8	–
7	−11.9	0.134	186	0.79		–
8	−16.0	0.16	225	0.796	32.5	–
9	−16.0	0.16	225	0.796	32.5	–
10	−15.54	0.159	376	0.62	30	–
11	−8.7	0.132	115	0.82		–
12						23.1
13	−16.6	0.157	261	0.65	30.8	–
14	−16.00	0.159	240	0.64		5.6
15	−11.5	0.175	202	0.79	29.3	6.5
16	−12.4	0.194	209	0.66	27.6	7.2
17			60		35	23.6

[a] Energy density are units of normal nuclear matter density beyond which the velocity of sound in neutron matter becomes larger (superluminal) than the velocity of light. The symbol "–" indicates that causality is not violated.

falls to a value 0.2–0.3 at the star's equator.

The Kepler angular velocities themselves vary appreciably between models; there is about a 50% difference between the slowest and fastest, not counting case 17, for which the compression modulus is unrealistically low. The corresponding range in period is 0.42 ms to 0.68 ms. For the entire sequence of stars in most of the models studied, the Kepler frequency is shown in Fig. 6.2.

6.10 Gravitational-Wave Instabilities

We have discussed an absolute limit on rotation, the frequency at which the centrifugal force would overcome gravity at a star's equator. At higher frequencies, stars shed mass at the equator. There are additional means by which rotation may be limited which become relevant if they occur at frequency lower than the Kepler frequency. These instabilities create and

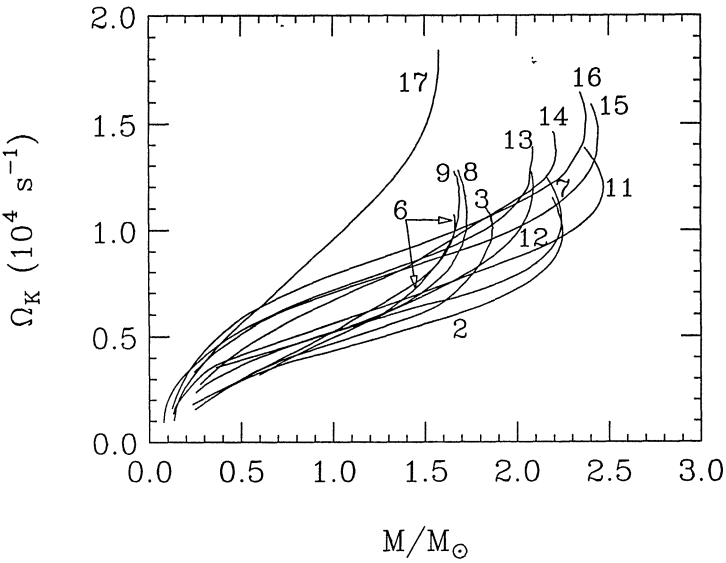

FIGURE 6.2. Kepler angular velocities as a function of the mass of the rotating star are shown for star sequences of a number of the equations of state[75].

are created by gravitational radiation moderated by the viscosity of the stellar material which tends to damp them.

In hot stars certain of these instabilities probably occur below the Kepler frequency in which case they establish the rotation limit. The fact that the viscosity of the star depends on its temperature, (being smallest in the hottest, and therefore youngest, newly born stars) suggests that gravitational-wave instabilities probably lead to the rapid spin-down of any neutron star born with high frequency near the Kepler frequency.

On the other hand, as we discussed in greater detail elsewhere, it is believed that another population of very fast millisecond pulsars are very old neutron stars that have been spun up by accretion from a companion. Being old, they are cold, say 10^5 K. These old stars are heated by accretion, to perhaps 10^6 K, but not likely anywhere near the temperature of newly born neutron stars of 10^{10} K. From this evolutionary perspective, it is important to have an acquaintance with gravitational-wave, radiation-reaction instabilities as moderated by viscosity.

Like most objects, a neutron star has normal modes of vibration. In realistic nonrotating stars, viscosity damps all vibrations. However, in ro-

TABLE 6.4. Calculated properties of rotating limiting-mass neutron star models [75]

Label	$\Omega_K{}^b$	$\frac{M_{\rm rot}}{M_\odot}$	$R_{\rm eq}$ (km)	$\frac{\epsilon_c}{\epsilon_0{}^a}$	I^c	$\frac{V_{\rm eq}}{c}$	e	$\frac{\omega_c}{\Omega_K{}^b}$	$\frac{\omega_{\rm surf}}{\Omega_K{}^b}$
1	0.93	2.04	13.60	7.16	1.89	0.50	0.70	0.58	0.17
2	0.99	2.25	13.43	7.83	2.15	0.54	0.69	0.67	0.20
3	1.01	1.87	12.42	9.43	1.33	0.51	0.69	0.61	0.16
4	1.01	1.72	12.17	10.3	1.16	0.49	0.69	0.60	0.15
5	1.02	2.06	12.87	8.67	1.81	0.54	0.69	0.64	0.19
6	1.03	1.67	11.91	10.8	1.07	0.48	0.69	0.60	0.15
7	1.04	2.24	12.97	7.96	2.12	0.55	0.69	0.67	0.22
8	1.06	1.73	11.91	10.6	1.16	0.50	0.69	0.61	0.16
9	1.13	1.69	11.31	12.1	1.02	0.51	0.68	0.64	0.17
10	1.16	2.47	12.34	7.12	2.45	0.60	0.69	0.76	0.28
11	1.18	2.47	12.24	7.66	2.44	0.61	0.68	0.76	0.29
12	1.12	2.09	11.59	10.8	1.61	0.57	0.68	0.72	0.22
13	1.29	2.09	10.97	10.0	1.53	0.59	0.69	0.74	0.27
14	1.37	2.21	10.82	10.6	1.73	0.62	0.68	0.77	0.29
15	1.45	2.44	10.70	10.1	2.21	0.66	0.64	0.82	0.35
16	1.51	2.38	10.31	10.5	2.02	0.67	0.65	0.82	0.36
17	1.81	1.58	7.98	20.7	0.64	0.61	0.67	0.76	0.27

[a]The quantity ϵ_0=140 MeV/fm^3 (= $2.5\cdot10^{14}$ g/cm^3) denotes the density of normal nuclear matter.
[b]Ω_K is in units of 10^4 s^{-1}.
[c]I is in units of 10^{45} g-cm^2.

tating stars, there are modes that are always unstable in inviscid stars and unstable in viscous stars above certain rotation frequencies.

The cause of instability in viscous stars above a critical frequency is the following. A vibration on a rotating star constitutes an aspherical flow of matter; it produces gravitational radiation. The vibration is unstable if the energy and angular momentum carried off in gravitational waves cause the mode to grow in amplitude. The rotation of the star is thereby damped by gravitational radiation. However, stars do rotate, which tells us the obvious: viscosity damps all rotational instabilities below some frequency of rotation.

This is a subject that we touch on in this chapter. We shall emphasize the physical ideas and illustrate some relevant results. The topic is too complex to treat in detail here and has a comparatively long history which the interested reader can trace through our more recent references. Some of the pioneering work on the subject can be found in Refs. [257, 258, 259, 260].

TABLE 6.5. Calculated properties of nonrotating, limiting-mass, neutron stellar models. The quantity ϵ_0 is defined in Table 6.4 [75]

Label	$\frac{M_s}{M_\odot}$	R_s (km)	$\frac{\epsilon_c}{\epsilon_0}$	I (10^{45}g $\cdot$ cm^2)
1	1.792	11.12	9.37	1.76
2	1.976	11.34	9.29	2.04
3	1.605	10.48	11.36	1.29
4	1.510	10.14	11.99	1.10
5	1.808	10.97	9.57	1.73
6	1.458	10.12	12.10	1.05
7	1.969	10.97	9.29	2.02
8	1.525	9.84	12.79	1.08
9	1.494	9.48	13.93	0.99
10	2.198	10.70	9.64	2.40
11	2.195	10.63	9.64	2.37
12	1.843	9.77	12.50	1.55
13	1.848	9.24	12.79	1.50
14	1.971	9.29	12.16	1.68
15	2.197	9.56	11.54	2.17
16	2.135	9.17	12.50	1.98
17	1.412	6.90	24.07	0.62

To understand the nature of the gravitational-radiation instability, let a neutron star rotate with angular velocity Ω, and consider a small perturbation with time and angular dependence $e^{i(m\phi-\omega t)}$. Let the perturbation propagate in the direction opposite to that in which the star itself rotates. First, consider slow rotation of the star. The angular velocity of the perturbation is ω/m. The aspherical transport of matter will disturb the spacetime continuum in the vicinity of the star's surface. The disturbance propagates as gravitational radiation at the speed of light.

The direction of the rotation of the aspherical flow will cause the resultant gravitational radiation to carry off angular momentum of sign opposite to that of the star. Since the only source for the sign of this angular momentum is the perturbation itself, the gravitational radiation will damp the perturbation. However, if the star rotates with sufficiently high angular velocity, the perturbation will be dragged forward in the direction of the star's rotation. In this case the gravitational radiation will have angular momentum of the same sign as the star, but the angular momentum of the perturbation is still in the opposite sense of that carried by the star since it is moving against the direction of flow of the star's fluid. Because the perturbation is the source of the disturbance of the spacetime continuum at the surface of the star, the amplitude of the perturbation grows to conserve

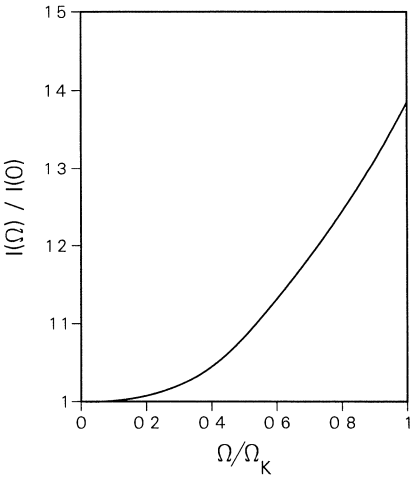

FIGURE 6.3. For fixed baryon number A of the star, the moment of inertia is shown as a function of rotational frequency. (Calculation kindly provided by F. Weber.)

the angular momentum of the gravitational radiation and perturbation.

The above discussion pertains to the damping or initial growth of a small perturbation. If the perturbation grows, it will eventually overwhelm the star. The star's angular momentum will then be carried off by the gravitational radiation. It is not our goal to follow the temporal development of the perturbation, but rather to estimate the rotational frequencies Ω_m of stars for which various counterrotating modes m become unstable. We seek to find the lowest such frequency. It is this frequency that places the upper limit on the angular velocity of the star (or lower limit on its period).

To be more precise, the modes that have turned out to be most important are the so-called $l = m$, f-modes. In the nonrotating limit, these reduce to the $l = m$ spherical harmonic indices, and the f refers to the zero-radial node disturbances. They are initially superficial surface waves with as many waves as the index $l = m$, and they rotate around the equator.

Here we attempt to give some physical idea of the origin of the instabilities without going into details. We would like to follow the initial evolution of the energy contained in a perturbation about equilibrium, such as discussed above. Schematically we can write the energy contained in the perturbation as

$$E(t) = \tfrac{1}{2} \sum_n \int \eta_n (\delta q_n \cdot \delta q_n^*) d^3 r \,, \tag{6.52}$$

where δq_n denotes a displacement from equilibrium associated with shear or bulk stress of the star, for some process labelled n, or a radial perturbation of density that departs from an axially symmetric flow of matter and therefore couples to some multipole of the gravitational field. The no-

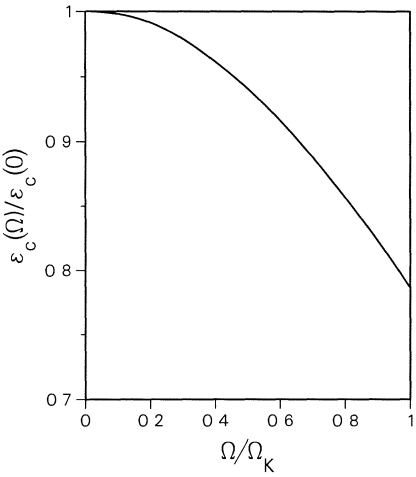

FIGURE 6.4. Comparison of central densities of stars with fixed baryon number A as a function of rotational frequency. (Calculation kindly provided by F. Weber.)

tation is schematic. In the case of shear stress, the product will denote a contraction of second-rank tensors.

We assume that all perturbations have a sinusoidal dependence $e^{i(m\phi-\omega t)}$ on time and azimuth where ω is the frequency of the mode and $m = l$ is an integer index of a spherical harmonic. The coefficient η_n denotes the shear or bulk coefficient or is a constant associated with coupling of the vibrations to the gravitational field. Since energy is dissipated by the stresses and added by the gravitational field as described above, the frequency has an imaginary part. Therefore,

$$\frac{dE}{dt} = 2\,\mathrm{Im}(\omega)\,E \equiv -\frac{2E}{\tau}\,. \tag{6.53}$$

Depending on the sign of $\mathrm{Im}(\omega)$, the perturbation is either damped or grows with a time scale τ. A mode m changes from instability to stability as $1/\tau$ passes through zero. If E and its time derivative can be evaluated, then a time scale for each of the processes n can be computed and the sum of their inverses is $1/\tau$. These zeros of $1/\tau$, like the surface waves and gravitational radiation from which they originate, depend on the rate of rotation of the star Ω. They will be different for each $m = l$ mode, so we denote them by Ω_m.

Stars are stable against the $l = m$ mode at rotational frequencies that are less than Ω_m. So the smallest of these critical frequencies sets the limit for the rotation of the star. A star with greater than this limiting frequency will develop an instability that causes a rapid loss of angular momentum through gravitational radiation until its frequency falls below the critical value. The problem then is to evaluate these critical frequencies

and determine the smallest of them for a given mass star.

This is a difficult program—to find the surface vibrations of a rotating star and determine the rotational frequency of the star at which they change from instability to stability. It has never been performed for a rotating star in General Relativity. Newtonian or post-Newtonian physics is sometimes used and frequently the modes of a nonrotating star have been investigated, the idea being that the frequencies of these superficial surface waves, as seen in the rotating frame fixed to the star, will be quite similar to those of a nonrotating star.

Suppose we consider, as an example, shear viscosity and gravitational radiation-reaction as the relevant phenomena in the perturbation. The problem is then to find the frequencies Ω_m that satisfy

$$0 = \frac{1}{\tau_{V,m}(\Omega_m)} + \frac{1}{\tau_{G,m}(\Omega_m)} \,. \tag{6.54}$$

The first term refers to viscosity and the second to gravitational radiation-reaction.

The viscous timescale was computed for a nonrotating spheroid by Lamb (1881):

$$\tau_{V,m} = \frac{1}{(2m+1)(m-1)} \frac{R^2 \overline{\rho}}{\eta} \tag{6.55}$$

where η is the viscosity coefficient, R is the radius of the spheroid and $\overline{\rho} = M/\big((3/4)\pi R^3\big)$ is the average density. To relate the viscosity to the temperature and average density of a star, we adopt the expression [261, 262]

$$\eta = 347\, \overline{\rho}^{9/4}/T^2 \tag{6.56}$$

where $\overline{\rho}$ is the density in g/cm^3, T is temperature in Kelvin, and η is the shear viscosity in g/(cm s).

Detweiler [263] computed the damping time for gravity waves due to a surface wave of frequency $\omega(0)$ traveling on a nonrotating fluid sphere of radius R and found that

$$\tau_{G,m} = \frac{4m(m-1)^2(2m+1)[(2m-1)!!]^2}{3(m+1)(m+2)\,\omega^{2m+2}(0)\,R^{2m+1}} \,. \tag{6.57}$$

The eigenfrequencies

$$\omega_m(0) = \sqrt{\frac{M}{R^3}\frac{2m(m-1)}{2m+1}} \tag{6.58}$$

were computed by Thomson (1863) [264] for an inviscid nonrotating star. Comins [265, 266] computed the timescale for damping or growth of a

perturbation on Maclaurin spheroids (incompressible, uniform density, hypothetical objects) including both viscosity and gravitational radiation-reaction. His complicated results were put into more tractable form by Lindblom [267] who expressed the solution of (6.54) in the form

$$\Omega_m = -\frac{\omega_m(0)}{m}\left[\alpha_m(\Omega_m) + \gamma_m(\Omega_m)\left(\frac{\tau_{G,m}}{\tau_{V,m}}\right)^{1/(2m+1)}\right]. \tag{6.59}$$

(By the conventions chosen, the counterrotating surface wave of angular velocity ω/m has a sign opposite to that of the star Ω.)

The functions α_m and γ_m are properties of the particular stellar model under consideration. In other words, they depend on the solution of the equations of stellar structure with a particular equation of state. In practice they have been computed for idealized equations of state, such as Maclaurin spheroids or polytropes. They do not depart far from unity over the entire frequency range Ω and in early work were approximated as such. Indeed, in a study of polytropes, it has been confirmed that Ω_m depends much more strongly on the radius and mass of the neutron star model (through $\tau_{V,m}$ and $\tau_{G,m}$) than on the polytropic index assumed in calculating α_m [268].

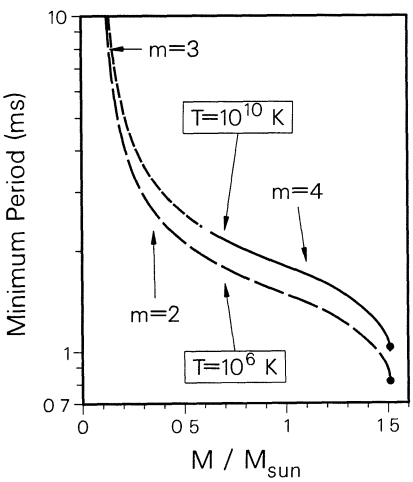

FIGURE 6.5. Minimum period that is stable against gravitational radiation-reaction moderated by viscosity for a hot and cold sequence of stars. The mode that establishes stability is shown by the value of m [248].

We illustrate the results of the above discussion for two temperatures in Fig. 6.5. As a typical example, we show the minimum stable period that a family of neutron stars can have in the face of viscosity-moderated gravitation, radiation-reaction instabilities [248]. The minimum stable period is a very strong function of the mass and radius of the star. For the limiting-mass star, the critical frequency varies typically by about 25%

among various models of the equation of state in theories for which the properties of symmetric nuclear matter are fixed within their known range [239].

A neutron star is born hot and cools during its life as an isolated star. If it is born with angular velocity above the limit established by the processes discussed above, the star will rapidly spin down until its frequency falls below that of the minimum stable mode. Thereafter, its frequency falls more slowly (due to the dipole radiation discussed in Chapter 5) on the timescale of the pulsar's active lifetime as a pulsar—an epoch of a few million years. Thus the minimum stable period of a hot star, illustrated in Fig. 6.5, establishes the rotational limit of the star during its lifetime as long as it remains isolated.[4]

For the limiting-mass star, the minimum period is about 1 ms as seen in Fig. 6.5. For comparison, the Kepler period of the limiting-mass star of this particular model is $P \sim 0.63$ ms [248]. Therefore, the gravitational wave instabilities set a more stringent limit on stable rotation than the mass-shedding limit for stars whose history has left them isolated from a companion.

On the other hand, the $T = 10^6$ K curve of Fig. 6.5 is relevant to old, cold stars that have acquired a companion and have been spun up and heated by accretion. In this case general relativistic instability is closer to the Kepler mass-shedding instability.

According to what has been said here, the typical limit on rotation of newly born stars is $P \geq P_{\rm limit} \sim 1$ ms and is set by the gravitational radiation-reaction instability as moderated by viscosity—not by the Kepler period. Typically we have found that the limit placed by gravitational wave instabilites on the rotational period is 30–40% larger than the Kepler period, according to the particular model of the star [146, 239]. However, the result mentioned is not firmly established. There are several reasons. One is that we are able to compute the Kepler period in General Relativity whereas the gravitational viscosity limits can be computed only under what might turn out to be severe limitations—Newtonian or post-Newtonian gravity, and under rough approximations to the actual structure of the star (such as Maclaurin spheroids or polytropes). If the gravitational viscosity limits were compared, instead, with the Newtonian Kepler frequency, the difference would be much smaller. What the difference would be if both were computed in the General Theory of Relativity taking full account of the structure of the star, we simply do not know.

There is a further complication. Ipser and Lindblom [269] have studied Newtonian models in which, in addition to the shear viscosity considered in this section, they have included, as well, estimates of the effect of bulk viscosity. They find that above $T \sim 10^{10}$ K the effects of bulk viscosity dom-

[4]Accretion from a low-mass companion may spin up an old cold star to a frequency higher than is possible for the stable rotation of a hot star.

inate and raise the critical frequency above the value it would otherwise have. Cutler, Lindblom, and Splinter have studied more general pulsations induced by the same processes in General Relativity for nonrotating stars and for a range of realistic stellar models rather than the idealized Maclaurin spheroids or polytropes [270]. They conclude that bulk viscosity will dominate over shear in the same high temperature era of the star which lasts for about a day [208].

Because of the absence of general relativistic calculations of possibly unstable modes in rotating stellar models, particularly realistic ones, it is unclear how important the gravitational-viscosity instability is—whether it causes, simply, a small reduction in stable frequency compared to the Kepler frequency or a large reduction as discussed above. From the point of view of fast pulsars and their evolutionary history, it appears to us that this is an important and fruitful area of investigation, albeit very complicated.

7

Limiting Rotational Period of Neutron Stars

7.1 Motivation

Pulsars have been identified with the theoretical objects called neutron stars. The identification is convincing—but not proved. The short rotational periods of millisecond pulsars inform us that the average density (and, therefore, the central density) must be very high—higher than the density of nuclei (5.8). The most obvious inference is that pulsars are the objects conceived of by Baade and Zwicky. However, there is another possibility that has such a fundamental implication that it should not be overlooked. We will find that the conventional interpretation of pulsars as neutron stars—or any any other type of star that is gravitationally bound—can be ruled out if any pulsar is found to rotate at a frequency above a certain limit.

The goal of this chapter is to establish the maximum rate of rotation sustainable by a neutron star. The Kepler frequency[1]—the frequency at which matter at the equator is shed—is the *absolute* limit for rotation. How large can that limit be for any conceivable neutron star model? What would be implied about a pulsar's constitution if it were observed to exceed such a limit?

Several authors have investigated how rapidly neutron stars can rotate based on particular theories of dense matter [185, 242, 243]. The minimum Kepler period for several neutron star models is $\sim$ 0.5 ms for $1.44M_{\odot}$ neutron stars.[2] Given the uncertainty in the equation of state in the high-density domain of matter, no decisive conclusion could be reached if a pulsar with a shorter period were found, save that none of those theories is correct. A decisive rotational limit for gravitationally bound (i.e., neutron) stars can be derived only from a set of constraints that do not exceed our certain knowledge and principles [188, 271].

Our approach is to formulate the least number of constraints that can

---

[1]Recall that the Kepler frequency is defined as the frequency of a particle in stable circular orbit at the circumference of a star. It is therefore also the frequency at which disruption of the star would occur.

[2]However it should not be concluded from the quoted literature that there are viable descriptions of neutron stars that can rotate at periods as low as 0.5 ms. It turns out that the central density of such models is so high as to invalidate the use of confined baryons in the calculation of the models (Section 10.3.3).

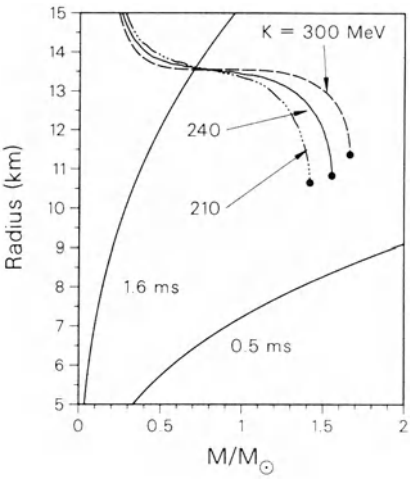

FIGURE 7.1. Generic relationships for neutron stars (or degenerate, relativistic, gravitationally bound stars in general) for several equations of state as labeled according to compression K (with $m^*_{sat.}/m = 0.78$). The limits imposed by a 1.6-ms and 0.5-ms pulsar are also shown by solid curves. Stars below them are stable for still shorter periods (see (7.1)).

be imposed with assurance on the equation of state and, within the class satisfying those constraints, find the highest possible rotational frequency of the corresponding neutron star models. The limit on rotation (as a function of stellar mass) is somewhat akin to the mass limit for neutron stars found by Rhoades and Ruffini [73].

So far we have spoken of neutron stars, but here we broaden the meaning of that name for the purpose of the limit derived in this chapter. A neutron star is bound by gravitational interaction. Above the density of approximately that of Fe^{56} atoms ($\sim$ 7.86 g/cm^3) the pressure of cold-catalyzed matter is positive and in the interior of the star, very large. The density is so great that nucleons reside in the range of the repulsive interaction of their neighbors. This repulsion (and the large Fermi energy) would blow the star apart into its constituents if gravity were turned off. As we know, relativistic stars have a limiting mass corresponding to any equation of state for dense matter. We also know the generic form of the mass–radius relationship for degenerate relativistic stars bound by gravity (Section 5.3.11). A star at the mass limit has the smallest radius, as illustrated in Fig. 7.1. It therefore can rotate more rapidly than any other star in the sequence according to the approximate expression for the Kepler frequency [185, 186, 75],

$$\Omega_K \approx 0.625(M/R^3)^{1/2}\,. \tag{7.1}$$

Although this result is Newtonian (5.7), reduced by the prefactor, it was justified for General Relativity in the proceeding chapter, and it is accurate to better than 10%. In this chapter, the term neutron star is used interchangeably with gravitationally bound star. We make a key distinction

between pulsars that are or can be gravitationally bound stars and those that cannot. The limit derived in the sequel is not only valid for neutron stars; it is valid for any conceivable star that is gravitationally bound.

One now glimpses the importance of the rotational limit. If it is violated by observation, then a type of star bound in the absence of gravity must exist—a self-bound star.[3] We discuss the possible existence and constitution of such stars in Chapter 10.

In the next sections, we enumerate the minimal constraints on the equation of state for finding the minimum rotational period of neutron stars, describe the variational ansatz and present the results that define the region in the mass-period plane inaccessible to neutron stars. We also derive a limit on rotational period for any star that follows from the structure of Einstein's equations alone [188]. Of course, such a limit lies below the limit for neutron stars since fewer constraints are involved. We then discuss the conclusion one would be forced to draw if a pulsar were found in the region forbidden to neutron stars but allowed by General Relativity.

7.2 The Minimal Constraints

We adopt the following as the minimal principles and constraints for finding the minimum rotational period of *gravitationally* bound stars (which means, in practice, neutron stars):

1. Einstein's general relativistic equations for stellar structure hold.

2. The matter of the star satisfies $dp/d\rho \geq 0$ which is a necessary condition that a body is stable, both as a whole and also with respect to the spontaneous expansion or contraction of elementary regions away from equilibrium (Le Chatelier's principle).

3. The equation of state satisfies the causal constraint for a perfect fluid; a sound signal cannot propagate faster than the speed of light, $v(\epsilon) \equiv \sqrt{dp/d\epsilon} \leq 1$, which is also the appropriate expression for sound signals in General Relativity [272].

4. The high-density equation of state, whatever it is, matches, continuously in energy and pressure, the low-density equation of state of Baym, Pethick, and Sutherland [61].

The first two constraints are most secure. The causal constraint, as expressed here, is frequently invoked; most theories of dense matter obey it, at least to densities expected in neutron stars. Some theories, like the (σ, ω, ρ)

[3]By self-bound star, we mean a star that would be bound even in the absence of gravity.

nuclear field theory of Chapter 4, explicitly obey it at all densities. Strictly speaking, the expression $v(\epsilon) \equiv \sqrt{dp/d\epsilon} \leq 1$, even for a perfect fluid, refers to the signal speed only in a homogeneous body, if v is dependent on ϵ, and, in an inhomogeneous body, only if v is independent of ϵ. Nevertheless, it is a general causal constraint for a perfect fluid. It is not known how to impose a causal constraint on an imperfect fluid. However, the effect, on our results, of lifting the constraint $\sqrt{dp/d\epsilon} \leq 1$ is easily examined. The results of these tests and others are given in Section 7.5. The effect of the fourth constraint is also easily examined.

7.3 Variational Ansatz

In the 'low-density' region, up to some fiducial density ρ_0 near nuclear density, we use the equation of state of Baym, Pethick, and Sutherland [61] (referred to as BPS) for charge-neutral nuclear matter. Results from the work of Baym, Bethe, and Pethick [64] and of Siemens [63] were also employed in the above reference. We take the BPS equation of state to be reasonably constrained by the bulk properties of nuclear matter at the saturation density of nuclei. A tabulated entry in the BPS tables that is suitable for the fiducial density occurs at $\rho_0 = 0.1625\ \mathrm{fm}^{-3}$. (We have used a subscript "0" to denote the conditions at normal nuclear matter saturation density in other parts of this book. Because the fiducial density ought to be chosen close to that state, we use the same notation again, but understand that, in the present context, it simply represents the fiducial density close to saturation density.)

Beyond the fiducial density we represent the unknown equation of state by a parameterized form. As an option we allow for the possibility of a first-order phase transition of the type where the pressure is constant and the energy density increases linearly with baryon density over a certain range. This is the most extreme allowable form of an equation of state since it satisfies the equality in Le Chatelier's principle. Above the fiducial density or the phase transition region as the case may be, we adopt a 'gamma law' form. At the density at which the equation of state becomes acausal, we replace it by its causal limit. In summary the equation of state is continuous and defined by the following equations:

(a) low density:

$$\epsilon(\rho) = \epsilon_{BPS}(\rho), \qquad p(\rho) = p_{BPS}(\rho), \qquad \rho < \rho_0. \tag{7.2}$$

(b) phase-transition region:

$$\epsilon(\rho) = \frac{\rho}{\rho_0}\left(\epsilon_0 + p_0\right) - p_0, \qquad p(\rho) = p_0, \qquad \rho_0 \leq \rho \leq \rho_1 \equiv \rho_0 + \Delta, \tag{7.3}$$

where $\epsilon_0 \equiv \epsilon_{BPS}(\rho_0)$, $p_0 \equiv p_{BPS}(\rho_0)$. This satisfies the condition that the baryon chemical potential, $\mu(\rho) \equiv d\epsilon/d\rho =$ constant in the interval

Δ. This segment satisfies Le Chatelier's principle at its limit, namely, the equality in the second constraint.

(c) parameterized region:

$$\begin{aligned} \epsilon(\rho) &= \frac{A}{\gamma-1}\left(u^\gamma - u\right) + u\epsilon_1 + (1-u)(A-p_0)\,, \\ p(\rho) &= A\left(u^\gamma - 1\right) + p_0, \qquad \text{for } \rho_1 < \rho < \rho_s, \end{aligned} \tag{7.4}$$

where $u = \rho/\rho_1$ and $\epsilon_1 \equiv (\rho_1/\rho_0)(\epsilon_0 + p_0) - p_0$ if $\Delta \neq 0$ while $u = \rho/\rho_0$ and $\epsilon_1 \equiv \epsilon_0$ if $\Delta \equiv 0$. The second constraint requires that $A\gamma \geq 0$. If the equation of state (7.4) becomes acausal at ρ_s defined by $\left(dp/d\epsilon\right)_{\rho_s} = 1$ (at which density we denote the energy density and pressure by ϵ_s, p_s), we replace it thereafter by

(d) causal limit:

$$\epsilon(\rho) = \epsilon_s - p_s + p(\rho),$$

and

$$p(\rho) = \frac{1}{2}\left\{p_s - \epsilon_s + (p_s + \epsilon_s)\left(\frac{\rho}{\rho_s}\right)^2\right\}, \qquad (\text{for } \rho \geq \rho_s). \tag{7.5}$$

In passing we note that Le Chatelier's principle at its extreme $dp/d\rho = 0$, or, equivalently, $p =$ constant, also corresponds to the mixed phase of a one-component system undergoing a first-order phase transition. This is a special and extreme example of a first-order phase transition. In multi-component systems with a first-order phase transition, in general, the pressure is not a constant in the mixed phase but rather is an increasing function of density on an isotherm [145]. Nevertheless, we shall refer to the special region, $p =$ constant as a condensate, or phase-transition region. Since compact baryon stars in equilibrium have particles carrying both baryon or electric charge or both, a first-order phase transition region, if it exists, will almost certainly be of the multicomponent type for which $dp/d\rho > 0$. (See Chapter 9.)

7.4 Limiting Value of Rotational Period as a Function of Mass

The maximum-mass star $M_{\max}$ in the sequence of gravitationally bound compact stars belonging to a given equation of state has the minimum Kepler period since the mass is largest and the radius is smallest (7.1). Therefore, we can incorporate the minimal constraints into a variational search over A, γ, and Δ for the lower limit on the rotational period of a neutron star as a function of maximum mass $M_{\max}$ by minimizing the function $f(M,P) = w_1(M - M_{\max})^2 + w_2 P^2$, where w_1 and w_2 are weights. We use a modified Levenberg–Marquardt method [273] for finding the minimum

of a nonlinear function of its arguments. The function has its minimum when $M = M_{\max}$ and P is the least possible Kepler period for that mass. Of course, $M_{\max}$ and P depend nonlinearly on the parameters mentioned above through the solution of Einstein's equations. An absolute limit on the angular velocity Ω or corresponding period of rotation $P = 2\pi/\Omega$ is

$$P_K \approx 10.1\left(\frac{R^3}{M}\right)^{1/2} = 0.0276\left(\frac{(R/\mathrm{km})^3}{M/M_\odot}\right)^{1/2} \quad \mathrm{ms}. \tag{7.6}$$

We have used the approximation (7.1).

The results are summarized in Fig. 7.2. We show the minimum Kepler periods for stellar sequences that are subject to the above constraints as a function of the corresponding maximum (limiting) mass star. Neutron stars cannot lie below the solid curve of this figure within the narrow limits discussed in detail below. We also show Kepler periods for the sequence whose maximum mass is $1.8M_\odot$. As an example, a neutron star of canonical mass $1.442M_\odot$ cannot have a rotational period less than 0.33 milliseconds if the equation of state does not have a first-order phase transition. If it does, the period can be further reduced by 0.01 ms, which falls within the uncertainty of (7.6). In Section 7.6 we derive a region forbidden by the structure of General Relativity. It is also shown in the figure.

We compare the two equations of state that yield the minimum period (within the 0.01 ms quoted above) for a $1.442M_\odot$ star in Fig. 7.3 (they are the bottom two curves, one having a constant pressure phase-transition region, the other not). The radii of the corresponding static stars are 6.19 and 6.32 km, respectively, and the central energy densities are 26.1 and 26.0 times normal nuclear saturation density ($\epsilon_0 \approx 2.5 \times 10^{14}$ g/cm^3 = 0.71 fm^{-4} = 140 MeV/fm^3). The high density required of neutron star models (see Fig. 7.4), if they are to withstand short rotational periods, has been cited as reason enough to suspect that short-period pulsars, if they exist, are not neutron stars [274, 275].

The energy density profiles at the edges of two optimally configured spherical neutron stars, the rotating counterparts of which are stable to mass shedding at $P \sim 0.33$ ms, are shown in Fig. 7.5. The notable features of these stellar profiles are the nearly uniform interior density and the rapid drop in density very close to the edge. These features are characteristic of an equation of state stiff at high density and very soft at intermediate, features that promote stability to fast rotation [243, 215].

The fiducial density is at $\epsilon \approx 0.7$ fm^{-4}, and the bulge in both profiles in Fig. 7.5 below this density corresponds to neutron star matter below the density of nuclear matter represented by the BPS equation of state. It should be noted that the subnuclear crust (magnified in this figure by the suppressed origin) is actually very thin ~ 0.2 km. (The radii of these stars, as quoted above, lie more than five decades in density below the lowest value of the abscissa in Fig. 7.5.) For comparison we show the profile of

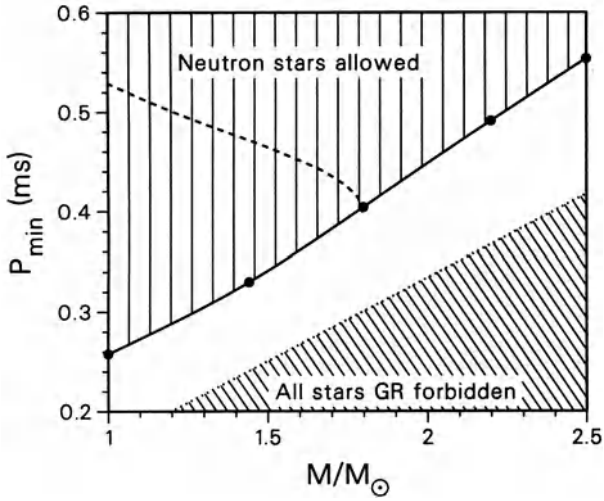

FIGURE 7.2. Minimum rotational period of neutron stars (solid curve). Calculated points are shown by dots. Periods of a sequence of stars whose maximum mass is $1.8M_\odot$ (dashed line). Region forbidden by structure of General Relativity (modulo the approximate formula (7.6)) (diagonal shaded region). [188]

a limiting star of the same mass whose Kepler period is 0.5 ms. This is a more conventional neutron star model. It is evident that, to attain the slightly smaller limiting period of 0.33 ms, the structure of the star and the underlying equation of state must be radically different. The central energy density of the spherical star, with the 0.5 ms Kepler period for the rotating counterpart, is $18.6\epsilon_0$.

It may be of some interest that the Oppenheimer–Volkoff limiting-mass star corresponding to an ideal neutron gas has $M = 0.72M_\odot$, $R = 9.6$ km and, for the rotating counterpart, a Kepler period of $P = 0.98$ ms. This star lies far above the scale of Fig. 7.2. The Rhoades–Pietronero–Ruffini maximum mass star has $M = 3.2M_\odot$, $R = 13.7$ km, and the rotating counterpart has Kepler period $P = 0.79$ ms and lies about 0.1 ms above the projection of our limiting curve.

7.5 Test of Sensitivity of Results

We discuss the accuracy with which the limiting curve dividing the period-mass plane into regions accessible and inaccessible to neutron stars is determined. Our tests are performed for a canonical mass of $1.442M_\odot$ since this

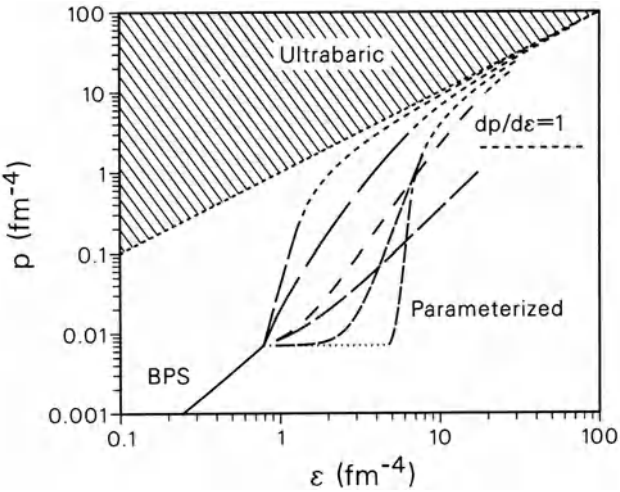

FIGURE 7.3. Bottom two equations of state produce minimum rotational period for a 1.442-$M_\odot$ neutron star, one with condensate ($p =$ constant region) and the other without. Others illustrate the flexibility of the simplest parameterization, (7.3–7.5). The three segments of each are (a) BPS, (b) parameterized region, and (c) causal limit, $dp/d\epsilon = 1$. Ultrabaric region has $p > \epsilon$. Its boundary is $p = \epsilon$. This region is inaccessible from below when $dp/d\epsilon \leq 1$.

is likely to be near the mass of most neutron stars produced in supernova. (It is commonly accepted that the favored mass lies in a rather narrow range (around the Chandrasekhar limit) which establishes the mass of the iron core of the progenitor star.)

The sensitivity of the results to the choice of a 'low-density' equation of state was tested by setting the pressure to zero at and below the fiducial density. The corresponding period is thereby reduced by a small amount, 0.014 ms. This extreme softening permits the greatest compaction at the surface and therefore the greatest stability to mass shedding. No other low-density equation of state, having the same pressure and energy at saturation, could give a lower value for the limiting period.

We remark here that some early calculations [78] of purely neutron matter which neglect the penalty of the high-isospin asymmetry imposed by the nuclear force actually predict bound neutron matter at a density near normal nuclear density. However, the Fermi energy contributes only about one-half of the value of the symmetry coefficient in the empirical mass formula, the remainder arising from the isospin part of the nuclear force. This part is neglected in the work that finds neutron matter to be bound. If neutron matter were bound, then $p = 0$ at its equilibrium density. This defines the

edge of the star which would occur near nuclear density ($\sim 2.5\ 10^{14}$ g/cm^3), as in the above test, instead of at the density of iron (~ 7.86 g/cm^3), as for the lowest energy state of cold-catalyzed matter [23]. So our test embraces the extreme case of bound neutron matter. However, there is no reason to expect neutron matter to be bound. Nuclei of Z very different from N become increasingly less bound with increasing $(N-Z)^2$, which gives rise to the well known "valley of stability" (4.106).

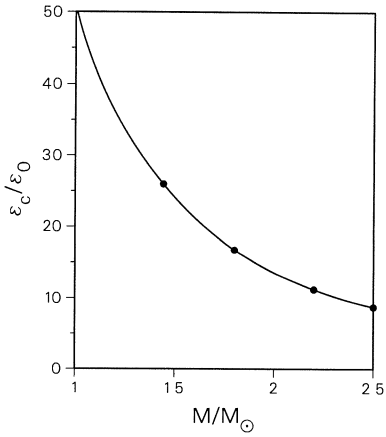

FIGURE 7.4. Least possible central energy density in units of normal nuclear saturation density for the nonrotating neutron stars whose rotating counterparts have the shortest possible Kepler period, namely those corresponding to Fig. 7.2.

We have already stated the result that the shortest period of a $1.442 M_\odot$ star can be reduced by 0.01 ms below 0.33 ms if the equation of state is allowed to have a region of constant pressure as a function of density. Such an equation of state satisfies Le Chatelier's principle at its limit (the equality in the second constraint). This is true whether we take the density of the onset of the constant pressure region lying near nuclear density or above. By the test of the second paragraph in this section, the maximum reduction in period that can be gained by having the onset of the region of constant pressure occur at a lower density than fiducial is < 0.014 ms.

The effect of a specific choice of fiducial density ρ_0 in the range 0.1484–0.1814 fm^{-3} near nuclear saturation amounts to an uncertainty in the minimum period of only ± 0.001 ms for our canonical neutron star.

The parameterization of the equation of state used above and the flexibility to reach the limit allowed by Le Chatelier's principle, through the inclusion of a phase transition with constant pressure, is illustrated by the extremes in Figs. 7.3 and 7.5. The parameterization apparently represents a very flexible family within which we search for a minimum period. To test this conjecture we also expanded the variational ansatz with two additional powers of density to find whether our limit can be significantly

lowered. The expanded ansatz is

$$\begin{aligned}\epsilon(\rho) &= \frac{A}{\gamma-1}(u^\gamma - u) + \frac{B}{\gamma-2}(u^{\gamma-1} - u) + \frac{C}{\gamma-3}(u^{\gamma-2} - u) \\ &\quad + u\epsilon_0 + (1-u)(A+B+C-p_0)\,, \\ p(\rho) &= A(u^\gamma - 1) + B(u^{\gamma-1} - 1) + C(u^{\gamma-2} - 1) + p_0\,, \end{aligned} \tag{7.7}$$

where $B > 0$, $C > 0$ are additional parameters that are varied to minimize the period at a given mass. (The restriction to positive values assures that the second constraint is always satisfied when $\gamma > 2$.) The result is that the period could be reduced by only 0.003 ms for a 1.442-$M_\odot$ star, a very small reduction (1%) for an ansatz with two additional parameters.

It is believed that a signal in any medium cannot propagate faster than the speed of light. Nevertheless, the principle of causality (the usual phrase employed to state this belief) does not follow from Lorentz invariance [276]. Although searches for tachyons have so far proved fruitless, the principle is not thereby proved. Moreover, it is not known what condition the equation of state of an imperfect fluid should satisfy so that superluminal signals are not attained. Therefore, we test the effect on the minimum rotational period if the causal constraint is lifted. The result is that the period can be reduced by 0.037 ms. This is the largest of the uncertainties.

All of the above quoted uncertainties are small and lie within the accuracy of the means of estimating the Kepler period (7.6), save the relaxation of the 'causal' constraint, which is slightly larger. We conclude that the solid line of Fig. 7.2 marks the lower boundary for neutron stars rather accurately. Moreover, as pointed out in Section 7.7, gravitational wave instabilities (section 6.10) are expected to occur at periods longer than the Kepler period. So, the latter is an absolute bound.

We have not questioned the validity of General Relativity as a theory underlying the structure of compact stars. The value of M/R for the limiting-mass star in various models of the equation of state is generally found to lie in the range of $0.2 - 0.3$. For our minimally constrained models designed to minimize the rotational period, the value of $M/R \approx 0.34$. Solar system phenomena (such as the advance of the perihelion of planets) test General Relativity only in the weak field limit where the surface gravitational field of the sun is $M/R < 2 \times 10^{-6}$.

Recent experimental results, derived from nearly two decades of accurate timing observations on the binary neutron star system PSR 1913+16 [4, 36], test the theory in much stronger gravitational fields. The conclusion is that correct theories of gravity are tightly constrained. Einstein's theory lies at the center of the constrained region. It appears that there is little ground for questioning the appropriateness of the usual equations for relativistic stellar structure. In any case, we do not know how to assess an error to the first constraint if the correct theory is even a small variant of the usual one.

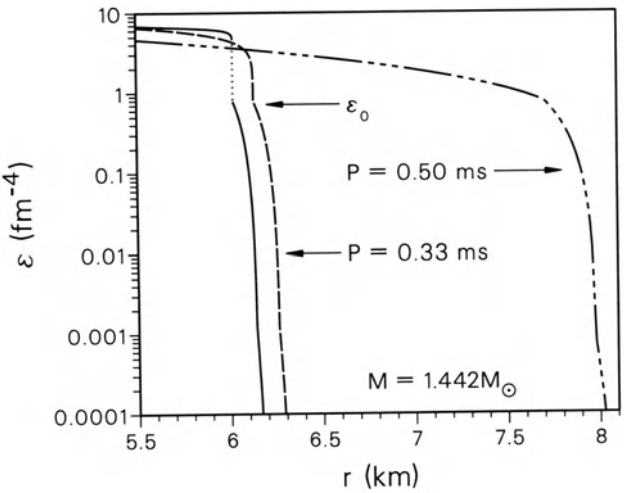

FIGURE 7.5. Density profiles of the edges ($R \sim 6.2$ km) of the two limiting-mass spherical stars corresponding to the bottom two equations of state of Fig. 7.3 each with mass $1.442 M_\odot$ and Kepler periods for rotating stars of 0.32 and 0.33 ms for the solid and dashed cases, respectively. The phase-transition region ($p =$ constant) corresponds to the discontinuity in density (dotted). The other profile is ($R \sim 8$ km) for the same limiting mass but Kepler period of 0.5 ms.

7.6 General Relativistic Limit on Rotation

Interestingly, a limit on rotation can be derived by assuming only that Einstein's equations of stellar structure hold [188]. Then $M/R < 4/9$ for any static star as, we saw in Section 3.12. Using the approximate relationship (7.6), we obtain

$$P \approx 10.1 M \left(\frac{M}{R}\right)^{3/2} > \frac{273}{8} M = 0.167 \frac{M}{M_\odot} \text{ ms} \qquad \text{(any star)}, \tag{7.8}$$

which, for a star of mass equal to that of PSR1913+16 yields $P > 0.24$ ms. Since the limit on M/R follows from the structure of Einstein's equations, the above limit on period applies both to neutron stars as well as to hypothetical stars made of self-bound matter. The forbidden region is marked in Fig. 7.2.

7.7 Discussion and Alternatives

So far as is known, all stars are bound by gravity including neutron stars and hybrid stars—the form neutron stars take if the pressure in the core is sufficiently high to convert nucleons to quark matter (Chapter 9). Other types of stars have been conceived but not identified [277, 278, 279]. They are made of hypothetical matter that is self-bound and absolutely stable at high density. Such stars would not be subject to the limit on rotation of a gravitationally bound star and could, if self-bound at sufficiently high density, rotate at periods below that limit [275]. We will return to this alternative in Chapter 10.

The purpose of this chapter is to provide a decisive means of distinguishing pulsars that can be (but are not necessarily) gravitationally bound, compact stars, like neutron or hybrid stars,[4] from those that cannot be bound by gravity alone. The limit that we have obtained for the rotational period as a function of stellar mass is necessarily more severe than would be obeyed by real neutron stars because there is no physical principle that requires the equation of state to minimize the rotation period. Moreover, there are unstable pulsation modes of a rotating star associated with gravitational radiation-reaction [260, 259, 280] which occur at periods larger than the Kepler period [267, 281, 239, 146, 269] (see Chapter 6). If a pulsar has a rotation period smaller than any of the periods for these critical modes, it will spin down by gravitational radiation until its period approaches that of the largest of the unstable modes (Section 6.10). However, the physics that enters the estimate of these instabilities is far less certain than that which determines the Kepler period, so we use this absolute lower bound of a uniformly rotating star. Therefore, if a pulsar with rotation period and mass falling below our limiting curve is found, it actually lies even further below the limit established by nature for neutron stars.

There is a region in the period-mass plane below that allowed to neutron stars and above that forbidden by General Relativity (Fig. 7.2). What could be the general nature of a star that might fall in this intermediate region? The only general category of stars that could have smaller rotation periods than neutron stars is the category of stars that are made of hypothetical matter that is stable and self-bound in bulk at sufficiently high equilibrium energy density [275, 215].

The limiting rotational period of a star composed of matter that is self-bound ($p = 0$) at the equilibrium energy density ϵ_e is trivial to establish. Since the density (and pressure) decrease monotonically from the center to the edge of a star, it follows that the energy density (and the average,

[4]Hybrid stars denote neutron stars in which the central part is composed of quark matter or the mixed phase of quark and neutron star matter. They are the subject of Chapter 9.

in particular) satisfies $\bar{\epsilon} \geq \epsilon_e$. The equality holds only when gravity is negligible, meaning that the mass is small. The average density also satisfies the identity $M \equiv (4\pi/3)R^3\bar{\epsilon}$. Using this relationship in (7.6), we have $P_K = 1.6(3\pi/\bar{\epsilon})^{1/2} < 1.6(3\pi/\epsilon_e)^{1/2}$. Observing also the limit imposed on M/R by General Relativity (7.8), we write

$$1.21\left(\frac{\epsilon_0}{\epsilon_e}\right)^{1/2} > \frac{P_K}{\text{ms}} > 0.167\,\frac{M}{M_\odot} \qquad \text{(self-bound star)}, \tag{7.9}$$

where $\epsilon_0 \approx 140$ MeV/fm^3 is the equilibrium energy density of normal nuclear matter.

From the above equation, it is clear that, if ϵ_e is large enough (a few times nuclear density), the period of a self-bound star can lie in the region prohibited to neutron stars. Such a star's energy profile is unlike those of Fig. 7.5; instead, the star has a sharp edge at which the energy density falls from the high equilibrium value of the bound matter to zero in a strong interaction length (Fig. 8.1). Such a star has a small radius for its mass as compared to a gravitationally bound star (Fig. 10.1). This is what permits it to rotate rapidly without shedding matter at its equator. In passing we note the limit placed on the equilibrium density of self-bound matter by the general relativistic inequality $M/R < 4/9$ (3.132):

$$\epsilon_e \leq \bar{\epsilon} < \left(\frac{4}{9}\right)^3 \frac{3}{4\pi}\frac{1}{M^2} = 52\left(\frac{M_\odot}{M}\right)^2 \epsilon_0\,. \tag{7.10}$$

In the event that self-bound matter exists in bulk, objects from microscopic nuggets to stars could exist, limited in mass only by gravitational collapse [282, 283]. Gravity plays the minor role of preventing self-bound stars from fissioning into smaller bound fragments except by the addition of sufficient energy to compensate for the creation of additional surface area.

The most likely candidates for stars made of matter that is self-bound at high density are strange stars, hypothetical stars composed of almost equal numbers of up, down, and strange quarks. Strange quark matter was hypothesized to be the absolute ground state of the strong interaction by Bodmer [284] and Witten [277, 285] independently. We will study the hypothesis and its consequences in detail in Chapter 10. Several recent accounts can be found in Refs. [275, 286]. As it turns out, the hypothesis is quite plausible on the basis of scale arguments—and very difficult either to prove or disprove (Chapter 10).

Another candidate in the category of self-bound stars is the so called Q-star [287, 279]. These have been discussed as exotic solutions of effective nuclear field theories. While exotic solutions of fundamental theories, such as the sphaleron [288] of the classical Weinberg–Salam theory of the electroweak interaction, must be taken seriously, the status of an exotic solution of an effective theory is much more tenuous. Moreover, the properties of hypothetical Q-stars, whether dilute, very large and of many solar masses, or

dense, small and of solar mass, are not delimited by any known physics. In contrast, the argument for the possible existence of strange stars depends on simple physics and the QCD energy scale which place the energy per nucleon of strange matter close to the nucleon mass, the only uncertainty being whether a fraction of a nucleon mass above or below [277, 275].

7.8 Summary

A neutron star cannot have a period for uniform rotation (the rotation that minimizes the mass-energy at fixed baryon number [244]) that lies more than a few percent below the solid curve of Fig. 7.2. For a 1.442-$M_\odot$ neutron star, this means that the period must exceed $0.33^{+0.03}_{-0.04}$ ms where the upper error is that of (7.6) and the lower is the largest of the test errors and corresponds to lifting the causal constraint appropriate for a perfect fluid (where 0.037 is rounded to 0.04). This curve refers to the mass-shedding limit (Kepler period). Gravitational-wave instabilities will actually set a more stringent lower bound that lies above our curve. The most conservative bound for the region excluded to neutron stars is the one adopted here.

If a pulsar is found with mass and period that place it below our critical curve, it must be an object different from a neutron star. It appears that the only alternative for breaking the limit on gravitationally bound stars is a state of matter that is self-bound in bulk at an energy density larger than normal nuclear matter by a factor of five to ten. The most plausible candidate to date, in our opinion, is strange quark matter. We introduce quark matter in the next chapter in preparation for a study of hybrid stars in Chapter 9 and strange stars in Chapter 10. Hybrid stars are gravitationally bound objects similar to neutron stars. Strange stars are entirely different objects. They would be bound by the strong interaction even in the absence of gravity.

8

Quark Stars

8.1 Introduction

Quark or hybrid neutron-quark stars are composed, in whole or in part, of quark matter. Such a state of matter was conceived soon after the realization that quarks, the constituents of nucleons, are asymptotically free. At the extreme of asymptotic momentum transfer, density, or temperature, quarks are free of interaction. Under such circumstances the individuality of nucleons is lost, and the quarks of nuclear matter are free to explore a much larger "colorless" region of space referred to as quark matter.

The deconfined phase of quark matter is of interest in astrophysics for a number of reasons. First, the universe likely passed through this phase in the first few seconds. Second, the conditions in the cores of neutron stars may be such that ordinary hadronic matter in which quarks are confined in individual hadrons is converted by high pressure to quark matter, forming a hybrid star—a star with a quark matter central region and a nuclear matter mantle. Third, it is conceivable that strange quark matter may actually be the ground state of the strong interaction rather than the state of nucleons and nuclei. In this case pulsars could be strange quark stars instead of neutron stars. In this chapter we introduce material for a discussion of both hybrid stars (Chapter 9) and strange stars (Chapter 10). Because the stellar structure of the latter is simpler than the former, the illustrations of this chapter are of quark stars rather than hybrids.

We do not have a rigorous theory of dense nuclear matter. Quantum chromodynamics (QCD)—although believed to be essentially the fundamental theory at the nuclear and subnuclear scale—is not a theory from which we can derive practical results for the equation of state. We shall begin, therefore, with a simple model of quark matter based on the notion of asymptotic freedom, namely the MIT bag model [289]. The bag model is a simple tool compared to the nuclear field theory with which we attacked the more difficult problem of hadronic matter and neutron stars in Chapters 4 and 5. As a result, our work with quark and hybrid stars will be correspondingly simplified.

8.2 Quark Matter Equation of State

We derive expressions for the bag model equation of state of quark matter in several approximations. These will be useful to us later in connection

with the possible existence of neutron stars with quark matter cores.

In the simple model of free quarks in a bag, we derive analytical expressions for pressure, energy density, and the other properties from a Fermi gas of quarks in two limits,

$$1)\ \ T=0, m\neq 0 \quad \text{and} \quad 2)\ \ T\neq 0, m=0\,. \tag{8.1}$$

The pressure, energy density, baryon number density, and entropy density are

$$\begin{aligned}
p &= \sum_f \frac{1}{3}\frac{\gamma_f}{2\pi^2}\int_0^\infty k\frac{\partial\epsilon_f(k)}{\partial k}\Big[n(k,\mu_f)+n(k,-\mu_f)\Big]k^2dk - B\,,\\
\epsilon &= \sum_f \frac{\gamma_f}{2\pi^2}\int_0^\infty \epsilon_f(k)\Big[n(k,\mu_f)+n(k,-\mu_f)\Big]k^2dk + B\,,\\
\rho &= \sum_f \frac{1}{3}\frac{\gamma_f}{2\pi^2}\int_0^\infty \Big[n(k,\mu_f)-n(k,-\mu_f)\Big]k^2dk\,,\\
s &= \frac{S}{V} = \Big(\frac{\partial p}{\partial T}\Big)_{V,\mu_f}\,,
\end{aligned} \tag{8.2}$$

where $\epsilon_f(k) = \left(m_f^2+k^2\right)^{1/2}$ and

$$n(k,\mu_f) = \left(\exp\{[\epsilon_f(k)-\mu_f]/T\}+1\right)^{-1} \tag{8.3}$$

is the Fermi distribution function. The factor 1/3 occurs in the baryon density because there are three quarks per baryon. The bag pressure is denoted by B. It represents the positive energy shift per unit volume in the deconfined vacuum relative to the confined vacuum. The quark degeneracy for each flavor is $\gamma_f = 2_{\text{spin}} \times 3_{\text{color}}$.

Other properties of possible interest are, for example, the electric charge density or the strangeness,

$$q = \sum_f \frac{\gamma_f}{2\pi^2}q_f\int_0^\infty \Big(n(k,\mu_f)-n(k,-\mu_f)\Big)k^2dk\,, \tag{8.4}$$

where q_f is the quark electric charge for flavor f.

8.2.1 Zero Temperature

For the first of the two limiting cases above, the distribution functions become step functions at energy μ_f. In that case we can use standard integrals (Ref. [45]. p. 87) to express the results. For example,

$$\begin{aligned}
&\int_0^k \frac{k^4}{\sqrt{m^2+k^2}}dk\\
&= \frac{1}{4}\left[k^3\sqrt{k^2+m^2} - \frac{3}{2}m^2k\sqrt{m^2+k^2} + \frac{3}{2}m^4\ln\left(\frac{\sqrt{k^2+m^2}+k}{m}\right)\right].
\end{aligned}$$

TABLE 8.1. The six known quarks, their masses and quantum numbers, baryon numbers, charges, isospin projections, strangeness, charm, beauty, and truth

Name	Mass (MeV)	b Number	q	i_3	s	c	b	t
u	5	1/3	2/3	1/2	0	0	0	0
d	7	1/3	−1/3	−1/2	0	0	0	0
s	150	1/3	−1/3	0	−1	0	0	0
c	1500	1/3	2/3	0	0	1	0	0
b	5000	1/3	−1/3	0	0	0	1	0
t	>100000	1/3	2/3	0	0	0	0	1

We find

$$
\begin{aligned}
p &= -B + \sum_f \frac{1}{4\pi^2}\left[\mu_f k_f(\mu_f^2 - \frac{5}{2}m_f^2) + \frac{3}{2}m_f^4 \ln\left(\frac{\mu_f + k_f}{m_f}\right)\right], \\
\epsilon &= B + \sum_f \frac{3}{4\pi^2}\left[\mu_f k_f(\mu_f^2 - \frac{1}{2}m_f^2) - \frac{1}{2}m_f^4 \ln\left(\frac{\mu_f + k_f}{m_f}\right)\right], \\
\rho &= \sum_f \frac{k_f^3}{3\pi^2}, \qquad (8.5)
\end{aligned}
$$

where k_f is the Fermi momentum for flavor f defined in terms of the chemical potential, $\mu_f = (m_f^2 + k_f^2)^{1/2}$. The above results are suitable for compact star calculations in which the nucleons are believed to be dissolved into quarks by the high pressure in the interior of the star; since temperatures of neutron stars, shortly after birth, have fallen to the KeV region (which is negligible on the nuclear scale), the zero temperature limit is appropriate.

8.2.2 Massless quark approximation

We can also obtain analytic expressions if the quarks are massless, even if the temperature is finite. After some manipulation and using the standard integrals,

$$
\int_0^\infty dx \frac{x}{1+e^x} = \frac{\pi^2}{12}, \qquad \int_0^\infty dx \frac{x^3}{1+e^x} = \frac{7}{120}\pi^4, \qquad (8.6)
$$

we obtain the explicit forms

$$
\begin{aligned}
p &= \sum_f \left(\frac{7}{60}\pi^2 T^4 + \frac{1}{2}T^2\mu_f^2 + \frac{1}{4\pi^2}\mu_f^4\right) - B, \\
\epsilon &= 3p + 4B,
\end{aligned}
$$

$$\begin{aligned}\rho &= \sum_f \frac{1}{3}\Big(T^2\mu_f + \frac{\mu_f^3}{\pi^2}\Big)\,,\\ s &= \sum_f \Big(\frac{7}{15}\pi^2 T^3 + T\mu_f^2\Big)\,.\end{aligned} \tag{8.7}$$

For the massless Bose gas of gluons of degeneracy $\gamma_g = 2\times 8_c$, we similarly obtain the contributions

$$\begin{aligned}p &= \frac{8\pi^2}{45}T^4\,,\\ \epsilon &= 3p\,,\\ s &= \frac{32\pi^2}{45}T^3\,,\end{aligned} \tag{8.8}$$

where we use

$$\int_0^\infty \frac{x^3\,dx}{e^x-1} = \frac{\pi^4}{15}\,. \tag{8.9}$$

As an example, the pressure for massless quarks and gluons is found to be

$$p = \frac{8\pi^2}{45}T^4 + \sum_f\Big(\frac{7}{60}\pi^2T^4 + \frac{1}{2}T^2\mu_f^2 + \frac{1}{4\pi^2}\mu_f^4\Big) - B\,, \tag{8.10}$$

with $\epsilon = 3p + 4B$ and no changes in ρ or s.

The lowest order gluon interactions have been calculated [290, 291, 292] and result in the following modification:

$$\begin{aligned}p = -B &+ \frac{8\pi^2}{45}T^4\Big(1-\frac{15\alpha_s}{4\pi}\Big)\\ &+\sum_f\Big[\frac{7}{60}\pi^2T^4\Big(1-\frac{50\alpha_s}{21\pi}\Big) + \Big(\frac{1}{2}T^2\mu_f^2 + \frac{1}{4\pi^2}\mu_f^4\Big)\Big(1-\frac{2\alpha_s}{\pi}\Big)\Big]\end{aligned} \tag{8.11}$$

with corresponding changes in ϵ, $s = \partial p/\partial T$, and $\rho = \frac{1}{3}\sum_f \partial p/\partial\mu_f$. The coupling constant is denoted by α_s.

8.2.3 First order in α_s

The thermodynamic potential to first order in the strong interaction coupling constant has been obtained in the literature (see [285] and references therein). Renormalized at the scale σ, the result is

$$\Omega_f = -\frac{\gamma_f}{24\pi^2}\Big\{\mu_f\sqrt{\mu_f^2-m_f^2}(\mu_f^2-\frac{5}{2}m_f^2) + \frac{3}{2}m_f^4\ln\Big[\frac{\mu_f+\sqrt{\mu_f^2-m_f^2}}{m_f}\Big]$$

$$
\begin{aligned}
- \quad & \frac{2\alpha_s}{\pi}\left[3\left(\mu_f\sqrt{\mu_f^2-m_f^2}-m_f^2\ln\left[\frac{\mu_f+\sqrt{\mu_f^2-m_f^2}}{\mu_f}\right]\right)^2\right. \\
- \quad & 2\left(\mu_f^2-m_f^2\right)^2-3m_f^4\ln^2\left(\frac{m_f}{\mu_f}\right) \qquad (8.12) \\
+ \quad & \left.\left.6\ln\left(\frac{\sigma}{\mu_f}\right)\left(\mu_f\sqrt{\mu_f^2-m_f^2}m_f^2-m_f^4\ln\left[\frac{\mu_f+\sqrt{\mu_f^2-m_f^2}}{m_f}\right]\right)\right]\right\},
\end{aligned}
$$

where μ_f, and m_f denote the chemical potential and mass of the quark flavor f, $(f = u, d, s, c)$ and $\gamma_f = 2 \times 3_{\text{color}}$ is the degeneracy. (A sign error in the quoted literature has been corrected in the above expression for Ω_f.) The renormalization scale σ should be typical of the chemical potentials of the problem, and we set $\sigma = 300$ MeV. The thermodynamic potentials for the electron (0.511 MeV) and muon (106 MeV) are given also by the above expression with the omission of the α_s terms and the replacement of the degeneracy factor γ_f by that of the leptons, $\gamma_\lambda = 2$. The quark number densities, baryon number density, charge density, energy density and pressure are given by

$$n_f = -\partial\Omega_f/\partial\mu_f\,, \tag{8.13}$$

$$\rho = \frac{1}{3}\sum_{u,d,s,c} n_f\,, \tag{8.14}$$

$$q = \sum_i n_i q_i\,, \tag{8.15}$$

$$\epsilon = B + \sum_i(\Omega_i + \mu_i n_i)\,, \tag{8.16}$$

$$p = -B - \sum_i \Omega_i\,, \tag{8.17}$$

where the sums over i extend over all four[1] quarks and the two leptons. The difference in the vacuum energy of confined and deconfined phases is denoted by B, and q_i denotes the electric charge on particle type $i = u, d, s, c, e^-, \mu^-$.

8.3 Quark Star Matter

As an example, we illustrate hypothetical stars made of quark matter. (We will discuss this topic at a more advanced level in the next two chapters.)

[1] We keep the charm quark only to be able to demsonstrate later that it is not a constituent of stable stars.

We have discussed the fact that stars are charge-neutral and in equilibrium; that is, they are a mixture of species in chemical equilibrium at a given temperature (effectively zero for a mature neutron star) and therefore in the lowest energy state at every density. Since the timescale of a star is effectively infinite compared to the weak interaction timescale, weak interactions violate strangeness conservation. The strangeness quantum number of quarks is therefore not conserved in a star. Any neutrinos or photons produced in the decay of a high-momentum u or d quark, near the top of the Fermi surface, to a low-momentum s quark will leak out of the star. The star's energy is thereby lowered both by loss of the neutrino and photon energy and by lowering of the average energy of the quarks. Chemical equilibrium is therefore found without regard to the conservation of quark strangeness. In other words, the strangeness chemical potential is set identically to zero.

We have derived expressions for the pressure and energy density of quark matter in terms of the quark chemical potentials above. To the energy density and pressure of quark matter, we need to add those of leptons so that charge neutrality can be achieved at the lowest energy. Expressions for these contributions can be found in the last terms of (5.47) and (5.48).

Let us consider how the chemical potentials are to be determined. According to the above discussion of strangeness nonconservation, the relationships between the quark chemical potentials are determined solely by conservation of electric charge and baryon charge. Possible transformations that conserve these charges (and not strangeness) can be inferred from Table 8.1:

$$\mu_u = (\mu_b - 2\mu_e)/3\,, \qquad \mu_d = (\mu_b + \mu_e)/3\,, \qquad \mu_s = (\mu_b + \mu_e)/3\,, \tag{8.18}$$

where, as usual, μ_e stands for the electron chemical potential (unit negative charge) and μ_b stands for the chemical potential for unit baryon charge (i. e., neutron, sometimes also denoted μ_n). From these we have the connections

$$\mu_d = \mu_u + \mu_e\,, \qquad \mu_s = \mu_d\,, \qquad \mu_c = \mu_u\,. \tag{8.19}$$

We can write the expression for the electric charge density of the quarks analogous to (8.5) and, taking account of leptons, write the condition for charge neutrality as

$$q = \sum_f \left(q_f \frac{k_f^3}{\pi^2} \right) - \frac{k_e^3}{3\pi^2} - \frac{k_\mu^3}{3\pi^2} = 0 \tag{8.20}$$

where the last two terms are the lepton contributions and

$$k_f = (\mu_f^2 - m_f^2)^{1/2}\,, \qquad k_e = (\mu_e^2 - m_e^2)^{1/2}\,. \tag{8.21}$$

Finally, the expression for the baryon number density in (8.5) or (8.13) provides a fifth relationship for the chosen density with which the six chemical

potentials $\mu_u, \mu_d, \mu_s, \mu_c, \mu_e$, and μ_μ can be determined at specified baryon density.

Knowing the quark chemical potentials, we can now compute the pressure and energy density of the quarks. Since the electron mass is small, it can be neglected or kept in expressions similar to (8.5) or (8.13–8.17) for the electron energy density and pressure contributions. The B should be dropped and electron statistical weight 2 substituted for quark weight 6; i.e., multiply p and ϵ by 1/3. The result is then added to the pressure and energy of the quarks to get the total. The procedure is similar for the muon whenever μ_e exceeds the muon mass. This provides a complete description in the approximation of the bag model to the equation of state for quark star matter.

8.4 Strange and Charm Stars

At first sight, the notion of pure quark matter stars may seem unrealistic. The normal expectation is that the phase of quarks confined in nucleons is the ground state of the strong interaction. Quark matter, if present in a neutron star, would exist only in the high-density interior. However, it is possible that three-flavor quark matter consisting of u, d, and s quarks may actually be the ground state of the strong interaction [284, 277]. In such a case, there could exist pure quark matter stars. We shall examine the *strange quark matter hypothesis* carefully in Chapter 10. In the meantime we use the simple equations of state developed above to discuss quark stars as hypothetical objects and contrast several of their features with neutron stars. (As a side issue, our study will be useful in bringing out some general points on stability.)

We employ the equation of state described above for cold quark star matter to compute the structure of quark stars. This is done by solving the Oppenheimer–Volkoff equations (3.21, 3.22) with the above equation of state for the pressure and energy density [293]. At low and moderate baryon densities (which we estimate from (8.5), putting $m_f = 0$ for ease), we shall find that the chemical potential for strange quarks (8.19) is larger than the strange quark mass. The strange quark must therefore be included in the description of quark stars having the density range typical of neutron stars.

The charm quark chemical potential (8.19) does not approach the magnitude of the charm quark mass in the same density range. Consequently, the charm quark is not populated except at density far above that found in neutron or analogous strange stars.[2] One is naturally led to ask if there is a

[2]We shall call a quark star after the most massive quark flavor with which it is populated. A strange star is composed of the three quark flavors u, d, s; a charm star of four flavors u, d, s, c.

sequence of stable charm stars above the neutron or strange star sequences. We address this question later in the chapter.

In the bag model of quark matter, the value of B determines whether strange quark matter has a lower ground state than hadronic matter in the confined phase. We will choose a value that yields a binding per baryon number $E/A \approx 928$ MeV for strange quark matter in equilibrium ($p = 0$). This value is slightly lower than the mass of the nucleon (and also of the energy per nucleon in the Fe^{56} nucleus ($\sim$ 931 MeV)). The value of B that yields $E/A = 928$, making strange matter absolutely stable (but just barely), is

$$B^{1/4} = 154.5$$

as in Fig. 1(a) of Ref. [285] for $m_s = 150$ MeV. In this case the star is devoid of nuclear matter. The entire compact star, including its surface region, is (strange) quark matter.

The edge of a star occurs at the radius where the pressure becomes zero. Zero pressure in the equation of state corresponds to equilibrium matter or else to zero density. Under the assumption of a bag constant that makes strange matter the absolute ground state, zero pressure corresponds to the equilibrium energy density of strange quark matter. Therefore the transition in a strange quark star at its edge is from a high interior density to zero on a length scale characterized by the strong interaction range—10^{-13} cm. The density at the inner edge is twice or more that of nuclear density ($\epsilon_0 \sim 2.5 \times 10^{14}$ g/cm^3; see (8.22) below). The strange star has an extremely abrupt edge; it probably has the hardest smoothest surface of any object in the universe.[3]

The edge of a neutron star is not nearly so abrupt as that of a strange star. Since neutron stars are made from material that has been processed in stellar evolution, ordinary iron forms their surface (page 73). The energy density of iron is only a few g/cm^3 or about 14 orders of magnitude less than the central energy density of the star. The density profile of a neutron star in contrast to a strange star therefore falls continuously from nuclear density to the density of iron. At the latter density, there is an abrupt transition to zero density on a length scale of atomic spacing in solid iron.

The density profile of three strange stars of differing mass are illustrated in Fig. 8.1. These results are similar to results of Haensel et al. [282] and of Alcock et al. [283]. Stellar edges all occur at $p = 0$ and therefore at the same (high) energy density corresponding to equilibrium. The stellar interiors are more or less compressed according to mass (weight of the overlying

[3]The skin thickness of a nucleus is also of the same order as that of a strange star, 10^{-13} cm. The cause is the same in each case—the range of the force that binds—the strong force. It is only the small radius of the one and the large radius of the other that makes the skin thickness of the star seem unusually small. Given the short range of the strong interaction, it is of course immaterial to the skin thickness how much matter lies interior to the skin.

matter). The quark populations of the most massive of them are shown in Fig. 8.2. There we see that electron populations are five orders of magnitude less than quark populations. This is another example in which charge neutrality is achieved more economically among the conserved baryon-carrying particles.

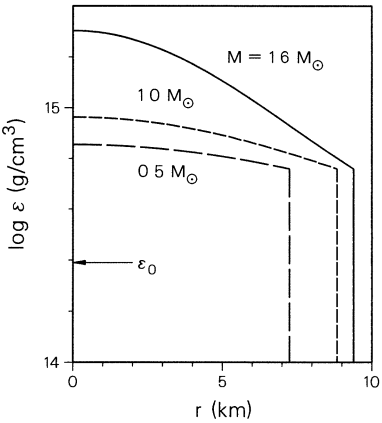

FIGURE 8.1. Density profiles of three strange quark stars of indicated masses.

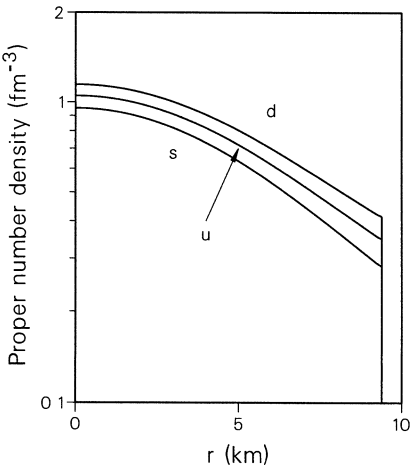

FIGURE 8.2. Quark populations of a $M = 1.6M_\odot$ strange star (close to the limiting mass of $1.64M_\odot$). The electron population lies far below the scale.

We use the massless quark approximation and zero temperature to discuss some of the results found above. This approximation should give a reasonable description at densities such that the chemical potentials are larger than the masses. From (8.7) we have that $\epsilon = 4B$ at equilibrium

($p = 0$) which occurs at the edge of the star. Translate this to nuclear units using $1 = \hbar c = 197.3$ MeV-fm, and find

$$\epsilon = 4B \sim \frac{4(154 \text{ MeV})^4}{(197 \text{ MeV} - \text{fm})^3} \sim 300 \text{ MeV/fm}^3 \sim 5 \times 10^{14} \text{ g/cm}^3 . \quad (8.22)$$

This is a little more than twice the energy density of normal nuclear matter (see the section in Chapter 3 on units). It is 14 orders of magnitude greater than the energy density at the edge of a neutron star, namely, the energy of ordinary solid iron (≈ 7.8 g/cm^3). So the density distribution of a strange quark star is quite unusual compared to that of a neutron star or any other star.

Aside from the first few moments of the life of the star, we can take $T = 0$. When we approximate the u, d, and s quark masses as zero, matter made from an equal population of each is identically charge-neutral; therefore $\mu_e \equiv 0$. From the expressions for the density and the pressure (8.5), we then obtain, at the edge of the star ($p = 0$),

$$\mu_u = \mu_d = \mu_s \equiv \mu = \left(4\pi^2 B/3\right)^{1/4} = 1.9 B^{1/4} . \quad (8.23)$$

We see that the chemical potential is about twice the strange quark mass in this approximation (it would be even larger had a finite strange quark mass been used in the estimate of μ). Consequently, strange quarks will be present, even at the edge of the star, in almost the same number as u and d quarks, not only in its higher density interior. In the same approximation, the baryon number density is $\rho = \mu^3/\pi^2$ and the energy per baryon number is

$$\epsilon/\rho = \left(108\pi^2 B\right)^{1/4} = 5.7 B^{1/4} = 880 \text{ MeV} . \quad (8.24)$$

This is smaller than the energy per nucleon in Fe required to make strange matter absolutely stable. We call such stable matter, with an approximately equal number of u, d, and s quarks, *strange quark matter*, or simply strange matter.

For a star governed by the simple equation of state $\epsilon = 3p + 4B$, the Oppenheimer–Volkoff equations take on a universal form independent of bag pressure when the following scaling is made [277, 294]:

$$\overline{p} = p/B, \quad \overline{\epsilon} = \epsilon/B, \quad \overline{r} = \sqrt{B}\, r, \quad \overline{M} = \sqrt{B}\, M . \quad (8.25)$$

In terms of the radii and masses of one sequence of stars, the radii and masses for any other choice of B can be found from

$$R(B') = \sqrt{B/B'}\, R(B), \qquad M(B') = \sqrt{B/B'}\, M(B) . \quad (8.26)$$

In Fig. 8.3 the sequence of star masses as a function of central density is

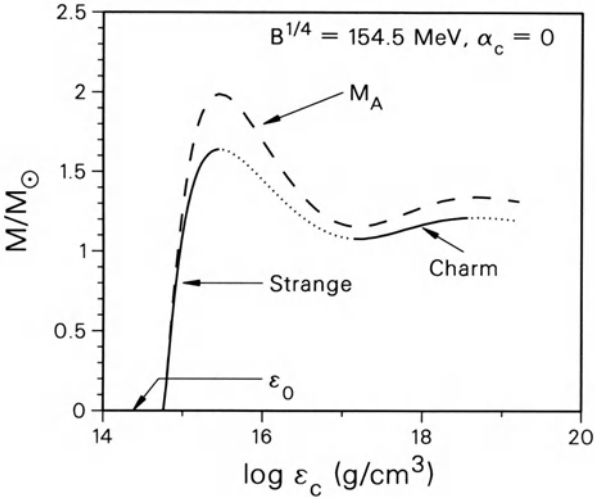

FIGURE 8.3. Gravitational mass of strange and charm stars compared to mass at infinity M_A of the equivalent number of neutrons corresponding to the quark number.

shown for the above choice of B. The lower curve is the gravitational mass of the star defined in (3.22), i. e.,

$$M = 4\pi \int_0^R \epsilon(r) r^2 \, dr \, . \tag{8.27}$$

The upper curve is the mass of the equivalent number of baryons if the star were disassembled into neutrons at infinity and is often referred to as the baryon mass of the star. It is obtained by integrating the baryon number density over proper volume (3.145) and multiplying by the neutron mass m_n:

$$M_A = 4\pi m_n \int_0^R \rho(r) \left[1 - \frac{2M(r)}{r} \right]^{-1/2} r^2 \, dr \, . \tag{8.28}$$

Such stars are stable against disassembly of their equivalent number of neutrons at infinity because the gravitational mass always lies below the baryon mass M_A. This is in contrast to the analogous high-density family of neutron stars studied in the 1960s [295].

On the gravitational mass curve as a function of central density, the regions of positive slope satisfy the necessary condition for stability (Section 3.9.5). The first sequence of stars with increasing mass as a function of central density can properly be called a strange star sequence, since these

stars are an approximately equal mixture of u, d, and s quarks. What of the next sequence having a positive slope which in addition contains the charm quark? An analogous sequence can be found for neutron stars by integrating the Oppenheimer–Volkoff equations to high density. However, stability studies carried out in the early 1960s showed that all configurations with central densities greater than that of the limiting neutron star are unstable to long-wavelength radial vibrations. Such vibrations carry high-density matter in the stellar core across its Schwarzschild radius; collapse to a black hole results [23]. A glance at Fig. 8.4 showing the very steep rise of the particle density (and therefore also mass density), suggests that

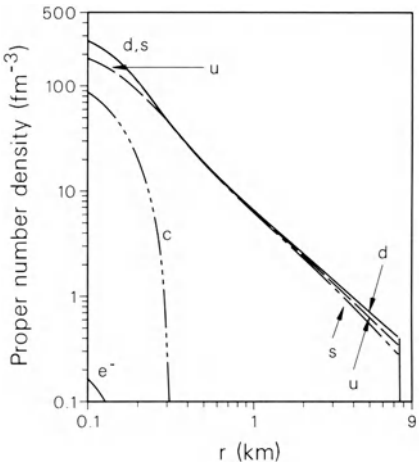

FIGURE 8.4. The distribution of quarks in a charm star near the limiting mass of the family.

these stars are indeed of the type of high-density star discussed by Harrison et al. [23] as being unstable to acoustical vibrations. This is also true for charm stars as we now show [148].

The pulsations of stellar configurations can be analyzed in terms of normal modes with time dependence $e^{\pm i\omega_n t}$. Unstable modes are those for which ω_n^2 is negative. (In this case there is an exponentially growing term $e^{\mathrm{Im}(\omega_n)t}$. A term with positive exponential time dependence implies unbounded growth of the mode.) As we shall see in Section 10.5.3, the modes are ordered $\omega_n^2 < \omega_{n+1}^2$. A function of ω_n^2 which is negative when the squared frequency is negative is shown in Fig. 8.5. We see that the lowest (nodeless) mode becomes unstable at the limiting mass of strange stars. Successive modes ($n = 1, 2, \cdots$) become unstable at those turning points that occur at increasing central density. Charm stars are therefore unstable.

An interesting study of stability can be found in Ref. [23]. There it is shown that a denumerable infinity of oscillations exists in the mass-density plot of compact stars described by a polytropic equation of state. While this is an idealization of the equation of state, it has the common prop-

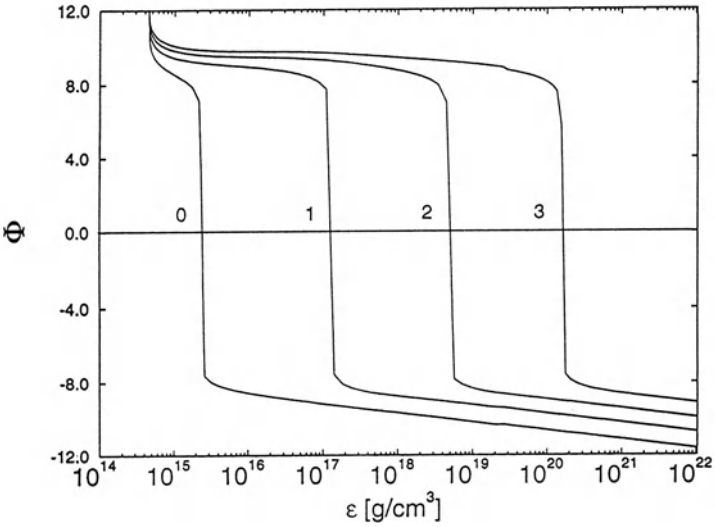

FIGURE 8.5. Pulsation frequencies for the lowest four ($n = 0, 1, 2, 3$) modes of quark stars as a function of central density. For convenience we plot $\Phi(x) \equiv \text{sign}(x)\ \log(1 + |x|)$ where $x \equiv (\omega_n/sec^{-1})^2$ as the abscissa. For $\Phi < 0$, the squared frequency is negative and the mode unstable. (From [148].)

erty of any realistic one—that the pressure never decreases with increasing density (Le Chatelier's principle). The lowest vibrational mode (nodeless) becomes unstable at the maximum of the stable sequence of neutron stars. An additional higher mode becomes unstable at each higher density where $dM/d\epsilon_c = 0$. There is no reason to expect a different result for quark stars. The first two maxima for quark stars seen in Fig. 8.3 are, no doubt, the beginning of such an infinite series. All, save the first (which are strange stars), are unstable.

8.5 Beyond White Dwarfs and Neutron Stars

Could there be in nature any stabilizing influence for a higher density sequence of stars beyond the neutron (or strange) stars? The question obviously cannot be answered definitively by reference to an equation of state in a regime in which we have no certain knowledge. However, we can give the following argument that higher density sequences cannot be expected.

At white dwarf densities the nucleons occupy nuclei which are ponderous and contribute little to the pressure—white dwarfs are stabilized against gravity by electron Fermi pressure. With increasing central density and stellar mass, electron capture onto protons reduces the supporting pressure. Beyond a critical mass—the Chandrasekhar mass—the white dwarf

sequence terminates. There is then a long region in central density for which stellar configurations are unstable. When the central density attains a value $\sim 10^{11}$ g/cm^3 (several orders of magnitude above that of the limiting-mass white dwarf), neutrons drip out of nuclei. At still higher density, the nuclei themselves are destroyed, and the Fermi pressure of nucleons (in the case of neutron stars) and quarks (in the case of quark stars) replaces that of electrons in stabilizing the next sequence of stable stars.

This next stable sequence consists of low-mass neutron stars or quark stars, respectively. These stars have about the same central density. At a little higher density, the short-range repulsion of the nuclear force lends additional resistance to the collapse of neutron stars. Just above the limiting mass of neutron or strange quark stars, all resistance to collapse is overcome by gravity.

What could be another stabilizing agent for higher density stars beyond that corresponding to the mass limit of neutron or strange stars? Quark Fermi pressures are won only at the expense of nucleon pressure in the case of neutron stars. In either case, for higher densities, the growth of pressure is relieved as each new quark flavor threshold is reached, since at such thresholds, baryon number is shared by an additional Fermi sea. There appears to be no physical means of reintroducing stability at higher density. Therefore, there are no grounds for expecting sequences of stable stars at densities higher than those of neutron stars or strange stars. Charm quarks are absent in strange stars—the charm chemical potential does not come close to the charm mass in the range of densities reached in strange stars. Therefore charm, truth, and beauty are flavors that do not appear in stable compact stars. These flavors have astrophysical interest only during the first few seconds of the universe.

The above conclusion seems to be in accord with the 1965 results of Ref. [23], whose authors studied the stellar configurations at all densities using a polytropic equation of state. Although such an equation of state is schematic, it is difficult to imagine how the general conclusion of that work could be modified by any other equation of state that obeys Le Chatelier's principle, especially in view of our discussion above .

9

Hybrid Stars

9.1 Introduction

Quark matter—which no doubt occupied the universe sometime in the first few seconds—may exist naturally today in the cores of neutron stars. The possibility was considered many years ago in the pioneering research of several authors (Itoh [296], Baym and Chin [297], Chapline and Nauenberg [298], and Keister and Kisslinger [299]). The earliest estimates suggested that hadronic matter would not convert to quark matter unless densities of the order $10\rho_0$ were achieved [297]. Such densities are only marginally attainable in stellar models, so for some years the existence of quark matter in neutron stars seemed doubtful.

In early research—and even in quite recent work—certain simplifications in some models and approximations in others had a profound effect on the resulting stellar models. In both cases the effect was to render the phase transition as one of constant pressure. Since pressure varies monotonically in a star, the mixed phase was strictly excluded in all of this research [300].

Constant pressure in the mixed phase—independent of the proportions of phases in equilibrium—is a special case which does not describe the matter of neutron stars. In general, constant pressure is characteristic of a first-order phase transition in a substance having a single independent component. Water is an example. The matter of neutron stars has two independent components—the conserved baryon number and total electric charge (which is zero). Generally, the pressure varies in the mixed phase of such multicomponent substances.[1] In addition, all properties, such as the densities of each phase, vary with proportion. Moreover, when one of the conserved quantities is electric charge, the long range of the Coulomb interaction introduces spatial order into the mixed phase [144, 145].

We now believe that quark matter—the deconfined[2] phase of quarks—is quite likely to occupy the inner regions of the more massive neutron stars. Quark matter may exist only in the mixed phase in equilibrium with the confined phase of hadronic matter or, possibly, also as a pure phase in the central region [144, 145]. We call neutron stars with quark or mixed

[1] The pressure may be constant in the mixed phase of a multicomponent substance only for special proportions of the components.

[2] Of course, we mean deconfined in the sense that the density or temperature of matter is so high that individual nucleons have dissolved into uncorrelated quarks which are free to explore the larger region of dense or hot matter. The whole region is colorless, and the liberation of individual quarks is not implied.

phase interiors *hybrid stars* when the quark aspect is emphasized. They are otherwise a variation of the concept of neutron stars, just as hyperon stars are a variation.

The mixed phase of confined and deconfined matter is most unusual [144, 145, 301, 302, 303]. It is expected to form a crystalline lattice of various geometries of the rarer phase immersed in the dominant one (see Figs. 1.1 and 9.1). The notion of a crystalline lattice that occupies the *crust* of a neutron star is familiar. In the crustal region interior to the edge of the star at densities high enough to ionize atoms, the nuclei are immersed in a background of electrons and assume a crystalline configuration so as to minimize the sum of Coulomb and surface energies. What is unusual about the crystalline mixed confined-deconfined phase is that the two forms of matter are simply different phases of one and the same substance, not different substances like nuclei and a gas of electrons.

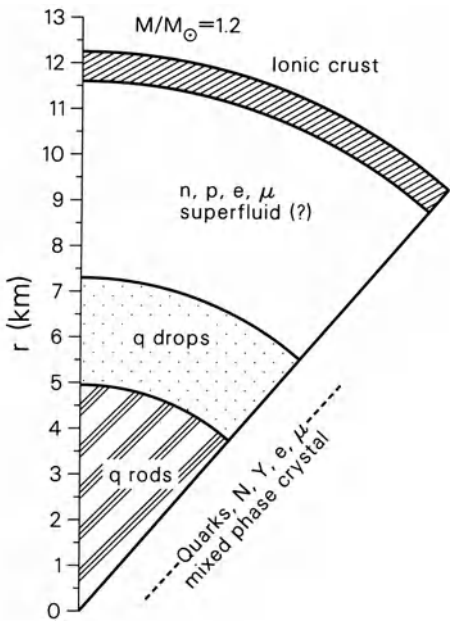

FIGURE 9.1. A section through a neutron star model that contains an inner region of mixed confined and deconfined phases. The innermost sphere consists of quark matter rods and a surrounding layer of quark matter drops immersed in the confined phase of hadronic matter. The particle composition of these regions consists of quarks, nucleons, hyperons, and leptons. A liquid of neutron star matter containing nucleons and leptons surrounds the mixed phase. A thin crust of heavy ions forms the stellar surface. See also Fig. 1.1 for a more massive and complex structured star.

The formation of a lattice in the confined-deconfined mixed phase occurs because the two phases in equilibrium are driven by the isospin symmetry energy of nuclear matter to have opposite charges. This does not violate the condition that a star must be electrically neutral. Charge neutrality of the star will be achieved *globally* $[\int \rho(r) d^3r = 0]$ not *locally* $[\rho(r) \equiv 0]$ if

that is energetically favored.[3] The distinction was not recognized in earlier work [300]. Nor was the distinction between first-order phase transitions in single and multicomponent substances recognized.

The crystalline structure of the mixed phase varies in geometry throughout the region that it occupies in neutron stars. There are likely consequences for all transport properties as well as for pulsar glitches. In this chapter we will discuss why the structure arises. We will then portray its properties and its variation in geometrical form through a star. In the last section, a novel consequence of the deconfinement phase transition and hyperonization of neutron stars (Chapter 5) in the possible formation of low-mass black holes is studied.

9.2 Constant-Pressure Phase Transition

As discussed above, the confined-deconfined phase transition is not expected to occur at constant pressure. Nonetheless, it is interesting to examine the consequences of the assumption of constant pressure so as to contrast the results with those for a variable pressure phase transition characteristic of multicomponent substances. The first case is familiar, the second not.

A familiar example of a single-component substance from the textbooks is the liquid–vapor transition in water, where the single conserved 'charge' or independent component is H_2O. First-order phase transitions in simple substances have well-known properties. As the substance is compressed at constant temperature or cooled at constant pressure, it begins condensing the other phase at a certain point. This phase of partial transformation from one pure phase to another, assumed to be always in equilibrium under whatever conditions of temperature or pressure prevail, is referred to as the mixed or coexistence phase.

A second notable property of a simple substance is that the mixed phase consists of the two phases in their respective unchanging states, no matter what their proportions. The water–vapor transition is a familiar example. In Fig. 9.2 an example is shown of the constancy of the pressure of a first-order phase transition in a simple substance. This particular example is for pure neutron matter in equilibrium with u-d-s quark matter, which is also identically charge-neutral in the limit of massless quarks (as is the case in Fig. 9.2).

In the language of Gibbs, the two phases are in equilibrium when their (baryon) chemical potentials, temperatures, and pressures are equal, cor-

[3] An atom is a familiar example of a system that is neutral but whose charge density is finite, i.e., globally neutral. A locally neutral atom would be a very highly excited state indeed.

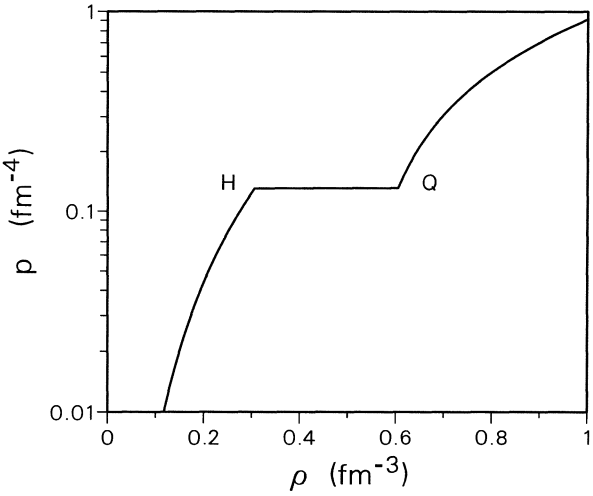

FIGURE 9.2. Behavior of pressure vs. density in the vicinity of a first-order phase transition in a simple substance having one chemical potential corresponding to conserved baryon number. Points labeled H and Q mark the end of the hadronic and beginning of the quark phase, the region between being the mixed phase. See text for further description and also Eq. 9.4

responding respectively to chemical, thermal, and mechanical equilibrium:

$$\begin{aligned} \mu_H &= \mu_Q = \mu\,, \\ T_H &= T_Q = T\,, \\ p_H(\mu, T) &= p_Q(\mu, T) = p\,. \end{aligned} \tag{9.1}$$

The subscripts H and Q denote the confined (hadronic) and deconfined (quark) phases. At constant temperature the last equation can be solved for the unique value of μ, independent of the proportion of the two phases in equilibrium. This value specifies the constant but unlike values of the energy density of each phase in equilibrium:

$$\epsilon_H \equiv \epsilon_H(\mu) \quad \neq \quad \epsilon_Q(\mu) \equiv \epsilon_Q\,. \tag{9.2}$$

The volume-weighted energy and baryon number density of the substance in the mixed phase, which we refer to for brevity as averages, are

$$< \epsilon > \;=\; (1-\chi)\epsilon_H + \chi\epsilon_Q\,, \tag{9.3}$$

$$< \rho > \;=\; (1-\chi)\rho_H + \chi\rho_Q\,. \tag{9.4}$$

Here $(1-\chi)$ and χ are the volume fraction of the hadronic and quark matter phases in coexistence. One can verify that these expressions, linear

in χ, imply that the pressure ($p = -\partial E/\partial V$) is constant in the mixed phase of a simple substance, as we already know. The pressure is shown as a function of the baryon (neutron) chemical potential in Fig. 9.3 for several cases. If both phases were described in terms of the same theory instead of one theory for the hadronic phase and one for the quark phase, the two solid lines would be joined, as shown schematically by the dashed line. In other words, the pressure as a function of chemical potential turns back and crosses itself at the point of phase equilibrium—the point where pressure, temperature (here zero), and chemical potential are equal in the two phases.

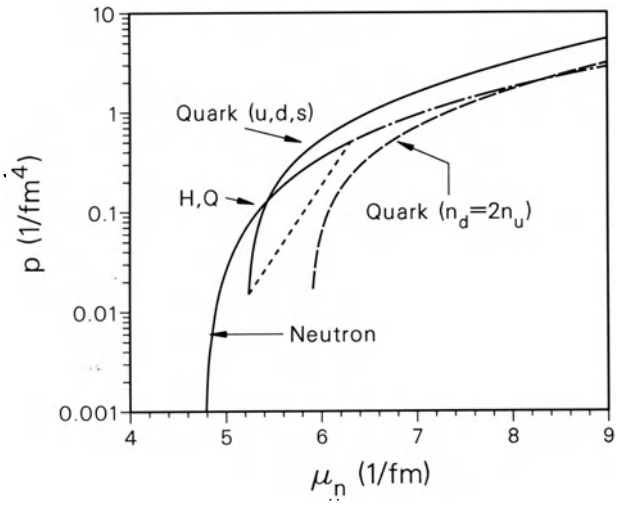

FIGURE 9.3. Pressure vs. baryon chemical potential for pure neutron matter, for u-d-s quark matter, and for quark matter with u-d quarks in the charge-neutral proportion indicated. Note the elevated chemical potential (and therefore baryon density) at which the latter curve crosses the neutron matter curve compared to that of equilibrated u-d-s quark matter. Note that here the points H and Q that denote the density of the beginning and end of the mixed phase in Fig. 9.2 coincide at the chemical potential common throughout the mixed phase in a simple substance [145].

The above properties lead to a particular structure for a star. We know from both the Newtonian and the Oppenheimer–Volkoff equations for stellar structure that the pressure is a monotonic decreasing function of the distance from the center of the gravitating object, just as in our atmosphere. Therefore, the equal pressure points (H and Q at the ends of the mixed phase of a simple substance and all points in between) would be mapped onto the same radial coordinate within the star. At that radial coordinate there would be a discontinuity in the density, (9.2). This is illustrated in Fig. 9.4 where matter interior to the radial point at H,Q would be purely

quark matter, and juxtaposed and exterior to it would be purely hadronic matter, each at its respective equilibrium density.

If local charge neutrality is enforced in the description of a first-order phase transition in a multicomponent substance, as has been frequently done in the literature, the transition is forced into the constant pressure mold. This can be seen as follows. The two conditions in which the charge density vanishes locally are

$$q_H(\mu_b, \mu_q) = 0\,, \qquad q_Q(\mu_b, \mu_q') = 0\,. \tag{9.5}$$

We can think of solving them, respectively, in the form

$$\mu_q = f(\mu_b), \qquad \mu_q' = g(\mu_b)\,. \tag{9.6}$$

Use these results in the Gibbs requirement for equality of pressure at equilibrium and find

$$p_H(\mu_b, f(\mu_b), T) \;=\; p_Q(\mu_b, g(\mu_b), T) \;=\; p\,. \tag{9.7}$$

We see that the problem has been reduced to one dimension: the pressure is a function of only one chemical potential. By demanding that each phase in equilibrium be separately charge-neutral—a demand that exceeds the global neutrality required by the physics—the phase transition has been made to resemble that of a simple substance in which the pressure remains constant independent of the proportion of the phases in equilibrium. It can be seen that the above demand of local neutrality is incompatible with Gibbs phase equilibrium, because one of the chemical potentials is forced to be discontinuous, as in (9.6).

9.3 The Confined-Deconfined Phase Transition in Neutron Stars

9.3.1 Conservation laws are global—not local

Real neutron stars have two conserved charges, electric and baryonic. Therefore, neutron star matter is not a 'simple' substance but a 'complex' one—it has more than one independent component. The characteristics of a first-order phase transition (which we assume the deconfinement transition to be[4]) are quite different in the two cases.

[4]Lattice gauge simulations of QCD are not conclusive on the issue of whether the confined-deconfined phase transition is first- or second-order because they deal generally with hot matter and vanishing baryon chemical potential. There is still great difficulty in dealing with finite quark masses. We shall assume that the transition is first-order.

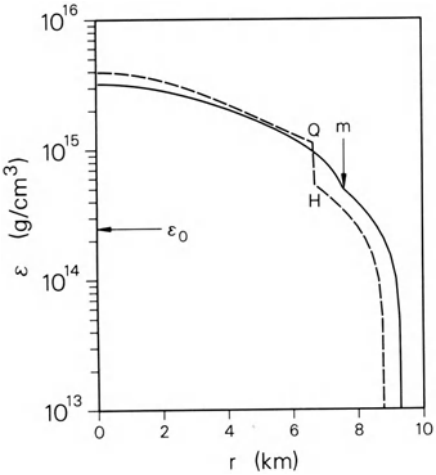

FIGURE 9.4. Density in a star in which the hadronic-quark matter phase transition is modeled as constant pressure (simple substance). A discontinuity in density, corresponding to the difference between H and Q in Fig. 9.2, occurs at the radial coordinate where the pressure is equal to that of the mixed phase. This contrasts with the continuous density distribution corresponding to the theory developed later in the chapter. For the particular coupling constants and bag constant B chosen to describe the two phases, the mixed phase extends from the center to the radius marked m. [145].

The difference arises because a complex substance possesses degrees of freedom unavailable to a simple substance. These degrees of freedom were frozen out in the early research [300]. Recall from (5.21) that stars must be charge-neutral. This statement pertains to the overall net charge on the star. It is a global restriction and not a local one which would correspond to identically vanishing charge density. Since nature requires only global neutrality, if it is energetically favorable to have charges separated, it will be so. We have examples of such systems. The neutron is one and the atom is another. Both have finite charge distributions; they simply integrate to zero.

9.4 Degrees of Freedom in a Multicomponent System

Consider a substance composed of two conserved 'charges' or independent components— Z of one kind[5], B of the other. In the case of a neutron star, these could denote the net electric charge number (in units of e) and net baryon charge number. Let the substance be closed and in a heat bath. Define the concentration by $c = Z/B$. The ratio is fixed only as long as the system remains in one pure phase or the other! When in the mixed phase, the concentration in each of the regions of one phase or the other

[5]If Z denotes the net electric charge, it would be zero for a star, but we retain the symbol for generality.

may be different and they are restricted only by the conservation on the total numbers,

$$c_1 = Z_1/B_1, \quad c_2 = Z_2/B_2, \qquad Z_1 + Z_2 = Z, \quad B_1 + B_2 = B\,. \tag{9.8}$$

If the internal forces can lower the energy of the system by rearranging the concentration, they will do so. The essential point is that conservation laws in chemical thermodynamics are global, not local. Moreover, the concentrations c_1, c_2 will be optimized by the internal forces of the system at each proportion of the phases, so that the properties of the phases *vary* in the mixed phase. This is in contrast with the liquid–vapor transition in water or in any other single-component substance.

The mathematical proof of the above properties is not nearly so illuminating as the physical verbal proof above, but we give it for completeness. The Gibbs condition for phase equilibrium is that the chemical potentials μ_b and μ_q corresponding to B and Z, temperature T, and the pressures in the two phases be equal,

$$p_H(\mu_b, \mu_q, T) = p_Q(\mu_b, \mu_q, T) \tag{9.9}$$

where the subscripts H and Q denote confined hadronic and quark phases, respectively. As discussed, the condition of local conservation is stronger than required. We apply the weaker condition of global conservation in a volume V comprising a bulk quantity of material

$$(1-\chi)\rho_H(\mu_b, \mu_q, T) + \chi\rho_Q(\mu_b, \mu_q, T) = B/V \equiv <\rho>\,, \tag{9.10}$$

$$(1-\chi)q_H(\mu_b, \mu_q, T) + \chi q_Q(\mu_b, \mu_q, T) = Z/V \equiv <q>\,, \tag{9.11}$$

$$\chi = V_Q/V, \qquad (V = V_H + V_Q)\,. \tag{9.12}$$

Given a temperature, the three equations (9.9–9.11) serve to determine the two independent chemical potentials μ_q and μ_b and V for a specified volume[6] fraction χ of quark phase in equilibrium with the hadronic phase. We note that the condition of global conservation expressed by (9.10) and (9.11) is compatible, together with (9.9), with the number of unknowns to be determined. It would *not* be possible to satisfy Gibbs conditions if local electric charge conservation were demanded, for that would replace (9.11) by two equations, such as $q_H(\mu_b, \mu_q, T) = Z_H/V_H$, $q_Q(\mu_b, \mu_q, T) = Z_Q/V_Q$, and the problem would be overdetermined.

It is important to note that, because of the freedom available to the system to rearrange the concentration(s) of the conserved charges, the solution of the equations for Gibbs equilibrium and charge conservation (9.9–9.11) is

[6]The volume V is not that of a star but of a local inertial frame whose extent in the star, as we have proven in Chapter 3, is large enough by far to validate the bulk approximation or the use of Lorentz frames to solve the equations describing matter.

different for each proportion of the phases χ so that all properties, including the common pressure, vary through the mixed phase.

There is another way in which the variation of pressure can be deduced. The energy density is not given by (9.3)—a linear function in χ—but by the highly nonlinear relationship

$$< \epsilon > \quad = \quad (1-\chi)\epsilon_H(\chi) + \chi\epsilon_Z(\chi)\,. \tag{9.13}$$

We refer to $< \epsilon >$ as the average density as a brief way of denoting the volume-weighted density of each phase. Because the relationship is nonlinear, the pressure varies ($p = -\partial E/\partial V$).

The internal force that can exploit the degree of freedom opened by global charge neutrality and which is closed to one in which local neutrality is artificially enforced, is the isospin-restoring force experienced by the confined phase of hadronic matter and which is manifested in the valley of beta stability (4.106). The hadronic regions of the mixed phase can arrange to be more isospin symmetric than in the pure phase by transferring charge to the quark phase in equilibrium with it.[7] Symmetry energy will be lowered thereby at only a small cost in rearranging the quark Fermi surfaces. Thus the mixed-phase region of the star will have positively charged regions of nuclear matter and negatively charged regions of quark matter.

Whether a phase transition takes place at constant or varying pressure has dramatic effects in the environment of a star or any gravitational field. No region of constant pressure can exist in the hydrostatic equilibrium of a gravitating body. Pressure is a monotonic function according to the Oppenheimer–Volkoff equations. By demanding either identical charge neutrality, as for a star made purely of neutrons, or local charge neutrality, the phase transition was forced to be of this type in the earlier research [300]. Fig. 9.4 compares the density profiles of neutron stars in which the mixed phase is treated as that of a simple or a complex substance. The properties of the mixed phase in a complex substance are illustrated in Fig. 9.5. Note that all quantities appropriately vary continuously.

A family of stars parameterized by central density and corresponding to the treatment of the present section is shown by the solid line in Fig. 9.6. The fictitious family, corresponding to a treatment of neutron stars as purely neutron and undergoing a constant pressure phase transition to u, d, s quark matter, is depicted by the dashed line. Hydrostatically stable,

[7]The ground state can be found in chemical thermodynamics without knowledge or specification of the particular reactions involved when a system decays from a state of higher energy to one of lower. To be clear, however, when we speak of regions of hadronic and quark matter exchanging charge, the exchange is mediated by the electro-weak interaction, for example the exchange of a W boson. In achieving the lowest energy, neither the electric nor strangeness charge need be conserved separately in confined and deconfined regions. The electric charge is overall conserved of course, but strangeness not longer than the weak interaction time.

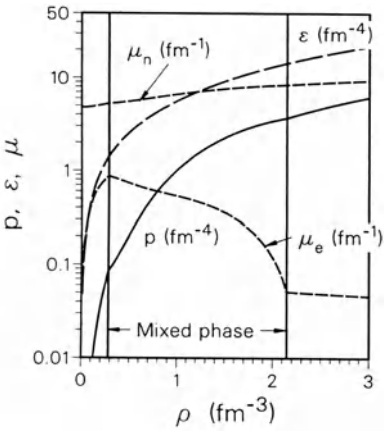

FIGURE 9.5. The pressure, weighted energy density (9.13), and chemical potentials as a function of density for the hadron-quark phase transition in the case that the star is correctly treated as one having two conserved charges, baryon and electric [145].

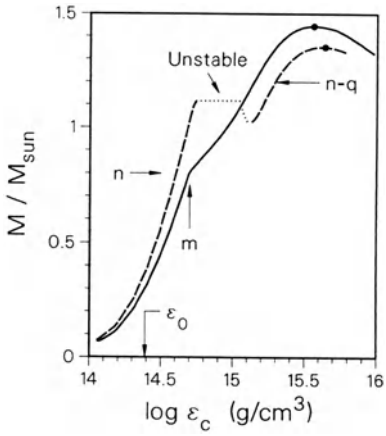

FIGURE 9.6. Dashed line shows a family of stars for which the hadron-quark phase transition takes place at constant pressure. 'n' denotes pure neutron stars; 'n-q' quark cores with neutron matter mantles. Solid line are stars in beta equilibrium treated properly with two continuous chemical potentials. Stars above 'm' have mixed-phase interiors and neutron star matter mantles; stars below 'm' are in the pure neutron star matter phase [145].

pure neutron stars correspond to the portion marked 'n'. The configurations with central densities lying in the flat region are unstable. We thus discern a clear difference in the two treatments, aside from the existence of the mixed phase: When the phase transition is treated as one taking place in a multicomponent substance, there is no region of instability in the sequence between minimum and maximum mass configurations.

It is worth noting in Fig. 9.6 that quark matter appears (in a mixed phase) in stars with mass as low as 0.8 $M_\odot$ (for the parameters used in the illustration). This contrasts with the incorrect treatment of neutron star matter as a simple substance for which quark matter appears first in a star of mass $1.2M_\odot$ and at much higher central density.

9.4.1 Coulomb lattice structure of the mixed phase

We described above how the isospin symmetry energy in neutron matter will exploit the degree of freedom of readjusting the charges between hadronic and quark phases in equilibrium so as to reduce the symmetry energy to the extent consistent with charge conservation. Regions of hadronic matter will have a net positive charge neutralized by a net negative charge on the quark matter regions (and to a much lesser degree by electrons).[8]

Coulomb repulsion will prevent the regions of like charge from growing too large, and the surface energy will act in the opposite sense in preventing them from becoming too small. We understand, therefore, that the mixed phase will form a particular Coulomb lattice so as to minimize the sum of Coulomb and surface interface energy at each proportion of phases [144, 145]. The proportion of phases will, of course, vary with depth in the star, and the lattice will accordingly vary.

We expect that the outer region of the neutron star will consist of hadronic matter. At a depth where the pressure is higher, some hadronic matter will have been converted to quark matter. The quark matter will consist of a lattice of droplets immersed in hadronic matter. Much deeper in the star, the roles will be reversed in accordance with the associated pressure. In between, other geometric phases may occur corresponding to intermediate pressures. Perhaps the pressure will be high enough in the inner core to convert all the matter to quark matter. The density profile of the star is continuous and, in general, consists of three regions: (1) the outer hadronic region, (2) the intermediate mixed-phase region with the proportion of phases and corresponding crystalline structure varying with depth in the star, and (3) the interior quark matter core. (See Figs. 1.1 and 9.1.) The picture is quite different from that when the second conserved charge is suppressed.

9.4.2 Phase diagram

In the case of a simple substance, the pressure is a function of one chemical potential, and we have seen its general form—the pressure increases with μ up to a point, backtracks below, and then crosses itself. The point of intersection corresponds to the mixed phase. The stable phase is the one with highest pressure (Fig. 9.3). In the case of two chemical potentials, the

[8]Electrons play a minor role in charge neutrality once densities are reached where neutrality can be achieved in large part among baryons. The conserved baryons must be present in an number equal to that with which the star was born but electrons must be present *only* to the extent of neutralizing any excess positive charge not already neutralized among particles carrying baryon charge [49, 86].

pressure is a surface, not a line, and the intersection of the surfaces is the line, rather than the point, corresponding to the mixed phase.

The analogue of Fig. 9.3 for two chemical potentials (corresponding to two conserved charges) is Fig. 9.7. In this example the hadronic phase is represented locally by the surface bounded by X A A′X′. Phase equilibrium occurs on the line A A′ which is the intersection of the hadronic and quark pressure surfaces. However, only a segment of that line pertains to any particular pair of conserved charges. In this schematic plot, the line 0a is the projection of the line defined in the chemical potential plane by the conservation equations

$$\rho_H(\mu_b, \mu_q) = B/V\,, \qquad q_H(\mu_b, \mu_q) = Z/V \tag{9.14}$$

for the pure hadronic phase. The end of the pure hadronic phase ($\chi = 0$) is denoted 0. Similarly, the line 1b is the projection onto the pressure surface of the line representing the solution of the conservation equations in the quark phase. The line 01 is the mixed phase for which χ, the proportion of quark phase, varies from zero to unity. In other words, for the given amount of conserved charges, the line a01b represents the system in the pure hadronic, mixed, and pure quark phases, respectively.

9.4.3 Two energy scales

The energy scale of stellar matter in bulk is large, being of the order of GeV per baryon charge. This is because such matter is highly compressed and includes the masses and Fermi energies as well as the compression energy. The energy density of each phase through the mixed phase region is shown in Fig. 9.8. In this chapter we have discussed how a substance possessing a first-order phase transition and having more that one conserved charge of which one is the electric charge, may develop a Coulomb lattice of the rarer phase immersed in the other. The energy scale of this geometrical structure is much smaller than the bulk energy scale since it involves surface and screened Coulomb energies (related by a factor of two as we shall see, and so of the same order). Therefore we approximate each problem separately:

(a) The mass and radius of the star, the pressures, chemical potentials, particle populations, indeed the gross structure of the star and the radial location of the mixed phase can be found independently of the crystalline structure of the mixed phase.

(b) The important crystalline properties of the mixed phase can be quantitatively evaluated with input of charge and energy densities of the two phases in equilibrium found in (a). The forms, dimensions, spacings, and location of the crystalline structure can be computed as they evolve with distance from the center of a particular mass star. This is so because all are a function of χ which is a function of pressure and hence of radial location in the star.

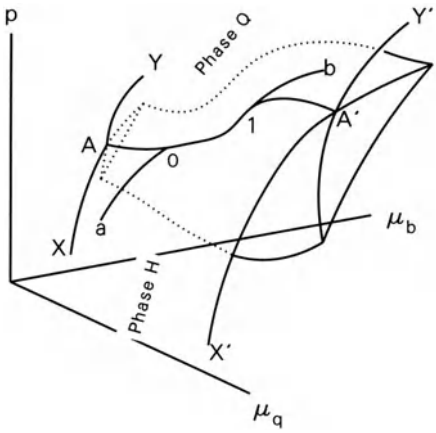

FIGURE 9.7. Schematic of pressure as a function of two chemical potentials. For chosen conserved charges, a0 represents the trajectory that the system will lie on in the pure hadronic phase, 01 in the mixed phase with proportion χ varying from 0 to 1, and 1b the trajectory on which the system will lie when in the pure quark phase [145].

9.5 Gross Structure of a Hybrid Star

We use the theories of dense neutron star matter and of cold quark matter developed in earlier chapters to compute the gross properties of stellar models including the phase-transition region. Each theory by itself represents a pure phase—hadronic or quark as the case may be. Each is to be solved subject to charge neutrality (as in (9.14) for the hadronic phase). At each step in density, the pressure of both phases (at equal chemical potentials) can be checked to identify the greater pressure (which identifies the physical phase) and to discover the point at which the pressures first become equal. That point identifies the beginning of the mixed phase.

Throughout the mixed phase, charge neutrality must be enforced only as an overall constraint, as in (9.11), and not separately on each of the phases as explained earlier. In the mixed phase the proportion or fraction χ of volume occupied by the quark phase is a more convenient independent variable than baryon density. The pressures of the two phases in equilibrium are equal, but vary with χ. When χ become equal to unity, the matter is in the pure quark phase.

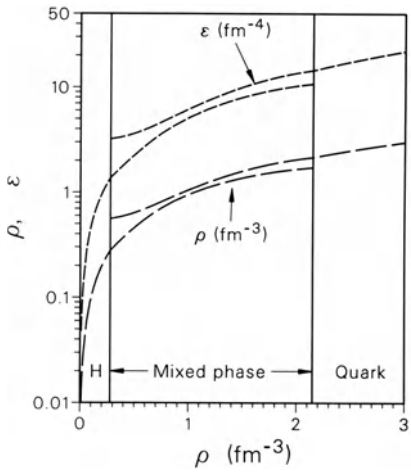

FIGURE 9.8. For the hadronic quark phase transition, the energy density and baryon density in each phase in equilibrium is shown through the mixed phase where the x axis is the volume-weighted density of the mixed phase [145].

Besides specifying the theories of the two separate phases, we need the relationship between the quark chemical potentials and those for the independent conserved quantities—baryon number $\mu_n(\equiv \mu_b)$ and electron charge $\mu_e(\equiv -\mu_q)$. The relationships are

$$\mu_u = \mu_c = (\mu_n - 2\mu_e)/3, \qquad \mu_d = \mu_s = (\mu_n + \mu_e)/3\,. \tag{9.15}$$

The quark chemical potentials can be obtained from the general rule relating particle chemical potentials to the independent potentials according to the content of the quarks (Table 8.1).

For a bag constant of $B^{1/4} = 180$ MeV and for nuclear matter properties lying in the range of accepted values, we show in Fig. 9.9 the population densities of baryons, quarks, and leptons. For the particular equations of state of hadronic and quark matter, the transition to the pure quark phase is attained because the central density is sufficiently high. The inner 4.6 km of the star forms a quark gas. The region between 4.6 km and 7.8 km is a shell of mixed phase containing, on the microscopic scale, regions of quark and hadronic matter with the rarer phase arranged in a crystalline lattice whose structure we will calculate latter. Exterior to this mixed phase is neutron star matter liquid. At the edge of the star at densities below neutron drip, a very thin crust of nuclei is arranged at lattice sites embedded in an electron gas [61].

Lepton populations in the star are quenched with decreasing radius as the quark populations rise since charge neutrality of the star is achieved in a more energetically favorable manner among the baryon carrying particles. Baryon number is conserved in the star. The same result was encountered in a purely hadronic star as discussed in Chapter 5. The phenomenon is quite

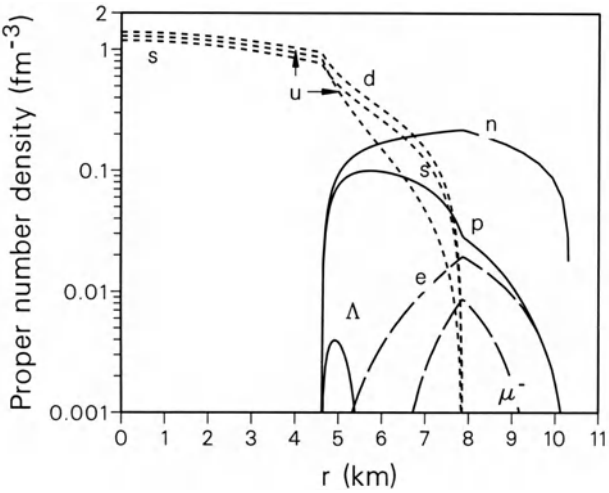

FIGURE 9.9. Population densities per unit volume (9.10) in a hybrid star at the mass limit $1.42M_\odot$ as a function of Schwarzschild radius. The nuclear properties defining the coupling constants in the hadronic phase are $K = 300$ MeV and $m^\star/m = 0.7$. Hyperon couplings are chosen as in Section 5.4.3 with $x_\sigma = 0.6$. Calculation is otherwise similar to [145].

general. Particular charged species of baryons however are not conserved. Only the net charge (zero) is conserved. Leptons produced or absorbed in beta decay or its inverse are not conserved in the star because neutrinos diffuse out.

We learned in Chapter 5 that the compression and effective nucleon mass at saturation are not precisely known and the structure of stars is fairly sensitive to the uncertainties. Therefore, particle populations are shown for other values of these parameters in Fig. 9.10. In this case the hyperons play a more important role in the mixed phase. The pure quark matter phase occupies a sphere of only 2-km radius while the crystalline mixed phase forms a shell of 6-km thickness.

9.5.1 Energy budget in the reapportionment of charge

We have emphasized the importance of the degree(s) of freedom corresponding to a reapportionment of conserved quantities among the phases in equilibrium. This degree of freedom is exploited by the internal forces at each proportion of phases in the coexistence phase, so as to minimize the energy. Figure 9.11 vividly illustrates this phenomenon.

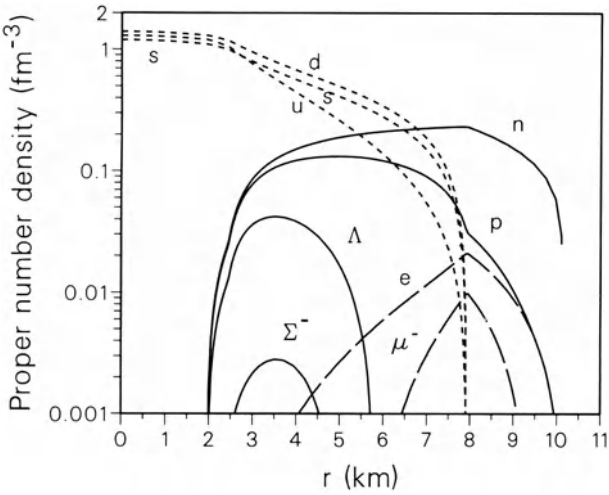

FIGURE 9.10. Population densities in a hybrid star at the mass limit $1.45M_\odot$. Nuclear properties defining the coupling constants in the hadronic phase are $K = 240$ MeV and $m^\star/m = 0.78$. Hyperon couplings are chosen as in Section 5.4.3 with $x_\sigma = 0.6$. Calculation is otherwise similar to [145].

Consider the electric charge densities on each phase, quark and hadronic, as a function of the volume proportion χ of quark matter. Matter is purely hadronic at $\chi \equiv 0$. At slightly finite values of χ, hadronic matter is in equilibrium with an infinitesimal amount of quark matter. The high isospin asymmetry of the hadronic matter at that point (and beyond) can be relieved by transferring charge between phases. Near the threshold for the phase transition, there is little quark matter; the relief is slight. The negative charge density carried by quark matter is largest near the threshold because the cost of arranging the u,d,s quark Fermi surfaces to provide positive charge to the regions of the confined hadronic phase is of little importance at the low-threshold proportion of the quark phase. This energy cost is balanced by relief in symmetry energy in the hadronic phase.

However, the cost in Fermi energy in the quark phase required to provide charge to the hadronic phase becomes increasingly important in the energy budget for greater proportions of quark matter. Therefore, as the proportion of quark matter grows, its charge density decreases. The charge density carried on baryons is the inverse of this, rising to its maximum value as the baryon density goes to zero (at $\chi = 1$). The total charge—the sum of the charge densities times the respective volumes of the phases—is zero. Neutrality is global, not local.

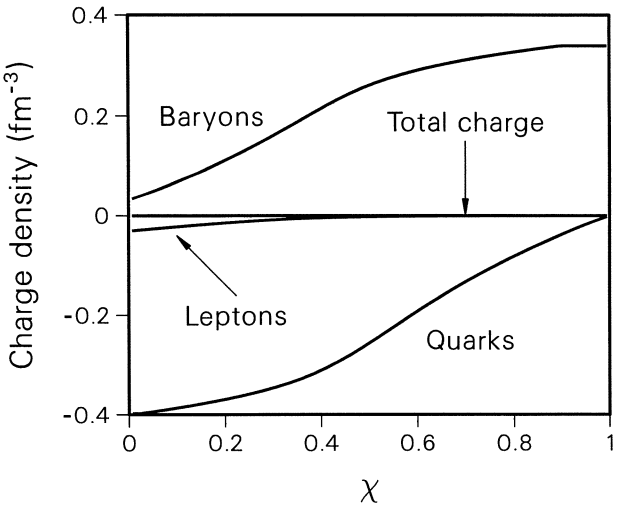

FIGURE 9.11. Charge densities in regions of hadronic and quark matter, respectively, in phase equilibrium as a function of quark matter volume proportion χ. ($K = 240$ MeV, $B^{1/4} = 180$ MeV, $m^\star/m = 0.78$, $x_\sigma = 0.6$)[303]

9.6 Crystalline Structure

We have discussed how a crystalline structure in the mixed phase of a complex substance is inevitable if the transition is first-order and the substance has electric charge as one of its conserved charges [145]. The Coulomb interaction will tend to break the regions of like charge into smaller ones, while this process is opposed by the surface interface energy. Their competition will be resolved by forming a lattice of the rare phase immersed in the dominant one whose form, size, and spacing will minimize the sum of surface and Coulomb energies. In other words, a crystalline lattice will be formed. It is not altogether certain that the lattice is rigid, but evidently an ordered phase is energetically favorable.

Consider a Wigner–Seitz cell of radius R containing the rare-phase object of radius r and an amount of the dominant phase that makes the cell charge neutral. The whole medium can be considered as made of such non-interacting cells. The solution to problems involving a competition between Coulomb and surface interfacial energies is universal.

Let us first see schematically how the varying crystalline structure can be calculated. The Coulomb and surface energies per unit cell volume can be written

$$E_C/V = C(\chi)r^2, \qquad E_S/V = S(\chi)/r\,. \tag{9.16}$$

Here the form of the functions $C(\chi)$ and $S(\chi)$ correspond to a specific geometry, such as spheres, rods, or slabs. Of course, the restriction to three discrete geometries is an idealization, but will serve the purpose of the next section.

When there is little of one phase immersed in the other, we expect the rare phase to form spherical droplets to minimize the surface. As an example, let us see what form the function S takes in this case. For a surface energy coefficient σ, we have

$$\frac{E_S}{V} = \frac{4\pi r^2 \sigma}{4\pi R^3/3} = 3\sigma\chi/r\,, \qquad \chi = (r/R)^3\,. \tag{9.17}$$

Now the function $S(\chi)$ can be read for the geometry of spheres. As the quark phase becomes more abundant, the droplets merge to form rods, and, at higher proportion, rods merge to form slabs. As the proportion further increases, a point is reached at which the two phases interchange roles, developing into nuclear droplets of positive charge immersed in a background of negatively charged quark matter at the other extreme of the mixed phase. In all cases the form of Coulomb and surface energies per unit volume have the general form as defined in (9.16). The minimum of their sum occurs when

$$E_S = 2E_C\,. \tag{9.18}$$

The radius of the droplets is then determined by

$$r^3 = \frac{S(\chi)}{2C(\chi)}\,, \tag{9.19}$$

which depends explicitly on the proportion of phases χ. Since $\chi = (r/R)^3$, the distance between droplets is also determined for this value of the proportion. For each geometry (drops, rods, or slabs), one can compute $(E_C + E_S)/V$ to find which geometry yields the lowest energy, its radius (or half-thickness) r, and spacing $2R$.

The process responsible for creating the conditions for the mixed-phase crystalline structure are quite different from those which create the structure in a mixture of nuclei and electron gas, as is found in the subsaturation matter in the crust of a neutron star. In the latter case atoms are ionized at the densities of the crust and positively charged nuclei find themselves immersed in an electron gas. A Coulomb structure seems quite natural. The unusual aspect of the situation we describe is that the structure consists of two phases of the same substance—hadronic matter in the confined and deconfined phases which carry opposite charges. The exchange of charge and strangeness is mediated by the weak interaction and driven by the symmetry energy of the confined phase. Nevertheless, the interplay of surface and Coulomb energies in defining the nature, size, and spacing of structure is identical.

Having shown schematically how the problem of structure may be solved, we now turn to the actual formulation. The electrostatics are trivial, but the details are tedious. We quote the results without derivation. Since the competition between surface and Coulomb energies is independent of the context, we may adapt the results of [212] to write the radius of the rare phase immersed in the other and the minimum of the sum of Coulomb and surface energies in the case of the three geometries:

$$\frac{1}{r^3} = \frac{4\pi[q_H(\chi) - q_Q(\chi)]^2 e^2 f_d(x)}{\sigma d}, \quad d = 1, 2, 3, \tag{9.20}$$

$$\frac{E_C + E_S}{V} = 6\pi x \Big(\frac{\{\sigma d\big[q_H(\chi) - q_Q(\chi)\big]e\}^2 f_d(x)}{16\pi^2} \Big)^{1/3}. \tag{9.21}$$

The charge densities of hadronic and quark matter (in units of e) at a given proportion χ are q_H and q_Q. Recall that χ is defined as the volume fraction of quark matter. So when hadronic matter is the background phase, the quark droplets (rods or slabs) of radius r and cell radius R are related by

$$\chi = (r/R)^d \quad \text{(hadronic matter background)}, \tag{9.22}$$

with $d = 1, 2, 3$ corresponding to slabs, rods, and drops, respectively. (In the case of slabs, r is the half-thickness and R is the half-distance between slabs.) In the opposite situation where quark matter is the background, the fraction of hadronic matter is

$$1 - \chi = (r/R)^d \quad \text{(quark matter background)}. \tag{9.23}$$

The ratio of droplet (rod or slab) to cell volume is defined as

$$x = (r/R)^d. \tag{9.24}$$

The function $f_d(x)$ is given in all three cases by

$$f_d(x) = \frac{1}{d+2}\Big[\frac{1}{(d-2)}(2 - dx^{1-2/d}) + x\Big], \tag{9.25}$$

where the singularity at $d = 2$ is well behaved and has the value

$$\lim_{d\to 2}\left[\frac{(2 - dx^{1-2/d})}{(d-2)}\right] = -(1 + \ln x). \tag{9.26}$$

We have supposed that the electrons are uniformly distributed throughout the mixed phase in both quark and hadronic regions. They therefore do not appear in the above expression.

The surface tension enters the above determination of the structure as a crucial factor, but it is not known. Fortunately, it is evident from (9.21) that the boundaries of the mixed phase are unaffected by its value since

the surface and Coulomb energies vanish at both boundaries; therefore the bulk properties of the medium determine the boundaries. It is also clear that because the structure size (r) and the sum of Coulomb and surface energies scale with the same power of σ independent of geometry (d), the locations in the star where the geometry changes from one form to another is independent of the value of the surface tension.

It is evident that the surface tension should be computed self-consistently with the two models of quark and hadronic matter at equilibrium. Moreover, unlike simple substances, such as water and vapor, the density of each phase changes as its proportion in the mixed phase changes (Fig. 9.12). So, the surface energy is not expected to be a constant.

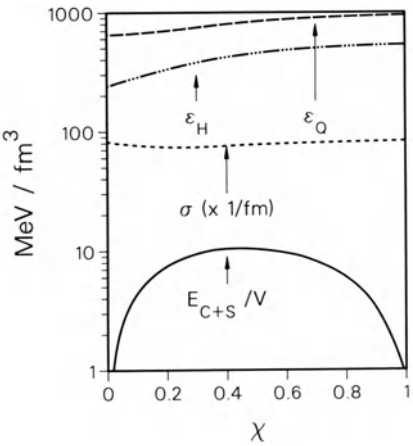

FIGURE 9.12. The energy densities of each phase, the surface interface energy σ (as approximated in the text), and the sum of surface and Coulomb energy densities are shown in the mixed phase of hadronic and quark matter as a function of the volume proportion of quark matter χ. See Fig. 9.9 for other details. See also Ref. [145].

In Fig. 9.12 note that the varying densities of the two phases, though unequal, tend to track one other. In a simple substance, by contrast, the density of each phase in equilibrium remains constant for all proportions of the phases, and the two phases often have significantly different densities. As a gross approximation, the surface energy is given by the difference in energy densities times a length scale typical of the surface thickness [304]. In the case of mixed quark and hadronic matter, the length scale is of the order of the strong interaction range, $L = 1$ fm. In other words, the surface interfacial energy should depend on the proportion of phases in phase equilibrium just as everything else does:

$$\sigma(\chi) = \text{constant} \times [\epsilon_Q(\chi) - \epsilon_H(\chi)] \times L\,. \tag{9.27}$$

Great care has to exercised in assigning a value to the constant in the above expression. If too large a value is chosen, the structured phase will

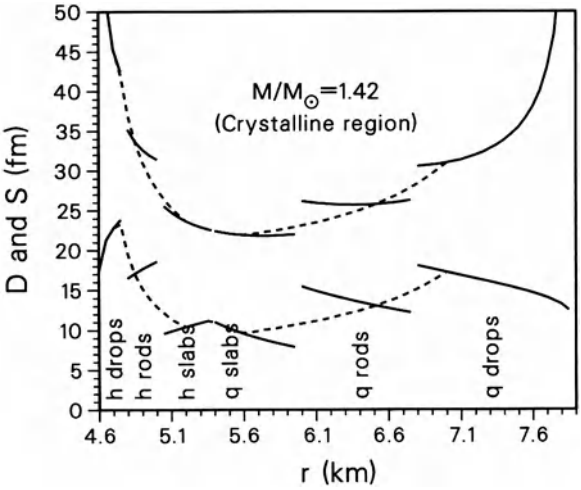

FIGURE 9.13. Crystalline mixed region in a neutron star showing the diameter D (lower curves) and spacing S (upper curves) of indicated geometric structures as a function of radial Schwarzschild coordinate. The region internal to 4.6 km is pure quark matter. Notation 'h drops' denotes hadronic drops immersed in quark matter, and so on. The stellar radius is 10.7 km. The dashed line is continuous dimensionality interpolation. See Fig. 9.9 for particle populations and other details. Taken from [302].

have an energy higher than the unstructured one. But this would violate the general fact that, when a degree of freedom is opened to a physical system, the energy will not be raised—it can remain unchanged (the degree of freedom remaining unexploited)—or it can and generally will be lowered. In Ref. [301] various arbitrary values of a constant σ were employed. In keeping with the above physical principle, we choose a value, as shown in Fig. 9.12, that gives a value not exceeding 10 MeV/fm^3 to the optimized sum of surface and Coulomb energy densities (which is a function of χ).

9.6.1 Crystalline structure as a function of stellar mass

In this section we study the crystalline, mixed-phase region of hybrid stars as a function of stellar mass to see how its geometry, dimensions, and location in the star vary. To demonstrate the extreme dependence of the crystalline structure on stellar mass, we compare two stars differing by only $0.02M_\odot$. In Fig. 9.13 we show the diameter of the geometrical objects, identify their forms, and plot the spacing between centers of the rare-phase objects immersed in the other phase. The mass of the star is at the mass

limit $M = 1.42M_\odot$. The pressure at the center and extending to 4.6 km is sufficiently high that this region is occupied by pure quark matter. The region between 4.6 and 7.8 km is in the crystalline, confined-deconfined phase. Since the phase transition is completed before the center of the star is reached, the geometrical structures span the full range of forms. At the outer edges of the mixed phase region, drops of *finite* diameter are spaced in the limit of $\chi = 0$ at *infinite* distance. In all cases the diameters of the geometric forms lie between about 10 and 25 fm. Of course, were it not for the restriction to three discrete geometries, the discontinuities in the diameters and spacings shown in the Figs. 9.13 and 9.14 would be interpolated by intermediate forms. In the formulae (9.20–9.26), d can be treated as a continuous variable in the range (1,3) for this purpose, and the result is shown in the one case.

For lower mass stars, the central density and pressure may be insufficient to fully convert quark matter to hadronic matter. This is the case for the neighboring mass star $M = 1.40M_\odot$ for which the geometries of the crystalline mixed phase are shown in Fig. 9.14. The crystalline phase extends to the center of the star, and the central geometry consists of rods of hadronic matter immersed in quark matter. For a mere $0.02M_\odot$ change in mass, the situation has changed radically from a star having a 4.6-km quark gas core enclosed by a 3-km thick crystalline shell to a star which is an 8-km crystalline sphere having no quark gas interior.

The extreme sensitivity of the crystalline structure to stellar mass is due to the high compression in neutron stars. Stellar density is a rather flat function of radial coordinates except near the edge of the star. A small change in central density (and therefore mass) has a large effect on where in the star a particular density occurs. Naturally, the details illustrated above are for the particular parameters chosen. The pattern of the results is, however, general.

The results for another parameter set are shown in Fig. 9.15. There the radial coordinates of the boundaries of various regions are shown for various stellar masses up to the limiting mass ($1.454M_\odot$). It is remarkable, as shown in the detail of Fig. 9.15, that, for only a small range in mass, the core is pure quark matter. For lower mass stars, the mixed phase extends from the center out to some few kilometers. The stars with mass between 0.84 and $1.07M_\odot$ contain only quark drops in a hadronic background.

Early research, by inadvertently closing off a degree of freedom, rendered the hadronic–quark transition as one of constant pressure for all proportions in the mixed phase [300]. In such a case the mixed phase cannot exist in the gravitational field in a star. The pure quark phase was found to occur only at high density or pressure and therefore concentrated near the center. That is true here also. However, the mixed phase extends to a rather low density of only several times nuclear saturation density, as has been found by several authors when the star is allowed to exploit the degree

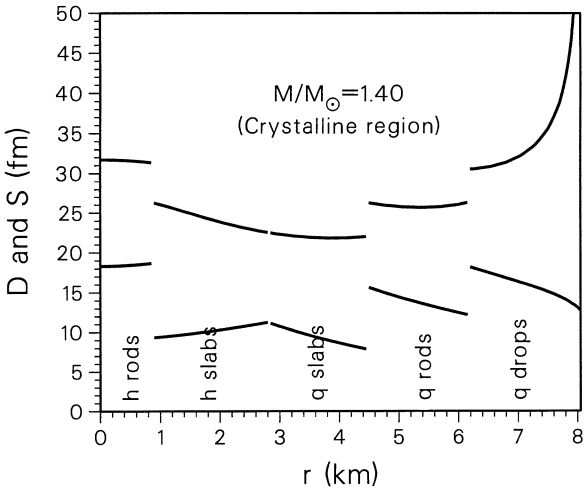

FIGURE 9.14. Similar to the previous figure but for a slightly less massive star. The pure quark phase is entirely absent and the mixed crystalline phase now extends to the star's center. Taken from [302]. The stellar radius is 12.3 km.

of freedom opened when charge neutrality is imposed globally rather than locally [144, 145, 301, 305, 302, 303].

9.6.2 Possible implications for glitches

There is a possible connection between the highly variable crystalline structure of the confined-deconfined mixed phase in neutron stars and the phenomenon of pulsar glitches. Glitches are irregular, unpredictable, and sudden small changes in a pulsar's period. They must therefore be associated with a sudden change in the moment of inertia. A purely liquid or gaseous star is mechanically unable to generate sudden changes in its moment of inertia or angular momentum by any conceivable mechanism. It is certain therefore that rigid regions in a pulsar play a role in the period glitch phenomenon.

Glitch behavior is highly individualistic from one pulsar to another [178]. We tentatively suggest that this may be due to the extreme sensitivity on stellar mass of the radial extent of the Coulomb lattice of the mixed phase region and the forms that occupy it as well as the moments of inertia associated with different gaseous (quark), liquid (nuclear), and lattice regions [302]. The interior crystalline region of the mixed phase and the crustal solid, separated by a nuclear liquid, offer interesting possibilities for inter-

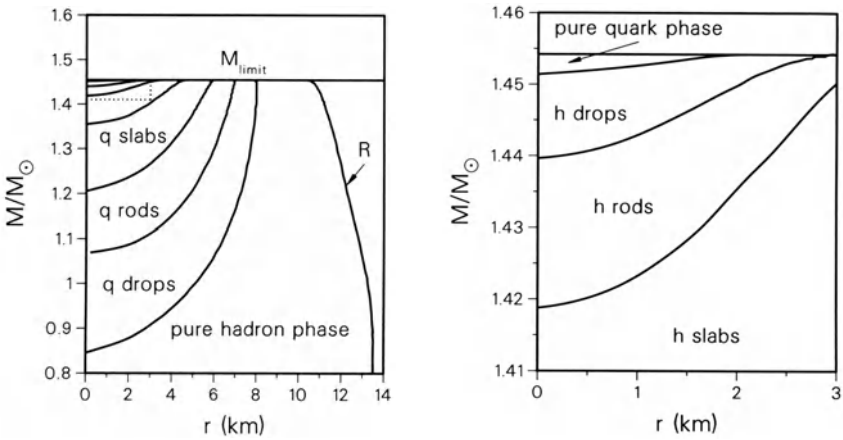

FIGURE 9.15. The left panel shows the radial boundaries of the various geometrical forms for stars above $0.8M_\odot$. The stellar radius is shown by R ($K = 240$ MeV, $m^*/m = 0.78$, $x_\sigma = 0.6$, $B^{1/4} = 180$ MeV). The right panel shows the detail of the dotted box of the left panel [306].

action or stimulated response at the time a glitch originates in one of them and in post-glitch recovery.

The crystalline form cannot fit uniformly into the axial symmetry of a rotating star without lattice imperfections. As the star cools we envision that the crystalline structure will develop with relatively few imperfections, but over time and successive glitches their number will grow, creating, eventually, a granular region. Thus, we also expect a long-term change in behavior with pulsar age.

9.7 Mechanism for Formation of Low-Mass Black Holes

The deconfinement phase transition and hyperonization of neutron star matter (Chapter 5) may play a crucial role in the formation of low-mass black holes ($M \sim 1.5$ to $2M_\odot$). In this section we study how collapse may be triggered in protoneutron stars whose mass falls within a certain range.

Evolved stars with masses $M > 8M_\odot$ are believed to collapse either directly into black holes of mass equal to the progenitor unaccompanied by a supernova and neutrino signal, or to a metastable protoneutron stars

with the remainder of the star ejected in a supernova to seed the universe with elements heavier than those produced in the big bang. (Recall Section 3.1.)

The protoneutron star is hot and lepton-rich. Neutrinos produced during the collapse of the core by the inverse beta decay of protons are thermalized with all favors of quarks and antiquarks as the core temperature rises upon continued contraction. An abundance of gamma rays produce electron pairs which annihilate, producing the neutrinos that will ultimately carry off the binding energy of the neutron star (about a 100 MeV per nucleon for a neutron star near the mass limit). The neutrinos are trapped for a duration of about ten seconds by the hot, dense material of the compact star [29]. The protostar core will otherwise contain a charge-neutral admixture of neutrons, protons, electrons, and muons in close to equilibrium proportions. If the baryon number is not too great, the protoneutron star will deleptonize, cool, and evolve quickly to a stable neutron star.

Alternatively, if the mass of the protoneutron star falls in a certain window above the limiting mass of the fully evolved neutron star that it will become upon deleptonization, it will suffer a *delayed* collapse to a low-mass black hole somewhat in excess of the neutron star limiting mass of $\sim 1.5 M_\odot$. Such a black hole is formed following escape of the initially trapped neutrinos on a timescale not longer than the diffusion time (~ 10 s) and after the processed stellar material of the progenitor star has been ejected in a supernova explosion [31].

In Chapter 5 we discussed the softening of the equation of state by hyperonization of nucleons and, in this chapter, a similar softening caused by the confined-deconfined phase transition compared to that of a charge-neutral mixture of neutrons, protons, and leptons. These processes reduce the limiting mass of neutron stars by an amount of the order of one-half a solar mass [89]. This reduction is the window spoken of above.

The observation of the neutrino signal from the 1987 supernova in the nearby Large Magellanic Cloud (SN1987A), but the absence of a pulsed signal or evidence of a neutron star in the light curve of the supernova remnant, suggests that a supercritical protoneutron star may have been formed which collapsed to form a black hole subsequent to neutrino emission. In any case, the processes described here are possibly responsible for the formation of black holes after the supernova explosion and neutrino signal. They may be relevant to any disparity in neutron star birthrates and type II supernova rates in the galaxy.

Brown and Bethe [232] have suggested that many stars in the mass range 18–30 $M_\odot$ produce black holes instead of neutron stars. They proposed kaon condensation as a possible destabilizing influence on protoneutron stars in a window of about $0.2 M_\odot$ [307] augmented by about $0.04-0.1 M_\odot$ by thermal and lepton pressure in the protoneutron star prior to deleptonization [308]. However, for reasons discussed in Chapter 5, we do not believe that kaon condensation occurs in neutron stars.

9.7.1 Hyperonization-Induced collapse

Neutrinos and gammas produced in the hyperonization reactions (5.25,-5.28) will diffuse out of the star, lowering its energy and making the conversion of nucleons to hyperons irreversible. However, this final ground state is not accessible to a newly formed neutron star until after the trapped neutrinos have escaped and the protostar has cooled and shrunk to its final density.

It takes only a few seconds for neutrinos to diffuse from the star thus cooling it. Prior to neutrino diffusion, it is possible that the collapsing core forms a more massive protoneutron star than ultimately can be supported by the softer equation of state of the fully equilibrated matter containing hyperons. The core mass that collapses increases roughly as the mass of the presupernova star [309, see Table 1]. Protoneutron stars formed in a certain mass and baryon number range will therefore suffer almost immediate collapse to a black hole [310, 31].

Sequences of stellar masses as functions of baryon number for the case of hyperon stars are shown in Fig. 9.16. The sequences for (n, p, e, μ) matter, which we take to be representative of protoneutron stars for which hyperonization is delayed by the presence of trapped neutrinos, are shown

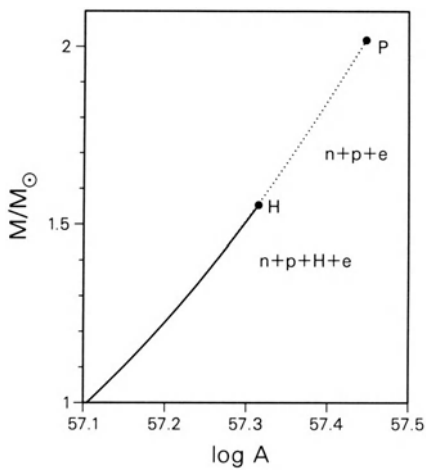

FIGURE 9.16. Masses of protoneutron stars represented by (n+p-+e+μ) and hyperonized neutron stars (n+p+e+μ+H) are shown as a function of baryon number A. The region between the two mass limits (marked by H and P) is the range of protoneutron stars having A for which there is no stable configuration after deleptonization. Parameters of theory are such that corresponding symmetric matter has $m^\star/m = 0.78$, $K = 240$ MeV, and $x_\sigma = 0.6$. (The short spur on each curve corresponds to stellar configurations that lie beyond the limiting mass in plots of mass vs. central density and are shown only for completeness—they are unstable in all cases.)(From [31]).

by dotted lines. The solid dots mark the mass limit for the sequences. The solid lines represent stars composed of hyperonized neutron star matter, the final ground state.

The nonoverlapping segment of the dotted lines H–P in Fig. 9.16 (which, on the scale shown, are otherwise coincident with the long solid lines) represents protoneutron stars whose baryon number exceeds that of any stable configuration of hyperonized stars. Therefore, when hyperonization commences during diffusion of neutrinos out of the protoneutron star, these initially stable configurations will begin to collapse. We see that the mass range of protoneutron stars that would suffer such a fate is about $\frac{1}{2}M_{\odot}$. Certainly, the lower part of the window for collapse, and perhaps all of it, is compatible with estimates of the masses involved in core collapse [309] and ejecta fallback [311].

One can say something qualitative about the lifetime of the protoneutron stars that have baryon number falling above the point H in Fig. 9.16. As explained above, protoneutron stars with baryon numbers that place them between the points H and P have no stable configuration after *complete* deleptonization. Those that lie closer to H will be stabilized for a longer time since intermediate stages of hyperonization will still support them.

In other words, there is a continuum of sequences of partially hyperonized stars between H and P with complete hyperonization corresponding to H and no hyperonization to P. Therefore, a star at P (or of greater A than corresponds to H) has no temporarily stable, partially hyperonized configuration, whereas one closer to H has a continuum of configurations differing in degree of hyperonization that can still support its baryon number against collapse (for some short time) before total deleptonization and hyperonization to the ground state. This process takes of the order of ten seconds and is the lifetime expected for a protoneutron star whose baryon number (or mass) just exceeds the limit at H, while a shorter life is expected for those nearer P.

As is clear from the discussion, those configurations lying below H are absolutely stable upon hyperonization, and form neutron stars while those above P suffer immediate collapse of the entire presupernova star to form massive black holes. Those configurations whose baryon number places them between H and P will suffer delayed collapse to low-mass black holes (~ 1.5 to $2M_{\odot}$).

9.7.2 Deconfinement-Induced collapse

An alternative possibility is that, upon deleptonization, the hadronic matter of the protoneutron star converts to the quark matter phase containing u, d, and s quarks [31, 312]. This also happens only because deleptonization softens the equation of state, as described above. In both cases we find a substantial window of roughly $0.5M_{\odot}$ into which a protoneutron star may fall and be temporarily stabilized prior to deleptonization and ultimate subsidence into a black hole. The mechanism is evidently robust. In Fig. 9.17 we compare the stable hybrid star sequence (solid line) with the sequence that is temporarily stabilized by the trapped neutrinos, similar to

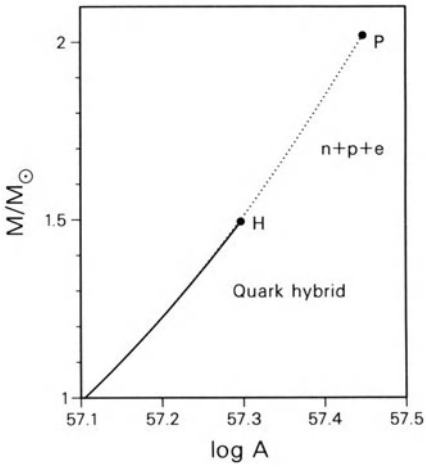

FIGURE 9.17. Similar to Fig. 9.16 but in which hadronic matter undergoes a transition to a mixed phase and a pure quark phase comprising the sequence labeled "hybrid" at greater depth in the star. The bag constant is $B^{1/4} = 185$ MeV and $\alpha_s = 0$. For the hadronic case the corresponding symmetric matter has $m^\star/m = 0.78$, $K = 240$ MeV, and $x_\sigma = 0.6$. (From [31].)

Fig. 9.16. Again there is an extensive range of baryon numbers above H for which the temporarily stabilized stars (n+p+e+μ) have no stable configuration when the matter undergoes the transition to the lower energy state. Protoneutron stars with masses above about $1.5M_\odot$ therefore collapse.

9.7.3 Density profiles

It is of some interest to see the change in the stellar configuration for those protoneutron stars that *do* have a stable final state of hyperonized matter or of quark matter, i. e., those that have a baryon number that falls in the range of the solid line below H in Figs. 9.16 and 9.17. The three configurations—the protoneutron star stage, and the two possible final ground states, hyperonized stars or hybrid stars—are compared in Fig. 9.18 for the same baryon number. (The temperature here is taken as zero. The temperature of the protoneutron star would be mainly reflected in the lower density tail of the star, giving it a larger radius. Thermal pressure is insignificant in comparison with compression and Fermi energy.) The comparison is made for stars of fixed $A = 1.974 \times 10^{57}$ and mass $1.49M_\odot$ (slightly larger for the (n, p, e, μ) configuration).

It can be seen that the protoneutron star composed of the (n, p, e, μ) charge-neutral matter subsides into a denser and more compact configuration as the matter in the interior hyperonizes or converts to quark matter. There will be a modest spin-up in angular velocity as this happens. The moments of inertia of protoneutron star, hyperonized, and hybrid stars are 11.95, 10.37, and 8.964 in units of $M_\odot$-km^2, so that the hyperonized and

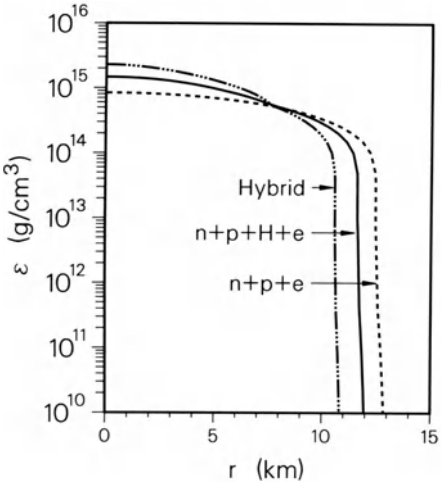

FIGURE 9.18. Mass-energy profile of protoneutron star (dashed) and hyperonized neutron star and hybrid star having the same A and mass $1.49M_\odot$ for the case $m^\star/m = 0.78$, $K = 240$ MeV. Note the more compact configuration of the ground state whether it be a hyperonized neutron star or a hybrid.

quark stars are spun up by factors of 1.15 and 1.33, respectively, over the angular velocity of protoneutron stars.

9.7.4 Discussion

It is believed that the core of a massive evolved star collapses either directly into a black hole or forms a hot, lepton-rich protoneutron star which deleptonizes to form a stable neutron star. A third possibility considered here is that the protoneutron star has a supercritical baryon number larger than that of stable evolved neutron stars and less than that which would lead to immediate collapse of the presupernova star. It is therefore accompanied by a supernova explosion and subsides into a low-mass black hole after deleptonization. The latter two eventualities would both eject heavy elements into the universe in a supernova event signaled by a neutrino pulse of a few seconds duration. They differ in the final fate of the core and in the duration of the neutrino signal. The width of the window for delayed subsidence and the frequency with which it is populated is relevant to the outcome of particular events (for example, SN1987A) as well as for understanding the statistics on supernova-pulsar associations.

Since subsidence of a protoneutron star to a black hole or to a stable hyperonized or hybrid star is triggered by deleptonization, it takes place during that era on its timescale—of the order of ten seconds. The process is regulated by neutrino loss since the other two timescales—hydrodynamic ($\tau_{\rm hydro} \approx 10^{-3}$ s) and weak interaction ($\tau_{\rm weak} \approx 10^{-10}$ s), which governs transformation of nucleons to hyperons—are small by comparison.

Neutrinos trapped in a core which undergoes direct collapse to a black hole (that is the baryon number lies above the point P) will be carried within the horizon by the collapsing core. In contrast, most or all of the neutrinos (depending on where between H and P the baryon number of the protoneutron star lies) will escape during the deleptonization that causes the delayed subsidence of the core into a black hole. However, if the mass is toward the upper end of the window for only temporary stability, the signal will be shortened and in any case the tail will be infinitely red-shifted as the star sinks toward the horizon (page 120). Whether the protoneutron star is subcritical and collapses to a stable hyperonized or hybrid star or is supercritical and collapses by one of the delayed mechanisms to a black hole, the neutrinos produced by hyperonization or formation of quark matter will form the tail of the neutrino signal in either case.

Neutron stars near the upper mass or baryon limit of stability may still suffer collapse to black holes on a much longer timescale of hours to months or years if they are hovering at the limit of evolved neutron stars and there is sufficient mass fallback ($\sim 0.1 M_{\odot}$). The process is complex. Because of the longer timescale, we do not include it as a broadening of the window for prompt subsidence. Moreover, the window for accretion-induced collapse in binary systems is small compared to the two mechanisms we include.

In the cases for which a neutron star is the final ground state, the contracting protoneutron star (Fig. 9.18) may execute damped oscillations about the final configuration, producing a surplus of hyperons (or quark matter) compared to the final equilibrium state of the star and then a deficit, as the density oscillates. Because the diffusion timescale for neutrinos and gammas, produced as decay products of associated kaons, is very long compared to the hydrodynamic timescale, no signature of the density oscillations would be observable in these signals.

If the oscillations were not purely radial pulsations, they would produce gravitational radiation since all stars rotate. Indeed, the density dependence of the shear viscosity in a rotating star would possibly cause deviations from purely radial pulsations. However, we will not explore this possibility here.

The neutrino signal from SN1987A informs us that a protoneutron star was formed [313], but, according to the processes discussed here, it does not inform us that an evolved neutron star was ultimately formed. No pulsed radiation has been observed, and the present evidence from the light curve of the supernova remnant is compatible with the presence of a low-mass black hole but not of a neutron star [314].

If continuing observation of the remnant and search for pulsed radiation from the site of SN1987A reveals no pulsar, one of the mechanisms discussed here may be responsible for turning high-mass protoneutron stars into black holes *after* the processed stellar material has been ejected in a supernova and the neutrino signal of the event has been emitted.

It has been estimated that about one-half of the supernovae in our galaxy leave no promptly observable star [315]. The mechanisms discussed here,

which have the immediate signature of neutron star formation—supernova and neutrino signal—but which are followed by the unannounced subsidence to a low-mass black hole ($M \sim 1.5$ to $2M_\odot$), may contribute to or be responsible for the apparent discrepancy.

9.8 Tables of Equation of State for Hybrid Stars

The following are equations of state for hybrid (neutron-quark) star matter corresponding to nuclear properties identified in Table 5.5. The octet of baryons comprise the composition of the confined phase as described in Chapter 5. The ratio of hyperon to nucleon coupling to the scalar meson field is $x_\sigma = 0.6$. The corresponding coupling to the vector fields can be found in table 5.4. Muons as well as electrons are included. Quark matter is described in Section 8.2.3. The quark masses are taken as $m_u = 0$, $m_d = 0$ and $m_s = 150$ MeV. The bag constants used are $B^{1/4} = 180$ MeV and $\alpha_s = 0$.

TABLE 9.1. Equation of state corresponding to matter with pure confined hadronic phase below a baryon number density 0.26 fm^{-3}, mixed confined-deconfined phase at intermediate densities and pure quark matter at high density above 1.17 fm^{-3}. Nuclear properties correspond to $K = 240$ MeV, $m^\star/m = 0.78$. See also Fig. 9.10.

ρ fm^{-3}	ϵ $\mathrm{g/cm}^3$	p $\mathrm{dyne/cm}^2$	ρ fm^{-3}	ϵ $\mathrm{g/cm}^3$	p $\mathrm{dyne/cm}^2$
0.010	1.6758 +13	7.4377 +30	0.692	1.3047 +15	1.5845 +35
0.015	2.5141 +13	8.9843 +30	0.725	1.3769 +15	1.7514 +35
0.020	3.3529 +13	1.2123 +31	0.759	1.4511 +15	1.9250 +35
0.025	4.1911 +13	1.9243 +31	0.793	1.5258 +15	2.1011 +35
0.030	5.0301 +13	3.2767 +31	0.826	1.5981 +15	2.2725 +35
0.060	1.0074 +14	3.6507 +32	0.856	1.6670 +15	2.4353 +35
0.090	1.5151 +14	1.3499 +33	0.885	1.7318 +15	2.5877 +35
0.120	2.0279 +14	3.1938 +33	0.911	1.7927 +15	2.7291 +35
0.150	2.5471 +14	5.9384 +33	0.936	1.8498 +15	2.8595 +35
0.180	3.0735 +14	9.6207 +33	0.959	1.9035 +15	2.9798 +35
0.210	3.6075 +14	1.4377 +34	0.981	1.9540 +15	3.0905 +35
0.240	4.1500 +14	2.0302 +34	1.001	2.0014 +15	3.1916 +35
0.264	4.5823 +14	2.5825 +34	1.020	2.0465 +15	3.2852 +35
0.286	5.0009 +14	2.7999 +34	1.038	2.0894 +15	3.3718 +35
0.309	5.4220 +14	3.0590 +34	1.055	2.1303 +15	3.4518 +35
0.331	5.8427 +14	3.3598 +34	1.072	2.1697 +15	3.5264 +35
0.354	6.2659 +14	3.7086 +34	1.087	2.2073 +15	3.5951 +35
0.376	6.6933 +14	4.1113 +34	1.103	2.2435 +15	3.6589 +35
0.399	7.1271 +14	4.5758 +34	1.117	2.2787 +15	3.7187 +35
0.422	7.5693 +14	5.1094 +34	1.201	2.4831 +15	4.1354 +35
0.445	8.0224 +14	5.7206 +34	1.231	2.5569 +15	4.3491 +35
0.469	8.4884 +14	6.4181 +34	1.261	2.6313 +15	4.5644 +35
0.494	8.9697 +14	7.2094 +34	1.291	2.7062 +15	4.7813 +35
0.519	9.4685 +14	8.1019 +34	1.321	2.7817 +15	5.0001 +35
0.545	9.9853 +14	9.1000 +34	1.351	2.8578 +15	5.2207 +35
0.571	1.0522 +15	1.0205 +35	1.381	2.9344 +15	5.4430 +35
0.598	1.1077 +15	1.1416 +35	1.411	3.0116 +15	5.6668 +35
0.627	1.1674 +15	1.2753 +35	1.441	3.0892 +15	5.8923 +35
0.659	1.2342 +15	1.4245 +35	1.471	3.1674 +15	6.1193 +35

TABLE 9.2. Equation of state corresponding to $K = 300$ MeV, $m^\star/m = 0.70$ See previous table caption for other details. Pure confined hadronic phase lies below baryon number density 0.25 fm^{-3} and pure deconfined quark matter above 0.86 fm^{-3} See also Fig. 9.9.

ρ fm^{-3}	ϵ g/cm^3	p dyne/cm^2	ρ fm^{-3}	ϵ g/cm^3	p dyne/cm^2
0.010	1.6758 +13	1.1176 +31	0.681	1.2971 +15	1.4839 +35
0.015	2.5151 +13	1.4722 +31	0.695	1.3268 +15	1.5214 +35
0.020	3.3542 +13	1.8839 +31	0.708	1.3558 +15	1.5563 +35
0.025	4.1936 +13	2.5248 +31	0.721	1.3841 +15	1.5889 +35
0.030	5.0326 +13	3.6529 +31	0.734	1.4119 +15	1.6194 +35
0.060	1.0078 +14	3.1818 +32	0.746	1.4391 +15	1.6478 +35
0.090	1.5153 +14	1.2460 +33	0.759	1.4659 +15	1.6745 +35
0.120	2.0278 +14	3.1400 +33	0.771	1.4922 +15	1.6995 +35
0.150	2.5472 +14	6.1711 +33	0.783	1.5181 +15	1.7229 +35
0.180	3.0746 +14	1.0508 +34	0.794	1.5437 +15	1.7449 +35
0.210	3.6114 +14	1.6446 +34	0.806	1.5689 +15	1.7655 +35
0.240	4.1591 +14	2.4246 +34	0.817	1.5938 +15	1.7850 +35
0.246	4.2671 +14	2.5998 +34	0.829	1.6185 +15	1.8033 +35
0.267	4.6611 +14	2.8467 +34	0.840	1.6429 +15	1.8206 +35
0.287	5.0428 +14	3.1158 +34	0.851	1.6671 +15	1.8370 +35
0.308	5.4216 +14	3.4243 +34	0.862	1.6910 +15	1.8524 +35
0.328	5.7994 +14	3.7756 +34	0.891	1.7574 +15	2.0431 +35
0.347	6.1769 +14	4.1721 +34	0.922	1.8246 +15	2.2360 +35
0.367	6.5551 +14	4.6153 +34	0.951	1.8924 +15	2.4311 +35
0.387	6.9343 +14	5.1060 +34	0.982	1.9610 +15	2.6284 +35
0.406	7.3153 +14	5.6422 +34	1.012	2.0302 +15	2.8277 +35
0.426	7.6977 +14	6.2211 +34	1.041	2.1001 +15	3.0291 +35
0.445	8.0811 +14	6.8369 +34	1.071	2.1706 +15	3.2324 +35
0.464	8.4656 +14	7.4841 +34	1.102	2.2417 +15	3.4379 +35
0.484	8.8508 +14	8.1578 +34	1.132	2.3135 +15	3.6450 +35
0.502	9.2318 +14	8.8367 +34	1.161	2.3859 +15	3.8543 +35
0.521	9.6061 +14	9.5082 +34	1.191	2.4589 +15	4.0655 +35
0.539	9.9733 +14	1.0164 +35	1.222	2.5325 +15	4.2783 +35
0.556	1.0332 +15	1.0797 +35	1.252	2.6067 +15	4.4929 +35
0.573	1.0683 +15	1.1404 +35	1.281	2.6814 +15	4.7095 +35
0.589	1.1028 +15	1.1983 +35	1.311	2.7568 +15	4.9277 +35
0.606	1.1371 +15	1.2534 +35	1.342	2.8326 +15	5.1477 +35
0.621	1.1707 +15	1.3057 +35	1.372	2.9091 +15	5.3694 +35
0.637	1.2035 +15	1.3548 +35	1.401	2.9860 +15	5.5926 +35
0.652	1.2356 +15	1.4008 +35	1.431	3.0635 +15	5.8177 +35
0.667	1.2667 +15	1.4438 +35	1.462	3.1416 +15	6.0443 +35

TABLE 9.3. Equation of state corresponding to $K = 300$ MeV, $m^\star/m = 0.78$. See previous table caption for other details. Pure confined hadronic phase lies below baryon number density 0.26 fm^{-3} and pure deconfined quark matter above 1.0 fm^{-3}.

ρ fm^{-3}	ϵ g/cm^3	p dyne/cm^2	ρ fm^{-3}	ϵ g/cm^3	p dyne/cm^2
0.010	1.6770 +13	1.4536 +31	0.741	1.4193 +15	1.8043 +35
0.015	2.5163 +13	2.1180 +31	0.761	1.4639 +15	1.8924 +35
0.020	3.3559 +13	2.7070 +31	0.781	1.5072 +15	1.9765 +35
0.025	4.1957 +13	3.4288 +31	0.800	1.5491 +15	2.0563 +35
0.030	5.0357 +13	4.4907 +31	0.818	1.5896 +15	2.1319 +35
0.060	1.0084 +14	2.9325 +32	0.836	1.6287 +15	2.2032 +35
0.090	1.5159 +14	1.1633 +33	0.853	1.6666 +15	2.2704 +35
0.120	2.0283 +14	2.9844 +33	0.869	1.7033 +15	2.3337 +35
0.150	2.5472 +14	5.8863 +33	0.884	1.7388 +15	2.3932 +35
0.180	3.0737 +14	9.9578 +33	0.900	1.7732 +15	2.4492 +35
0.210	3.6089 +14	1.5355 +34	0.914	1.8066 +15	2.5019 +35
0.240	4.1538 +14	2.2168 +34	0.929	1.8392 +15	2.5514 +35
0.257	4.4599 +14	2.6573 +34	0.942	1.8708 +15	2.5981 +35
0.278	4.8595 +14	2.8840 +34	0.956	1.9017 +15	2.6420 +35
0.300	5.2630 +14	3.1544 +34	0.969	1.9319 +15	2.6835 +35
0.321	5.6665 +14	3.4635 +34	0.982	1.9614 +15	2.7226 +35
0.343	6.0710 +14	3.8151 +34	0.994	1.9903 +15	2.7595 +35
0.364	6.4787 +14	4.2134 +34	1.007	2.0186 +15	2.7944 +35
0.386	6.8903 +14	4.6624 +34	1.036	2.0884 +15	2.9955 +35
0.407	7.3075 +14	5.1657 +34	1.066	2.1588 +15	3.1986 +35
0.429	7.7311 +14	5.7269 +34	1.097	2.2298 +15	3.4035 +35
0.451	8.1620 +14	6.3482 +34	1.127	2.3015 +15	3.6105 +35
0.473	8.6010 +14	7.0314 +34	1.156	2.3738 +15	3.8195 +35
0.496	9.0485 +14	7.7762 +34	1.186	2.4467 +15	4.0301 +35
0.518	9.5044 +14	8.5815 +34	1.217	2.5202 +15	4.2429 +35
0.541	9.9695 +14	9.4465 +34	1.247	2.5943 +15	4.4572 +35
0.564	1.0442 +15	1.0364 +35	1.276	2.6690 +15	4.6735 +35
0.587	1.0916 +15	1.1312 +35	1.306	2.7442 +15	4.8913 +35
0.610	1.1389 +15	1.2281 +35	1.337	2.8200 +15	5.1111 +35
0.632	1.1859 +15	1.3259 +35	1.367	2.8963 +15	5.3323 +35
0.654	1.2325 +15	1.4234 +35	1.396	2.9732 +15	5.5556 +35
0.676	1.2792 +15	1.5206 +35	1.426	3.0506 +15	5.7801 +35
0.698	1.3266 +15	1.6176 +35	1.457	3.1286 +15	6.0064 +35
0.720	1.3734 +15	1.7124 +35	1.487	3.2070 +15	6.2344 +35

10

Strange Stars

10.1 The Strange Matter Hypothesis

It is conventionally assumed that the *ground state* of hadronic matter is the state in which quarks are confined in individual hadrons. This phase of matter occupies the observable universe. Even though we look to the farthest reaches of the cosmos, we recognize spectral lines—whether Doppler, gravitationally or cosmologically shifted—identifiable with transitions of atoms and nuclei known on earth. Most of the mass of every object we can experimentally study resides in its nuclear constituents. Indeed, our experience so firmly affirms the confined phase as the normal phase of matter that we usually do not question it. However, there is presently no evidence to show that the ground state of matter must be that of quarks confined in hadrons. The confined state may simply be a very long-lived state, but not an absolutely stable one. Indeed, it is not possible to prove otherwise save by the discovery of a lower energy state.

In this chapter a very different possibility is considered—*the strange matter hypothesis*—due to Bodmer [284] and Witten [277] independently. According to the hypothesis, the true and absolute ground state of the strong interactions is the deconfined state of quark matter consisting of an approximately equal proportion of up, down, and strange quarks. Matter in such a state is called strange matter.

The strange matter hypothesis may seem manifestly incorrect since all that we know is the confined state. Nevertheless, as we study the hypothesis more deeply we shall see that it is compatible with all known facts including the present appearance of the universe. We will find that the universe would have evolved along the path that it is presumed to have followed and would appear essentially as it is to-day if the hypothesis is true [215, 275, 316, 317]. Only on a very long timescale—that of stellar evolution—is it possible for the confined state of individual hadrons to transform into strange matter.

One way in which the confined phase could slowly evolve into strange matter is through the formation of neutron stars. Neutron stars possess dense cores in which the phase transition to quark matter is likely to occur. In this process the weak interaction would convert about a third of the quarks to the strange flavor because at high density such a state has a lower energy than two-flavor quark matter (because baryon number is shared among three Fermi seas instead of two). If strange matter were the true ground state, then no barrier would exist for the conversion of the *entire* star, once the core has converted. In this way neutron stars would

be converted to strange stars.

How could one tell a strange star from a neutron star? In Chapter 8 it was found that neutron and strange stars have about the same mass and radius. However, in Chapter 7 we established a lower bound on the rotational period of *gravitationally* bound stars (such as neutron stars). We shall see that stars made of matter that is saturated and self-bound,[1] at sufficiently high-energy density, can rotate faster than gravitationally bound stars (for which neutron stars, by reason of their compactness, are the fastest). Consequently, *if a pulsar with a period falling below the limit of gravitationally bound stars were discovered, the conclusion that the confined hadronic phase of nucleons and nuclei is only metastable would be virtually inescapable.*[2]

We shall study the strange matter hypothesis because strange matter is the most likely candidate for the substance of any pulsar found to rotate faster than is possible for a neutron star. First, we examine the compatibility of the hypothesis with our present knowledge of matter, the present nature of the universe, and its evolution in the confined hadronic phase. We will find that there is no scientific basis on which the hypothesis can presently be confirmed or refuted. We derive a condition on strange matter that would allow a star made of it to rotate rapidly—more rapidly than a neutron star. If the hypothesis were true, a host of rare but exotic phenomena could exist some of which we explore in later parts of this chapter. The discovery of any phenomenon that would confirm the hypothesis would be a fundamental discovery.

10.2 Compatibility of the Hypothesis with Present Knowledge

10.2.1 Energetic considerations

From many aspects of nuclear physics, we know that nuclei are composed of nucleons containing up and down quarks—not quark matter. Therefore two-flavor (nonstrange) quark matter lies above the energy per nucleon of nuclear matter. However, what if the equilibrium (normal) state of three-flavor quark matter is at a density sufficiently high that the quark chemical potential is large compared to the strange quark mass? In that case the

[1]By saturated we mean that a bound system's density does not increase with particle number; instead its size increases (as with nuclei). By self-bound we mean matter that is bound in bulk by the strong interaction and does not require gravity for the stability of stellar objects made from it. In contrast, nuclei are unstable above about $A = 250$. By "self-bound" we also imply saturated matter. The pressure of self-bound matter is zero in the equilibrium (normal) state.

[2]Metastable refers to a state of a system that is not its ground configuration but is possibly very long-lived.

baryon number can be shared among three Fermi seas, thus lowering the energy per baryon number.

The available energy scale for comparison is that of QCD, say 100 MeV, established by lattice simulations. As an order of magnitude estimate, treat the quarks as a Fermi gas. The energy density scales as $\epsilon \sim \gamma\mu^4$ and the baryon density as $\rho \sim \gamma\mu^3$, where $\gamma = 2, 3$ is the degeneracy. (Use the zero temperature approximation to Section 8.2.2 and neglect B.) Compare the two types of quark matter at the same baryon density: since $\mu \sim \gamma^{-1/3}$, three-flavor quark matter has an energy per baryon ϵ/ρ of approximately $(2/3)^{1/3} \sim 0.9$ times that of 2-flavor, or about 100 MeV lower. This places the energy per nucleon of strange quark matter in the vicinity of that of nuclear matter. Whether it lies above the nucleon mass or below the energy per nucleon in iron ($\sim$ 930 MeV) may be a matter of only one percent.

Clearly, under the circumstance that the phases of hadronic and strange quark matter lie so close in energy per baryon, models of confinement such as the bag model or even lattice QCD[3] cannot provide even a hint as to which phase is lower. While it is certainly interesting to explore the predictions of models, they are not sufficiently precise to portray either the limitations or possibilities for strange stars.

10.2.2 The universe and its evolution

The strange matter hypothesis could be true even though the universe evolved along a path which brought it to its present phase—a metastable one if the hypothesis is true. The fact that most of the mass in every object that we know—from our own bodies to all the visible galaxies—resides in nucleons and nuclei tells us for certain only that this is one possible state of matter and that it is very long-lived—not necessarily that it is the lowest energy state. How misleading the present composition of the universe is in revealing the nature of the ground state is immediately exposed by noting that the lowest energy state of the confined phase is Fe^{56}—and there is little of that in the universe. We understand perfectly well why this is so. Only a few of the lightest elements were produced in the primordial nucleosynthesis. Heavier elements are fused very slowly in massive stars on the timescale of their evolution ($\geq 10^7$ years).

Witten [277] hypothesized that strange quark matter is absolutely stable as a possible solution to the so-called missing mass or dark matter problem. It is believed by most astronomers, based both on a cosmological argument (observed flatness of the universe) and on the observations that the visible matter of the universe is subject to greater gravitational forces than the visible matter itself would exert, that there is much more matter in the

[3]Solutions of QCD, the confined theory of hadronic matter, are simulated on a spacetime lattice on computers. Even so, attention has been focused only on a very restricted class of problems.

universe, indeed within our own galaxy, than can be seen. Such matter is referred to as dark matter, and has been the subject of much speculation. It is believed to amount to 90% of the total mass of the universe.

In the early high-temperature era, the universe almost certainly passed through the deconfined quark matter phase, of which three-flavor quark matter is lower in energy than two-flavor. Witten reasoned that, if strange matter were the ground state, much matter would have remained in this phase. If it is truly the ground state, then objects from microscopic to star-like would be stable. Such matter in microscopic and macroscopic lumps, called strange nuggets, would be nonluminous and therefore invisible as objects in space. Hence, the suggestion that strange matter formed the dark matter of the universe.

However, it was soon shown that, even if strange matter is the ground state, all (or almost all) strange matter would have evaporated in the high-temperature era into ordinary hadrons. There would be little or no relic strange matter [318, 319]. Strange matter as a candidate for dark matter did not turn out to be a viable suggestion. Nevertheless, it may still be true (in view of the energetic reasons given above) that it is the ground state. Because of the evaporation of hot primordial strange matter into hadrons, we understand why the subsequent evolution of the universe is undisturbed by the question as to which is the absolute ground state of cold matter—the confined or deconfined strange matter state. And we understand why there can be little strange matter present now: it can be recreated only in the interiors of neutron stars and therefore on the timescale of stellar evolution.

10.2.3 Stability of nuclei against decay to strange matter

We know from the arguments presented above that strange quark matter likely has an energy per nucleon that places it close to that of Fe^{56} (~ 930 MeV per nucleon). Theory is not accurate enough to decree whether it is above or below, making it unstable or absolutely stable. Even if strange matter is lower in energy per baryon number, ordinary nuclei can decay into the strange quark phase only on a timescale that is long in comparison with the age of the universe.

The decay is inhibited by the need for A *simultaneous* strangeness-changing weak interactions, where A is the atomic number of the nucleus [285]. It is energetically unfavorable for the transition to take place one quark at a time since this would initially produce only hypernuclei—which are higher in energy than the original ordinary nuclei. It is important in the above argument to realize that surface and shell effects place a lower but uncertain bound ($A = 10 - 1000$) on the baryon number for which small nuggets of strange matter are bound even if strange matter in bulk is absolutely stable [285, 320]. Thus, low-mass nuclei are stable even though

only a few simultaneous weak interactions are required to convert them to strange nuclear nuggets. The lower energy of the nucleon compared to the lambda is an extreme example.

10.2.4 Stability of nuclei to conversion by strange nuggets

Although the mass of the strange quark is larger than that of the up and down quarks, the quark chemical potential exceeds the mass difference at any density above several times nuclear (8.23). All three quarks are therefore almost equally populous (Chapter 8, Section 8.4). Because of the mass difference, a slight deficit of strange quarks exists which provides a nugget with a positive charge but with low Z/A.

The positive charge of strange matter insures that a nugget will repel nuclei. As a result, nuggets will be inert except in a neutron-rich environment, such as neutron stars, in massive stars in the late stage of collapse when the density exceeds the neutron drip density, or in very high-temperature matter where the kinetic energy of charged particles may overcome the Coulomb barrier. Any strange nuggets present on earth will not grow to become conspicuous. Moreover, because of their high density (a few times nuclear density), the surface gravitational force acting on nuggets with $A > 10^{17}$ would exceed the electrostatic forces holding solid material together so that such nuggets would sink toward the center of the earth [285]. The anomalously low charge-to-mass ratio Z/A provides a signature for their identification if they occur on earth with sufficient concentration to be found. However, as we shall see in the next section, the concentration expected on earth is small.

10.2.5 Terrestrial searches

If strange stars exist, there will be some abundance of strange nuggets present on Earth, accumulated as cosmic rays over Earth's lifetime. We now estimate an upper limit to see if strange matter as the ground state is ruled out by present experimental limits. For nearly 20 years of observations on the Hulse–Taylor binary pair of compact stars (one of which is the pulsar with celestial coordinates 1913+16), the observed decay of the binary orbit has confirmed Einstein's gravitational radiation to an accuracy of less than one percent [36, 4]. Eventually, the decay of this orbit will cause the compact stars to collide, and some fraction of their material will be injected into the galaxy. The decay time is short compared to the galactic age.

In our estimate of the abundance of such material that has accumulated on earth, we employ accepted cosmological figures for those items that are available and overestimates of others, so as to get an upper bound on the concentration of strange nuggets. For this purpose we need the age of the

galaxy (10^{10} years), the frequency of galactic type II supernovae[4] ($\sim 1/(100$ yr)) [321], the fraction of pulsars that occur in binary compacts ($\approx 1/100$), and the fraction of mass ejected from a collision (1/10) [322]. We find a mass of debris of $10^5 M_\odot$ spread over the galaxy from compact star collisions. We can translate this into baryon number by noting that $M_\odot \approx 10^{57} m$ where m is the nucleon mass.

For the galaxy volume we take its luminous radius of 15 kpc and approximate the thickness uniformly as 2 kpc. This yields $V_G = 4 \times 10^{67} \mathrm{cm}^3$. We find, for the mass density of debris, $\rho < \frac{1}{2} 10^{-29}$ g/cm^3 or a baryon number density $n < \frac{1}{4} 10^{-5}/$ cm^3 . As an extreme overestimate, assume that all such compacts were strange and that all mass is ejected in minimum mass fragments ($A \approx 1000$ [285]). We find a number density of strange nuggets of $N_G < \frac{1}{4} 10^{-8}/\mathrm{cm}^3$. Assuming a typical galactic velocity of 10^7 cm/s, there would be an influx of $< 10^{15}/\mathrm{cm}^2$ over the age of the earth (5×10^9 yr). (However, the velocity assumed corresponds to the measured typical velocity of pulsars transverse to the galactic plane [323]. If the isotropic component is less, then our flux is an overestimate.)

The earth's crust is not tranquil. Mountains are cast up, then eroded; continents drift; tectonic plates collide and slide over one another. Material that can be recognized as once having been at the earth's surface resurfaces in the lava of volcanic eruptions, having been subducted to the molten core below the mantle. We estimate a geologic mixing depth of the order of ten kilometers (a conservative estimate). Even if all cosmic nuggets were stopped at the earth's surface, they would be diluted to a concentration of $10^9/\mathrm{cm}^3$ or less over geologic times, or $< 10^{-15}$ nuggets per nucleon given an earth density of $5\mathrm{g}/\mathrm{cm}^3$. This extreme overestimate is to be compared with the upper limit of 10^{-14} established by experiment [324].

We conclude the strange matter hypothesis cannot be ruled out by present experimental limits on the abundance of strange nuggets in the earth's crust! There are probably no favorable samples on earth for strange nugget searches, in view of the high degree of dilution. Meteorites have their surfaces burned off in traversing the atmosphere if they are not completely destroyed, and are also not favorable. However, the moon's surface has been exposed to the hypothetical strange cosmic rays without geologic mixing. In addition, only minor meteoritic activity has disturbed the lunar surface since early times. Moon rock might prove to be a favorable sample for mass spectroscopy (because of the anomalously small Z/A of strange matter) or for a Coulomb back scattering experiment such as that of ref. [324].

---

[4]Type II supernovae are the fates of massive stars. The core produces a neutron star or black hole.

10.2.6 Summary, prospects and challenges

Since shortly after Witten's paper, it has been understood that, even if strange matter is the lowest energy state when cold and that the early universe passed through this phase, it was so hot at the time that strange matter would have evaporated into hadrons [319, 318]. Little if any primordial material is expected to have survived [325]. For these reasons and those developed in the preceding paragraphs, we understand that the universe would have evolved along essentially the same path, and, aside from very subtle signals, would appear the same now, no matter which is the ground state. Only at the death of massive stars (when dense matter that is cold on the nuclear scale is produced in the resulting neutron stars) may conditions for the creation of *cold* strange matter occur for the first time. Whether such conditions have ever been achieved depends on the unknown phase-transition density and whether it has been reached in the core of any neutron star. In Chapter 9 we have estimated that it does.

We are only just now entering an era in which advances in technology may allow the detection of the necessarily subtle signals that might be present if the universe exists in a metastable (albeit long-lived) phase instead of the ground state. There being little or no relic strange matter, strange matter can be recreated now, only in the cores of dense neutron stars and only slowly on the scale of evolution of massive stars—about 10^7 years or more.

From the discussion in the introduction to this chapter, we understand that the discovery of a very rapidly rotating pulsar with period smaller than could plausibly be attributed to a neutron star would signal that the universe is in a metastable phase of matter [326, 274]. Detection of the proposed signal is feasible. We expand upon this theme in the next section.

10.3 Submillisecond Pulsars

No submillisecond pulsar has yet been discovered; this is not surprising in view of the detection biases that have been imposed on large-scale searches (Section 5.2.4). As commented on before, the limits on search sensitivity are not easily overcome, but they are not insurmountable. In this section we discuss the difficulties that would be encountered in a conventional interpretation if a submillisecond pulsar were discovered. We then show how its interpretation as a strange star would be natural and, under a certain circumstance, inevitable. A discovery of this sort would be fundamental, so we carefully lay out the arguments in the following sections.

10.3.1 The fine-tuning problem

The mass–radius relationship has a characteristic form shown in Fig. 10.1 for compact stars that are bound only by gravity (like neutron stars). For

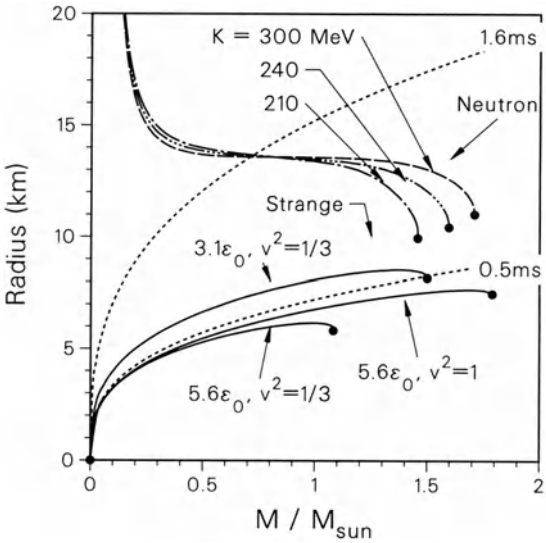

FIGURE 10.1. Generic relationships for compact stars bound only by gravity (neutron stars) and stars made of self-bound matter (strange). Stars below solid lines can rotate at or faster than the indicated period. These curves are representations of (7.1). The equation of state for self-bound matter is parameterized as $\epsilon = p/v^2 + \epsilon_b$, and star families are labeled by the value of ϵ_b and v^2. (From [275].)

low masses where the gravitational attraction is weak, the star is large. For higher masses (near the limit for collapse to a black hole), the radius decreases rapidly with increasing mass. For such stars, only those very close to the mass limit can rotate rapidly because their radius is smallest and mass greatest (see (5.7),(5.8)). In other words, to rotate rapidly a neutron (or hybrid) star must be finely tuned in mass or, equivalently, baryon number. In contrast, the entire sequence of self-bound stars can rotate rapidly, as the figure shows. We discuss the reason for this shortly.

10.3.2 Limits to neutron star rotation

Concerning the question of what is the minimum rotational period of a neutron or hybrid star, we refer to Chapter 7. There we derived the lower limit on the period as a function of stellar mass using only well established principles and minimal constraints on the equation of state. We found, for example, that a canonical neutron star of mass $1.44M_\odot$ cannot have a period of less than $\sim$ 0.3 ms. This is a very conservative and absolute

limit, because there is no physical principle requiring that the structure of stars be optimized so as to minimize their rotational period. Stars with periods below this limit must be made of material that is self-bound at a high equilibrium density. The most plausible candidate is strange matter. Because the absolute limit is extremely conservative, it is worth exploring a less stringent constraint that would still constitute a strong case that a pulsar violating the constraint could not be a neutron star. We did this in Chapter 6, page 273 and found a realistic limit based on numerous models of neutron stars imposed by gravitational-wave instabilities [239]. We concluded that the discovery of a pulsar with period less than ~ 1 ms would constitute strong evidence that the star is not a neutron star or any star bound only by gravity.

10.3.3 Implausibly high central densities

It is true that some neutron star models have been found to posses Kepler periods around 0.5 ms [185]. However, the central densities for such models are so high that their description as neutron stars is implausible. In other words, the basis of the calculation on which such stars are founded is contradicted by the outcome. To underline the situation, in Fig. 10.2 we show the *minimum* possible value of the central density of gravitationally bound stars of canonical mass $1.44M_{\odot}$ as a function of Kepler period [275]. We see that a 0.5 ms pulsar must have an anomalously large density if its matter is in the form of baryons.

It is not known either from experiment or from lattice simulations of QCD at what density the confined hadronic phase would dissolve into the unconfined phase of quark matter. We have found fairly low transition densities in Chapter 9 but those findings are not definitive. We could enquire concerning the density of hadronic matter if compressed to such a degree that all nucleons, treated as spheres of radius equal to the experimental charge radius of the proton (0.8 fm), were in contact. That density is less than three times normal nuclear density. It is quite possible that confinement persists to higher densities. However, it seems hard to reconcile densities of ten or more with confinement of quarks in individual hadrons.

We conclude that such high central densities, as are required for stable rotation at a period of 0.5 ms, are unreasonably high for the confined phase but quite natural for the deconfined phase. At first sight the conclusion reached would seem compatible with hybrid stars. But since hybrids are gravitationally bound, they are subject to the rotational constraints discussed for such stars; in particular, gravitational-wave instabilities moderated by viscosity set the limit, as it appears, of $P \geq 1$ ms (Section 6.10). A strange (self-bound) star is not likely to be subject to the same constraint because the viscosity of quark matter is computed to be high [327]. The surface modes that give rise to gravitational radiation are expected to be

damped and the instability deferred to much higher rotational frequency (Section 6.10).

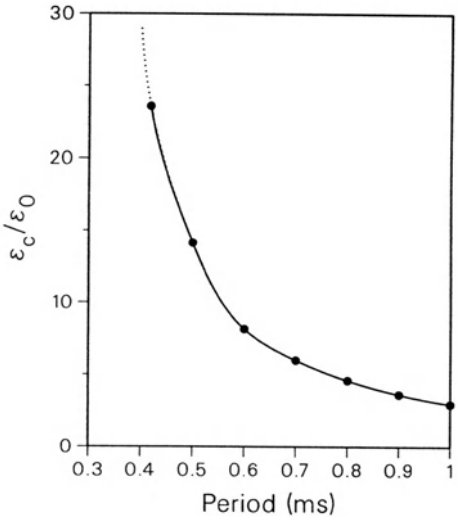

FIGURE 10.2. The least possible central density of 1.44-$M_\odot$ stars required for stable rotation as a function of rotational period. (From [275].)

10.3.4 Strange stars as fast rotors

If strange quark matter is self-bound and absolutely stable, as has been suggested [277, 284], the structure of a compact star composed of such matter would be entirely different from that of a neutron star because of QCD confinement [277, 283, 282]. Such a star is called a strange star, or a strange quark star. While gravity binds all known stars, it merely prevents strange stars from fissioning into smaller bodies, compresses them, and of course, imposes a mass limit that cannot be evaded by relativistic stars (Section 2.8.6). Strange stars are otherwise bound by the strong interaction. They form an entirely distinct and disconnected branch of compact stars and are not part of the continuum of equilibrium configurations that include white dwarfs and neutron or hybrid stars (Fig. 3.2).

Gravitational binding diminishes with lower mass, so that the radius of gravitationally bound stars, like neutron stars, increases as the mass decreases. Below a critical mass ($M \lesssim \frac{1}{10} M_\odot$), neutron stars are unstable. The mass–radius relation is shown in Fig. 10.1. This relation is in sharp contrast to that of hypothetical self-bound stars, such as strange stars. We see this formally as follows. Denote the normal energy density of self-bound matter (the density at which the internal pressure vanishes) by ϵ_b. A small nugget therefore has mass

$$M = \frac{4}{3}\pi R^3 \epsilon_b \qquad \text{(no gravity)} \tag{10.1}$$

so that, unlike neutron stars (or more generally stars bound only by gravity), the mass radius relationship for small mass is

$$R \propto M^{1/3}. \tag{10.2}$$

This dependence of the radius on mass has a generically different form from that of gravitationally bound stars as shown in Fig. 10.1. Because of the relationship between M and R, the entire family of strange stars can rotate rapidly, as can be seen from (7.1), not just those near the limit of collapse to a black hole [274]. This is so because, for such a radius–mass relationship as depicted in the figure, the expression for the Kepler frequency (7.1) is a constant for low-mass strange stars (use (10.1)) and only increases for those near the mass limit because gravity compresses the star to a smaller radius. From (7.1) we can derive a condition on the normal density of self-bound stable matter that will allow all such stars to rotate with period P [215, 275]:

$$\epsilon_b \geq \frac{3}{4\pi G}\left(\frac{\Omega}{\zeta}\right)^2 = 1.4\epsilon_0\left(\frac{\mathrm{ms}}{\mathrm{P}}\right)^2. \tag{10.3}$$

(The empirical factor $\zeta \approx 0.625$ for General Relativity was discussed in connection with (5.7).) For example, all strange stars can rotate with $P = \frac{1}{2}$ ms if $\epsilon_b > 5.6\epsilon_0$ (where $\epsilon_0 = 2.5 \times 10^{14}\mathrm{g/cm}^3$ is normal nuclear density).

Gravitational radiation-reaction instabilities are unimportant for quark stars because of the expected high viscosity [327]. Therefore the Kepler frequency sets the limit.

10.3.5 Out of the impasse

Fast rotation poses problems for understanding a pulsar as a neutron star. On the other hand, four difficulties would be solved by the interpretation of the discovery of a submillisecond pulsar as a strange star.

(1) Very short periods are possible for strange stars provided only the normal density satisfies the above relationship.
(2) Rotation of strange stars is not likely to be limited by gravitational radiation-reaction instabilities because of the expected high viscosity of quark matter.
(3) High central densities, as required by fast rotation (see (5.8)), are natural for quark matter but implausible for confined hadronic matter.
(4) A strange star does not have to be finely tuned in mass (as does a neutron star) to be stable at very fast rotation as illustrated in Fig. 10.1. The whole sequence can rotate rapidly subject to (10.3).

10.3.6 Motivation for searches and prospects for discovery

The factors that presently limit the sensitivity of searches for short-period radio pulsars were discussed in Section 5.2.4. The dispersion of the radio signal by the interstellar medium forces compromises to be made in the search techniques.[5] These compromises cause a sharp roll-off in sensitivity to pulsars with periods below about a millisecond [171, 172]. The limit is not absolute and will be lowered in time, as the search technology is further improved.

Because of the observational bias, the cutoff in short periods that appears in Fig. 5.3 is possibly an artifact. It would indeed be a coincidence if the present technical cutoff in sensitivity coincided with the true lower range of pulsar periods. Therefore, the growing number of pulsar discoveries[6] with periods right down to the search cutoff suggests the tantalizing possibility that pulsars with still shorter periods really do exist.

A special opportunity and challenge exists for radio astronomy. The discovery of additional millisecond pulsars is exciting, both because of their novelty and for what they may reveal of the evolutionary processes involved in their creation and the environment of galactic globular clusters. (Globular clusters are now understood to provide an environment that is especially favorable for the incubation of fast pulsars [166]) But the discovery of a single sub-millisecond pulsar, especially below $\frac{1}{3}$ ms [188] or even below 1 ms (with less decisiveness), would be an experimental result of fundamental importance. A successful search would inform us that the true ground state of the strong interaction is not that of quarks confined in hadrons, but of deconfined strange quark matter. It would also tell us that the universe is in a very long-lived but excited state. This possibility cannot be ruled out at the present time. Aside from a few subtle signals, such as the possible existence of submillisecond pulsars, the universe would have evolved in the manner it did, no matter the ground state (Section 10.2).

10.4 Structure of Strange Stars

We can use the results of Chapter 8 to compute the structure of strange stars and to gain further insight into why self-bound stars can rotate rapidly, provided the equilibrium energy density of the matter from which they are made is high enough. The pressure is zero at equilibrium. That is what equilibrium requires and implies. As we have learned, zero pressure marks the edge of a star. It occurs very abruptly—the mass-energy density falls from $\sim 10^{15}$ g/cm^3 to zero in a distance characteristic of the range of

[5]So far, all millisecond pulsars are observed only at radio frequencies.

[6]The number of known millisecond pulsars tripled between 1992 and 1996.

the force that binds it—the strong interaction length (10^{-13} cm).

The mass-energy profiles of a self-bound star and a neutron star are compared in Fig. 10.3 for stars of the same mass. Because a self-bound star is clearly much more compact, it is more stable to centrifugal disruption. (The edges of neutron stars also terminate abruptly, but on a length scale of atomic spacing and at the much lower density of solid iron—about 7.85 g/cm^3 (see page 73). It is at this density that neutron star matter has zero pressure.)

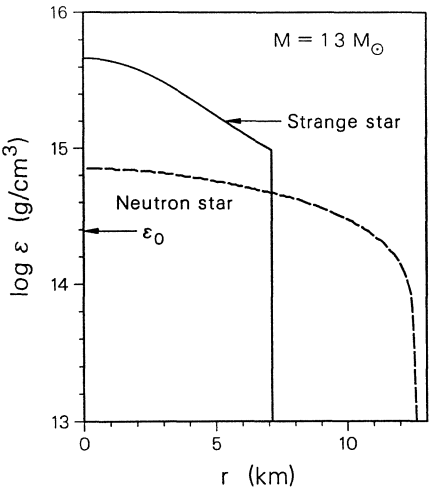

FIGURE 10.3. Mass-energy profile as a function of Schwarzschild coordinate r for a neutron star and a strange star.

Based on the bag model of confinement and the range placed on its parameters by the condition that strange quark matter is the ground state, several authors have asserted that strange stars cannot rotate rapidly [243, 186] or can do so only marginally [328]. This is an unfortunate confusion in logic in translating a statement that is true of a crude model to a statement about nature. We have emphasized elsewhere that whether or not strange stars can rotate very rapidly is entirely an experimental question, not a theoretical one [274]. For to determine on theoretical grounds whether the energy per nucleon in strange matter lies below that in Fe^{56} with $E/A =$ 930 MeV, which would make it absolutely stable, or lies above the nucleon mass at 939 MeV, would require one percent accuracy, an accuracy certainly not possessed by the bag model, nor indeed by lattice QCD now or in the foreseeable future. Neither lattice QCD nor models of confinement can rule out the hypothesis that strange matter is stable, nor conversely can they be used to assert that it is the ground state. Nor can they predict the equilibrium energy density of strange matter.

If the strange matter hypothesis is true, then some or all pulsars may be strange stars rather than neutron stars. Strange stars can be produced in at

least two ways [319, 329]: (1) If the density in the core of the more massive neutron stars exceeds the transition density to quark matter (as seems likely from Chapter 9), the core will spontaneously convert to nonstrange quark matter. In turn, this matter will weak-decay to strange matter. Conversion of the entire star will then occur on a short timescale. (2) If a nugget of strange matter falls into a main sequence star, it will gravitate to the center and lie dormant until the star collapses. When the density exceeds the neutron drip density, the nugget will grow and then convert the entire neutron star produced in the supernova. It is possible that the universe is sufficiently contaminated by strange nuggets (whose abundance is discussed in the next section) that the second process will always preempt the first [330].

10.5 Strange Stars to Strange Dwarfs

10.5.1 Strange stars with nuclear crusts

A strange star has a sharp edge of thickness defined by the range of the strong interaction (cf. Fig. 8.1). Such 'bare' strange stars were discussed in Chapter 8. However, strange stars can also carry a crust of nuclear material which is suspended from contact with the strange star by a strong electric dipole field. This was noted by Alcock, Farhi, and Olinto [283] who pointed out that the electrons (which neutralize the positive charge of strange quark matter and are bound to it by the Coulomb attraction) extend several hundred fermis beyond the edge.[7] In consequence, just inside the surface, there is a positively charged layer (because strange matter by itself is slightly positively charged[8]). Together with the electrons that extend outside the sharp surface of the strange matter, a dipole layer of high voltage is created. The surface dipole layer supports ordinary matter (which it polarizes) out of contact with the core.

The gap between the core and its crust of heavy ions is estimated to be of the order of several hundred fermis [283]. Effects of finite temperature have been investigated in ref. [148]. The maximum density of the nuclear 'crust' is strictly limited by the neutron drip density ϵ_{drip} above which free neutrons would gravitate to the strange core and be converted to quark matter. It is likely that strange stars do have such crusts of various inner crust densities depending on their histories and ages. Interstellar space is not empty.

---

[7]Because electrons are not subject to the strong interaction, their distribution can extend beyond the sharp edge of the quark distribution over a region of the order of the de Broglie wave length.

[8]Because of the strange quark mass, slightly less than 1/3 of the quarks in strange matter are strange.

The above situation—an inner, high-density medium and an outer low-density one separated by a vacuum—is different than ordinarily encountered in stellar structure. However, because the gap between core and crust is negligible on the scale of the size of the star, the situation can be simulated by an effective equation of state [147].

The effective equation of state should consist of two parts: (1) The nuclear crust should be represented by a low-density equation of state of charge-neutral nuclear matter such as forms the crust of neutron stars (Section 5.3.7). The most significant aspect of this density domain is that it consists of a Coulomb lattice of heavy ions immersed in an electron gas. The heavy ions become ever more neutron rich as the neutron drip density is approached from below. The equation of state at subnuclear density down to very low density has been calculated by Baym, Pethick, and Sutherland (BPS) [61]. We use the BPS equation of state to describe the crust having a density at its inner edge at a value below or equal to the neutron drip,

$$\epsilon_{\text{crust}} \leq \epsilon_{\text{drip}} \approx 4 \times 10^{11}\ \text{g/cm}^3 . \tag{10.4}$$

(2) At pressures above that corresponding to ϵ_{crust}, the equation of state corresponds to strange quark matter. We use the simplest form of the bag model equation of state for strange matter because, as far as the relationship of energy density and pressure is concerned, it is accurate to within 4% of the more complicated form involving quark masses [283]. The simplest form is $P = (\epsilon - 4B)/3$.

The edge of stars occurs at $P = 0$, and, if a strange star is bare, the corresponding energy density is $\epsilon = 4B$. In the presence of a crust, the quark core will be slightly compressed by the weight of the crust, and the pressure at the edge of the core will be small but positive and equal to the pressure of the crustal material at the density ϵ_{crust}. Correspondingly, the energy density at the edge of the core will be slightly larger than $4B$. The equation of state is illustrated in Fig. 10.4 for the case that $P_{\text{crust}} = P_{\text{drip}}$. For other inner crust densities the equation of state is represented by

$$P(\epsilon) = \begin{cases} P_{\text{BPS}}(\epsilon) & \text{if } P < P_{\text{crust}} \\ \frac{1}{3}(\epsilon - 4B) & \text{if } P \geq P_{\text{crust}} . \end{cases} \tag{10.5}$$

We adopt a representative value for the bag constant for which 3-flavor strange matter is stable, $B^{1/4}$=145 MeV. This value will serve to illustrate the general features of a nuclear crust on strange stars. For massless strange quarks, this bag constant corresponds to an equilibrium energy per baryon number of about 830 MeV. For strange quarks of 150 MeV mass, it corresponds to about 880 MeV [285]. In other words, this choice represents strongly bound ($\geq$ 50 MeV/nucleon) strange matter that is absolutely bound with respect to ^{56}Fe. Results for more weakly bound but stable strange quark matter can be found in ref. [147].

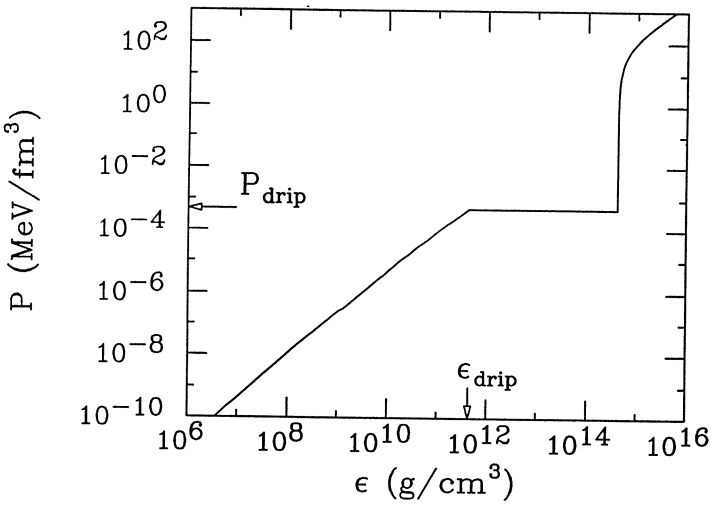

FIGURE 10.4. Equation of state of a strange star surrounded by a nuclear crust with inner density below neutron drip. The symbols $P_{\rm drip}$ and $\epsilon_{\rm drip}$ refer to drip pressure and drip energy density. The quark matter equation of state is calculated for $B^{1/4}$=145 MeV. (From [147].)

Normally, there is one unique sequence of stars for a given equation of state, the mass increasing as the central density is increased—a single-parameter family. However, the density of the crust $\epsilon_{\rm crust}$ (which is arbitrary save that it cannot exceed the drip density) constitutes a second parameter corresponding to the discontinuity in density at the surface of the strange core. The value of the crust density is arbitrary. In any particular case the crust depends on the particular circumstances under which the bare strange star acquired its crust.

Thus, strange stars with nuclear crusts form a two-parameter sequence corresponding to the central density and the inner crust density. In practice we fix the inner density of the crust and vary the central density to generate a corresponding sequence. For a particular equation of state of core and crust material, each pair of such parameters defines a unique stellar structure with a particular mass and radius.

Pressure in a star is a continuous and monotonically decreasing function of the Schwarzschild radial coordinate. However, there is a discontinuity in energy density between strange quark matter and hadronic matter at the pressure corresponding to the inner crust density because the density of quark matter is much higher than nuclear matter at a common pressure. The energy discontinuity between hadronic matter at the crust pressure

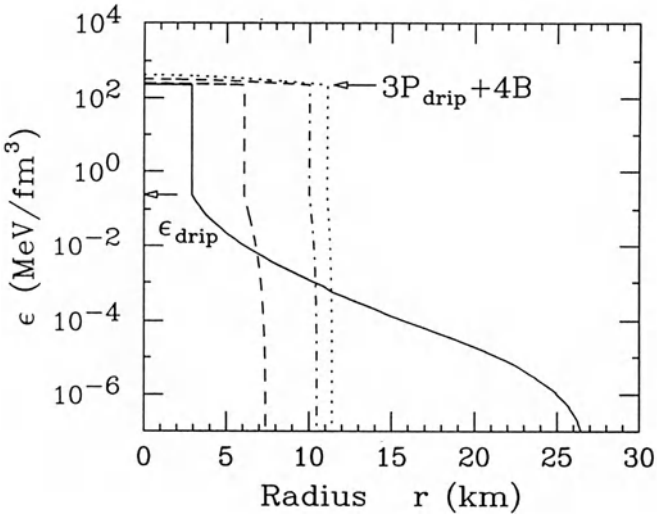

FIGURE 10.5. Strange stars with nuclear crusts at the drip density: energy density as a function of radial distance from the star's center for gravitational masses $M/M_\odot$=0.020 (solid line), 0.20 (dashed), 1.00 (dash-dotted), and 1.50 (dotted). The bag constant $B^{1/4} = 145$ MeV. (From [147].)

and strange quark matter at the same pressure is (Fig. 10.4)

$$\Delta\epsilon \equiv (3P_{\text{crust}} + 4B) - \epsilon_{\text{crust}} \ . \tag{10.6}$$

The energy density of the star will suffer this discontinuity (across the several hundred fermi gap described above) at the radius where the pressure of the star falls from its central value to P_{crust}. The energy density and pressure profiles of several nonrotating sample stars are shown in Figs. 10.5 and 10.6 for gravitational masses in the range of $0.020 \leq M/M_\odot \leq 1.50$. The ends of this range correspond, respectively, to a light star close to the lower mass limit and one closer to the upper mass limit. The sharp fall in the energy profile marks the boundary between the quark core and the nuclear crust.

If strange matter is the absolute ground state, stable objects of strange matter from microscopic nuggets to stars could exist. The nuclear crust, suspended out of contact with the core by the electric dipole layer, is attached to the star by the gravitational interaction. For a given inner density of the crust, the maximum of which is the drip density, the crust will be thinner the more massive the strange quark core, and thicker the less massive it is.

The above behavior of the crust thickness can be understood as a consequence of the way the core radius scales with mass. For masses too small

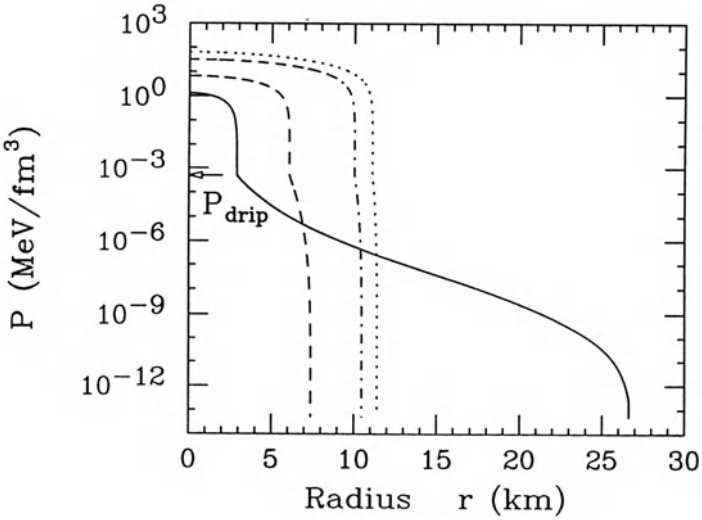

FIGURE 10.6. Pressure as a function of radial distance from the star's center for different gravitational masses (the labeling is the same as in Fig. 10.5). The bag constant $B^{1/4} = 145$ MeV. (From [147].)

for gravity to play an important role, the relationship is $M = (4\pi/3)\, R^3 \epsilon_0$ where $\epsilon_0 = 4B$ is the equilibrium density of strange matter. This relationship is only somewhat modified near the most massive star in the sequence which gravity terminates. Since $R \propto M^{1/3}$, the (Newtonian) gravitational force acting on a unit mass at the surface of the core is $M/R^2 \propto M^{1/3}$. When the inner crust density is the neutron drip density, we find a minimum mass star of $\sim 0.015 M_\odot$, to be compared to $0.1 M_\odot$ for neutron stars [61]. Thus, the thickening of the crust illustrated in Fig. 10.5 for the $M/M_\odot = 0.02$ case (which is close to the lower mass limit for an inner crust density equal to the neutron drip density) illustrates profiles very close to the lower end point of stable strange stars with nuclear crusts of maximum density.

A comparison of these figures for different bag constants B can be facilitated by noting the scaling laws that apply to strange stars [277, 294]. For a central energy density that is some fixed multiple of B, the mass and radius of bare strange stars correspond to different assumptions about the bag constant scale as

$$M \propto 1/\sqrt{B}, \qquad R \propto 1/\sqrt{B}. \tag{10.7}$$

The maximum-mass strange star for a given B corresponds to a central density of $19.2B$.

The mass–radius relationship for strange stars with a nuclear crust is

shown in Fig. 10.7. Because the crust is bound by gravitational interaction, the relationship is qualitatively similar to the one for neutron stars, the radius being largest for the lightest and smallest for the heaviest in the sequence. Just as for neutron stars, the relationship is not necessarily monotonic at intermediate masses. The radius of the strange quark core is also shown, and it follows the inevitable behavior of objects that are self-bound, namely, the one mentioned above, $R \propto M^{1/3}$, which is only somewhat modified near the mass where gravity terminates the stable sequence.

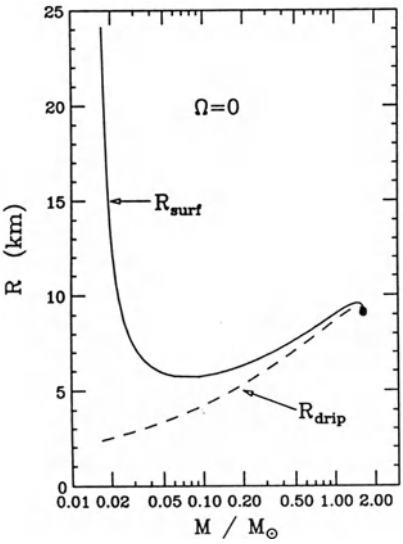

FIGURE 10.7. The radius of the strange core (dashed curve) and the radius of the star including nuclear crust (solid curve) as a function of stellar mass. (From [147].)

10.5.2 Strange dwarfs with nuclear crusts

Strange stars—the counterparts of neutron stars—with central densities above nuclear saturation density, have been extensively discussed in Chapter 8 and in the literature [286]. Here we want to trace the connection between strange stars and strange dwarfs—stars falling in the mass and radius range of white dwarfs but having a core of strange quark matter. We find a possible new class of very dense white dwarfs whose stability is established solely by a strange quark core [149, 66].

The mass–radius relationship for a sequence extending from ordinary neutron stars to ordinary white dwarfs and then to planets is shown in Fig. 10.8. The stable neutron stars are the configurations extending from the maximum-mass neutron star (marked by a bullet) to the minimum-mass star (marked by a vertical line). The stable white dwarf configurations extend from the maximum-mass dwarf toward stars of larger radius.

By comparison, two out of a continuum of strange star sequences extending from strange stars to strange dwarfs are shown. In the one case

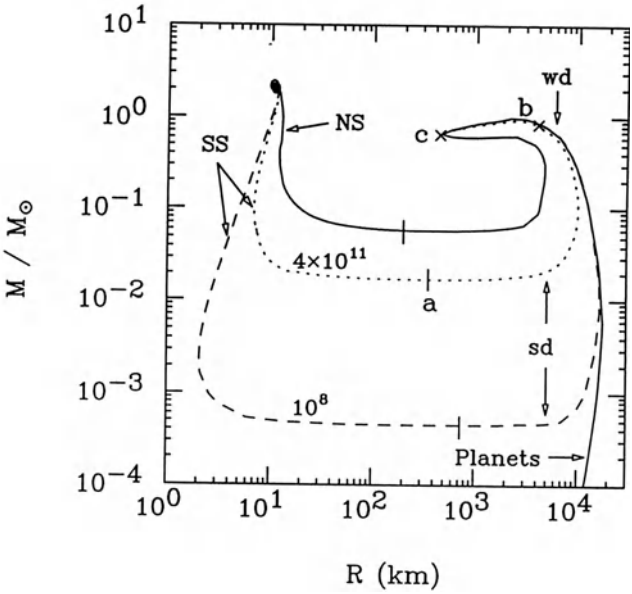

FIGURE 10.8. Neutron star (NS)–white dwarf (wd) sequence, (solid line). Two strange star (SS)–strange dwarf (sd) sequences, for which the inner crust density of nuclear material has the indicated values (in gm/cm^3). The higher value is the drip density. Vertical bars mark minimum mass stars. Crosses mark termination of the strange star sequences where the strange core shrinks to zero. At those points, strange dwarfs become identical to ordinary white dwarfs. (From [149])

the inner crust density is equal to the neutron drip density (the maximum possible value) and, in the other, a much smaller density.

The minimum-mass star on any strange-star sequence (marked by a vertical line in Fig. 10.8) divides it into strange stars analogous to neutron stars and strange dwarfs. The strange stars in these sequences consist primarily of a strange quark core surrounded by a thin nuclear crust of up to a few kilometers. The strange dwarfs consist of a small core and an envelope of nuclei arrayed in a Coulomb lattice region that is up to a few thousand kilometers thick.

Of course, the central density (and therefore the radius of the strange core) shrinks along members of a sequence from the maximum mass strange star toward the dwarfs. In the limit that the radius has shrunk to zero, the star is identical to a white dwarf, and therefore the strange sequence terminates at a point on the white dwarf sequence.

Ordinary white dwarfs could exist which envelop a strange quark core. These would lie on sequences whose inner crust density falls at or below the maximum density of ordinary white dwarfs which is $\epsilon_{\rm wd} \approx 10^9$ gm/cm^3

[61]. One such sequence whose strange dwarf branch is of this class is shown in Fig. 10.8 and labeled by the crust density of 10^8 g/cm^3. Such dwarfs are not very interesting since they would differ imperceptibly from white dwarfs of similar mass but without the core.

Aside from the trivial configurations mentioned above, there are also highly novel ones [149]. There are acoustically and hydrostatically stable strange dwarfs having crustal densities of nuclear material higher by orders of magnitude than is possible for the central densities of ordinary white dwarfs. These stable sequences can have nuclear material with densities as high as the neutron drip density—a few hundred times larger than would be found in the maximum-mass white dwarf and 4×10^4 times larger than in a typical $M = 0.6 M_\odot$ white dwarf. The stable sequences include and lie below the one marked 4×10^{11} and above the one marked 10^8 in Fig. 10.8. These stellar sequences terminate on the *unstable* sequence between white dwarfs and neutron stars. Such stars owe their stability solely to the quark core. Their stability is proved in the next section and some of their characteristics in the following.

10.5.3 Stability

The only astronomically interesting objects are those in hydrostatic equilibrium and stable against radial oscillations. We solve for the eigenfrequencies of the normal radial modes of vibration. (Any other vibrations can be analyzed in terms of the normal modes.) We refer to the catalogue of methods provided by Bardeen, Thorne, and Meltzer [331].

For the metric of a spherically symmetric star (2.169), the adiabatic motion of the star in its nth normal mode (where $n = 0$ is the fundamental mode) is expressed in terms of an amplitude $u_n(r)$ by $\delta r(r,t) = e^\nu u_n(r) e^{i\omega_n t}/r^2$ which denotes small perturbations in r. The quantity $\omega_n(t)$ is the star's oscillatory frequency, which we want to compute. The eigenequation for $u_n(r)$ which governs the nth normal mode—first derived by Chandrasekhar [55]—has the Sturm–Liouville form

$$\frac{d}{dr}\left(\Pi \frac{du_n}{dr}\right) + \left(Q + \omega_n^2 W\right) u_n = 0\,, \tag{10.8}$$

where the functions

$$\begin{aligned}
\Pi &= e^{(\lambda+3\nu)} r^{-2} \Gamma P\ , \\
Q &= -4 e^{(\lambda+3\nu)} r^{-3} \frac{dP}{dr} - 8\pi e^{3(\lambda+\nu)} r^{-2} P\left(\epsilon + P\right)\ , \\
&\quad + e^{(\lambda+3\nu)} r^{-2} \left(\epsilon + P\right)^{-1} \left(\frac{dP}{dr}\right)^2\ , \\
W &= e^{(3\lambda+\nu)} r^{-2} \left(\epsilon + P\right)\ , \\
\Gamma &= \frac{(\epsilon + P)}{P} \frac{\partial P}{\partial \epsilon}
\end{aligned} \tag{10.9}$$

are expressed in terms of the equilibrium configuration of the star. The quantities ϵ, P, and dP/dr denote the energy density, the pressure, and pressure gradient as measured by a local observer. They are obtained from the Oppenheimer–Volkoff equations. The symbol Γ denotes the varying

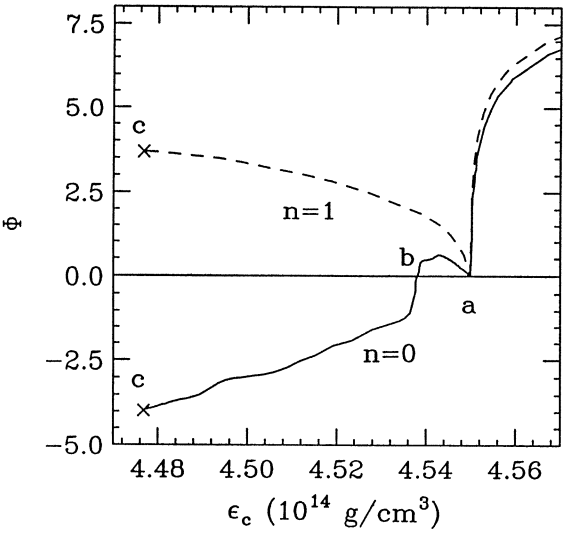

FIGURE 10.9. Pulsation frequencies for $n = 0, 1$ measured by $\Phi(x) \equiv \mathrm{sgn}(x) \log(1 + |x|)$ where $x \equiv (\omega_n/\mathrm{s}^{-1})^2$ as a function of central star density in the vicinity of strange dwarfs having inner crust density equal to neutron drip. For $\Phi < 0$, the squared frequency is negative and the mode unstable. (From [149].)

adiabatic index at constant entropy. The boundary conditions are $u_n \sim r^3$ at the star's origin and $du_n/dr = 0$ at the star's surface. The second of these assures that the Lagrangian change[9] in the pressure at the surface is zero. Solving the eigenvalue equation leads to the frequency spectrum ω_n^2 ($n = 0, 1, 2, \ldots$) of the normal radial modes.

A characteristic feature of the solutions is that the squared eigenfrequencies ω_n^2 form an infinite discrete sequence, $\omega_0^2 < \omega_1^2 < \omega_2^2 < \cdots$. If any of these is negative for a particular star, the frequency is complex and its imaginary part yields an exponentially growing amplitude of oscillation $e^{\mathrm{Im}(\omega)t}$. Such stars are unstable.

We have computed the frequencies for sequences of strange stars (exhibited in Fig. 10.8) having an inner crust density equal to the drip density [149, 66]. For the central density range relevant to the strange dwarfs, a

[9]The Lagrangian perturbation follows moving fluid elements in the perturbed and unperturbed configurations that correspond to one another. In contrast, Eulerian perturbations refer to changes at fixed points in space.

convenient function of the vibrational frequencies is shown in Fig. 10.9. Point 'a' corresponds to the minimum-mass star and 'b' to the maximum-mass strange dwarf of the sequence with crust equal to the drip density. It will be noticed that, at the minimum mass (point 'a'), the squared frequency of the fundamental mode becomes zero, but does not change sign. So the strange star configurations to the left of 'a' and the strange dwarf configurations to the right are all stable. However, at 'b', the squared frequency of the fundamental mode does change sign. Configurations to the right of 'b' are stable and those to the left unstable.

A similar result holds for all other strange sequences with values of inner crust density lower than the drip density. The entire portion of the sequences of strange stars to strange dwarfs with crusts between the maximum-mass star of each class is stable. This is an interesting contrast with ordinary neutron stars and white dwarfs shown by the solid line of Fig. 10.8. In this case all stars in the sequence from the minimum mass neutron star to the maximum mass white dwarf are unstable. The stable part of the branch of white dwarfs are those that extend from the maximum mass toward the region labeled 'planets'—namely, the dwarfs with larger radii than that possessed by the one at the maximum mass. The unstable region spans about five orders in magnitude of central density.

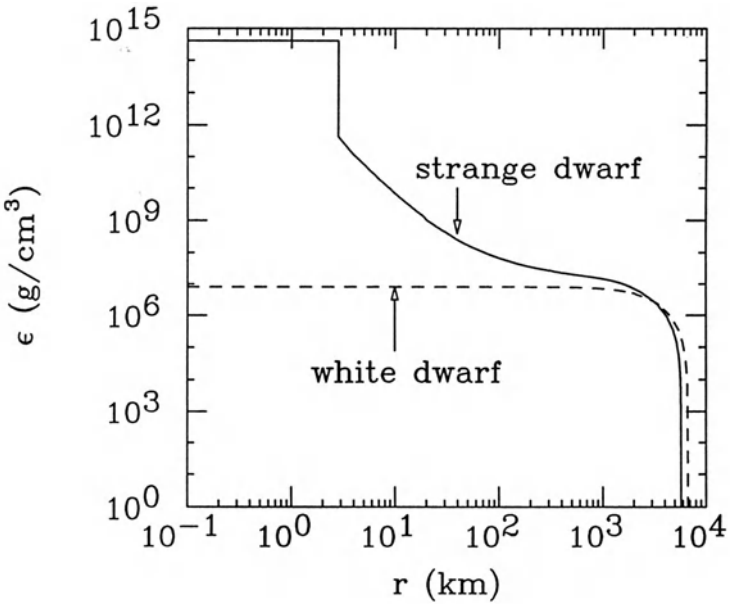

FIGURE 10.10. Mass–energy profile of a strange dwarf and a white dwarf of the same mass $0.6M_{\odot}$. The quark core of the strange dwarf is the structure within 3 kilometers. Outside is nuclear material of 'nner density equal to the neutron drip density. (From [149].)

10.5.4 Possible new class of dense white dwarfs

As just proved, stellar configurations with inner crust densities in the range from the neutron drip density down to the central density of the limiting-mass white dwarf,

$$4 \times 10^{11}\ \mathrm{g/cm^3} \approx \epsilon_{\mathrm{drip}} > \epsilon_{\mathrm{crust}} > \epsilon_{\mathrm{wd}} \approx 10^9\ \mathrm{g/cm^3}\,, \tag{10.10}$$

are stabilized by the presence of the strange core. Without the strange quark matter core, these stars would have central densities that correspond to the unstable sequence of configurations that lie between the stable white dwarfs and neutron stars. We call these stars *strange dwarfs* and distinguish them from the trivial configurations consisting of a strange core and a white dwarf envelope $\epsilon_{\mathrm{crust}} < \epsilon_{\mathrm{wd}}$ which would be stable with or without the core [149].

The masses of the strange dwarfs range from values of about $10^{-4} M_\odot$ to about a solar mass—interesting candidates for gravitational microlensing searches. The lower limit can be compared to $\sim \frac{1}{10} M_\odot$ for a neutron star. They have strange cores of only several kilometers in radius and a baryon number in the range $54.2 < \log A < 55.4$, compared to $\log A \sim 57$ for a neutron star or white dwarf. The mass-energy profile of a strange dwarf is compared to a white dwarf profile in Fig. 10.10. In both cases they correspond to stable stars of a mass $0.6 M_\odot$ (typical of observed white dwarfs). In the case of the strange dwarf, the inner crust density is chosen to have its maximum possible value, the drip density. The inner density of nuclear material can be enormous—up to a few hundred times the maximum density possible in ordinary white dwarfs and about 4×10^4 times larger than the central density in the prevalent mass ($\sim 0.6 M_\odot$) of white dwarfs.

We will say a few words about ways in which the objects described here might be formed. There may be others which we have not imagined, and the history of astronomical discovery cautions us that the laws of nature are explored by the universe in many unanticipated ways. The capture of strange nuggets by main-sequence stars is probably an inevitable consequence if Witten's hypothesis is correct [332, 333]. The galaxy would be filled with a flux of strange nuggets (Section 10.2.5) which would contaminate every object with which they come in contact—planets, neutron stars, white dwarfs, main-sequence stars, etc. Main-Sequence stars are ideal large-surface, long-integration-time detectors for the strange-matter flux because of their large size[332, 333]. In contrast to neutron stars and ordinary white dwarfs (whose material is characterized by a large structural constant so that the nuggets never reach their cores), nuggets accreted onto main-sequence stars can indeed gravitate to their centers, accumulate, and form a strange-matter core that grows with time until the star's demise as a main-sequence star. Those whose mass lies in the approximate mass range ($\sim 1 - 5 M_\odot$) would then give birth to a strange dwarf.

There are other possible modes of formation of dense strange dwarfs. As

discussed in the literature, primordial bodies of mass between $\frac{1}{100}$ and 1 $M_\odot$ may be formed in the early universe and may survive to the present epoch [325]. Such objects will occasionally be captured by a main-sequence star and form a significant core in a single and singular event. Finally, we mention that, in the very early evolution of the universe, lumps of hot, strange quark matter evaporated nucleons which are plausibly gravitationally bound to the lump. The evaporation continues until the quark matter has cooled sufficiently. Depending on the original baryon number of the quark lump, a strange star or a dwarf—both with nuclear crusts, is formed.

10.6 Conclusion

The strange matter hypothesis is compatible with our knowledge of laboratory physics and with all that is known of the universe. It constitutes the most startling possibility conceived for the nature of dense matter. If it is true, all the visible matter of the universe is in a long-lived but metastable state—not the ground state of hadronic matter. The hypothesis has broad implications of great importance for cosmology, the early universe, its evolution, for compact stars, and for laboratory physics of high energy nuclear collisions. Present searches of evidence for the truth of the hypotheses take place in several arenas. There are cosmic ray searches for strange nuggets having an anomalous charge-to-mass ratio [334, 335], there are laboratory searches for low-mass nuggets, possibly only metastable, that may be produced in the collisions of high energy nuclei [336], and searches for submillisecond pulsars as signals of strange stars [337].

Appendix A
Useful Astronomical Data

1. Distance: 1 ly (light year) = 9.4605 $\times 10^{12}$ km.
2. Distance: 1 pc (parsec) = 3.2615 ly (light year) = 3.0856 $\times 10^{13}$ km.
3. Solar mass: $M_\odot = 1.989 \times 10^{33}$ g = 1.477 km.
4. Solar radius: $R_\odot = 6.9598 \times 10^5$ km.
5. Astronomical unit (au) = Sun–Earth distance = 1.4960×10^8 km.
6. Milky Way galaxy mass: $4 - 10 \times 10^{11} M_\odot$.
7. Milky Way galaxy disk radius (luminous matter): ~ 15 kpc.
8. Sun–galactic center distance: 10 kpc.
9. Universe age: $> 1.8 \times 10^{10}$ yrs.
10. Milky Way galaxy age (oldest disk stars): $\sim 10^{10}$ yrs.
11. Earth age: 5×10^9 yrs.
12. Time since extinction of dinosaurs: 7×10^7 yrs.
13. Lifetime of 10 $M_\odot$ stars: 10^7 yrs.

Some useful general references to astrophysical data and phenomena:

Encyclopedia of Astronomy and Astrophysics, R. A. Meyers, ed. Academic Press, San Diego, 1989.

The Astronomy and Astrophysics Encyclopedia, S. T. Maran, ed. Van Nostrand Reinhold, New York, 1992.

Astrophysical Data in two volumes, K. R. Lang, *Planets and Stars* and *Galaxies and the Universe*. Springer-Verlag, New York, 1991.

Books for Further Study

On Relativity:

B. K. Harrison, K. S. Thorne, M. Wakano and J. A. Wheeler, *Gravitation Theory and Gravitational Collapse* (University of Chicago Press, Chicago, 1965).

Ya. B. Zel'dovich and I. D. Novikov, *Relativisitc Astrophysics, Vol. 1, Stars and Relativity* (University of Chicago Press, Chicago, 1971).

S. Weinberg, *Gravitation and Cosmology* (John Wiley & Sons, New York, 1972).

C. W. Misner, K. S. Thorne and J. A. Wheeler, *Gravitation* (W. H. Freeman, San Francisco, 1973).

P. A. M. Dirac, *General Theory of Relativity* (John Wiley & Sons, New York, 1975).

On Theory of Compact Stars:

S. L. Shapiro and S. A. Teukolsky, *Black Holes, White Dwarfs, and Neutron Stars* (John Wiley & Sons, New York, 1983).

On Observations on Compact Stars:

R. N. Manchester and J. H. Taylor, *Pulsars* (W. H. Freeman, San Francisco, 1977).

A. G. Lyne and F. Graham-Smith, *Pulsar Astronomy* (Cambridge University Press, 1990).

References

[1] W. Baade and F. Zwicky, Phys. Rev. **45** (1934) 138.

[2] A. Einstein, Annalen der Phys., **49** (1916) 769.

[3] A. Einstein, *The Meaning of Relativity* (Methuen and Co., London) 5th ed., (A lecture series at Princeton University, 1921, with several revisions in later editions) 1951.

[4] J. H. Taylor, A. Wolszczan, T. Damour and J. M. Weisberg, Nature, **355** (1992) 132.

[5] C. M. Will, *Was Einstein Right?* (Oxford University Press, 1995).

[6] A. A. Michelson and E. W. Morley, Am. J. Sci. **34** (1887) 333.

[7] W. J. Swiatecki, Phys. Scripta **28** (1983) 349.

[8] R. v. Eötvös, Math. Nat. Ber. Ungarn **8** (1890) 65.

[9] K. Nordvedt, Phys. Rev. **169** (1968) 1017; op. cit. **180** (1969) 1293; Phys. Rev. D **3** (1971) 1683.

[10] R. V. Pound and G. A. Rebka, Phys. Rev. Lett. **4** (1960) 337.

[11] A. Schild, Texas Quarterly **3** (1960) 42.

[12] A. Schild, in *Evidence for Gravitational Theories*, ed. by C. Möller, (Academic Press, New York, 1962).

[13] A. Schild, in Relativity Theory and Astrophysics ed. by J. Ehlers, (American Mathematical Society, Providence, R. I., 1967).

[14] S. Weinberg, *Gravitation and Cosmology*, (Johen Wiley & Sons, New York, 1972).

[15] M. Berry, *Principles of Cosmology and Gravitation*, (Adam Hilgar Publ., Bristol, 1989, 1st ed. 1976).

[16] A. Einstein and W. de Sitter, Proc. Nat. Acad. Sci. **18** (1932) 213.

[17] C. W. Misner, K. S. Thorne and J. A. Wheeler, *Gravitation* (Freeman & Co., San Francisco, 1973).

[18] J. R. Oppenheimer and H. Snyder, Phys. Rev. **56** (1939) 455.

[19] M. A. Abramowicz and A. R. Prasanna, Mon. Not. R. Astron. Soc., **245** (1990) 720.

[20] M. D. Kruskal, Phys. Rev. **119** (1960) 1743.

[21] G. Szerkeres, Publ. Mat. Debrecen. **7** (1960) 285.

[22] J. B. Hartle in *Relativity, Astrophysics and Cosmology*, W. Israel ed. (D. Riedel Publishing Co., Dordrecht, Holland), 1973.

[23] B. K. Harrison, K. S. Thorne, M. Wakano and J. A. Wheeler, *Gravitation Theory and Gravitational collapse*, (University of Chicago Press, Chicago, 1965).

[24] N. K. Glendenning, T. Kodama and F. R. Klinkhamer, Phys. Rev. D **38** (1988) 3226.

[25] A. S. Eddington, Observatory **30** (1920) 353.

[26] E. M. Burbidge, G. R. Burbidge, W. A. Fowler and F. Hoyle, Rev. Mod. Phys. **29** (1957) 547.

[27] S. A. Colgate and R. W. White, Astrophys. J. bf 143 (1966) 626.

[28] S. Bludman, D. H. Feng, T. Gaisser and S. Pittel, eds. *The Physics of Supernovae*, Phys. Reports **256** (1995) 1.

[29] A. Burrows and J. M. Lattimer, Astrophys. J. **307** (1986) 178.

[30] N. K. Glendenning, Phys. Lett. **114B** (1982) 392; Astrophys. J. **293** (1985) 470; Z. Phys. A **326** (1987) 57; Z. Phys. A **327** (1987) 295.

[31] N. K. Glendenning, Astrophys. J. **448** (1995) 797.

[32] J. R. Ipser, Astrophys. J. **158** (1969) 17.

[33] D. N. Schramm and R. V. Wagoner, Ann. Rev. Nucl. Part. Sci. **27** (1979) 37.

[34] S. M. Austin, Prog. Part. Nucl. Phys. **7** (1981) 1.

[35] R. A. Hulse and J. H. Taylor, Astrophys. J. (Letters) **191** (1974) L 59; op.cit., **195** (1975) L 51; **201** (1975) L 55.

[36] J. H. Taylor and J. M. Weisberg, Astrophys. J. **345** (1989) 434.

[37] J. M. Weisberg and J. H. Taylor, Phys. Rev. Lett. **52** (1984) 1348.

[38] T. Kodama, Prog. Theor. Phys. bf 47 (1972) 444.

[39] Ya. B. Zel'dovich and I. D. Novikov, *Relativistic Astrophysics, Vol. 1, Stars and Relativity* (University of Chicago Press, 1971).

[40] A. S. Eddington, Observatory **58** (1935) 37.

[41] S. Chandrasekhar, from the Eddington Centenary Lectures, 1982, reprinted in *Truth and Beauty*, University of Chicago Press, 1987, Ch. 6.

[42] K. R. Lang, *Astrophysical Data, Planets and Stars*, (Springer-Verlag, New York, Berlin, 1992).

[43] E. E. Salpeter and H. M. Van Horn, Astrophys. J. **155** (1969) 183.

[44] S. L. Shapiro and S. A. Teukolsky, *Black Holes, White Dwarfs, and Neutron Stars*, John Wiley & sons, N. Y., 1983.

[45] I. S. Gradshteyn and I. M. Ryzhik, *Tables of Integrals, Series and Products*, (Academic Press, N. Y., 1965).

[46] P. M. Morse and H. Feshbach, *Methods of Theoretical Physics*, (McGraw-Hill, New York, 1953).

[47] L. D. Landau and E. M. Lifshitz, *Statistical Physics*, Chapter VIII, (Addison-Wesley, Reading, 1969).

[48] N. K. Glendenning, Phys. Lett. **114B** (1982) 392.

[49] N. K. Glendenning, Astrophys. J. **293** (1985) 470.

[50] R. H. Fowler, Mon. Not. R. Astron. Soc. **87** (1926) 114.

[51] S. Chandrasekhar, Astrophys. J. **74** (1931) 81.

[52] S. Chandrasekhar, Mon. Not. R. Astron. Soc. **95** (1935) 207.

[53] Rev. John Michell, Phil. Trans. R. Soc. (London) **74** (1784) 35-57.

[54] L. D. Landau, Phys. Z. Sowjetunion **1** (1932) 285.

[55] S. Chandrasekhar, Phys. Rev. Lett. **12** (1964) 114.

[56] E. Schatzman, Astron. Zhur. **33** (1956) 800.

[57] B. K. Harrison and J. A. Wheeler, cited in B. K. Harrison et al., *Gravitation Theory and Gravitational Collapse*, (University of Chicago Press, Chicago, 1965).

[58] S. Chandrasekhar and R. F. Tooper, Astrophys. J. **139** (1964) 1396.

[59] J. R. Oppenheimer and G. M. Volkoff, Phys. Rev. **55** (1939) 374.

[60] T. Hamada and E. E. Salpeter, Astrophys. J. **134** (1961) 683.

[61] G. Baym, C. Pethick and P. Sutherland, Astrophys. J. **170** (1971) 299.

[62] V. Weidemann, Annu. Rev. Astron. Astrophys. **28** (1990) 103.

[63] P. J. Siemens, Nucl. Phys. **A141** (1970) 225.

[64] G. Baym, H. A. Bethe, and C. J. Pethick, Nucl. Phys. **A175** (1971) 225.

[65] D. Koester, H. Shultz and V. Weidemann, Astron. and Astrophys. **76** (1979) 262.

[66] N. K. Glendenning, Ch. Kettner, and F. Weber, Astrophys. J. **450** (1995) 253.

[67] R. C. Tolman, *Relativity, Thermodynamics and Cosmology*, (Clarendon Press, Oxford, 1934).

[68] H. Bondi, Proc. R. Soc. (London) **A282** (1964) 303.

[69] J. E. McClintock, in *Physics of the Accretion onto Compact Objects*, K. O. Mason et al., eds. (Springer-Verlag, Berlin, 1986).

[70] A. P. Cowley, Annu. Rev. Astron. Astrophys. **30** (1992) 287.

[71] J. Casares, P. A. Charles and T. Naylor, Nature, **355** (1992) 614.

[72] F. Zwicky, Phys. Rev. **55** (1939) 726.

[73] C. E. Rhoades and R. Ruffini, Phys. Rev. Lett. **32** (1974) 324,
M. Nauenberg and G. Chapline, Astrophys. J. **179** (1973) 277,
L. Pietronero and R. Ruffini, in *Physics and Astrophysics of Neutron Stars and Black Holes*, R. Giacconi and R. Ruffini, eds. (North-Holland, Amsterdam, 1978),
J. B. Hartle, Phys. Rep. **46** (1978) 201,
J. L. Friedman and J. R. Ipser, Astrophys. J. **314** (1987) 594.

[74] J. L. Friedman, J. R. Ipser and L. Parker, Astrophys. J. **304** (1986) 115.

[75] F. Weber and N. K. Glendenning, Astrophys. J. **390** (1992) 541.

[76] M. H. Johnson and E. Teller, Phys. Rev. **98** (1955) 783.

[77] H. P. Duerr, Phys. Rev. **103** (1956) 469;.

[78] J. D. Walecka, Ann. of Phys. **83** (1974) 491.

[79] B. D. Serot and J. D. Walecka, The Relativistic Nuclear Many-Body Problem, in *Advances in Nuclear Physics*, J. W. Negele and E. Vogt, eds. (Plenum Press, New York, 1986).

[80] W. Koepf and P. Ring Nucl. Phys. A493 (1989) 61.

[81] J. König and P. Ring Phys. Rev. Lett. 71 (1993) 3079.

[82] M.M. Sharma, G.A. Lalazissis, W. Hillebrandt, and P. Ring Phys. Rev. Lett. 72 (1994) 1431.

[83] P. Ring Progr. Part. Nucl. Phys. 37 (1996) 193.

[84] H. Toki, Y. Sugahara, D. Hirata, and B.V. Carlson Nucl. Phys. A524 (1991) 633.

[85] V. Blum, J.A. Maruhn, P.-G. Reinhard, W. Greiner Phys..Lett. B323 (1994) 262.

[86] N. K. Glendenning, Nucl. Phys. **A493** (1989) 521.

[87] N. K. Glendenning, Phys. Lett. **114B** (1982) 392; Z. Phys. A **326** (1987) 57; ibid. **327** (1987) 295.

[88] J. Ellis, J. I. Kapusta and K. A. Olive, Nucl. Phys. **B348** (1991) 345.

[89] N. K. Glendenning and S. A. Moszkowski, Phys. Rev. Lett. **67** (1991) 2414.

[90] L. Lindblom, Astrophys. J. **398** (1992) 569.

[91] J. D. Bjorken and S. D. Drell, *Relativistic Fields*, (McGraw Hill, New York, 1965).

[92] H. Goldstein, *Classical Mechanics*, (Addison-Wesley, Cambridge, Mass., 1951).

[93] I. J. R. Aitchison, *An Informal Introduction to Gauge Field Theories*, (Cambridge University Press, Cambridge, 1982).

[94] C. Quigg, *Guage Theories of the Strong, Weak, and Electromagnetic Interactions*, (The Benjamin Cummings Publ. Co., Menlo Park, CA., 1983).

[95] E. Noether, Nachr. Kgl. Ges. Wiss. Gottingen, (1918) 235.

[96] P. A. M. Dirac, *The principles of Quantum Mechanics*, (The Clarendon Press, Oxford, 1947).

[97] P. Möller, W. D. Myers, W. J. Swiatecki and J. Treiner, Atomic Data and Nuclear Data Tables, **39** (1988) 225.

[98] P. M. Möller and J. R. Nix, Nucl. Phys. **A361** (1981) 17.

[99] J. P. Blaizot, D. Gogny and B. Grammiticos, Nucl. Phys. **A265** (1976) 315; J. P. Blaizot, Phys. Rep. **64** (1980) 171.

[100] H. Krivine, J. Treiner and O. Bohigas, Nucl. Phys. **A336** (1980) 155.

[101] N. K. Glendenning, Phys. Rev. Lett. **57** (1986) 1120.

[102] N. K. Glendenning, Phys. Rev. C **37** (1988) 2733.

[103] M. M. Sharma, W. T. A. Borghols, S. Brandenburg, S. Crona, A. van der Woude and M. N. Harakeh, Phys. Rev. C **38** (1988) 2562.

[104] W. D. Myers and W. J. Swiatecki, Nucl. Phys. **A601** (1996) 141.

[105] C. H. Johnson, D. J. Horen and C. Mahaux, Phys. Rev. C **36** (1987) 2252.

[106] C. Mahaux and R. Sartor, Nucl. Phys. **A475** (1987) 247.

[107] M. Jaminon and C. Mahaux, Phys. Rev. C **40** (1989) 354.

[108] H. A. Bethe and J. Goldstone, Proc. R. Soc. (London) **A238** (1957) 551.

[109] L. C. Gomes, J. D. Walecka and V. F. Weiskopf, Ann. of Phys. (New York) **3** (1958) 241.

[110] B. Banerjee, N. K. Glendenning and M. Gyulassy, Nuc. Phys. **A361** (1981) 326.

[111] N. K. Glendenning, B. Banerjee and M. Gyulassy, Ann. Phys. (New York) **149** (1983) 1.

[112] L. D. Landau and E. M. Lifshitz, *Fluid Mechanics*, ch. XV, (Pergamon Press, Oxford, 1959, reprinted, 1982).

[113] J. Boguta and A. R. Bodmer, Nucl. Phys. **A292** (1977) 413.

[114] Gao Shang-hui, Ge Zun-Zao, Y. C. Leung, Li Zong-Wei, and Liang Shao-Rong, Astrophys. J. **245** (1981) 1110.

[115] R. B. Wiringa, V. Fics and A. Fabriconi, Phys. Rev. C **38** (1988) 779.

[116] S. I. A. Garpman, N. K. Glendenning and Y. J. Karant, Nuc. Phys. **A322** (1979) 382.

[117] N. K. Glendenning, Phys. Lett. **185B** (1987) 275;
N. K. Glendenning, Nucl. Phys. **A469** (1987) 600.

[118] N. K. Glendenning, Nucl. Phys. **A512** (1990) 737.

[119] Ya. B. Zel'dovich, Soviet Physics—JETP, **14** (1962) 1143.

[120] N. K. Glendenning, Phys. Lett. B **208** (1988) 335.

[121] S. A. Chin, Ann. Phys. (New York) **108** (1977) 301.

[122] R. C. Tolman, Phys. Rev. **55** (1939) 364.

[123] L. Woltjer, Astrophys. J. **140** (1964) 1309.

[124] F. Pacini, Nature, **216** (1967) 567.

[125] A. Hewish, S. J. Bell, J. D. H. Pikington, P. F. Scott and R. A. Collins, Nature **217** (1968) 709.

[126] R. E. Rothchild, S. R. Kulkarni, R. E. Lingenfelter, Nature, **368** (1994) 432;
T Murakami, Y. Tanaka, S. R. Kulkarni, Y. Ogasaka, T. Sonabe Y. Ogawara, T Aoki and A. Yoshida, op. cit. 127.

[127] T. Gold, Nature, **218** (1968) 731.

[128] V. Canuto in *Proc. Int. Sch. of Phys. "Enrico Fermi"* Course **LXV** (North Holland, N.Y. 1978) 448.

[129] M. A. Ruderman, Nature **223** (1969) 597.

[130] M. A. Ruderman and P. G. Sutherland, Astrophys. J. **196** (1975) 51.

[131] E. Flowers and M. A. Ruderman, Astrophys. J. **215** (1977) 302.

[132] J. P. Ostriker and J. E. Gunn, Astrophys. J. **157** (1969) 1395.

[133] J. E. Gunn and J. P. Ostriker, Phys. Rev. Lett. **22** (1969) 728.

[134] J. E. Gunn and J. P. Ostriker, Astrophys. J. **160** (1970) 979.

[135] D. Pines and J. Shaham, Nature Phys. Sci. **235** (1972) 43.

[136] D. Pines and J. Shaham, Phys. Earth and Planet. Inter., **6** (1972) 103.

[137] J. Shaham, Astrophys. J. **310** (1986) 780.

[138] M. A. Alpar, P. W. Anderson, D. Pines, and J. Shaham, Astrophys. J. Lett. **249** (1981) L29 (1987) 2152.

[139] A. G. W. Cameron, Astrophys. J. **130** (1959) 884.

[140] V. A. Ambartsumyan and G. S. Saakyan, Astron. Zh. **37** (1963) 193 [Soviet Ast. – AJ,**4** (1960) 187].

[141] V. R. Pandharipande, Nucl. Phys. **A178** (1971) 123.

[142] H. A. Bethe and M. Johnson, Nucl. Phys. **A230** (1974) 1.

[143] S. A. Moszkowski, Phys. Rev. D **9** (1974) 1613.

[144] N. K. Glendenning, Nuclear Physics B (Proc. Suppl.) **24B** (1991) 110.

[145] N. K. Glendenning, Phys. Rev. D, **46** (1992) 1274.

[146] F. Weber, N. K. Glendenning and M. K. Weigel, Astrophys. J., **373** (1991) 579.

[147] N. K. Glendenning and F. Weber, Astrophys. J. **400** (1992) 647.

[148] Ch. Kettner, F. Weber, M. K. Weigel and N. K. Glendenning, Phys. Rev. D. **51** (1995) 1440.

[149] N. K. Glendenning, Ch. Kettner and F. Weber, Phys. Rev. Lett. **74** (1995) 3519.

[150] R. N. Manchester and J. H. Taylor, *Pulsars*, (W. H. Freeman and Co., San Francisco, 1977).

[151] A. G. Lyne and F. Graham-Smith, *Pulsar Astronomy*, (Cambridge University Press, 1990).

[152] D. H. Staelin and E. C. Reifenstein, Science **162** (1968) 1481.

[153] M. I. Large, A. F. Vaughan and B. Y. Mills, Nature, **220** (1968) 340.

[154] J. H. Taylor, in *Pulsars as Physical Laboratories*, Blandford, Hewish, Lyne and Mestel, eds. (The Royal Society, Oxford University Press, 1993).

[155] A. Wolszczan, Nature **350** (1991) 688.

[156] D. C. Backer, S. Kulkarni, C. Heiles, M. M. Davis, W. M. Goss, Nature **300** (1982) 615.

[157] M. A. Alpar, A. F. Cheng, M. A. Ruderman and J. Shaham, Nature **300** (1982) 728.

[158] P. R. Bachus, J. H. Taylor and M. Damashek, Astrophys. J. Lett. **255** (1982) L63.

[159] V. Boriakoff, R. Buccheri and F. Fauci, Nature **304** (1983) 417.

[160] A. S. Fruchter, D. R. Stinebring and J. H. Taylor, Nature, **333** (1988) 237.

[161] R. N. Manchester, A. G. Lyne, C. Robinson, N. D'Amico, M. Bailles and J. Lim, Nature, **352** (1991) 219.

[162] A. Wolszczan and D. A. Frail, Nature, **355** (1992) 145.

[163] A. Wolszczan, Science, **264** (1994) 538.

[164] J. F. Bell, M. Bailes, R. N. Manchester, J. M. Weisberg and A. G. Lyne, Astrophys. J. Part 2 - Letters **440** (1995) L81.

[165] L. A. Rawley, J. H. Taylor, and M. M. Davies, Astrophys. J. **326** (1988) 947.

[166] D. C. Backer and S. R. Kulkarni, Phys. Today, **43** (1990) 26.

[167] R.D. Blandford, A. Hewish, A. G. Lyne and L. Mestel, eds., *Pulsars as Physical Laboratories*, (The Royal Society, Oxford University Press, 1993).

[168] N. K. Glendenning, Astrophys. J. **359** (1990) 186.

[169] A. G. Lyne R. N. Manchester and J. H. Taylor, Mon. Not. R. Astron. Soc. **185** (1985) 409.

[170] A. G. Lyne, in *High Energy Phenomena Around Collapsed Stars*, F. Pacini, ed. (D. Riedel Publ., Dordrecht, 1987).

[171] J. H. Taylor and D. R. Stinebring, Annu. Rev. Astron. Astrophys. **24** (1986) 285.

[172] S. R. Kulkarni, in *Pulsars as Physical Laboratories*, R. D. Blandford, A. Hewish, A. Lyne and L. Mestel, eds. (The Royal Society, Oxford University Press, 1993).

[173] D. Bhattacharya and E. P. J. van den Heuvel, Physics Reports, **203** (1991) nos. 1 & 2.

[174] A. G. Lyne and D. R. Lorimer, Nature **369** (1994) 127.

[175] D. A. Frail, W. M. Goss and J. B. Z. Whiteoak, Astrophys. J. **437** (1994) 781.

[176] D. A. Frail and S. R. Kulkarni, Nature **352** (1991) 785.

[177] J. M. Cordes, G. S. Downes and J. Krauss–Polstorff, Astrophys. J. **330** (1988) 847.

[178] R. N. Manchester, in *The Structure and Evolution of Neutron Stars*, D. Pines, R. Tamagaki and S. Tsurata, eds. (Addison-Wesley, Redwood City, Calif., 1992).

[179] J. McKenna and A. G. Lyne, Nature, **343** (1990) 349.

[180] P. Goldreich and W. H. Julian, Astrophys. J. **157** (1969) 869.

[181] A. Hewish and S. E. Okoye, Nature **203** (1964) 171.

[182] F. Pacini, Nature **219** (1968) 145.

[183] J. M. Rankin, Astrophys. J. **274** (1983) 333; loc. cit. **301** (1986) 901.

[184] J. M. Rankin and J. A. Gil, Comments Astrophys. **14** (1989) 1.

[185] J. L. Friedman, J. R. Ipser and L. Parker, Phys. Rev. Lett. **62** (1989) 3015.

[186] P. Haensel and J. L. Zdunik, Nature **340** (1989) 617.

[187] J. W. Negele and D. Vautherin, Nucl. Phys. **A178** (1973) 123.

[188] N. K. Glendenning, Phys. Rev. D **46** (1992) 4161.

[189] S. E. Thorsett, Z. Arzoumanian, M. M. McKinnon and J. H. Taylor, Astrophys. J. **405** (1992) L29.

[190] P. C. Joss and S. A. Rappaport, Ann. Rev. Astr. Astrophys. **22** (1984) 537.

[191] F. Nagase, Publ. Astron. Soc. Japan, **41** (1989) 1.

[192] E. J. Groth, Astrophys. J. Suppl. **29** (1975) 453.

[193] A. G. Lyne, R. S. Pritchard, and F. G. Smith, Mon. Not. R. Astron. Soc. **233** (1988) 667.

[194] A. G. Lyne, R. S. Pritchard, F. Graham-Smith and F. Camilo, Nature **381** (1996) 497.

[195] R. Manchester, J. Durdin, and L. Newton, Nature **331** (1985) 374.

[196] V. M. Kaspi, R. N. Manchester, B. Siegman, S. Johnston, and A. G. Lyne, Astrophys. J. **422** (1994) L83.

[197] R. N. Manchester and B. A. Peterson, Astrophys. J. **342** (1989) L23.

[198] H. Ögelman and G. Hasinger, Astrophys. J. **353** (1990) L21.

[199] F. Nagase, J. Deeter, W. Lewis, T. Dotani, F. Makino, and K. Mitsuda, Astrophys. J. **351** (1990) L13.

[200] Ch. Gouiffes, J. P. Finley, and H. Ögelman, Astrophys. J. **394** (1992) 581.

[201] N. K. Glendenning and F. Weber, Phys. Rev. D **50** (1994) 3836.

[202] B. D. Serot and J. D. Walecka, Phys. Lett. **87B** (1980).

[203] C. J. Horowitz and B. D. Serot, Nucl. Phys. **A368** (1981) 413.

[204] J. Boguta, Nucl. Phys. **A372** (1981) 386.

[205] P.-G. Reinhard, M. Rufa, J. Maruhn, W. Greiner and J. Friedrich, Z. Phys. **A323** (1986) 13.

[206] Liu Zhi-cheng, Liang Shao-rong and Gao Shang-hui, Act. Astrophys. Sin. **5** (1986) 310.

[207] O. V. Maxwell, Astrophys. J. **316** (1987) 691.

[208] K. Nomoto and S. Tsuruta, Astrophys. J. **312** (1987) 711.

[209] M. Prakash, M. Prakash, J. M. Lattimer and C. J. Pethick, Astrophys. J. **390** (1992) L77.

[210] D. Vautherin and P. Bonche, Nucl. Phys. **A372** (1981) 496.

[211] D. Q. Lamb, J. M. Lattimer, C. J. Pethick and D. G. Ravenhall, Nucl. Phys. **A360** (1981) 459.

[212] D. G. Ravenhall, C. J. Pethick and J. R. Wilson, Phys. Rev. Lett. **50** (1983) 2066;
D. G. Ravenhall, C. J. Pethick and J. M. Lattimer, Nucl. Phys. **A407** (1983) 571, and references cited.

[213] R. D. Williams and S. E. Koonin, Nucl. Phys. **A435** (1985) 844.

[214] L. Lindblom, Astrophys. J. **317** (1987) 325.

[215] N. K. Glendenning, in *Relativistic Aspects of Nuclear Physics*, Rio de Janeiro, August 1989, T. Kodama K. Chung, S. Duarte and M. Nemes, eds. (World Scientific, Singapore, 1990).

[216] J. I. Kapusta, and K. A. Olive, Phys. Rev. Lett. **64** (1990) 13.

[217] J. Boguta and S. Bohrmann, Phys. Lett. **102B** (1981) 93.

[218] G. E. Walker, Nucl. Phys. **A450** (1986) 287c.

[219] M. Rufa, H. Stocker, P. G. Reinhardt, J. Maruhn and W. Greiner, J. Phys. **G13** (1987) L143.

[220] M. Rufa, J. Schaffner, J. Marhun, H. Stocker, W. Greiner and P.–G. Reinhard, Phys. Rev. C **42** (1990) 2469.

[221] D. J. Millener, C. B. Dover and A. Gal, Phys. Rev. C **38** (1988) 2700.

[222] N. M. Hugenholtz and L. Van Hove, Physica **24** (1958) 363.

[223] M. M. Sharma. W. Stocker, P. Gleissl, and M. Brack, Nucl. Phys. **A504** (1989) 337.

[224] N. K. Glendenning, D. Von–Eiff, M. Haft, H. Lenske, and M. K. Weigel, Phys. Rev. C **48** (1993) 889.

[225] J. Mares and B. K. Jennings, Phys. Rev. C **49** (1994) 2472.

[226] E. Gudmundson, C. Pethick and R. Epstein, Astrophys. J. **272** (1983) 286.

[227] K. A. Van Riper, Astrophys. J. Suppl. **75** (1988) 449.

[228] N. K. Glendenning, Z. Phys. A, **327** (1987) 295.

[229] H. A. Bethe and G. E. Brown, Astrophys. J. Lett. 445 (1995) L129.

[230] N. K. Glendenning, in *Proceedings of the 1989 International Nuclear Physics Conference*, Sao Paulo, Brasil, Vol. 2, M. S. Hussein et al., eds. (World Scientific, Singapore, 1990).

[231] D. B. Kaplan and A. Nelson, Phys. Lett. **175 B** (1986) 57.

[232] G. E. Brown and H. A. Bethe, Astrophys. J. **423** (1994) 659.

[233] P. J. Ellis, R. Knorren and M. Prakash, Phys. Lett. **B349**, (1995) 11.

[234] J. Schaffner and I. N. Mishustin, Phys. Rev. C **53** (1006) 1416.

[235] N. K. Glendenning, P. Hecking and V. Ruck, Ann. Phys. (New York) **149** (1983) 22.

[236] J. B. Hartle, Astrophys. J. **150** (1967) 1005.

[237] J. B. Hartle and K. S. Thorne, Astrophys. J. **153** (1968) 807.

[238] B. Datta, Nature **308** (1984) 338;
B. Datta and Kapoor, Nature **315** (1985) 557;
B. Datta and Ray, Mon. Not. R. Astron. Soc. **204** (1983) 75P.

[239] F. Weber and N. K. Glendenning, Z. Phys. A **339** (1991) 211.

[240] F. Weber and N. K. Glendenning, Phys. Lett. B **265** (1991) 1.

[241] M. Salgado, S. Bonazzola, E. Gourgoulhon and P. Haensel, Astron. Astrophys. **291** (1994) 155.

[242] K. Sato and H. Suzuki, Prog. Theoret. Phys. (Tokyo) **81** (1989) 997.

[243] J. M. Lattimer, M. Prakash, D. Masak and A. Yahil, Astrophys. J. **355** (1990) 241.

[244] J. B. Hartle and D. Sharp, Astrophys. J. **147** (1967) 317.

[245] D. J. Hegyi, Astrophys. J. **217** (1977) 244.

[246] F. Weber, *Hadron Physics and Neutron Star Properties*, Habilitation Thesis, Ludwig-Maximilians University of Munich, 1992.

[247] F. Weber and M. K. Weigel, Nucl. Phys. **A505** (1989) 779, and references contained therein.

[248] N. K. Glendenning, F. Weber and S. A. Moszkowski, Phys. Rev. C. **45** (1992) 844.

[249] B. Friedman and V. R. Pandharipande, Nucl. Phys. **A361** (1981) 502.

[250] P. Poschenrieder and M. K. Weigel, Phys. Lett. **200B** (1988) 231; P. Poschenrieder and M. K. Weigel, Phys. Rev. C **38** (1988) 471.

[251] R. Machleidt, K. Holinde, and Ch. Elster, Phys. Rep. **149** (1987) 1.

[252] K. Holinde, K. Erkelenz, and R. Alzetta, Nucl. Phys. **A194** (1972) 161; **A198** (1972) 598.

[253] L. S. Celenza and C. M. Shakin, *Relativistic Nuclear Structure Physics*, World Scientific Lecture Notes in Physics, Vol. 2, World Scientific, Singapore, 1986.

[254] C. J. Horowitz and B. D. Serot, Nucl. Phys. **A464** (1987) 613.

[255] B. ter Haar and R. Malfliet, Phys. Rep. **149** (1987) 208.

[256] F. Weber and N. K. Glendenning, *Hadronic Matter and Rotating Relativistic Neutron Stars*, in Proc. of the Nankai Summer School on Astrophysics and Neutrino Physics, Tianjin, China 1991, D. H. Feng, G. Z He and X. Q. Li, eds. (World Scientific, Singapore, 1993).

[257] S. Chandrasekhar, Phys. Rev. Lett. **24** (1970) 611.

[258] S. Chandrasekhar, Astrophys. J. **161** (1970) 561.

[259] J. L. Friedman and B. F. Schutz, Astrophys. J. bf 222 (1978) 281.

[260] L. Lindblom and S. L. Detweiler, Astrophys. J. **211** (1977) 565.

[261] E. Flowers and N. Itoh, Astrophys. J. **206** (1976) 218.

[262] C. Cutler and L. Lindblom, Astrophys. J. **314** (1987) 234.

[263] S. L. Detweiler, Astrophys. J. **197** (1975) 203.

[264] W. Thomson, Phil. Trans. R. Soc. (London), **153** (1863) 608.

[265] N. Comins, Mon. Not. R. Astron. Soc. **189** (1979) 233.

[266] N. Comins, Mon. Not. R. Astron. Soc. **189** (1979) 255.

[267] L. Lindblom, Astrophys, J. **303** (1986) 303.

[268] R. A. Managan, Astrophys. J. **309** (1986) 598.

[269] J. R. Ipser and L. Lindblom, Astrophys. J. **373** (1991) 213.

[270] C. Cutler, L. Lindblom and R. J. Splinter, Astrophys. J. **363** (1990) 603.

[271] S. Koranda, N. Stergioulas and J. L. Friedman, Astrophys. J. (Preprint 1996, to be published).

[272] A. R. Curtis, Proc. R. Soc. (London), A **200** (1950) 248.

[273] J. E. Dennis, Jr. and R. B. Schnabel, *Numerical Methods for Unconstrained Optimization and Non-Linear Equations*, (Prentis–Hall, New Jersey, 1983).

[274] N. K. Glendenning, Phys. Rev. Lett. **63** (1989) 2629.

[275] N. K. Glendenning, Mod. Phys. Lett. A, **5** (1990) 2197.

[276] S. A. Bludman and M. A. Ruderman, Phys. Rev. **170** (1968) 1176; Phys. Rev. D **1** (1970) 3243.

[277] E. Witten, Phys. Rev. D **30** (1984) 272.

[278] S. Bahcall, B. W. Lynn and S. B. Selipsky, Nucl. Phys. B **325** (1989) 606.

[279] B. W. Lynn, A. E. Nelson and N. Tetradis, Nucl. Phys. B **345** (1990) 186.

[280] J. L. Friedman, Phys. Rev. Lett. **51** (1983) 11.

[281] J. R. Ipser and L. Lindblom, Phys. Rev. Lett. **62** (1989) 2777.

[282] P. Haensel, J. L. Zdunik and R. Schaeffer, Astron. Astrophys. **160** (1986) 121.

[283] C. Alcock, E. Farhi and A. V. Olinto, Astrophys. J. **310** (1986) 261.

[284] A. R. Bodmer, Phys. Rev. D **4** (1971) 1601.

[285] E. Farhi and R. L. Jaffe, Phys. Rev. D **30** (1984) 2379.

[286] *Strange Quark Matter in Physics and Astrophysics*, J. Madsen and P. Haensel, eds. Nuclear Physics B (Proc. Suppl.) **24B** (1991).

[287] S. Bahcall, B. W. Lynn and S.B. Selipsky, Nucl. Phys. B **331** (1990) 67.

[288] F. R. Klinkhamer, and N. S. Manton, Phys. Rev. C **30** (1984) 2212.

[289] A. Chodos, R. L. Jaffe, K. Johnson, C. B. Thorne and V. F. Weisskopf, Phys. Rev. D **9** (1974) 3471.

[290] S. A. Chin, Phys. Lett. **78B** (1978) 552.

[291] J. I. Kapusta, Nucl. Phys. **B148** (1979) 461.

[292] O. K. Kalashnikov and V. V. Klimov, Phys. Lett. **88B** (1979) 328.

[293] N. K. Glendenning, in *1990 Summer School on the Structure of Hadrons and Hadronic Matter,* Dronton, The Netherlands, O. Scholten and J. H. Koch, eds. (World Scientific, Singapore, 1991).

[294] C-S. Wang and W. Wang, Commun. Theor. Phys. (China) **15** (1991) 347.

[295] C. W. Misner and H. S. Zapolsky, Phys. Rev. Lett. **12** (1964) 635.

[296] N. Itoh, Prog. Theor. Phys. (Tokyo) **44** (1970) 291.

[297] G. Baym and S. Chin, Phys. Lett. **62B** (1976) 241.

[298] G. Chapline and M. Nauenberg, Nature **264**.

[299] B. D. Keister and L. S. Kisslinger, Phys. Lett. **64B** (1976) 117.

[300] G. Baym and S. A. Chin, Phys. Lett. **62B** (1976) 241.
G. Chapline and M. Nauenberg, Nature **264** (1976) 235; Phys. Rev. D **16** (1977) 456.
B. D. Keister and L. S. Kisslinger, Phys. Lett. **64B** (1976) 117.
W. B. Fechner and P. C. Joss, Nature **274** (1978) 347.
B. Freedman and L. McLerran, Phys. Rev. D **17** (1978) 1109.
H. A. Bethe, G. E. Brown and J. Cooperstein, Nucl. Phys. **A462** (1987) 791.
B. D. Serot and H. Uechi, Ann. Phys. (New York) **179** (1987) 272.
N. K. Glendenning, in *Proceedings of the 1989 International Nuclear Physics Conference*, Sao Paulo, Brasil, Vol. 2, p. 711, M. S. Hussein et al., eds. (World Scientific, Singapore, 1990).
J. Ellis, J. Kapusta and K. A. Olive, Nucl. Phys. **B348** (1991) 345.
A. Rosenhauer, E. F. Staubo, L. P. Csernai, T. Overgard, and E. Ostgaard, Nucl. Phys. **540** (1992) 630.

[301] H. Heiselberg, C. J. Pethick, and E. F. Staubo, Phys. Rev. Lett. **70** (1993) 1355.

[302] N. K. Glendenning and S. Pei, Phys. Rev. C **52** (1995) 2250.

[303] N. K. Glendenning and S. Pei, (in the Eugene Wigner Memorial Issue of) Heavy Ion Physics (Budapest)**1** (1995) 1.

[304] W. D. Myers, W. J. Swiatecki and C. S. Wang, Nucl. Phys. **A436** (1985) 185.

[305] V. R. Pandharipande and E. F. Staubo, in *Proc. 2'nd International Conf. of Physics and Astrophysics of Quark-Gluon Plasma,* Calcutta, 1993, Eds. B. Sinha, Y. P. Viyogi and S. Raha, (World Scientific, 1994).

[306] N. K. Glendenning, in *International Conference on Nuclear Physics at the Turn of the Millennium*, E. Stein and H. Stocker, eds. 1996 (World Scientific Press, to be published) Structure of Vacuum and Elementary Matter, March 10 to March 16 1996, Wilderness/George, South Africa.

[307] V. Thorsson, M. Prakash, and J. M. Lattimer, Nucl. Phys. **A572** (1994) 693.

[308] I. Bombaci, M. Prakash, M. Prakash, P. J. Ellis, J. M. Lattimer and G. E. Brown, Nucl. Phys. **A583** (1995) 623.

[309] S. E. Woosley and T. A. Weaver, Ann. Rev. Astron. Astrophys. **24** (1986) 205.

[310] W. Keil and H. T. Janka, Astron & Astrophys. **296** (1994) 145.

[311] F. C. Michel, Nature, **333** (1988) 644.

[312] M. Prakash, J. R. Cooke and J. M. Lattimer, Phys. Rev. D **52** (1995) 661.

[313] A. Burrows, Astrophys. J. **335** (1988) 891.

[314] G. E. Brown and J. C. Weingartner, Astrophys. J. **436** (1994) 843.

[315] D. J. Helfand and R. H. Becker, Nature, **307** (1994) 215.

[316] J. Madsen in *Strange Quark Matter in Physics and Astrophysics*, J. Madsen and P. Haensel, eds. Nucl. Phys. B, Proc. Suppl. **24** (1991).

[317] J. Madsen, *Physics and Astrophysics of Strange Quark Matter*, Proceedings of the 2nd International Conference on Physics and Astrophysics of Quark-Gluon Plasma, January 19-23, 1993, Calcutta, India, B. Sinha, Y. P. Viyogi, and S. Raha, eds. (World Scientific Press, Singapore, 1994).

[318] C. Alcock and E. Farhi, Phys. Rev. D **32** (1985) 1273.

[319] C. Alcock and A. V. Olinto, Ann. Rev. Nucl. Part. Sci. **38** (1988) 161.

[320] J. Madsen, Phys. Rev. D **47** (1993) 5156.

[321] E. Cappellaro and M. Turatto, Astron. Astrophys. **190** (1988) 10.

[322] J. P. A. Clark and D. M. Eardley, Astrophys. J. **215** (1977) 311.

[323] A. G. Lyne, B. Anderson, and M. Salter, Mon. Not. R. Astron. Soc. **201** (1982) 503.

[324] M. Brugger, K. Lutzenchirchen, S. Polikanov, G. Hermann, M. Overbeck, N. Trautmann, A. Breskein, R. Chechnik, Z. Fraenkel and U. Smilansky, Nature **337** (1989) 434.

[325] W. N. Cottingham, D. Kalafatis and R. Vinh Mau, Phys. Rev. Lett. **73** (1994) 1328.

[326] N. K. Glendenning, J. of Phys. G, **15** (1989) L255.

[327] R. F. Sawyer, Phys. Lett. **233** (1989) 412.

[328] J. A. Frieman and A. V. Olinto, Nature **341** (1989) 633.

[329] A. V. Olinto, Phys. Lett. **192B** (1987) 71.

[330] R. R. Caldwell and J. L. Friedman, Phys. Lett. B **264** (1991) 143.

[331] J. M. Bardeen, K. S. Thorne, and D. W. Meltzer, Astrophys. J. **145** (1966) 505.

[332] J. Madsen, Phys. Rev. Lett. **61** (1988) 2909.

[333] J. Madsen, *Quark Nuggets, Dark Matter and Pulsar Glitches*, Proceedings of the XXIVth Rencontre de Moriond, Les Arcs, Savoie, France, March 5–12, 1989, J. Audouze and J. Tran Thanh Van, eds. (Edition Frontiers, Paris, 1990).

[334] T. Saito, Y. Hatano, Y. Fukuda, and H. Oda, Phys. Rev. Lett. **65** (1990) 2094.

[335] T. Saito, *Search for Strange Quark Nuggets in Galactic Cosmic Rays*, Proceedings of the International Symposium on Strangeness and Quark, Crete, Greece, G. Vassiliadis, A. D. Panagiotou, S. Kumar, and J. Madsen, eds. (World Scientific, Singapore 1995).

[336] C. Greiner, D. H. Rischke, H. Stocker and P. Koch, Phys. Rev. D **38** (1988) 2797.

[337] A. Wolszczan, private communication.

Index

Accretion
  disk, 118, 185
  and pulsar spin-up, 191, 266, 273
Action principle in gravity, 52
Active galactic nuclei, 60, 118
Affine connection, 24, 26, 31, 43, 45
  symmetry, 24

Baryon current, 140
Baryon density, 151
Baryon mass of star, 50, 299
Baryon number, proper, 110
Baryon, octet, 124
Beta equilibrium, 207, 212, 241; *see also* General beta equilibrium
Bianchi identities, 38
Big bang, 61, 327
Binding energy, neutron star, 66, 111, 112, 206
Black dwarf, 57
Black hole, 4, 41, 45, 50, 52, 60, 62, 64, 95, 97, 99, 118, 185, 224, 226, 300
  density, 123
  formation of low-mass, 305, 326–328
  horizon, 45
  low-mass, 332
  massive, 329
Bohr radius, 74, 104
Bondi, 110
BPS equation of state, 101, 243
Braking index, 201, 202–205

Causal limit, 96
Causality, 98, 109, 115, 277
Chandrasekhar mass, 58, 199
  limit for white dwarf, 94, 97
Charge favored baryon, 221
Charge neutrality
  among baryons, 240, 297, 313, 317
  global, 304, 308
  local, 304, 305, 308, 309
  of stars, 71, 207, 228, 240
Charge symmetry energy, 144; *see also* Isospin symmetry; Nuclear symmetry energy
Chemical equilibrium, 83, 208, 209, 217; *see also* Chemical potential
Chemical potential, 72, 83, 209, 217
  and conserved charges, 212
  independent, 209
Christoffel symbol, 25, 43; *see also* Affine connection
Clouds, interstellar gas, 55
Cold catalyzed matter, 100, 105, 222
Comma subscript notation, 16
Complex substance, several conserved charges, 308, 311, 319
Compression modulus, 234
Conservation laws
  baryon, 140
  global, 308
Conserved charge, 208, 209
  global, 308
Contraction of tensor indices, 17
Contravariant vector, 9, 14
Contravariant vector, law of transformation, 15
Cosmological constant, 40
Coulomb lattice, 223, 356
Coulomb stability of star, 207
Covariance, Lorentz, 132, 139
Covariant derivative, 31

Covariant divergence, 34, 35
and conservation law, 35
Covariant vector, 10, 14
law of transformation, 15
Crab pulsar, 184, 195, 196, 201, 203
Curvature tensor, 36; *see also* Einstein's curvature tensor; Riemann's curvature tensor
Curved spacetime, 17, 20, 22, 23, 26, 27, 36, 40, 45
and conservation of energy, 22
and tidal gravity, 21

Dark matter, 339
Death line, 191, 192
Deconfinement phase transition, 305, 306, 308, 326
Degenerate baryons and neutron stars, 59, 70, 94–98, 106, 182, 208, 210, 225–226
Degenerate electrons and white dwarfs, 70, 96, 100
Delta baryon, 214
Dipole age, 201
Dirac adjoint spinor, 140
Dirac effective mass, 146, 149
Dirac eigenvalues, 152
Dirac equation, 139, 149, 165, 170
Dirac gamma matrices, 139
Dirac Hamiltonian, 150
Dirac momentum eigenvalues, 149
Dirac spinor, 139
Dispersion measure, 190
Dispersion
DM, 190
due to interstellar plasma, 189
limits due to, 189
of pulsar signal, 185, 189, 190
Doppler shift, 182; *see also* Pulsar
Dragging of local inertial frame, 247, 249, 251, 255
Dust, interstellar, 55

Eötvös, 18
Earth, 64
Eddington, A., 58
Effective nucleon mass, 149, 234
at saturation density, 146, 155
See also Dirac effective mass; Landau effective mass
Einstein's curvature tensor, 39–41, 47, 54
Einstein's field equations, 40, 45, 48, 54, 67
from action principle, 52
and hydrostatic equilibrium, 68
in static isotropic spacetime, 42
outside a star, 44
Schwarzschild solution, 44
vanishing covariant divergence, 41
Einstein's general theory of relativity, 8, 68, 197
Electron capture, 97
Electron chemical potential, 238, 241
Electron pressure, 70, 88, 89, 93, 97
Element synthesis, in stars, 56
Energy-momentum tensor, 12, 46, 52, 54, 67, 134, 153, 155
Equality of inertial and gravitational mass, 18, 19
Equation of state, 61, 67, 113, 161, 167, 171, 218
BPS, 101, 243
causality, 113, 173
Fermi gas, 81
and first order phase transition, 113
Harrison–Wheeler, 101, 242
high density limit, 173
and limiting neutron star mass, 113
at low density, 221, 222
of neutron star matter, 216
satisfies $p < \epsilon$, 115
stiff, 113
See also Nuclear field theory
Equivalence principle, 19, 20, 23, 25, 28, 32, 61, 124
strong, 19
Euler–Lagrange equations, 130, 148; *see also* Nuclear field theory
Event, in spacetime, 9

Fermi momentum at nuclear saturation, 144
Four-vector, 9
Four-velocity, 11, 12, 31, 118
of fluid in a static star, 47, 48
Frame dragging, 247; *see also* Dragging of local inertial frame
Freely falling frame, 19, 23, 24, 27, 120; *see also* Lorentz frame; Inertial frame
Fundamental tensor, 18

Galilean metric, 9; *see also* Minkowski metric
Gamma-ray burster, 181
Gaussian curvature, 37
General beta equilibrium, 207, 214, 229; *see also* Neutron star matter
General covariance, 30, *see* Principle of general covariance
General relativity, 7, 197
strong field test, 341
Geodesic, 21, 22, 24, 25, 27, 32, 118, 121, 257
Gibbs's conditions, 305
Glitch, *see* Pulsar, glitch
Globular cluster, 185, 187, 190, 192, 348
Gravitational field, photon in, 20
Gravitational wave, 267, 270, 271
instabilities of rotating stars, 265, 273
limit on rotation of pulsars, 273
Gravitational action principle, 53
Gravitational binding, 180
Gravitational collapse, 51, 56, 59, 70, 97, 117, 223, 224, 227, 327
role of pressure, 52
Gravitational energy of a star, 66
Gravitational field, 67
Gravitational mass, 48, 50, 51, 69, 299
Gravitational, maximum, stellar redshift, 77
Gravitational radiation, 8, 68, 270
Gravitational radius, 51, 64
Gravitational redshift, 20, 21, 73, 77, 78, 120
Gravitational time dilation, 21, 73, 77, 253
Gravitational units, 62, 196
Gravity, partial decoupling of matter fields, 67

Hamilton's principle, 129
Harrison–Wheeler equation of state, 101
Hilbert, D., 53
Horizon, 120
Hulse–Taylor pulsar, 8, 68; *see also* Pulsar 1913+16
Hybrid star, 200, 286, 303, 304, 315
Hyperon, 124
in neutron star, 182, 210, 213, 229, 234
Hyperon coupling constants, 230, 231, 233
Hyperon fraction in neutron star, 234
Hyperon star, 229, 233
Hyperonization, 224, 229

Inertial frame
dragging by rotating star, 247
local, 19, 21, 25, 31, 110
Interstellar dust, 55
Invariant interval, 8, 9, 11, 13, 14, 23, 24, 43, 45, 119; *see also* Proper time
Invariant volume element, 33, 110
Iron
end point of fusion in stars, 56
and surface of neutron star, 70
Isospin current, 138, 164
baryon, 141
Isospin favored baryon, 221
Isospin invariance, 137
Isospin symmetry, 86, 145, 164, 207, 311
and crystalline structure in hybrid stars, 318
see also Nuclear symmetry energy

Jacobian, 33
Jeans instability, 56
Jupiter, 64

Kaon, 210, 211
Kaon condensation, 212, 238, 239
Kepler frequency, 256, 258
  in GR, 257
  self-consistency condition in GR, 248
Kiloparsec, 189

Lagrange multipliers, 83
Lagrangian density, 129
Lagrangian of matter, 53, 66, 213, 214
Lagrangian of nuclear matter, 147
Landau effective mass, 146
Lane–Emden equation, 90
Le Chatelier's principle, 91, 113, 277–279, 283, 301, 302
Light cone, 13, 121
Limit of $M/R < 4/9$ for static star, 109
Limiting mass, 52, 64, 69, 93, 95, 97–99, 106, 108, 109, 112, 145, 197, 199, 200, 218, 224, 227, 229, 233, 234
Limiting mass, Ruffini, 112
Limiting of M/R by Bondi, 110
Line element, 8, 14; *see also* Invariant interval
Lorentz boost, 9
Lorentz frame, 14, 22
  local, 19, 124
  local, mathematical definition, 26
Lorentz invariance, 8
Lorentz scalar, 130
Lorentz transformation, 8
Low-mass X-ray binaries, 118

Main sequence stars, 56
Mass limit, *see* Limiting mass
Maximum mass, *see* Limiting mass
Mean field approximation, 148, 173
Measurement precision, 26
Mercury, 8
Meson, *see* Nuclear field theory, Scalar meson, Rho meson, Omega meson
Metallicity of stars, 61
Metric tensor, 10, 14, 17, 24–26, 29, 31, 33, 36, 37, 53, 64, 67, 74, 111, 118, 120
  for axial symmetric spacetime, 249
  See also Minkowski and Schwarzschild, 14
Minkowski, 8, 10, 62
Minkowski metric, 9, 12, 14, 22, 28, 33, 53
Mixed phase, 303, 308, 315
  of complex substance, 308
  Coulomb lattice in, 313, 314, 316
  crystalline, 303, 313, 314, 317, 319, 323–325
  of hadronic and quark matter, 305
  of simple substance, 305
  of simple substance excluded in gravitational field, 308
Molecular cloud, 55
Moment of inertia, 203
  in GR, 254

Neutrino chemical potential, 209
Neutrino
  diffusion from protoneutron star, 328, 329, 331
  signal of Supernova, 327, 331, 332
  in stellar collapse, 58, 59
  thermalized in collapsing core, 327
  trapped, 327–329
Neutron drip density, 87, 100, 350, 351
Neutron star, 1, 70, 79, 81, 99, 181
  average density, 197
  baryon mass, 111, 299
  baryon number, 64
  binding energy per nucleon, 111, 112, 206
  birth, 59
  central density, 69, 97
  charge neutrality, 207, 211
  composition, 85, 208, 212, 213, 229
  compression energy per nucleon, 106, 111

Coulomb lattice, 313
crystalline interior, 303, 313, 314, 317, 319, 323–325
density, 1
distribution of mass-energy, 106
evolution, 210, 266
evolution of strangeness, 210
frozen state, 209
hyperons in, 229, 233
limiting mass, 182
limiting mass estimated, 234
mass, 64
mass-energy profile, 197
mass-radius relationship, 94, 106, 225
matter, 101, 183, 207, 208, 214, 217, 235, 237
hyperonization, 224
low density, 222
theory, 214
minimum Kepler period, 226
mixed phase, 315
moment of inertia, 196, 203
net electric charge, 207
pion condensation in, 237
quarks in, 315
radius, 64
resistance to collapse, 70
rotational limit, 275
sequence, 51, 234
stability, 70, 91
stability against removal of single nucleons, 112
temperature, 80, 208, 210, 216, 217, 266, 271, 272, 274
See also Limiting mass; Deconfinement phase transition
Neutronization, 97, 100, 104
in stellar collapse, 58
Newtonian approximation, 44
Newtonian physics, 41, 197
and connection to spacetime metric, 29
Newtonian star, 68, 87, 89
Nordtvedt experiments, 19
Nuclear binding energy, 144
Nuclear compression modulus, 145, 159
Nuclear equation of state, 144, 153, 155
Nuclear field theory, 127, 147, 214, 215
algebraic determination of couplings, 158, 218
equation of state, 167, 171
equation of state in high-density limit, 173
Euler–Lagrange equations, 171
ground-state expectation, 150
isospin force, 164
nuclear matter properties, 158
octet baryons, 169, 170
scalar self-interactions, 156
symmetry energy, 168
Nuclear force, 70, 207
Nuclear fusion in stars, 56
Nuclear mass formula, 144
Nuclear matter, 208, 214, 215, 237
properties, 143, 144, 218
theory, 54, 214
symmetric, 143
Nuclear saturation, 143, 153
density, 114, 144
Nuclear symmetry energy, 144, 145, 155, 168, 213, 214, 216, 228
Null cone, 121

Omega meson, 124, 136, 147
Euler–Lagrange equation, 157
Oppenheimer–Volkoff equations, 47, 50, 67–69
and one parameter family of stars, 51
scaling, 114
See also Limiting mass
Oppenheimer–Volkoff star, 98

Pauli blocking, 208–210
Pauli exclusion principle, 81, 207, 223, 227
Perfect fluid, 12, 46
Phase equilibrium, *see* Gibbs's conditions
Phase transition, 308
phase diagram for complex substance, 313

Phase transition (*cont.*)
See also Deconfinement phase transition; Mixed phase
Photon
in gravitational field, 20, 21
trajectory bent by gravity, 21
Pion condensation, 212, 213, 237
Planck scale, 122
Planetary companions of pulsar, 185
Planetary nebula, 57, 81, 95
Polytrope, 86, 87, 90
Pound–Rebka experiment, 20
Precession of orbit, 8, 41, 68, 184
Principle of equivalence, *see* Equivalence principle
Principle of general covariance, 30, 32, 46
Principle of relativity, 21, 32
Proper baryon number, 110
Proper time, 13, 76, 78; *see also* Invariant interval
Proton fraction in neutron star, 234
Protoneutron star, 59, 210, 326–332
Protostar, 56
Pulsar, 181, 184
Pulsar 1534+12, 185
Pulsar 1757−24, 193
Pulsar 1913+16, 8, 68, 184, 186, 203, 284
mass, 200
tests of general relativity, 8
Pulsar 1937+21, 186
Pulsar
angular spread of signal, 196
beaming, 183
binary, 68
braking index, 202
dipole age, 201, 203
discovery, 181
Doppler shift and companion star, 182
evolution, 191
fast, 338, 343, 347
glitch, 176, 193, 325
individual pulses, 188
integrated pulse, 188
magnetic field, 1, 195, 204
masses, 199
millisecond, 185, 187, 191, 266
mode switching, 189
nulling, 189
periods, 186
periods and dispersion, 189
planetary companion, 185
pulse profile, 188
recycled, 191, 266
subpulse drifting, 188
supernova association, 191
time variation of period, 201
velocity, 192
Pulsars, two populations, 190

QCD, 125, 289; *see also* Quark matter
Quark matter, 126, 289, 293, 303; *see also* Phase transition; Strange quark matter
Quark properties, 291
Quark star, *see* Strange stars

Radio telescope, 181
Radius of the galaxy, 189
Red giant, 57
Redshift, *see* Gravitational redshift
Relativistic mean-field approximation, 148
Rho meson, 124, 137
Euler–Lagrange equation, 165
isospin current, 138
Ricci scalar curvature, 53
Ricci tensor, 37, 43, 44, 47
symmetry, 37
Riemann curvature tensor, 36, 45
Riemann tensor, Bianchi identities, 38
Rotating star, 247
line element, 249
uniform rotation, 249, 252
See also Dragging of local inertial frame
Rotation of stars, 5
Rotational limit, 256
absolute, 275
GR, 285

Scalar curvature, 37, 47
Scalar density, 33, 152

Scalar meson, 135, 147
in nuclear matter, 153
Schwarzschild metric, 43, 45
Schwarzschild radius, 45, 122, 300
Schwarzschild singularity, 118, 120
Schwarzschild solution, 44, 64
Schwarzschild stars, 50
Self-bound star, 285, 286, 338; *see also* Strange star, 286
Separation formula, *see* Invariant interval
Sequence of neutron stars, 51, 223
Shapiro time delay, 8
Sigma meson, 124
Euler–Lagrange equation, 157
Simple substance, 305
Solar mass, 64
Special theory of relativity, 8, 13, 26, 29, 40, 41, 46
Spectral line and strong gravitational field, 73
Stability beyond neutron stars, 301
Stability of stars, 91, 93, 96, 256, 300
Stability of strange dwarfs, 357
Star formation, 55
Star surface and zero pressure, 73
Star
main sequence, 56
protostar, 56
Stellar evolution
end points, 55
low mass stars, 57
massive stars, 58
Stellar radius, 51
Stellar sequence, 70
Stellar structure, *see* Oppenheimer–Volkoff equations
Stellar surface and zero pressure, 51, 70
Strange dwarf, 355, 360
dense, 360
Strange matter hypothesis, 6, 337
Strange quark matter, 289, 296, 298
Strange star, 6, 337, 346, 350
Strange star with nuclear crust, 350
Strangeness, not conserved in stars, 207, 208
Stress-energy tensor, *see* Energy-momentum tensor
Sun, 64
Supergiants, 55
Supernova, 1, 59, 61, 95, 180, 191, 195, 199, 200, 207, 210, 327
remnant, 59, 180, 192
1987A, 327
Symmetries
global, 131
local, 131
Symmetry energy, *see* Nuclear symmetry energy

Tensor, 16
antisymmetric, 35
law of transformation, 17
Thermonuclear fusion, 56
Thermonuclear reactions, 58
Tidal gravity, 21
Time dilation, *see* Gravitational time dilation

Ultrabaric region, 109, 115
Units
gravitational, 62
nuclear and particle physics, 178

Vector meson, in nuclear matter, 153
Vector, *see* Contravariant vector; Covariant vector
Vela pulsar, 184, 193, 195, 203
Volume element, invariant, 33, 110

Weak interaction
role of in neutron star, 207, 211
timescale and hyperons in neutron stars, 207
White dwarf, 6, 57, 70, 79–81, 86, 90, 93, 94, 97, 99, 102, 181, 185, 197, 221, 222
He, O and C, 81, 87, 99, 102
limiting mass and electron capture, 97
mass, 80, 94
mass-radius relation, 94
maximum central density, 106, 357

White dwarf (*cont.*)
nature of limiting mass, 95, 96
stability, 91; *see also* Electron pressure
strange, 355
temperature, 80
World line, 28

X-ray binary, 181
X-ray pulsar Vela X-1, mass, 200'